U-007-105.5

*4379*

# *GROUNDWATER MODELING REPORT SUMMARY OF MODEL DEVELOPMENT APRIL 1993 FINAL*

*05/12/93*

*DOE-FN/EPA*
*500 REPORT*

# GROUNDWATER MODELING REPORT
# SUMMARY OF MODEL DEVELOPMENT

FERNALD ENVIRONMENTAL MANAGEMENT PROJECT
FERNALD, OHIO

REMEDIAL INVESTIGATION and FEASIBILITY STUDY

PREPARED FOR:

U.S. DEPARTMENT OF ENERGY
FERNALD FIELD OFFICE

PREPARED BY:

IT CORPORATION

April 1993

FINAL

01

4379

# GROUNDWATER MODELING REPORT
# SUMMARY OF MODEL DEVELOPMENT

FERNALD ENVIRONMENTAL MANAGEMENT PROJECT
FERNALD, OHIO

REMEDIAL INVESTIGATION and FEASIBILITY STUDY

PREPARED FOR:

U.S. DEPARTMENT OF ENERGY
FERNALD FIELD OFFICE

PREPARED BY:

IT CORPORATION

April 1993

FINAL

02

# TABLE OF CONTENTS


| | Page |
|---|---|
| List of Tables | iv |
| List of Figures | vi |
| List of Acronyms | xii |
| List of Abbreviations | xiii |
| 1.0 Introduction | 1-1 |
| 1.1 Objectives of the Modeling Program | 1-2 |
| 1.2 Support to Remedial Investigations | 1-3 |
| 1.3 Support to Risk Assessment | 1-4 |
| 1.4 Support to Feasibility Study | 1-4 |
| 2.0 Hydrologic and Geologic Characterization of the FEMP Area | 2-1 |
| 2.1 Introduction | 2-1 |
| 2.2 Surface Water Hydrology | 2-4 |
| 2.2.1 Great Miami River | 2-4 |
| 2.2.1.1 Great Miami River Hydrologic Characterization | 2-6 |
| 2.2.2 Paddys Run | 2-12 |
| 2.2.3 Storm Sewer Outfall Ditch | 2-15 |
| 2.3 Geologic Characterization of the FEMP Area | 2-15 |
| 2.3.1 Physiographic Province | 2-16 |
| 2.3.2 Regional Bedrock Geology | 2-16 |
| 2.3.3 Regional Glacial Geology | 2-17 |
| 2.4 Local Geology and Topography | 2-19 |
| 2.4.1 Bedrock Valley | 2-22 |
| 2.4.2 Great Miami Aquifer | 2-24 |
| 2.4.3 Glacial Overburden | 2-24 |
| 2.5 Local Geologic Trends | 2-29 |
| 3.0 Hydrogeologic Characterization of the FEMP Area | 3-1 |
| 3.1 Great Miami Aquifer | 3-7 |
| 3.2 Glacial Overburden Groundwater System | 3-10 |
| 3.3 Groundwater Elevations and Flow | 3-14 |
| 3.4 Surface Water/Groundwater Interaction | 3-20 |
| 3.4.1 Great Miami River/Groundwater Interaction | 3-22 |
| 3.4.2 Paddys Run/Groundwater Interaction | 3-22 |
| 4.0 Model Design | 4-1 |
| 4.1 Groundwater Model for the FEMP | 4-1 |

TABLE OF CONTENTS
(continued)


| | Page |
|---|---|
| 4.1.1 Model Code Selection | 4-7 |
| 4.1.2 Model Code Verification | 4-8 |
| 4.1.3 Overview of Technical Approach | 4-8 |
| 4.2 Hydrologic Parameter Estimation | 4-10 |
| 4.2.1 Regional Aquifer | 4-10 |
| 4.2.1.1 Transmissivities and Hydraulic Conductivities | 4-10 |
| 4.2.1.2 Porosity | 4-11 |
| 4.2.1.3 Infiltration/Recharge Rates | 4-11 |
| 4.2.1.4 Great Miami River Leakage | 4-12 |
| 4.2.1.5 Paddys Run Leakage | 4-12 |
| 4.2.1.6 Pumping Rates | 4-12 |
| 4.2.1.7 Contaminant Loading Periods | 4-13 |
| 4.2.1.8 Background Uranium Concentrations | 4-13 |
| 5.0 Groundwater Flow Model | 5-1 |
| 5.1 Preliminary Two-Dimensional Flow Model | 5-1 |
| 5.1.1 Regional Model Grid and Boundary Conditions | 5-1 |
| 5.1.2 Steady-State Flow Option | 5-3 |
| 5.1.3 Input Data | 5-4 |
| 5.1.4 Model Calibration Approach | 5-5 |
| 5.1.5 Model Calibration Results | 5-14 |
| 5.1.6 Sensitivity Analysis | 5-21 |
| 5.2 Three-Dimensional Flow Model | 5-21 |
| 5.2.1 Extension of Input Data | 5-24 |
| 5.2.2 Model Calibration Approach | 5-24 |
| 5.2.3 Model Calibration Results | 5-28 |
| 5.2.4 Sensitivity Analysis | 5-41 |
| 6.0 Solute Transport Model | 6-1 |
| 6.1 Analytical Solute Transport Modeling | 6-1 |
| 6.1.1 Approach | 6-1 |
| 6.1.2 Results - Waste Storage Area | 6-2 |
| 6.1.3 Results - South Plume Area | 6-3 |

TABLE OF CONTENTS
(continued)


| | Page |
|---|---|
| 6.2 Two-Dimensional Solute Transport Model | 6-8 |
| 6.2.1 Telescoping Regional Flow Model | 6-10 |
| 6.2.2 Model Grid | 6-10 |
| 6.2.3 Initial Conditions | 6-13 |
| 6.2.4 Input Data | 6-13 |
| 6.2.5 Source Loading Estimation | 6-15 |
| 6.2.6 Model Calibration | 6-18 |
| 6.2.7 Sensitivity Analysis | 6-22 |
| 6.3 Three-Dimensional Solute Transport Model | 6-22 |
| 6.3.1 Model Grid and Boundary Conditions | 6-23 |
| 6.3.2 Input Data and Groundwater Recalibration | 6-23 |
| 6.3.3 Model Calibration | 6-24 |
| 6.3.3.1 Preliminary Calibration Testing | 6-24 |
| 6.3.3.2 Final Calibration | 6-29 |
| References | |
| Appendix A - Geochemical Programs: Issues 3 and 5 Report | |
| Appendix B - 2DFLOW Model Evaluation | |
| Appendix C - 3DSOL Calibration Using Retardation Factor of 9 | |

## LIST OF TABLES


| Table | Title | Page |
|---|---|---|
| 2-1 | A Summary of Values Calculated From HEC-2 Model for the Site Reach of the Great Miami River, Used as a Basis for Input to STRIP1B Model | 2-10 |
| 3-1 | Summary, Hydraulic Conductivity Testing | 3-12 |
| 4-1 | Results of Literature Review for Model Development | 4-2 |
| 4-2 | Estimated Uranium Loss to Storm Sewer System and Storm Sewer Outfall Ditch | 4-14 |
| 4-3 | Background Uranium Concentrations | 4-17 |
| 5-1 | Observed Groundwater Elevations for 2D and 3D Model Calibration April 1986 | 5-7 |
| 5-2 | Statistical Tests for 2DFLOW Model Calibration Based on April 1986 Data | 5-11 |
| 5-3 | Initial Input Hydraulic Conductivity and Recharge Values Used in the 2DFLOW Model | 5-13 |
| 5-4 | Water Balance in the Vicinity of the Southwestern Ohio Water Company Collector Wells for the Two-Dimensional FLOW Model | 5-18 |
| 5-5 | Results of the Sensitivity Analysis for the Two-Dimensional Flow Model Utilizing Run 2DFLOW | 5-22 |
| 5-6 | Statistical Tests for 3DFLOW Model Calibration | 5-39 |
| 5-7 | Water Balance in the Vicinity of the Southwestern Ohio Water Company Collector Well for the Three-Dimensional Flow Model | 5-40 |
| 5-8 | Results of the Sensitivity Analysis for the Three-Dimensional Flow Model Utilizing Run 3DFLOW | 5-48 |
| 5-9 | Results of the Sensitivity Analysis for the Three-Dimensional Flow Model Utilizing Run 3DFLOW | 5-49 |
| 6-1 | Comparison of the Measured and Predicted Concentrations for Shallow Wells in the Waste Pit Area | 6-4 |

## LIST OF TABLES
(continued)


| Table | Title | Page |
|---|---|---|
| 6-2 | Outlier Data Eliminated for Uranium Concentration Model Calibration | 6-27 |
| 6-3 | Observed Concentrations 95 Percent Confidence Intervals for the Means, and Calculated Concentrations for the Three-Dimensional Finite-Difference Solute Transport Model Retardation Factor 12 | 6-32 |
| 6-4 | Uranium Loading Rates for Source Areas in the Three-Dimensional Finite-Difference Solute Transport Model, Retardation Factor 12, Longitudinal Dispersivity 100 Feet, and Transverse Dispersivity 10 Feet | 6-46 |
| 6-5 | Total Uranium Loading for Source Areas in the Three-Dimensional Finite-Difference Solute Transport Model, Retardation Factor 12, Longitudinal Dispersivity 100 Feet, and Transverse Dispersivity 10 Feet | 6-47 |
| C-1 | Inlier Concentrations Calculated by the Three-Dimensional Finite-Difference Solute Transport Model Retardation Factor 9 | C-2 |
| C-2 | Outlier Concentrations Calculated by the Three-Dimensional Finite-Difference Solute Transport Model Retardation Factor 9 | C-5 |
| C-3 | Uranium Loading Rates for Source Areas in the Three-Dimensional Finite-Difference Solute Transport Model, Retardation Factor 9, Longitudinal Dispersivity 50 Feet, and Transverse Dispersivity 1 Foot | C-11 |
| C-4 | Total Uranium Loadings for Source Areas in the Three-Dimensional Finite-Difference Solute Transport Model, Retardation Factor 9, Longitudinal Dispersivity 50 feet, and Transverse Dispersivity 1 Foot | C-12 |
| C-5 | Results of the Sensitivity Analysis for the Three-Dimensional Finite-Difference Solute Transport Model Retardation Factor 9 | C-18 |

## LIST OF FIGURES


| Figure | Title | Page |
|---|---|---|
| 2-1 | Five Mile Radius Map, FEMP | 2-2 |
| 2-2 | Location of Major Features at the FEMP | 2-3 |
| 2-3 | Surface Water Hydrology | 2-5 |
| 2-4 | River Stage at Hamilton and Ross, Ohio 1985 and 1986 | 2-8 |
| 2-5 | Location of River Cross Sections Used to Obtain Hydraulic Characteristics | 2-9 |
| 2-6 | Topographic Map of the FEMP | 2-14 |
| 2-7 | Schematic Diagram of the Deep Stage Drainage System and the Present Drainage System | 2-18 |
| 2-8 | Generalized Stratigraphic Column of the FEMP Region | 2-20 |
| 2-9 | Generalized Geologic Cross-Section, FEMP Area | 2-21 |
| 2-10 | 3-Dimensional Bedrock Configuration | 2-23 |
| 2-11 | Bedrock Topography | 2-25 |
| 2-12 | Clay Interbed Isopach | 2-26 |
| 2-13 | Clay Interbed Topographic Surface | 2-27 |
| 2-14 | Glacial Overburden Isopach | 2-28 |
| 2-15 | Study Area Geologic Cross Section Locations | 2-30 |
| 2-16 | Geologic Cross Section A-A' Study Area | 2-31 |
| 2-17 | Geologic Cross Section B-B' Study Area | 2-32 |
| 2-18 | Geologic Cross Section C-C' Study Area | 2-33 |
| 2-19 | Geologic Cross Section D-D' Study Area | 2-34 |
| 2-20 | Geologic Cross Section E-E' Study Area | 2-35 |
| 2-21 | Geologic Cross Section F-F' Study Area | 2-36 |

## LIST OF FIGURES
(continued)


| Figure | Title | Page |
|---|---|---|
| 2-22 | Geologic Cross Section G-G' Study Area | 2-37 |
| 2-23 | Geologic Cross Section H-H' Study Area | 2-38 |
| 2-24 | Geologic Cross Section I-I' Study Area | 2-39 |
| 2-25 | Geologic Cross Section J-J' Study Area | 2-40 |
| 2-26 | Geologic Cross Section K-K' Study Area | 2-41 |
| 2-27 | Geologic Cross Section L-L' Study Area | 2-42 |
| 3-1 | Groundwater Monitoring Well Completion Depths | 3-2 |
| 3-2 | Monitoring Well Locations, 1000 Series Wells | 3-3 |
| 3-3 | Monitoring Well Locations, 2000 Series Wells | 3-4 |
| 3-4 | Monitoring Well Locations, 3000 Series Wells | 3-5 |
| 3-5 | Monitoring Well Locations, 4000 Series Wells | 3-6 |
| 3-6 | Hydrogeologic Environments | 3-9 |
| 3-7 | Generalized Groundwater Flow Direction in Great Miami Aquifer | 3-15 |
| 3-8 | Regional Groundwater Elevations, August 1982 | 3-16 |
| 3-9 | Regional Groundwater Elevations, April 1986 | 3-17 |
| 3-10 | Regional Groundwater Elevations, May 1988 | 3-18 |
| 3-11 | Hydrograph of Well O2E, January 1981 - December 1989 | 3-21 |
| 3-12 | Areas of Surface Water Infiltration to the Great Miami Aquifer Along Paddys Run | 3-23 |
| 3-13 | Hydrograph of Paddys Run and Great Miami Aquifer at Well Location 14, February 24, 1989 - June 26, 1989 | 3-25 |

## LIST OF FIGURES
(continued)


| Figure | Title | Page |
|---|---|---|
| 3-14 | Hydrograph of Paddys Run and Great Miami Aquifer at Well Location 14, April 27, 1989 - April 30, 1989 | 3-26 |
| 4-1 | Background Monitoring Well Locations | 4-18 |
| 5-1 | Swift III Flow Model Grid for RI/FS Model Area | 5-2 |
| 5-2 | Refined 2-Dimensional Flow Model, Model Zones | 5-6 |
| 5-3 | Refined 2-Dimensional Flow Model Residual Heads for Calibrated Run, April 1986 Data | 5-15 |
| 5-4 | Refined 2-Dimensional Flow Model Calibrated Run, Flow Vectors and Potentiometric Surface | 5-16 |
| 5-5 | Refined 2-Dimensional Flow Model, Hydraulic Conductivity Zones | 5-19 |
| 5-6 | Refined 2-Dimensional Flow Model Recharge Zones, Pumping Rates, and Boundary Heads | 5-20 |
| 5-7 | Swift III Model Grid for RI/FS Model Area with Cross Section Locations | 5-25 |
| 5-8 | Geologic Cross Section Q-Q Showing Model Layers | 5-26 |
| 5-9 | Geologic Cross Section R-R Showing Model Layers | 5-27 |
| 5-10 | 3-Dimensional Flow Model, Hydraulic Conductivity Zones - Layer 1 | 5-29 |
| 5-11 | 3-Dimensional Flow Model, Hydraulic Conductivity Zones - Layer 2 | 5-30 |
| 5-12 | 3-Dimensional Flow Model, Hydraulic Conductivity Zones - Layer 3 | 5-31 |
| 5-13 | 3-Dimensional Flow Model, Hydraulic Conductivity Zones - Layer 4 | 5-32 |
| 5-14 | 3-Dimensional Flow Model, Hydraulic Conductivity Zones - Layer 5 | 5-33 |
| 5-15 | 3-Dimensional Flow Model Recharge Zones, Pumping Rates, and Boundary Heads | 5-35 |
| 5-16 | 3-Dimensional Flow Model, Residual Heads for Calibrated Run, April 1986 Data, Layer 1 | 5-36 |

## LIST OF FIGURES
(continued)


| Figure | Title | Page |
|---|---|---|
| 5-17 | 3-Dimensional Flow Model, Residual Heads for Calibrated Run, April 1986 Data, Layer 2 | 5-37 |
| 5-18 | 3-Dimensional Flow Model, Residual Heads for Calibrated Run, April 1986 Data, Layer 3,4,5 | 5-38 |
| 5-19 | 3-Dimensional Flow Model, Calibrated Run, Layer 1, Flow Vectors and Potentiometric Surface | 5-42 |
| 5-20 | 3-Dimensional Flow Model, Calibrated Run, Layer 2, Flow Vectors and Potentiometric Surface | 5-43 |
| 5-21 | 3-Dimensional Flow Model, Calibrated Run, Layer 3, Flow Vectors and Potentiometric Surface | 5-44 |
| 5-22 | 3-Dimensional Flow Model, Calibrated Run, Layer 4, Flow Vectors and Potentiometric Surface | 5-45 |
| 5-23 | 3-Dimensional Flow Model, Calibrated Run, Layer 5, Flow Vectors and Potentiometric Surface | 5-46 |
| 5-24 | Collector Wells, Combined Average Annual Pumping Rate | 5-50 |
| 6-1 | Analytical Solute Transport Model Observed and Predicted Normalized Uranium Concentrations for North Plume Area Varying Source Widths | 6-5 |
| 6-2 | Analytical Solute Transport Model Predicted Normalized Uranium Concentration Distribution for Waste Storage Area in 1988 | 6-6 |
| 6-3 | Analytical Solute Transport Model Time Versus Uranium Mass Loss at Storm Sewer Outfall Ditch Area with Fitted Curves | 6-7 |
| 6-4 | Analytical Solute Transport Model Predicted Normalized Uranium Concentration Distribution for Southern Plume Area in 1988 | 6-9 |
| 6-5 | Groundwater Modeling Grid Boundaries | 6-11 |
| 6-6 | Solute Transport Model Grid | 6-12 |
| 6-7 | Comparison of Simulated Groundwater Contours from 2DFLOW and 2DSOL Models | 6-14 |

## LIST OF FIGURES
(continued)


| Figure | Title | Page |
|---|---|---|
| 6-8 | Solute Transport Model Source Loading Locations and Pumping Well Rates | 6-17 |
| 6-9 | Two-Dimensional Solute Transport Model Simulated Uranium Concentrations Present Conditions | 6-20 |
| 6-10 | Observed Uranium Concentrations - 2000 Series Wells | 6-21 |
| 6-11 | Three-Dimensional Solute Transport Model Nondetect Well Locations | 6-26 |
| 6-12 | Three-Dimensional Solute Transport Model Calibration Well Locations | 6-28 |
| 6-13 | Three-Dimensional Solute Transport Model Residual Concentrations for Calibrated Run, Layer 1, Retardation Factor 12 | 6-37 |
| 6-14 | Three-Dimensional Solute Transport Model Residual Concentrations for Calibrated Run, Layers 2 through 5, Retardation Factor 12 | 6-38 |
| 6-15 | Three-Dimensional Solute Transport Model Source Loading Rates, Source Period 1, Retardation Factor 12 | 6-41 |
| 6-16 | Three-Dimensional Solute Transport Model Source Loading Rates, Source Period 2, Retardation Factor 12 | 6-42 |
| 6-17 | Three-Dimensional Solute Transport Model Source Loading Rates, Source Period 3, Retardation Factor 12 | 6-43 |
| 6-18 | Three-Dimensional Solute Transport Model Source Loading Rates, Source Period 4, Retardation Factor 12 | 6-44 |
| 6-19 | Three-Dimensional Solute Transport Model Source Loading Rates, Source Period 5, Retardation Factor 12 | 6-45 |
| 6-20 | Three-Dimensional Solute Transport Model Simulated Uranium Concentrations Present Conditions, Layer 1, Retardation Factor 12 | 6-49 |
| 6-21 | Three-Dimensional Solute Transport Model Simulated Uranium Concentrations Present Conditions, Layer 2, Retardation Factor 12 | 6-50 |
| 6-22 | Three-Dimensional Solute Transport Model Simulated Uranium Concentrations Present Conditions, Layer 3, Retardation Factor 12 | 6-51 |

## LIST OF FIGURES
(continued)


| Figure | Title | Page |
|---|---|---|
| 6-8 | Solute Transport Model Source Loading Locations and Pumping Well Rates | 6-17 |
| 6-9 | Two-Dimensional Solute Transport Model Simulated Uranium Concentrations Present Conditions | 6-20 |
| 6-10 | Observed Uranium Concentrations - 2000 Series Wells | 6-21 |
| 6-11 | Three-Dimensional Solute Transport Model Nondetect Well Locations | 6-26 |
| 6-12 | Three-Dimensional Solute Transport Model Calibration Well Locations | 6-28 |
| 6-13 | Three-Dimensional Solute Transport Model Residual Concentrations for Calibrated Run, Layer 1, Retardation Factor 12 | 6-37 |
| 6-14 | Three-Dimensional Solute Transport Model Residual Concentrations for Calibrated Run, Layers 2 through 5, Retardation Factor 12 | 6-38 |
| 6-15 | Three-Dimensional Solute Transport Model Source Loading Rates, Source Period 1, Retardation Factor 12 | 6-41 |
| 6-16 | Three-Dimensional Solute Transport Model Source Loading Rates, Source Period 2, Retardation Factor 12 | 6-42 |
| 6-17 | Three-Dimensional Solute Transport Model Source Loading Rates, Source Period 3, Retardation Factor 12 | 6-43 |
| 6-18 | Three-Dimensional Solute Transport Model Source Loading Rates, Source Period 4, Retardation Factor 12 | 6-44 |
| 6-19 | Three-Dimensional Solute Transport Model Source Loading Rates, Source Period 5, Retardation Factor 12 | 6-45 |
| 6-20 | Three-Dimensional Solute Transport Model Simulated Uranium Concentrations Present Conditions, Layer 1, Retardation Factor 12 | 6-49 |
| 6-21 | Three-Dimensional Solute Transport Model Simulated Uranium Concentrations Present Conditions, Layer 2, Retardation Factor 12 | 6-50 |
| 6-22 | Three-Dimensional Solute Transport Model Simulated Uranium Concentrations Present Conditions, Layer 3, Retardation Factor 12 | 6-51 |

## LIST OF FIGURES
(continued)


| Figure | Title | Page |
|---|---|---|
| 6-23 | Three-Dimensional Solute Transport Model Simulated Uranium Concentrations Present Conditions, Layer 4, Retardation Factor 12 | 6-52 |
| 6-24 | Three-Dimensional Solute Transport Model Simulated Uranium Concentrations Present Conditions, Layer 5, Retardation Factor 12 | 6-53 |
| C-1 | Three-Dimensional Solute Transport Model Source Loading Rates, Source Period 1 Retardation Factor 9 | C-7 |
| C-2 | Three-Dimensional Solute Transport Model Source Loading Rates, Source Period 2 Retardation Factor 9 | C-8 |
| C-3 | Three-Dimensional Solute Transport Model Source Loading Rates, Source Period 3 Retardation Factor 9 | C-9 |
| C-4 | Three-Dimensional Solute Transport Model Source Loading Rates, Source Period 4 Retardation Factor 9 | C-10 |
| C-5 | Three-Dimensional Solute Transport Model Simulated Uranium Concentrations Present Conditions, Layer 1, Retardation Factor 9 | C-13 |
| C-6 | Three-Dimensional Solute Transport Model Simulated Uranium Concentrations Present Conditions, Layer 2, Retardation Factor 9 | C-14 |
| C-7 | Three-Dimensional Solute Transport Model Simulated Uranium Concentrations Present Conditions, Layer 3, Retardation Factor 9 | C-15 |
| C-8 | Three-Dimensional Solute Transport Model Simulated Uranium Concentrations Present Conditions, Layer 4, Retardation Factor 9 | C-16 |
| C-9 | Three-Dimensional Solute Transport Model Simulated Uranium Concentrations Present Conditions, Layer 5, Retardation Factor 9 | C-17 |

# LIST OF ACRONYMS

| | |
|---|---|
| 2DSOL | Two-dimensional analytical solution for solute transfer in groundwater |
| 2DFLOW | Two-dimensional flow modeling |
| 3DSOL | Three-dimensional analytical solution for solute transfer in groundwater |
| 3DFLOW | Three-dimensional flow modeling |
| A&W | Albright and Wilson Company |
| CIT/CIS | Centered in Time/Central in Space |
| DOE | U.S. Department of Energy |
| EPA | U.S. Environmental Protection Agency |
| ERDA | U.S. Energy Research and Development Administration |
| FEMP | Fernald Environmental Management Project |
| FMPC | Fernald Materials Processing Center |
| HEC-2 Model | Hydraulic Engineering Center |
| IT | IT Corporation |
| NAVFAC | Naval Facilities Engineering Command |
| NLO | National Lead Company of Ohio |
| ODNR | Ohio Department of Natural Resources |
| OU | Operable unit |
| QAPP | Quality Assurance Project Plan |
| RCRA | Resource Conservation and Recovery Act |
| RI/FS | Remedial Investigation/Feasibility Study |
| SOWC | Southwestern Ohio Water Company |
| USGS | U.S. Geological Survey |
| WEMCO | Westinghouse Environmental Management Company of Ohio |
| WMCO | Westinghouse Materials Company of Ohio |

# LIST OF ABBREVIATIONS

| | |
|---|---|
| cfs | cubic feet per second |
| Ci | curie |
| cm/s | centimeters per second |
| ft/day | feet per day |
| ft | feet |
| $ft^2$/day | square feet per day |
| $ft^2$ | square feet |
| $ft^3$ | cubic feet |
| $ft^3$/lb | cubic feet per pound |
| $ft^3$/s | cubic feet per second |
| g/cc | grams per cubic centimeter |
| gpd/$ft^2$ | gallons per day per square foot |
| gpd | gallons per day |
| gpm/ft | gallons per minute per foot |
| gpm | gallons per minute |
| in./yr | inches per year |
| kg | kilogram |
| km | kilometers |
| lbs | pounds |
| mgd | million gallons per day |
| msl | Mean sea level |
| µg/L | micrograms per liter |
| N | north |
| psi | pounds per square inch |
| $R_f$ | retardation factor |
| s | seconds |
| $UF_4$ | uranium tetrafluoride |
| $UO_2$ | uranium dioxide |
| $UO_3$ | uranium trioxide |
| W | west |

# 1.0 INTRODUCTION

Groundwater modeling studies were initiated at the Fernald Environmental Management Project (FEMP) by IT Corporation (IT) at the request of the U.S. Department of Energy (DOE). These studies were to support interim activities and different aspects of the remedial investigation/feasibility study (RI/FS) and associated risk assessments. The work plan covering these studies was developed by IT (1988a). This report describes the construction, calibration, and model evaluation of the finite-difference groundwater flow and solute transport models developed for use in the FEMP RI/FS. Model construction is the development of computer input files that constitute the model. Model calibration is the adjustment of parameters in the input file until the model is an adequate representation of the real system. Model evaluation involves the prediction of future conditions through the application of the model to simulate a particular site. Model calibration was completed in December 1990, and this report only addresses modeling work and FEMP studies done up to this time. Tasks performed after December 1990 are addressed in their individual operable unit reports.

The modeling program began with the development of a conceptual model using available site studies and literature sources. This conceptual model is presented in Chapter 2.0, along with the development of the initial modeling parameters derived from the literature used in the program. This conceptual model was modified during the modeling process as more of the FEMP's geology and hydrogeology was understood, but essentially provided the baseline understanding of the hydrogeologic system. Incorporated into this conceptual model is an interpretation of the FEMP's geology and hydrogeology as of December 1990, which is presented in Chapters 3.0 and 4.0. The final solute transport calibration also used the results of an IT geochemical study of the FEMP, which is reproduced in Appendix A.

A total of two groundwater flow models were built on a regional scale using a regional model grid. A two-dimensional model was initially built, which was later modified to become three dimensional and updated with additional stratigraphy. These regional scale models are discussed in Chapter 5.0. The resulting flow fields obtained from these models were imported into a local scale model grid which was used to simulate solute transport. Additional evaluation of the three-dimensional flow model was also undertaken using a different data set, which is discussed in Appendix B.

Two successive solute transport model calibrations using the local model grid are reported herein. The first calibration was developed before the results of the geochemical modeling were available from the report reproduced in Appendix A. It was a provisional calibration that was adequate for use in supporting a removal action for mitigating contamination south of the FEMP pending final action under the RI/FS and is presented in Appendix C. The second calibration was completed when the results of the geochemical modeling were available and is presented in Chapter 6.0. The second

calibration produced a more refined model that benefitted from the geochemical results and from additional uranium concentration data that had become available. Its degree of calibration is higher, and it has been used to support ongoing RI/FS activities. The solute transport model calibration was completed for total dissolved uranium only, since uranium is the principal contaminant of concern at the FEMP, although other contaminants do exist.

The scope of the report is limited to a description of those modeling activities, data, and results necessary to establish the validity and applicability of the model to FEMP conditions. It excludes such technical details as descriptions of all minor data preprocessing and postprocessing computer programs and procedures, descriptions of numerous individual model calibration runs, and other routine modeling activities and technicalities. These details are recorded in project files and computer files stored on magnetic tapes.

## 1.1 OBJECTIVES OF THE MODELING PROGRAM

The overall objective of the modeling program at the FEMP is to supplement the existing geologic, hydrogeologic, and geochemical database in order to support the RI/FS process. The hydrologic regime impacted by the FEMP activities encompasses a large area with complex geologic and hydrologic conditions. The development of the model was necessary to supplement direct field observations so that the combined informational base would be sufficient to support the understanding of the current situation in the RI, the projection of future conditions in the public health and environmental risk assessment, and the evaluation of the remedial action alternatives in the FS. The specific support to be provided to these activities is described in Sections 1.2 through 1.4.

The field observations, including groundwater monitoring, establish whether contamination may be present at a specific location and to what level. Groundwater modeling provides a systematic means to interpolate between and extrapolate beyond the field observations of the contaminant concentration throughout the area of interest. In particular, the information from the modeling is used in conjunction with available field observations to:

- Estimate the location and value of the maximum uranium concentration
- Estimate the mass of the contaminant present in the aquifer
- Explain the occurrence of the field observations
- Indicate whether or not any field observations should be considered as anomalies.

The following hydrologic, geologic, and geochemical issues are addressed by the models described in this report:

- Groundwater flow rates and directions relative to the FEMP waste storage area, waste discharge areas, and areas of postulated releases
- Recharge to the regional aquifer, including the interrelationship between the aquifer and the principal surface water courses
- Relationship between water quality data and the identified potential contaminant sources
- The relative importance of the identified sources in terms of uranium loading rates to the aquifer
- The effects of geochemical variability in the aquifer system as it relates to contaminant mobility.

## 1.2 SUPPORT TO REMEDIAL INVESTIGATIONS

The purpose of the RI is to determine the nature and extent of any release, or threat thereof, of hazardous or radioactive substances, pollutants, or contaminants, and to gather all necessary data to support the FS. The RI is intended to satisfy the following specific objectives that are supported by the groundwater modeling:

- Identify and characterize any sources of radiological and chemical contamination
- Determine the nature and extent of radiological and chemical contaminants
- Identify the pathways and mechanisms for radiological and chemical constituent migration, and conduct public health risk assessments and environmental impact studies
- Develop, validate, and apply various site models to augment the current understanding of the site environment, and to predict future impacts with and without remedial actions
- Provide necessary information for the identification, evaluation, and selection of the most environmentally and economically acceptable alternatives in the FS.

For the purposes of the RI, a principal use of the groundwater flow and solute transport models is to develop an understanding of the nature and extent of the contamination. Significant pathways associated with past and current releases are evaluated to refine the assessment of current risk posed by contaminated groundwater. A key application of the model is to augment the existing database by

providing a systematic means to fill in the gaps between the single-point observations. Prediction of the locations of the maximum concentration resulting from the integration of the contributions from multiple sources, as well as the approximate extent of coalesced contaminant plumes, represent the types of information that can be most effectively generated via the application of the models. It is these types of information that are critical to the evaluation of current and future risks.

Uranium has been designated as the principal contaminant of concern at this time and is the only contaminant selected for detailed modeling. Other contaminants including radionuclides, metals, and organics have been detected in regions underlying the FEMP, but are not as regionally extensive as the uranium contamination. If deemed necessary at a later date, other contaminants could be considered through an appropriate adjustment of the solute transport model, by adjusting parameters such as retardation, contaminant decay constants, source loading areas, and source loading rates.

## 1.3 SUPPORT TO RISK ASSESSMENT

The baseline risk assessment evaluates the no-action alternative for the FEMP considering both the radionuclides and indicator chemicals. The baseline risk assessment is comprised of an assessment of the exposure pathways and an evaluation of the risk posed by the intake of the contaminants of concern by hypothetical off-FEMP individuals or population groups.

An evaluation of the no-action alternative requires the prediction of future conditions and associated risks if all sources and pathways are unaltered from their current status. Since past and current field observations cannot yield such predictions directly, the results of the models become a critical input to the no-action assessment. The groundwater flow and solute transport models will be used to predict whether concentrations in groundwater at critical receptor locations will increase and whether additional receptors will be impacted to a significant extent.

The initial condition for the no-action model is equated to the model output in the evaluation of current conditions, thus the effects of any past releases are accounted for by existing concentrations in the groundwater. Current and potential future releases are quantified as sources to the extent possible with available data.

## 1.4 SUPPORT TO FEASIBILITY STUDY

The objective of the FS is to develop and evaluate remedial action alternatives to protect public health, public welfare, and the environment from releases or threatened releases of hazardous or radioactive substances, pollutants, or contaminants at or from the FEMP. The groundwater flow and solute transport models are used to support the evaluation of the remedial action alternatives in the FS.

One application of the model in the FS involves using the groundwater flow and solute transport models to evaluate the technical feasibility of remedial actions, including evaluating the locations and pumping rates of extraction wells, and determining the areas that could serve as sources of water for any potable water replacement wells. The modification of pathways by depressing the groundwater levels through pumping to control groundwater flow can also be accounted for in the groundwater flow model. The resultant flow field, however, influences contaminant transport patterns; thus, impacts at receptor locations must be further examined by application of the solute transport model.

The second type of model application in the FS involves the solute transport model for the prediction of future conditions under various remedial action alternatives. Actions that are source control measures are simulated by eliminating current or future releases from the model input. However, since full source control is rarely realized in practice, the model is also used to assess the effects of incomplete source control and to evaluate various source reduction measures to determine the most cost-effective program. The temporal and spatial variations of uranium concentration resulting from the different remedial actions are predicted.

The groundwater flow model in conjunction with the solute transport model also finds use as a tool for the conceptual design phase of the FS. For example, the models can be used to determine the number, location, orientation, and pumping rates of extraction wells to most cost-effectively capture a contaminant plume.

# 2.0 HYDROLOGIC AND GEOLOGIC CHARACTERIZATION OF THE FEMP AREA

A basic understanding of the hydrologic surface water system and the geologic environment on both a regional and site-specific basis is essential prior to initiating a groundwater modeling effort. It is with this reasoning that the following section presents: (1) a general introduction describing the former operations and the current waste management areas at the FEMP, (2) a general characterization of the surface water resources that occur in the vicinity of the FEMP facility, and (3) a brief description of the geology in the FEMP area. The surface water and geologic interpretations presented in this section are those that were used in the selection of parameters and modeling conditions for use in the groundwater modeling effort. The interpretations are based on information that was available as of December 1990.

## 2.1 INTRODUCTION

The FEMP is located on 1050 acres in a rural area of Hamilton and Butler counties, approximately 17 miles northwest of Cincinnati, Ohio. There are scattered residences and several villages, including Fernald, New Baltimore, Ross, New Haven, and Shandon, located within a 5-mile radius of the FEMP (Figure 2-1). Activities such as farming and raising dairy and beef cattle account for the majority of the land use in the surrounding area.

The FEMP is a government-owned, contractor-operated, federal facility formerly used for the production of pure uranium materials for the DOE. A variety of chemical and metallurgical processes were used at the FEMP to manufacture uranium products. During the manufacturing process, high-quality uranium compounds were introduced into the FEMP process at several points. Impure starting materials were dissolved in nitric acid and the uranium was purified through solvent extraction to yield a solution of uranyl nitrate. Evaporation and heating converted the nitrate solution to uranium trioxide ($UO_3$) powder. This compound was reduced with hydrogen to uranium dioxide ($UO_2$) and then converted to uranium tetrafluoride ($UF_4$) by reaction with anhydrous hydrogen fluoride. Uranium metal was produced by reacting $UF_4$ and magnesium metal in a refractory-lined vessel. The primary uranium metal was then remelted with scrap uranium metal to yield a purified uranium ingot. Various uranium metal working processes were also conducted at the site. In addition, the FEMP served as the thorium repository for the DOE and maintains long-term storage of these materials.

Uranium production at the FEMP was suspended in July 1989, and all subsequent activities have been focused on environmental restoration. Waste and effluent management practices at the FEMP played a significant role in determining the nature and extent of contamination at the facility and the potential for future contamination events. Before 1984, solid and slurried wastes from FEMP processes were disposed of in the on-property waste storage areas (Figure 2-2).

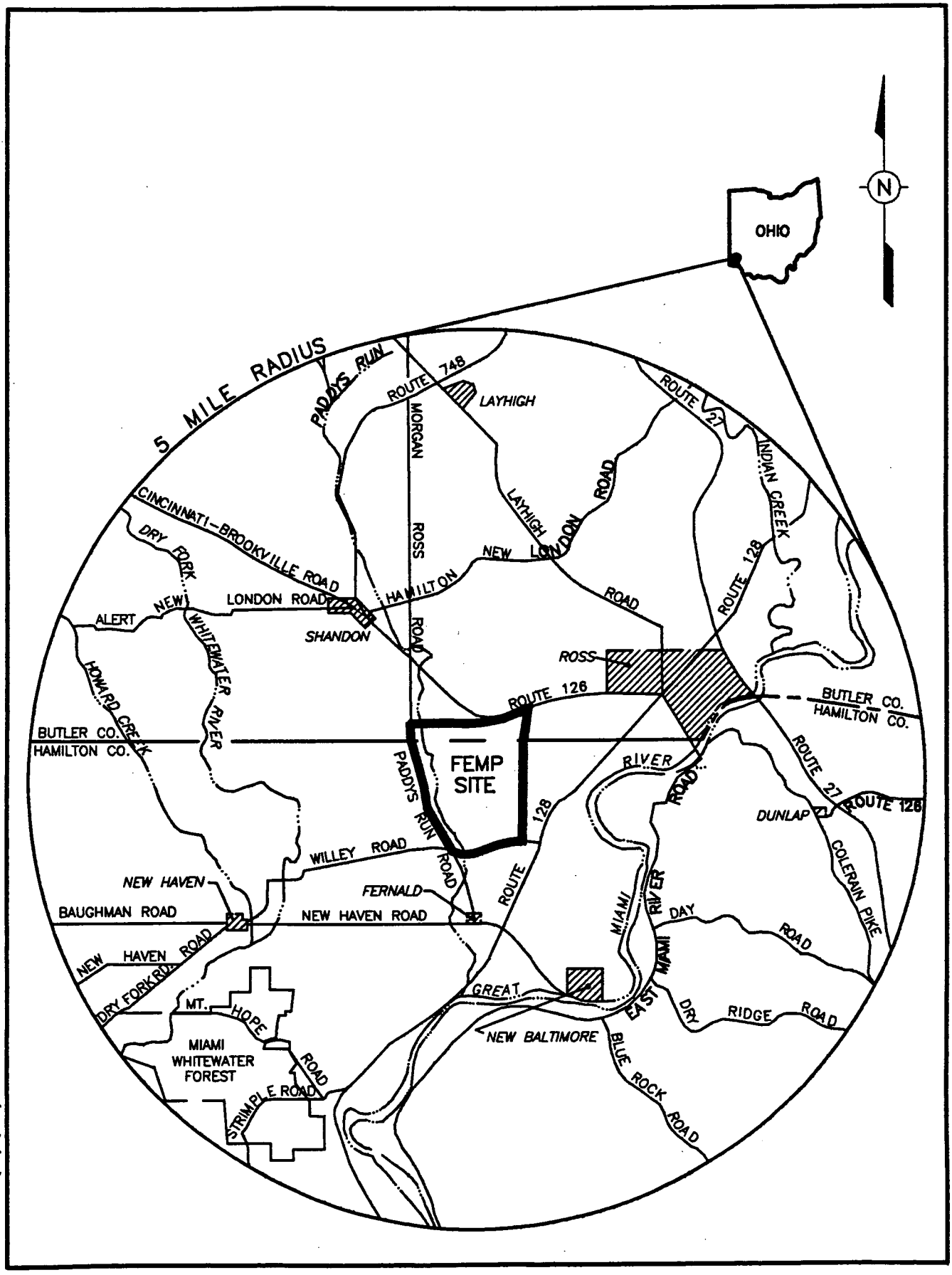


409195-A41 (GW) (PGH)

FIGURE 2-1 FEMP FIVE-MILE RADIUS MAP

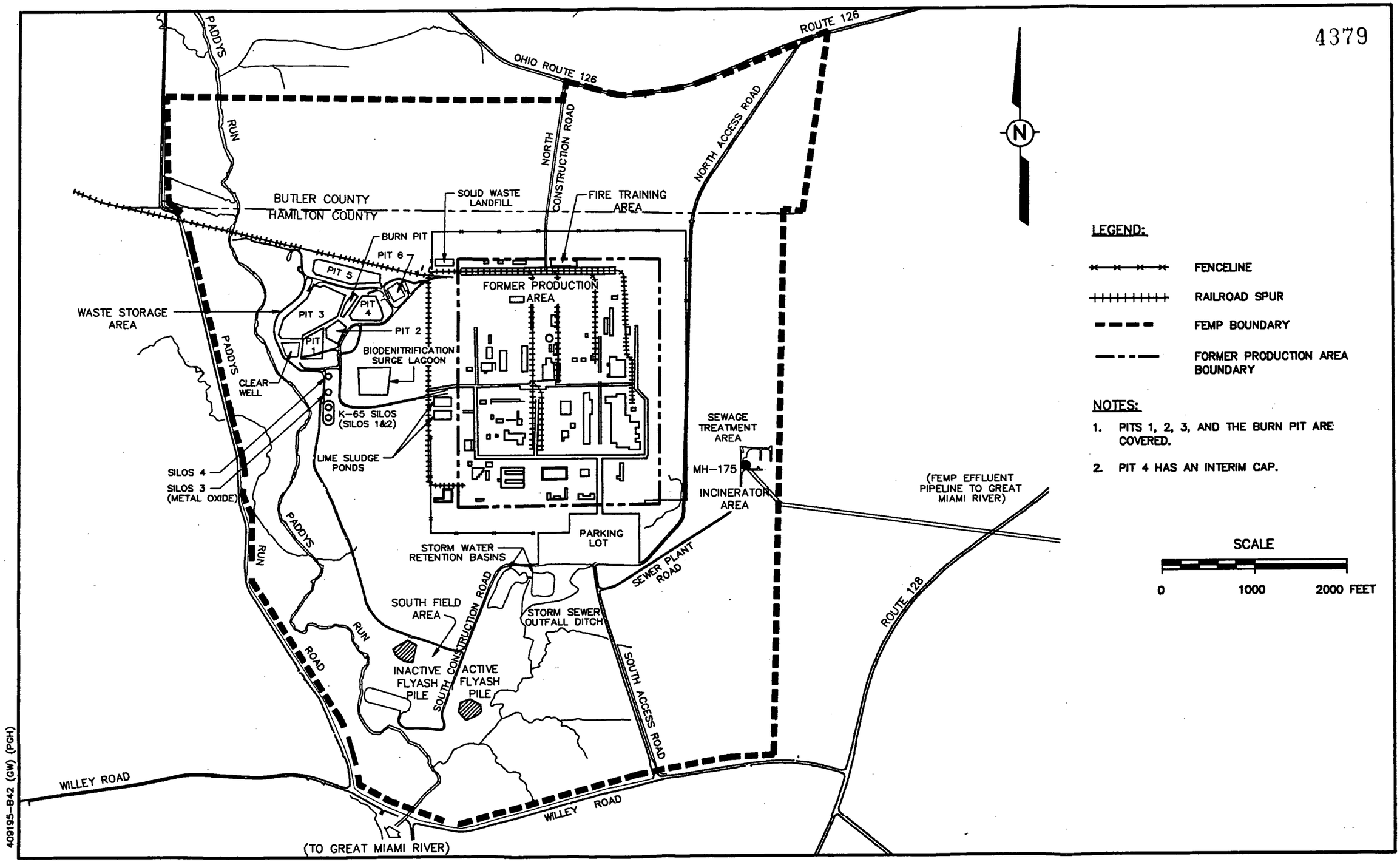


FIGURE 2-2
LOCATION OF MAJOR FEATURES AT THE FEMP

These areas included:

- Six low-level radioactive waste storage pits
- Two earthen-bermed concrete silos containing K-65 residues, which are high-specific activity, radium-bearing materials produced during the refining of Belgian Congo pitchblende ore
- One silo containing metal oxides
- One unused concrete silo
- Two lime sludge ponds,
- One solid waste landfill.

Although numerous actions at the FEMP have been taken to abate, minimize, stabilize, mitigate, or eliminate the release or threat of release of hazardous substances, pollutants, contaminants, or hazardous constituents at or from the FEMP, the former uranium processing activities at the FEMP have resulted in uranium contamination of the groundwater beneath and to the south of the facility. This groundwater modeling report serves as a primary source to document the baseline groundwater modeling efforts for the FEMP groundwater investigation.

## 2.2 SURFACE WATER HYDROLOGY

Three principal surface water courses, the Great Miami River, Paddys Run, and the storm sewer outfall ditch are the main constituents of the hydrologic flow on and adjacent to the FEMP. Other components involve a variety of man-made surface water drainage pathways in the waste storage areas and the former production area.

### 2.2.1 Great Miami River

The FEMP is located within the Great Miami River Basin drainage, but above the river's present day flood plain. The Great Miami River is the receiving stream for the FEMP effluent discharge and represents the main surface water feature in the vicinity of the FEMP (Figure 2-3). The river flows generally to the southwest and has a drainage area of approximately 3360 square miles at the Hamilton gage, which is located about 10 miles upstream from the FEMP discharge outfall. Only a small portion in the northeast corner of the FEMP drains directly to the Great Miami River.

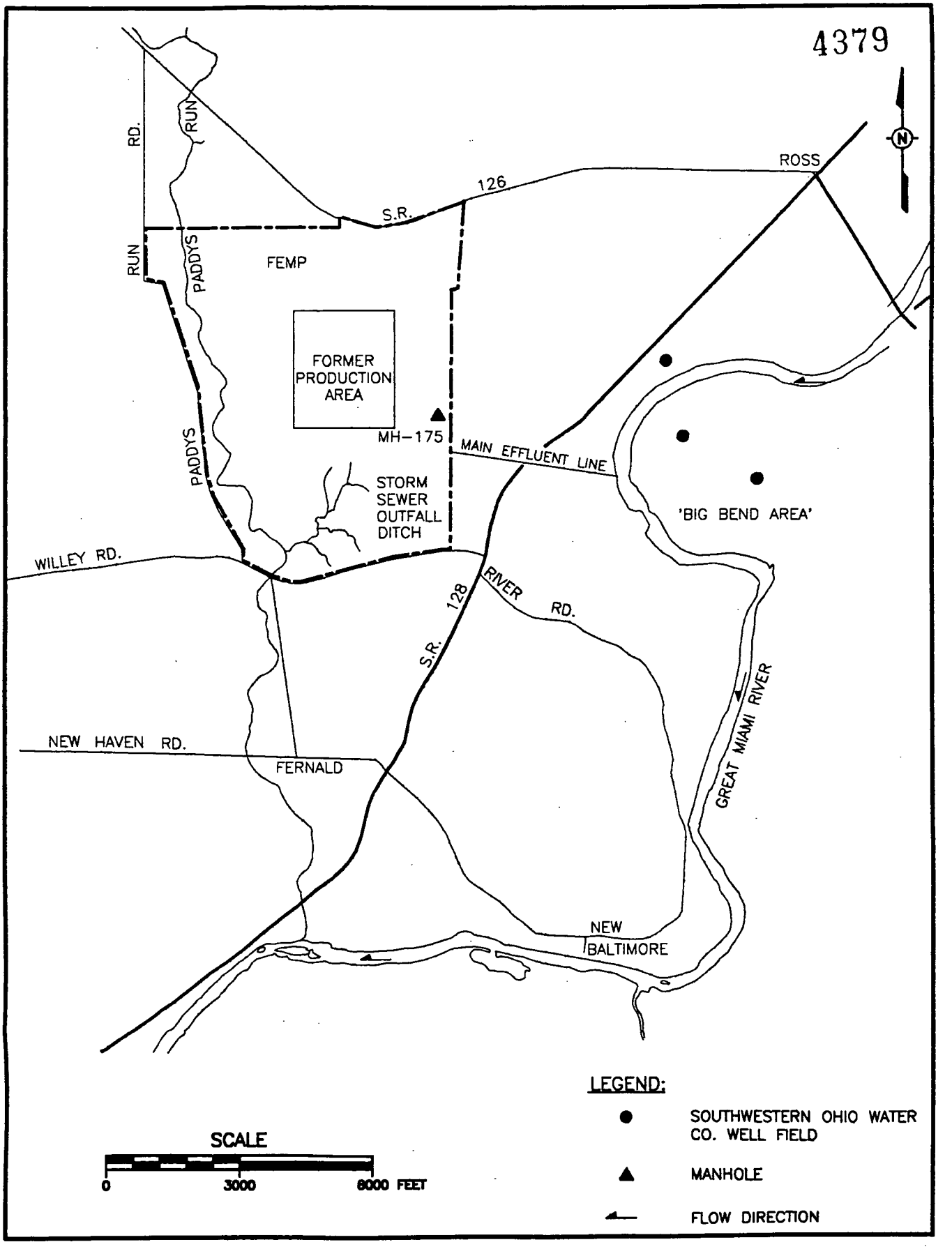


409195-A56 (GW) (PGH.)

FIGURE 2-3 SURFACE WATER HYDROLOGY

The Great Miami River exhibits meandering patterns that result in sharp directional changes over distances of less than 3000 feet. Directly east of the FEMP, the river passes through a 180-degree curve known as the "Big Bend." A 90-degree bend in the river also occurs near New Baltimore, approximately two miles downstream from the FEMP point of discharge.

The average discharge of the Great Miami River at Hamilton, based on 55 years of records, is 3305 cubic feet per second ($ft^3/s$) (IT 1988). Using drainage area scaling, the corresponding average flow at the FEMP point of discharge has been estimated to be 3460 $ft^3/s$. The maximum discharge ever recorded for the Great Miami River at Hamilton occurred on March 26, 1913 and was estimated to be 352,000 $ft^3/s$. The maximum discharge since the construction in 1922 of five retarding basins, located approximately seven miles upstream of Ross, was 108,000 $ft^3/s$ and occurred on January 21, 1959. The 10-year-flood discharge has been calculated to be 81,455 $ft^3/s$ for the FEMP reach. This value is approximately half of the 7-day, 10-year flow value ($Q_{7\text{-}10}$) of 267 $ft^3/s$, as computed by the U.S. Geological Survey (USGS) for the Hamilton gage. This translates to 280 $ft^3/s$ at the FEMP river reach. The Great Miami River fluctuates by only a few feet over most of the year, with periodic increases up to approximately 12 feet above normal flow conditions.

The Great Miami River has eroded through the overburden deposits and is in contact with the well-sorted sand and gravel valley fill deposits which underlie much of the river's bed. Under natural conditions, groundwater would flow from the aquifer into the river system. However, the Southwest Ohio Water Company (SOWC) extraction wells located in the Big Bend area reverse this pattern and induce recharge from the Great Miami River to the aquifer.

The rate of such recharge by stream infiltration varies widely with respect to both place and time. Factors which influence the recharge rate include fluctuating river levels, different hydraulic gradients, and changing streambed conditions. Seasonal changes in water temperature can also affect the infiltration rate since the viscosity of the water varies with temperature.

Two studies of riverbed infiltration rate were conducted during the summers of 1956 near Ross (Dove 1961), and 1962 in Fairfield Township (Speiker 1968a). Infiltration rates were calculated to be 240,000 and 492,000 gallons per day (gpd) per acre of streambed, respectively. Both tests were performed in similar terrains under low streamflow conditions at water temperatures of approximately 80 degrees Fahrenheit (°F).

2.2.1.1 Great Miami River Hydrologic Characterization

The surface water system in the FEMP area is dominated by the Great Miami River to the east and south of the site and Paddys Run which flows along the western edge of the FEMP. Other minor drainages, such as the storm sewer outfall ditch, convey surface flow to Paddys Run, and eventually

the Great Miami River, which is the receiving stream for all FEMP surface flow. These surface water systems are described in Section 2.2.2 and Section 2.2.3. The following discussion presents the characterization effort for the Great Miami River.

Figure 2-4 presents the continuous record of river stage at the Hamilton gage for 1985 and 1986. The stage is shown to fluctuate by only a few feet over most of the year, with periodic increases up to approximately 12 feet above normal flow conditions. Also shown in Figure 2-4 are the flow values recorded at the Ross Bridge during the Westinghouse Environmental Management Company of Ohio (WEMCO) routine monitoring program. The general pattern of variability is similar to that observed at the Hamilton gage.

The hydrologic characteristics of the Great Miami River throughout the FEMP area were investigated using the HEC-2 computer model developed by the Hydrologic Engineering Center of the U.S. Army Corps of Engineers (USACE). The program was developed for the calculation of water surface profiles and related hydrologic parameters such as flow velocity for steady, gradually varied flow in natural or man-made channels. The effects of various obstructions such as bridges, culverts, weirs, and structures in the flood plain were considered in the computations. The computational procedure is based on the solution of the one-dimensional energy equation, with energy loss due to friction evaluated using Manning's equation.

The input data for the HEC-2 program included flow regimes, discharges, cross-sectional geometry, starting surface water elevation, reach lengths, and energy loss coefficients. All data for the Great Miami River were obtained from the USACE, Louisville District. Data were provided on 21 sections in a reach extending over five miles from a point downstream from the City of New Baltimore to a point just upstream of the Ross Bridge (Figure 2-5). Of particular interest were the five sections spanning a river distance of approximately 1.5 miles near the FEMP discharge, with two sections (I and J) located upstream from the discharge and three river sections (F, G, and H) located downstream. A starting water surface elevation of 455.0 feet above mean sea level (msl) at the confluence of the Ohio River and the Great Miami River was used to initiate the program for average flow conditions. Various river surface elevation values and river discharges were used to represent high flow (10-year flood stage) conditions, low flow (7-day, 10-year flow) conditions, and observed field conditions for the period of September 11 through 14, 1987. The hydrologic parameters used for purposes of this study are summarized in Table 2-1.

Representative values for water depth, velocity, channel width, and hydraulic radius were computed using an average of the values for the aforementioned five river sections (F-J). The following values were obtained for the mean flow case:

Water Depth = 5.4 feet

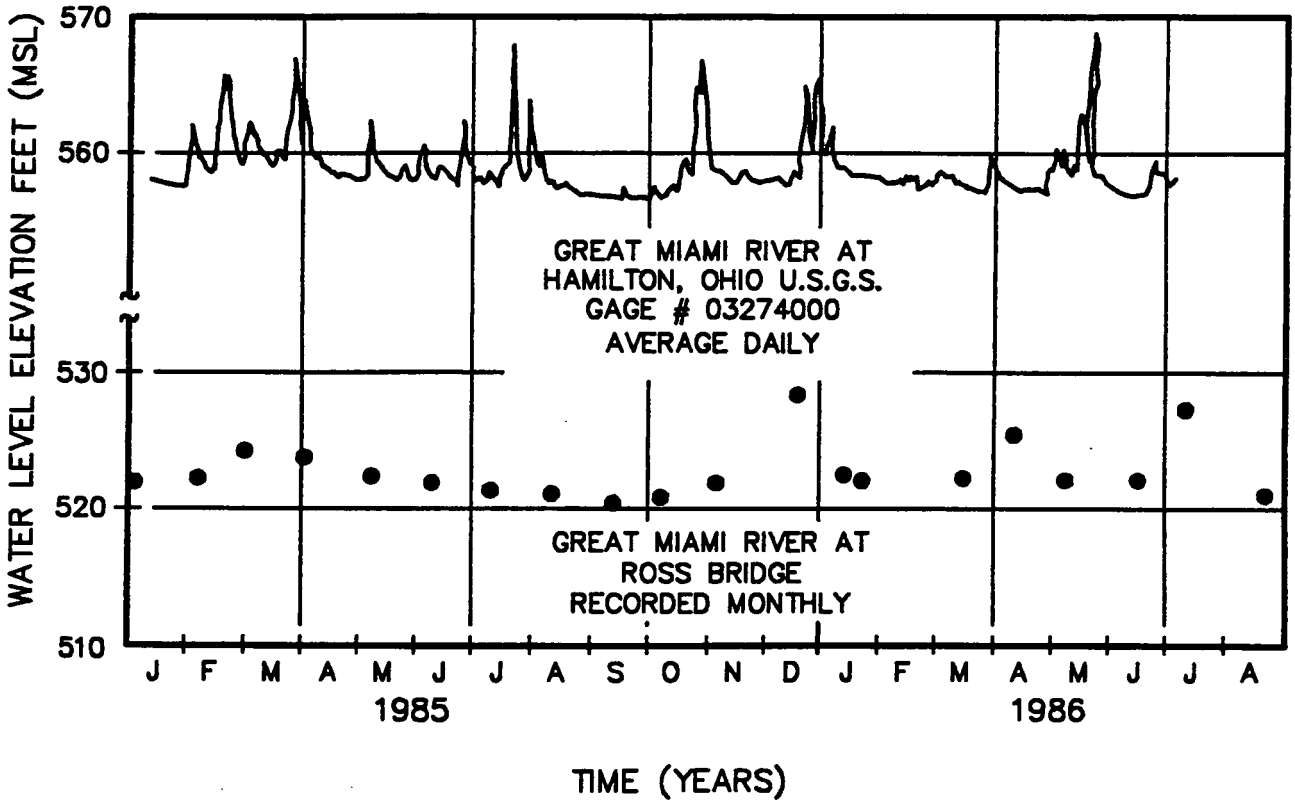


409195-A55 (GW) (PGH)

FIGURE 2-4 RIVER STAGE AT HAMILTON AND ROSS, OHIO
1985 AND 1986

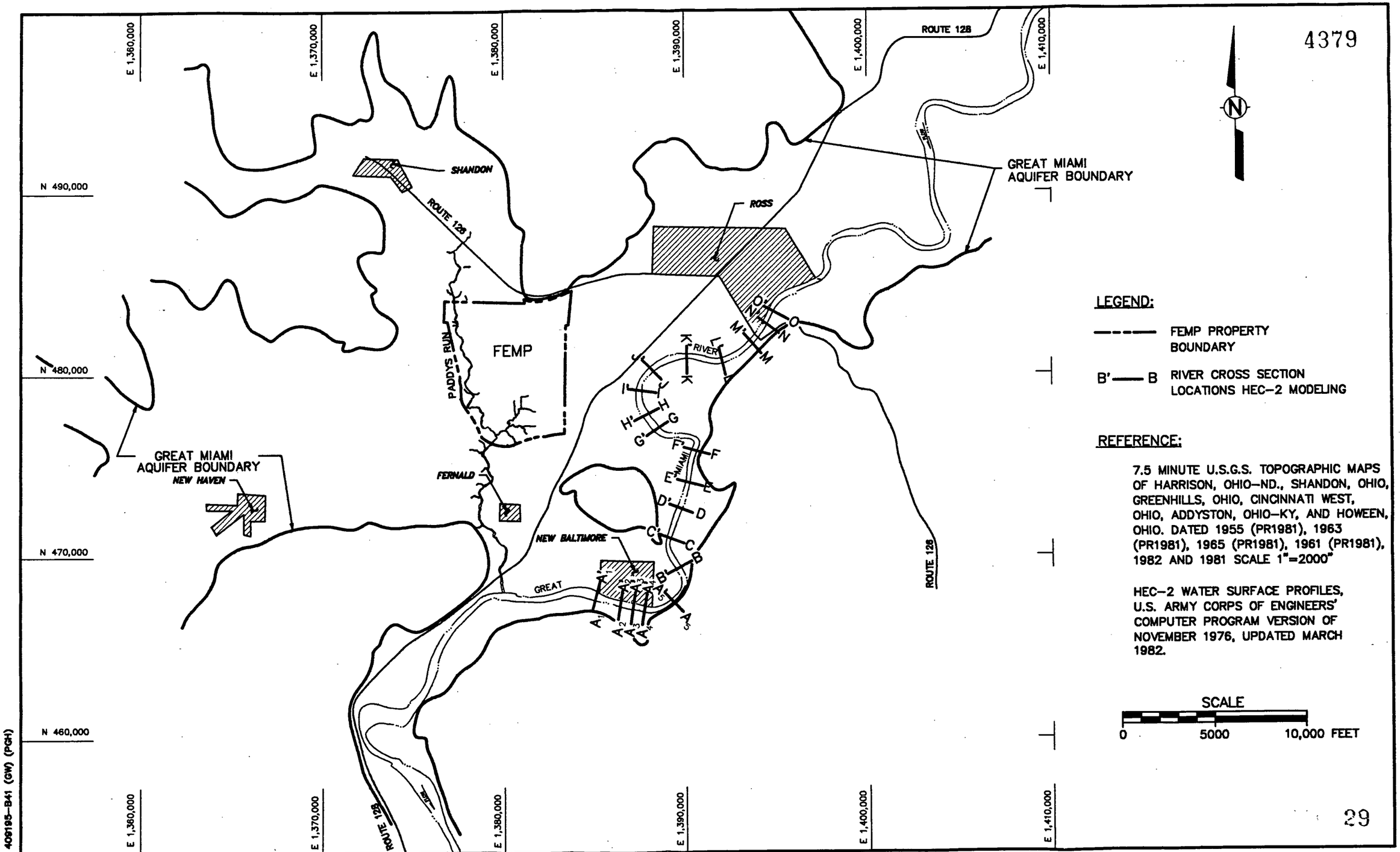




FIGURE 2-5
LOCATION OF RIVER
CROSS SECTIONS USED TO OBTAIN
HYDRAULIC CHARACTERISTICS

## TABLE 2-1

## A SUMMARY OF VALUES CALCULATED FROM HEC2 MODEL FOR THE SITE REACH OF THE GREAT MIAMI RIVER, USED AS A BASIS FOR INPUT TO STRIP1B MODEL

1. High Flow Conditions (10-year flood)
   River Discharge,[a] Q = 81,455 $ft^3/s$

| Section | F | G | H | I | J | Mean of Five Sections |
|---|---|---|---|---|---|---|
| Velocity of flow, V ($ft^2/s$) | 3.94 | 3.56 | 3.71 | 5.06 | 6.95 | 4.64 |
| Water surface elevation (ft MSL) | 541.31 | 542.69 | 543.39 | 543.79 | 544.14 | - |
| River width, W (ft) | 3,600 | 5,410 | 6,335 | 5,686 | 5,166 | 5,239 |
| River depth, H (ft) | 11.84 | 9.38 | 8.81 | 5.74 | 5.40 | 8.2 |
| Hydraulic radius (ft)[b] | 11.80 | 9.36 | 8.80 | 4.80 | 6.33 | 8.22 |

2. Low Flow Conditions (7-day, 10-year low flow)
   River Discharge,[c] Q = 280 $ft^3/s$

| Section | F | G | H | I | J | Mean of Five Sections |
|---|---|---|---|---|---|---|
| Velocity of flow, V ($ft^2/s$) | 0.65 | 1.52 | 4.97[d] | 0.84 | 0.22 | 0.81 |
| Water surface elevation (ft MSL) | 511.70 | 513.04 | 518.08 | 520.17 | 520.19 | - |
| River width, W (ft) | 188 | 39[e] | 80 | 262 | 276 | 202 |
| River depth, H (ft) | 3.00 | 6.89 | 0.75 | 1.47 | 3.6 | 3.1 |
| Hydraulic radius (ft)[b] | 2.33 | 4.37 | 0.71[d] | 1.30 | 4.76 | 3.19 |

See footnotes at end of table.

**TABLE 2-1**
(Continued)

3. Average Flow Conditions (Mean flow for period of record)
River Discharge,[c] Q = 3,460 $ft^3/s$

| Section | F | G | H | I | J | Mean of Five Sections |
|---|---|---|---|---|---|---|
| Velocity of flow, ($ft^2/s$) | 1.77 | 2.16 | 3.08 | 2.19 | 1.39 | 2.12 |
| Water surface elevation (ft MSL) | 517.30 | 520.06 | 522.78 | 524.26 | 524.48 | - |
| River width, W (ft) | 306 | 420 | 322 | 365 | 312 | 345 |
| River depth, H (ft) | 6.48 | 4.19 | 4.03 | 4.55 | 7.92 | 5.4 |
| Hydraulic radius (ft)[b] | 6.49 | 3.82 | 3.55 | 4.41 | 8.08 | 5.27 |

4. Field Conditions (September 11 through 14, 1987)
River Discharge,[c] Q = 534 $ft^3/s$

| Section | F | G | H | I | J | Mean of Five Sections |
|---|---|---|---|---|---|---|
| Velocity of flow, V ($ft^2/s$) | 0.79 | 1.81 | 3.20 | 1.06 | 0.37 | 1.45[f] |
| Water surface elevation (ft MSL) | 512.78 | 514.83 | 519.14 | 520.82 | 520.87 | - |
| River width, W (ft) | 256 | 47[e] | 119 | 273 | 274 | 230 |
| River depth, H (ft) | 2.61 | 4.78 | 0.97 | 2.12 | 4.30 | 3.0 |
| Hydraulic radius (ft)[b] | 2.66 | 3.18 | 0.95 | 1.76 | 5.35 | 2.78 |

[a]Extrapolated from data for river mouth provided in HEC2 model.

[b]Hydraulic radius (ft) = $\frac{\text{Total Area of Channel } (ft^2)}{\text{Total Wetted Perimeter (ft)}}$

[c]Extrapolated from Hamilton gage data.

[d]Critical depth assumed in HEC2. Value not used for calculation of mean value.

[e]Channel is split into two deep, but narrow channels; therefore, the value was not included in calculating the mean.

[f]Field measurement, V = 1.35 $ft^2/s$ (Station 4, 9/12/87) was used as model input.

Flow Velocity = 2.1 feet per second (ft/s)
Channel Width = 345 feet
Hydraulic Radius = $\frac{\text{area of channel}}{\text{wetted perimeter}}$ = 5.3 feet

The average depth of water in the Great Miami River under mean flow conditions in the vicinity of the FEMP discharge is 5.4 feet, based on model results from the USACE HEC-2 computer program for calculating water surface profiles. Additionally, the parameter values for high, low, and field flow conditions are also shown in Table 2-1 and were used along with the average flow values for surface water modeling of contaminant transport in the Great Miami River to indicate the sensitivity of the model to input parameters.

As a check of the appropriateness of the averaged (Sections F to J) flow parameter values, these values were compared to the other values that were derived by averaging the values of all 21 sections along the Great Miami River for mean flow case:

Water Depth = 5.7 feet
Flow Velocity = 2.3 ft/s
Channel Width = 302 feet
Hydraulic Radius = $\frac{\text{area of channel}}{\text{wetted perimeter}}$ = 5.6 feet

This comparison of values indicates that the hydrologic characteristics of the river in the vicinity of the FEMP discharge point are similar to the overall river conditions. Consequently, the use of the weighted average values for the five local stations is justified for subsequent model studies. Additional details describing the HEC-2 modeling effort are presented in the Hydrogeologic Study of the FMPC Discharge to the Great Miami River report (IT 1988).

### 2.2.2 Paddys Run

Paddys Run is an ungaged, intermittent stream that originates north of the FEMP property, drains southward along the west side of the FEMP, and eventually enters the Great Miami River approximately 1.5 miles south of the FEMP (Figure 2-3). Paddys Run is critical in the evaluation of contaminant transport at the FEMP, as it is the discharge point for a majority of the natural drainage at the facility.

Paddys Run drains a 16-square-mile basin and loses flow to the underlying aquifer along much of its course, due to its highly permeable channel bottom which is carved into the Great Miami Aquifer. Paddys Run flows primarily between January and May, with an estimated average discharge for this period ranging from of 0.2 to 4.0 cubic feet per second (cfs) (Dames and Moore 1985). High-water marks have suggested a water stage of up to 4 feet during peak flows. Although actual peak flows

have not been measured, calculated maximum peak flows for 100-year 24-hour, and two-year 24-hour rain events are 5000 cfs and 1000 cfs, respectively.

The banks of Paddys Run are steep to near vertical and display up to 20 feet of glacial till, loess, and lacustrine overburden deposits. The streambed also exposes the underlying sand and gravel alluvium of the Great Miami Aquifer. This alluvium is particularly exposed along the stretch between the K-65 silo area and the Great Miami River. The contact with the buried valley deposits results in the infiltration of surface flow downstream of the K-65 silos. Periods of constant flow typically occur in January and May and following heavy precipitation events. Moist zones at various elevations on the cut banks are evidence of groundwater seepage from the perched aquifer zones that occur in the overburden material beneath the waste pits and K-65 silos.

The overland flow from the FEMP runs east to west into Paddys Run, except for the northeast corner which drains eastward to the Great Miami River. The FEMP production and waste storage areas rest on a relatively level plain at about 580 feet above msl. This plain slopes from 600 feet msl along the eastern boundary of the FEMP to 570 feet msl at the silos (Figure 2-6). The surface elevation drops off to the west, into the depression occupied by Paddys Run at an elevation of 550 feet msl.

The course of Paddys Run has been artificially modified by FEMP activities at least two times. Part of Paddys Run previously flowed close to the waste pit area but, in 1961, it was diverted to the west, away from the waste pits. The now swampy, abandoned stretch of Paddys Run near the waste pit berms catches and retains surface runoff (WMCO 1987). A second modification occurred in 1970, downstream of the K-65 silos. In this case, Paddys Run was straightened to prevent erosion of Paddys Run Road. One additional modification was the removal of approximately 700 cubic yards of sand and gravel from the bed of Paddys Run, near the K-65 silos, between 1952 and 1985 for FEMP construction activities (WMCO 1987).

There are several tributaries which contribute significantly to the flow in Paddys Run. The most significant tributary is the storm sewer outfall ditch, which receives all the surface water from east of the former production area, the southeast quarter of the FEMP reservation, and a considerable area southeast of the FEMP. The second largest tributary to Paddys Run drains the area north of the former production area and flows west into Paddys Run on the north side of the railroad tracks, northwest of the waste pits. Surface water runoff from the waste storage area enters Paddys Run via three tributaries. The larger of the three tributaries enters Paddys Run just north of the silos and south of the Clearwell. The two smaller tributaries drain the area north of Pit 5, including the northwest corner of the former production area and the area between Pit 5 and Pit 3. These two drainages enter Paddys Run immediately south of the railroad tracks and about 100 yards south of the tracks,

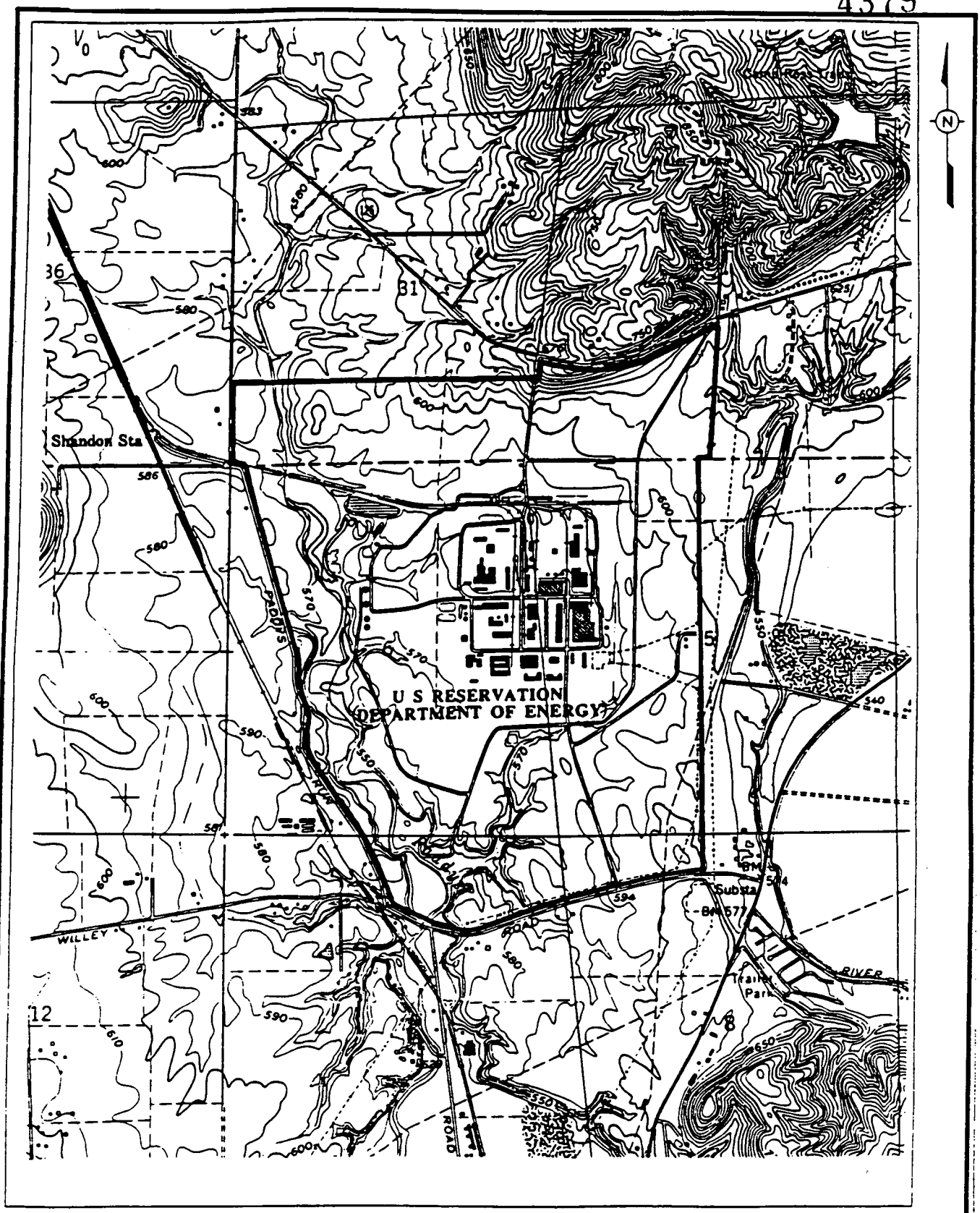


SOURCE:
USGS (1981)
SHANDON, OHIO
QUADRANGLE

SCALE
1:24,000

409195-A43 (GW) (PGH)

FIGURE 2-6 TOPOGRAPHIC MAP OF THE FEMP

respectively. There is also a tributary that drains the area west of the former production area and south of the waste storage area. This tributary enters Paddys Run just south of the K-65 silos.

### 2.2.3 Storm Sewer Outfall Ditch

A principal drainage feature of the FEMP is a tributary to Paddys Run known as the storm sewer outfall ditch. This drainage course originates east of the former production area, flows southwest across the southern portion of the FEMP property, and enters Paddys Run near the southwest corner of the property (Figures 2-2 and 2-3). Much of the stream bottom of this drainage course, which also collects runoff from an area east of the former production area, is composed of sand and gravel. Similar to Paddys Run, the storm sewer outfall ditch has eroded through the veneer of surficial glacial overburden, so that the base of the ditch directly overlies the valley fill deposits from the stormwater retention basins to the confluence with Paddys Run. Vertical seepage rates through the outfall ditch bottom are similar to Paddys Run, in that the permeable bed materials directly overlying the sand and gravel valley fill permit free infiltration of surface flow into the Great Miami Aquifer. This drainage course is generally dry throughout most of the year, with flows occurring during and immediately following precipitation events.

Generally, the storm water flow was conveyed to the storm sewer lift station, which diverts low flow storm water to Manhole 175. However, the storm sewer outfall ditch has historically conveyed surface water runoff from the former production area directly to Paddys Run when the capacity of the storm water collection system was exceeded. In addition, the storm sewer outfall ditch provided local drainage for the area east and southeast of the former production area. Two storm water retention basins were constructed and became operational in October 1986 and December 1989 at the head of the storm sewer outfall ditch. These basins significantly reduced the contribution of the former production area storm water to the outfall ditch. Storm water runoff from the former production area is now conveyed to these retention basins. The basins are designed to retain the runoff from a 10-year, 24-hour rainfall event; only in the event of an overflow would storm water from the former production area enter the outfall ditch. After at least a 24-hour retention period to allow for settling of suspended solids, the water is pumped out of the basins to the Great Miami River via the FEMP main effluent line. Overflows have occurred on a minimum of seven occasions since 1986.

## 2.3 GEOLOGIC CHARACTERIZATION OF THE FEMP AREA

The following discussion presents a broad overview of the lithologic, stratigraphic, and structural geologic conditions of the FEMP site in Fernald, Ohio, and the surrounding region.

### 2.3.1 Physiographic Province

The FEMP facility is located at coordinates latitude N 39° 18' and longitude W 84° 41' (Beavers et al. 1982), on the eastern edge of the Central Stable physiographic province. The Central Stable region is mostly low, rolling landscape and nearly level plains. The Central Stable physiographic province (also known as the Central Lowland physiographic province) is characterized by structural and sedimentary basins and domes. Among these features, the Cincinnati Geoanticline or "Cincinnati Arch" is structurally significant in the region. The FEMP is located near the axis of this structural arch, and this area displays exposures of some of the oldest bedrock in the State of Ohio. The underlying bedrock in the region consists of nearly horizontal, thin-bedded shale and fossiliferous limestone, of Middle and Late Ordovician age (Fenneman 1916). The main physiographic features in the area are gently rolling uplands, steep hillsides along the major streams, and the Great Miami River Valley, which is a relatively broad, flat-bottomed valley flanked on either side by bluffs that rise to a maximum of 300 feet above the general level of the valley floor.

### 2.3.2 Regional Bedrock Geology

The bedrock in the FEMP region consists of indurated shales and limestones of Upper Ordovician Age. The bedrock geology of the FEMP and the surrounding area has been previously described by Fenneman (1916), Durrell (1961), and Spieker (1968a). Previous reports by the above-mentioned authors and Watkins and Spieker (1971) and Swinford (1990 and in preparation) provide detailed geologic descriptions. Based on these studies, with modifications and extensions resulting from data collected during the RI studies, a comprehensive geologic history has been developed for the FEMP region area. This geologic history is summarized below in relation to those aspects of principal importance to the RI/FS.

In Late Ordovician time, approximately 450 million years ago, sediments which would become predominantly flat-lying shale with thin interbedded limestone were deposited in a shallow sea. These fine-grained, interbedded clayey and silt-rich shales and limestone, were at one time reduced to an almost level peneplain, which was then uplifted to an elevation of approximately 900 feet above sea level, and subsequently dissected some 400 or more feet by several large through flowing rivers and their dendritic tributaries (Fenneman 1916). This shale forms the relatively impermeable bedrock which now underlies the FEMP site and forms the core of the surrounding highland areas.

2.3.3 Regional Glacial Geology

The FEMP lies on the boundary between the southernmost extent of Pleistocene glaciation and the ancient unglaciated upland. During the Pleistocene Epoch, the bedrock topography of Southwestern Ohio was modified several times by the erosional and depositional action of continental ice sheets. Three major continental glaciers advanced as far south as Cincinnati. These were the Kansan or pre-Illinoian (approximately more than 1,200,000 years ago), the Illinoian (approximately 400,000 to 125,000 years ago), and the Wisconsin (approximately 70,000 to 11,000 years ago) glacial episodes. The FEMP is located within a 2- to 3-mile-wide subterranean bedrock valley known as the New Haven Trough. This valley formed as a result of Pleistocene glaciation and subsequently filled with glacial outwash materials and till (Brockman 1986). The geological history of the FEMP area, as presented by Fenneman (1916), is summarized in the following paragraphs.

During continental glaciation, much of the earth's available water was stored as ice on the continents, causing a significant depression of the earth's crust and a significant drop in sea level. The earth's crust rebounds between glacial events when the weight is removed. This crustal rebounding, coupled with lower sea levels, allowed the rivers to carve a series of deep bedrock valleys in the Cincinnati area. Part of the entrenched bedrock drainage system located in the vicinity of the FEMP was much larger than the present day Great Miami River system and cut to a level more than 200 feet below the present-day Great Miami River, forming the Deep Stage Drainage System. This system is typical of many of the major waterways in the glaciated parts of the midwest.

During the Kansan-Illinoian interglacial period, a large watercourse (larger than the present-day Great Miami River) cut a valley into this shale bedrock to a level of more than 200 feet below the present-day Great Miami River, forming the Deep Stage Drainage System. During continental glacial events, sea levels drop because of the large amount of water stored as ice on the continents. This drop in sea level allowed the rivers in the Deep Stage Drainage System to carve valleys roughly 200 feet deeper into the bedrock in the Cincinnati area than could happen under current sea level conditions.

As the Illinoian glacier advanced further into the Cincinnati area, the ancestral Ohio River (Figure 2-7A) flowing in the bedrock Deep Stage Valley was dammed by the glacier. The lake that formed behind the dam overflowed at the low divide in the vicinity of present day Anderson's Ferry and at what is now downtown Cincinnati. As the divide eroded, the present course of the Ohio River was established (Figure 2-7B). A subsequent ice advance forced the ancestral Great Miami River out of the Deep Stage Valley and the displaced river carved a new, narrow, deep valley from just north of New Baltimore to about one mile west of Cleves, where it returned to the original Deep Stage Valley. Because only water from the Great Miami River and its tributaries' drainage basin carved this valley, it is much smaller than the ancestral Ohio River Valley. The FEMP is located within this 2-mile-wide valley, termed the New Haven Trough by Fenneman (1916).

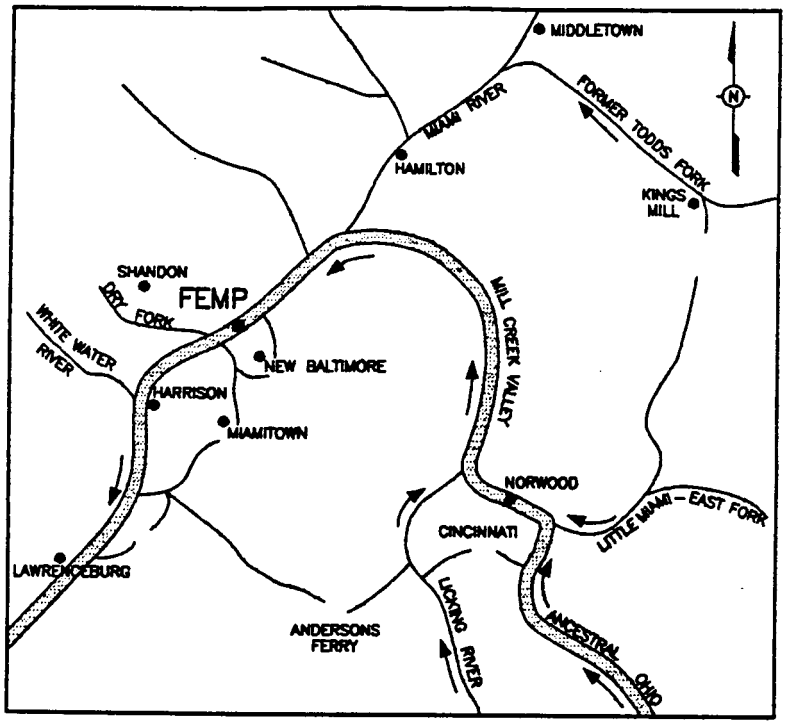


FIGURE 2-7A. DEEP STAGE DRAINAGE SYSTEM

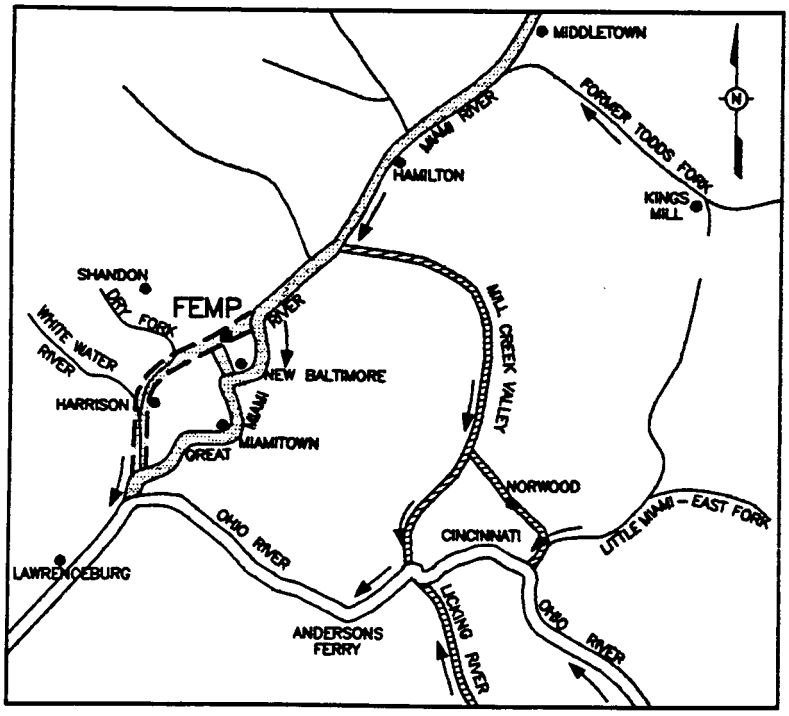


FIGURE 2-7B. PRESENT DRAINAGE SYSTEM

LEGEND:

- DIRECTION OF FLOW
- ANCESTRAL OHIO RIVER

LEGEND:

- DIRECTION OF FLOW
- GREAT MIAMI RIVER
- PRESENT OHIO RIVER
- NEW HAVEN TROUGH
- MILL CREEK BASIN

SOURCE:

FENNEMAN, N.M., 1916 "THE GEOLOGY OF CINCINNATI AND VICINITY", GEOLOGICAL SURVEY OF OHIO, BULLETIN 19.

NOT TO SCALE

409195-A53 (GW) (PGH)

FIGURE 2-7 SCHEMATIC DIAGRAM OF THE DEEP STAGE DRAINAGE SYSTEM AND THE PRESENT DRAINAGE SYSTEM

During the Illinoian glacial retreat about 125,000 years ago, the Deep Stage Valley, including the New Haven Trough, was filled with about 200 feet of glaciofluvial sediments. These sediments were deposited by water running from the margins of the glaciers and consisted mainly of well-sorted sand and gravel. The thick sand and gravel deposits in the bedrock troughs formed the present-day Great Miami Aquifer. A blanket of poorly-sorted, clay-rich glacial overburden was then deposited on top of these sediments during the Wisconsin ice advance, about 70,000 years ago.

Loess deposits formed as an accumulation of wind-borne dust, originally derived from vegetation-free areas around the ice sheet. Since the last retreat of continental glaciers, the streams in the area have removed much of the glacial overburden and lacustrine mantle left by the ice sheets. Postglacial erosion by the Great Miami River and its tributaries removed significant portions of the glacial overburden and left terrace remnants which stand topographically higher than surrounding bottom lands. The Great Miami River has eroded through the glacial overburden and is now in direct contact with the glaciofluvial outwash deposits that comprise the buried valley (Great Miami) aquifer. Paddys Run is also in direct contact with these deposits in its lower reaches. The FEMP itself is located on a dissected till plain and lacustrine deposits left by the Wisconsin glaciation.

## 2.4 LOCAL GEOLOGY AND TOPOGRAPHY

The FEMP site is located on glacial overburden above the terrace remnants left after the establishment of the present-day Great Miami River channel. The geologic history of bedrock erosion and subsequent filling in of the valley with glacial outwash and till gave rise to the present-day deposits within the FEMP area.

The Great Miami River flows south from Middleton to just north of New Baltimore in the former Deep Stage Valley. At the present time, there is no surface stream occupying the New Haven Trough segment of the Deep Stage Valley between the Great Miami River east of the FEMP and the Whitewater River west of the FEMP.

The bedrock in the vicinity of the FEMP consists predominantly of flat-lying, olive-gray Ordovician shales with thin, interbedded layers of limestone. This shale forms the relatively flat floor and steep valley walls of the New Haven Trough. The buried channel was eroded into this shale bedrock by the ancestral Ohio River and occurs between 60 to more than 200 feet below the pre-erosional land surface in the vicinity of the FEMP.

During the retreat of the glacial ice sheets, the valley was filled with approximately 150 feet of regionally extensive Pleistocene glacial valley fill deposits. Figure 2-8 is a generalized stratigraphic column of the valley fill deposits. As indicated by the generalized cross section (Figure 2-9), the buried valley is about one-half to two miles wide and is U-shaped, having a broad, relatively flat

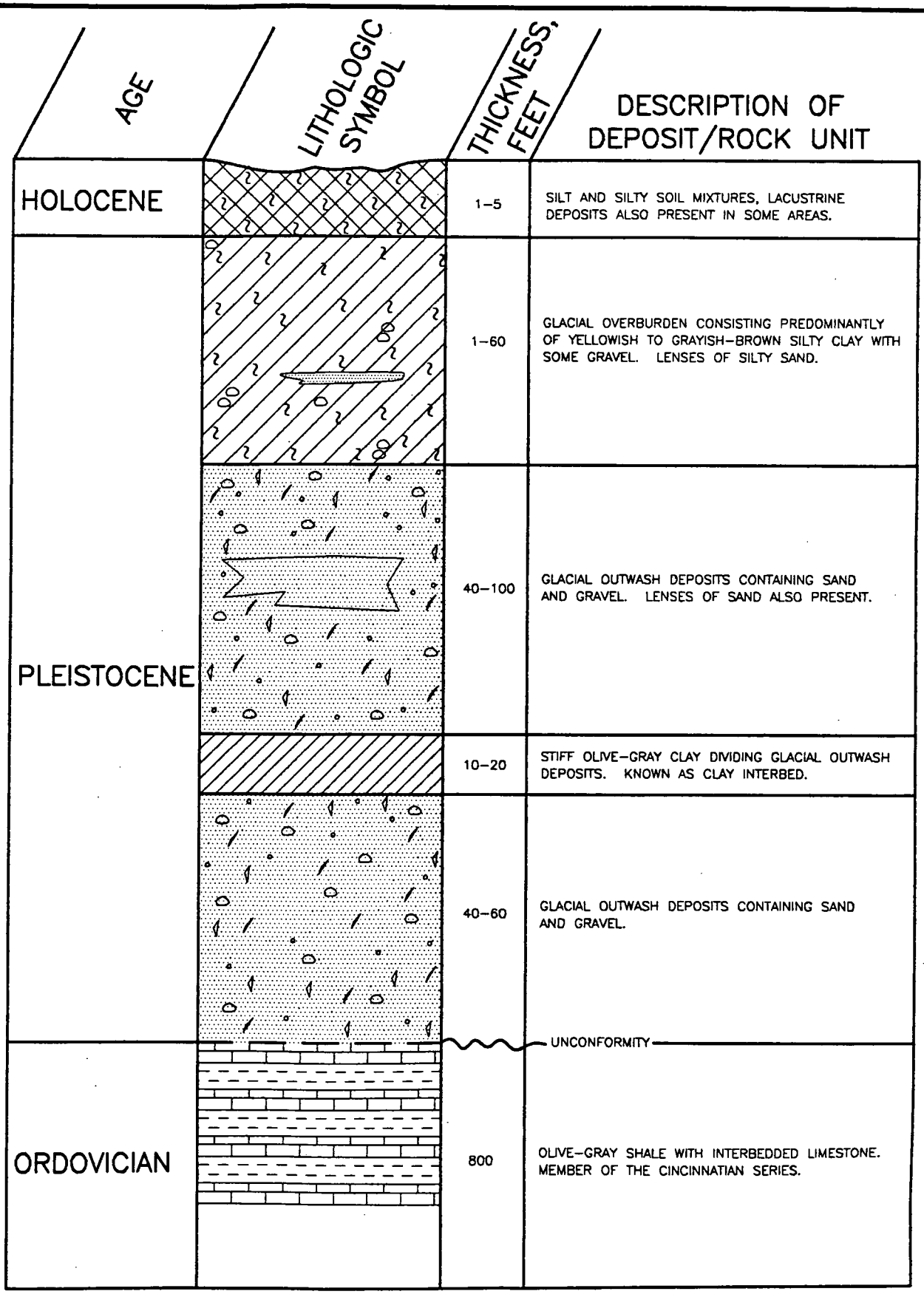


409195–A45 (GW) (PGH)

FIGURE 2–8 GENERALIZED STRATIGRAPHIC COLUMN OF THE FEMP REGION

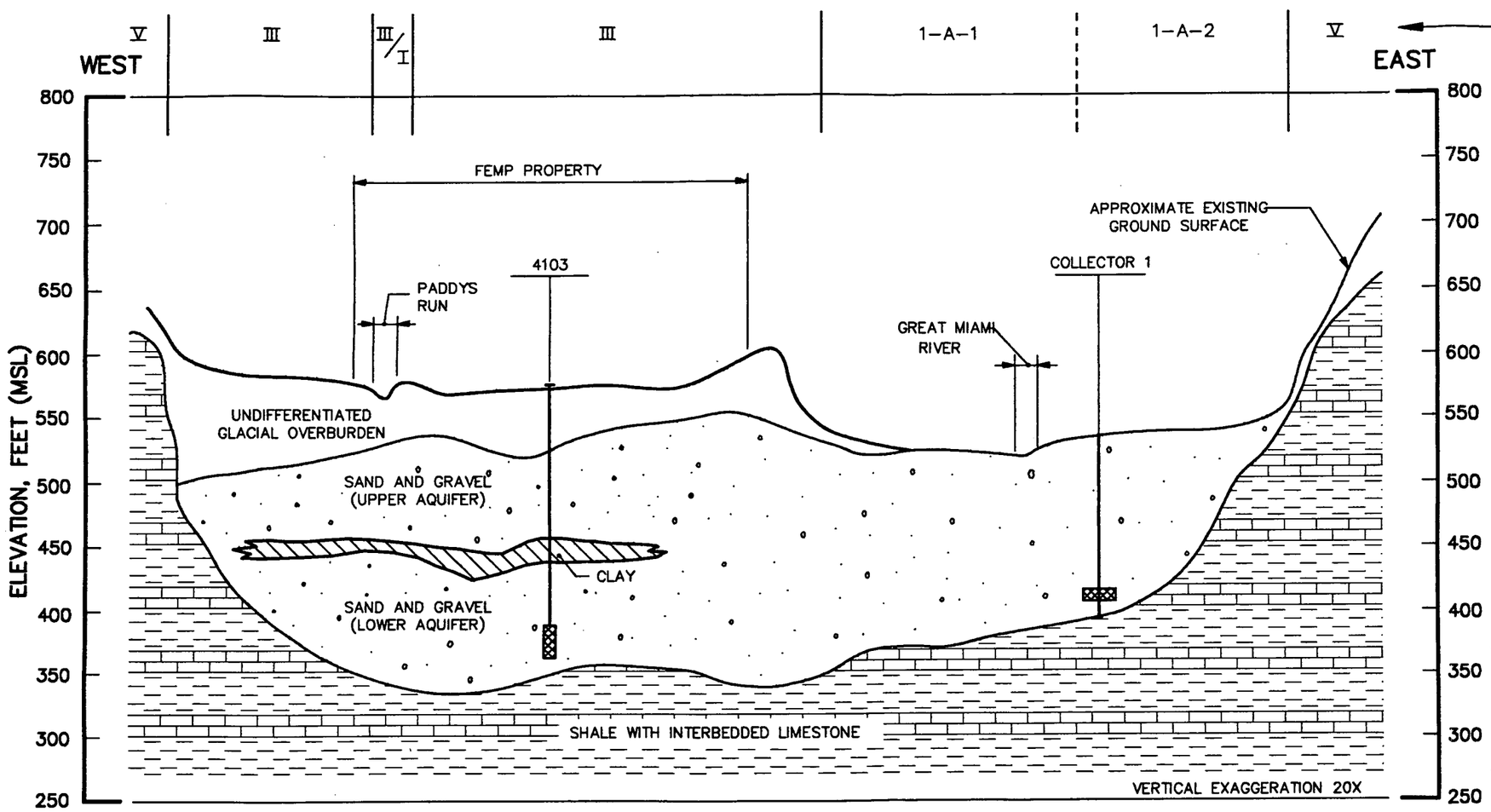


THE BORING LOGS AND RELATED INFORMATION DEPICT SUBSURFACE CONDITIONS ONLY AT THE SPECIFIC LOCATIONS AND DATES INDICATED. SOIL CONDITIONS AND WATER LEVELS AT OTHER LOCATIONS MAY DIFFER FROM CONDITIONS OCCURRING AT THESE BORING LOCATIONS. ALSO, THE PASSAGE OF TIME MAY RESULT IN A CHANGE IN THE CONDITIONS AT THESE BORING LOCATIONS.

THE DEPTH AND THICKNESS OF THE SUBSURFACE STRATA INDICATED ON THE SECTIONS WERE GENERALIZED FROM AND INTERPOLATED BETWEEN THE TEST BORINGS. INFORMATION ON ACTUAL SUBSURFACE CONDITIONS EXISTS ONLY AT THE LOCATION OF THE TEST BORINGS AND IT IS POSSIBLE THAT SUBSURFACE CONDITIONS BETWEEN THE TEST BORINGS MAY VARY FROM THOSE INDICATED.

VERTICAL SCALE

0 100 200 FEET

HORIZONTAL SCALE

0 2000 4000 FEET

LEGEND:

OPEN OR SCREENED INTERVAL

REFERENCES:

MODIFIED FROM U.S.G.S. PROFESSIONAL PAPER NO. 605-A USING AVAILABLE OHIO STATE WATER WELL RECORDS, SOWC WATER WELL DATA, DAMES & MOORE'S "FEED MATERIALS PRODUCTION CENTER GROUNDWATER STUDY, TASK C REPORT" FOR THE DOE (1985), AND IT (1986) RI/FS BORING LOGS.

NOTE:

REFER TO FIGURE 3-6 FOR DESCRIPTION OF HYDROGEOLOGIC ENVIRONMENT

## GENERALIZED CROSS SECTION

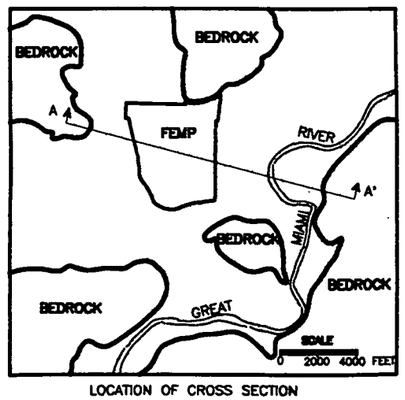


LOCATION OF CROSS SECTION

409195-B15 (GW) (PGH)



FIGURE 2-9
GENERALIZED GEOLOGIC CROSS SECTION
FEMP AREA

bottom and steep valley walls. Interbedded glacial till deposits occur within the outwash deposits, but in most cases are of limited lateral extent. The till deposits are composed primarily of poorly sorted pebbles, cobbles, and boulders in a predominately clay matrix.

The Pleistocene glacial activity deeply eroded the larger river valleys and subsequently deposited glacially-derived till and outwash sands and gravels in sufficient quantities to fill these valleys and displace and redirect master streams in the area. The veneer of glacial material in the area is such that bedrock exposures typically occur along the numerous waterfalls and steep valley walls of the tributary streams that drain into the Great Miami River. In some of the deeply eroded bedrock valley areas, the thickness of the glacial deposits may range to as much as 200 feet of glaciofluvial sand and gravel, which today is the Great Miami Aquifer.

In some areas, glacial overburden deposits overlie the bedrock uplands and portions of the outwash materials where they form the thick, unconsolidated sediment layers beneath the soil zone. This glacial till is composed of dense, silty clay that varies in composition vertically and laterally. The glacial overburden contains lenses of poorly sorted fine- to medium-grained sand and gravel, silty sand, and silt with layers of silty clay. The postglacial erosion of the overburden has resulted in the Great Miami River and the lower reaches of Paddys Run being in direct contact and hydraulic communication with the sands and gravels of the Great Miami Aquifer.

Postglacial erosion by the Great Miami River and its tributaries removed significant portions of the glacial overburden and left terrace remnants which stand topographically higher than surrounding bottom lands. The maximum elevation along the northern boundary of the FEMP property is a little more than 700 feet above msl. The former production area and waste storage area rest on a relatively level plain at about 580 feet elevation. The plain slopes from 600 feet along the eastern boundary of the FEMP to 570 feet at the K-65 silos, and then drops off toward Paddys Run at an elevation of 550 feet. All drainage on the FEMP is from east to west into Paddys Run, with the exception of the extreme northeast corner which drains east toward the Great Miami River.

### 2.4.1 Bedrock Valley

The eroded bedrock beneath the Great Miami Aquifer consists of predominantly flat-lying Ordovician shales with thin, interbedded layers of limestone. This bedrock unit reaches a total thickness of approximately 800 feet. During Pleistocene interglacial periods prior to the Illinoian and Wisconsin glacial advances, the ancestral Ohio River eroded a valley in the bedrock. This bedrock valley has a broad, relatively flat bottom and steep valley walls (Figure 2-10). During the retreat of the Illinoian ice sheets, the valley was filled with 200 feet of glaciofluvial sand and gravel, which today is the Great Miami Aquifer.

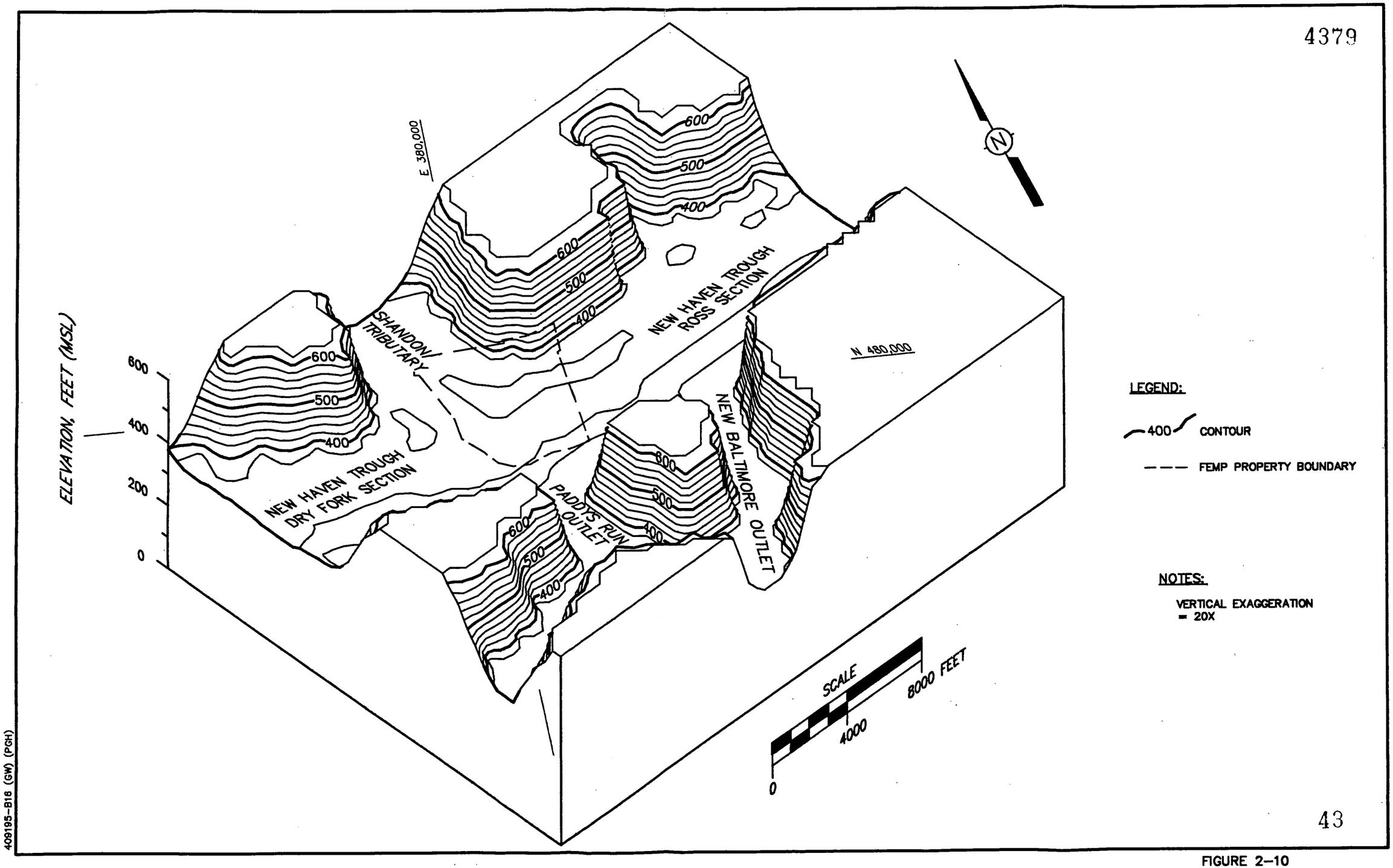


409195-B18 (GW) (PGH)



FIGURE 2-10
3-DIMENSIONAL BEDROCK CONFIGURATION

Watkins and Spieker (1971) performed extensive seismic refraction surveys to determine the thickness and extent of the sand and gravel deposits filling the bedrock valley. Test drilling was used in conjunction with the refraction surveys to verify the accuracy of the seismic determinations of the depth of the valley floor. The map of the top of bedrock (Figure 2-11) was derived from the bedrock map produced by Watkins and Spieker (1971), with additional information provided by Leow (1985) and Vormelker (1985), and monitoring wells constructed for the RI.

### 2.4.2 Great Miami Aquifer

The portion of the Great Miami Aquifer that underlies the FEMP study area consists primarily of glaciofluvial sand and gravel outwash deposited during the latest two Pleistocene glaciations. These deposits lie unconformably on the Ordovician shales, filling the bedrock valley to a depth of 200 feet in places. In the study area, the thickness of the Great Miami Aquifer varies from 120 to 200 feet in the valley and tributary valley centers to only a few feet along the valley walls. Although the glaciofluvial deposits are heterogeneous, they are typically well-sorted sands and gravels with only minor amounts of silt and clay. Within the coarse-grained sediments of the Great Miami Aquifer lies an interbedded clay layer that underlies most of the FEMP and parts of the surrounding areas (Figure 2-12). The clay interbed lies about 100 to 125 feet below the surface and generally about 60 to 80 feet below the water table (Figure 2-13). It ranges from 1 to 20 feet in thickness and consists of a low permeability homogeneous clay which acts as an aquitard within the Great Miami Aquifer. Because of this interbed, the aquifer is divided into upper and lower halves.

The clay of the interbedded layer is uniform in texture and contains only a small amount of silt and sand. It was deposited in a lacustrine or low-energy fluvial environment and displays varying (alternating light and dark sediment layers) in some samples. The interbed pinches out to the south and east, extends an unknown distance to the west, and grades into other lacustrine, glaciofluvial, and glacial till deposits to the north in the Shandon Tributary.

### 2.4.3 Glacial Overburden

Glacial overburden covers the Great Miami Aquifer throughout most of the study area. It is of varying composition, including loess, lacustrine deposits, till, and glaciofluvial sediments. The overburden itself cannot be classified on a regional basis, as it is composed of varying amounts of the four materials, differing in structure and extent from location to location. For this reason, these materials are grouped into one unit for the purposes of both this discussion and future explanations of how the glacial overburden materials are modeled.

Within the FEMP study area, the glacial overburden ranges up to 5 and 50 feet in thickness, but most commonly averages between 20 and 30 feet (Figure 2-14). It extends to the north and west outside of the study area, but ends within the study area to the south and east where the Great Miami River has

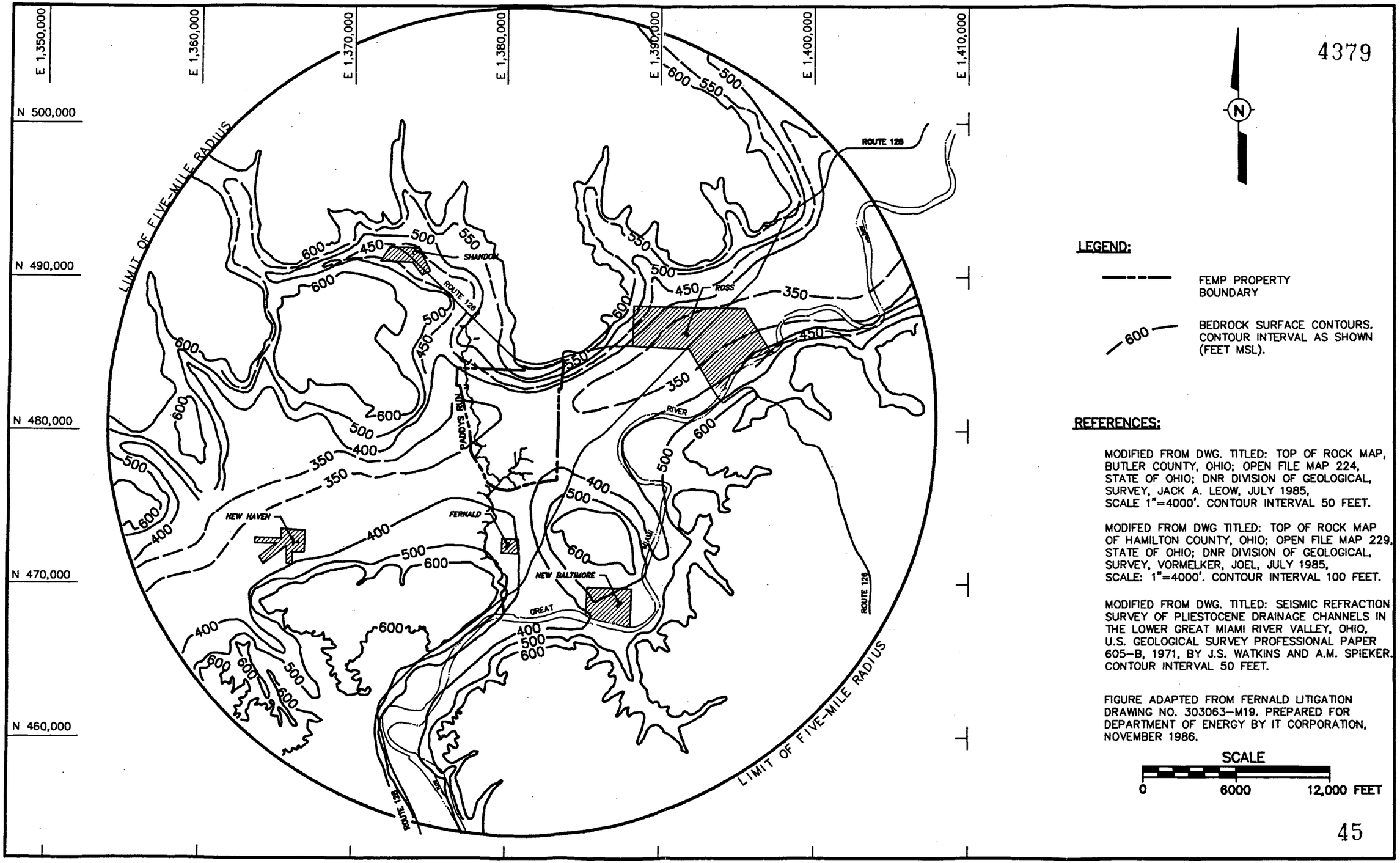




FIGURE 2-11
BEDROCK TOPOGRAPHY

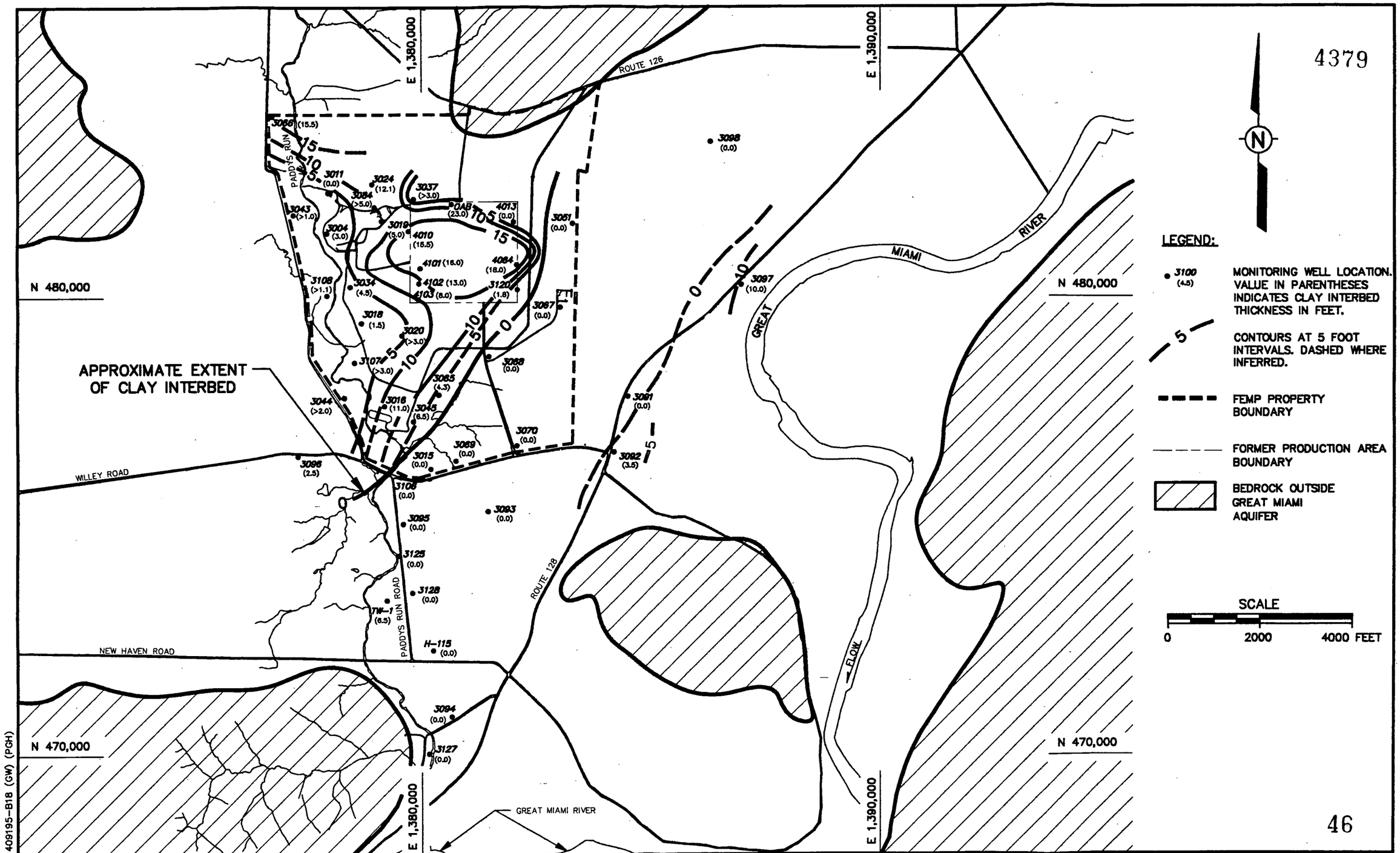


FIGURE 2-12
CLAY INTERBED ISOPACH

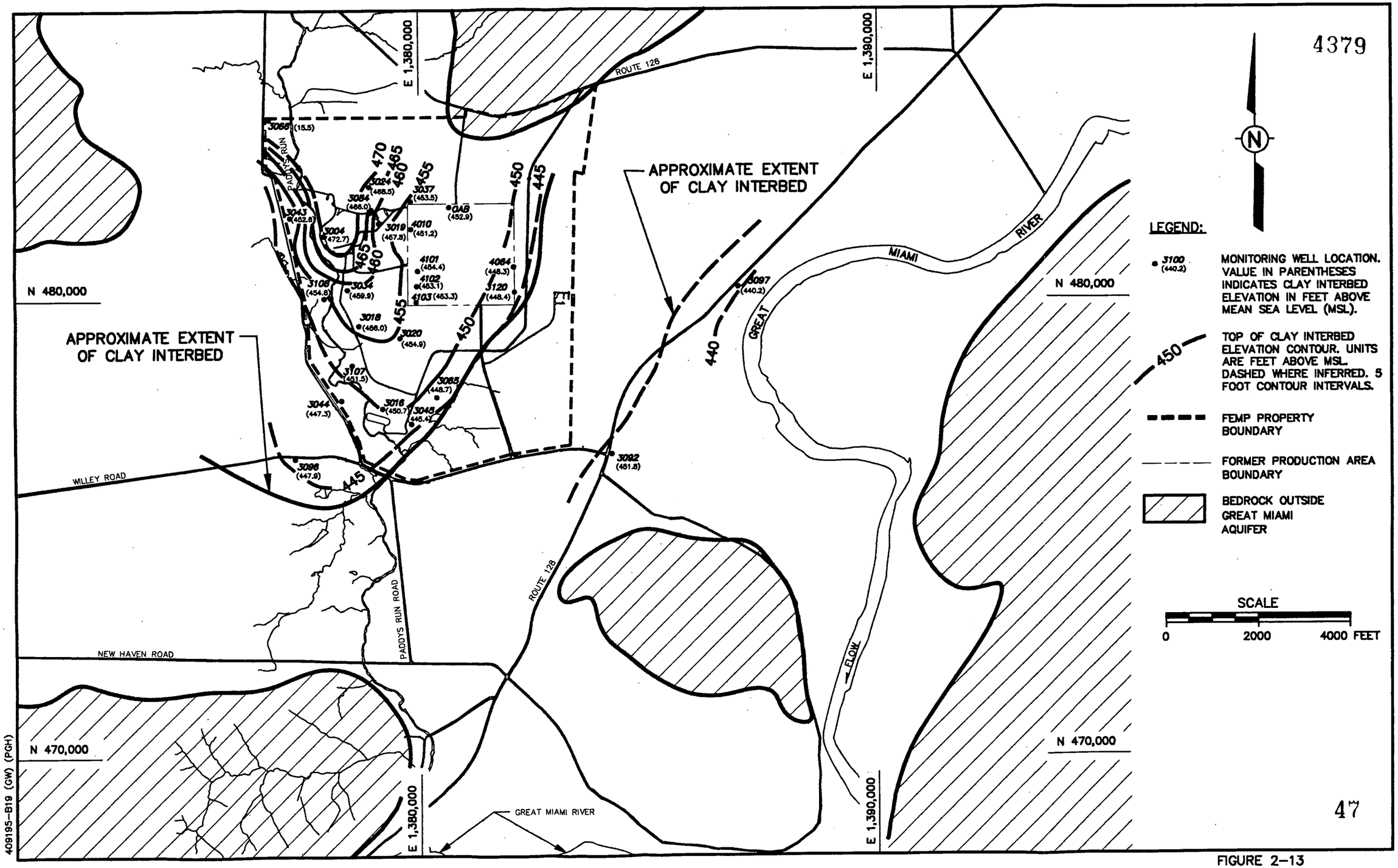


FIGURE 2-13
CLAY INTERBED
TOPOGRAPHIC SURFACE

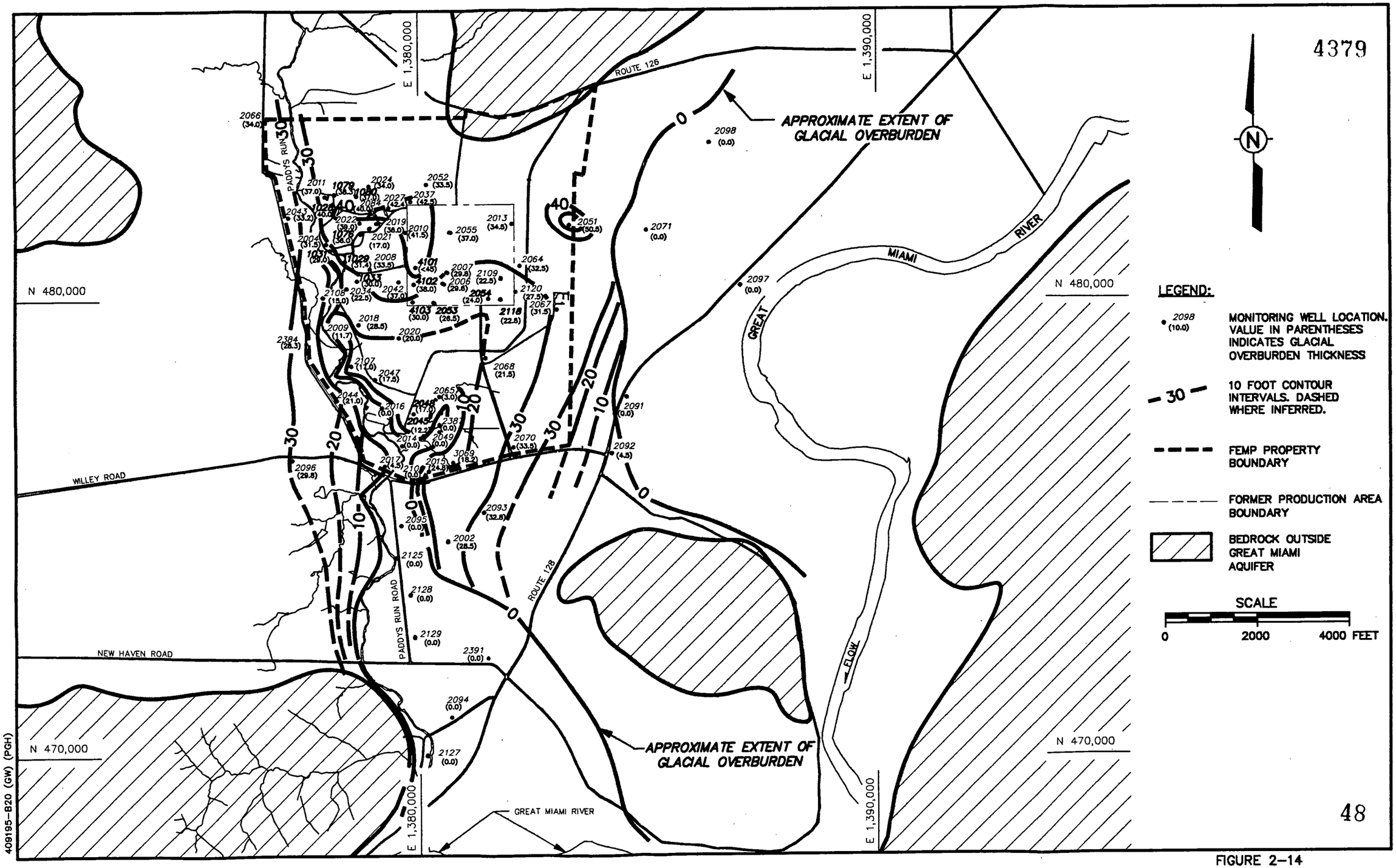




FIGURE 2-14
GLACIAL OVERBURDEN ISOPACH

stripped off the glacial overburden as it carved its present channel. The types of materials included as glacial overburden are described below:

- Loess: Loess is an aeolian deposit consisting of homogenous, silt-sized particles. It blankets large areas within the study area and is derived from wind erosion of unconsolidated glacial and glaciofluvial sediments. The loess is typically a buff to light yellow or yellow-brown silt bed between 1-1/2 to 3 feet thick.

- Lacustrine Deposits: The lacustrine deposits present in the study area consist of well-sorted, stratified fine sands, silts, and clays, often with varying present. The clays may be interbedded with wave-sorted beach deposits along the margins of a former lake basin. Lacustrine deposits are found primarily along Paddys Run and are generally several feet in thickness.

- Till: Undifferentiated till makes up the bulk of the glacial overburden materials in the study area. The tills were deposited either subglacially or at the melting margins of the glaciers and consist of a heterogeneous mixture of clays, silts, and pebbles. Tills may be of several types, including moraine deposits, ablation tills, and subglacial till sheets. The tills in the FEMP study area range in color from tan to brown to gray and are between 10 and 40 feet in thickness. They occur throughout most of the study area, but are not present in areas close to the Great Miami River, where they have been removed by erosion or were not deposited.

- Glaciofluvial Deposits: Glaciofluvial beds deposited by marginal or subglacial meltwater streams are interbedded within the till deposits. These beds consist of well-sorted sands and fine gravels. They are regionally discontinuous within the till and occur throughout the study area. They range in thickness from between a few inches to over 10 feet. Locally, interconnection of these beds may allow migration of groundwater within the glacial overburden.

## 2.5 LOCAL GEOLOGIC TRENDS

Due to the large number of borings available from the RI, extensive correlation of the geologic units is possible within the FEMP area. Figure 2-15 shows the cross section locations, and Figures 2-16 through 2-27 are the cross sections derived from bedrock maps, topographic maps, RI borings, and pre-RI monitoring wells. These cross sections exhibit the following trends and correlations:

- Cross-Section A-A' (Figure 2-16) is a typical cross section obliquely cutting the bedrock valley. Glacial overburden is seen on the western half of the section; on the eastern half it has been eroded away by the Great Miami River. The Great Miami Aquifer is fairly constant in thickness throughout the section, averaging about 150 to 200 feet thick, with the clay interbed occurring in the western area beneath the FEMP. Bedrock erosional topography is shown in this cross section.

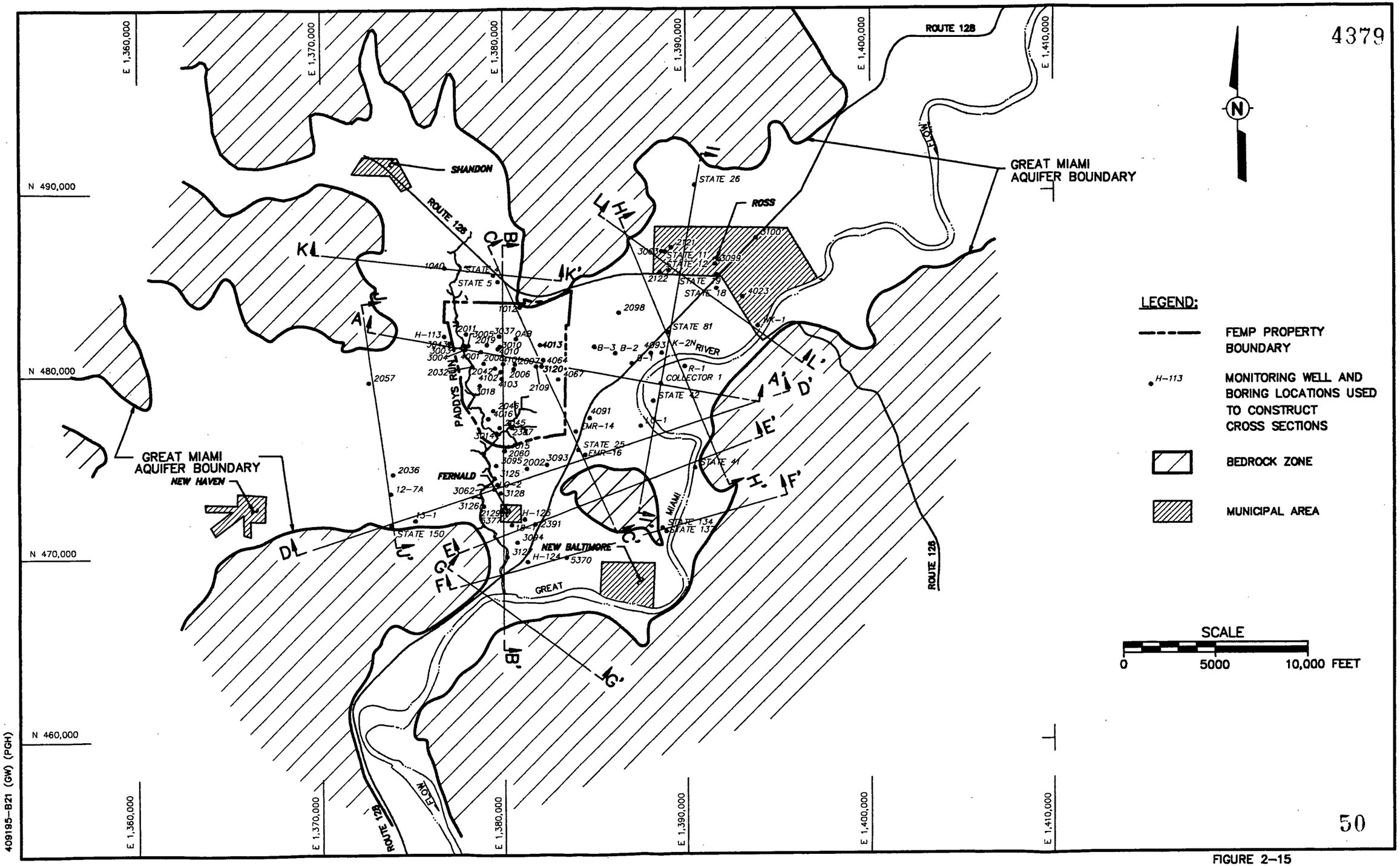


FIGURE 2-15
STUDY AREA GEOLOGIC CROSS SECTION LOCATIONS

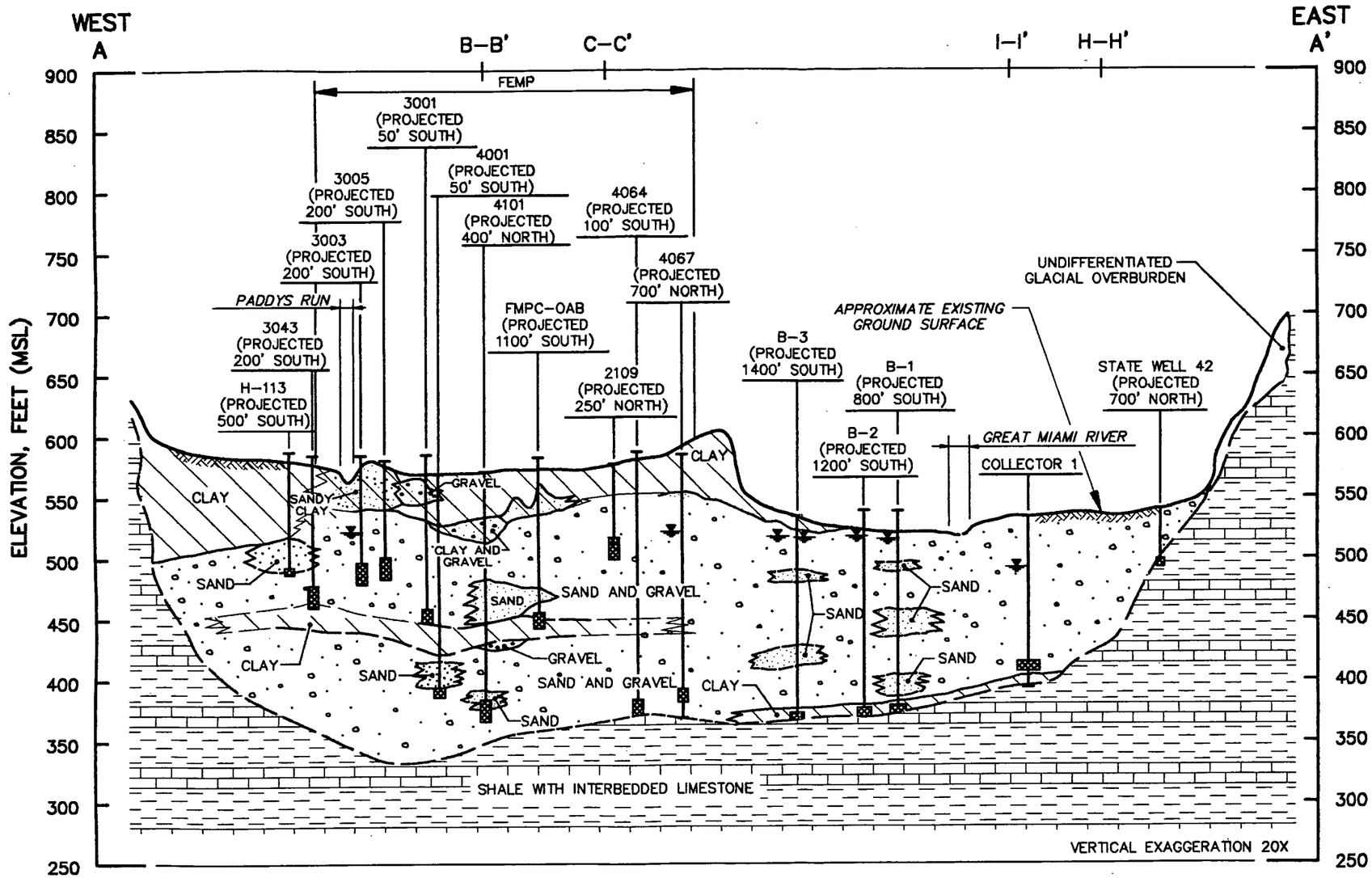


## CROSS SECTION A–A'

(LOOKING NORTH)

THE BORING LOGS AND RELATED INFORMATION DEPICT SUBSURFACE CONDITIONS ONLY AT THE SPECIFIC LOCATIONS AND DATES INDICATED. SOIL CONDITIONS AND WATER LEVELS AT OTHER LOCATIONS MAY DIFFER FROM CONDITIONS OCCURRING AT THESE BORING LOCATIONS. ALSO THE PASSAGE OF TIME MAY RESULT IN A CHANGE IN THE CONDITIONS AT THESE BORING LOCATIONS.

THE DEPTH AND THICKNESS OF THE SUBSURFACE STRATA INDICATED ON THE SECTIONS WERE GENERALIZED FROM AND INTERPOLATED BETWEEN THE TEST BORINGS. INFORMATION ON ACTUAL SUBSURFACE CONDITIONS EXISTS ONLY AT THE LOCATION OF THE TEST BORINGS AND IT IS POSSIBLE THAT SUBSURFACE CONDITIONS BETWEEN THE TEST BORINGS MAY VARY FROM THOSE INDICATED.

VERTICAL SCALE

0 100 200 FEET

HORIZONTAL SCALE

0 2000 4000 FEET

**LEGEND:**

WATER LEVELS (MEASURED 3/27/86 THROUGH 4/11/86)

INFERRED CONTACT

OPEN OR SCREENED INTERVAL

**NOTE:**

FOR LOCATION OF CROSS SECTION A–A', SEE FIGURE 2–15.

**REFERENCES:**

MODIFIED FROM U.S.G.S. PROFESSIONAL PAPER NO. 605–A USING AVAILABLE OHIO STATE WATER WELL RECORDS, SOWC WATER WELL DATA, DAMES & MOORE'S "FEED MATERIALS PRODUCTION CENTER GROUNDWATER STUDY, TASK C REPORT" FOR THE DOE (1985), AND IT (1986) RI/FS BORING LOGS.

FIGURE ADAPTED FROM FERNALD LITIGATION DRAWING NO. 303063–B16. PREPARED FOR U.S. DEPARTMENT OF ENERGY BY IT CORPORATION, NOVEMBER 1986.

409195–B22 (GW) (PGH)



FIGURE 2–16
GEOLOGIC CROSS SECTION A–A'
STUDY AREA

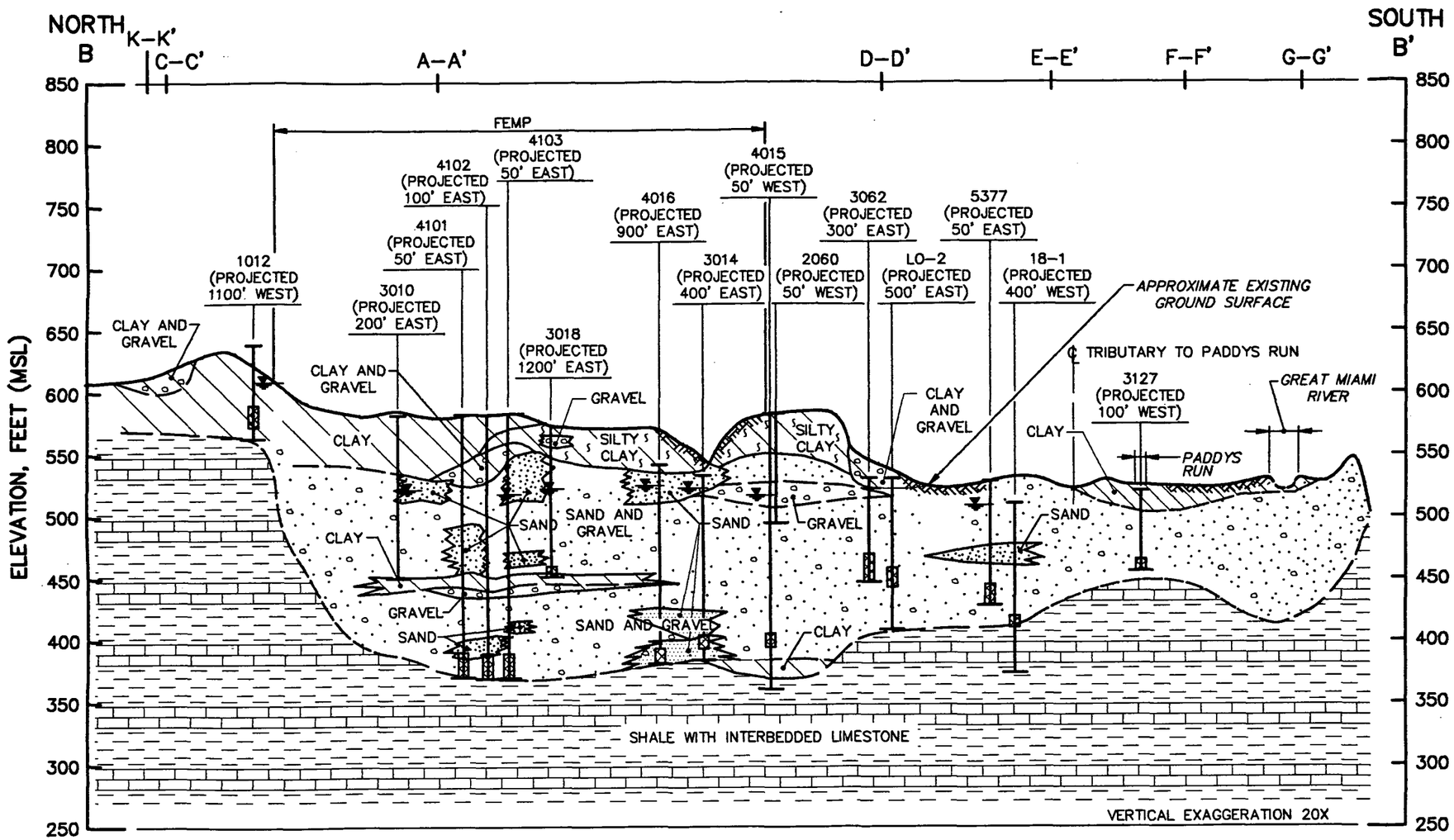


## CROSS SECTION B–B'

(LOOKING EAST)

THE BORING LOGS AND RELATED INFORMATION DEPICT SUBSURFACE CONDITIONS ONLY AT THE SPECIFIC LOCATIONS AND DATES INDICATED. SOIL CONDITIONS AND WATER LEVELS AT OTHER LOCATIONS MAY DIFFER FROM CONDITIONS OCCURRING AT THESE BORING LOCATIONS. ALSO THE PASSAGE OF TIME MAY RESULT IN A CHANGE IN THE CONDITIONS AT THESE BORING LOCATIONS.

THE DEPTH AND THICKNESS OF THE SUBSURFACE STRATA INDICATED ON THE SECTIONS WERE GENERALIZED FROM AND INTERPOLATED BETWEEN THE TEST BORINGS. INFORMATION ON ACTUAL SUBSURFACE CONDITIONS EXISTS ONLY AT THE LOCATION OF THE TEST BORINGS AND IT IS POSSIBLE THAT SUBSURFACE CONDITIONS BETWEEN THE TEST BORINGS MAY VARY FROM THOSE INDICATED.

VERTICAL SCALE

0 100 200 FEET

HORIZONTAL SCALE

0 2000 4000 FEET

LEGEND:

- WATER LEVELS (MEASURED 3/27/86 THROUGH 4/11/86)
- INFERRED CONTACT
- OPEN OR SCREENED INTERVAL

NOTE:

FOR LOCATION OF CROSS SECTION B–B', SEE FIGURE 2–15.

REFERENCES:

MODIFIED FROM U.S.G.S. PROFESSIONAL PAPER NO. 605–A USING AVAILABLE OHIO STATE WATER WELL RECORDS, SOWC WATER WELL DATA, DAMES & MOORE'S "FEED MATERIALS PRODUCTION CENTER GROUNDWATER STUDY, TASK C REPORT" FOR THE DOE (1985), AND IT (1986) RI/FS BORING LOGS.

FIGURE ADAPTED FROM FERNALD LITIGATION DRAWING NO. 303063–B17. PREPARED FOR U.S. DEPARTMENT OF ENERGY BY IT CORPORATION, NOVEMBER 1986.

409195–B23 (GW) (PGH)



FIGURE 2–17
GEOLOGIC CROSS SECTION B–B'
STUDY AREA

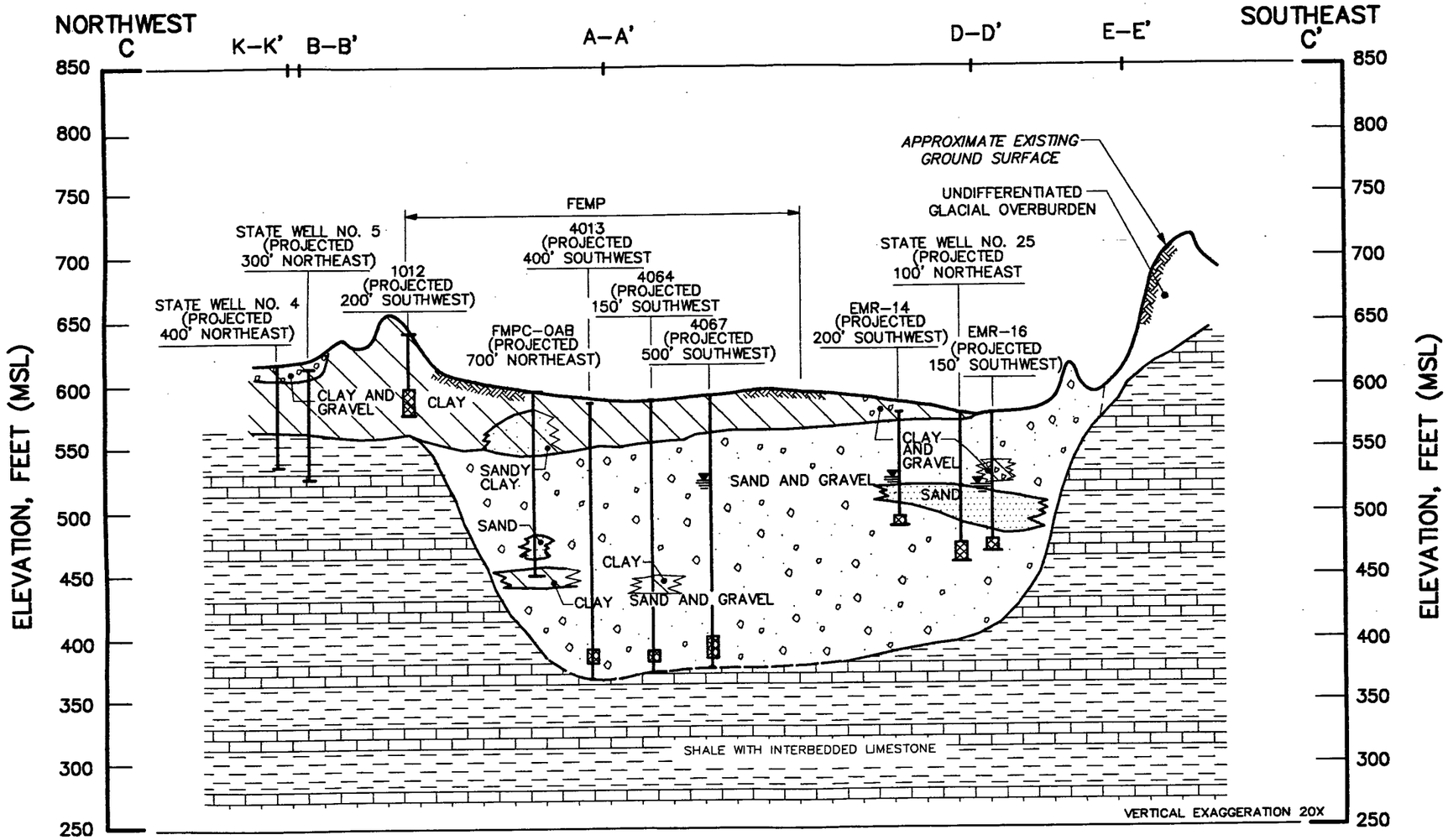


## CROSS SECTION C–C'

(LOOKING NORTHEAST)

THE BORING LOGS AND RELATED INFORMATION DEPICT SUBSURFACE CONDITIONS ONLY AT THE SPECIFIC LOCATIONS AND DATES INDICATED. SOIL CONDITIONS AND WATER LEVELS AT OTHER LOCATIONS MAY DIFFER FROM CONDITIONS OCCURRING AT THESE BORING LOCATIONS. ALSO THE PASSAGE OF TIME MAY RESULT IN A CHANGE IN THE CONDITIONS AT THESE BORING LOCATIONS.

THE DEPTH AND THICKNESS OF THE SUBSURFACE STRATA INDICATED ON THE SECTIONS WERE GENERALIZED FROM AND INTERPOLATED BETWEEN THE TEST BORINGS. INFORMATION ON ACTUAL SUBSURFACE CONDITIONS EXISTS ONLY AT THE LOCATION OF THE TEST BORINGS AND IT IS POSSIBLE THAT SUBSURFACE CONDITIONS BETWEEN THE TEST BORINGS MAY VARY FROM THOSE INDICATED.

VERTICAL SCALE

0 100 200 FEET

HORIZONTAL SCALE

0 2000 4000 FEET

LEGEND:

- WATER LEVELS (MEASURED 3/27/86 THROUGH 4/11/86)
- INFERRED CONTACT
- OPEN OR SCREENED INTERVAL

NOTE:

FOR LOCATION OF CROSS SECTION C–C', SEE FIGURE 2–15.

REFERENCES:

MODIFIED FROM U.S.G.S. PROFESSIONAL PAPER NO. 605–A USING AVAILABLE OHIO STATE WATER WELL RECORDS, SOWC WATER WELL DATA, DAMES & MOORE'S "FEED MATERIALS PRODUCTION CENTER GROUNDWATER STUDY, TASK C REPORT" FOR THE DOE (1985), AND IT (1986) RI/FS BORING LOGS.

FIGURE ADAPTED FROM FERNALD LITIGATION DRAWING NO. 303063–B18. PREPARED FOR U.S. DEPARTMENT OF ENERGY BY IT CORPORATION, NOVEMBER 1986.

409195–B24 (GW) (PGH)



FIGURE 2–18
GEOLOGIC CROSS SECTION C–C'
STUDY AREA

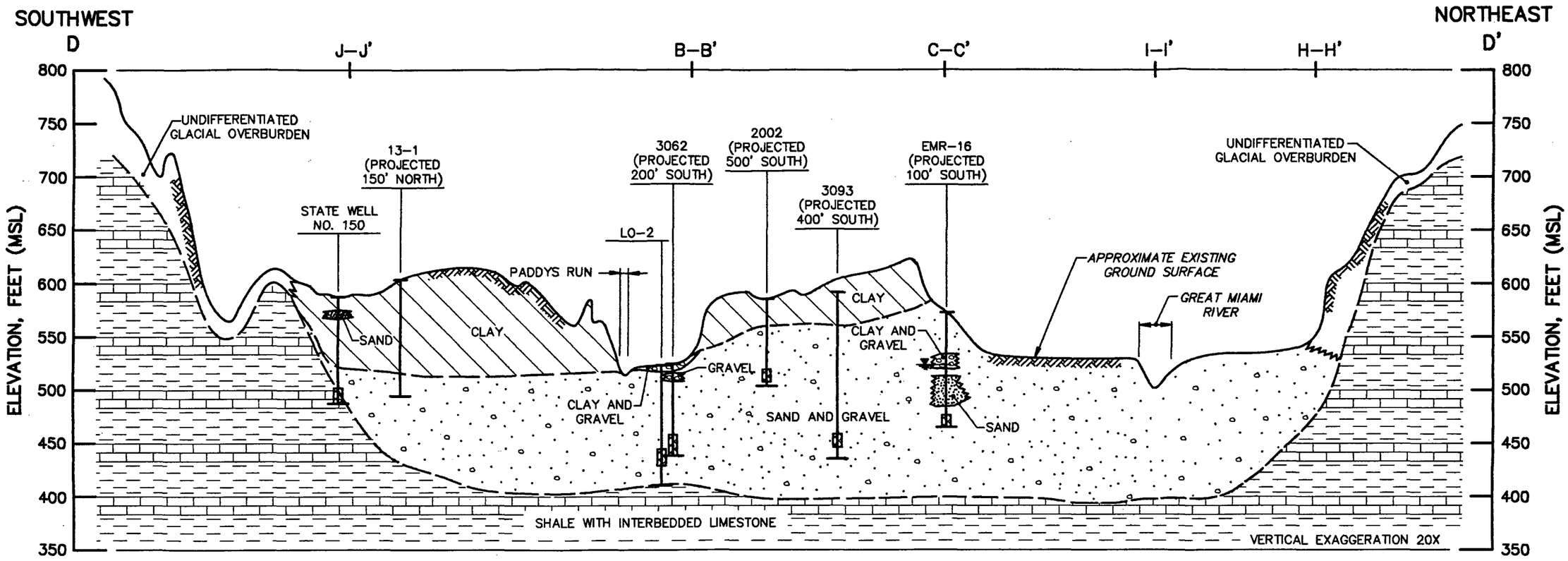


## CROSS SECTION D–D'

(LOOKING NORTHWEST)

THE BORING LOGS AND RELATED INFORMATION DEPICT SUBSURFACE CONDITIONS ONLY AT THE SPECIFIC LOCATIONS AND DATES INDICATED. SOIL CONDITIONS AND WATER LEVELS AT OTHER LOCATIONS MAY DIFFER FROM CONDITIONS OCCURRING AT THESE BORING LOCATIONS. ALSO THE PASSAGE OF TIME MAY RESULT IN A CHANGE IN THE CONDITIONS AT THESE BORING LOCATIONS.

THE DEPTH AND THICKNESS OF THE SUBSURFACE STRATA INDICATED ON THE SECTIONS WERE GENERALIZED FROM AND INTERPOLATED BETWEEN THE TEST BORINGS. INFORMATION ON ACTUAL SUBSURFACE CONDITIONS EXISTS ONLY AT THE LOCATION OF THE TEST BORINGS AND IT IS POSSIBLE THAT SUBSURFACE CONDITIONS BETWEEN THE TEST BORINGS MAY VARY FROM THOSE INDICATED.

VERTICAL SCALE

0 100 200 FEET

HORIZONTAL SCALE

0 2000 4000 FEET

**LEGEND:**

- WATER LEVELS (MEASURED 3/27/86 THROUGH 4/11/86)
- INFERRED CONTACT
- OPEN OR SCREENED INTERVAL

**NOTE:**

FOR LOCATION OF CROSS SECTION D–D', SEE FIGURE 2–15.

**REFERENCES:**

MODIFIED FROM U.S.G.S. PROFESSIONAL PAPER NO. 605–A USING AVAILABLE OHIO STATE WATER WELL RECORDS, SOWC WATER WELL DATA, DAMES & MOORE'S "FEED MATERIALS PRODUCTION CENTER GROUNDWATER STUDY, TASK A REPORT" FOR THE DOE (1985), AND IT (1986) RI/FS BORING LOGS.

FIGURE ADAPTED FROM FERNALD LITIGATION DRAWING NO. 303063–B19. PREPARED FOR U.S. DEPARTMENT OF ENERGY BY IT CORPORATION, NOVEMBER 1986.

409195–B25 (GW) (PGH)



FIGURE 2–19
GEOLOGIC CROSS SECTION D–D'
STUDY AREA

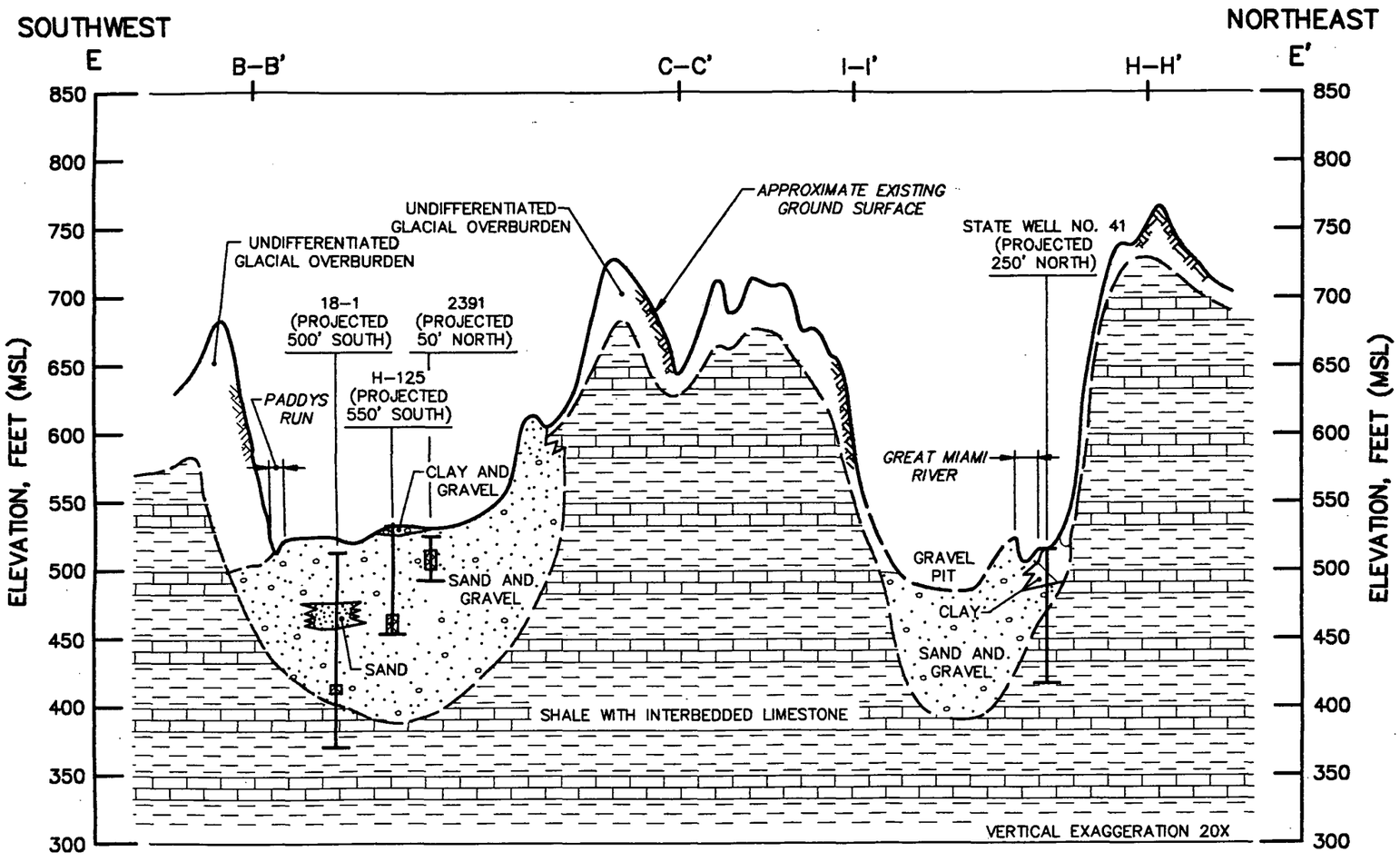


## CROSS SECTION E–E'

(LOOKING NORTHWEST)

THE BORING LOGS AND RELATED INFORMATION DEPICT SUBSURFACE CONDITIONS ONLY AT THE SPECIFIC LOCATIONS AND DATES INDICATED. SOIL CONDITIONS AND WATER LEVELS AT OTHER LOCATIONS MAY DIFFER FROM CONDITIONS OCCURRING AT THESE BORING LOCATIONS. ALSO THE PASSAGE OF TIME MAY RESULT IN A CHANGE IN THE CONDITIONS AT THESE BORING LOCATIONS.

THE DEPTH AND THICKNESS OF THE SUBSURFACE STRATA INDICATED ON THE SECTIONS WERE GENERALIZED FROM AND INTERPOLATED BETWEEN THE TEST BORINGS. INFORMATION ON ACTUAL SUBSURFACE CONDITIONS EXISTS ONLY AT THE LOCATION OF THE TEST BORINGS AND IT IS POSSIBLE THAT SUBSURFACE CONDITIONS BETWEEN THE TEST BORINGS MAY VARY FROM THOSE INDICATED.

VERTICAL SCALE

0 100 200 FEET

HORIZONTAL SCALE

0 2000 4000 FEET

**LEGEND:**

- WATER LEVELS (MEASURED 3/27/86 THROUGH 4/11/86)
- INFERRED CONTACT
- OPEN OR SCREENED INTERVAL

**NOTE:**

FOR LOCATION OF CROSS SECTION E–E', SEE FIGURE 2–15.

**REFERENCES:**

MODIFIED FROM U.S.G.S. PROFESSIONAL PAPER NO. 605–A USING AVAILABLE OHIO STATE WATER WELL RECORDS, SOWC WATER WELL DATA, DAMES & MOORE'S "FEED MATERIALS PRODUCTION CENTER GROUNDWATER STUDY, TASK C REPORT" FOR THE DOE (1985), AND IT (1986) RI/FS BORING LOGS.

FIGURE ADAPTED FROM FERNALD LITIGATION DRAWING NO. 303063–B20. PREPARED FOR U.S. DEPARTMENT OF ENERGY BY IT CORPORATION, NOVEMBER 1986.

409185–B26 (GW) (PGH)



FIGURE 2–20
GEOLOGIC CROSS SECTION E–E'
STUDY AREA

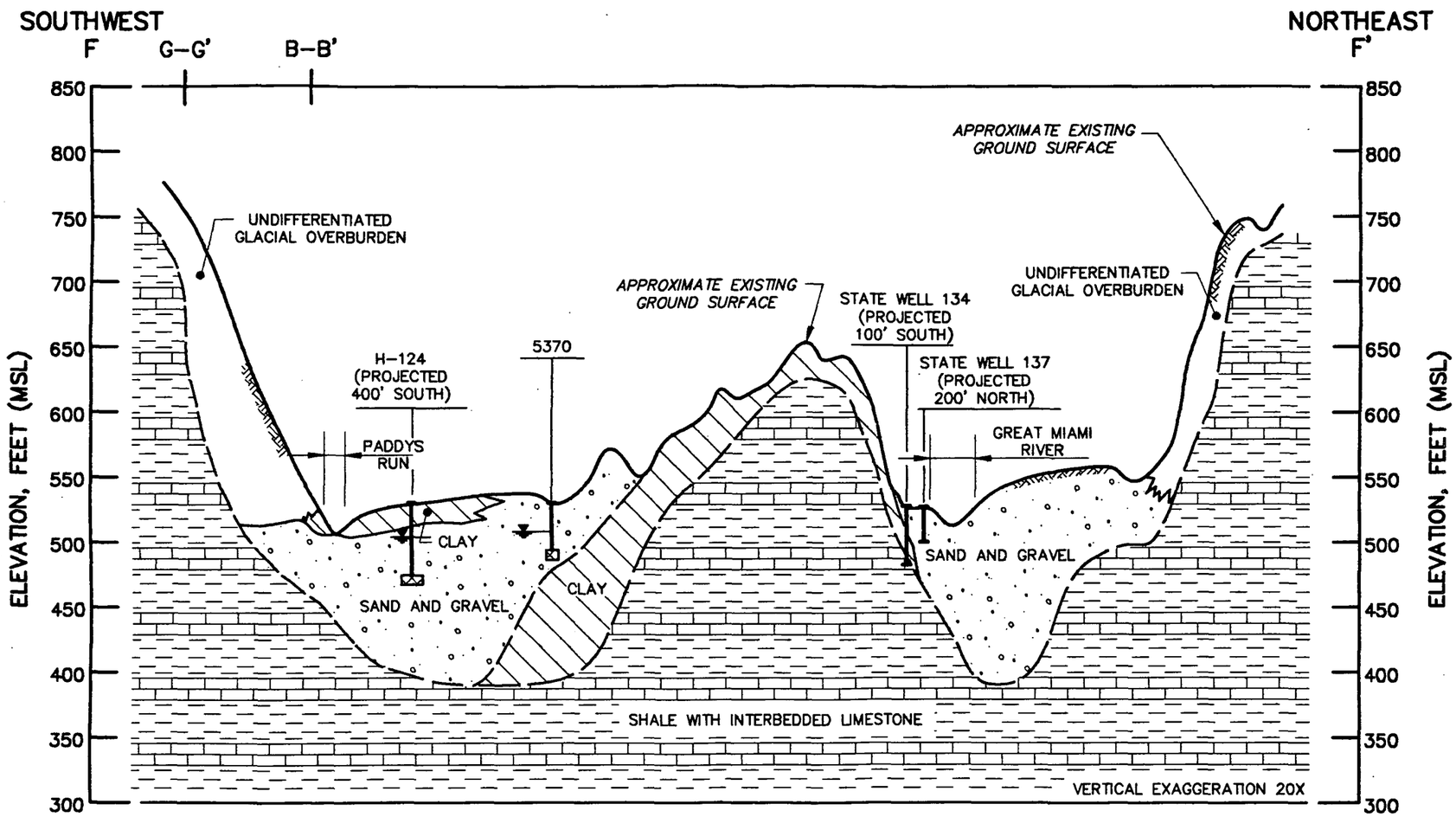


## CROSS SECTION F–F'

(LOOKING NORTHWEST)

THE BORING LOGS AND RELATED INFORMATION DEPICT SUBSURFACE CONDITIONS ONLY AT THE SPECIFIC LOCATIONS AND DATES INDICATED. SOIL CONDITIONS AND WATER LEVELS AT OTHER LOCATIONS MAY DIFFER FROM CONDITIONS OCCURRING AT THESE BORING LOCATIONS. ALSO THE PASSAGE OF TIME MAY RESULT IN A CHANGE IN THE CONDITIONS AT THESE BORING LOCATIONS.

THE DEPTH AND THICKNESS OF THE SUBSURFACE STRATA INDICATED ON THE SECTIONS WERE GENERALIZED FROM AND INTERPOLATED BETWEEN THE TEST BORINGS. INFORMATION ON ACTUAL SUBSURFACE CONDITIONS EXISTS ONLY AT THE LOCATION OF THE TEST BORINGS AND IT IS POSSIBLE THAT SUBSURFACE CONDITIONS BETWEEN THE TEST BORINGS MAY VARY FROM THOSE INDICATED.

VERTICAL SCALE

0 100 200 FEET

HORIZONTAL SCALE

0 2000 4000 FEET

**LEGEND:**

- WATER LEVELS (MEASURED 3/27/86 THROUGH 4/11/86)
- INFERRED CONTACT
- OPEN OR SCREENED INTERVAL

**NOTE:**

FOR LOCATION OF CROSS SECTION F–F', SEE FIGURE 2–15.

**REFERENCES:**

MODIFIED FROM U.S.G.S. PROFESSIONAL PAPER NO. 605–A USING AVAILABLE OHIO STATE WATER WELL RECORDS, SOWC WATER WELL DATA, DAMES & MOORE'S "FEED MATERIALS PRODUCTION CENTER GROUNDWATER STUDY, TASK C REPORT" FOR THE DOE (1985), AND IT (1986) RI/FS BORING LOGS.

FIGURE ADAPTED FROM FERNALD LITIGATION DRAWING NO. 303063–B21. PREPARED FOR U.S. DEPARTMENT OF ENERGY BY IT CORPORATION, NOVEMBER 1986.

409195–B27 (GW) (PGH)



FIGURE 2–21
GEOLOGIC CROSS SECTION F–F'
STUDY AREA

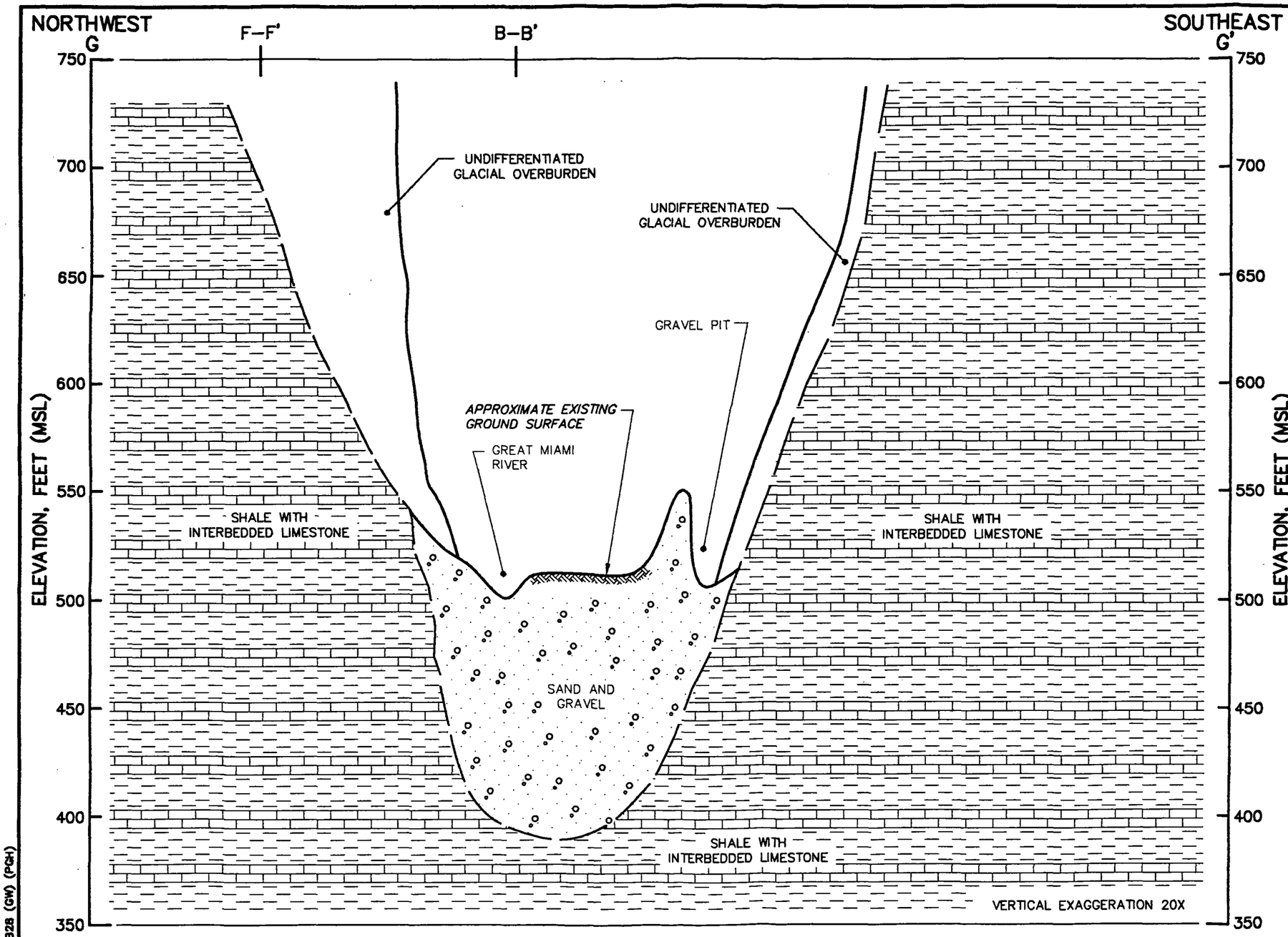


## CROSS SECTION G–G'

(LOOKING NORTHEAST)

THE BORING LOGS AND RELATED INFORMATION DEPICT SUBSURFACE CONDITIONS ONLY AT THE SPECIFIC LOCATIONS AND DATES INDICATED. SOIL CONDITIONS AND WATER LEVELS AT OTHER LOCATIONS MAY DIFFER FROM CONDITIONS OCCURRING AT THESE BORING LOCATIONS. ALSO THE PASSAGE OF TIME MAY RESULT IN A CHANGE IN THE CONDITIONS AT THESE BORING LOCATIONS.

THE DEPTH AND THICKNESS OF THE SUBSURFACE STRATA INDICATED ON THE SECTIONS WERE GENERALIZED FROM AND INTERPOLATED BETWEEN THE TEST BORINGS. INFORMATION ON ACTUAL SUBSURFACE CONDITIONS EXISTS ONLY AT THE LOCATION OF THE TEST BORINGS AND IT IS POSSIBLE THAT SUBSURFACE CONDITIONS BETWEEN THE TEST BORINGS MAY VARY FROM THOSE INDICATED.

VERTICAL SCALE

0 50 100 FEET

HORIZONTAL SCALE

0 1000 2000 FEET

**LEGEND:**

INFERRED CONTACT

**NOTE:**

FOR LOCATION OF CROSS SECTION G–G' SEE FIGURE 2–15.

THE SUBSURFACE CONDITIONS DEPICTED ARE BASED ON THE REFERENCES. THE DEPTH AND THICKNESS OF SUBSURFACE STRATA INDICATED ON THE SECTION ARE BASED ON THESE REFERENCES AND IT IS POSSIBLE THAT SUBSURFACE CONDITIONS MAY VARY SINCE TEST BORINGS HAVE NOT BEEN CONDUCTED AT THESE LOCATIONS.

**REFERENCES:**

MODIFIED FROM U.S.G.S. PROFESSIONAL PAPER NO. 605–A USING AVAILABLE OHIO STATE WATER WELL RECORDS, SOWC WATER WELL DATA, DAMES & MOORE'S "FEED MATERIALS PRODUCTION CENTER GROUNDWATER STUDY, TASK C REPORT" FOR THE DOE (1985), AND IT (1986) RI/FS BORING LOGS.

FIGURE ADAPTED FROM DRAWING NO. 303317–A104, FROM "HYDROGEOLOGIC STUDY OF THE GREAT MIAMI RIVER" PREPARED FOR U.S. DEPARTMENT OF ENERGY BY IT CORPORATION, AUGUST 1988.

409195–B28 (GW) (PGH)



FIGURE 2–22
GEOLOGIC CROSS SECTION G–G'
STUDY AREA

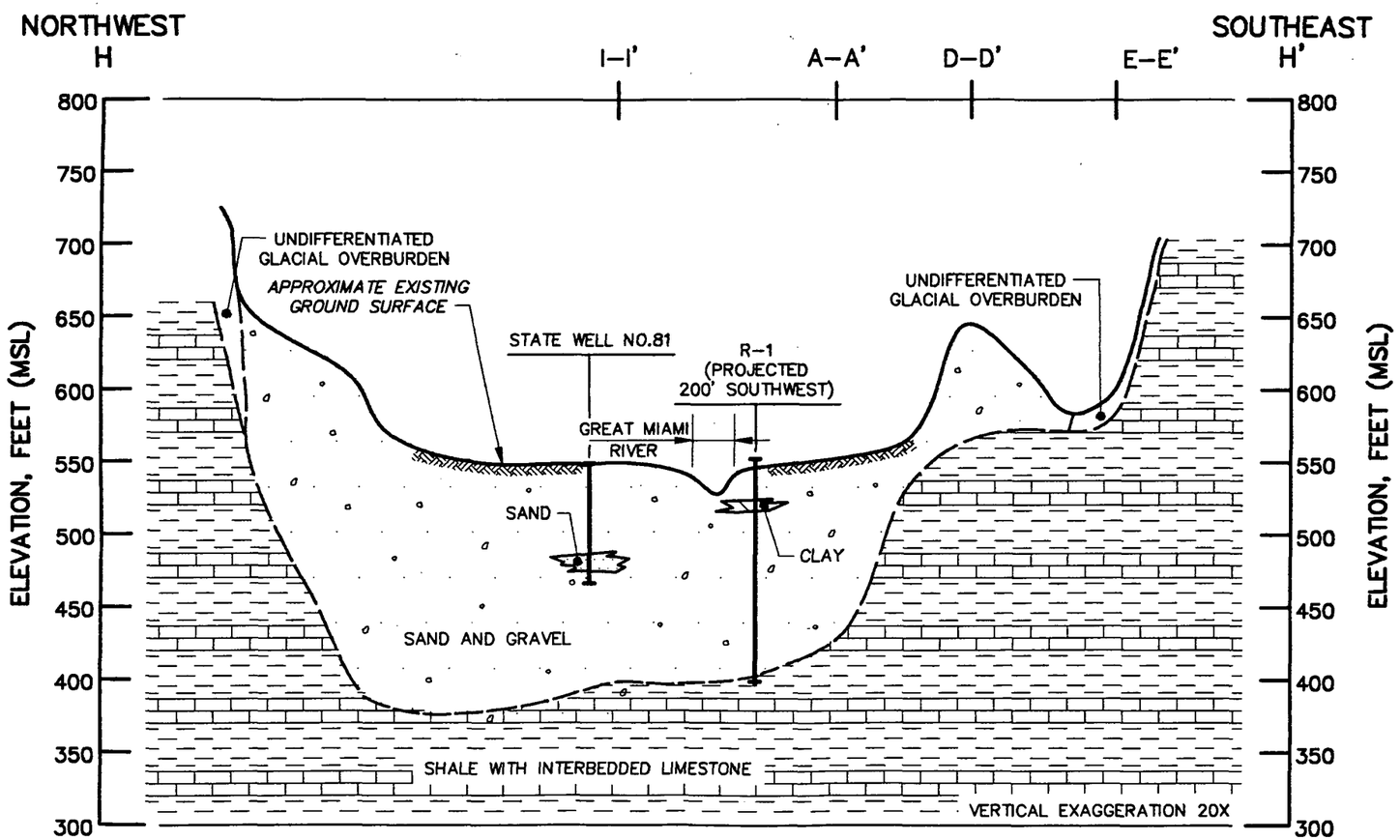


## CROSS SECTION H–H'

(LOOKING NORTHEAST)

THE BORING LOGS AND RELATED INFORMATION DEPICT SUBSURFACE CONDITIONS ONLY AT THE SPECIFIC LOCATIONS AND DATES INDICATED. SOIL CONDITIONS AND WATER LEVELS AT OTHER LOCATIONS MAY DIFFER FROM CONDITIONS OCCURRING AT THESE BORING LOCATIONS. ALSO THE PASSAGE OF TIME MAY RESULT IN A CHANGE IN THE CONDITIONS AT THESE BORING LOCATIONS.

THE DEPTH AND THICKNESS OF THE SUBSURFACE STRATA INDICATED ON THE SECTIONS WERE GENERALIZED FROM AND INTERPOLATED BETWEEN THE TEST BORINGS. INFORMATION ON ACTUAL SUBSURFACE CONDITIONS EXISTS ONLY AT THE LOCATION OF THE TEST BORINGS AND IT IS POSSIBLE THAT SUBSURFACE CONDITIONS BETWEEN THE TEST BORINGS MAY VARY FROM THOSE INDICATED.

VERTICAL SCALE

0 100 200 FEET

HORIZONTAL SCALE

0 2000 4000 FEET

**LEGEND:**

INFERRED CONTACT

**NOTE:**

FOR LOCATION OF CROSS SECTION H–H' SEE FIGURE 2–15.

**REFERENCE:**

MODIFIED FROM U.S.G.S. PROFESSIONAL PAPER NO. 605–A USING AVAILABLE OHIO STATE WATER WELL RECORDS.

409195–B29 (GW) (PGH)



FIGURE 2–23
GEOLOGIC CROSS SECTION H–H'
STUDY AREA

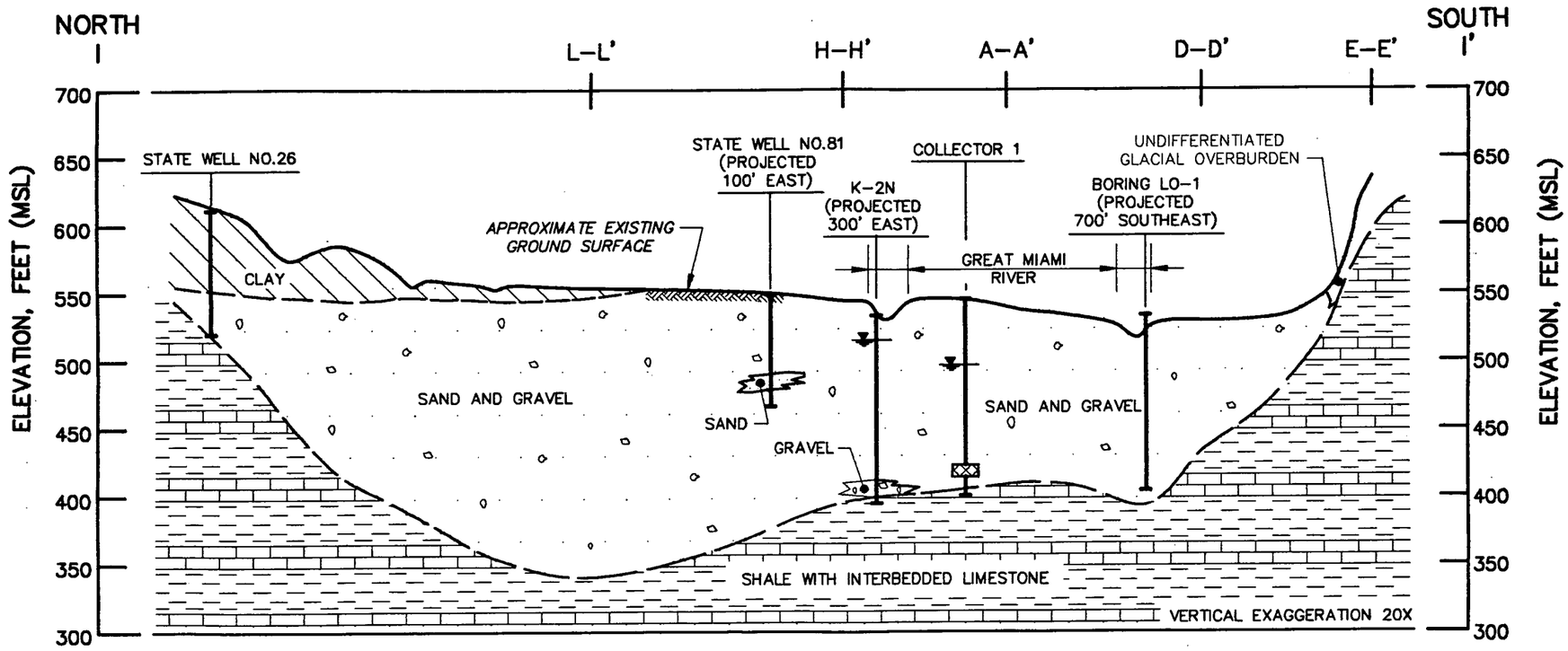


## CROSS SECTION I–I'

(LOOKING EAST)

THE BORING LOGS AND RELATED INFORMATION DEPICT SUBSURFACE CONDITIONS ONLY AT THE SPECIFIC LOCATIONS AND DATES INDICATED. SOIL CONDITIONS AND WATER LEVELS AT OTHER LOCATIONS MAY DIFFER FROM CONDITIONS OCCURRING AT THESE BORING LOCATIONS. ALSO THE PASSAGE OF TIME MAY RESULT IN A CHANGE IN THE CONDITIONS AT THESE BORING LOCATIONS.

THE DEPTH AND THICKNESS OF THE SUBSURFACE STRATA INDICATED ON THE SECTIONS WERE GENERALIZED FROM AND INTERPOLATED BETWEEN THE TEST BORINGS. INFORMATION ON ACTUAL SUBSURFACE CONDITIONS EXISTS ONLY AT THE LOCATION OF THE TEST BORINGS AND IT IS POSSIBLE THAT SUBSURFACE CONDITIONS BETWEEN THE TEST BORINGS MAY VARY FROM THOSE INDICATED.

VERTICAL SCALE

0 100 200 FEET

HORIZONTAL SCALE

0 2000 4000 FEET

**LEGEND:**

- WATER LEVELS (MEASURED 3/27/86 THROUGH 4/11/86)
- INFERRED CONTACT
- OPEN OR SCREENED INTERVAL

**NOTE:**

FOR LOCATION OF CROSS SECTION I–I', SEE FIGURE 2–15.

**REFERENCES:**

OHIO STATE WATER WELL RECORDS, STATE OF OHIO DEPARTMENT OF NATURAL RESOURCES DIVISION OF WATER TECHNICAL REPORT NO. 4, AND REPORT PREPARED FOR OHIO ENVIRONMENTAL PROTECTION AGENCY BY GEOTRANS, INC.

409195–B30 (GW) (PGH)



FIGURE 2–24
GEOLOGIC CROSS SECTION I–I'
STUDY AREA

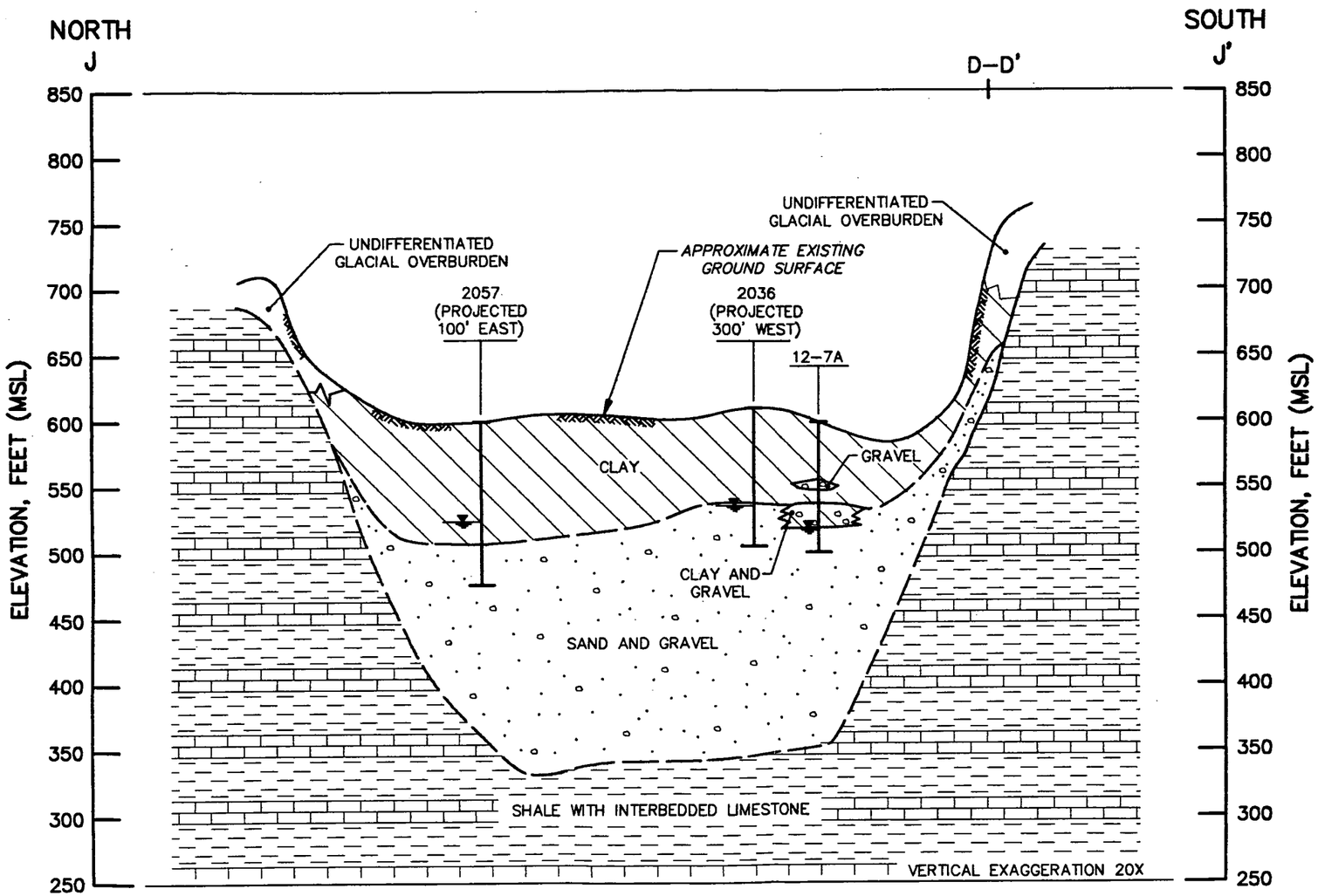


## CROSS SECTION J–J'

(LOOKING EAST)

THE BORING LOGS AND RELATED INFORMATION DEPICT SUBSURFACE CONDITIONS ONLY AT THE SPECIFIC LOCATIONS AND DATES INDICATED. SOIL CONDITIONS AND WATER LEVELS AT OTHER LOCATIONS MAY DIFFER FROM CONDITIONS OCCURRING AT THESE BORING LOCATIONS. ALSO THE PASSAGE OF TIME MAY RESULT IN A CHANGE IN THE CONDITIONS AT THESE BORING LOCATIONS.

THE DEPTH AND THICKNESS OF THE SUBSURFACE STRATA INDICATED ON THE SECTIONS WERE GENERALIZED FROM AND INTERPOLATED BETWEEN THE TEST BORINGS. INFORMATION ON ACTUAL SUBSURFACE CONDITIONS EXISTS ONLY AT THE LOCATION OF THE TEST BORINGS AND IT IS POSSIBLE THAT SUBSURFACE CONDITIONS BETWEEN THE TEST BORINGS MAY VARY FROM THOSE INDICATED.

VERTICAL SCALE

0 100 200 FEET

HORIZONTAL SCALE

0 2000 4000 FEET

**LEGEND:**

WATER LEVELS (MEASURED 3/27/86 THROUGH 4/11/86)

INFERRED CONTACT

**NOTE:**

FOR LOCATION OF CROSS SECTION J–J', SEE FIGURE 2–15.

**REFERENCES:**

MODIFIED FROM U.S.G.S. PROFESSIONAL PAPER NO. 605–A USING AVAILABLE OHIO STATE WATER WELL RECORDS, SOWC WATER WELL DATA, DAMES & MOORE'S "FEED MATERIALS PRODUCTION CENTER GROUNDWATER STUDY, TASK C REPORT" FOR THE DOE (1985), AND IT (1986) RI/FS BORING LOGS.

409195–B31 (GW) (PGH)



FIGURE 2–25
GEOLOGIC CROSS SECTION J–J'
STUDY AREA

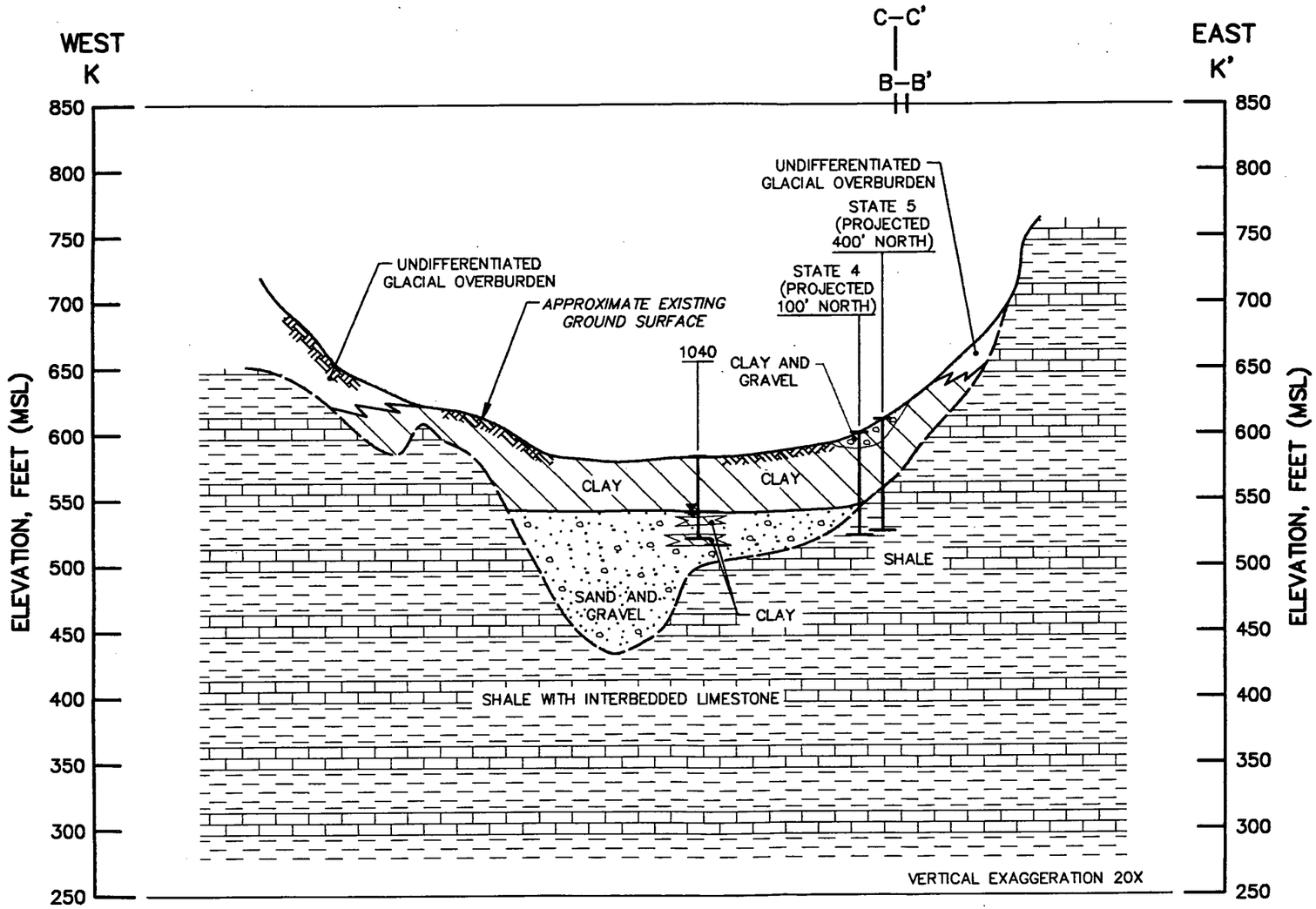


## CROSS SECTION K–K'

(LOOKING NORTH)

THE BORING LOGS AND RELATED INFORMATION DEPICT SUBSURFACE CONDITIONS ONLY AT THE SPECIFIC LOCATIONS AND DATES INDICATED. SOIL CONDITIONS AND WATER LEVELS AT OTHER LOCATIONS MAY DIFFER FROM CONDITIONS OCCURRING AT THESE BORING LOCATIONS. ALSO THE PASSAGE OF TIME MAY RESULT IN A CHANGE IN THE CONDITIONS AT THESE BORING LOCATIONS.

THE DEPTH AND THICKNESS OF THE SUBSURFACE STRATA INDICATED ON THE SECTIONS WERE GENERALIZED FROM AND INTERPOLATED BETWEEN THE TEST BORINGS. INFORMATION ON ACTUAL SUBSURFACE CONDITIONS EXISTS ONLY AT THE LOCATION OF THE TEST BORINGS AND IT IS POSSIBLE THAT SUBSURFACE CONDITIONS BETWEEN THE TEST BORINGS MAY VARY FROM THOSE INDICATED.

VERTICAL SCALE

0 100 200 FEET

HORIZONTAL SCALE

0 2000 4000 FEET

**LEGEND:**

WATER LEVELS (MEASURED 3/27/86 THROUGH 4/11/86)

INFERRED CONTACT

**NOTES:**

FOR LOCATION OF CROSS SECTION K–K', SEE FIGURE 2–15.

DUE TO INSUFFICIENT BORING LOG DATA IN THE CROSS SECTION AREA, FURTHER DEFINITION WAS ADDED BY USING BORING LOG 3066 TO EXPAND THE INTERBEDS OF CLAY IN THE BURIED CHANNEL.

**REFERENCES:**

MODIFIED FROM U.S.G.S. PROFESSIONAL PAPER NO. 605–A USING AVAILABLE OHIO STATE WATER WELL RECORDS, SOWC WATER WELL DATA, DAMES & MOORE'S "FEED MATERIALS PRODUCTION CENTER GROUNDWATER STUDY, TASK C REPORT" FOR THE DOE (1985), AND IT (1986) RI/FS BORING LOGS.



400185–B32 (GW) (PGH)

FIGURE 2–26
GEOLOGIC CROSS SECTION K–K'
STUDY AREA

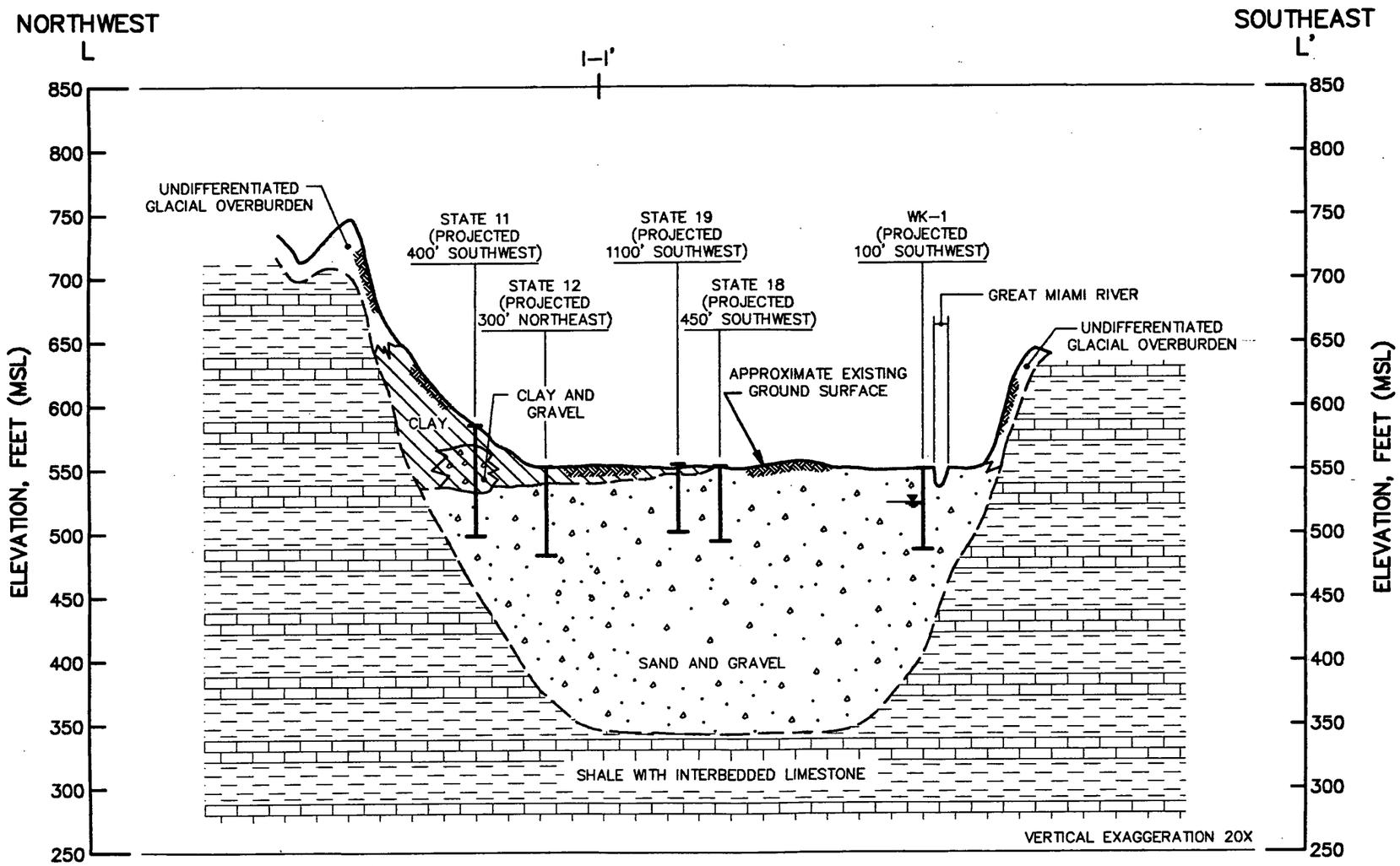


## CROSS SECTION L–L'

(LOOKING NORTHEAST)

THE BORING LOGS AND RELATED INFORMATION DEPICT SUBSURFACE CONDITIONS ONLY AT THE SPECIFIC LOCATIONS AND DATES INDICATED. SOIL CONDITIONS AND WATER LEVELS AT OTHER LOCATIONS MAY DIFFER FROM CONDITIONS OCCURRING AT THESE BORING LOCATIONS. ALSO THE PASSAGE OF TIME MAY RESULT IN A CHANGE IN THE CONDITIONS AT THESE BORING LOCATIONS.

THE DEPTH AND THICKNESS OF THE SUBSURFACE STRATA INDICATED ON THE SECTIONS WERE GENERALIZED FROM AND INTERPOLATED BETWEEN THE TEST BORINGS. INFORMATION ON ACTUAL SUBSURFACE CONDITIONS EXISTS ONLY AT THE LOCATION OF THE TEST BORINGS AND IT IS POSSIBLE THAT SUBSURFACE CONDITIONS BETWEEN THE TEST BORINGS MAY VARY FROM THOSE INDICATED.

VERTICAL SCALE

0 100 200 FEET

HORIZONTAL SCALE

0 2000 4000 FEET

**LEGEND:**

WATER LEVELS (MEASURED 3/27/86 THROUGH 4/11/86)

INFERRED CONTACT

**NOTE:**

FOR LOCATION OF CROSS SECTION L–L', SEE FIGURE 2–15.

**REFERENCES:**

MODIFIED FROM U.S.G.S. PROFESSIONAL PAPER NO. 605–A USING AVAILABLE OHIO STATE WATER WELL RECORDS, SOWC WATER WELL DATA, DAMES & MOORE'S "FEED MATERIALS PRODUCTION CENTER GROUNDWATER STUDY, TASK C REPORT" FOR THE DOE (1985), AND IT (1986) RI/FS BORING LOGS.

409195–B33 (GW) (PGH)



FIGURE 2–27
GEOLOGIC CROSS SECTION L–L'
STUDY AREA

- Cross-Sections A-A', B-B', and C-C' (Figures 2-16, 2-17, and 2-18, respectively) illustrate the geology underlying the FEMP. Thick deposits of glacial overburden overlie the Great Miami Aquifer. The Great Miami Aquifer is thickest in the area which lies underneath the FEMP where it approaches 200 feet. The clay interbed underlies the northwestern half of the FEMP, dividing the aquifer almost equally into upper and lower halves. The FEMP Production Monitoring Well 4103, shown in Cross-Section B-B', pumps an average of 292 gpm from the lower half of the aquifer.

- Cross-Section C-C' (Figure 2-18) shows a typical cross section perpendicular to the valley trend. The glacial overburden again thins in the direction of the Great Miami River where erosion has stripped much of it away. The Great Miami Aquifer remains fairly constant in thickness. The clay interbed is present beneath a portion of the FEMP.

- Section D-D' (Figure 2-19) shows a longitudinal view of the southern portion of the New Haven Trough. A topographic expression of the moraine which dammed a glacial lake in Paddys Run Valley appears on either side of Paddys Run. It should also be noted that the clay interbed is not present this far to the south of the FEMP.

- Cross-Section E-E' (Figure 2-20) is a section across the Paddys Run Outlet in the west and the current channel of the Great Miami River in the east. The Paddys Run Outlet here has had its glacial overburden eroded away by the Great Miami River. Only small remnants of clay interbeds (probably fluvial in origin) are still present in this area. This region of the Great Miami River Valley also exhibits erosion and terracing and has levees along the river channel.

- Cross-Section F-F' (Figure 2-21) exhibits nearly the same features as Cross Section E-E', but contains an additional clay lens present in the Fernald Outlet adjacent to the bedrock knob which separates the two valleys. This clay pocket may be a remnant of the glacial overburden which was protected from erosion by the bedrock knob. The bedrock topographic map (Figure 2-11) shows an elevated terrace which lies above the present stream valley and on which the town of New Baltimore is located.

- Cross-Section G-G' (Figure 2-22) shows the bedrock valley further downstream from the Paddys Run Outlet.

- Cross-Section H-H' (Figure 2-23) is almost perpendicular to the New Haven Trough and is upstream of the FEMP. The bedrock valley is relatively narrow here, and the surface topography is dominated by fluvial terraces and the flood plain of the Great Miami River. A small interbed of clay is found in this area; otherwise, the aquifer is fairly homogeneous.

- Cross-Section I-I' (Figure 2-24) is a north-south section located to the east of the Great Miami River where the SOWC's large collector wells are located. Collector Well No. 1 is included on the cross section, and pumps an average of 6026 gpm of water from the aquifer. Collector Well No. 2 (not shown) is located west of the section and has the same average pumping rate and design as Collector Well No. 1. The aquifer in this area ranges in thickness from 150 to 200 feet, and is composed almost exclusively of sand and gravel with no silt or clay lenses. As it is hydraulically connected with the

riverbed, the aquifer receives induced infiltration from the Great Miami River which is available for use by the collector wells.

- Cross-Section J-J' (Figure 2-25) shows the area west of the FEMP site in the buried valley. As at the FEMP, the valley is basically U-shaped with the Great Miami Aquifer filling it. The presence or absence of the clay interbed is uncertain due to lack of borings in the area. The glacial overburden is much thicker in this region, approaching 100 feet through part of the section, and is not breached by stream erosion.

- Cross-Section K-K' (Figure 2-26) shows a section through a typical region of the Shandon Tributary, which lies north of the FEMP. This is a tributary valley to the New Haven Trough; thus, the cross-sectional area of the aquifer is smaller than in other regions, primarily because of the decreasing bedrock valley depth. The Great Miami Aquifer has more interbedded clays present within its upper portions. Thick deposits of undissected glacial overburden also reduce recharge rates and further reduce groundwater flow in this area.

- Cross-Section L-L' (Figure 2-27) is perpendicular to the New Haven Trough at Ross, east of the FEMP, and upstream of the SOWC collector wells. A thin layer of glacial overburden overlies the northwestern half of this area. The Great Miami Aquifer is well sorted and homogeneous with high transmissivity.

# 3.0 HYDROGEOLOGIC CHARACTERIZATION OF THE FEMP AREA

A general description of the hydrologic surface water system and the geologic environment on both a regional and site-specific basis was presented in Chapter 2.0. Chapter 3.0 synthesizes that general information into the components necessary for characterizing the hydrogeologic conditions of the FEMP area and initiating a groundwater modeling effort. The following section presents: (1) a general characterization of the hydrogeological environments that occur in the vicinity of the FEMP facility, (2) a brief description of the Great Miami Aquifer and the perched glacial overburden groundwater systems, (3) the observed groundwater elevations and the projected groundwater flow directions, and (4) a general characterization of the Great Miami River and Paddys Run surface water system interactions with the groundwater systems in the FEMP area. The hydrogeologic interpretations presented in this section are those that were used in the selection of parameters and modeling conditions for use in the groundwater modeling effort. The interpretations are based on information that was available as of December 1990.

As presented in Chapter 2.0, there are two major types of geologic material that underlie the FEMP site:

- The Ordovician shale and limestone bedrock in which the New Haven Trough has been excavated
- The unconsolidated glacial and fluvial deposits which overlie the Ordovician bedrock and fill the New Haven Trough.

Saturated zones occur in the glacial overburden and the valley fill deposits. These saturated zones were monitored for water level and water quality using a series of monitoring wells (Figures 3-1 through 3-5). The 1000-Series monitoring wells were used to monitor the perched groundwater system located in the glacial overburden, while the 2000- through 4000-Series monitoring wells were used to monitor successively deeper levels within the Great Miami Aquifer. The monitoring wells depicted in Figures 3-2 through 3-5 are those monitoring wells that were available for the December 1990 groundwater modeling effort. Since 1990, the FEMP environmental characterization and groundwater monitoring programs have added numerous monitoring wells, and Figures 3-2 through 3-5 represent only a portion of the currently available monitoring well network.

Both the classic and regulatory definitions of an aquifer were considered when evaluating the hydrogeology of the study area. The classic definition of an aquifer is "a water-saturated unit that will yield water to wells or springs at a sufficient rate so that the wells or springs can serve as practical sources of water supply" (Driscoll 1986). Saturated zones occur that cannot sustain withdrawals sufficient for water supplies, but meet the regulatory definition of an aquifer; that is, "the uppermost formation nearest to the ground surface that is capable of yielding a significant amount of groundwater

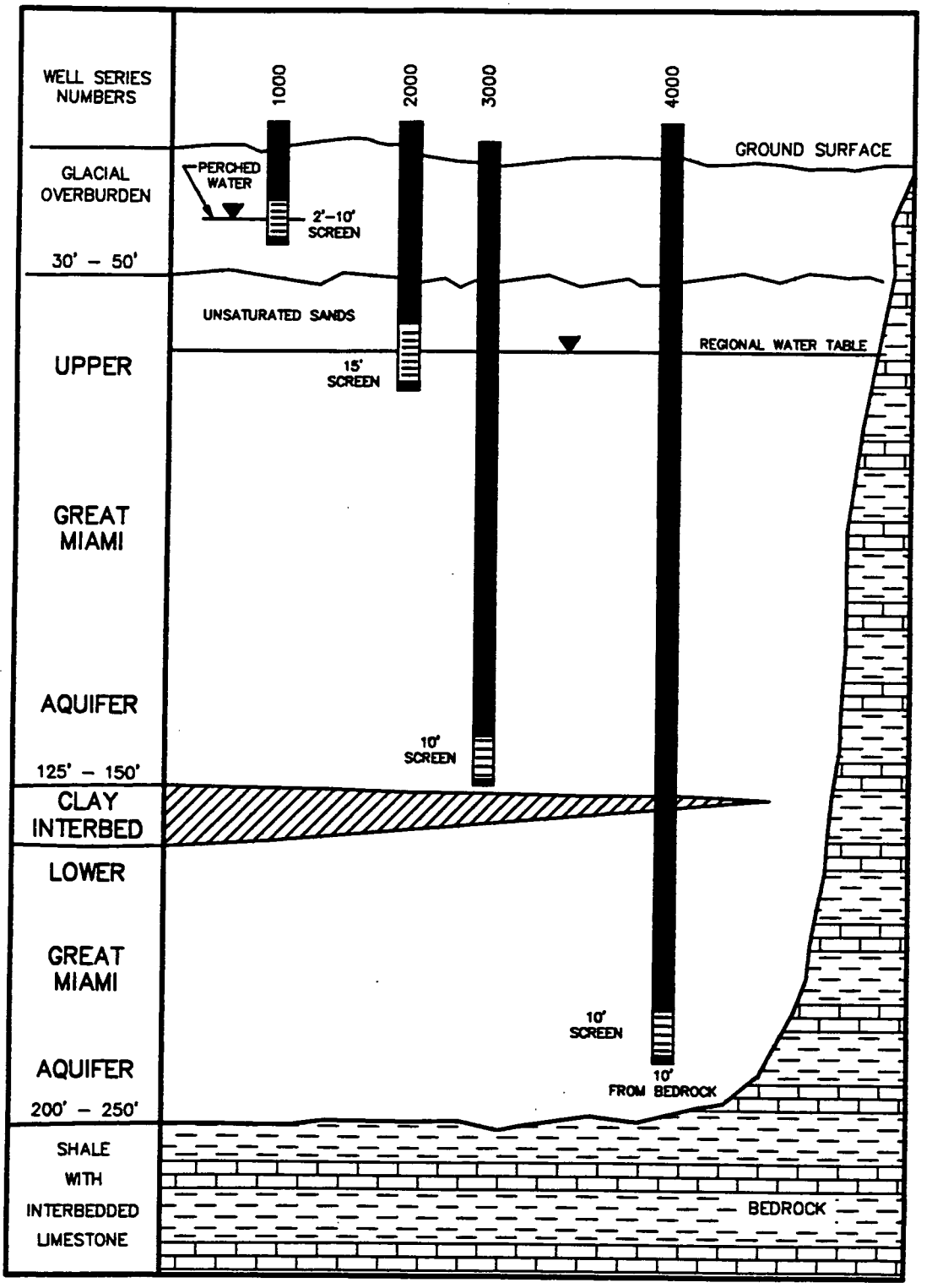


409195-A48 (GW) (PGH)

FIGURE 3-1 GROUNDWATER MONITORING WELL COMPLETION DEPTHS

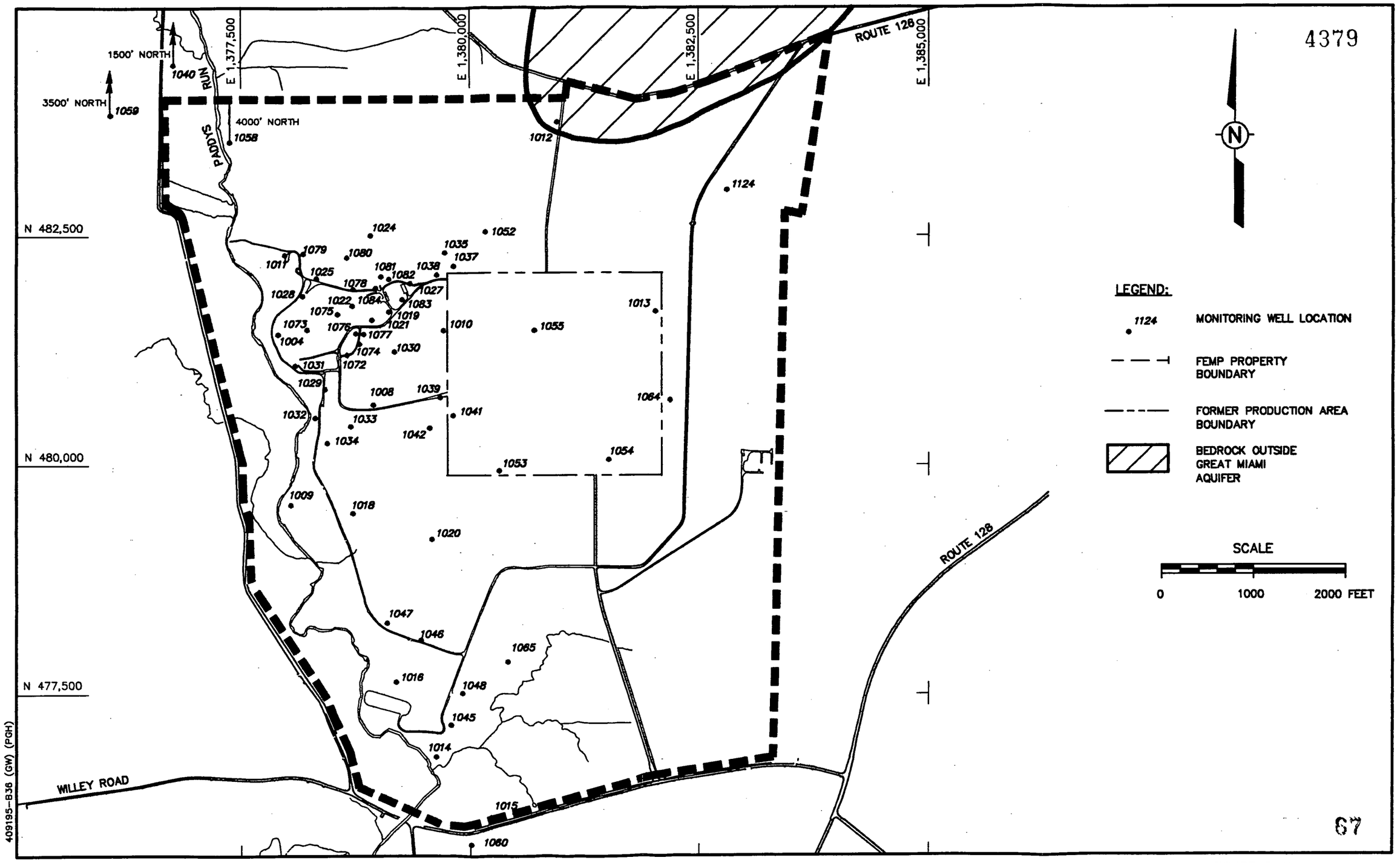


FIGURE 3-2
MONITORING WELL LOCATIONS
1000 SERIES WELLS

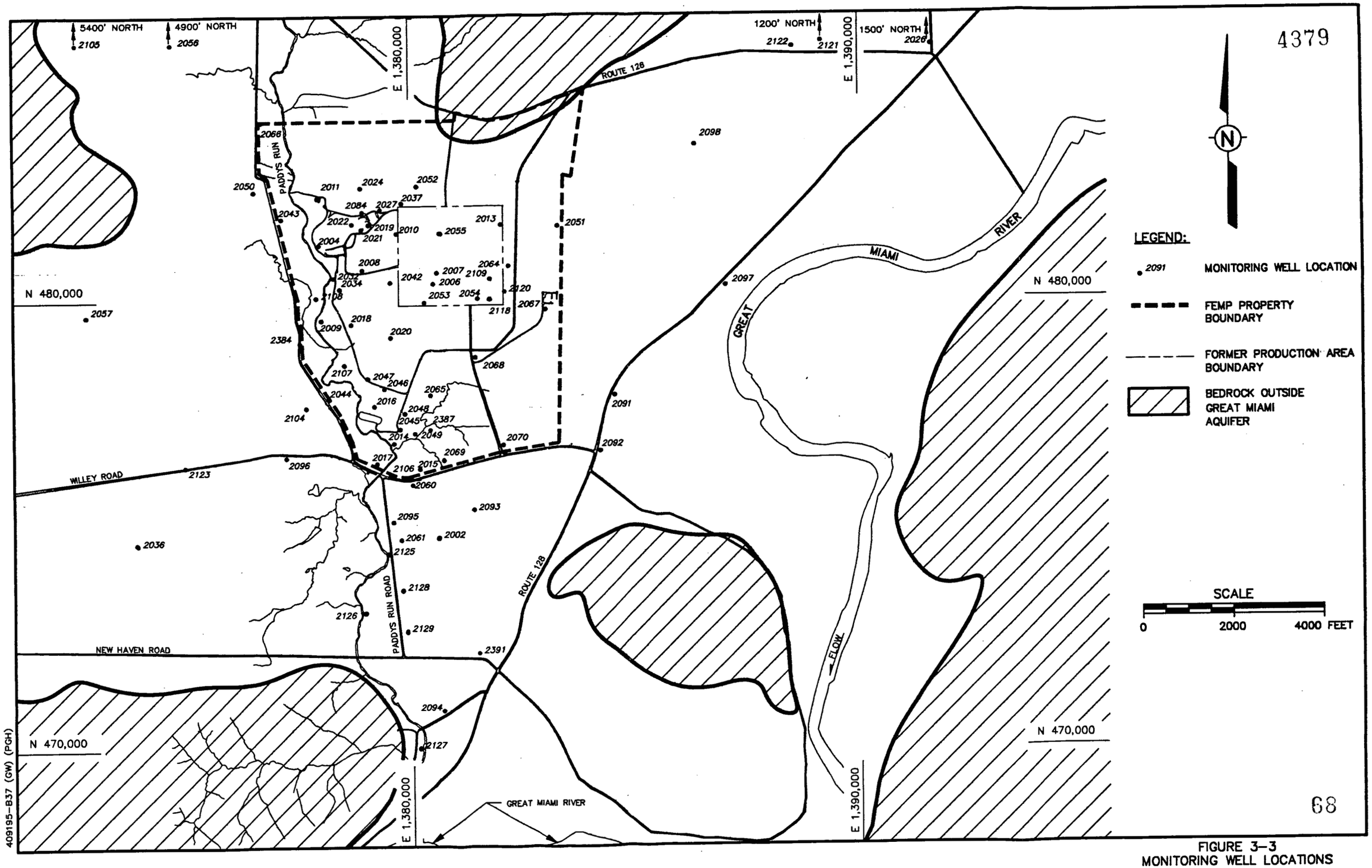


FIGURE 3-3
MONITORING WELL LOCATIONS
2000 SERIES WELLS

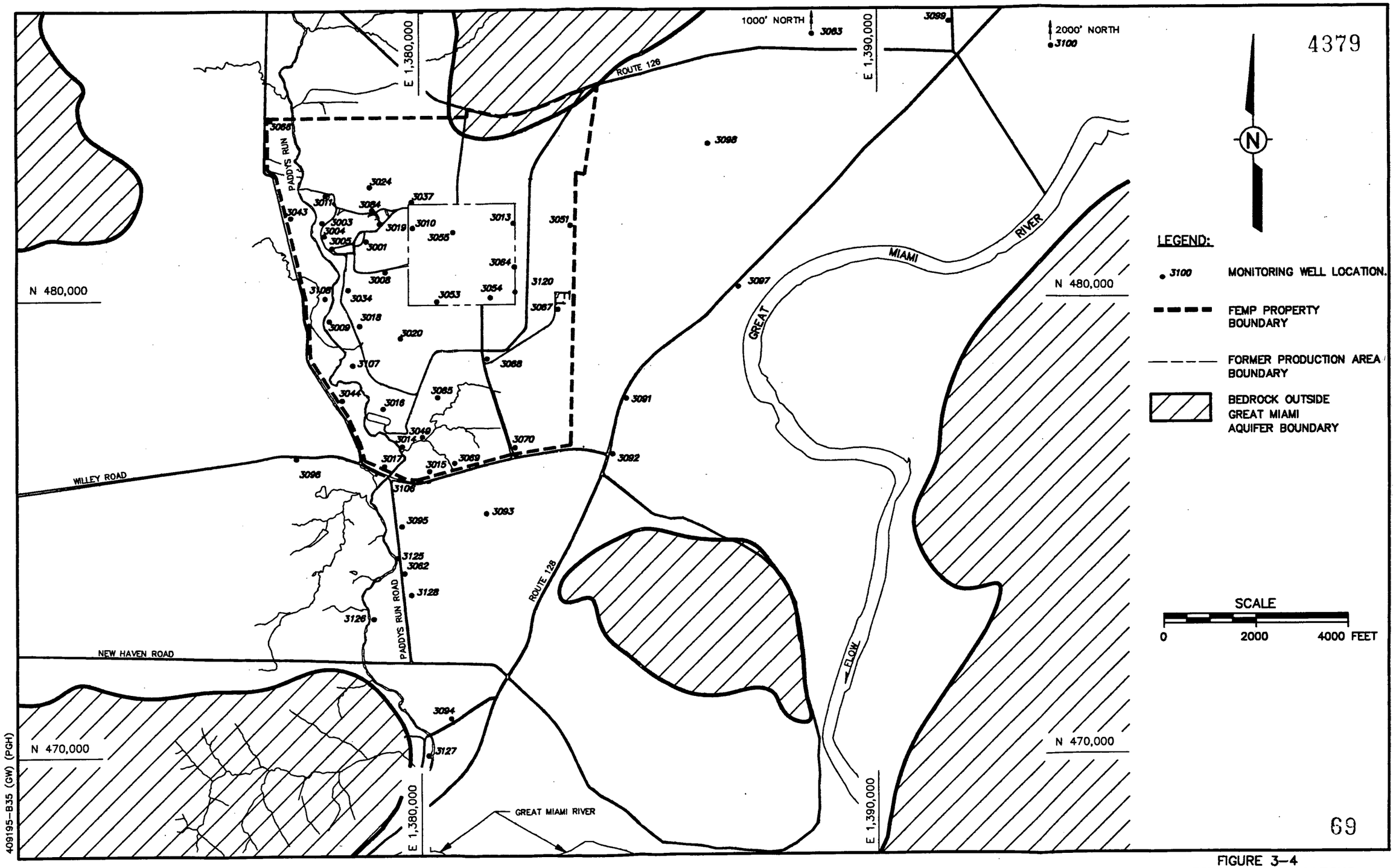


FIGURE 3-4
MONITORING WELL LOCATIONS
3000 SERIES WELLS

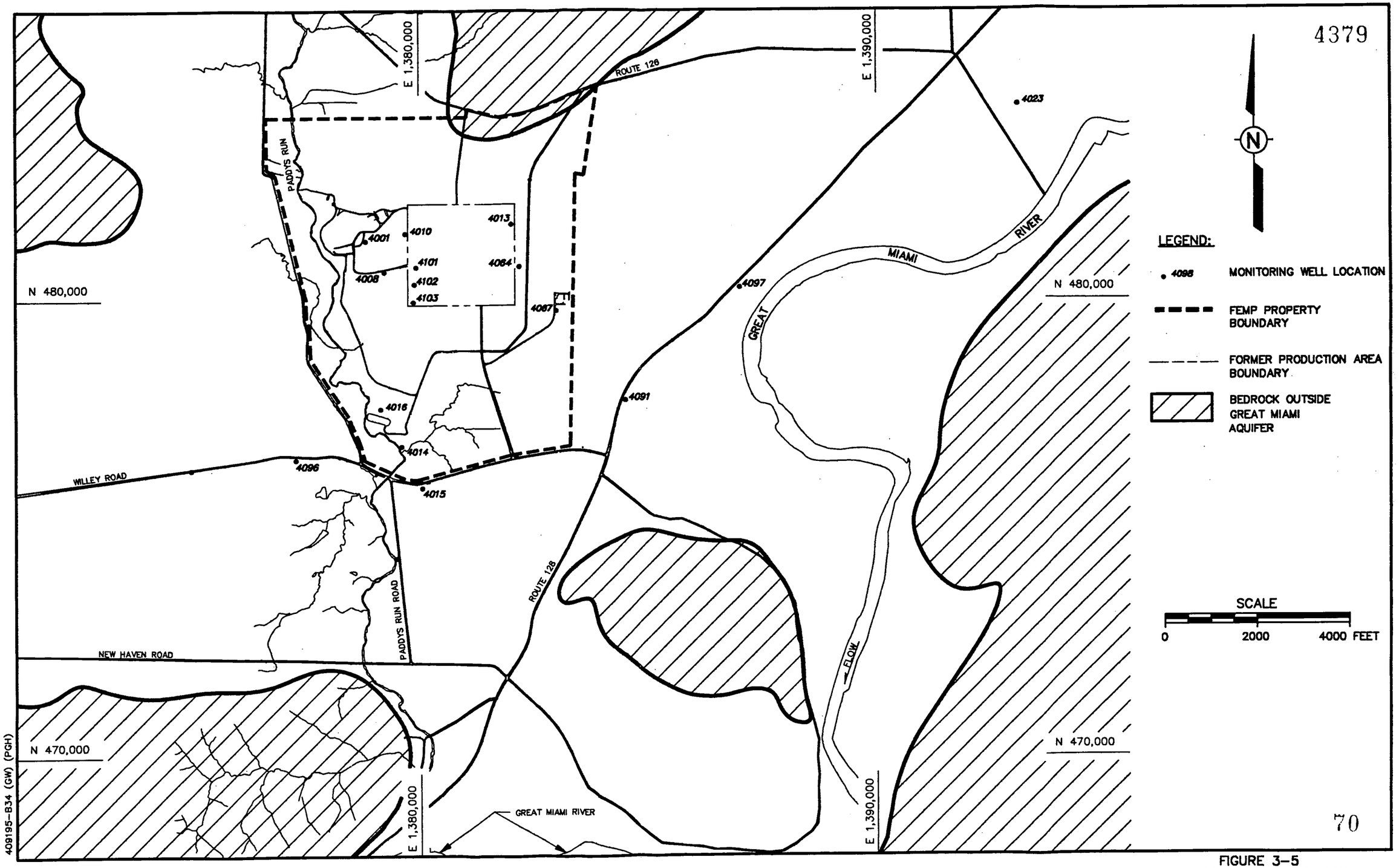


FIGURE 3-5
MONITORING WELL LOCATIONS
4000 SERIES WELLS

to wells or springs" (EPA 1986). Saturated zones that do not yield significant water may still be important as contaminant pathways.

In the FEMP study area, the sand and gravel deposits of the Great Miami Aquifer represent a classic aquifer. The perched groundwater system within the glacial overburden, while not representing a practical water supply, is important as a potential contaminant pathway to the regional aquifer, streams, and springs.

The principal sources of recharge to these aquifer units are:

- Recharge from bedrock
- Recharge from direct precipitation
- Recharge from induced stream infiltration.

Recharge due to groundwater occurring in the shale and limestone bedrock is limited. The shale itself is nearly impermeable, with water movement limited to fractures within thin limestone lenses. Average yearly recharge from the bedrock to the valley fill is approximately 200,000 gallons per day per linear mile (0.03 gpm/ft) along the valley (Dove 1961).

Precipitation falling within the basin is the dominant source of groundwater recharge. Infiltration of rainfall provides approximately 570,000 gallons per day per square mile (12 in./yr) of recharge to the unconsolidated aquifer systems (Dove 1961). This includes recharge through the glacial overburden, river terraces, and flood plain deposits.

Induced stream infiltration resulting from pumping water supply wells near the Great Miami River causes a portion of the surface water to infiltrate through the bed of the river into the groundwater system. The rate of recharge by stream infiltration varies based upon fluctuating river levels, hydraulic gradients, streambed conditions, and water temperature (Section 3.4.1). Natural recharge from Paddys Run along the west side of the FEMP and the Dry Fork of the White Water River west of the site also provides significant amounts of recharge on a seasonal basis.

## 3.1 GREAT MIAMI AQUIFER

The Great Miami Aquifer can be divided into areas with similar hydrologic and geologic properties that are distinct from other adjacent areas of the aquifer. These subdivisions have been designated as hydrogeologic environments (Spieker 1968a). A hydrogeologic environment describes a portion of an aquifer possessing hydrologic and geologic properties that differ from the properties of the aquifer in

adjacent areas. During these investigations, five major hydrogeologic environments were identified and mapped in the Great Miami River Valley (Figure 3-6). These environments include:

- Type I (Subtypes I-A-1 and I-A-2): Sand and gravel aquifer; recharge by induced stream infiltration potentially available.
- Type II: Sand and gravel aquifer without the possibility of stream recharge.
- Type III: Sand and gravel aquifer overlain by clay; stream recharge generally not available.
- Type IV: Buried valleys filled with clay; large water supplies generally not available (not present in Figure 3-6).
- Type V: Shale and limestone bedrock overlain by till; large water supplies generally not available.

Two characteristics of unconfined aquifers are used. These characteristics are transmissivity and specific yield, which describe the ability of water to move through the aquifer material and the ability of the aquifer to produce water, respectively. The higher the transmissivity the greater the ability to transmit water. The specific yield is a measure of the quantity of water an aquifer will yield from storage when the hydraulic head declines, and is related to the porosity and the grain size. The smaller the grain size, the more water that will be retained in the aquifer and not available to a pumping well. Conversely, coarser sediment will retain less water and have a larger specific yield.

The Type I hydrogeologic environment describes the Great Miami Aquifer along the flood plain of the Great Miami River to the south and east of the FEMP facility, and also in the valley of Paddys Run west and south of the FEMP former production area. The Type I-A-1 aquifer is 150 to 200 feet thick, and the Type I-A-2 aquifer is less than 150 feet thick; both are underlain by bedrock. The aquifer sediments crop out at the surface; thus, stream infiltration is possible in areas proximal to local streams. The lithology of the aquifer consists primarily of well-sorted sand with gravel, although scattered lenses of clay or fine-grained material are also present. In the main valley, these lenses are not of sufficient thickness or areal extent to act as semiconfining layers or to significantly affect groundwater movement. Aquifer transmissivity generally ranges from 40,000 to 67,000 square feet per day ($ft^2$/day), with a specific yield of about 0.2. Individual pumping wells can yield as much as 3000 gpm.

The Type II hydrogeologic environment is characterized by having less than 150 feet of sand and gravel, with no areally extensive interstratified clay layers present. Recharge by stream infiltration is not available. The specific yield for the aquifer is about 0.2. Large groundwater supplies are not generally available from the Type II aquifer. Those portions of the Great Miami Aquifer that exhibit

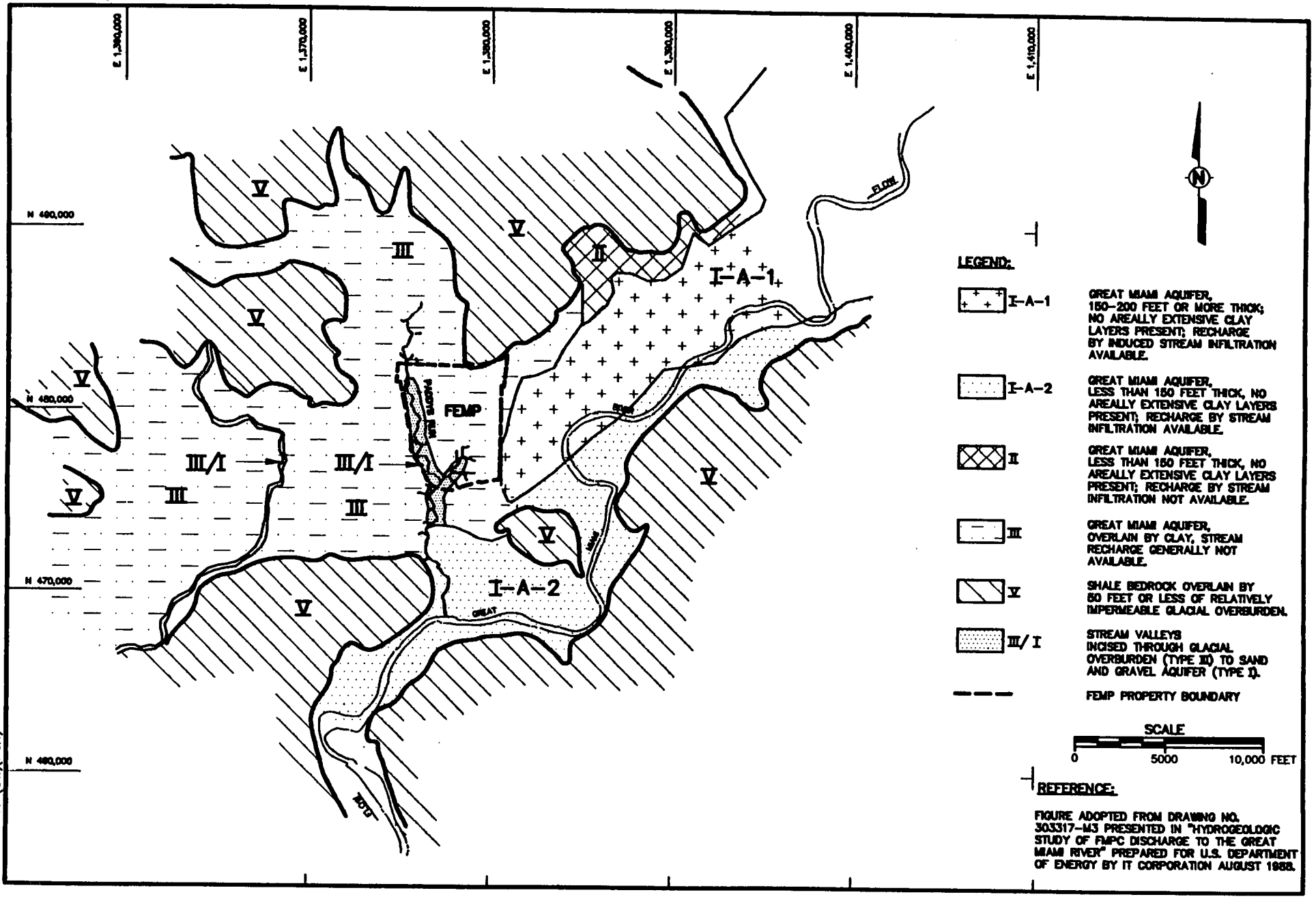


FIGURE 3-6 HYDROGEOLOGIC ENVIRONMENTS

characteristics of a Type II environment are of limited areal extent within the study area. They are generally located in close proximity to bedrock valley walls.

The Type III hydrogeologic environment is characterized by clayey glacial overburden overlying the Great Miami Aquifer. In the region directly beneath the FEMP, the aquifer is divided into upper and lower parts by a clay interbed approximately 10 to 20 feet thick occurring approximately 140 feet below land surface. Hence, the lower aquifer is classified as a semiconfined or leaky confined aquifer. Spieker and Norris (1962) have estimated a coefficient of storage of 0.001 for the lower sand and gravel aquifer. Spieker (1968a) estimated a transmissivity range of 4700 to 40,000 $ft^2$/day. Small streams such as Paddys Run occur in areas overlain by the clay-rich glacial overburden (Type III environment), where stream recharge to the underlying sand and gravel aquifer generally does not occur. However, in the lower reaches, these streams have incised through the clay overburden, resulting in the recharge of the sand and gravel aquifer from stream infiltration (Type I environment). This occurrence of Type III and Type I environments (related to overburden erosion) are indicated on Figure 3-6 as Type III/I.

The Type IV hydrogeologic environment is typified by valleys filled largely with clay. No examples of this environment are found within the study area.

The Type V hydrogeologic environment includes all of the areas outside of the buried valley of the Great Miami Aquifer. These areas are bedrock uplands consisting of shale with interbedded limestone overlain by 50 feet or less of clay-rich glacial overburden. Large quantities of groundwater are not generally transported through this material. Pumping well yields vary widely, generally ranging from 0 to 10 gpm. However, sand and gravel lenses are erratically distributed throughout this glacial overburden and, in some cases, pumping wells completed in these units may yield up to 50 gpm.

## 3.2 GLACIAL OVERBURDEN GROUNDWATER SYSTEM

In addition to the regional hydrogeologic environments in the Great Miami Aquifer, localized perched groundwater occurs in the glacial overburden. The perched groundwater system is not described by the USGS as a separate environment type, but is described as the uppermost, recharge-restricting layer of the Type III hydrogeologic environment.

As part of the FEMP site characterization program, short-term hydraulic conductivity tests (slug tests) were conducted on selected 1000-Series monitoring wells. These hydraulic conductivity tests were conducted to measure the hydraulic conductivity of the glacial overburden in and around the waste storage area and the flyash pile areas. Test results were reported in the RI reports for these areas (Operable Unit 1 and Operable Unit 2, respectively).

Hydraulic conductivity testing could not be performed on preselected Wells 1004, 1009, 1014, and 1045 because these monitoring wells were observed to be dry since their installation. A hydraulic conductivity test was not performed on Well 1022 because this monitoring well was constructed prior to the RI/FS in a test pit that was backfilled with gravel. The results from the hydraulic conductivity testing of these preselected monitoring wells would yield meaningless values. Alternative monitoring wells were, therefore, selected (Table 3-1).

Falling-head slug tests were conducted by injecting a known volume of water into the monitoring well and recording the water level decline with time. The procedures used to conduct these tests followed Sampling Plan Section 3.4.2, and Quality Assurance Program Plan (QAPP) Section 5.6 (DOE 1988). A duplicate rising-head hydraulic conductivity test was conducted on Monitoring Well 1018 to validate the falling-head slug test results.

Slug test data were analyzed following the procedures outlined in NAVFAC DM7, Design Manual, Soil Mechanics, Foundations and Earth Structures, (Department of the Navy 1971). The data were analyzed manually using the Hvorslev Method. The hydraulic conductivity results are summarized in Table 3-1. The variability in the values reflects the local variation in subsurface soil properties in the till.

Dense, fine-grained glacial till and glaciolacustrine deposits of silt and clay classify the overburden as an aquitard in most locations. However, small-scale fluvial and beach deposits interbedded within the till form layers of relatively high hydraulic conductivity. Hydraulic conductivities in the perched zones at the site range from $8 \times 10^{-3}$ ft/day to 0.85 ft/day ($2.8 \times 10^{-6}$ centimeters per second [cm/s] to $3.0 \times 10^{-4}$ cm/s), based on falling-head tests in 1000-Series monitoring wells (Table 3-1). The hydrogeologic characteristics of the overburden vary with the season and specific locations. At the FEMP, depth to perched groundwater in the glacial overburden ranged from 1 to 15 feet. A perched water table can seasonally fluctuate by up to 10 feet at a single location, with the highest water levels occurring during the early spring and the lowest during the late fall.

The four glacial overburden materials present in the regional geologic setting have the following hydrogeologic characteristics:

- Loess: Blanket deposits of loess deposited during Pleistocene and post-Pleistocene time generally consist of silt with small amounts of clay. These deposits are moderately cohesive with a porosity of 40 to 50 percent. Hydraulic conductivity for loess is reported as 0.028 ft/day to 2.8 ft/day ($1.0 \times 10^{-5}$ cm/s to $1.0 \times 10^{-3}$ cm/s), without secondary permeability. Near-surface deposits of loess have an enhanced secondary permeability due to fracturing, animal burrows, and root tubes, as indicated by site borings. These features can impart a secondary

**TABLE 3-1**
**SUMMARY**
**HYDRAULIC CONDUCTIVITY TESTING**

| Monitoring Well No. | Subsurface Soil Type | Hydraulic Conductivity (cm/s) | Hydraulic Conductivity (ft/day) |
|---|---|---|---|
| 1008 | Clay, Trace Gravel | $1.3 \times 10^{-4}$ | 0.37 |
| 1012 | Clay w/Gravel, Shale Bedrock | $1.6 \times 10^{-3}$ | 4.53 |
| 1018 | Sand, Silt, Clay | $5.7 \times 10^{-4}$ | 1.61 |
| 1025 | Clay, Trace Gravel | $2.5 \times 10^{-6}$ | 0.01 |
| 1034 | Clay, Fine Sand, Some Silt and Gravel | $2.5 \times 10^{-5}$ | 0.07 |
| 1035 | Clay, Some Silt | $2.5 \times 10^{-5}$ | 0.07 |
| 1041 | Clay, Some Silt | $1.1 \times 10^{-4}$ | 0.31 |
| 1046 | Clay, Silt, Sand | $6.8 \times 10^{-5}$ | 0.19 |
| 1048 | Clay, Silt, Sand, Gravel | $1.6 \times 10^{-4}$ | 0.45 |
| 1065 | Silt, Some Clay, Some Sand | $2.2 \times 10^{-5}$ | 0.06 |
| 1079 | Clay, Some Sand, Some Gravel | $1.8 \times 10^{-5}$ | 0.05 |

permeability that greatly exceeds the unenhanced permeability (Freeze and Cherry 1979).

- Lacustrine Deposits: Offshore silt and clay with interbedded near-shore beach sands were deposited in meltwater lakes that existed during Pleistocene time. Unfractured, fine-grained lacustrine deposits can form large aquitards as evidenced by the clay interbed within the Great Miami Aquifer, while near-surface deposits are generally fractured. The interbedded sand and gravel beach deposits can form aquifers, but these are limited in extent and yield.

- Till: Till consists of sediments that are deposited directly under, from within, or from the top of a glacier without the sorting action of water. At the site, no attempt has been made to differentiate the till types or to determine if individual till sheets exist. Till is a heterogenous mixture of silt, clay, sand, gravel, and boulder-sized materials. Although the coarser materials are present, the till in the study area is too fine grained to be a permeable hydrogeologic unit.

  Within the FEMP area where shale and limestone comprise the regional bedrock, glacial erosion has produced till comprised mainly of silt and clay which, therefore, has low permeability. Water supply investigations which included the FEMP site (Spieker 1968a, 1968b) considered the glacial overburden as an aquitard which restricted surface recharge to the Great Miami Aquifer. Investigations in similar geologic settings (Hendry 1988; Cravens and Ruedisili 1987; Barari and Hedges 1985; Grisak et al. 1976; Hendry 1982) indicate that till deposits can be divided from a hydrogeologic standpoint into an oxidized near-surface weathered zone and a deeper, reduced unweathered zone. These studies indicate that infiltration occurs only in the weathered till, in which much of the infiltrating water is lost to evapotranspiration. In addition to this loss, some water discharges laterally to seeps or drainages. This latter type of loss is evident in the FEMP study area along Paddys Run, where small seeps occur during periods of high rainfall.

- Glaciofluvial Deposits: Most of the large productive aquifers found in areas covered by continental glaciation are found in the glaciofluvial outwash deposits left by the meltwater of receding glaciers. These deposits, which consist of well-sorted sand and gravel, occur as extensive blanket valley fill deposits. At the FEMP, these deposits are confined by surface layers of till or glaciolacustrine silts and clays and may also have interbedded tills which act as aquitards.

The perched groundwaters in the glacial overburden at the FEMP occur under both confined and unconfined conditions. As seen from the 1000-Series monitoring wells data, the general groundwater movement in the perched system in the vicinity of the FEMP is toward Paddys Run and the storm sewer outfall ditch. However, because the shallow perched zones are not interconnected across the facility, the movement of fluids is likely to be discontinuous with different areas affected by different

influences. The flow patterns within these zones vary seasonally due to variations in recharge. Shallow groundwater flow may also be influenced by the widespread presence of drain tiles installed by the previous owners of the property in support of agricultural activities of the surrounding areas.

## 3.3 GROUNDWATER ELEVATIONS AND FLOW

The generalized groundwater flow pattern in the Great Miami Aquifer is shown in Figure 3-7. Groundwater enters the study area from three directions. In the northeast, groundwater moves southwest from the Ross area into the portion of the New Haven Trough now occupied by the Great Miami River. For simplicity, this report will refer to flow from the northeast as flow from the Ross Section of the New Haven Trough. The second source of groundwater is the Shandon Tributary to the north of the FEMP, which contains a tributary of the New Haven Trough under the town of Shandon. The majority of the groundwater from the Shandon Tributary flows under the waste storage area and the former production area and leaves along the eastern boundary of the FEMP to discharge into the Great Miami River. This flow is strongly influenced by the pumping of the collector wells. The groundwater and surface water exit this area via the Great Miami River Valley at what will be referred to in this report as the New Baltimore Outlet. The third source of groundwater is from the west. The recharge from the Dry Fork of the Whitewater River, located about two miles west of the FEMP, causes groundwater to move to the east toward the FEMP. This flow turns southward under the southern part of the FEMP and flows to the Great Miami River in the glaciofluvial deposits under the southern part of Paddys Run, termed the Paddys Run Outlet. A portion of the groundwater from the Shandon Tributary also reaches the Great Miami River via Paddys Run. Although these general flow patterns dominate the regional flow system, local and short-term variations do occur within it.

Regional groundwater maps constructed from more comprehensive water elevation surveys in August 1982, April 1986, and May 1988 are presented in Figures 3-8, 3-9, and 3-10, respectively.

Within the context of these flow patterns, the following conclusions can be reached:

- Groundwater enters the FEMP from the north, west, and northwest and exits toward the Great Miami River Valley to the south and toward the Great Miami River and SOWC production wells to the east (Figure 3-7).

- The large SOWC pumping wells, located in the "Big Bend" meander on the Great Miami River east of the FEMP, produce a pronounced and persistent cone of depression. This cone of depression creates an induced eastward flow of groundwater in the northern and central portions of the FEMP (Figures 3-7 and 3-9), resulting in a groundwater divide trending northwest to southeast across the south-central portion of the FEMP.

- Paddys Run affects local groundwater flow along the western boundary and in the area south of the FEMP. During dry seasons when there is little recharge to the regional aquifer, groundwater flows southeastward. During

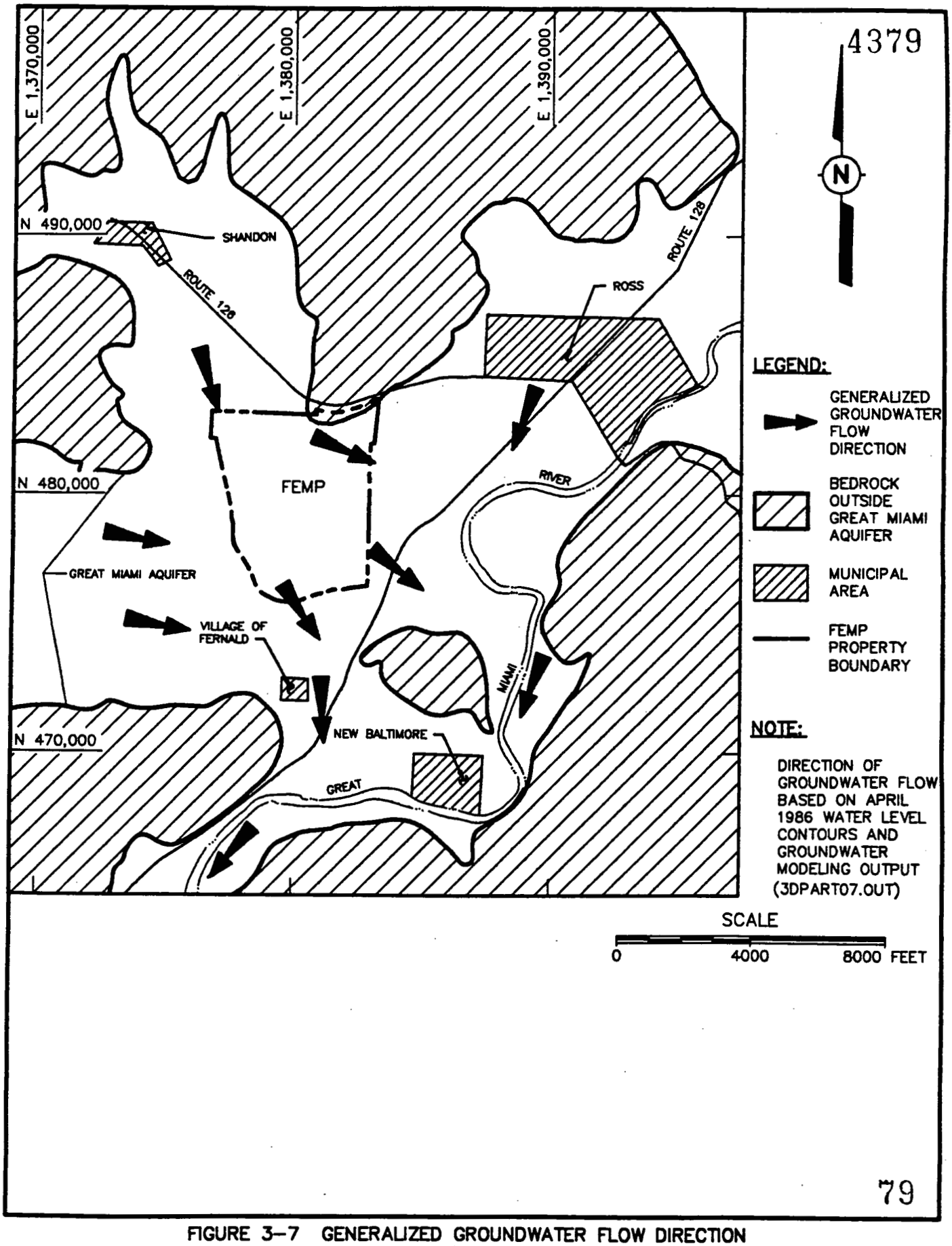


409185-A47 (GW) (PGH)

FIGURE 3-7 GENERALIZED GROUNDWATER FLOW DIRECTION IN GREAT MIAMI AQUIFER

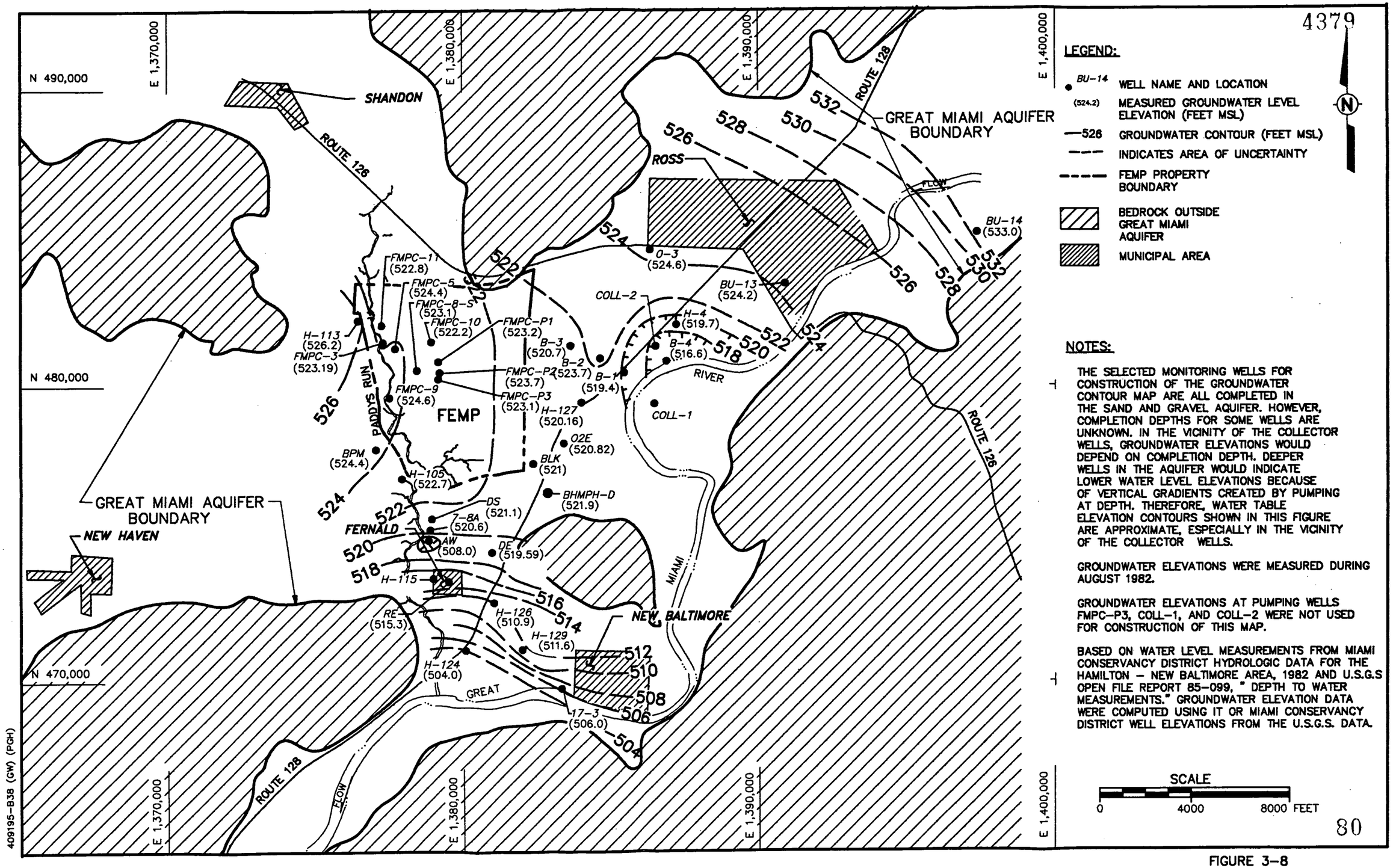


NOTES:

THE SELECTED MONITORING WELLS FOR CONSTRUCTION OF THE GROUNDWATER CONTOUR MAP ARE ALL COMPLETED IN THE SAND AND GRAVEL AQUIFER. HOWEVER, COMPLETION DEPTHS FOR SOME WELLS ARE UNKNOWN. IN THE VICINITY OF THE COLLECTOR WELLS, GROUNDWATER ELEVATIONS WOULD DEPEND ON COMPLETION DEPTH. DEEPER WELLS IN THE AQUIFER WOULD INDICATE LOWER WATER LEVEL ELEVATIONS BECAUSE OF VERTICAL GRADIENTS CREATED BY PUMPING AT DEPTH. THEREFORE, WATER TABLE ELEVATION CONTOURS SHOWN IN THIS FIGURE ARE APPROXIMATE, ESPECIALLY IN THE VICINITY OF THE COLLECTOR WELLS.

GROUNDWATER ELEVATIONS WERE MEASURED DURING AUGUST 1982.

GROUNDWATER ELEVATIONS AT PUMPING WELLS FMPC-P3, COLL-1, AND COLL-2 WERE NOT USED FOR CONSTRUCTION OF THIS MAP.

BASED ON WATER LEVEL MEASUREMENTS FROM MIAMI CONSERVANCY DISTRICT HYDROLOGIC DATA FOR THE HAMILTON – NEW BALTIMORE AREA, 1982 AND U.S.G.S OPEN FILE REPORT 85-099, " DEPTH TO WATER MEASUREMENTS." GROUNDWATER ELEVATION DATA WERE COMPUTED USING IT OR MIAMI CONSERVANCY DISTRICT WELL ELEVATIONS FROM THE U.S.G.S. DATA.

FIGURE 3-8

REGIONAL GROUNDWATER ELEVATIONS
AUGUST 1982

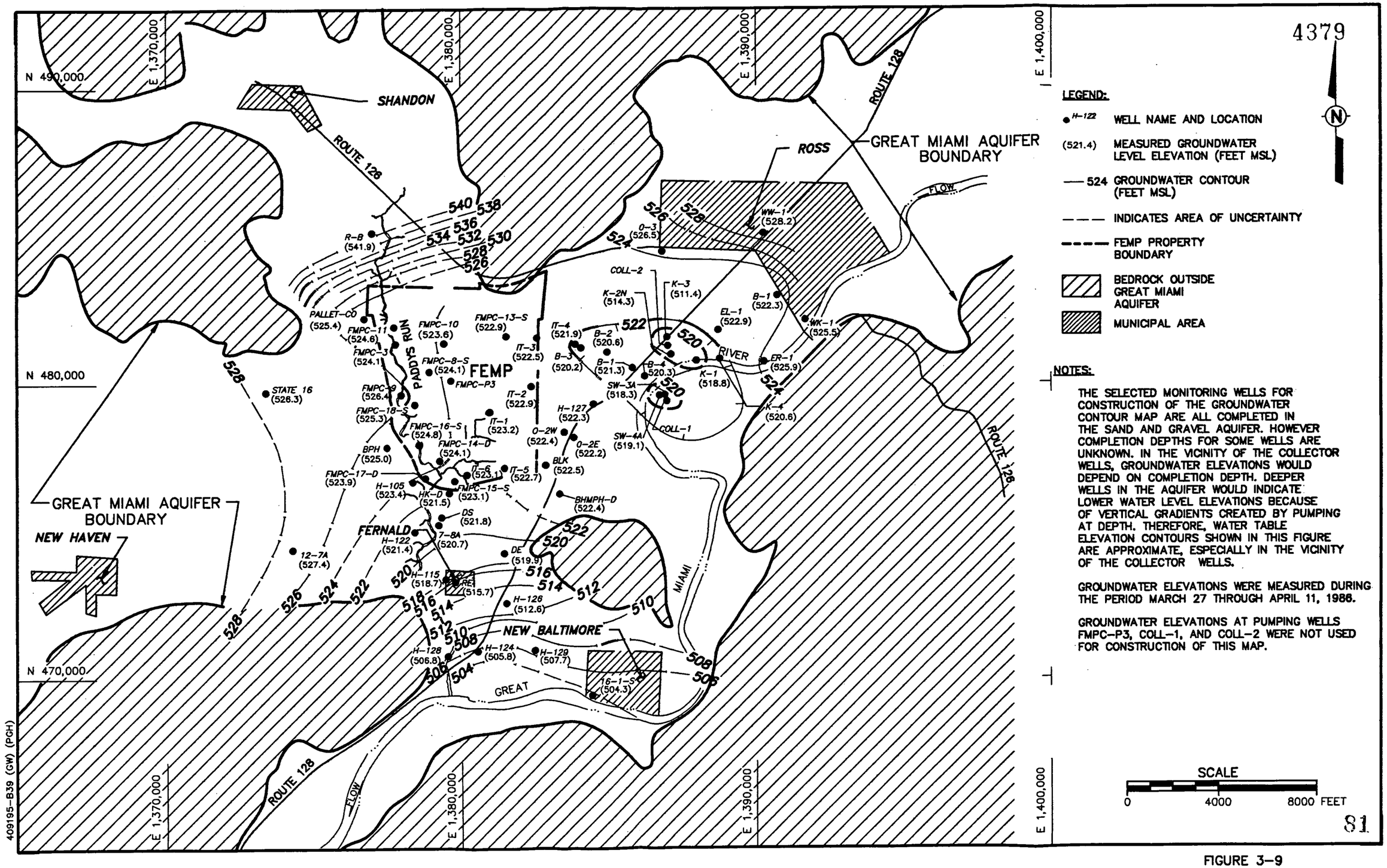




FIGURE 3-9
REGIONAL GROUNDWATER ELEVATIONS
APRIL 1986

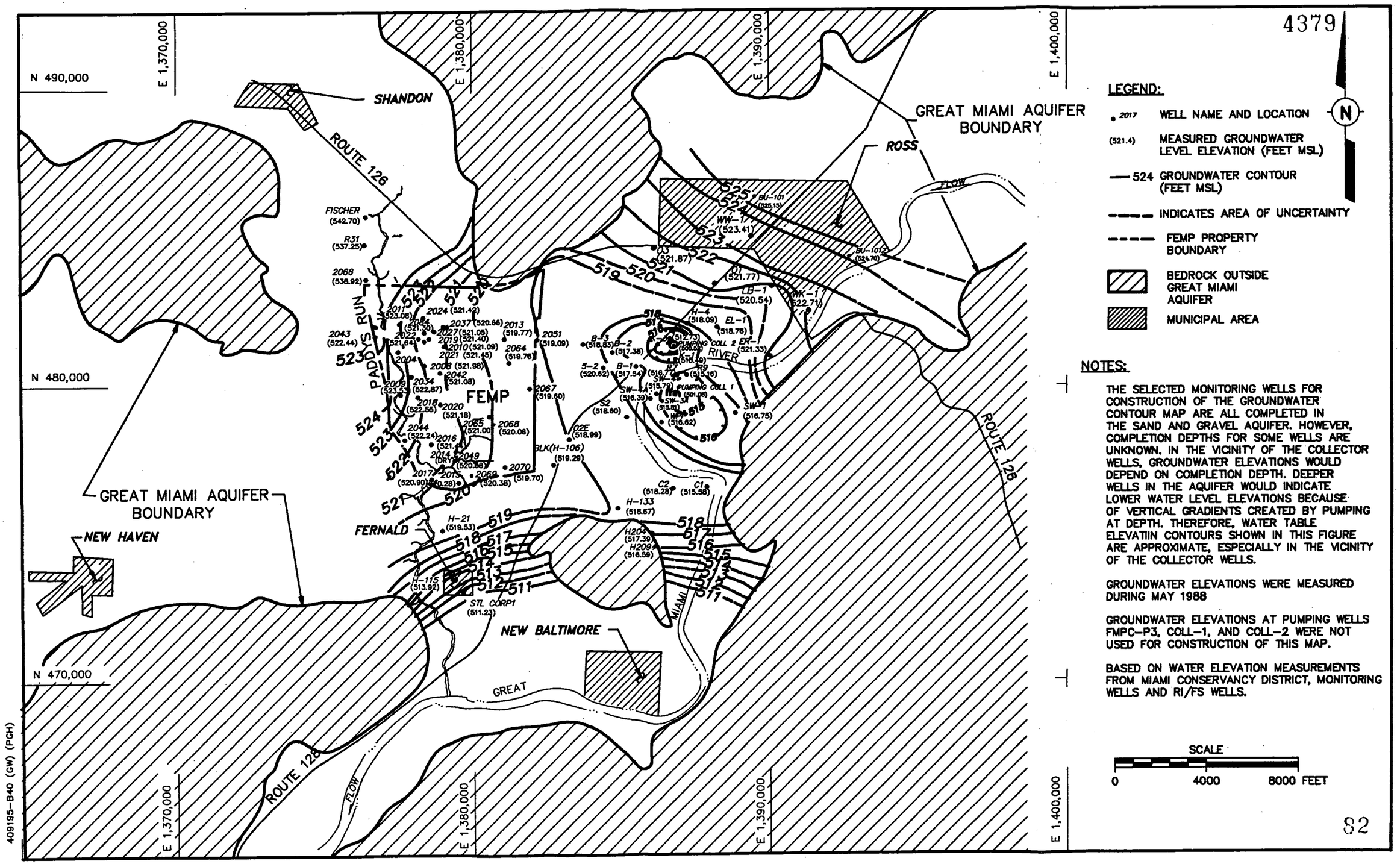


LEGEND:

- • 2017 WELL NAME AND LOCATION
- (521.4) MEASURED GROUNDWATER LEVEL ELEVATION (FEET MSL)
- — 524 GROUNDWATER CONTOUR (FEET MSL)
- ---- INDICATES AREA OF UNCERTAINTY
- ---- FEMP PROPERTY BOUNDARY
- BEDROCK OUTSIDE GREAT MIAMI AQUIFER
- MUNICIPAL AREA

NOTES:

THE SELECTED MONITORING WELLS FOR CONSTRUCTION OF THE GROUNDWATER CONTOUR MAP ARE ALL COMPLETED IN THE SAND AND GRAVEL AQUIFER. HOWEVER, COMPLETION DEPTHS FOR SOME WELLS ARE UNKNOWN. IN THE VICINITY OF THE COLLECTOR WELLS, GROUNDWATER ELEVATIONS WOULD DEPEND ON COMPLETION DEPTH. DEEPER WELLS IN THE AQUIFER WOULD INDICATE LOWER WATER LEVEL ELEVATIONS BECAUSE OF VERTICAL GRADIENTS CREATED BY PUMPING AT DEPTH. THEREFORE, WATER TABLE ELEVATIIN CONTOURS SHOWN IN THIS FIGURE ARE APPROXIMATE, ESPECIALLY IN THE VICINITY OF THE COLLECTOR WELLS.

GROUNDWATER ELEVATIONS WERE MEASURED DURING MAY 1988

GROUNDWATER ELEVATIONS AT PUMPING WELLS FMPC-P3, COLL-1, AND COLL-2 WERE NOT USED FOR CONSTRUCTION OF THIS MAP.

BASED ON WATER ELEVATION MEASUREMENTS FROM MIAMI CONSERVANCY DISTRICT, MONITORING WELLS AND RI/FS WELLS.

SCALE

0 4000 8000 FEET



FIGURE 3-10
REGIONAL GROUNDWATER ELEVATIONS
MAY 1988

periods of high flow in Paddys Run, stream water infiltrates the Great Miami Aquifer and creates a groundwater mound and strong southward gradients. In the northern portion of the study area, the mound creates a local reversal causing a northward component of flow. Both of these flows are transient conditions which only last for the duration of seasonal high flow in Paddys Run.

- Bedrock highs south of the FEMP on the east and west also control groundwater flow direction. The combination of the eastern and western bedrock highs forces groundwater to flow due south toward the Great Miami River. The groundwater gradient steepens in the narrow bedrock channel.

- Monthly groundwater elevations show seasonal fluctuation, as seen in hydrographs of the FEMP monitoring wells. The short-term fluctuations are due to surface water/groundwater interaction, which is discussed in Section 3.4.

Examination of the groundwater data from January 1988 through April 1990 shows some of the transient effects resulting from both drought and flood conditions. These features are prevalent throughout the 2000-Series groundwater elevation maps, although they can be seen in the 3000- and 4000-Series maps as well. Using these maps, the following trends and conditions can be identified:

- Flow conditions across much of the FEMP generally trend almost due east. These flow patterns are relatively stable, although they tend to shift slightly northward during periods of extended recharge (April to May 1989).

- Peak groundwater levels generally occur during the spring and early summer months, which are also the major groundwater recharge months. For the period of record, the highest groundwater contours occurred during the month of June 1989, when unusually large amounts of rainfall caused much recharge to occur. This caused groundwater elevations to rise to approximately 4 to 5 feet above their mean levels. Monitoring wells proximal to Paddys Run exhibited elevations as much as 10 feet over their normal levels due to the large amount of groundwater recharge entering from Paddys Run.

- Minimum groundwater levels generally occur during the late fall and early winter months of the year. This corresponds with the dry season for southern Ohio, which generally starts in late summer or early fall and runs to late fall. For the January 1988 through April 1990 time period, minimum groundwater levels occurred during the months of November 1988 through January 1989. Levels during this time were unusually low due to drought conditions that occurred from spring through fall of 1988. This caused groundwater levels to fall to approximately 2 to 3 feet below their normal seasonal lows.

- Recharge events occurring in Paddys Run can be seen in May to June 1989 and March to April 1990. Leakage from Paddys Run can be seen to cause a "mound" in the groundwater as it infiltrates through the streambed and enters the groundwater system. This effect is transient, although it appears to occur on an annual basis as part of the recharge during the spring and early summer months (Section 3.4.2).

The hydrograph of a representative monitoring well located in the flood plain of the Great Miami River is shown in Figure 3-11. This monitoring well exhibits behavior identical to trends in the FEMP monitoring wells and has the largest database of any monitoring well within the regional area. As previously discussed, the water level readings show a broad cyclic trend on a yearly basis. High-water levels generally occur in the spring or early summer, and low-water levels generally occur in the late fall or early winter. Monitoring Well O2E to the east of the site exhibits this characteristic behavior, with seasonal fluctuations visible as cyclic patterns in the monitoring well's hydrograph. For most years, the groundwater experiences a fluctuation on the order of 4 to 6 feet, with increases occurring faster than decreases. The average recharge period is 4 to 5 months, while the average discharge period lasts 7 to 8 months. This is a typical water cycle for southern Ohio.

The drought experienced by the Cincinnati area in 1987 to 1988 is visible on the hydrograph as the two lowest points on its curve. Although recharge did occur during the spring of 1988, it was not enough to counteract the water lost by the groundwater system during 1987. Thus, the peak groundwater level in 1988 was approximately the same as the minimum groundwater levels from previous years. The regional groundwater map for May 1988 (Figure 3-10) was developed from data taken during this drought period. Two other maps, one in August 1982 (Figure 3-8) and the other in April 1986 (Figure 3-9), show similar water level conditions. The August 1982 levels were taken approximately midway through the dry season, while the April 1986 values were taken just after peak groundwater season. These two data sets represent very similar types of flow regime. Primary influences on hydraulic head in the Great Miami Aquifer during these periods were the pumping rates of the collector wells, precipitation recharge, recharge from Paddys Run, and the stage of the Great Miami River.

## 3.4 SURFACE WATER/GROUNDWATER INTERACTION

The geomorphic setting of the Great Miami River and Paddys Run provides for interaction between the surface water and groundwater. Both surface water systems have eroded through the low permeability glacial overburden material to the Great Miami Aquifer. This contact allows for the direct exchange of water between the surface water and groundwater, which is important in relation to increased usage of the aquifer for water supplies and contaminant transport in the FEMP Study Area.

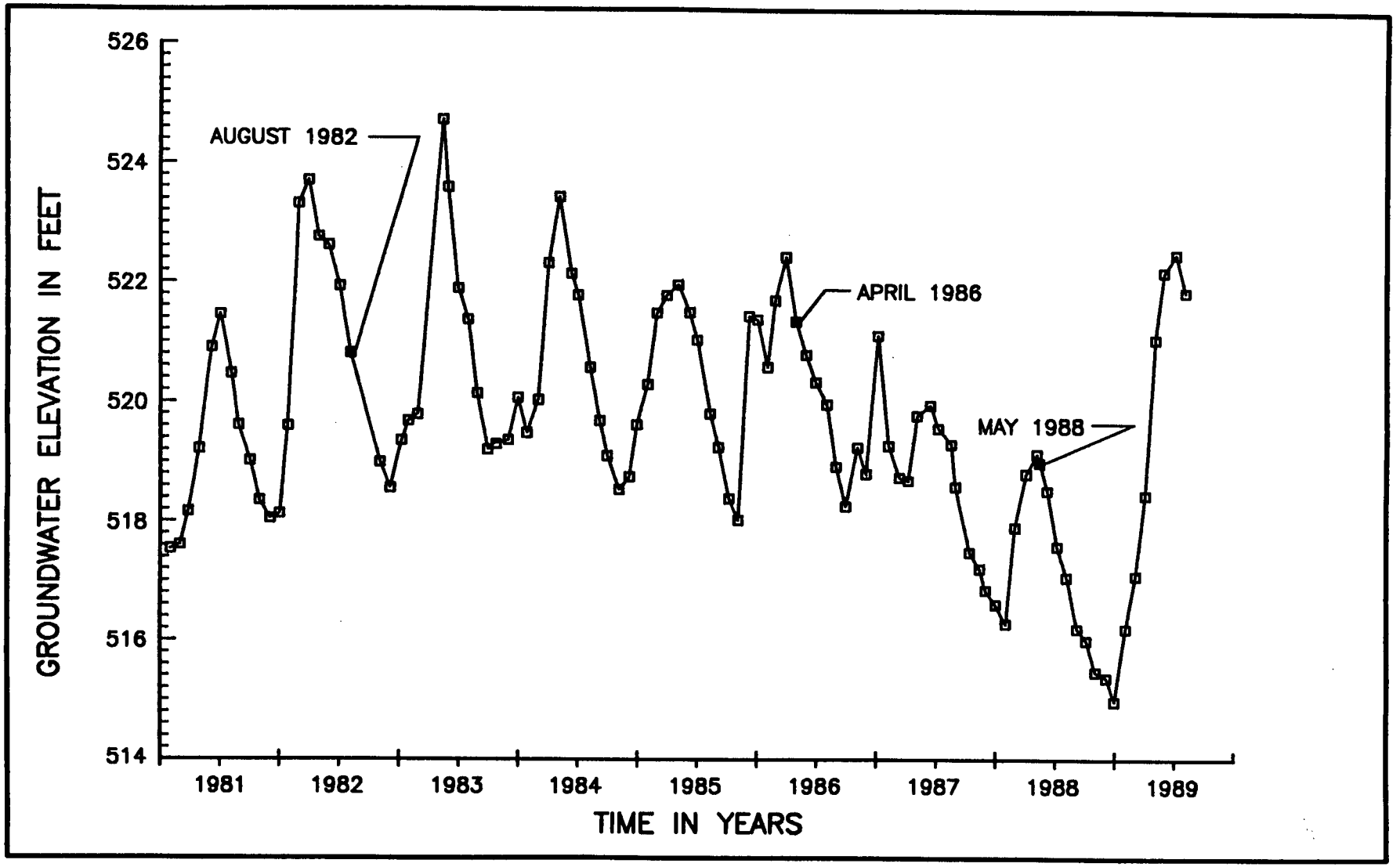


FIGURE 3-11 HYDROGRAPH OF WELL O2E
JANUARY 1981 – DECEMBER 1989

4379

### 3.4.1 Great Miami River/Groundwater Interaction

The Great Miami Riverbed is in contact with the sand and gravel deposits of the Great Miami Aquifer. Because the Great Miami River partially penetrates the water table, a portion of its flow originates from surface water, while a portion also comes from the aquifer beneath the river. The natural groundwater flow is generally from the aquifer to the river; that is, groundwater discharges into the river. However, pumping of the collector wells, which are located close to the river, induces recharge to the aquifer by stream infiltration. This occurs by creating a local hydraulic gradient, which causes flow from the river to the aquifer. This induced infiltration allows the collector wells to maintain a higher yield from the aquifer than could be achieved if the river was not present.

The rate of induced infiltration varies with respect to the season and the location on the stream. Factors which influence the infiltration rate include:

- River stage
- Hydraulic gradient
- Streambed characteristics
- Water temperature.

The riverbed infiltration rate had been investigated during the summer of 1956 near Ross (Dove 1961), and in Fairfield Township in the summer of 1962 (Spieker 1968a). Infiltration rates were calculated to be 240,000 and 492,000 gpd per acre (3,200 and 6,600 in./yr) of streambed, respectively. Both tests were performed in similar terrains, under low stream flow conditions, at water temperatures of approximately 80°F

The effects of the FEMP effluent discharge on groundwater quality due to the induced infiltration of Great Miami River water has been evaluated in a separate report (IT 1988). This study concluded that the FEMP discharge did not have a quantifiable effect on the groundwater system due to the high degree of induced infiltration that occurred upstream from the discharge point.

### 3.4.2 Paddys Run/Groundwater Interaction

Paddys Run interacts with the Great Miami Aquifer in several different ways that affect groundwater flow and discharge. The stream has eroded through the glacial overburden and into the top of the Great Miami Aquifer from its confluence with the Great Miami River to about the position of the silos (Figure 3-6). It is, therefore, directly connected with the Great Miami Aquifer in that reach. South of the FEMP, the elevation of the water table is close to or above the elevation of the stream bottom (Figure 3-12); consequently, during most of the year, the stream receives groundwater in this reach. In the vicinity of the FEMP, however, the stream is above the water table and loses water to the regional aquifer. It is generally dry, except during runoff periods following rainfall and snow-melt events. Sustained flow has been reported in Paddys Run during the winter and spring by Dames and Moore

86

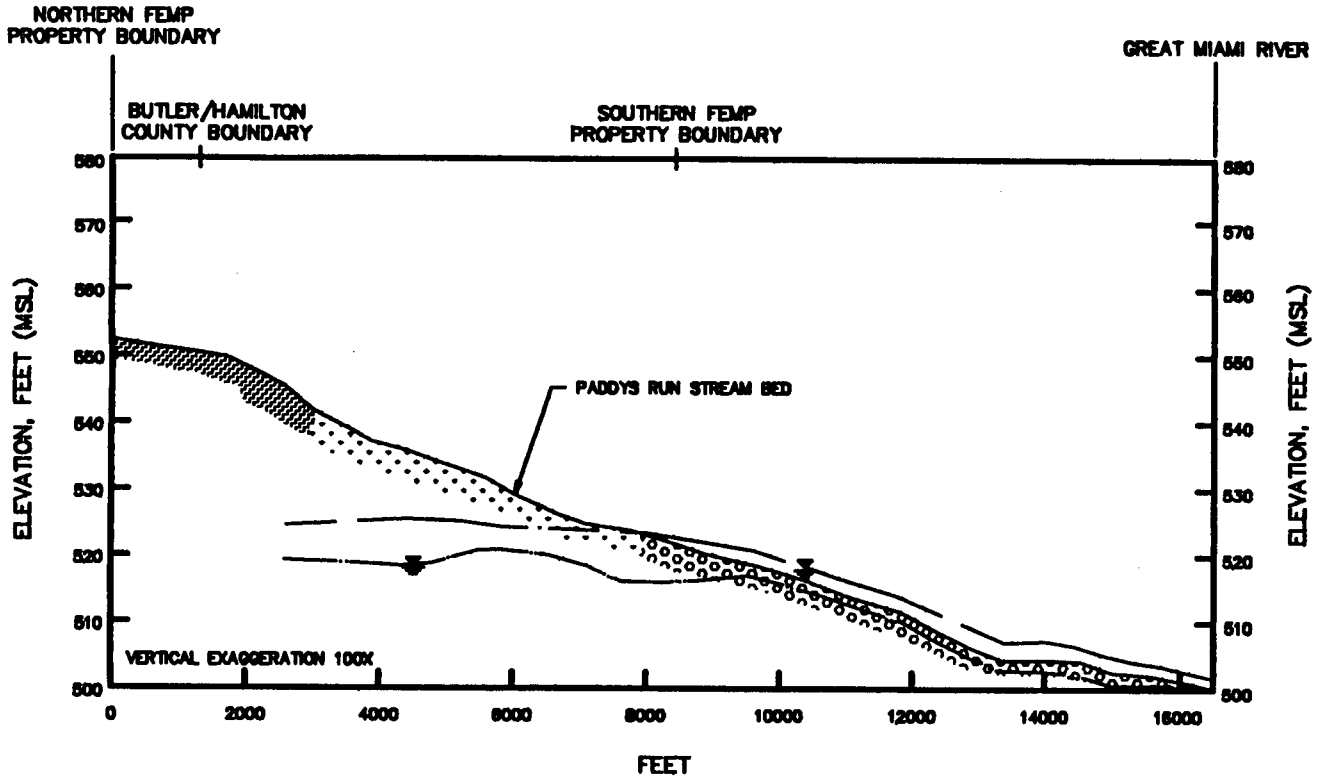


**LEGEND:**

- HIGH WATER TABLE (FEBRUARY TO JUNE, 1989 TO 1990)
- LOW WATER TABLE (SEPTEMBER TO DECEMBER, 1988 TO 1989)
- GLACIAL OVERBURDEN PRESENT; MINIMUM STREAM WATER INFILTRATION EXPECTED
- SURFACE WATER INFILTRATION OCCURS REGARDLESS OF WATER TABLE ELEVATION
- POSSIBLE SURFACE WATER INFILTRATION DEPENDING ON WATER TABLE ELEVATION

**NOTE:**

WATER TABLES SHOWN ARE BASED ON READINGS COLLECTED FROM WELLS 2004, 2009, 2014, 2107, 2125, 2126 AND 2127 FROM JANUARY 1988 TO APRIL 1990. PADDYS RUN STREAM BED AND GROUNDWATER TABLE ELEVATIONS ARE PROJECTED ONTO A VERTICAL PROFILE BETWEEN THE NORTHERN FMPC BOUNDARY AND THE GREAT MIAMI RIVER WHERE PADDYS RUN INTERSECTS.

VERTICAL SCALE: 0 — 20 — 40 FEET

HORIZONTAL SCALE: 0 — 2000 — 4000 FEET

FIGURE 3–12 AREAS OF SURFACE WATER INFILTRATION TO THE GREAT MIAMI AQUIFER ALONG PADDYS RUN.

409195–A52 (GW) (PGH)

87

4379

(1985) and by stream gaging stations monitored during the RI. Relatively little recharge of the Great Miami Aquifer occurs where Paddys Run is on clayey till north of the silos.

Groundwater elevation contour maps derived from the 2000- and 3000-Series monitoring wells show that the regional water table fluctuated, based on monthly readings, as much as 8 feet during the period of January 1988 to June 1989. This water table fluctuation may be considered extreme, since the FEMP experienced drought conditions from spring 1988 to early winter 1989, followed by an extended period of higher than average precipitation from late winter to early summer 1989. The cycle repeats in the winter of 1989/1990.

As shown in Figures 3-13 and 3-14, there is a high degree of correlation between the Paddys Run hydrograph and the regional aquifer hydrographs. These figures are based on continuous 60-minute readings using pressure transducers and a data logger. As the Paddys Run hydrograph peaks, the groundwater hydrograph shows a peak a very short time later, which indicates the hydrologic connection between the stream and the regional aquifer.

Increases in runoff in Paddys Run leads to the formation of a groundwater mound typically centered on Monitoring Wells 2108 or 2009, but under extremely wet conditions extending from Monitoring Well 2004 to Monitoring Well 2107. A slight influence is seen in the dry months of a normal (nondrought) year, but the mound is most pronounced during periods of high precipitation, such as from March to June 1989. This increased recharge forms a large transient groundwater mound in the regional water table, which affects the direction of flow in the vicinity of the mound. As the flow in Paddys Run decreases, and therefore the infiltration to the aquifer is reduced, the mound decreases in size until the flow patterns show only slight influence.

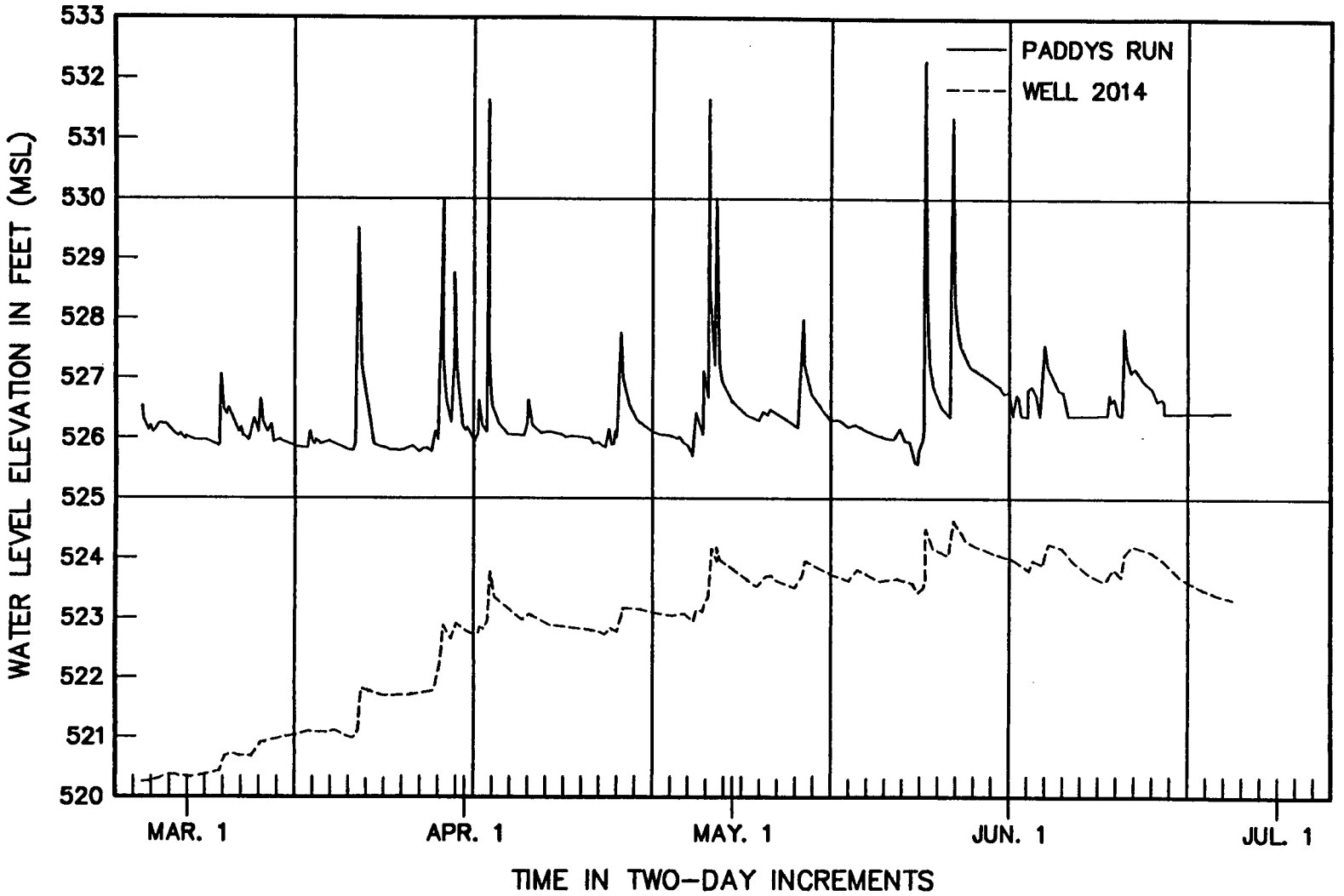


FIGURE 3-13 HYDROGRAPH OF PADDYS RUN AND GREAT MIAMI AQUIFER AT WELL LOCATION 14, FEBRUARY 24,1989 – JUNE 26, 1989

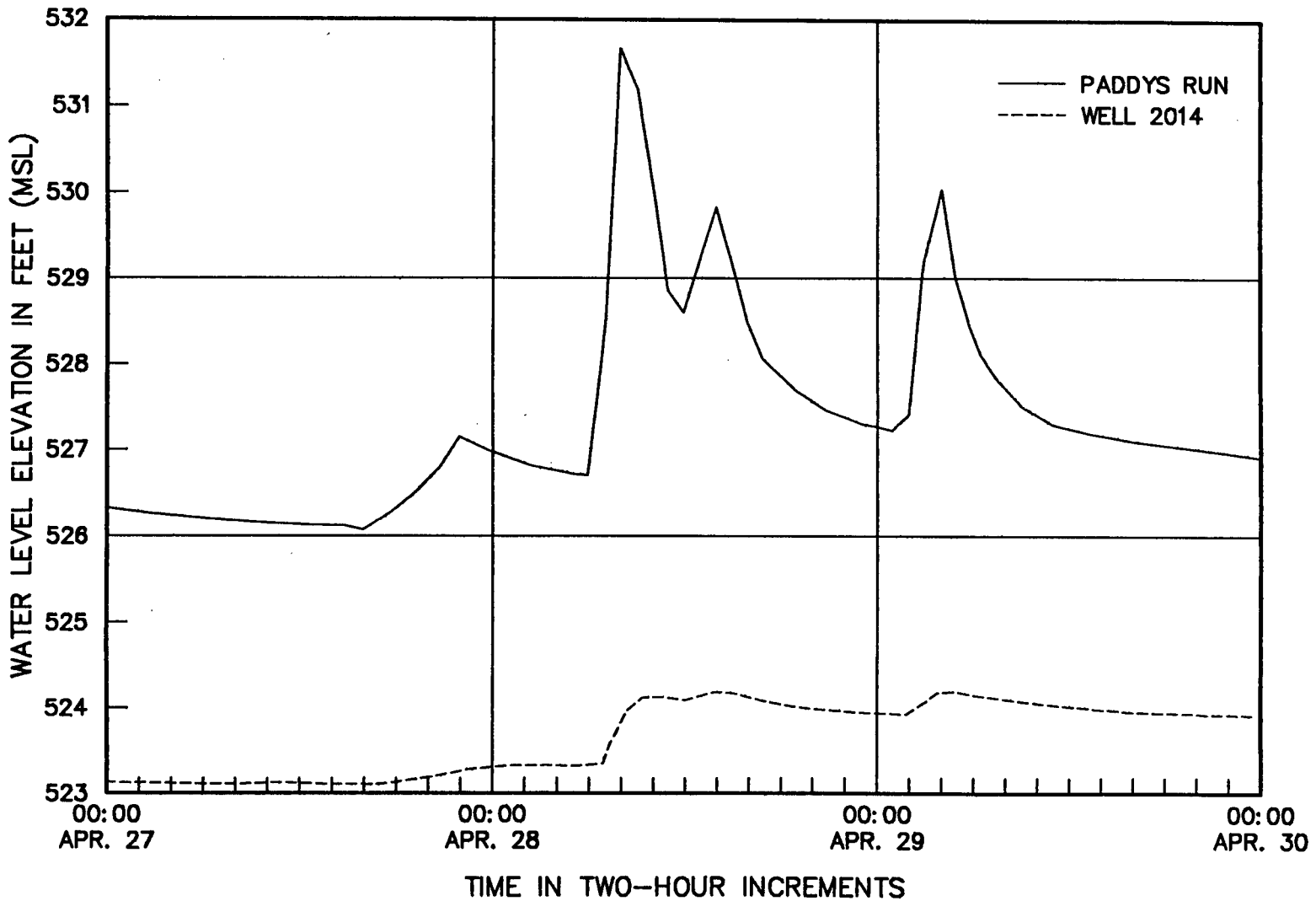


FIGURE 3-14 HYDROGRAPH OF PADDYS RUN AND GREAT MIAMI AQUIFER
AT WELL LOCATION 14, APRIL 27, 1989 – APRIL 30, 1989

409195-A51 (GW) (PGH)

# 4.0 MODEL DESIGN

The groundwater model for the FEMP and surrounding area was developed following a literature review of site-specific and regional geology reports. The goal of the literature review was to assemble a historical perspective of the FEMP with respect to potential waste discharge periods and to characterize the geologic materials in and around the FEMP to allow for detailed flow and solute transport modeling. The results of this literature review are presented in Table 4-1. This table summarizes the results of the literature review and shows reported ranges for input parameters used by the models. Along with these input parameter ranges, a basic understanding of the FEMP's geology and hydrogeology was gained. These geologic and hydrogeologic interpretations are presented in Chapters 2.0 and 3.0, respectively.

## 4.1 GROUNDWATER MODEL FOR THE FEMP

Groundwater modeling is a technique for producing a representation of a groundwater system that behaves in a manner similar to the real groundwater system. Many types of models are available. Mathematical models range from the solution of simple equations to very complex computer programs. In general, the more complex the model, the closer its behavior approaches that of the real system. Therefore, more complex models tend to produce better estimates of the actual behavior of the system than simpler models since the physical systems and processes can be more completely represented. The selection of a groundwater model is guided by the complexity of the real aquifer system, the amount and quality of data available, and the degree of representativeness needed.

In the case of the FEMP, the system is complex, numerous data are available, and a good representation of the aquifer system is required due to the importance of the decisions that will be at least partially based on model results. The complexity of the aquifer system is caused by the following site conditions:

- Location of the site over a thick, highly-permeable, irregularly-shaped aquifer in a bedrock valley with low-permeability walls
- Presence of horizontal and vertical variations in hydraulic conductivity
- Presence of a clay interbed beneath the site that separates the aquifer into upper and lower parts, but does not extend far from the site
- Presence of several potential contaminant source areas with different strengths and periods of release
- Presence of water supply wells that serve potential receptors and draw water from various depths within the aquifer
- The irregular course of the Great Miami River, which is a potential receptor location

## TABLE 4-1
## RESULTS OF LITERATURE REVIEW FOR MODEL DEVELOPMENT

| Model Input Parameter | Value or Range | Reference(s) |
|---|---|---|
| Subsurface Stratigraphy | Variable | RI Borings |
| | | Dames & Moore (1985) |
| | | State Well Logs |
| Bedrock Topography | Variable | RI Borings |
| | | State Well Logs |
| | | Leow (1985), Vormelker (1985) |
| | | Watkins & Spieker (1971) |
| Great Miami Aquifer | 2466 gpd/ft$^2$ | Dove (1961) |
| Hydraulic Conductivity | 2460 gpd/ft$^2$ | Smith (1962) |
| | 900 gpd/ft$^2$ | Klaer (1968) |
| | 2380-2760 gpd/ft$^2$ | Kazmann (1950) |
| | 2440-2780 gpd/ft$^2$ | Shaefer & Walton (1956) |
| | 2340-2420 gpd/ft$^2$ | Klaer & Kazmann (1943) |
| | 2000 gpd/ft$^2$ | Spieker & Norris (1962) |
| | 2500-3020 gpd/ft$^2$ | Lewis (1968) |
| | 5790 gpd/ft$^2$ | Smith (1960) |
| | 4000 gpd/ft$^2$ | Smith (1962) |
| | 270-450 ft/day | Spieker (1968a) |
| | 350 ft/day | GeoTrans (1985) |
| Clay Interbed | 2.5-3.2 gpd/ft$^2$ | Spieker & Norris (1962) |
| Hydraulic Conductivity | 0.25 gpd/ft$^2$ | GeoTrans (1985) |
| Clay Interbed Leakage | 0.25 gpd/ft$^3$ | Spieker & Norris (1962) |
| Bedrock Hydraulic Conductivity | $3 \times 10^{-5}$ to $3 \times 10^{-1}$ ft/day | Freeze & Cherry (1979) |

TABLE 4-1
(Continued)

| Model Input Parameter | Value or Range | Reference(s) |
|---|---|---|
| Great Miami Aquifer Porosity | 0.25 | Fetter (1980) |
| | 0.25 | Freeze & Cherry (1979) |
| | 0.25 | RI Boring Logs |
| Clay Interbed Porosity | 0.6 | Freeze & Cherry (1979) |
| Bedrock Porosity | 0.1 | Freeze & Cherry (1979) |
| Storage Coefficient | 0.2 | Dove (1961) |
| | 0.23 | Smith (1962) |
| | 0.2 | Spieker & Norris (1962) |
| | 0.2 | Spieker (1968a) |
| | 0.2 | Spieker (1968b) |
| Aquifer Recharge: | | |
| Into Sand & Gravel | 15 in/yr | GeoTrans (1985) |
| | 21 in/yr | Smith (1962) |
| | 12 in/yr | Dove (1961) |
| | 8.5 in/yr | Shaefer & Walton (1956) |
| | 6-21 in/yr | Spieker (1968b) |
| | (Average 15.2 in/yr) | |
| Through Till | 6 in/yr | GeoTrans (1985) |
| | 6 in/yr | Spieker (1968b) |
| From Bedrock | 200000 gpd/mile | Dove (1961) |
| Great Miami River Loss | 240000 gpd/acre | Dove (1961) |
| to Collector Wells | 168000 gpd/acre | Shaefer & Walton (1956) |
| | 325000 gpd/acre | Spieker (1968a) |
| | 75% of total pumping | Spieker (1968a) |

**TABLE 4-1**
(Continued)

| Model Input Parameter | Value or Range | Reference(s) |
|---|---|---|
| Great Miami River Heads | Variable | U.S. Army Corps of Engineers (1988)[a] |
| Water Supply Well Pumping Rates | | |
| SOWC Collector Wells | Variable (From 1984-1988) | SOWC (1984, 1985, 1986, 1987, 1988)[a] |
| Well P3 | 0.42-0.48 Mgd | WMCO (1988) |
| A & W Wells | 0.14 Mgd | Albright & Wilson (1987, 1988)[a] |
| Ruetger-Nease | 0.1 Mgd | Ruetgers-Nease (1988)[a] |
| Water Supply Well Radii | | |
| SOWC Collector Wells | 210 ft - Collector 1 | SOWC (1984)[a] |
| | 216 ft - Collector 2 | |
| Well P3 | 13 inch | WMCO (1988) |
| A&W Wells | 6 inch | Albright & Wilson (1987)[a] |
| Aquifer Potentiometric Heads | Variable | IT (1986 & 1988), Miami Conservancy District (1985) |
| Great Miami Aquifer Thickness | 150 ft | Dove (1961) |
| | 120-125 ft | Kazmann (1950) |
| | 120 ft | Shaefer & Walton (1956) |
| | 150-202 ft | Klaer & Kazmann (1943) |
| | 90 ft | Smith (1960) |
| | 178 ft | Smith (1962) |
| | 150-200 ft | Spieker (1968a) |
| | 150-250 ft | Spieker (1968b) |
| Compressibility of Water | $3.13 \times 10^{-6}$/psi | Streeter (1961) |
| Source Areas | Variable | Dames & Moore (1985) |

TABLE 4-1
(Continued)

| Model Input Parameter | Value or Range | Reference(s) |
|---|---|---|
| Initial Loading Rates | Variable | Thatcher (1972)[b] |
| Source Time Periods | Variable | Eye (1961) |
| | | WMCO (1988) |
| | | Theis (1951)[b] |
| | | Spieker (1950) |
| | | Spieker & Norris (1962) |
| | | GeoTrans (1985) |
| | | Facemire (1959) |
| Retardation Factor | Variable | GeoTrans (1982) |
| | 11-40.5 | IT (1989) |
| | (26 average) | |
| Dispersivity | 39-200 feet | Walton (1985) |
| | (100 Average) | |
| Radiocative Decay | 4.468E09 years | Steiger & Jager (1977)[b] |
| | (Halflife for U238) | |
| Background Uranium | Variable | WMCO (1988) |
| Concentration | | Eye (1961) |
| | | Sedom (1985) |
| | | RI Investigation Results |

[a]Cited reference is a technical memoranda to project files.
[b]Cited reference identified in GeoTrans (1985).

- A river and aquifer interrelationship that involves flow from the river to the groundwater near the collector wells and flow of water from the groundwater to the river in other reaches
- Presence of the collector wells, which influence the groundwater flow over a large area
- Presence of large changes in horizontal hydraulic gradients across the study area
- Presence of significant vertical hydraulic gradients within the study area
- Variation of areal recharge through different surficial materials composed of glacial overburden, flood plain, and alluvial deposits
- Presence of periodic significant recharge to the aquifer from Paddys Run.

Chemical and radiological contaminants associated with the FEMP site have been introduced to the Great Miami Aquifer from one or more of the following:

- Leakage from the waste pits in the waste storage area
- Discharges to and leakage from Paddys Run
- Discharges to and leakage from the storm sewer outfall ditch
- Waste or product spills in the former production area as well as from "suspect areas" within the FEMP site
- Facilities in the former production area used for the storage, containment, or transfer of radiological or chemical materials
- Seepage from Southfield, sanitary landfill, fly ash piles, and lime sludge ponds.

Figure 2-2 shows the FEMP site and these possible source areas.

Calibration of the model was accomplished through a series of successive modeling simulations, each of which modified model input parameters to more closely simulate the natural system. The calibration process should continue until the model is sufficiently refined as to be suitable for application to studies of the site, and to support the goals of the project. In the present case, these objectives are the following:

- To characterize the groundwater system by calculating groundwater flow rates and directions, supplying rates of recharge via infiltration of precipitation and stream water, relating contamination to possible sources and receptors, supplying contaminant source loading rates, estimating uranium concentrations between monitoring wells, and evaluating uranium mobility in the system

- To support evaluations of the need for additional groundwater monitoring and field investigations

- To estimate future concentrations at potential receptor locations under the no-action remedial alternative

- To evaluate the feasibility of different remedial actions

- To estimate temporal and spatial variations in uranium concentration that would result from different remedial actions.

### 4.1.1 Model Code Selection

For purposes of the RI/FS modeling, minimum requirements for the model code were determined to be:

- Three-dimensional modeling capability. This capability is necessary to account for possible vertical flow through the clay interbed at the FEMP site and to simulate the effects of vertical hydraulic gradients caused by pumping at depth.

- The capacity to quantitatively predict contaminant concentration at receptor locations as necessary to fully satisfy the requirements of the RI/FS. Therefore, only codes with options to model solute transport and associated attenuation/retardation processes were considered.

- Adequate verification of the code and previous applications under similar project settings.

- The availability of the modeling code and accompanying documentation.

- The capacity to model water table aquifer conditions.

- The capacity to model decay chains. Although the study of uranium does not require the consideration of daughter products, this would become a consideration if other radionuclides are found to be important.

- The ability to represent adsorption and biological decay processes so as to provide flexibility in the range of constituents that can be modeled.

- The option to consider density variations and temperature or concentration effects on fluid viscosity. Although not considered necessary at this time, this option could be beneficial to best simulate certain critical processes (e.g., leakage through the riverbed).

SWIFT III was determined to best satisfy the full set of selection criteria. Therefore, a decision was made to select SWIFT III as the code for use in the hydrogeologic investigation of the FEMP site-wide RI/FS (IT 1988b).

4.1.2 Model Code Verification

The SWIFT code was originally developed by Sandia National Laboratories for the Nuclear Regulatory Commission for use in the high-level nuclear waste isolation program. The first extension of the SWIFT code was made by GeoTrans, Inc. (GeoTrans), and was given the title SWIFT II.

Comparisons of results from the SWIFT II model code and analytical solutions appear in many documents. Results of the SWIFT II model applications have also been compared with data collected in numerous field studies. The comparisons provide evidence that the equations solved in the model are numerically correct and properly simulate the physical processes controlling groundwater system behavior. Applications of the code to these sites have appeared in several reports, including those appearing in Ward, et al. (1984), and Reeves, et al. (1986), which are summaries of the model verification process and field comparisons. Particularly noteworthy are previous applications of the SWIFT II code to the FEMP (GeoTrans 1985) and to a nearby site with a similar hydrogeologic setting (Ward et al. 1987).

Modifications to the SWIFT II code were made by GeoTrans in 1986. The modifications included changing the code from FORTRAN IV to FORTRAN 77, and making modifications in data input and output routines. The resulting model was termed the SWIFT III code.

Pursuant to the modifications, GeoTrans and IT conducted verification work that tested the validity of several features of the SWIFT III code. The results of GeoTrans' most recent model code verification work are presented in "SWIFT III Quality Assurance Benchmark Problem Execution Fiche" (GeoTrans 1988). IT's verification program included comprehensive testing of those SWIFT III features of importance to the FEMP. Both the groundwater flow and solute transport components of the SWIFT III code were tested against analytical solutions and the results from other established numerical models for a wide range of hypothetical conditions. The results of the IT verification program showed the model was capable of simulating hydrogeologic systems similar to the FEMP's. The IT code verification work is documented in a separate report (IT 1990).

4.1.3 Overview of Technical Approach

The products of the model development process, using the SWIFT III code, are a regional three-dimensional groundwater flow model and a local three-dimensional solute transport model. The process by which these models were constructed followed a progressive development that passed through simpler two-dimensional numerical and analytical models to arrive at the final, more complex models. The simpler models were used in the early stages of model development because of their relative ease of utilization. They had short computer execution times and required no significant waiting time for results of runs, and the computer input and output files were relatively short and easy to handle. Consequently, the simpler models were used both to develop a general understanding of

model conditions and to generate initial estimates of input parameters for calibrating the more complex models. Also, the two-dimensional models provided a relatively easy way to obtain information on the sensitivity of model results to variations in the values of input parameters.

The SWIFT III numerical code was used in the modeling effort for this study. The notations 2DFLOW and 3DFLOW are used to represent the simulation of the two- and three-dimensional flow modeling utilizing the SWIFT III code. For the solute transport modeling effects, the notations 2DSOL and 3DSOL are used to represent the two- and three-dimensional modeling simulations.

The modeling progression is summarized as follows:

- A preliminary 2DFLOW model developed to support a previously completed hydrogeologic study of FEMP discharge to the Great Miami River (IT 1988b), was refined using subsequently collected field data to establish the initial 2DFLOW model. The finite-difference grid used in the previous study was not changed. (Hereafter, the previous study will be referred to as the Zone of Influence Study.)

- A 3DFLOW model was produced by introducing five model layers, thereby representing the aquifer system as five distinct zones in the vertical direction. River stages and well pumping rates were imported from 2DFLOW. Hydraulic conductivities, boundary heads, recharge rates, and river leakage factors from 2DFLOW were used to provide initial estimates of the related parameters in 3DFLOW. (Recharge rates in this report refer to recharge due to infiltration of rainfall and snow melt as well as seepage from Paddys Run, unless another source is specifically mentioned.)

- Two-dimensional analytical solute transport models were produced to roughly simulate and better understand the uranium plumes that are present in the groundwater system downgradient from the waste storage area and within and downgradient from the southwest portion of the FEMP.

- A 2DSOL transport model was produced. It covered a smaller area than 2DFLOW and 3DFLOW and had much smaller cells in the finite-difference grid. Boundary heads, recharge rates, and hydraulic conductivities were imported from equivalent cells in 2DFLOW. An initial estimate for the uranium distribution coefficient was obtained from the two-dimensional analytical modeling.

- A 3DSOL transport model was produced. Boundary heads, recharge rates, and hydraulic conductivities were imported from equivalent cells in 3DFLOW. Initial estimates of contaminant source loading rates (rate of discharge of uranium to the aquifer) and a distribution coefficient for uranium were obtained from the calibrated 2DSOL model.

This model development was accompanied by a review of pertinent literature and reports of previous studies. These studies are referenced in Section 4.2, addressing the results of the literature review. The purpose of the review was to make the model consistent with available information on the site.

Parameter values were maintained within reasonable ranges during the model calibration. SWIFT III code verification work (IT 1990) preceded and accompanied the model development work. Preliminary results of concurrent geochemical analyses and geochemical modeling studies were incorporated into the calibration of the solute transport model as they became available and are presented in Appendix A, which reproduces the FEMP's Issues 3 and 5 Geochemical Report.

Radioactive decay is not considered in the present modeling. While uranium is radioactive and will decay to other radioisotopes and ultimately to stable lead, the half-lives of the uranium-238, -235, and -234 isotopes are $4.9 \times 10^9$, $7.04 \times 10^8$, and $2.47 \times 10^5$ years, respectively. The uranium has been present in the regional aquifer less than 40 years, a time period that is inconsequential relative to the reported half-lives. Therefore, modeling of uranium migration can be conducted without considering radioactive decay, and it can be concluded that the total mass of uranium within the aquifer will not decrease significantly as a result of radioactive decay during any period of interest.

Only two models, 3DFLOW and 3DSOL, are being applied to the RI/FS and risk assessment. The analytical models and the two-dimensional flow and solute transport models were only prepared as parts of the procedure for constructing the three-dimensional models and facilitating sensitivity analyses. The 3DFLOW and 3DSOL models are better representations of the real physical system. Nevertheless, the results of the models should be treated as estimates. Consequently, the use of models should be confined to treating the results as estimates and taking appropriate action to accommodate any error in the estimates. Such action could include monitoring the groundwater system around extraction wells to see if they are producing the expected results, monitoring uranium concentrations at receptor locations, and continuing the sampling of selected existing monitoring wells.

## 4.2 HYDROLOGIC PARAMETER ESTIMATION

This section presents the informational and analytical basis for the selection of initial values for those hydrologic parameters required as input to the groundwater flow model. Final values for these parameters were established based on the results of model calibration.

### 4.2.1 Regional Aquifer

This section discusses the hydrologic parameters of the regional aquifer, including transmissivity, porosity, and infiltration. In addition, the interaction of the Great Miami River and Paddys Run with the regional aquifer is discussed.

#### 4.2.1.1 Transmissivities and Hydraulic Conductivities

Spieker (1968a) mapped 11 units in the Great Miami Aquifer with distinctive physical and hydraulic properties. He reported that transmissivity values generally ranged from 300,000 to 500,000 gpd/ft (40,000 to 67,000 $ft^2$/day), and that individual pumping wells can yield as much as 3000 gpm.

GeoTrans (1985) summarized hydraulic properties for the Great Miami Aquifer near Hamilton, Ohio, approximately 10 miles north of the FEMP. Transmissivities ranging from 30,000 to 700,000 gpd/ft (4000 to 94,000 $ft^2$/day)) were reported for a site in the northern part of the city of Hamilton. Most values are reported in the range of 100,000 to 300,000 gpd/ft (approximately 13,000 to 40,000 $ft^2$/day). The aquifer at the site is 180 feet thick (Ward et al. 1987). Consequently, hydraulic conductivities range from 20 to 520 ft/day ($7.05 \times 10^{-3}$ to 0.18 cm/s), with most values being in the range of 75 to 225 ft/day (0.026 to 0.079 cm/s). The highest hydraulic conductivity reported for the aquifer near Hamilton was 774 ft/day (0.27 cm/s). Ward et al. (1987), stated that slug tests showed hydraulic conductivity increases with depth in the Great Miami Aquifer at Hamilton.

Hydraulic conductivities derived from pumping tests of the collector wells have ranged from 318 to 391 ft/day (0.11 to 0.14 cm/s) (GeoTrans 1985).

The pumping tests of the Great Miami Aquifer at the FEMP are described by Spieker and Norris (1962). They performed tests that utilized the FEMP water supply wells, which were screened below the clay interbed. They used the leaky aquifer method of analysis and obtained a hydraulic conductivity of 270 ft/day (0.095 cm/s). Two separate pumping tests were performed and estimates of the vertical hydraulic conductivity of the clay interbed, 0.43 ft/day ($1.5 \times 10^{-4}$ cm/s) and 0.33 ft/day ($1.16 \times 10^{-4}$ cm/s) were obtained. These values are far outside of the typical range of values for clay which is usually about $10^{-4}$ to $10^{-3}$ ft/day ($3.5 \times 10^{-7}$ cm/s) (Freeze and Cherry 1979, p. 29).

It is unlikely that the various analyses of the pumping tests reported for the Great Miami Aquifer adequately allowed for the combined effects of partial penetration and vertical anisotropy of the aquifer. Consequently, the transmissivities and hydraulic conductivities reported are probably lower than the true values for these parameters.

4.2.1.2 Porosity

No estimates of porosity in the Great Miami Aquifer were found in the literature. However, some estimates of specific yield have been made, and porosity of such deposits tends to be only slightly greater than specific yield. Spieker (1968a) stated that the aquifer may be classified with a specific yield of about 0.2. A three-day pumping test reported by GeoTrans (1985) provided a specific yield of 0.23. The average specific yield for aquifers composed of gravelly sand was reported to be 0.25 by Johnson (1967).

4.2.1.3 Infiltration/Recharge Rates

Spieker (1968a) estimated recharge to the Great Miami Aquifer throughout the study area at 6 to 21 in./yr, and used a recharge value of 15.2 in./yr in his electric analog model calibration (Spieker 1968b). Walton and Schaefer (1956) estimated that recharge in the area of the SOWC pumping wells

was 8.5 in./yr at the time of their study, which was a year of near-average precipitation. Smith (1962) estimated a recharge maximum of 21 in./yr in the Fairfield area northeast of Ross. GeoTrans (1985) produced a preliminary three-dimensional finite-difference flow model with a recharge of 15 in./yr where the Great Miami Aquifer is exposed at the ground surface, and 6 in./yr where glacial overburden covers the aquifer. A recharge value of 6 in./yr implies a vertical hydraulic conductivity of $1.4 \times 10^{-3}$ ft/day ($4.9 \times 10^{-7}$ cm/s), under unit hydraulic gradient, which is in the middle of the range for hydraulic conductivities given for glacial till (Freeze and Cherry, Table 2.2).

4.2.1.4 Great Miami River Leakage

The Great Miami River loses water by induced infiltration as it flows past the SOWC pumping wells. Walton and Schaefer (1956) investigated this stream leakage using a flow net approach. They estimated induced infiltration at 10,550,000 gpd, 62 percent of the water pumped from the SOWC pumping wells. Based on an electric analog model, Spieker (1968) estimated that 75 percent of the pumping was from induced infiltration.

4.2.1.5 Paddys Run Leakage

The main surface water drainage for the FEMP is Paddys Run, which flows along the western edge of the site. This is an intermittent stream which gains and loses flow along its course to the Great Miami River. A major tributary of Paddys Run is the storm sewer outfall ditch, which is a natural gully that has eroded through the glacial overburden in the southern portion of the FEMP. Surface water infiltrates through the sandy and gravelly beds of Paddys Run and the storm sewer outfall ditch, providing recharge to the Great Miami Aquifer.

Leakage from Paddys Run to the Great Miami Aquifer was assumed to occur along the reach of the streambed south of the Clearwell to a point about 2000 feet to the south of the FEMP. Leakage from the storm sewer outfall ditch to the Great Miami Aquifer was assumed to occur along the stream channel south of the storm water retention basins to its confluence with Paddys Run. The actual amount of leakage is variable, depending on the magnitude and duration of flows in each of these channels.

4.2.1.6 Pumping Rates

The only pumping wells determined to have a significant effect on the groundwater flow system are the collector wells. The discharge rate of 6025 gpm used for each of these wells in the 3DFLOW model is the average collector well pumping rate for March and April 1986, divided equally between the wells (Miami Conservancy District, unpublished data). The water level data used for calibration of the model were collected in these months. SOWC well pumping records for the period from 1952 through 1989 indicate that an equal allocation of the discharge rates between the pumping wells would be realistic for average long-term conditions. Pumping rates for the Albright & Wilson Company's

pumping wells are not accurately known; the value used in the three-dimensional flow model was 225 gpm, considered to be the upper limit of Albright & Wilson Company's pumping. This value was obtained from WMCO (1988).

4.2.1.7 Contaminant Loading Periods

Uranium contaminant loading rates and periods were determined using site historical release estimates. Since 1956, reports have documented estimated releases through the storm sewer system. These estimates were compiled and are presented in Table 4-2. These initial estimates were used to derive starting loading rates and loading periods for the solute transport models. This table records losses to the surface water system only; loading to the aquifer through Paddys Run would be a smaller percentage of the reported losses.

4.2.1.8 Background Uranium Concentrations

Background uranium concentrations at the FEMP were investigated using a number of monitoring wells screened upgradient of the FEMP site. Table 4-3 presents reported concentrations of the background wells and Figure 4-1 shows their locations. As can be seen in the table, most of the values reported are below 1 microgram per liter (µg/L) for the background monitoring wells. The highest reported concentration is 2.7 µg/L and the lowest value is below 0.03 µg/L.

## TABLE 4-2
## ESTIMATED URANIUM LOSS TO STORM SEWER SYSTEM AND STORM SEWER OUTFALL DITCH

| Year | Recorded Annual Uranium Loss to Storm Sewer System (lbs) | Recorded Annual Loss to Storm Sewer Outfall Ditch (lbs) | Assumed Annual Loss to Storm Sewer Outfall Ditch[a] (lbs) | (kg) | Source |
|---|---|---|---|---|---|
| 1956 | 1,800 | -- | 373 | 169 | b |
| 1957 | 2,600 | -- | 538 | 244 | b |
| 1958 | 5,400 | -- | 1,118 | 507 | b |
| 1959 | 6,300 | 1,400 | 1,400 | 635 | b |
| 1960 | 11,200 | 2,000 | 2,000 | 907 | b |
| 1961 | 11,800 | 2,600 | 2,600 | 1,179 | b |
| 1962 | 14,760 | -- | 2,624 | 1,190 | c |
| 1963 | 12,180 | -- | 2,580 | 1,170 | d |
| 1964 | 9,600 | -- | 2,470 | 1,120 | c |
| 1965 | 7,070 | -- | 1,464 | 664 | c |
| 1966 | 9,490[e] | 2,400[f] | 1,863 | 845 | c |
| 1967 | 4,190 | -- | 867 | 393 | c |
| 1968 | 4,080 | -- | 845 | 383 | c |
| 1969 | 5,568 | -- | 1,153 | 523 | c |
| 1970 | 2,976 | -- | 622 | 282 | c |
| 1971 | 4,184 | -- | 867 | 393 | c |
| 1972 | 2,584 | -- | 536 | 243 | c |
| 1973 | 2,605 | -- | 540 | 245 | c |
| 1974 | 1,752 | -- | 395[g] | 179 | c |

See footnotes at end of table.

**TABLE 4-2**
(Continued)

| Year | Recorded Annual Uranium Loss to Storm Sewer System (lbs) | Recorded Annual Loss to Storm Sewer Outfall Ditch (lbs) | Assumed Annual Loss to Storm Sewer Outfall Ditch[a] (lbs) | (kg) | Source |
|---|---|---|---|---|---|
| 1975 | 1,584[h] | -- | 725[i] | 329 | c |
| 1976 | -- | 98.5 | 194 | 88 | j |
| 1977 | -- | 157.6 | 320 | 145 | j |
| 1978 | -- | 46.0 | 95 | 43 | j |
| 1979 | -- | 75.5 | 154 | 70 | j |
| 1980 | -- | 16.4 | 33 | 15 | j |
| 1981 | -- | 4.3 | 9 | 4 | j |
| 1982 | -- | 42.7 | 24 | 11 | j |
| 1983 | -- | 98.5 | 97 | 44 | j |
| 1984 | -- | 124.8 | 123 | 56 | j |
| 1985 | -- | 85.4 | 85.4 | | k |
| | | TOTAL | 26,629 | 12,076 | |

[a]The assumed annual uranium loss to the Storm Sewer Outfall Ditch is calculated, if not recorded, as 21.85 percent of the annual loss to the Storm Sewer System. The 21.85 percent figure is the average ratio of the recorded annual loss to the Storm Sewer Outfall Ditch to the recorded loss to the Storm Sewer System for the years 1959, 1960, 1961, and 1966.

[b]NLO Report of FMPC Ground Contamination Study Committee, September 30, 1962.

[c]NLO Aquifer Contamination Control Reports, dated January 21, 1965 to October 1, 1975.

[d]Data for 1963 are not available. Value presented is the average of 1962 and 1964 data.

**TABLE 4-2**
(Continued)

[e]Value presented is calculated based on a loss of 8,700 pounds for the period January 1 to November 30, 1966.

[f]Value presented is calculated based on a loss of 2,200 pounds for the period January 1 to November 30, 1966.

[g]For January-November 1974, uranium loss to the Storm Sewer Outfall Ditch was 21.85 percent of the loss to the Storm Sewer System. For December 1974, the uranium loss to the Storm Sewer Outfall Ditch was 100 percent of the loss to the Storm Sewer System. Value presented is calculated accordingly.

[h]Value presented is calculated based on a loss of 132 pounds per month for the first four months of 1975.

[i]For January-June 1975, uranium loss to the Storm Sewer Outfall Ditch was 100 percent of the loss to the Storm Sewer System. For July-December 1975, the uranium loss to the Storm Sewer Outfall Ditch was 21.85 percent of the loss to the Storm Sewer System. Value presented is calculated accordingly.

[j]NLO FMPC Environmental Monitoring Report for 1976-1984. Values presented are converted from Ci to pounds by 1 Ci = 3283.5 pounds.

[k]WMCO FMPC Environmental Monitoring Report for 1985. Value presented is converted from Ci to pounds by 1 Ci = 3283.5 pounds.

# TABLE 4-3
## BACKGROUND URANIUM CONCENTRATIONS

| Well Number | Uranium Concentration, µg/L (through March 1989) |
|---|---|
| 2026 | < 1, 0.3, < 1, < 1 |
| 2036 | < 1, 0.3, 0.3, < 1 |
| 2056 | < 0.03, 0.18, < 1, < 0.1, < 1, 2.7 |
| 2057 | 0.30, < 0.25, < 1, 0.3, 0.1, 0.2 |
| 2105 | < 0.07, < 0.04, < 1, < 1, < 0.1, < 0.1 |
| 2121 | < 1, 0.9, 0.6, < 1 |
| 2123 | 0.30, < 1, 0.4, 0.3, < 1 |
| 3063 | < 1, 0.4, < 1, 0.6 |
| 3099 | < 1, 0.5, 0.6, < 1 |
| 3100 | < 1, 0.5, 0.6, 1.1 |
| 4023 | < 1, 0.6, 0.4, 1.7 |

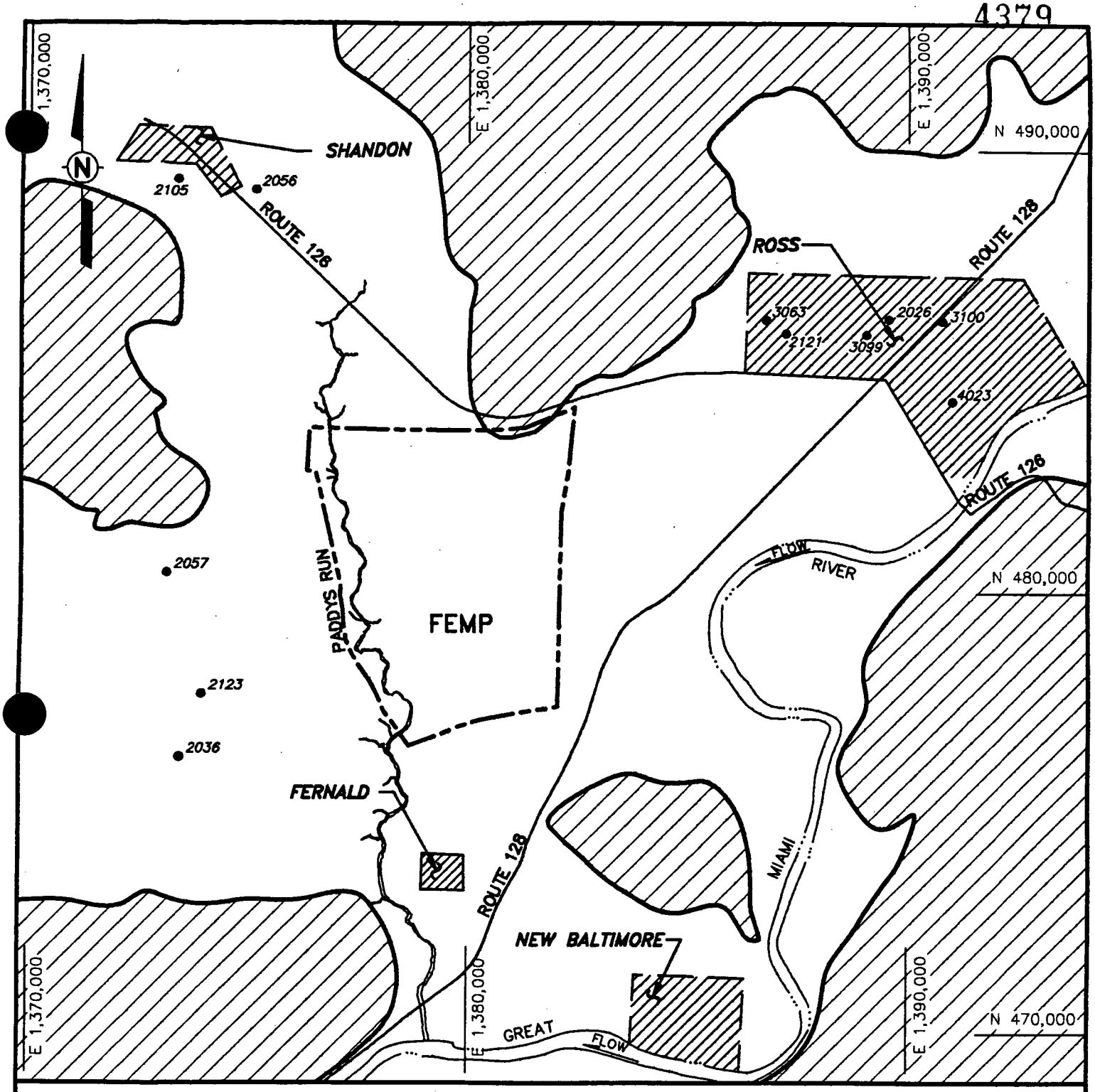


**LEGEND:**

- 2026 — WELL NAME AND LOCATION
- FEMP PROPERTY BOUNDARY
- BEDROCK OUTSIDE GREAT MIAMI AQUIFER
- MUNICIPAL AREA

SCALE: 0 — 4000 — 8000 FEET

409195 A91 (GW) (PGH)



FIGURE 4–1
BACKGROUND MONITORING WELL LOCATIONS

# 5.0 GROUNDWATER FLOW MODEL

Groundwater modeling at the FEMP was initiated with the construction of a regional groundwater flow model. The initial step in this modeling effort was the creation of the 2DFLOW model. This model was updated and refined to create the 2DFLOW model using an earlier flow model reported in the Zone of Influence Study (IT 1988b). The 2DFLOW model was calibrated to regional groundwater information from April 1986, obtained from monitoring wells within the Great Miami Aquifer. Following this calibration, a model evaluation study was also done using data obtained from May 1988. This is reported in Appendix B.

After calibration and validation of the 2DFLOW model, the model was expanded by adding a multilayered stratigraphy and creating a 3DFLOW. This model was also calibrated using an April 1986 database and was later incorporated into the solute transport modeling discussed in Chapter 6.0.

This chapter presents the construction, calibration, and results of the 2DFLOW and 3DFLOW models. These regional models were both created using the conceptual model discussed previously in Chapter 4.0. However, the parameters presented earlier were only used as starting input values; model calibration modified many of these parameters to achieve a final result.

## 5.1 PRELIMINARY TWO-DIMENSIONAL FLOW MODEL

The 2DFLOW model was developed by refining the model that was used in the Zone of Influence Study (IT 1988b). The refinements were based on an increasing database and resulted in some degree of modification to all features of the model except the grid and the stream stages applied to cells representing the Great Miami River. The refinements included adjusting well pumping rates and bedrock elevations to include values obtained subsequent to the Zone of Influence Study. A more refined calibration was also performed, which involved successive trial adjustments of hydraulic conductivity, recharge rates, river leakage factors, and boundary heads to produce simulated hydraulic heads that achieved a better fit to hydraulic heads measured in the actual system. The measured hydraulic heads were from water level data gathered in a comprehensive regional study in April 1986. An independent check of model performance was based on new water level data from May 1988. A sensitivity analysis was also performed. The construction, calibration, and sensitivity analyses of the preliminary flow model are described below.

### 5.1.1 Regional Model Grid and Boundary Conditions

The regional model grid imported from the Zone of Influence Study is shown in Figure 5-1. The exterior boundary lines of the grid are located far enough from the site to include the collector wells, the Great Miami River, and important features of the bedrock valleys. The boundaries are considered to be outside the area of influence of any pumping wells that affect the flow regime within the study

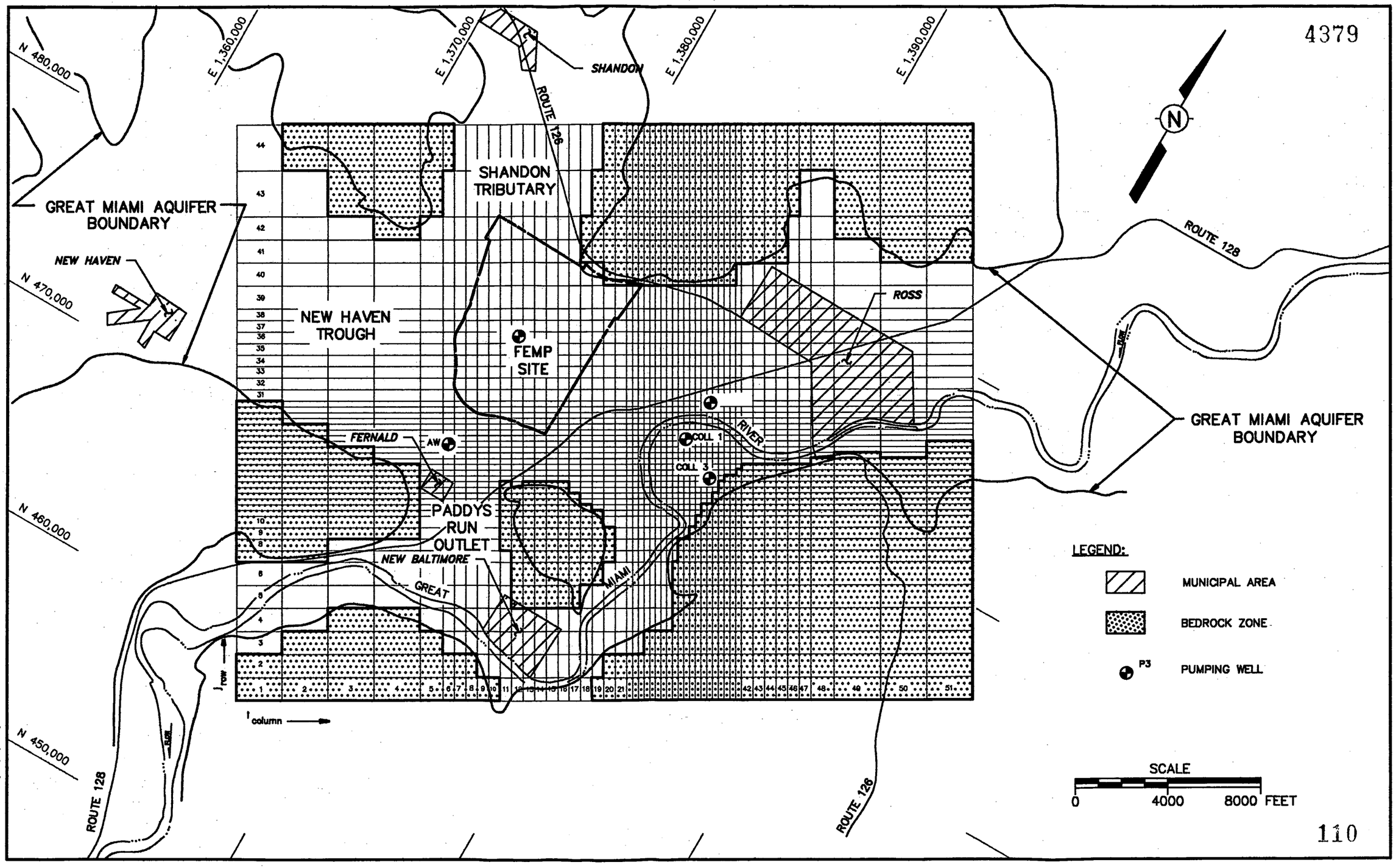




FIGURE 5-1
SWIFT III FLOW MODEL GRID
FOR RI/FS MODEL AREA

409195-B44 (GW) (PGH)

area. The Shandon Tributary is a bedrock valley that enters the model north of the FEMP and the Paddys Run Outlet is a bedrock valley south of the FEMP (Figure 3-10). Both valleys are included in the model. The groundwater conditions in the Shandon Tributary affect flow under the northern part of the FEMP, and the Paddys Run Outlet channels groundwater flowing from the FEMP southward toward the Great Miami River.

The model regional grid is oriented 30 degrees west of north to approximately align it with the axis of the main bedrock valley. This orientation also aligns the grid with the axes of the New Haven Trough and Shandon Tributary, which are roughly normal to the main valley. In the grid east-west direction, the grid extends from about two miles west of the FEMP to approximately 1/2 mile east of Ross. In the grid north-south direction, it extends from about 3/4 of a mile south of Shandon to about 1/2 mile south of New Baltimore. The exterior boundary of the grid is a rectangle, about 32,000 feet by 25,000 feet (6.1 by 4.7 miles). The regional grid covers an area of approximately 29 square miles.

The cell sizes in the grid vary from 250 feet by 250 feet in the vicinity of the collector wells to 2000 feet by 2000 feet at the northeastern and northwestern corners of the grid. This arrangement places relatively small cells where the hydraulic gradients are highest. Using large cells in peripheral parts of the model, where the cell size has little effect on the modeling, reduces the total number of cells that must be handled.

The flow system in the glacial overburden which overlies the Great Miami Aquifer across much of the study area was not included in the model. The overburden contains only localized flow systems and provides limited recharge to the Great Miami Aquifer by downward percolating water. The effects of the low permeability overburden are included in the model by using lower values for recharge where the low permeability overburden is present than in areas where it is not present.

The bedrock underlying the regional aquifer has a much lower permeability than the Great Miami Aquifer. The bottom faces of the cells within the grid system were treated as a no-flow boundary. Vertical faces representing bedrock at the exterior model boundaries were also treated as no-flow boundaries because recharge due to groundwater occurring in the shale and limestone bedrock is limited. Constant-head boundary conditions were supplied at cell faces representing the Great Miami Aquifer at the exterior boundaries of the model grid. These aquifer boundary conditions were subject to change during the calibration process.

### 5.1.2 Steady-State Flow Option

A steady-state groundwater flow option of SWIFT III was used for the modeling. This option was considered adequate since the long-term behavior of the groundwater system is the principal interest in the application of the model. The short-term fluctuations in configuration of the hydraulic head

distribution in the aquifer are not representative of the long-term behavior of the aquifer. Such short-term fluctuations are caused by temporary changes in well pumping rates, recharge rates, and stream stage. Monthly contoured maps of hydraulic head in the groundwater system in the FEMP area show little change in the general configuration of groundwater elevations for the period of observation. Three such maps are shown in Figures 3-8 through 3-10.

5.1.3 Input Data

Stratigraphic data and other information related to the model input were obtained from the reported results of previous investigations in the area (Fenneman 1916; Durrell 1961; Dove 1961; Spieker and Norris 1962; Spieker 1968a; Watkins and Spieker 1971; Leow 1985). Pertinent data and information were also obtained from boring logs of monitoring wells constructed for the RI.

A map of the elevation of the top of the bedrock that had been prepared for the Zone of Influence Study was refined by incorporating additional bedrock data from new monitoring wells constructed for the RI and some additional preexisting bedrock data. Also, cells treated as bedrock in the model were redefined as those that contained less than 25 feet of saturated Great Miami Aquifer, which resulted in minor modification of the bedrock distribution in the model.

The assigned discharge rates for the Collector Wells 1 and 2 were 8.68 million gallons per day (mgd) each for March and April 1986, based on an approximate equal distribution of flow among the wells (Miami Conservancy District unpublished data). The collector well pumping records for the period from 1952 through 1989 indicate that an equal allocation of the discharge rates would also be realistic for average long-term conditions. Flow rates for the other production wells within the study area were based on estimates obtained from well owners by WMCO. No production rate records were supplied. The combined discharge rate for the Albright & Wilson Company pumping wells (Monitoring Well 3062) in 2DFLOW was initially estimated at 100 gpm. This rate was changed in subsequent models as new information became available. The rate for the FEMP Production Well P3 (also referred to as Monitoring Well 4103) was 292 gpm, which is the average pumping rate for the period from March 26 through April 6, 1986 (WMCO 1986). Residential water wells were not included in the model, because their pumping rates are too small to significantly affect flow in the highly permeable Great Miami Aquifer and with discharge from private septic systems there is an approximate net-zero withdrawal from the aquifer. Even the pumping rates of the Albright & Wilson Company wells and the FEMP production wells were found not to have a significant effect on the flow. Particle tracing around these pumping wells show the wells to have only a limited capture radius. This is due in part to the high transmissivity of the Great Miami Aquifer.

River stages input to the model were derived from a calculation of the water surface profile of the Great Miami River under average flow conditions using HEC-2 (USACE 1984), a surface water flow

code (Section 2.2.1.1). These stages were calculated for the Zone of Influence Study. The input for the HEC-2 program included flow regime, discharge for average flow conditions, cross-sectional geometry, starting water surface elevation, reach lengths, and energy loss coefficients. All input data for the Great Miami River were obtained from USACE, Louisville District (1987). The average flow conditions from HEC-2 were for the same time period as the groundwater elevations. The groundwater elevations used represented an average flow condition by comparing them to Monitoring Well O2E hydrograph data, which represents regional groundwater elevations. Stages for each river cell chosen to represent the influence of the river were calculated by interpolation between river cross sections used in the HEC-2 modeling. The river cells are shown in Figure 5-2.

During monthly monitoring from January 1989 through July 1989, a seasonal rise in hydraulic head was identified near Paddys Run for the period March to June 1989. An analysis of hydrographs and monthly groundwater elevation maps during the period indicates that this rise in water levels, which is due to recharge along Paddys Run, is an annual occurrence with varying duration up to five or six months. An investigation of the effect of this seasonal change in potentiometric surface configuration shows that it causes very little deflection of the normal long-term movement of a solute that is subject to retardation processes in groundwater. The solute movement deviates only slightly from the long-term path movement as a result of the transient rise in hydraulic head under Paddys Run. The observed lack of a large effect by transient phenomena is a result of the slow movement of solutes in groundwater.

### 5.1.4 Model Calibration Approach

The purpose of model calibration is to produce a realistic representation of the groundwater system that behaves in a manner similar to the real system. The 2DFLOW model calibration started with the same values for hydraulic conductivity, recharge rate, river leakage factor, and boundary heads that were used in the final production runs of the Zone of Influence Study model. Subsequently, the parameters were changed through successive trials to produce an improved match between computed hydraulic heads and hydraulic heads observed in monitoring wells that represent conditions in the Great Miami Aquifer. Table 5-1 listed the observed hydraulic heads in 55 monitoring wells which were used in the model calibration, and locations of these monitoring wells are shown in Figure 3-9. Successive trials involved comparing computed and observed hydraulic heads at each monitoring well and checking the magnitude, distribution, and sign of residuals; i.e., observed head minus computed head. These residual values were analyzed with respect to reasonable changes in hydrological and geological parameters. The input was then revised for the succeeding run. The results of the succeeding simulation were then analyzed, and the process was repeated until model results adequately matched the field data in accordance with prescribed statistical criteria.

409195-B67 (GW) 1, 100% BLU
409195-B67 (GW) 2, 100% RE



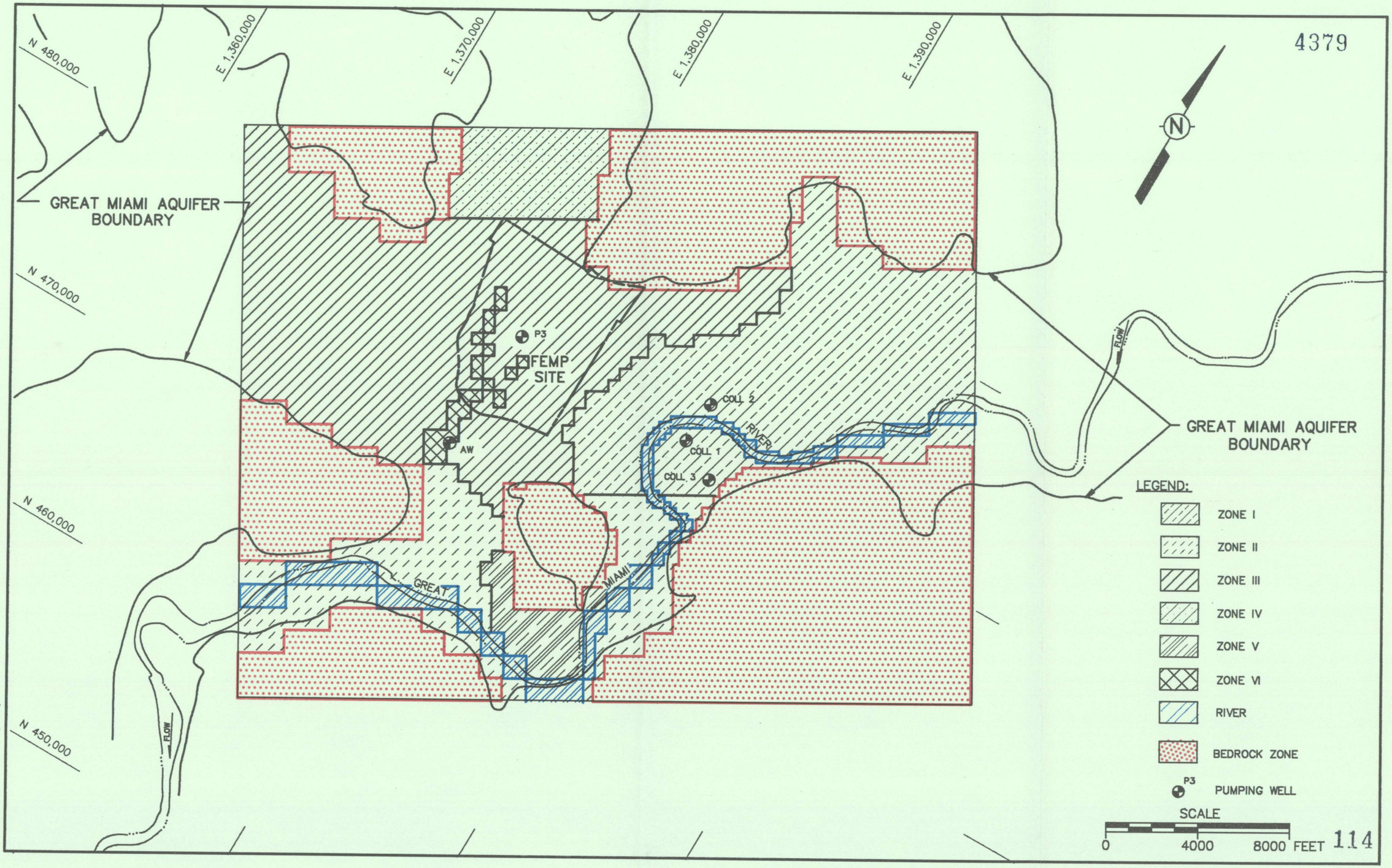




FIGURE 5-2
REFINED 2-DIMENSIONAL FLOW MODEL
MODEL ZONES

409195-B67 (GW) (PGH)

# TABLE 5-1
## OBSERVED GROUNDWATER ELEVATIONS FOR 2-D AND 3-D MODEL CALIBRATION APRIL, 1986

| Well Number | Groundwater Elevation (ft) | Synonym I.D. |
|---|---|---|
| 16-1-S | 504.31 | |
| 7-8A | 520.71 | |
| B-1 | 521.32 | |
| B-2 | 520.63 | |
| B-3 | 520.23 | |
| B-4 | 518.23 | |
| BHMHP-D | 522.36 | EMR-16 |
| BLK | 522.49 | EMR-14 |
| BPH | 524.96 | EMR-10, 2104 |
| DE | 519.87 | EMR-18 |
| DS | 521.81 | EMR-15, OS-2, MW-OS2, 2061 |
| EL1 | 522.89 | |
| ER1 | 525.89 | |
| FMPC-11 | 524.56 | T11, 11, MW-11, W-11, 211, 2011 |
| FMPC-13-D | 522.75 | 13D, MW-13D, W-13D, 313, 3013 |
| FMPC-13-S | 522.73 | 13S, MW-13S, W-13S, 213, 2013 |
| FMPC-14-D | 524.17 | 14D, W-14D, MW-14D, 314, 3014 |
| FMPC-14-S | 523.95 | 14S, W-14S, MW-14S, 214, 2014 |
| FMPC-16-S | 524.76 | 16S, W-16S, MW-16S, 216, 2016 |
| FMPC-17-D | 523.9 | 17D, W-17D, MW-17D, 317, 3017 |
| FMPC-17-S | 523.57 | 17S, W-17S, MW-17S, 217, 2017 |
| FMPC-18-D | 528.05 | 18D, MW-18D, W-18D, 318, 3018 |

**TABLE 5-1**
(Continued)

| Well Number | Groundwater Elevation (ft) | Synonym I.D. |
|---|---|---|
| FMPC-18-S | 525.26 | 18S, MW-18S, W-18S, 218, 2018 |
| FMPC-3 | 524.94 | T3, W-3, MW-3, 303, 3003 |
| FMPC-8-D | 523.43 | T8D, 8D, W-8D, MW-8D, 408, 4008 |
| FMPC-8-S | 524.08 | T8S, 8S, W-8S, MW-8S, 308, 3008 |
| FMPC-9 | 526.37 | T9, 9, W-9, MW-9, 309, 3009 |
| H-115 | 518.69 | |
| H-122A | 521.35 | |
| H-124 | 505.8 | |
| H-126 | 512.64 | |
| H-127 | 522.26 | |
| H-128 | 506.78 | |
| H-129 | 507.72 | |
| HK-D | 521.48 | 15D, EMR-26, W-15D, MW-15D, HK15D, FMPC15D, 415, 4015 |
| IT-1 | 523.15 | 268, 2068 |
| IT-2 | 522.87 | 267, 2067 |
| IT-5 | 522.66 | |
| K1 | 520.25 | |
| K2(N) | 514.36 | |
| K3 | 517.231 | |
| LB2 | 522.26 | |
| O-3 | 526.53 | |
| O2E | 522.22 | |
| 02W | 522.6 | |

**TABLE 5-1**
(Continued)

| Well Number | Groundwater Elevation (ft) | Synonym I.D. |
|---|---|---|
| PALLECT CO. | 525.38 | 2050 |
| R-7 | 520.7 | |
| RE | 515.69 | EMR-19 |
| State 16 | 526.34 | 2057 |
| SW 1 | 521.03 | |
| SW3A | 518.34 | |
| SW4A | 519.12 | |
| WK1 | 525.49 | |
| WW1 | 528.22 | Robert James, 3099 |

The adequacy of the calibration was determined through the use of GEOSTAT, a statistical program for examining the goodness of fit of groundwater modeling data (IT 1987). GEOSTAT yields nine statistical measures. Five of these measures were used as statistical criteria for flow model calibration (Table 5-2). The criteria were defined in the Groundwater Model Work Plan (IT 1988a), and were satisfied by the calibrated model. Furthermore, within the constraints of the criteria, the acceptability of the calibration was also based on the judgment of engineers and geologists working on the project.

A brief summary of the statistics used as predetermined criteria for flow model calibration follows:

- Mean Residual: A negative value indicates that computed hydraulic heads are, on the average, greater than observed hydraulic heads. A positive value has the opposite meaning. The value of this parameter must be reasonably close to zero, otherwise bias exists in the computed hydraulic heads. The predetermined criterion was $\pm 0.5$ foot.

- Mean of the Absolute Values of the Residuals. This parameter is a measure of the average difference between the observed and computed values without regard to the sign of these deviations. The optimal value is zero. The predetermined criterion was $\pm 2$ feet.

- Residual Standard Deviation: This is a measure of the degree of variance of the residuals from their mean. The optimal value is zero. The greater the value, the poorer the fit. The predetermined criterion was 3 feet.

- Regression Coefficient Between Measured and Computed Values: This is a measure of the tendency of computed hydraulic heads to increase as corresponding measured hydraulic heads increase. The optimal value is one, indicating a 1:1 correspondence between computed and measured values. The predetermined criterion was 0.95.

- Nearest Neighbor Autocorrelation, Unit Normal Deviate: This value is used to test for significant spatial clustering of positive or negative residuals. Significant spatial clustering is indicated by a value greater than 1.645 (IT 1987). This value was used for the predetermined criterion.

Other statistics were inspected for evidence of poor fit. They included mean observed head, mean computed head, coefficient of skewness of the residuals, error variance of the residuals, correlation coefficient between computed and observed heads, and correlation and regression coefficients between residuals and computed heads.

The 2DFLOW model was calibrated using April 1986 data. The primary reason for using the April 1986 data was that a large number of water level measurements over an extensive area were made at that time. The degree of representativeness of these water level data is indicated by the hydrograph shown in Figure 3-11. This hydrograph is for Monitoring Well O2E, located next to Highway 128 about 1/2 mile north of Willey Road, over 2000 feet from the Great Miami River, and over 4000 feet from the nearest collector well. This monitoring well is located in the Great Miami Aquifer with no

TABLE 5-2

STATISTICAL TESTS FOR 2DFLOW MODEL CALIBRATION BASED ON APRIL 1986 DATA

| Statistical Measure | Predetermined Criteria | 2-D Flow 1986 (2DFLOW) |
|---|---|---|
| Mean Residual (Observed Minus Computed Head) (ft) | $\pm$ 0.5 | 0.083 |
| Mean of The Absolute Residuals (ft) | $\leq$ 2 | 1.080 |
| Standard Deviation of Differences (ft) | $\leq$ 3 | 0.20 |
| Regression Coefficient Between Measured and Computed Values | 1 $\pm$ 0.05 | 1.02 |
| Nearest Neighbor Autocorrelation Unit Normal Deviate | < 1.645 | 0.636 |

clay interbeds present in the area. It is far enough from the river and the collector wells that neither dominates the water level fluctuations. This well has the longest record of monitoring wells in the local area. Comparison to other local and site monitoring wells shows it responds in the same manner as other monitoring wells to seasonal fluctuations and is representative of historical water levels. It shows both drought and high rainfall conditions. Some influence from the Great Miami River may exist, but comparison to on-site monitoring wells shows Monitoring Well O2E to be representative of site conditions. Inspection of the hydrographs shows that a median value for the water level prior to the 1987 to 1988 drought is about 520.5 feet. The water level at this monitoring well during the period of measurement (March 27 through April 11, 1986) was about 1.5 feet above the medial level. This 1.5-foot difference is small and should have very little effect on the application of the calibrated model to average conditions in the aquifer. Water levels measured in the drought of 1987 and 1988 are not representative water levels. As such, the May 1988 collected water levels provided an excellent database for an independent test of the model (Appendix B).

Initial values for hydraulic conductivity supplied to the model at the start of the calibration runs were differentiated according to hydrogeologic zones described by Spieker (1968a). The zones for the present model were numbered as shown in Figure 5-2. Zone I is an area where the Great Miami Aquifer is not overlain by clayey overburden. It is located in the eastern part of the model around Ross. Zone II is also an area where clayey deposits do not overlie the Great Miami Aquifer, located in this case along the Great Miami River where it bends southward in the vicinity of New Baltimore. Zone III is the upland area around the FEMP and west of the FEMP, where the Great Miami Aquifer is covered by glacial overburden. Zone IV is in the Shandon Tributary, and Zone V is an area near New Baltimore. The Great Miami Aquifer contains an abnormal number of clay interbeds in Zones IV and V. Zone VI is where Paddys Run has eroded through the clayey glacial deposits to the Great Miami Aquifer. Table 5-3 listed the initial hydraulic conductivity values used in the 2DFLOW model. The initial value for hydraulic conductivity assigned to Zones I, II, and V was 400 ft/day ($1.4 \times 10^{-1}$ cm/s). A hydraulic conductivity of 300 ft/day ($1.1 \times 10^{-1}$ cm/s) was assigned to Zones III and VI, and 150 ft/day ($5.3 \times 10^{-2}$ cm/s) was assigned to Zone IV. These values were based on a review of available data on aquifer transmissivity and stratigraphy, as modified by model calibration in the Zone of Influence Study. Bedrock was assigned a hydraulic conductivity of 0.003 ft/day ($1.0 \times 10^{-6}$ cm/s), which is in the lower part of the range for limestone and above the range for shale given by Freeze and Cherry (1979, p. 29).

Initial values for infiltration were applied to these same zones (Table 5-3). Recharge in Zones I, II, VI, and the river cells was assigned a value of 14 in./yr; and recharge in the remainder of the area, where the aquifer is overlain by glacial overburden, was assigned a value of 6 in./yr. These values came from the Zone of Influence Study. The value of 14 in./yr for the alluvial area is generally

## TABLE 5-3
## INITIAL INPUT HYDRAULIC CONDUCTIVITY AND RECHARGE VALUES USED IN THE 2DFLOW MODEL

| Locations[a] | Hydraulic Conductivity (ft/day) | Hydraulic Conductivity (cm/s) | Recharge (in/yr) |
|---|---|---|---|
| Zone I | 400 | $1.4 \times 10^{-1}$ | 14 |
| Zone II | 400 | $1.4 \times 10^{-1}$ | 14 |
| Zone III | 300 | $1.1 \times 10^{-1}$ | 6 |
| Zone IV | 150 | $5.3 \times 10^{-2}$ | 6 |
| Zone V | 400 | $1.4 \times 10^{-1}$ | 6 |
| Zone VI | 300 | $1.1 \times 10^{-1}$ | 14 |
| Bedrock | 0.003 | $1.0 \times 10^{-6}$ | 0 |

[a]See Figure 5-2

consistent with the value of 12 in./yr estimated by Dove (1961) and the slightly high monitoring well water levels mentioned earlier in this section.

The initial value assigned to the river leakage factor was 0.35 $day^{-1}$. This value was obtained by hydraulic conductivity divided by the thickness of the riverbed. The same value was assigned to all river cells. This value was imported from the Zone of Influence Study. Its initial value in that study was set at about three orders of magnitude below the aquifer hydraulic conductivity.

Initial values for hydraulic heads at the exterior boundaries of the model grid were imported from the Zone of Influence Study, where they were estimated by extrapolating hydraulic heads from the hand-contoured groundwater elevation map of April 1986. This method of estimating the boundary heads avoided introducing sharp changes in hydraulic gradient between the boundary and the nearest monitoring well. The external boundaries of the model in the bedrock areas were treated as no-flow boundaries in the regional models.

### 5.1.5 Model Calibration Results

The degree of calibration achieved is indicated in Figure 5-3, which shows the magnitude and distribution of the residuals. The aim of the calibration was to produce small residuals, without producing clusters of positive or negative values. Further reduction of the residuals would not have increased the representativeness of the model significantly. The predetermined statistical criteria previously described in this section were also satisfied, as shown in Table 5-2.

The performance of the model was also subjectively evaluated by examining the map of hydraulic head and flow vectors, an example of which is presented in Figure 5-4. The groundwater elevation contours shown in Figure 5-4 and all other potentiometric contour maps of computer model results were produced by SURFER, Version 4 (Golden Software, Inc. 1989), using Kriging. All of the contouring options of SURFER were tested, and Kriging produced the most accurate contours for these particular maps as compared to hand-contoured field data. The vectors shown in Figure 5-4 were produced by postprocessing programs written by IT to prepare data output from SWIFT III for AutoCad vector plots. Each vector points in the direction of horizontal groundwater movement at that location, and its length is proportional to the horizontal component of the average velocity. Horizontal velocities beneath the FEMP are so low compared to velocities in the Paddys Run Outlet and near the collector wells that they appear as dots on the map.

In Figure 5-4, the flow directions and the hydraulic head distribution around the collector wells are shown to be reasonable. Flow is directed toward the collector wells and accelerates as it approaches the wells. The channeling of flow in the Paddys Run Outlet results in a relatively high hydraulic gradient and large flow vectors. Differences between this map and the hand-contoured map in

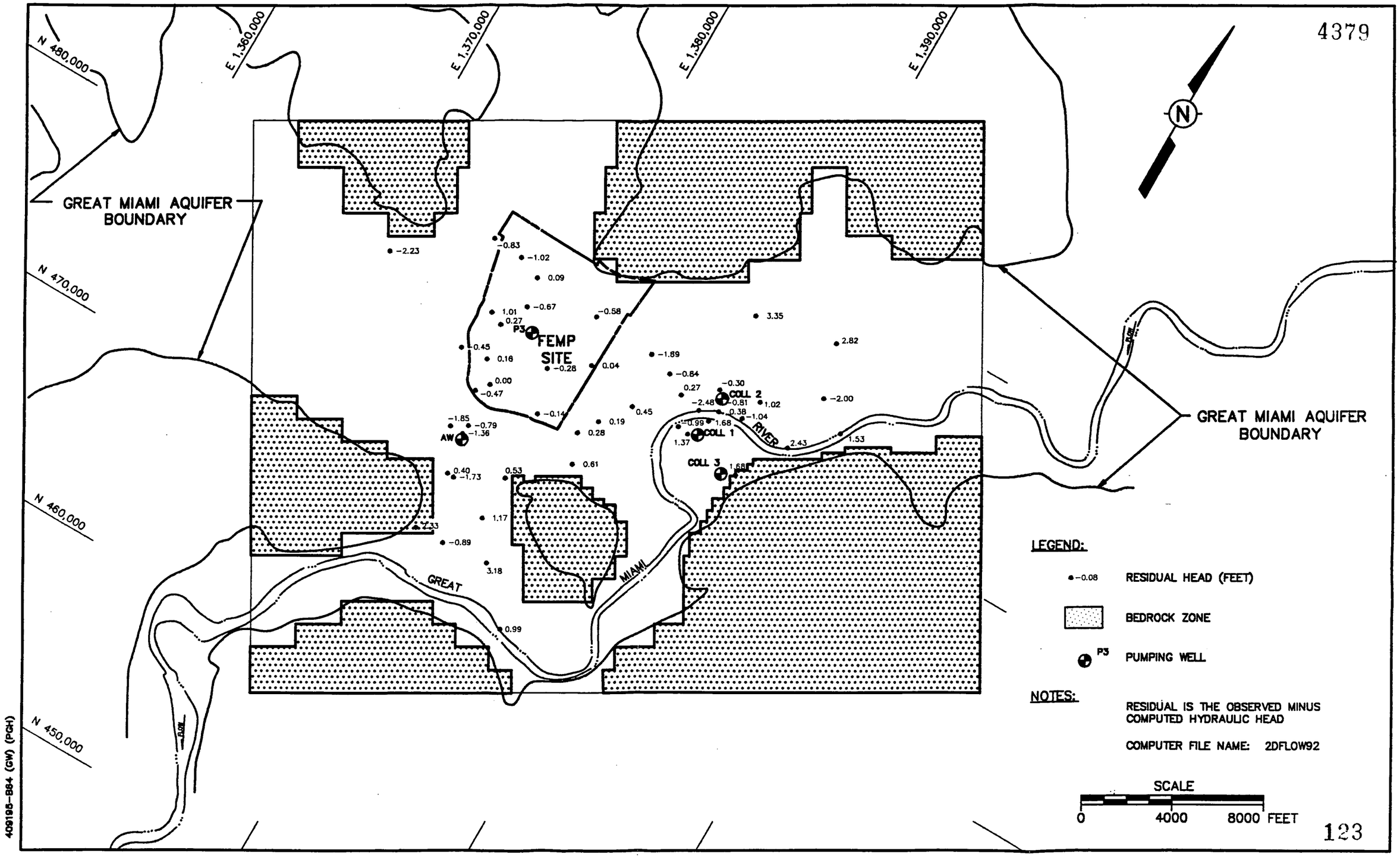




FIGURE 5-3

REFINED 2-DIMENSIONAL FLOW MODEL
RESIDUAL HEADS FOR CALIBRATED RUN
APRIL 1986 DATA

409195-B53 (GW) /01 100% BLUE



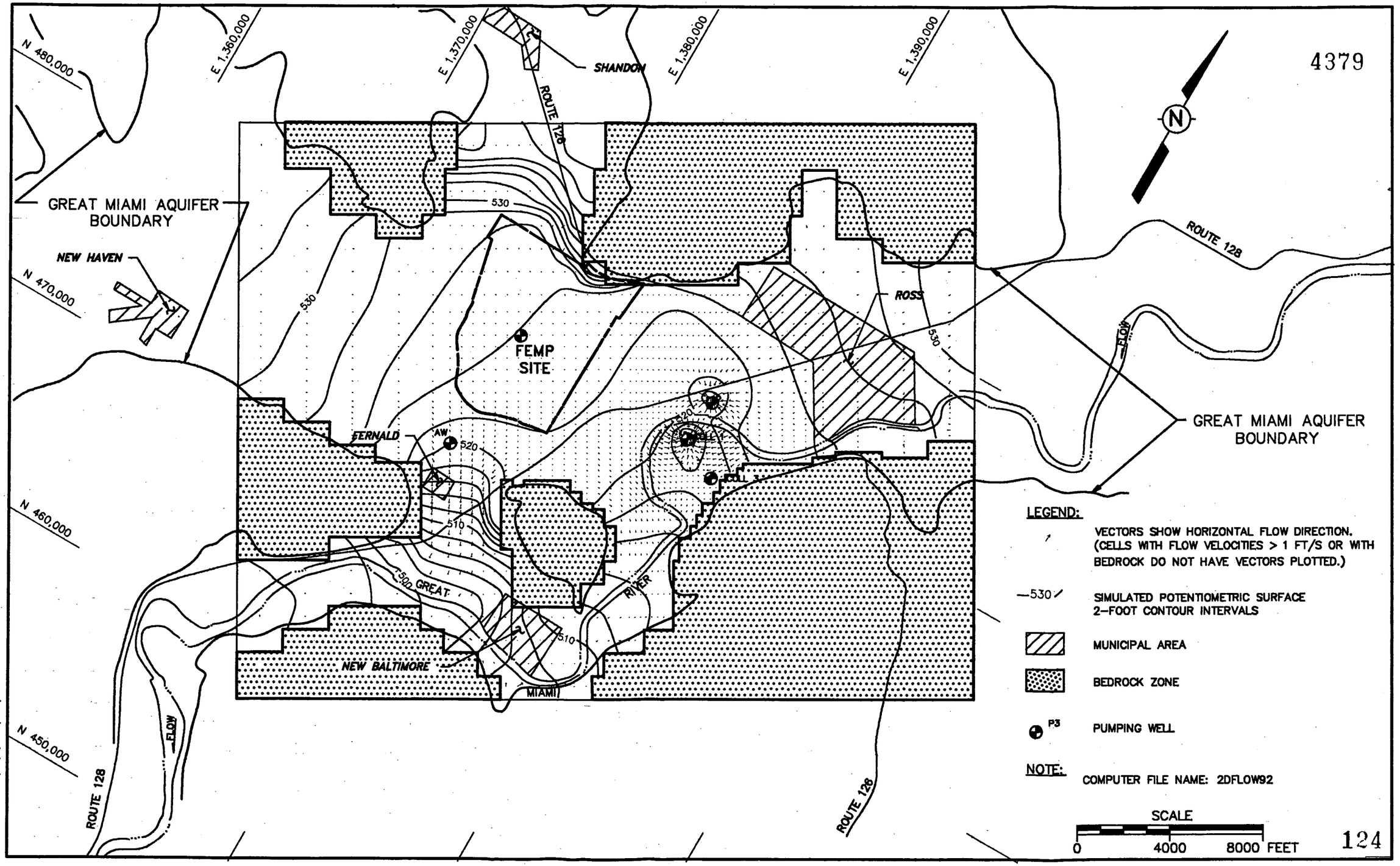




FIGURE 5-4
REFINED 2-DIMENSIONAL FLOW MODEL
CALIBRATED RUN
FLOW VECTORS AND POTENTIOMETRIC SURFACE

409195-B53 (GW) /01 (PGH)

Figure 3-9 are a result of the smoothing effect of allowing model heads at the monitoring wells to deviate from the field measurements as long as the deviations are within the guidelines discussed above.

The performance of the model was also checked by calculating a water balance for a large area around the collector wells. This balance was performed for the 1986 calibrated run described below. The area included in the balance covered the entire width of the bedrock valley from the eastern boundary of the FEMP to the western edge of Ross (Figures 5-1 and 5-4). The calculated inflows and outflows are reported in Table 5-4. The inflow/outflow ratio is 1.02, or within 2 percent of flow balance. Flow balance is a necessary check on the performance of a flow model calibration.

The distribution of hydraulic conductivities resulting from the model calibration is shown in Figure 5-5. The hydraulic conductivities in the Shandon area and in an area near the New Baltimore Outlet south of the FEMP were reduced to 30 ft/day ($1.0 \times 10^{-2}$ cm/s). These areas are known to contain more clay interbeds in the aquifer, so this reduction not only benefitted the calibration but correlates to observed conditions.

Infiltration rates are shown in Figure 5-6. Within the FEMP site, near the site west boundary and in the south part of the site, the recharge rate of 14 in./yr was used in the recharge zone of 6 in./yr. These cells represent the Paddys Run and storm sewer outfall ditch. Changes were not needed for calibration. The river leakage factor was increased to 0.5 $day^{-1}$ for all river cells. This change was needed to improve the calibration near the collector wells. Some hydraulic heads at external boundaries of the model were modified to provide a better calibration. Ranges of boundary heads in the Great Miami Aquifer are shown in Figure 5-6.

The simulated groundwater flow system that resulted from the model calibration is shown in Figure 5-4. Features of the flow system include the following:

- Groundwater flowing beneath the FEMP comes from the Shandon Tributary and the Dry Fork of the Whitewater River. Groundwater leaving the northern part of the FEMP flows eastward toward the collector wells.

- Groundwater leaving the southwestern corner of the FEMP moves toward the Great Miami River through the Paddys Run Outlet, where a high hydraulic gradient and high velocities result from the constriction of the flow within the bedrock trough.

- Other groundwater flow from the FEMP moves toward the Great Miami River south of the collector wells.

- Potentiometric contours swing around the collector wells, indicating that they have a pronounced effect on the flow system.

## TABLE 5-4
## WATER BALANCE IN THE VICINITY OF THE SOUTHWESTERN OHIO WATER COMPANY COLLECTOR WELLS FOR THE TWO-DIMENSIONAL FLOW MODEL

| Inflow Locations | Inflow Rates (Cubic Feet Per Day) | (Mgd) |
|---|---|---|
| West Boundary, I - 21, J = 10-39 | 181,358 | 1.36 |
| East Boundary, I = 50, J = 22-40 | 292,509 | 2.19 |
| North Boundary, I = 46-49, J = 41 | 26,886 | 0.20 |
| Great Miami River Leakage | 1,788,381 | 13.38 |
| Recharge | 308,227 | 2.30 |
| Total Inflow | 2,597,361 | 19.43 |
| **Outflow Locations** | **Outflow Rates (Cubic Feet Per Day)** | **(Mgd)** |
| South Boundary, I = 21-32, J = 10 | 101,818 | 0.76 |
| Collector Wells | 2,317,307 | 17.33 |
| Discharge to Great Miami River | 117,603 | 0.88 |
| Total Outflow | 2,536,728 | 18.97 |
| Inflow/Outflow Ratio | 1.024 | |
| Inflow/Outflow Imbalance | 2 % | |

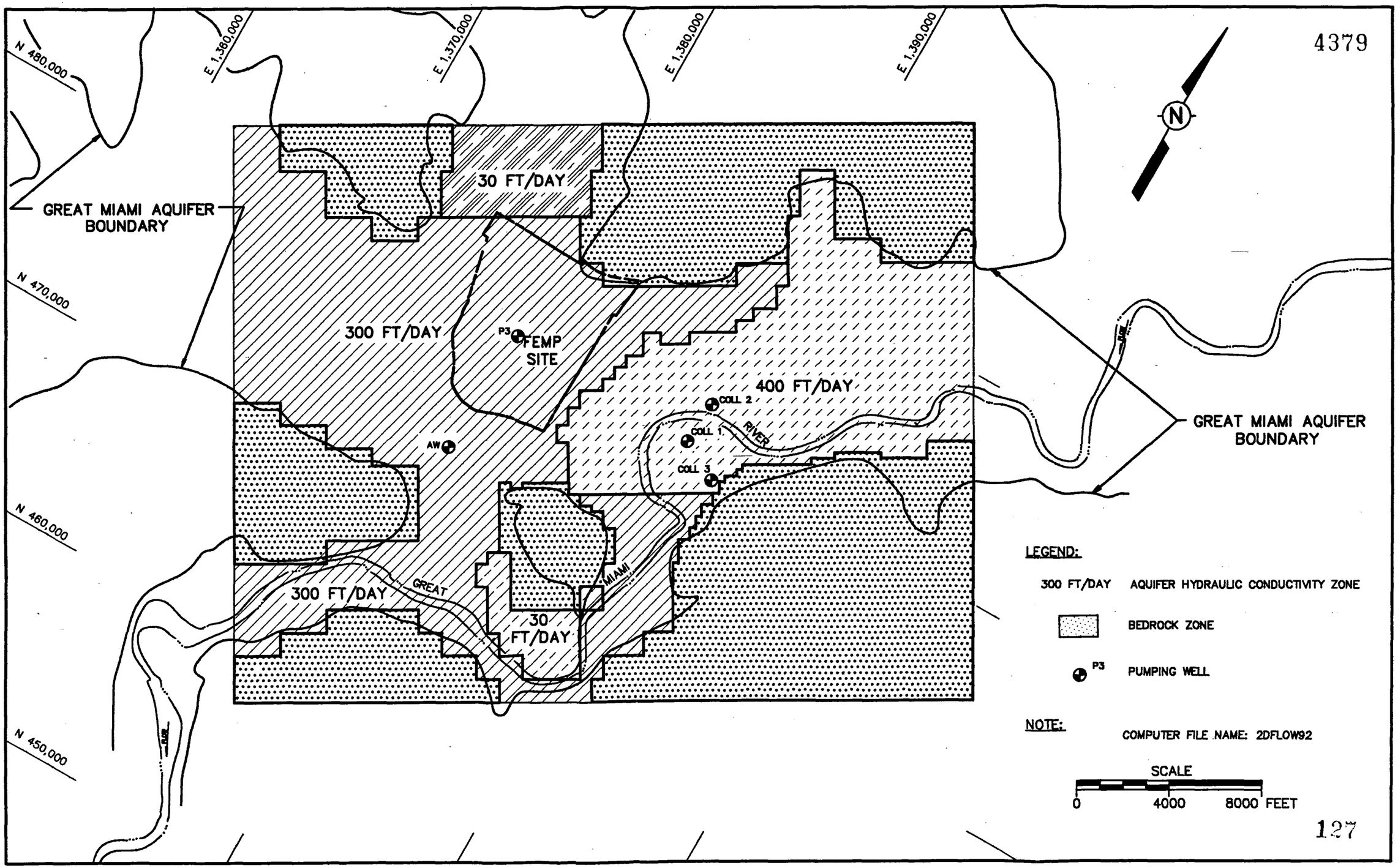




FIGURE 5-5
REFINED 2-DIMENSIONAL FLOW MODEL
HYDRAULIC CONDUCTIVITY ZONES

409195-B63 /01.02 % RED
409195-B63 /02,100% BLUE



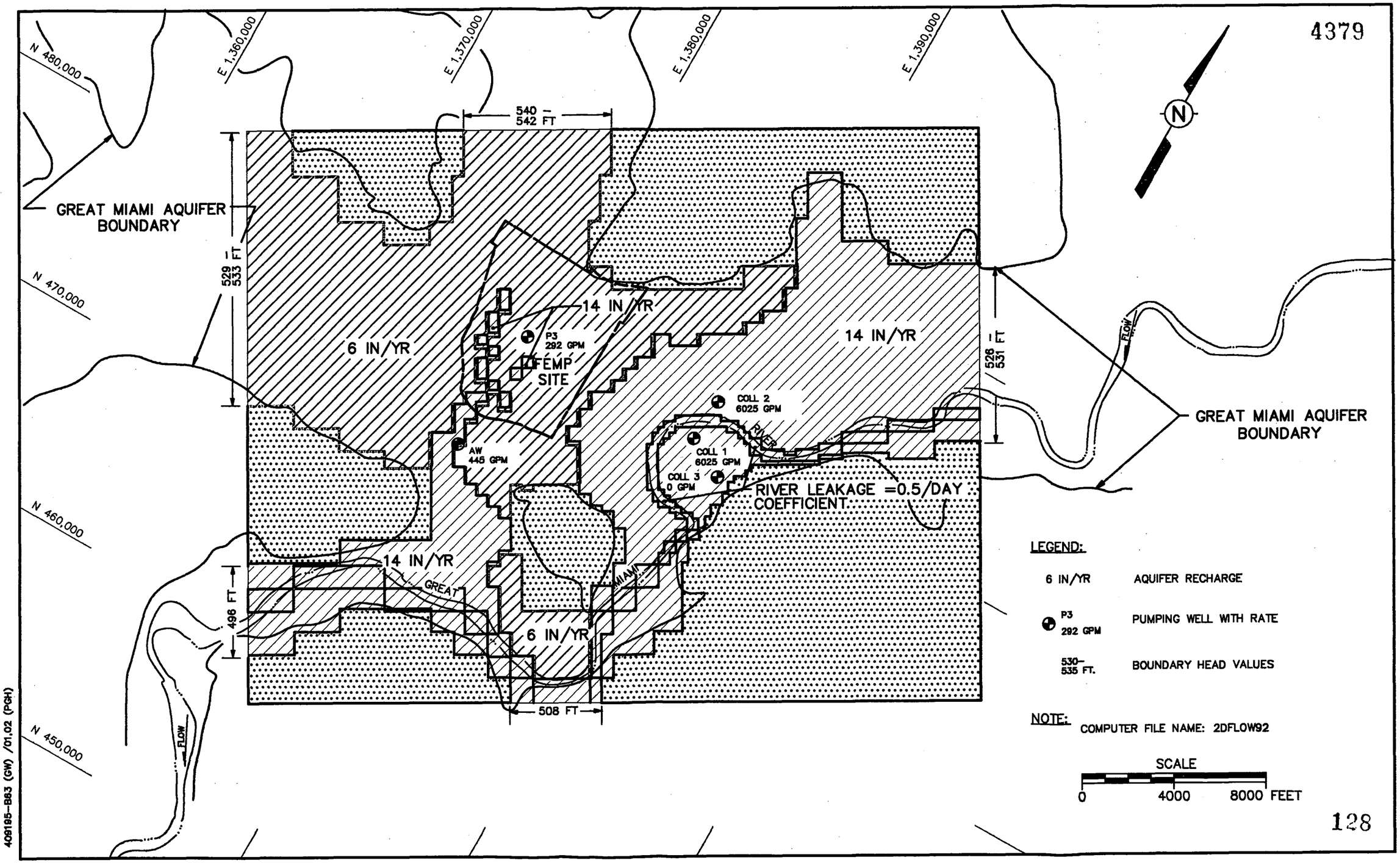


409195-B63 (GW) /01.02 (PGH)



FIGURE 5–6
REFINED 2–DIMENSIONAL FLOW MODEL RECHARGE ZONES, PUMPING RATES, AND BOUNDARY HEADS

- The effects of the FEMP water well and the Albright & Wilson Company pumping wells on the potentiometric contours are small and are not discernible on this map.

- A high hydraulic gradient is indicated in the Shandon Tributary to compensate for the low hydraulic conductivity where the aquifer material is relatively high in clay content as compared to the main valley.

### 5.1.6 Sensitivity Analysis

The sensitivity analysis applied to the 2DFLOW model investigated the effects of varying the input values of significant parameters. These parameters included hydraulic conductivity, recharge rate, and river leakage factor. The purpose of the sensitivity analysis was to determine the effect of parameter uncertainty on the representativeness of the calibrated model. Consequently, the degree to which the parameters were varied was based on the degree of uncertainty associated with each parameter. The results of the sensitivity analysis applied to the calibrated model are shown in Table 5-5. They are summarized as follows:

- Variation of hydraulic conductivity within the range of likely regional values (Table 4-1) has only a minor effect on model calibration. Consequently, even though varying hydraulic conductivity may be used to refine model calibration, further changes in hydraulic conductivity would not result in a significantly better representation of the groundwater system.

- Variation of recharge rates within the range of likely values also has only a minor effect on model calibration. Consequently, further changes in the rates would not result in a significantly better representation of the groundwater system.

- The range of likely values of river leakage factor is difficult to establish from published information. Hydraulic heads calculated by the model are shown to be very sensitive to this factor when the value assigned is low. In addition, because model results are not very sensitive to variation of other parameters within reasonable ranges, there is little freedom in the selection of the river leakage factor. As a result, the model itself can be used to establish a reasonable range of leakage values since values outside of this range produce meaningless results. The sensitivity of this particular model to the river leakage factor is caused by the effect of the collector wells, which obtain much of their water by induced infiltration from the river. When the induced infiltration is reduced by decreasing the leakage factor, drawdown due to pumping the wells increases greatly. Since the wells have been operating for more than 35 years, the riverbed clogging should not increase significantly in the future. Therefore, the river leakage factor considered to best represent the real system based on model results is not expected to change.

## 5.2 THREE-DIMENSIONAL FLOW MODEL

The 2DFLOW model was modified into a 3DFLOW model and updated with additional stratigraphy in order to better represent the real physical system.

TABLE 5-5

RESULTS OF THE SENSITIVITY ANALYSIS
FOR THE TWO-DIMENSIONAL FLOW MODEL
UTILIZING RUN 2DFLOW

| Sensitivity Run Number | Parameter | 2DFLOW Value | Sensitivity Run Value | Sensitivity Run[a] Statistics: Mean Residual (ft) | Sensitivity Run[a] Statistics: Mean Absolute Residual (ft) |
|---|---|---|---|---|---|
| 1 | Hydraulic Conductivity Zone I (ft/day) | 400 | 300 | 0.174 | 1.175 |
| 2 | Hydraulic Conductivity Zone I (ft/day) | 400 | 600 | 0.023 | 1.099 |
| 3 | Hydraulic Conductivity Zone III (ft/day) | 300 | 200 | 0.466 | 1.127 |
| 4 | Hydraulic Conductivity Zone VI (ft/day) | 300 | 200 | -0.447 | 1.36 |
| 5 | River Bed Leakage Factor ($day^{-1}$) | 0.5 | 0.05 | 3.694 | 3.839 |
| 6 | River Bed Leakage Factor ($day^{-1}$) | 0.5 | 0.25 | 0.745 | 1.240 |
| 7 | River Bed Leakage Factor ($day^{-1}$) | 0.5 | 1.0 | -0.284 | 1.186 |
| 8 | River Bed Leakage Factor ($day^{-1}$) | 0.5 | 5.0 | -0.638 | 1.416 |
| 9 | River Bed Leakage Factor ($day^{-1}$) | 0.5 | 50.0 | -0.729 | 1.494 |
| 10 | Recharge Rate Zone I (in/yr) | 14 | 20 | | |
| 10 | Recharge Rate Zone III (in/yr) | 6 | 8 | | |
| 10 | Recharge Zone IV (in/yr) | 6 | 8 | | |
| 10 | Recharge Rate Zone V (in/yr) | 6 | 8 | | |
| 10 | Recharge Rate Zone VI (in/yr) | 14 | 20 | | |
| 10 | | | | -0.434 | 1.301 |
| 11 | Recharge Rate Zone I (in/yr) | 14 | 10 | | |

See footnotes at end of table.

TABLE 5-5
(Continued)

| Sensitivity Run Number | Parameter | 2DFLOW Value | Sensitivity Run Value | Sensitivity Run[a] Statistics: Mean Residual (ft) | Sensitivity Run[a] Statistics: Mean Absolute Residual (ft) |
|---|---|---|---|---|---|
| 11 | Recharge Rate Zone III (in/yr) | 6 | 4 | | |
| 11 | Recharge Rate Zone IV (in/yr) | 6 | 4 | | |
| 11 | Recharge Rate Zone V (in/yr) | 6 | 4 | | |
| 11 | Recharge Rate Zone VI (in/yr) | 14 | 10 | | |
| 11 | | | | 0.534 | 1.117 |
| | | 2DFLOW STATISTICS: | | 0.083 | 1.080 |

[a]Mean Residual is the mean of the differences between observed heads and calculated heads. Mean Absolute Residual is the mean of the absolute differences between observed heads and calculated heads.

### 5.2.1 Extension of Input Data

The 3DFLOW model was developed by using the 2DFLOW model grid and separating the vertical extent of the aquifer into five distinct layers. The layers were designed in accordance with the following guidelines:

- Simulate the hydrologic effects of a clay interbed that is present beneath much of the FEMP property.
- Provide sufficient layers for realistic three-dimensional simulation of contaminant plumes originating from sources at the ground surface.
- Avoid causing pumping wells and monitoring wells to be screened in more than one layer. While the SWIFT III code can handle pumping wells that have screened intervals in more than one layer, model construction is slightly easier. Calibration is also simpler if each monitoring well is assigned to a single layer.

The layers were developed through the use of 12 intersecting cross sections, described in Section 2.5, taking care to maintain consistency across adjacent sections. The result was layers of fairly consistent thickness and elevation throughout the model, but with some variation in layer thicknesses and elevations resulting from the above guidelines. The elevations of the base of each layer were then interpolated between cross sections and entered into the model input data.

Figure 5-7 shows the locations of Cross-Sections Q-Q' and R-R'. The layers created for the model are shown in Figures 5-8 and 5-9. The top layer, Layer 1, represents the upper part of the Great Miami Aquifer that contains the water table. Layer 3 represents the clay interbed that is present beneath the FEMP. Where the clay is not present, Layer 3 is treated as sand and gravel material of the Great Miami Aquifer and assigned an appropriate hydraulic conductivity. Layer 2 represents the lower part of the upper aquifer, which is immediately above the clay interbed. Layers 4 and 5 divide the lower aquifer into two parts to realistically simulate the part of the aquifer serving the pumping wells, and to provide for better simulation of vertical contaminant dispersion.

### 5.2.2 Model Calibration Approach

The layout of grid rows and columns used in the 2DFLOW model (Figure 5-1) was also assigned to the 3DFLOW model. Values for the Great Miami River stage, water well pumping rates, boundary heads, elevation of the bedrock surface, and hydraulic conductivity of the bedrock were imported from the calibrated 2DFLOW model. The combined pumping rate for the Albright & Wilson Company wells was changed from 100 gpm to 445 gpm to 225 gpm during the course of the modeling as new information was received. The value used for final calibration was 225 gpm. Initial values for horizontal hydraulic conductivity, recharge rates, and river leakage factor were also derived from the 2DFLOW model; however, hydraulic conductivity and recharge rates were subsequently changed, as necessary, during the 3DFLOW model calibration.

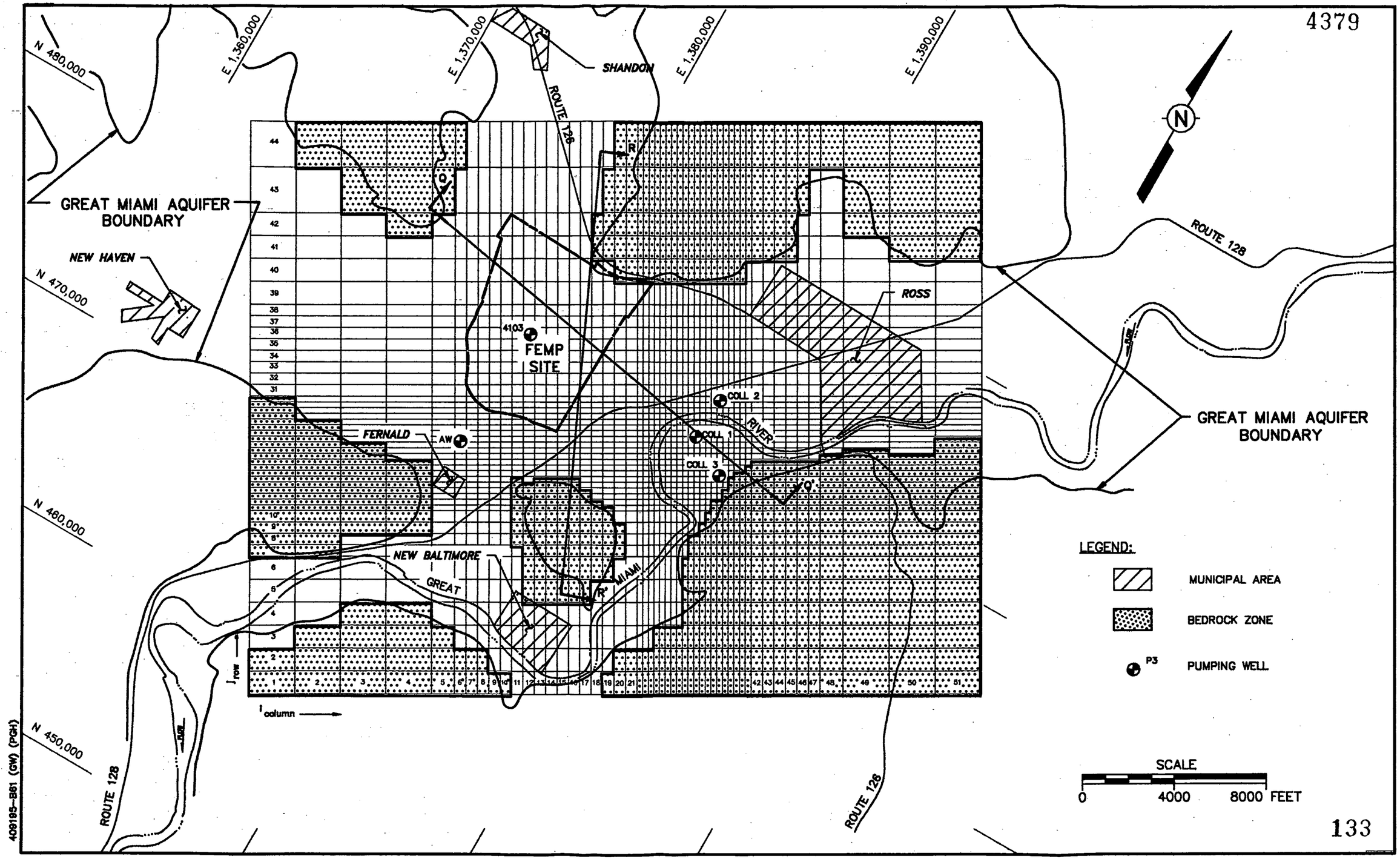


FIGURE 5-7
SWIFT III FLOW MODEL GRID
FOR RI/FS MODEL AREA
WITH CROSS SECTION LOCATIONS

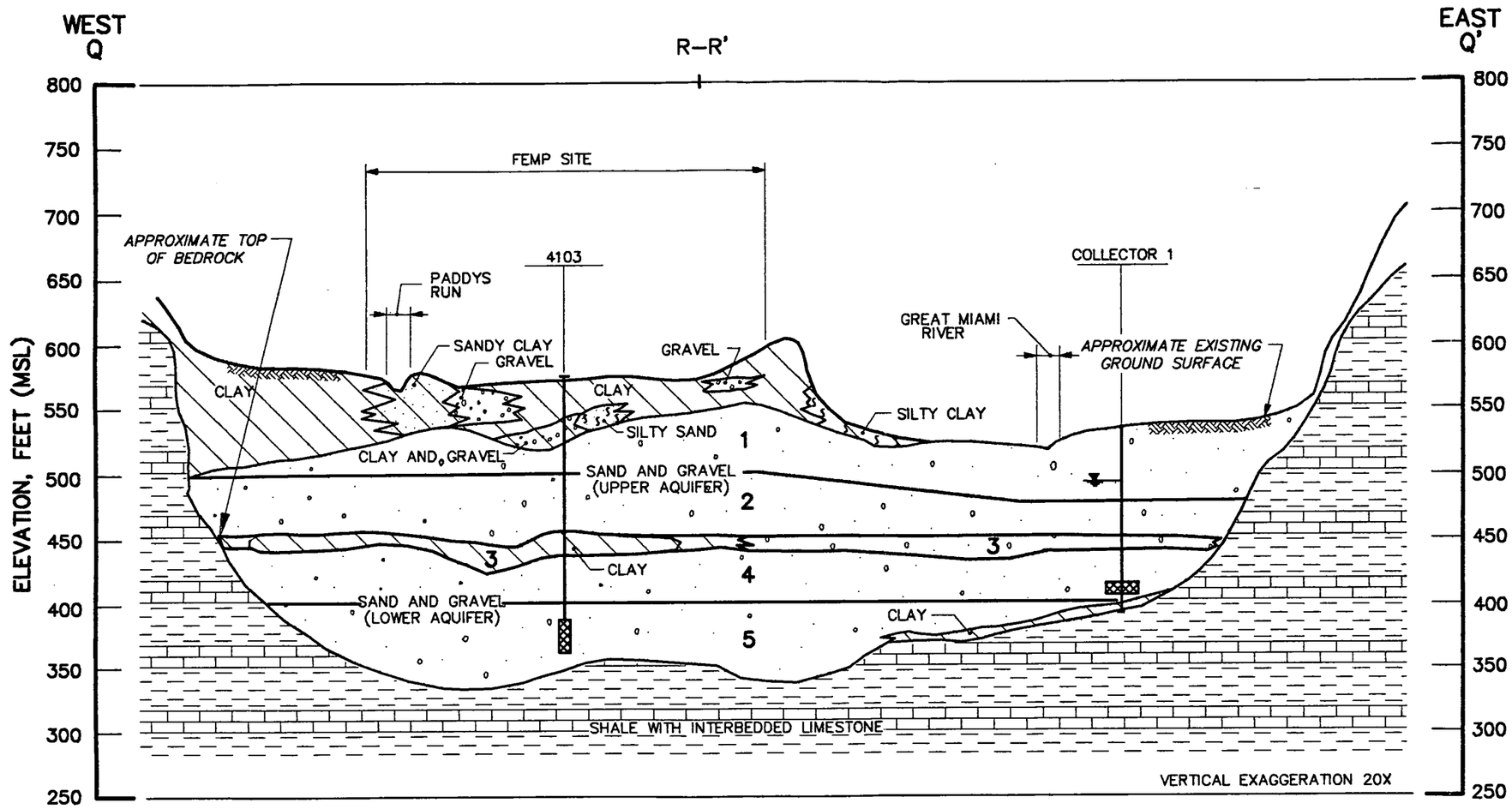


THE BORING LOGS AND RELATED INFORMATION DEPICT SUBSURFACE CONDITIONS ONLY AT THE SPECIFIC LOCATIONS AND DATES INDICATED. SOIL CONDITIONS AND WATER LEVELS AT OTHER LOCATIONS MAY DIFFER FROM CONDITIONS OCCURRING AT THESE BORING LOCATIONS. ALSO THE PASSAGE OF TIME MAY RESULT IN A CHANGE IN THE CONDITIONS AT THESE BORING LOCATIONS.

THE DEPTH AND THICKNESS OF THE SUBSURFACE STRATA INDICATED ON THE SECTIONS WERE GENERALIZED FROM AND INTERPOLATED BETWEEN THE TEST BORINGS. INFORMATION ON ACTUAL SUBSURFACE CONDITIONS EXISTS ONLY AT THE LOCATION OF THE TEST BORINGS AND IT IS POSSIBLE THAT SUBSURFACE CONDITIONS BETWEEN THE TEST BORINGS MAY VARY FROM THOSE INDICATED.

VERTICAL SCALE

0 100 200 FEET

HORIZONTAL SCALE

0 2000 4000 FEET

LEGEND:

WATER LEVELS (MEASURED 3/27/86 THROUGH 4/11/86)

2 HYDROGEOLOGIC LAYER USED IN SWIFT III MODELS

OPEN OR SCREENED INTERVAL

NOTE:

FOR LOCATION OF CROSS SECTION Q–Q', SEE FIGURE 5–7

REFERENCES:

MODIFIED FROM U.S.G.S. PROFESSIONAL PAPER NO. 605–A USING AVAILABLE OHIO STATE WATER WELL RECORDS, SOWC WATER WELL DATA, DAMES & MOORE'S "FEED MATERIALS PRODUCTION CENTER GROUNDWATER STUDY, TASK C REPORT" FOR THE DOE (1985), AND IT (1986) RI/FS BORING LOGS.

## CROSS SECTION Q–Q'

(LOOKING NORTH)

409195–B45 (GW) (PGH)



FIGURE 5–8
GEOLOGIC CROSS SECTION Q–Q'
SHOWING MODEL LAYERS

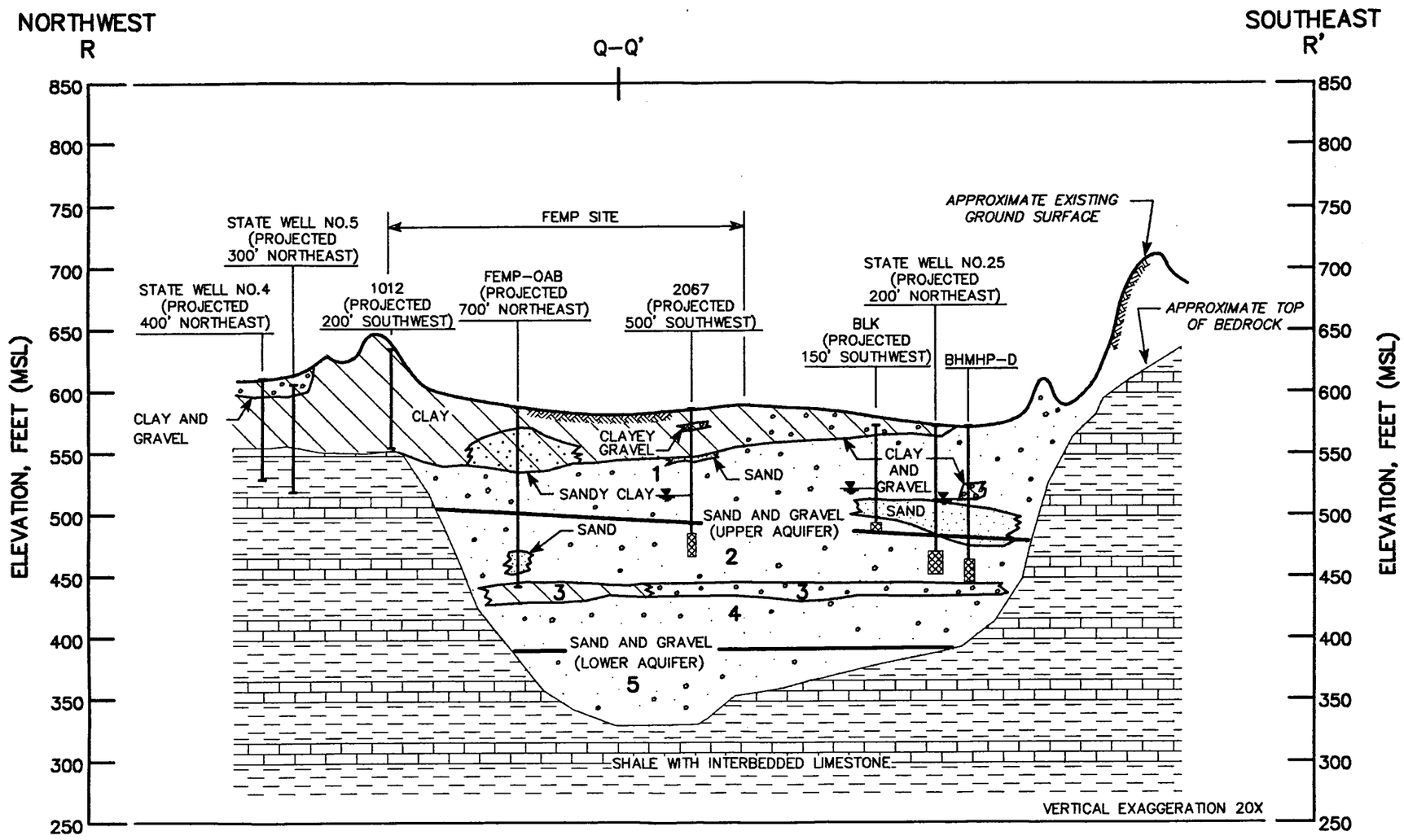


## CROSS SECTION R–R'

(LOOKING NORTHEAST)

THE BORING LOGS AND RELATED INFORMATION DEPICT SUBSURFACE CONDITIONS ONLY AT THE SPECIFIC LOCATIONS AND DATES INDICATED. SOIL CONDITIONS AND WATER LEVELS AT OTHER LOCATIONS MAY DIFFER FROM CONDITIONS OCCURRING AT THESE BORING LOCATIONS. ALSO THE PASSAGE OF TIME MAY RESULT IN A CHANGE IN THE CONDITIONS AT THESE BORING LOCATIONS.

THE DEPTH AND THICKNESS OF THE SUBSURFACE STRATA INDICATED ON THE SECTIONS WERE GENERALIZED FROM AND INTERPOLATED BETWEEN THE TEST BORINGS. INFORMATION ON ACTUAL SUBSURFACE CONDITIONS EXISTS ONLY AT THE LOCATION OF THE TEST BORINGS AND IT IS POSSIBLE THAT SUBSURFACE CONDITIONS BETWEEN THE TEST BORINGS MAY VARY FROM THOSE INDICATED.

VERTICAL SCALE

0 100 200 FEET

HORIZONTAL SCALE

0 2000 4000 FEET

**LEGEND:**

- WATER LEVELS (MEASURED 3/27/86 THROUGH 4/11/86)
- 2 — HYDROGEOLOGIC LAYER USED IN SWIFT III MODELS
- OPEN OR SCREENED INTERVAL

**NOTE:**

FOR LOCATION OF CROSS SECTION R–R', SEE FIGURE 5–7

**REFERENCES:**

MODIFIED FROM U.S.G.S. PROFESSIONAL PAPER NO. 605–A USING AVAILABLE OHIO STATE WATER WELL RECORDS, SOWC WATER WELL DATA, DAMES & MOORE'S "FEED MATERIALS PRODUCTION CENTER GROUNDWATER STUDY, TASK C REPORT" FOR THE DOE (1985), AND IT (1986) RI/FS BORING LOGS.

409195–B48 (GW) (PGH)



FIGURE 5–9
GEOLOGIC CROSS SECTION R–R'
SHOWING MODEL LAYERS

The clay interbed was given an initial horizontal hydraulic conductivity of 0.0003 ft/day ($1 \times 10^{-7}$ cm/s) and a vertical hydraulic conductivity of 0.00003 ft/day ($1 \times 10^{-8}$ cm/s). The value for horizontal hydraulic conductivity was estimated from published information on the range of hydraulic conductivity values for clay (Freeze and Cherry 1979, p. 29; Fetter 1980, p. 75; Todd 1959, p. 53). The initial ratio of vertical to horizontal hydraulic conductivity was assumed to be 1/10 throughout the model. This value resulted in adequate simulation of the vertical hydraulic gradient across the interbed. This ratio was based on typical published values and was subject to calibration and sensitivity analysis, as described below.

Calibration of the 3DFLOW model was performed against the same April 1986 data (Table 5-1) that were used for the 2DFLOW model. The calibration procedure was also similar to the procedure followed for 2DFLOW. Each observed monitoring well water level was compared to the computed hydraulic head in the appropriate cell in the layer that represented the depth of the well or screened interval; that is, residuals were assigned to their locations in the appropriate layer of the model. Wells where data were not available to ascertain the well depth or screened interval were assumed to be completed at the midpoint between the base of the aquifer and the water table. The statistical criteria used to test for the adequacy of calibration were the same as those used for 2DFLOW, and the judgment of the engineers and geologists working on the project was still applied.

### 5.2.3 Model Calibration Results

The distribution of hydraulic conductivities upon calibration of the 3DFLOW model are shown for the five layers in Figures 5-10 through 5-14. The figures show the increase in hydraulic conductivity and the decrease in width of the bedrock valley with depth.

In general, hydraulic conductivities were increased compared to those in 2DFLOW. While there is no direct way to determine why the increase was necessary for improved model performance, the features of 3DFLOW that would tend to affect hydraulic conductivity are (1) the effect of the clay interbed, which inhibited the effects of recharge in the FEMP area and movement of water coming from the Shandon Tributary; and (2) hydraulic head losses due to vertical flow components that are not represented in 2DFLOW. Hydraulic conductivities were increased more in the lower layers than in the upper layers. This redistribution helped avoid clustering of negative residuals at the FEMP site, which indicated that calculated hydraulic heads were too high. The distribution also helped to increase the vertical hydraulic gradient across the clay interbed and decrease the hydraulic head in the lower aquifer. The latter condition resulted in a better hydraulic connection between the lower aquifer and the collector wells and other downgradient discharge locations. Changes in hydraulic conductivities in the upper part of the Great Miami Aquifer produced small modifications in the hydraulic gradient, thereby effecting a better match between calculated and observed water levels within the FEMP site.

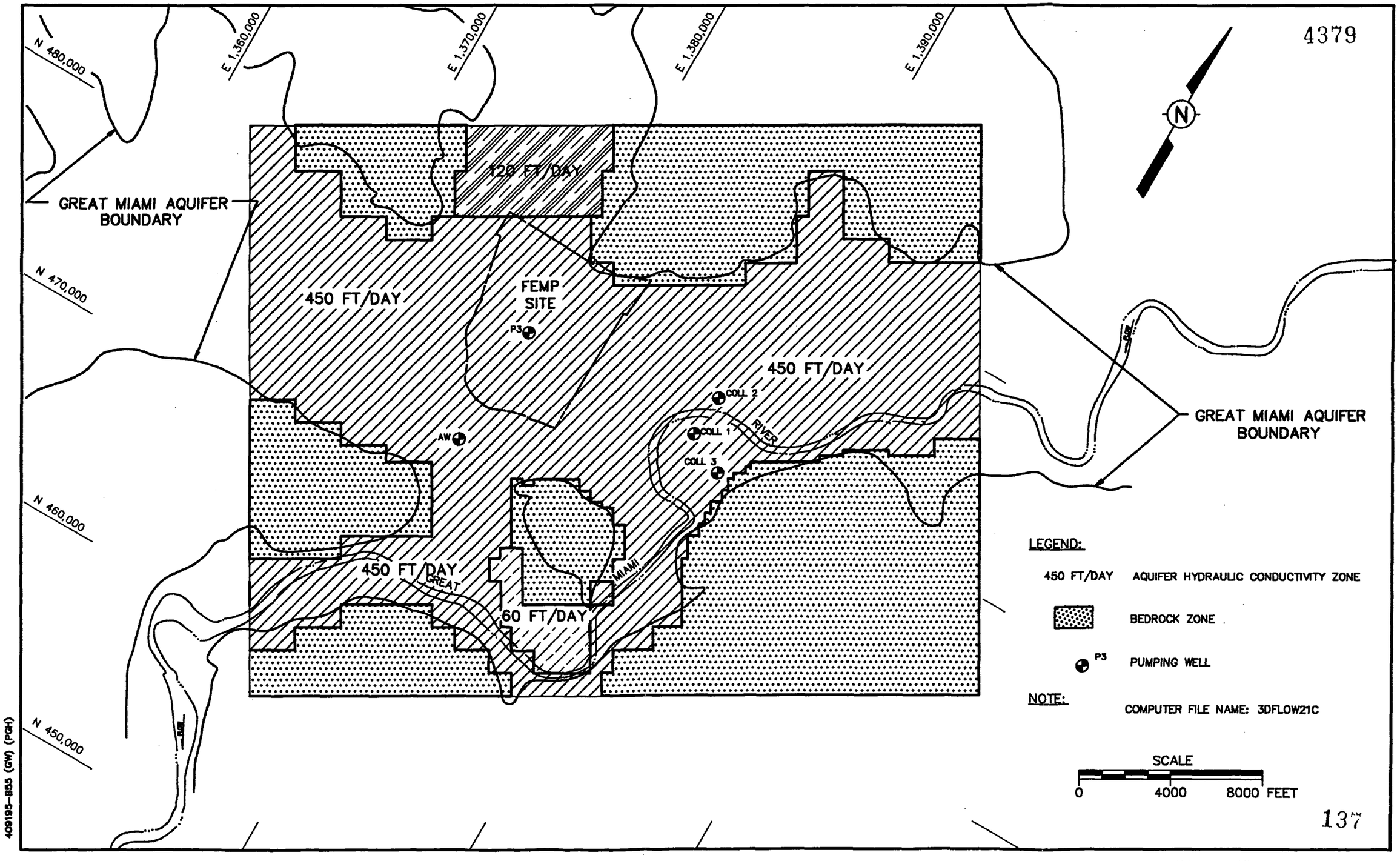




FIGURE 5-10
3-DIMENSIONAL FLOW MODEL
HYDRAULIC CONDUCTIVITY ZONES
LAYER 1

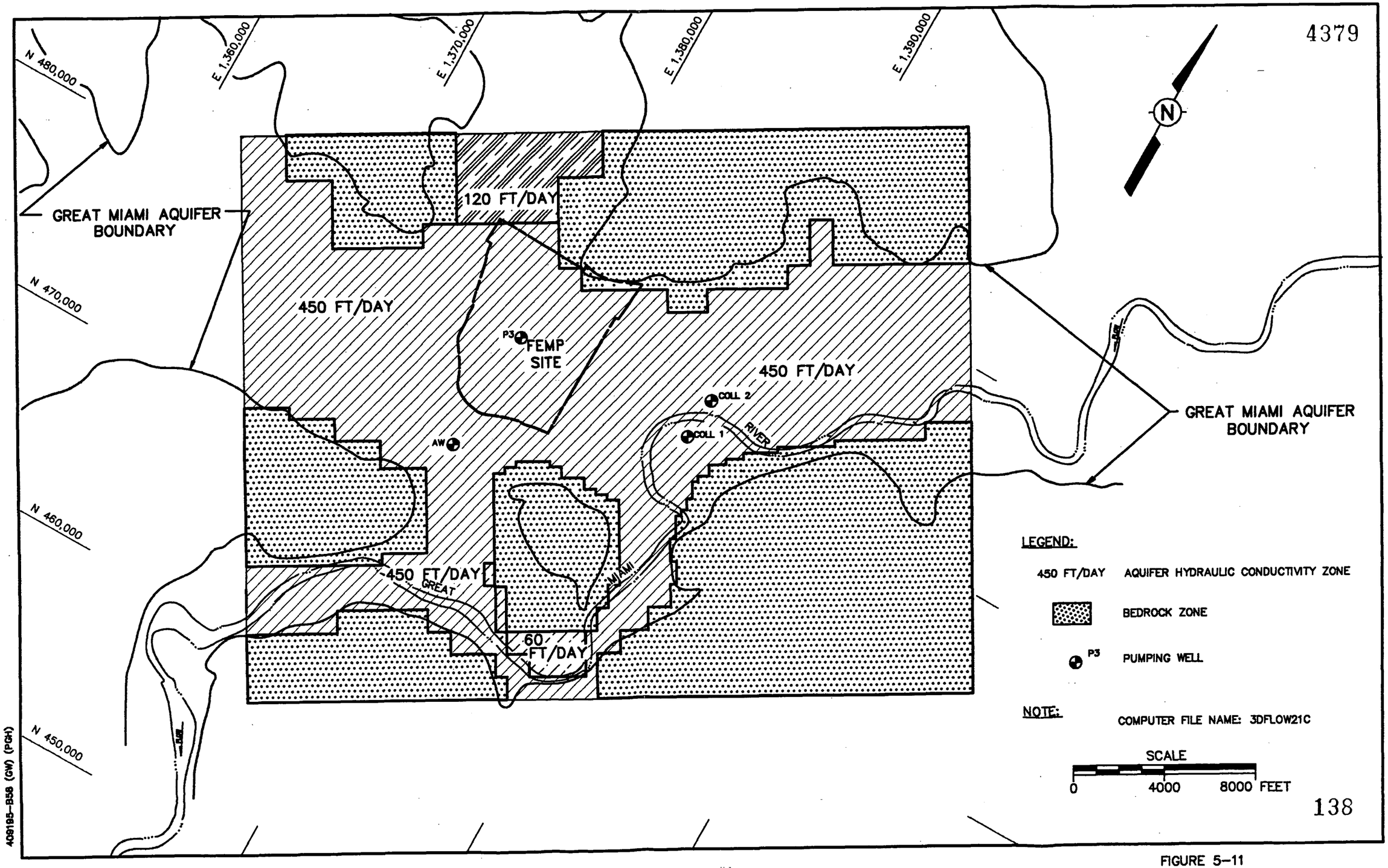




FIGURE 5-11
3-DIMENSIONAL FLOW MODEL
HYDRAULIC CONDUCTIVITY ZONES
LAYER 2

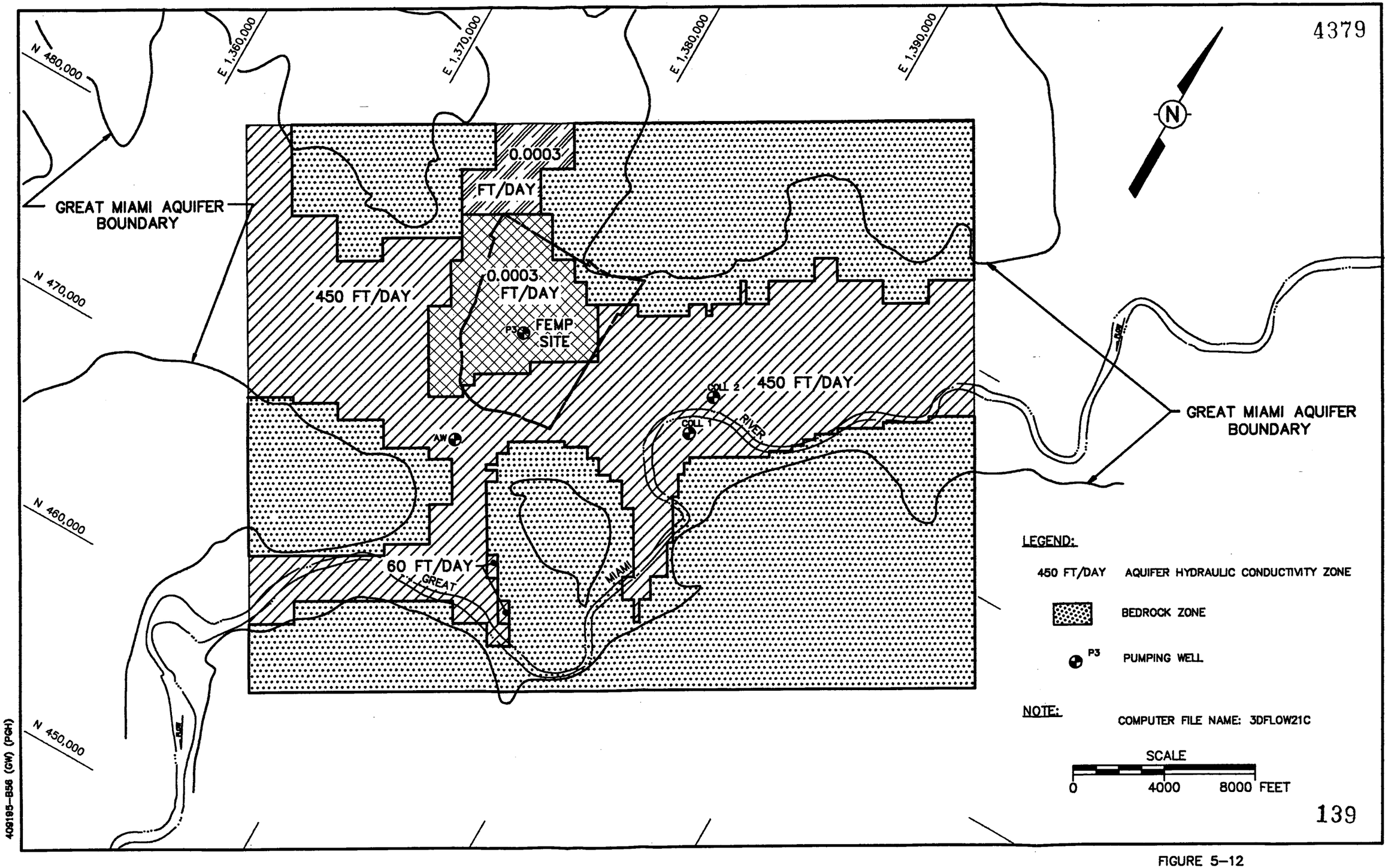




FIGURE 5-12
3-DIMENSIONAL FLOW MODEL
HYDRAULIC CONDUCTIVITY ZONES
LAYER 3

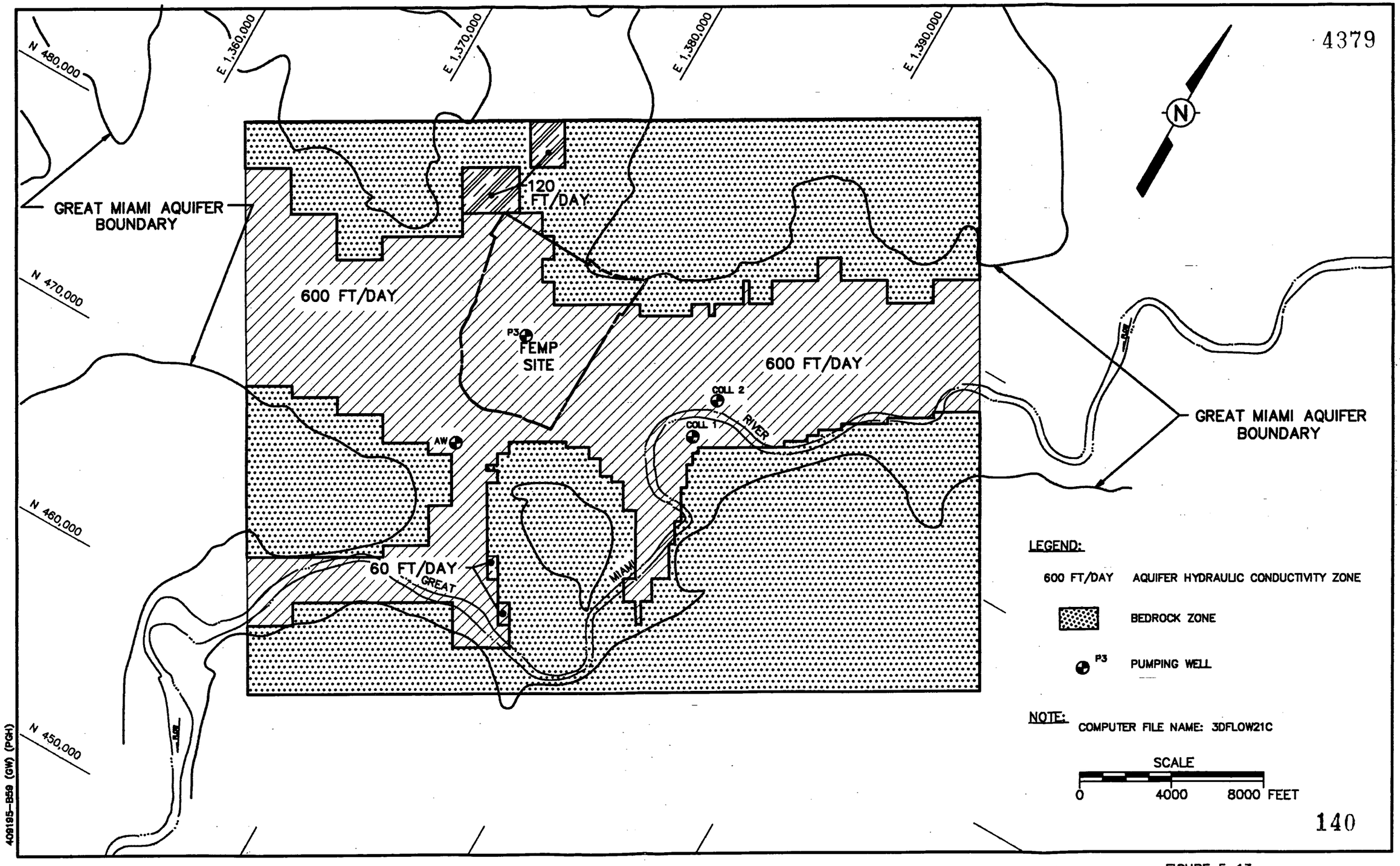




FIGURE 5-13
3-DIMENSIONAL FLOW MODEL
HYDRAULIC CONDUCTIVITY ZONES
LAYER 4

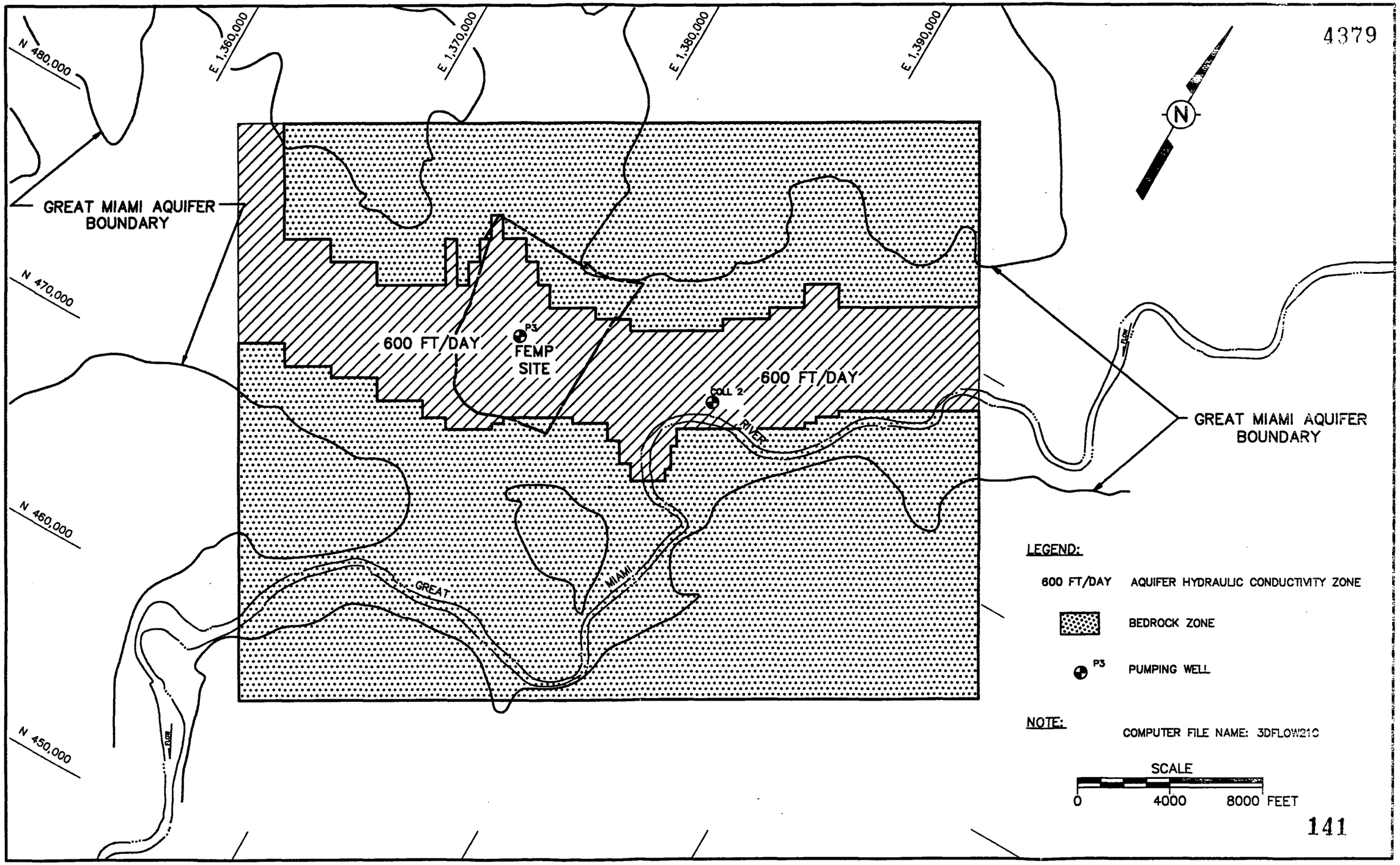




FIGURE 5–14
3–DIMENSIONAL FLOW MODEL
HYDRAULIC CONDUCTIVITY ZONES
LAYER 5

Recharge rates were also changed to help remove clustering of negative residuals across the FEMP site. The recharge rate over part of the site was reduced to 2 in./yr so that less water would have to drain from the aquifer above the clay interbed to maintain the hydraulic head values near observed levels. This reduction in simulated recharge rate is consistent with the industrial use of the site. Factors reducing recharge include water carried away from the site by storm sewers draining roofed and paved areas, precipitation falling on lined ponds, runoff and evaporation from roads, and increased runoff and evaporation from soils compacted by the industrial activities at the site. The recharge rates used in the calibrated model are shown in Figure 5-15.

Some small refinements were made where the north boundary of the model intersects the Shandon Tributary. Boundary heads were lowered by 0.5 foot and the bedrock configuration was modified to produce a more realistic valley cross section. These changes were in conjunction with changes in hydraulic conductivity in the tributary to refine the calibration in the northern part of the FEMP. The boundary heads elsewhere in the model remained the same as those in 2DFLOW. The river leakage factor remained at 0.5 $day^{-1}$, unchanged from 2DFLOW.

The residual heads achieved by the calibration runs are indicated in Figures 5-16 through 5-18, which show the magnitude and distribution of the residuals. Further reduction of the residuals was not warranted. The predetermined statistical criteria described in Section 5.1.4 were satisfied, with a minor deviation observed for the regression coefficient, as shown in Table 5-6. In addition, a water balance was calculated for the same area covered by the water balance for 2DFLOW. The calculated inflows and outflows are shown in Table 5-7. The inflow/outflow ratio is 1.002; imbalance is 0.2 percent.

The model results were also compared to field data by checking computed versus observed vertical hydraulic gradients. Hydraulic heads measured at different depths in monitoring well clusters were compared to calculated heads at those depths. Seven suitable monitoring well clusters were available for this comparison. One was in the area of the clay interbed at the FEMP site. This cluster had a monitoring well completed above the clay layer at the depth of Model Layer 2 and another monitoring well completed below the clay layer at the depth of Layer 5. The head difference measured in the field was 0.65 foot. The corresponding computed head difference was 1.04 feet. Given the greater complexity of the prototype system compared to model system, this result indicates that vertical gradients are being adequately represented. The other clusters were outside of the area of the clay interbed. For these clusters, measured head differences were very low because the vertical hydraulic conductivity of the aquifer is high and a large vertical gradient is not required to maintain vertical flow components. The maximum measured vertical head difference in these clusters was 0.38 foot. The computed head difference at that location was zero. This result may be due to the presence of some minor clay bed that would be impractical to simulate. Comparisons between observed and computed

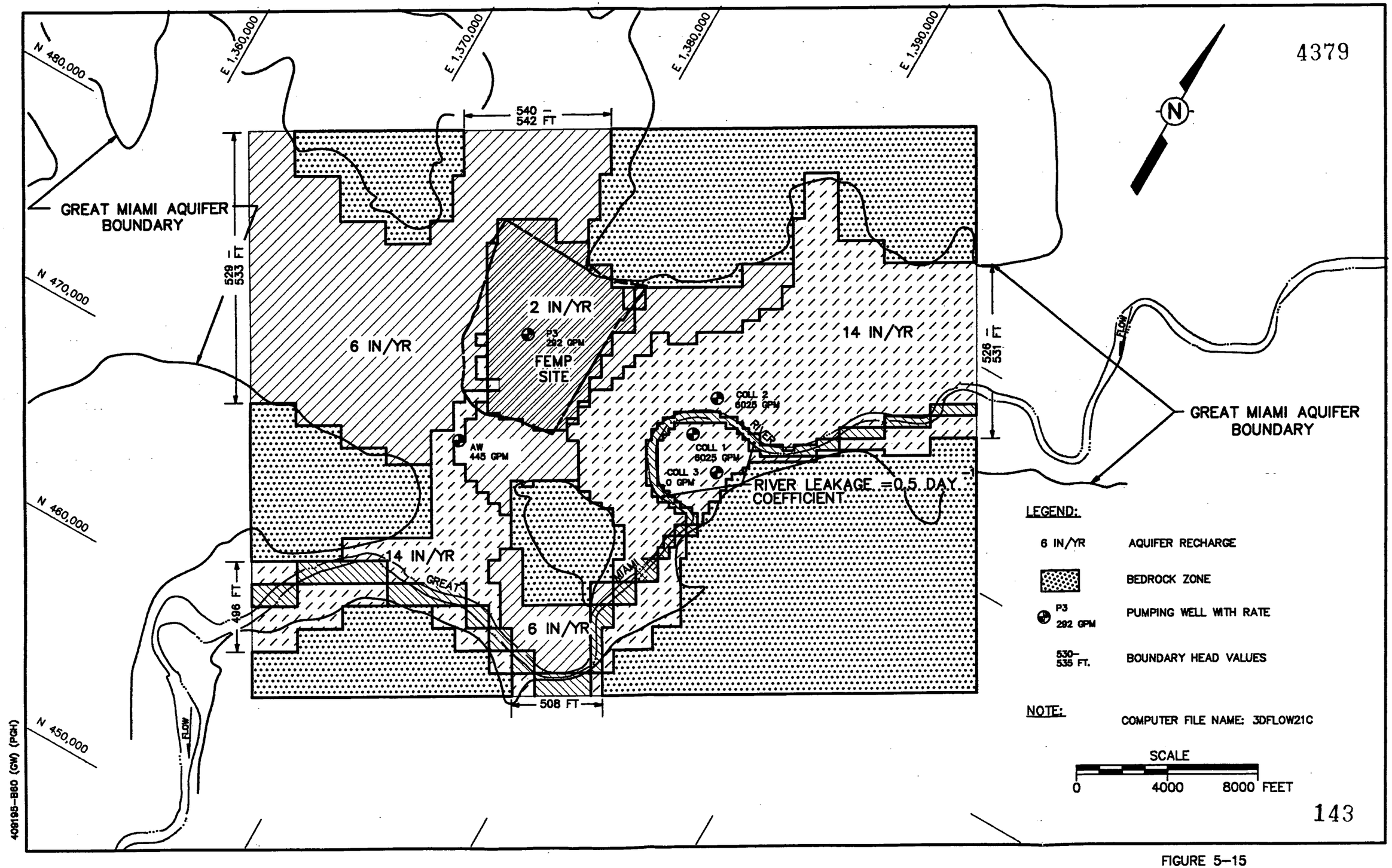




FIGURE 5–15
3–DIMENSIONAL FLOW MODEL
RECHARGE ZONES, PUMPING RATES,
AND BOUNDARY HEADS

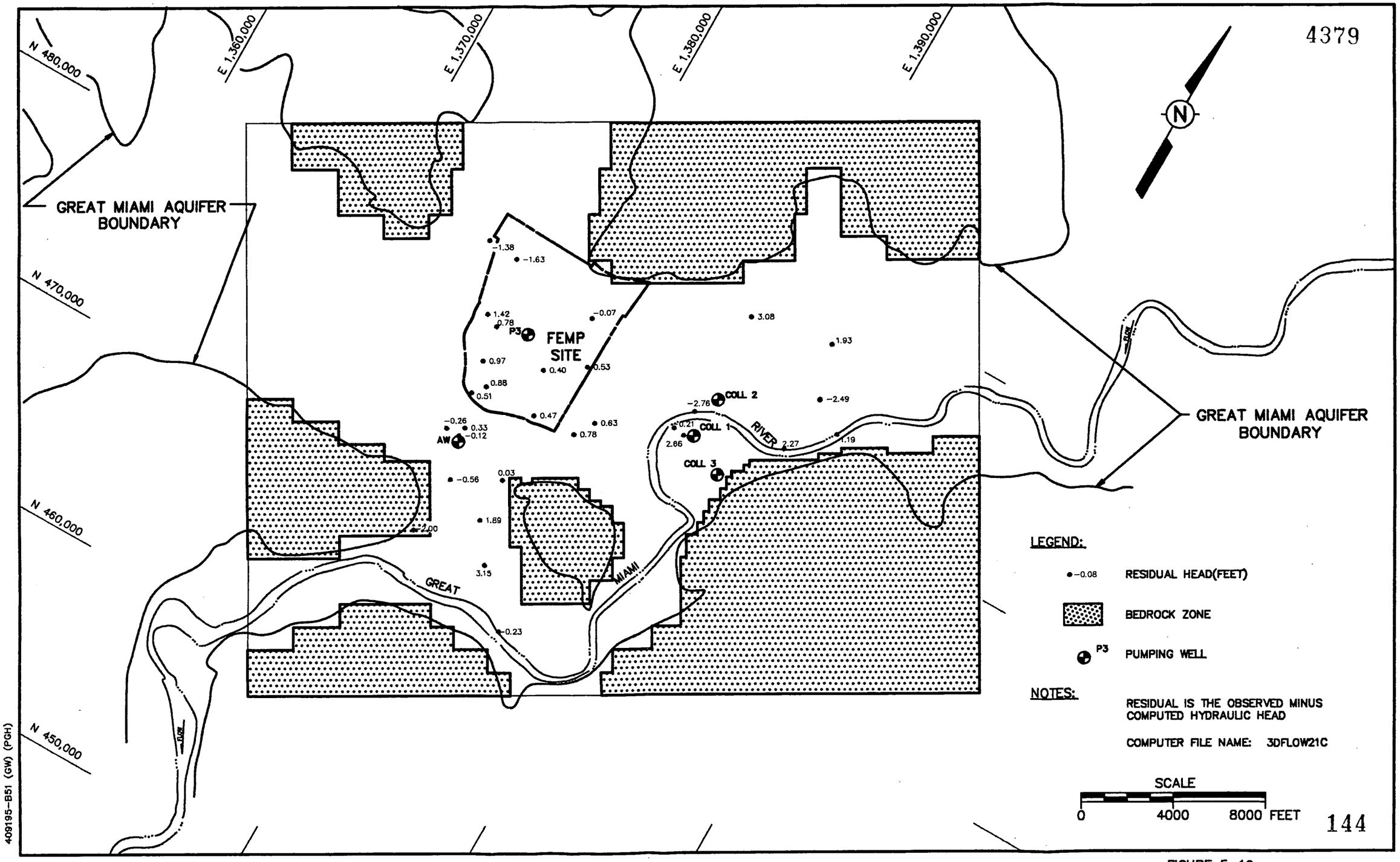




FIGURE 5-16
3-DIMENSIONAL FLOW MODEL
RESIDUAL HEADS FOR CALIBRATED RUN
APRIL 1986 DATA
LAYER 1

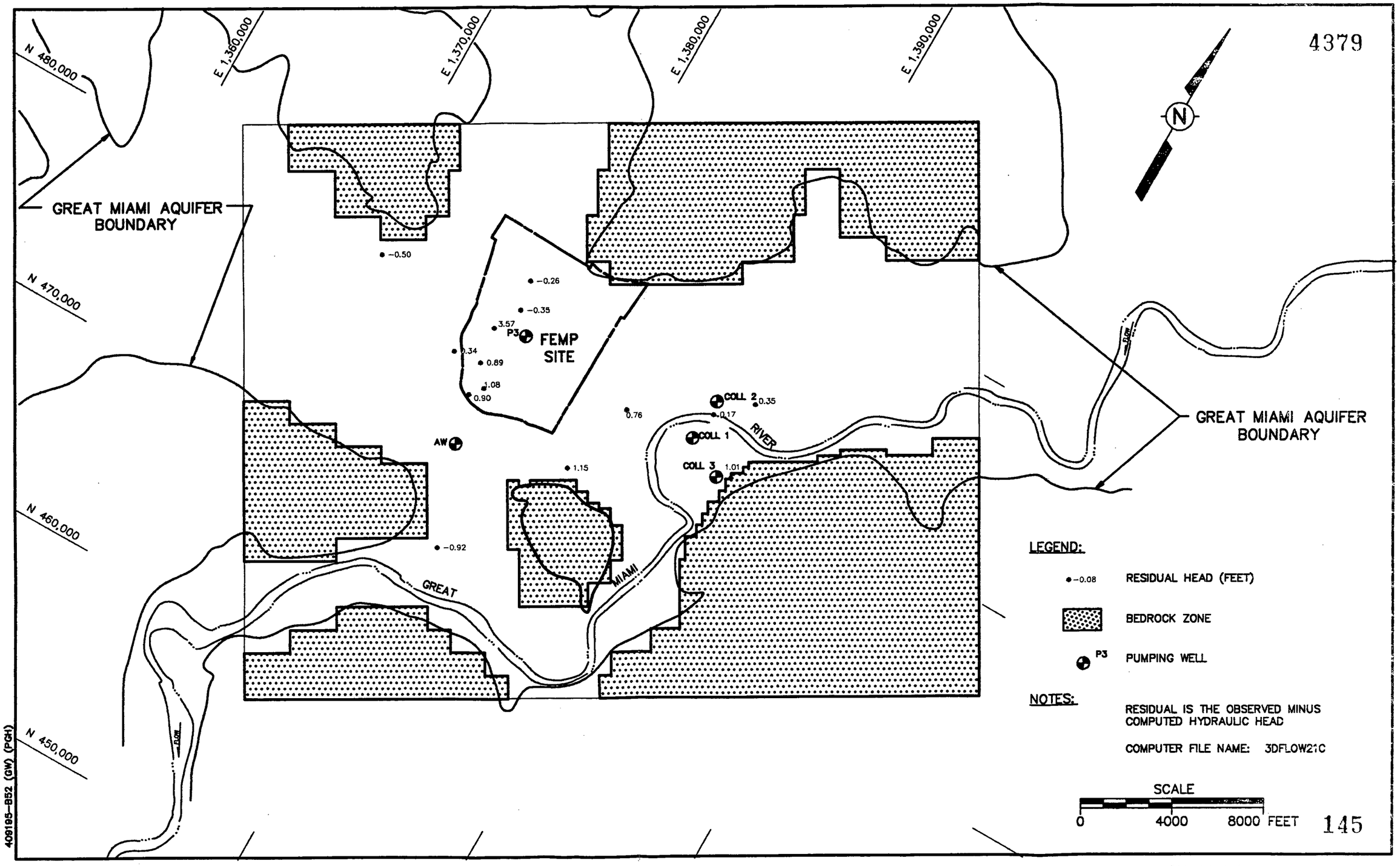




FIGURE 5-17
3-DIMENSIONAL FLOW MODEL
RESIDUAL HEADS FOR CALIBRATED RUN
APRIL 1986 DATA
LAYER 2

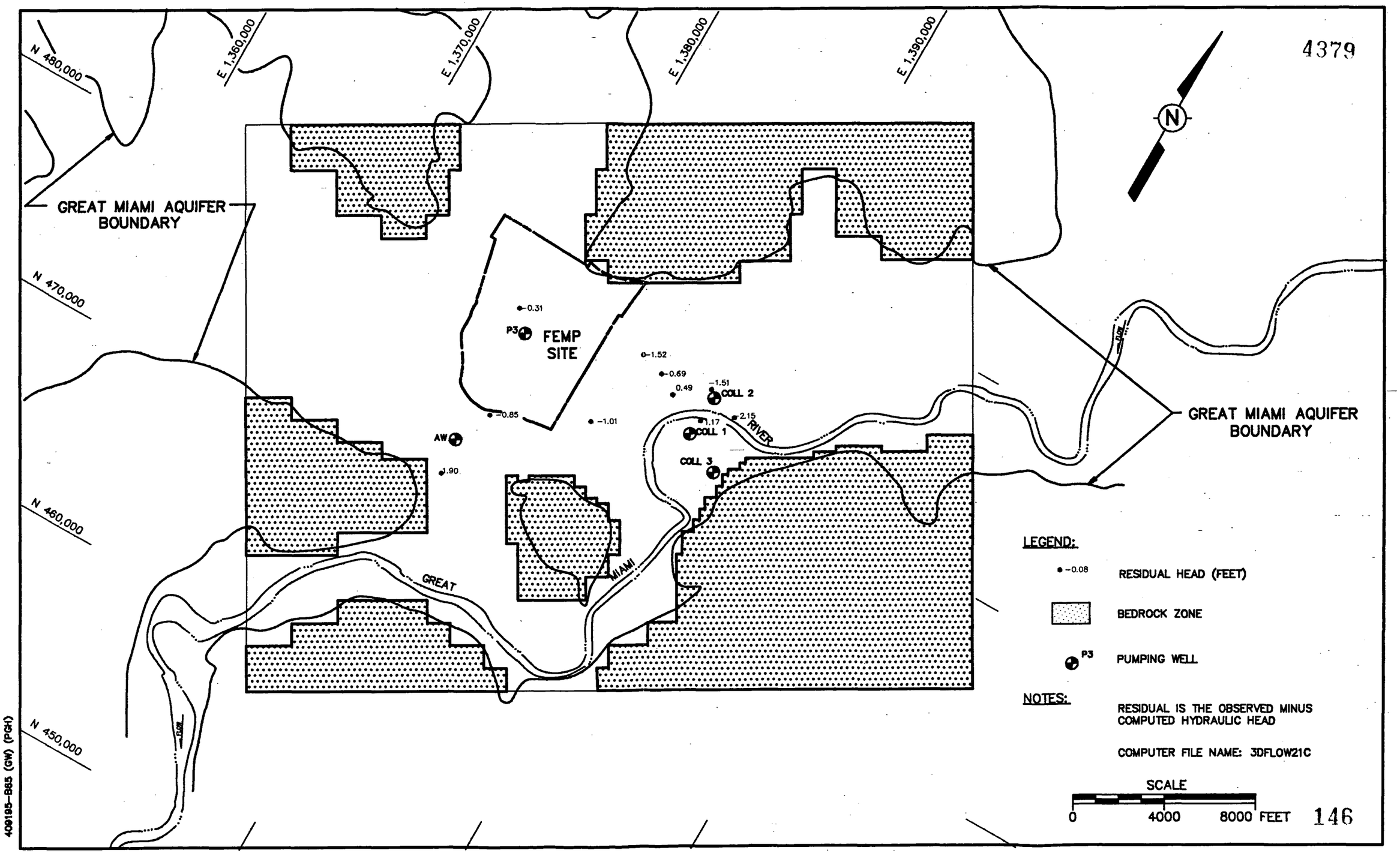




FIGURE 5-18
3-DIMENSIONAL FLOW MODEL
RESIDUAL HEADS FOR CALIBRATED RUN
APRIL 1986 DATA
LAYERS 3,4,5

## TABLE 5-6
## STATISTICAL TESTS FOR 3DFLOW MODEL CALIBRATION

| Statistical Measure | Predetermined Criteria | 3-D Flow 1986 (3DFLOW) |
|---|---|---|
| Mean Residual (Observed Minus Computed Head) (ft) | $\pm$ 0.5 | 0.326 |
| Mean of The Absolute Residuals (ft) | $\leq$ 2 | 1.083 |
| Standard Deviation of Differences (ft) | $\leq$ 3 | 1.365 |
| Regression Coefficient Between Measured and Computed Values | 1 $\pm$ 0.05 | 0.937 |
| Nearest Neighbor Autocorrelation Unit Normal Deviate | < 1.645 | 0.673 |

# TABLE 5-7
## WATER BALANCE IN THE VICINITY OF THE SOUTHWESTERN OHIO WATER COMPANY COLLECTOR WELL FOR THE THREE-DIMENSIONAL FLOW MODEL

| Inflow Locations | Inflow Rates (Cubic Feet Per Day) | (Mgd) |
|---|---|---|
| West Boundary, I - 21, J = 10-39 | 235,128 | 1.76 |
| East Boundary, I = 50, J = 22-40 | 327,720 | 2.45 |
| North Boundary, I = 46-49, J = 41 | 26,671 | 0.20 |
| Great Miami River Leakage | 1,693,089 | 12.66 |
| Recharge | 308,227 | 2.31 |
| Total Inflow | 2,590,835 | 19.38 |
| **Outflow Locations** | **Outflow Rates (Cubic Feet Per Day)** | **(Mgd)** |
| South Boundary, I = 21-32, J = 10 | 101,327 | 0.76 |
| Collector Wells | 2,317,307 | 17.33 |
| Discharge to Great Miami River | 166,676 | 1.25 |
| Total Outflow | 2,585,310 | 19.34 |
| Inflow/Outflow Ratio | 1.002 | |
| Inflow/Outflow Imbalance | 0.2% | |

head differences were better at other clusters. In summary, the model is adequately representing vertical head differences, and further calibration to match local influences on vertical hydraulic gradient is not warranted.

The simulated groundwater flow system that resulted from the 3DFLOW model calibration is shown for Layers 1 through 5 in Figures 5-19 through 5-23, respectively. Some large vectors were automatically deleted from the vector maps to improve their appearance and legibility. Such anomalies occur in areas near the collector wells and in the Paddys Run Outlet. The circles on the tails of the vectors indicate the vertical velocity component. The sizes of the circles are proportional to the rates of vertical movement. Over much of the area, the vertical velocities are so low that the circles are not discernible. Features of the simulated flow system include the following:

- Most of the groundwater in the Great Miami Aquifer above the clay interbed at the FEMP comes from the Shandon Tributary, while the groundwater in the Great Miami Aquifer below the interbed comes from the main bedrock valley to the west.

- Groundwater flow directions above and below the clay interbed beneath the FEMP are different. For example, the direction of the horizontal component of flow in a representative cell in the waste storage area differs by about 60 degrees between Layer 1 and Layer 4, which are above and below the clay interbed, respectively. Further south, the difference decreases, but it is as great as 20 degrees under much of the FEMP.

- The horizontal hydraulic gradient above the clay interbed is slightly higher than the horizontal gradient below the interbed.

- The hydraulic head difference across the clay interbed ranges to more than a foot, with the hydraulic head above the interbed being greater than the head below (i.e., downward flow component).

The difference in flow directions above and below the clay interbed has a noteworthy consequence when compared to the vertically integrated results of the 2DFLOW model. That is, the flow direction in Layer 1 in the waste storage area is found to be about 35 degrees different from the corresponding flow direction in 2DFLOW. Furthermore, consideration of vertical variants results in a simulated source-receptor relationship in 3DFLOW that is different from that of 2DFLOW. The 2DFLOW model shows virtually all of the groundwater from beneath the waste storage area moving toward the collector wells; but 3DFLOW shows much of the water from beneath the waste storage area moving toward the Great Miami River downstream from the collector wells. The results of the 3DFLOW model in the FEMP area are more representative of the natural system than the 2DFLOW results.

### 5.2.4 Sensitivity Analysis

Sensitivity analysis for 3DFLOW was performed on two interim calibrated runs that were available prior to completion of the calibration. This sensitivity analysis not only provided information on the

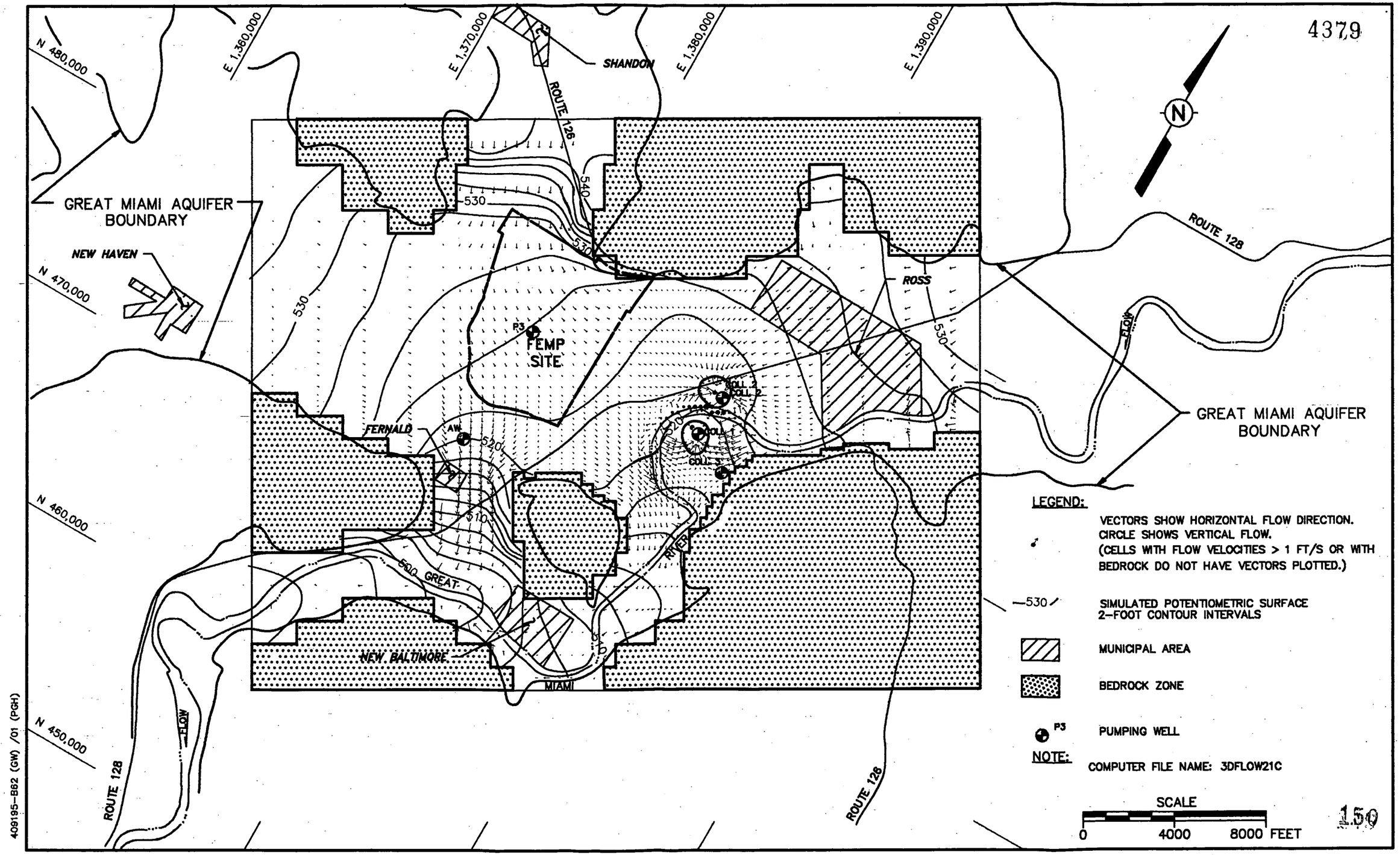




FIGURE 5-19

3-DIMENSIONAL FLOW MODEL
CALIBRATED RUN, LAYER 1
FLOW VECTORS AND POTENTIOMETRIC SURFACE

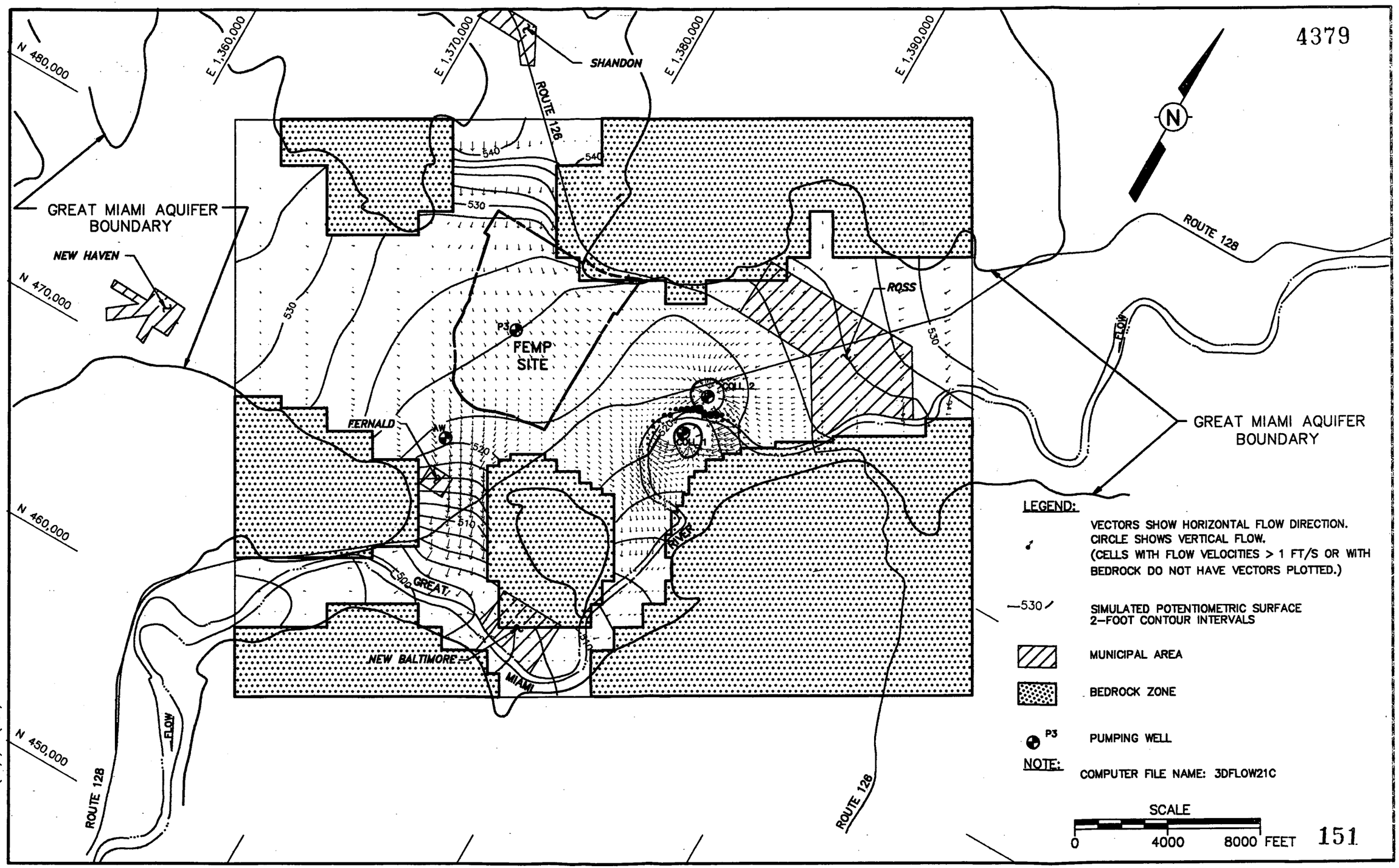




FIGURE 5-20

3-DIMENSIONAL FLOW MODEL
CALIBRATED RUN, LAYER 2
FLOW VECTORS AND POTENTIOMETRIC SURFACE

409195-B54 (GW) /01 (PGH)

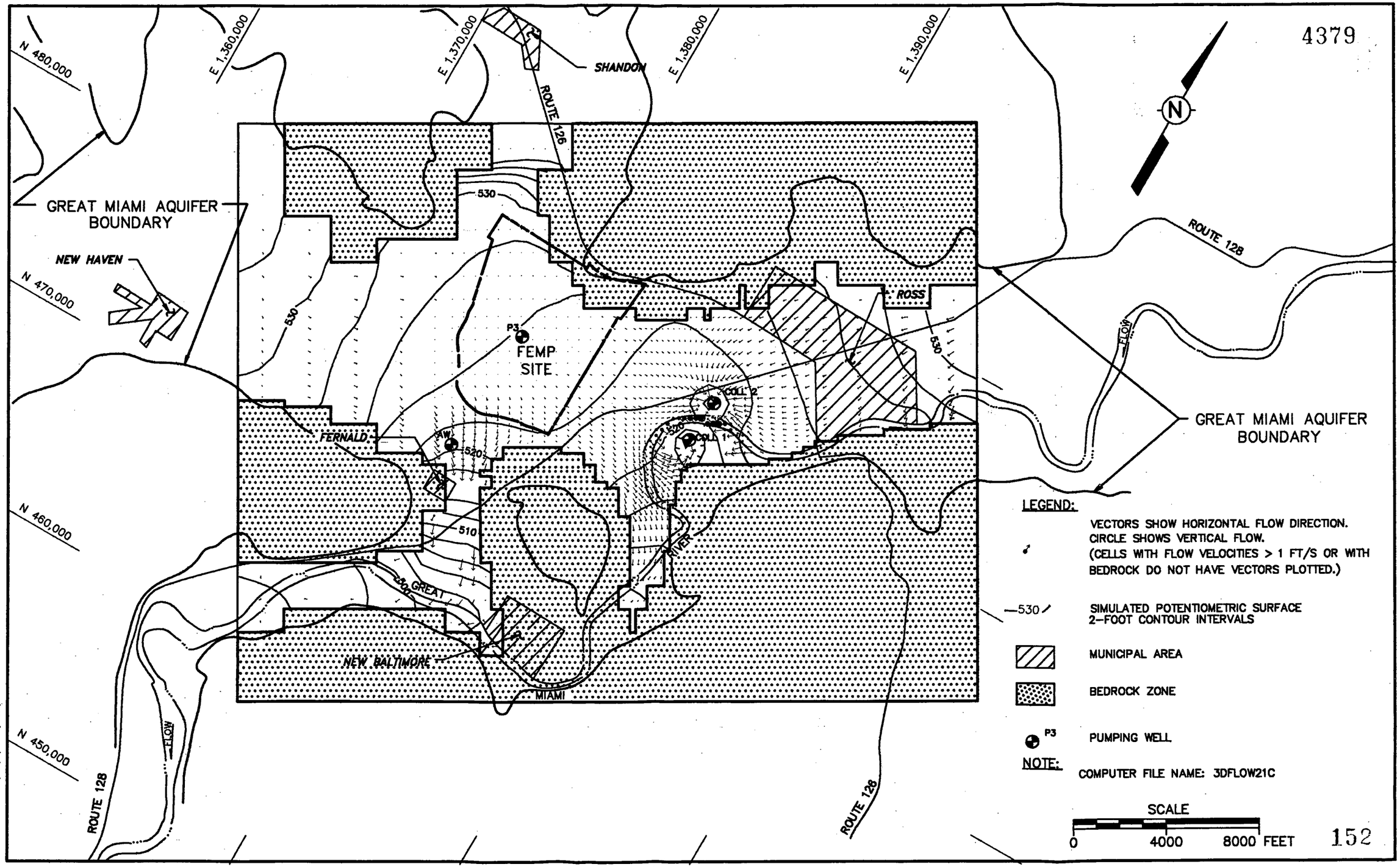


FIGURE 5-21

3-DIMENSIONAL FLOW MODEL
CALIBRATED RUN, LAYER 3
FLOW VECTORS AND POTENTIOMETRIC
SURFACE

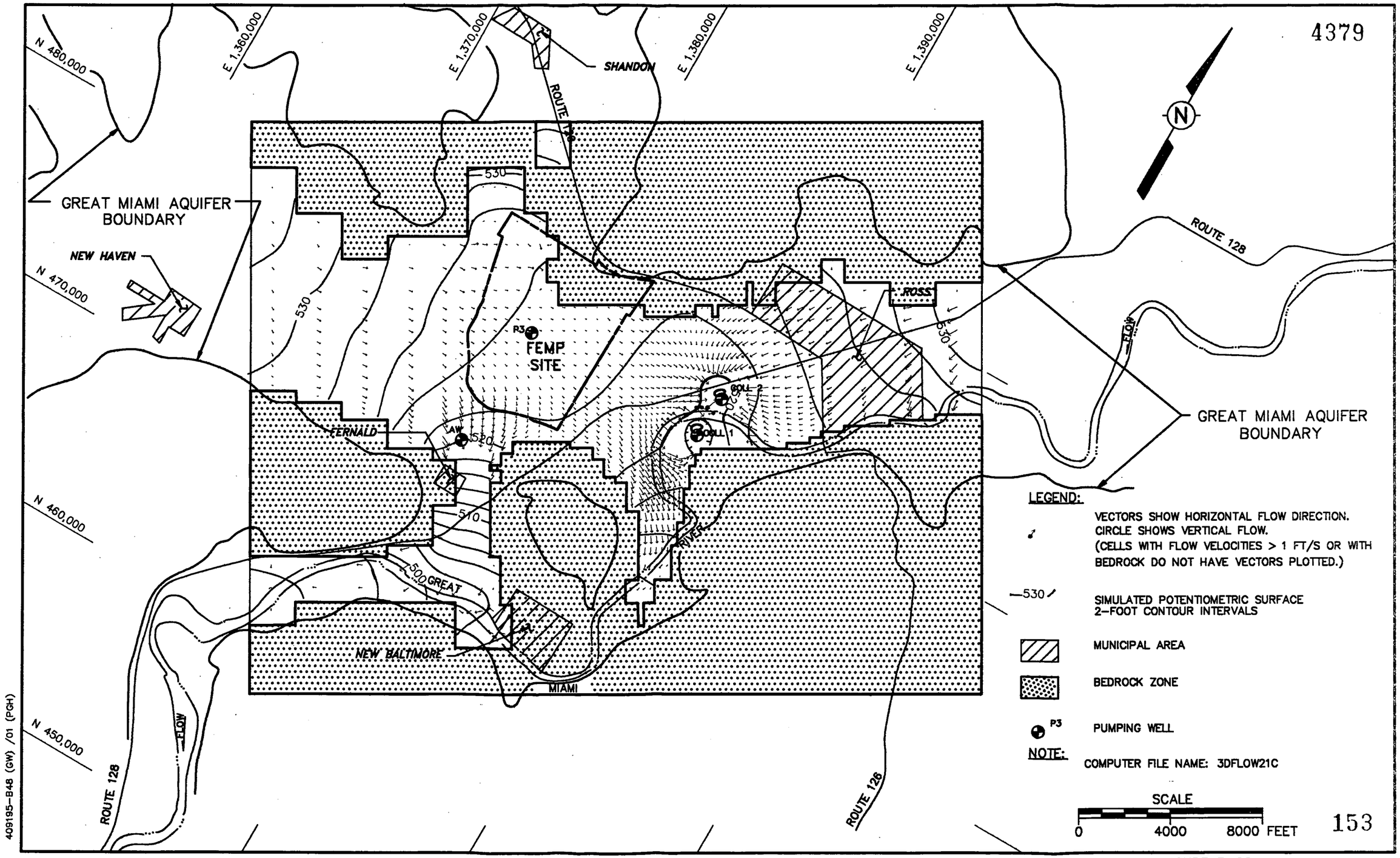




FIGURE 5-22

3-DIMENSIONAL FLOW MODEL
CALIBRATED RUN, LAYER 4
FLOW VECTORS AND POTENTIOMETRIC SURFACE

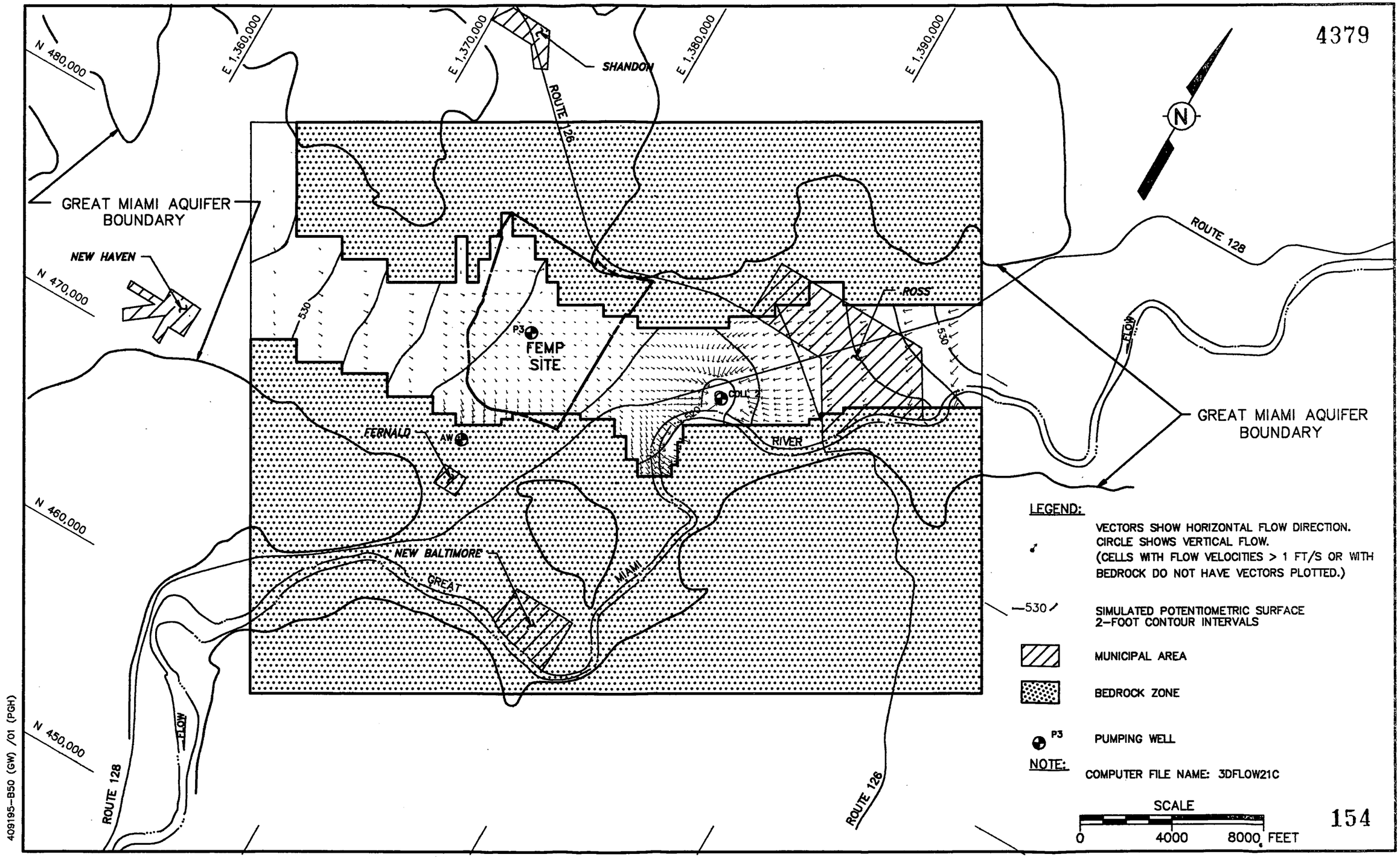




FIGURE 5-23
3-DIMENSIONAL FLOW MODEL
CALIBRATED RUN, LAYER 5
FLOW VECTORS AND POTENTIOMETRIC SURFACE

effect of parameter changes on model results, but also provided information pertinent to planning further calibration efforts for the purpose of producing minor improvements that make the calibration even better. The results of the sensitivity analysis applied to 3DFLOW are shown in Tables 5-8 and 5-9. They may be summarized as follows:

- A large increase in hydraulic conductivity in the lower aquifer (Layers 4 and 5) resulted in both a greater variation of values of residuals and undesirable clustering. This indicates that a large increase in hydraulic conductivity in the lower part of the aquifer would cause the degree of calibration (i.e., the model performance) to begin to decline.

- Variation of the vertical hydraulic conductivity of the clay interbed by an order of magnitude had no significant effect on the overall model calibration. Indeed, increasing the vertical hydraulic conductivity to 0.4 ft/day ($1.4 \times 10^{-4}$ cm/s) had no significant effect on the overall calibration.

- Decreasing the ratio of vertical to horizontal hydraulic conductivity by an order of magnitude had a small adverse effect on model calibration. Setting the vertical hydraulic conductivity equal to horizontal hydraulic conductivity had negligible effect on the degree of calibration.

- Variation of recharge rates within the area of the clay interbed beneath the FEMP site also had negligible effect on overall model calibration. However, it did result in reduced residuals near the FEMP, which is an important part of the model.

- One test of sensitivity to river leakage factor was performed, and the result was similar to the results obtained in 2DFLOW. That is, the model is sensitive to reduction of the river leakage factor.

The results of increasing and decreasing the pumping rates of the collector wells by 25 percent are discussed below. The mean residual and the mean absolute residual that resulted from increasing the pumping rate were 0.73 foot and 1.19 feet, respectively. The mean residual and the mean absolute residual that resulted from decreasing the pumping rate were -0.12 foot and 1.08 feet, respectively. The historical records indicate no significant trend of increasing or decreasing pumping rate versus time since 1967 (Figure 5-24). There may, however, be future changes in the pumping rates of these wells that could cause a significant departure from the predicted contaminant migration based on the present models. Even if the pumping rates of the collector wells should increase by 25 percent, the effect on flow velocities would be less than 20 percent beyond a distance of 750 feet from a collector well.

## TABLE 5-8
## RESULTS OF THE SENSITIVITY ANALYSIS FOR THE THREE-DIMENSIONAL FLOW MODEL UTILIZING RUN 3DFLOW

| Sensitivity Run Number | Parameter | 3DFLOW Value | Sensitivity Run Value | Sensitivity Run Statistics[a] Mean Residual (ft) | Sensitivity Run Statistics[a] Mean Absolute Residual (ft) |
|---|---|---|---|---|---|
| 1 | Hydraulic Conductivity in Layers 4 and 5 (Excluding the Zone at the FMPC) (ft/day) | 500<br>600 | 1150<br>1530 | 0.08 | 1.33 |
| 2 | River Bed Leakage Factor | 0.50 | 0.35 | 0.29 | 1.11 |
| 3 | Recharge Rates in the Northwest Corner of the FMPC (in/yr) | 6 | 4 | 0.05 | 1.08 |
| 4 | Recharge Rates across the FMPC (in/yr) | 6 | 2 | 0.23 | 1.06 |
| 5 | Boundary Condition along North Boundary (ft) | 542 | 541.5 | 0.21 | 1.06 |
| | | 3DFLOW STATISTICS: | | 0.04 | 1.08 |

[a]Mean Residual is the mean of the differences between observed head and calculated head. Mean Absolute Residual is the mean of the absolute difference between observed heads and calculated heads.

## TABLE 5-9
## RESULTS OF THE SENSITIVITY ANALYSIS FOR THE THREE-DIMENTIONAL FLOW MODEL UTILIZING RUN 3DFLOW

| Sensitivity Run Number | Parameter | 3DFLOW Value | Sensitivity Run Value | Sensitivity Run Statistics[a] Mean Residual (ft) | Sensitivity Run Statistics[a] Mean Absolute Residual (ft) |
|---|---|---|---|---|---|
| 6 | Vertical Hydraulic Conductivity Through Clay Interbed (ft/day) | 0.00003 | 0.0003 | 0.36 | 1.06 |
| 7 | Vertical Hydraulic Conductivity Through Clay Interbed (ft/day) | 0.00003 | 0.003 | 0.38 | 1.05 |
| 8 | Ratio of Vertical to Horizontal Hydraulic conductivity ($k_v/k_h$) | 1/10 | 1/100 | 1.03 | 1.45 |
| 9 | Ratio of Vertical to Horizontal Hydraulic Conductivity ($k_v/k_h$ | 1/10 | 1 | 0.19 | 1.04 |
| 10 | Collector Wells 1 and 2 Pumping Rates (gpm) | 6025 | 4520 | -0.12 | 1.08 |
| 11 | Collector Wells 1 and 2 Pumping Rates (gpm) | 6025 | 7530 | 0.73 | 1.19 |
| | | 3DFLOW STATISTICS: | | 0.36 | 1.06 |

[a]Mean Residual is the mean of the differences between observed heads and calculated heads. Mean Absolute Residual is the mean of the absolute differences between observed heads and calculated heads.

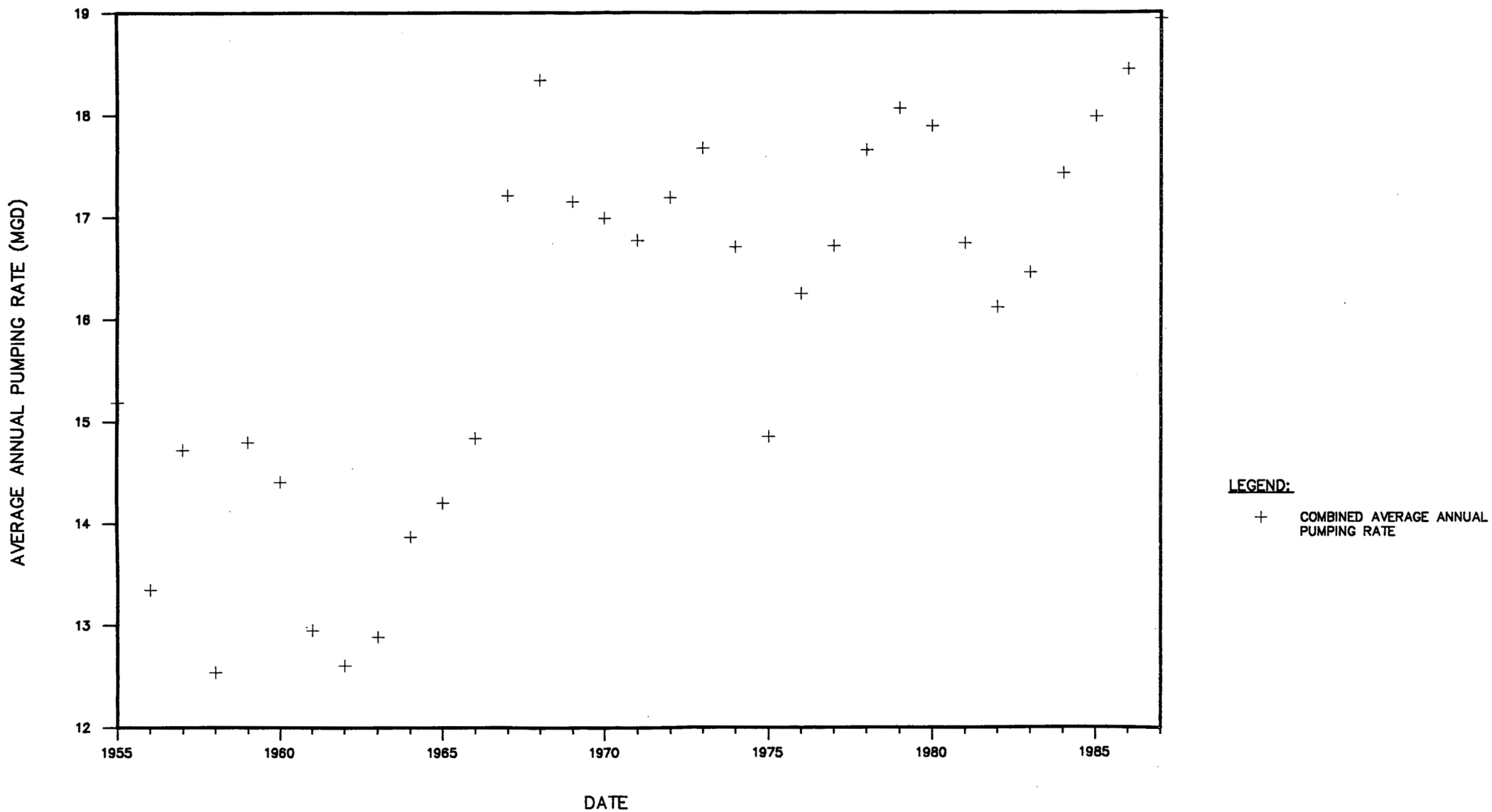


409195-B47 (GW) (PGH)



FIGURE 5-24
COLLECTOR WELLS
COMBINED AVERAGE ANNUAL PUMPING RATE

# 6.0 SOLUTE TRANSPORT MODEL

Solute transport modeling at the FEMP was initially started using an analytical solution to simulate uranium transport. This initial model was used to determine the likely range of values for dispersion and retardation in the Great Miami Aquifer for uranium. Following the completion of the analytical model and the 2DFLOW and 3DFLOW models, the numerical solute transport models were built. Like the groundwater flow models, solute transport models were constructed for both two- and three-dimensional systems in order to reduce modeling time by building increasingly complex models using the results of simpler simulations. Both solute transport codes were built on a local scale and directly imported groundwater flow systems from their corresponding two- and three-dimensional flow models.

The following sections discuss the development of the solute transport models built for the FEMP. They are presented in the order of their development, from the analytical solution to the 2DSOL and 3DSOL models. Only the final calibration of 3DSOL is presented here. An interim calibration was also done which is presented in Appendix C.

## 6.1 ANALYTICAL SOLUTE TRANSPORT MODELING

The development of the numerical solute transport model was preceded by the development of an analytical solute transport model to provide a preliminary evaluation of parameters for the numerical modeling. Analytical solute transport modeling was applied to two areas: (1) the waste storage area; and (2) the south plume area, which contains elevated uranium concentrations on and south of the FEMP. The analytical models only treat solute transport under simplified conditions. Due to the need to achieve closed form mathematical solutions, analytical models can only calculate concentrations for a physical system that is a highly simplified representation of the real system. Consequently, they are only used as an efficient transition to the more complex finite-difference models. The degree of calibration of the analytical models is adequate only for initial parameter estimates for use in the two-dimensional finite-difference solute transport model.

### 6.1.1 Approach

For the purposes of this analytical modeling, the flow directions of the models were aligned with the primary direction of groundwater flow in each area where the modeling was applied. Because the distance of observation wells away from the axis of the natural plume is a significant factor in determining uranium concentrations at the wells, two-dimensional analytical models had to be used. The two-dimensional analytical modeling was based on the following assumptions:

- Groundwater flow is uniform

- Effective porosity, longitudinal and transverse dispersivities, and retardation factor are constant
- The aquifer is infinite in all directions (i.e., no boundary effects)
- A line source of uranium is perpendicular to the direction of groundwater flow
- The source is continuous through the thickness of the aquifer
- The contaminant concentrations are initially zero
- Molecular diffusion is negligible.

The models were developed using the STRIP1B and STRIP1FBCG computer codes (IT 1986a, 1986b). These codes were developed by IT and have been extensively verified with the use of IT's finite element groundwater flow and solute transport code, GEOFLOW (IT 1986), and the Princeton Transport Code (PTC) developed at Princeton University (Babu 1987). The verifications, as well as the theoretical bases for STRIP1B and STRIP1FBCG, are published in the technical literature (Batu 1989; Batu and van Genuchten 1990). These two-dimensional analytical solutions were developed to calculate solute transport in a uniform groundwater flow field bounded by two impervious boundaries. The strip source can be located at any place between the impervious boundaries and oriented perpendicular to the flow direction. STRIP1B corresponds to the concentration-type (first type) boundary condition at the strip source. All of the initial and boundary conditions for STRIP1FBCG are the same except that it uses a flux-type (third-type) boundary condition at the strip source.

### 6.1.2 Results - Waste Storage Area

The principal direction of flow and the average hydraulic gradients were determined from hand-contoured potentiometric surface maps that were available at the time of the analytical modeling. Using Darcy's Law, a preliminary estimate of hydraulic conductivity of 400 ft/day (0.14 cm/s) was used to calculate an average groundwater velocity of 0.64 ft/day. The longitudinal dispersivity selected was 100 feet, and the transverse dispersivity was taken to be 10 feet. The use of 100 feet for longitudinal dispersivity was based on information on scale-dependent dispersivity in the scientific literature. Walton 1985 presents a graph of mean travel distance versus longitudinal dispersivity. If the mean travel distance in the plume area is 2500 feet, Walton's graph yields a longitudinal dispersivity of a little over 100 feet. The transverse dispersivity was held constant at 10 feet, because the ratio 1/10 for longitudinal to transverse dispersivity is commonly reported in the scientific literature (Walton 1985, p. 38).

A line source was placed at the waste storage area. The starting time of the uranium release was assumed to be 1955, and the measured concentrations corresponded to 1988 RI/FS sampling data.

Therefore, a total simulation period of 33 years was used for the model. An appropriate source width perpendicular to the groundwater flow field was unknown, and the retardation factor was also unknown. Successive trials were used to calibrate the model by varying the source width and the retardation factor. The calibration targets were the monitoring wells listed in Table 6-1. The 2000-Series monitoring wells were screened in the intervals below the water table and above the clay interbed. The relatively higher contaminant concentrations were found in these monitoring wells. Through the calibration processes, efforts were made to match the calculated concentrations with the sampled concentrations in the 2000-Series monitoring wells. The 2000-Series wells were used as they represented conditions at the top of the aquifer, where vertical dispersion effects were lowest. The calibrated result was a source width of 400 feet and a retardation factor of 3.5. (As will be discussed later in this chapter, the results of subsequent geochemical modeling and solute transport model calibration increased the retardation factor to 12.)

Figure 6-1 shows the relationship between retardation factor, source width, and the degree of calibration relative to two monitoring wells that are located closest to the axis of the simulated plume, about 250 feet away. Figure 6-2 shows the line source and the normalized concentration in the simulated plume at 33 years.

Table 6-1 shows the comparison between measured and calculated concentrations at monitoring wells in the vicinity of the plume. The calculated concentrations are based on a source concentration of uranium of 78 µg/L, which was a preliminary value measured at Monitoring Well 2010 at the point of entry into the regional aquifer. The value of 78 µg/L was the highest previously measured at Monitoring Well 2010.

### 6.1.3 Results - South Plume Area

A representative groundwater velocity of 1.33 ft/day was calculated for the south plume area using the method described above for the waste storage area. The value of 3.5 for the retardation factor determined for the waste storage area was used for the south plume area because the same constituent and aquifer materials are involved. Values for dispersivity were also kept the same. The source location was assumed to be the storm sewer outfall ditch. The source concentration and source width were unknown. These quantities were estimated as described below.

As can be seen in Figure 6-3, which was developed from reported estimates of discharge to the storm sewer outfall ditch (Table 4-2), the mass of uranium released to the storm sewer outfall ditch between 1961 and 1984 may be represented by the following formula:

$$M(t) = M_0 \exp(\gamma t) \qquad (1)$$

## TABLE 6-1
## COMPARISON OF THE MEASURED AND PREDICTED CONCENTRATIONS FOR SHALLOW WELLS IN THE WASTE PIT AREA

| Well No.[a] | Measured Concentration[b] (µg/L) | Predicted Concentration[c] (µg/L) |
|---|---|---|
| 2042 | 4 | < 0.08 |
| 2037 | 4 | < 0.08 |
| 2013 | < 1 | < 0.08 |
| 2051 | 3 | < 0.08 |
| 2068 | 3, < 1 | < 0.08 |
| 2064 | 3 | 2.6 |
| 2010 | 21 | 24.4 |

[a]See Figure 3-3 for well locations.

[b]Based on RI/FS data that have not been validated.

[c]For 400-foot source width.

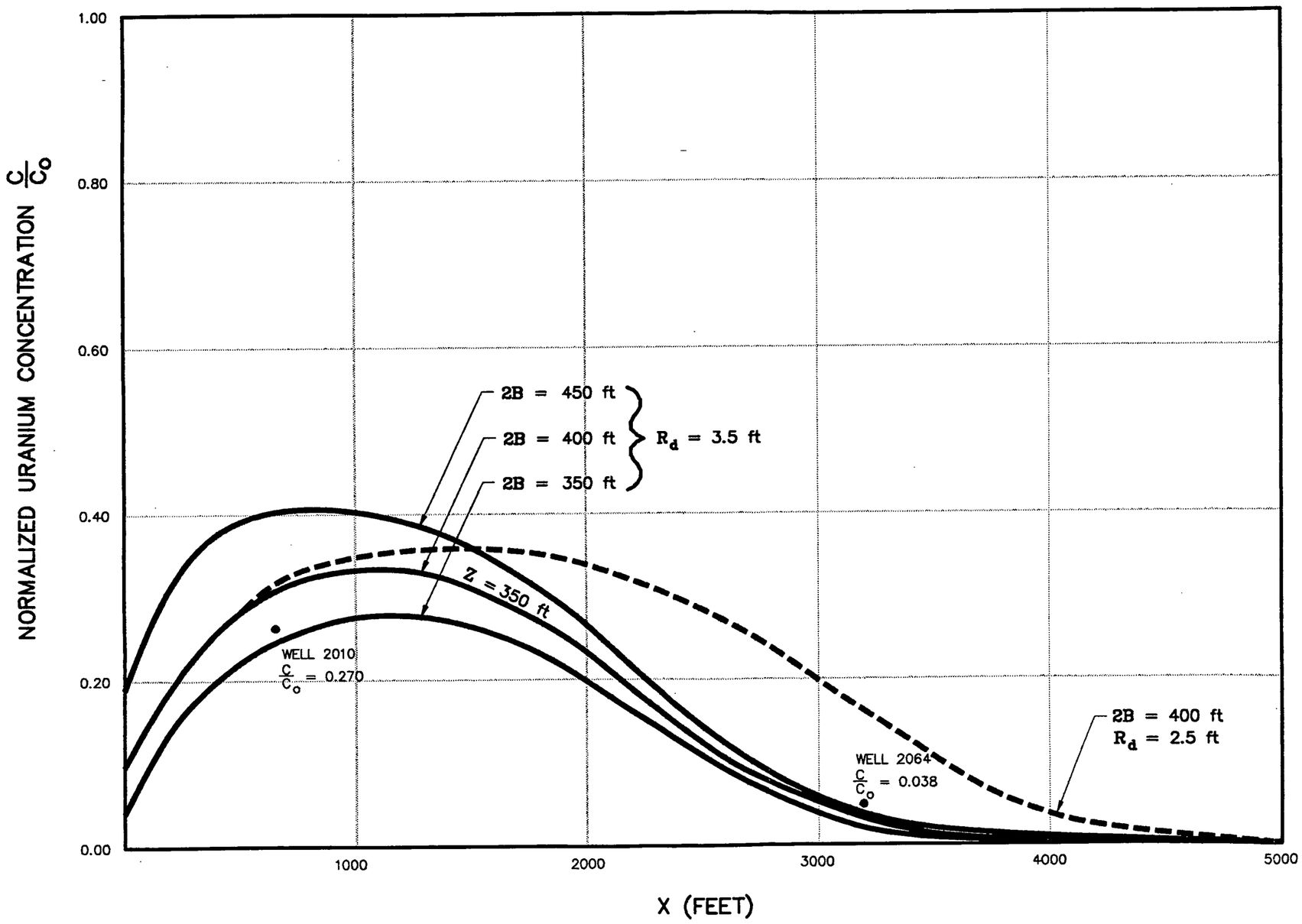


LEGEND:

$C_o$ = 78 μg/L

U = 0.64 ft/day

$\alpha_L$ = 100 ft

$\alpha_T$ = 10 ft

● OBSERVED NORMALIZED CONCENTRATION

NOTE:

COMPUTER FILE NAME: STRIP1FBCG.OUT

409195-B75 (GW) (PGH)



FIGURE 6-1
ANALYTICAL SOLUTE TRANSPORT MODEL
OBSERVED AND PREDICTED NORMALIZED
URANIUM CONCENTRATIONS
FOR NORTH PLUME AREA
VARYING SOURCE WIDTHS

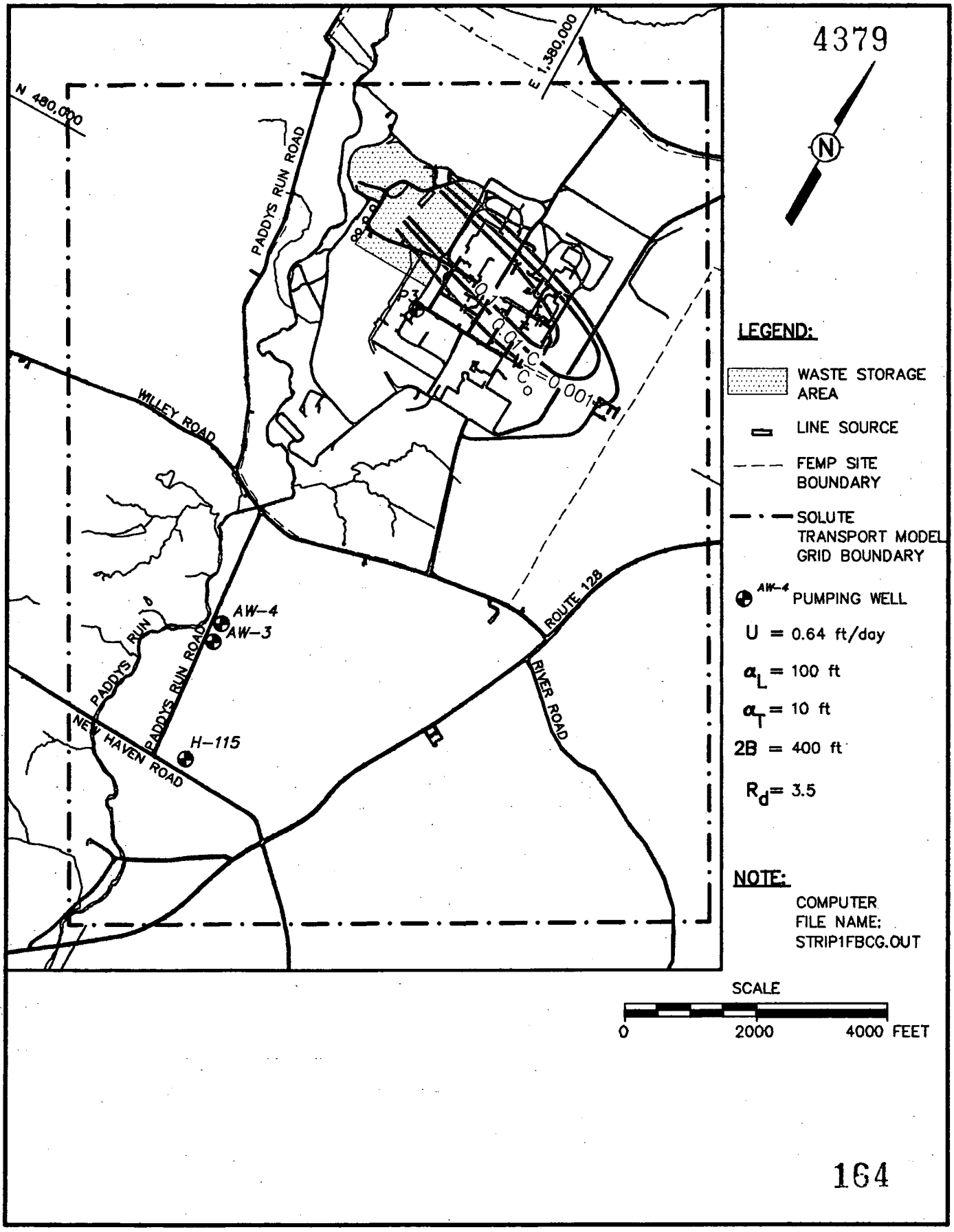


FIGURE 6-2 ANALYTICAL SOLUTE TRANSPORT MODEL PREDICTED NORMALIZED URANIUM CONCENTRATION DISTRIBUTION FOR WASTE STORAGE AREA IN 1988

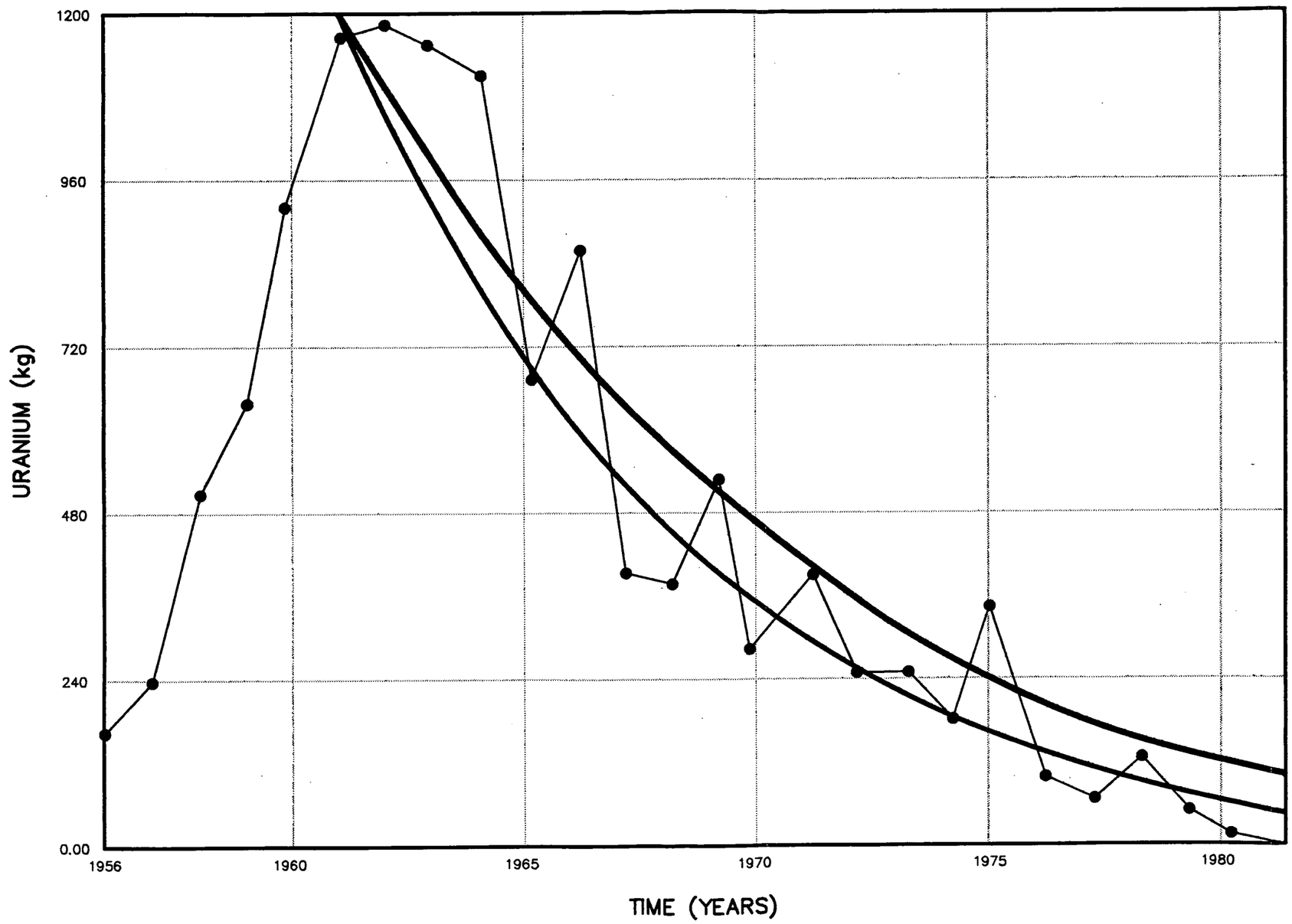


LEGEND:

● ASSUMED URANIUM MASS LOSS TO STORM SEWER OUTFALL DITCH

M(T) URANIUM MASS (Kg)

(t) TIME (DAYS)

FITTED CURVES

NOTE:
COMPUTER FILE NAME: STRIP1FBCG.OUT

409195-B76 (GW) (PGH)



FIGURE 6-3
ANALYTICAL SOLUTE TRANSPORT MODEL
TIME VERSUS URANIUM MASS LOSS
AT STORM SEWER OUTFALL DITCH AREA
WITH FITTED CURVES

where M(t) is the uranium mass in kilograms (kg), t is time (days), and $M_o$ and $\gamma$ ($day^{-1}$) are parameters. Two fitted curves are shown in Figure 6-3. The selected fit is the case in which $M_o$ equals 1200 kg and $\gamma$ equals -0.0004 $day^{-1}$. Therefore, Equation 1 takes the form:

$$M(t) = 1200\exp(-0.0004t) \tag{2}$$

Equation 2 corresponds to the period of 1961 to 1984 and describes the reduction in the rate at which uranium was discharged to the storm sewer outfall ditch. With the assumption that the source concentration decreases in the same form as Equation 2, the following expression can be written:

$$C_0(x=0,z,t) = C_m\exp(\gamma t) \qquad -B \le z \le B \tag{3}$$

in which $C_o$ is the source concentration, $C_m$ is the maximum concentration corresponding to the situation in 1961, and B is half the length of the line source. Equation 3 is the source condition used in the STRIP1B computer program.

Successive trials using different source widths were used to find a plume configuration that caused roughly equal source concentrations to be back-calculated from measured concentrations at Monitoring Wells 2060 and 2061 located downgradient of the storm sewer outfall ditch. The result was a source width (2B) of 1000 feet, and an initial concentration ($C_o$) corresponding to 1961 of about 4500 µg/L in order to fit present-day concentrations. Figure 6-4 shows the normalized concentration in the plume at the simulation period of 27 years (actual south plume contours are presented in Section 6.2.6 [Figure 6-10]). The extent of the simulated plume is very similar to the south plume, which implies that the major source of the south plume is the storm sewer outfall ditch.

## 6.2 TWO-DIMENSIONAL SOLUTE TRANSPORT MODEL

The purpose of the 2DSOL model was to provide a transitional step toward the 3DSOL transport model. This transitional step was included to promote efficiency in the development of 3DSOL, which is more complex and required more intensive use of labor and computer resources. The analytical model provided the initial estimate of loading sources and related transport parameters. Further estimates of model parameters were made by calibration of 2DSOL, and then these estimates were supplied as initial values in the three-dimensional model. Application of the 2DSOL model also provided valuable insight into the processes affecting uranium concentration so that key geochemical studies could be planned and initiated.

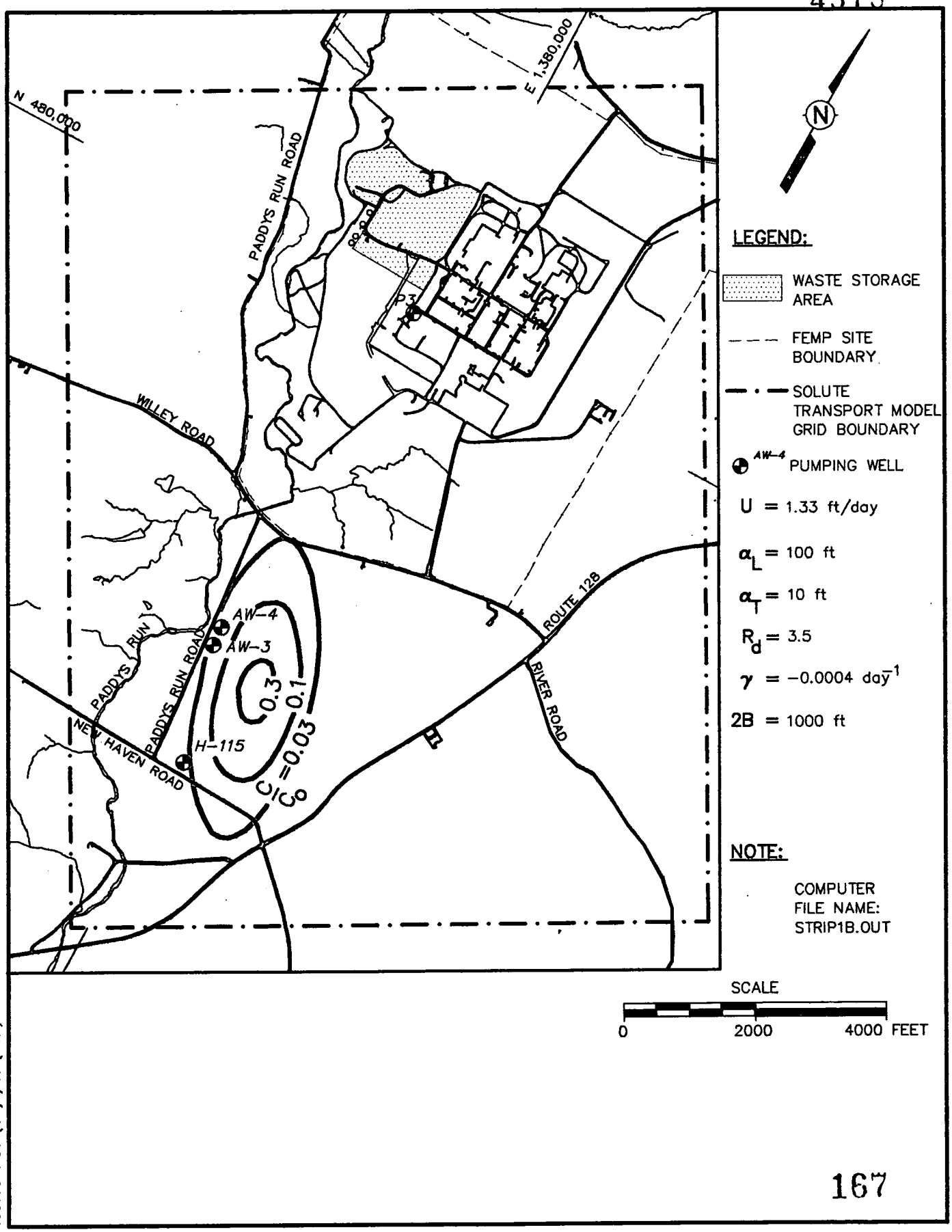


409195-A85 (GW) /01 (PGH)



FIGURE 6-4 ANALYTICAL SOLUTE TRANSPORT MODEL PREDICTED NORMALIZED URANIUM CONCENTRATION DISTRIBUTION FOR SOUTHERN PLUME AREA IN 1988

### 6.2.1 Telescoping Regional Flow Model

The grid for the solute transport model covers a smaller area around the FEMP site than the flow model grid (Figure 6-5). Such a reduction not only promotes efficient modeling, but can be justified by the fact that uranium migration occurs at a much slower rate than groundwater flow due to various retardation processes. The model area was reduced to the area that would be expected to maximize the value of information gained relative to the level of modeling effort. To this end, the grid area was made as small as possible while including all monitoring wells that would be used in the calibration with observed uranium concentrations. This procedure allowed for simultaneous calibration of all contaminant plume areas, which is important in case plumes from more than one source area coalesce. The proper grid size for the transport model should be designed so that importing the parameters used in the regional flow model, such as bedrock elevation, can be facilitated (Figure 6-6). The pressure heads calculated in the regional flow model at the boundaries of the transport model were assigned as constant pressure head boundaries for the transport model. For this condition, SWIFT III sets a convective flux boundary condition on radionuclide transport, which was the transport option used in the transport modeling. The output contains a contaminant mass-balance that includes the cumulative flux across the external boundary. The computed heads from the two models were compared to verify that the flow system in the solute transport model was successfully telescoped from the regional flow model (Figure 6-7).

### 6.2.2 Model Grid

The cell size in the solute transport model had to be reduced to ensure numerical stability. It was chosen to conform to guidelines presented by Reeves et al. (1986). The critical criterion was that cell dimensions are no more than twice the longitudinal dispersivity. This is the overshoot/undershoot criterion for finite-difference equations that are centered in time and central in space (CIT-CIS). The CIT-CIS difference scheme is provided to reduce numerical dispersion in model solutions. Numerical dispersion is very difficult to assess, but overshoot/undershoot if occurred can be closely monitored by mass balance calculation. The chosen cell size was 125 feet. This cell size had several advantages:

- It allowed for some deviation from the original estimate of 100 feet for longitudinal dispersivity. The guideline for overshoot/undershoot would remain satisfied for longitudinal dispersivities as low as 62.5 feet. It should be noted that the overshoot/undershoot criterion is only a guideline, and it may be possible to use smaller dispersivities without introducing significant contaminant mass losing or increasing.

- It allowed the grid to cover the desired area without introducing so many cells that computer run times and the size of input and output files would become intolerable.

- All flow model cell sizes were multiples of 125 feet; thus, each regional flow model cell corresponded exactly to four or more solute transport model cells.

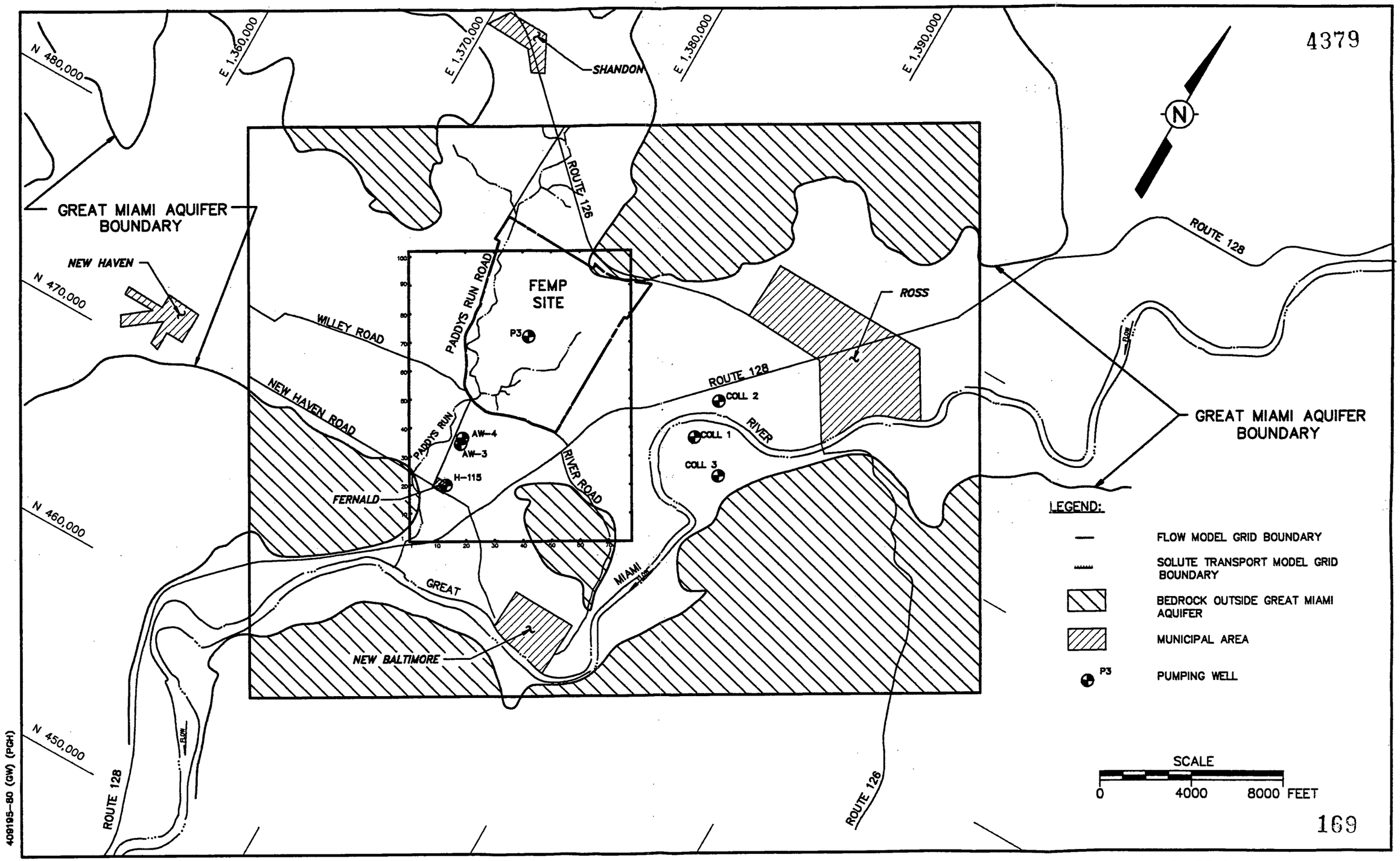


FIGURE 6-5
GROUNDWATER MODELING GRID BOUNDARIES

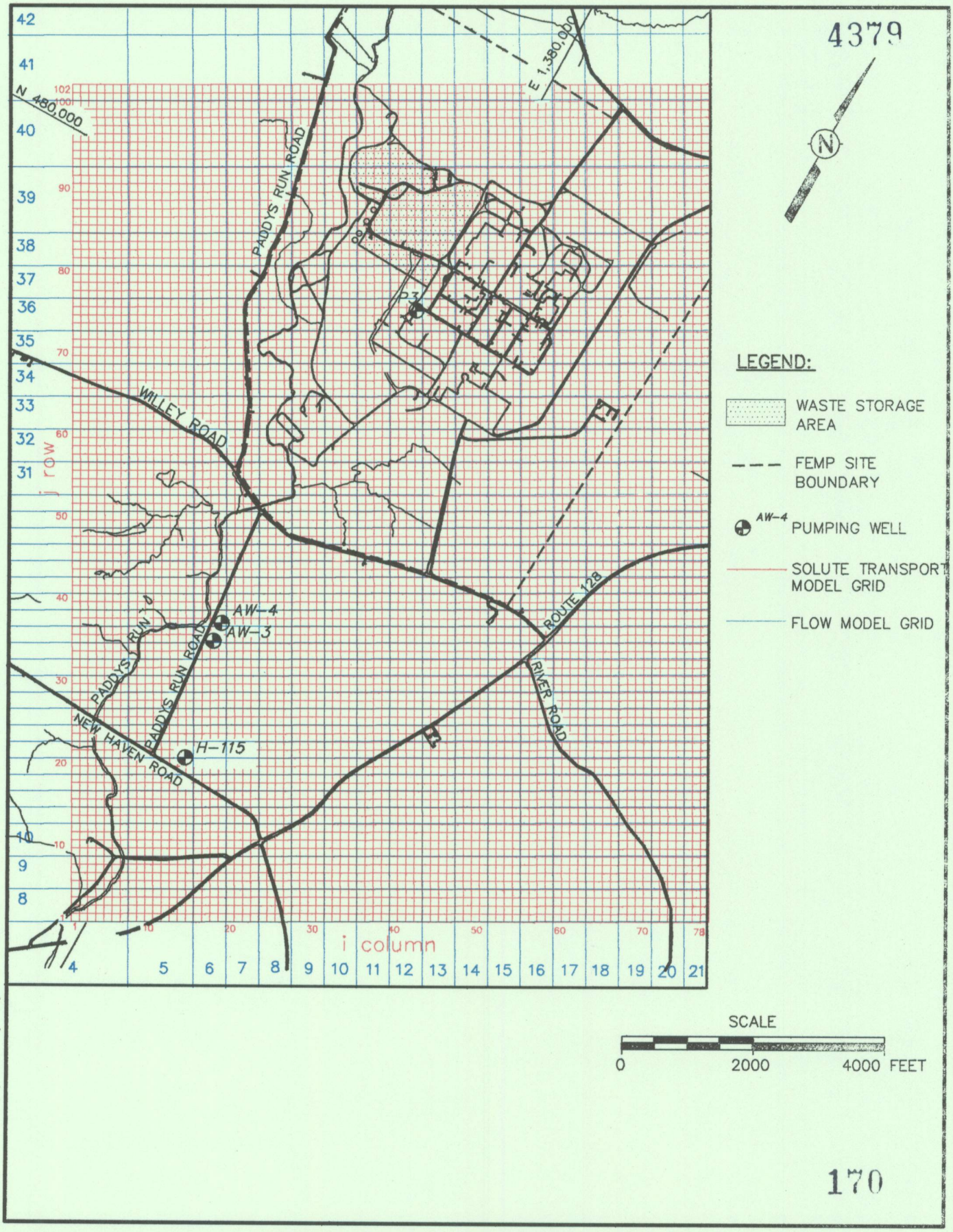


409195-A83 (GW) /01.02 (PGH)

FIGURE 6-6 SOLUTE TRANSPORT MODEL GRID

This condition facilitated telescoping process as discussed in the previous section.

The resulting model grid is shown in Figure 6-7. The 125-foot-by-125-foot cell size was used throughout the model. While using larger cell sizes outside of the area of primary interest would allow the model to be spatially extended, there was no way to substantiate whether such large cells would cause overshoot prior to running the model. If overshoot did occur, it would cause errors to be propagated throughout the model. Since setting up a model of this size uses a large amount of labor and computer resources, the reduced risk associated with smaller peripheral cells seemed to outweigh the advantage of covering a larger area.

### 6.2.3 Initial Conditions

The solute transport is modeled as a transient process using steady-state flow conditions. Initial uranium concentrations throughout the aquifer are set at the default value of zero, which is reasonably close to the average background value of about 0.4 µg/L. Uranium concentrations reported for observation wells located upgradient from the FEMP are given in Table 4-3. These wells are located west of the FEMP, north of the FEMP, and in the vicinity of the village of Ross (Figure 4-1). The values 2.7 and 1.7 µg/L test as statistical outliers using the methods described by Grubbs (1969). When these are rejected, the highest remaining concentration is 1.1 µg/L. Values reported as less than 1 µg/L are not informative and were not included in any statistical calculations. Other nondetection limits in the table were included in the calculations at the limiting value, which would tend to cause the representative background concentration to be overestimated.

### 6.2.4 Input Data

Hydraulic conductivities, bedrock elevations, recharge rates, and pumping rates were imported from 2DFLOW. Since one cell in the flow model corresponds to four or more cells in the solute transport model, simple computer programs were written to create relevant parts of the solute transport model input files from the flow model input files. The smaller cell size allowed the Albright & Wilson Company pumping wells to be represented individually in different cells, and the 225 gpm combined pumping rate was divided equally by assigning 112.5 gpm for each well. The flow model calibrated to the April 1986 data was used because this model was a better representation of average conditions of the groundwater system. As mentioned in Section 5.1.4, the model calibrated to the May 1988 data represents abnormal drought conditions.

The time increment initially used was 180 days. This increment satisfies the guideline for overshoot and undershoot at groundwater velocities up to about 0.5 foot per day. In some areas, groundwater velocity is greater than this criterion and undershooting occurred, as shown by a global mass balance. Therefore sensitivity of the model to the time increment was tested by lowering it to 60 days. The

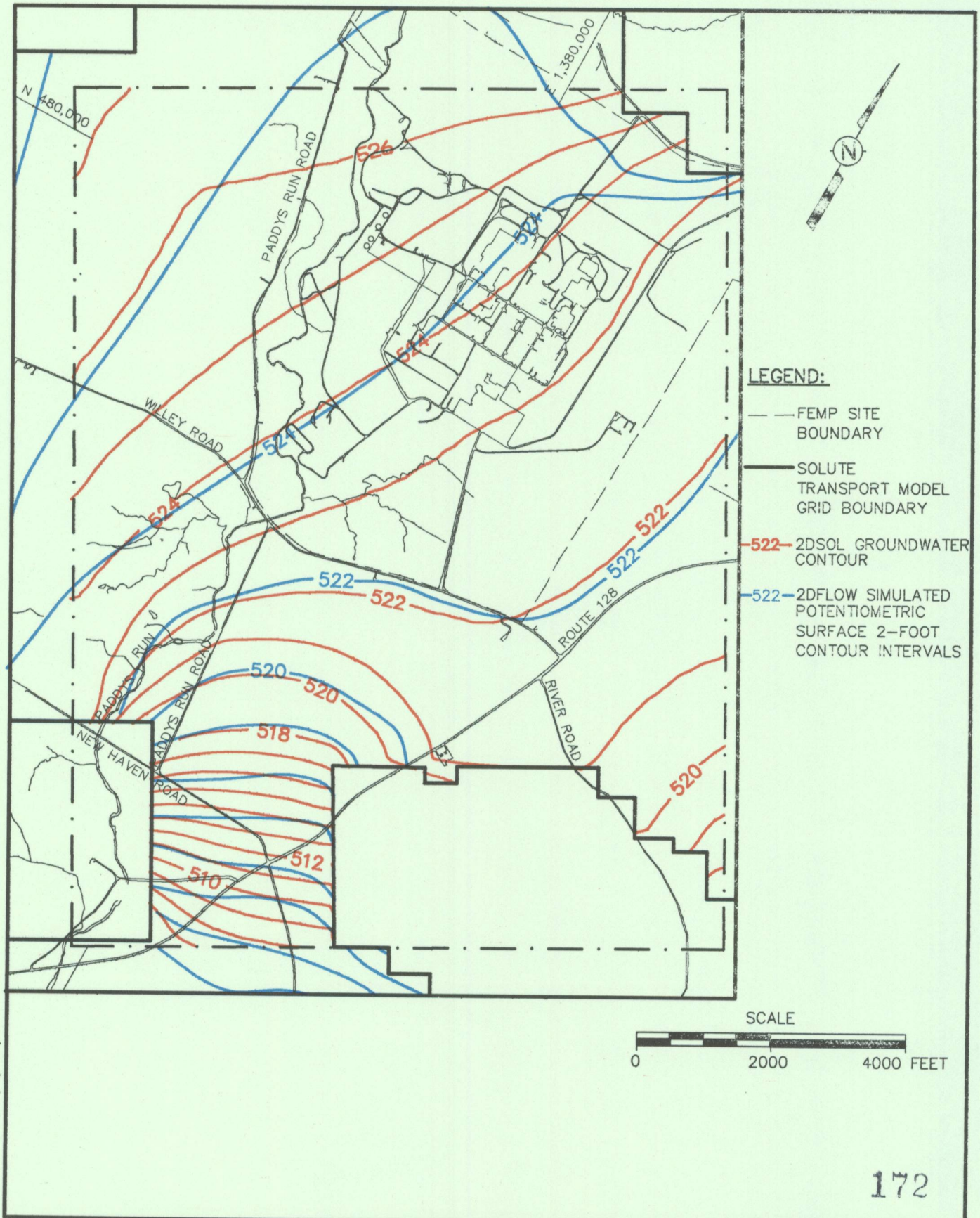


409195-A57 (GW) (PGH)



FIGURE 6-7 COMPARISON OF SIMULATED GROUNDWATER CONTOURS FROM 2DFLOW AND 2DSOL MODELS

result was that the distribution pattern of calculated uranium concentrations did not change, the mass balance ratio improved from 0.92 to 0.99, and computer execution time was greatly increased. The small increase in accuracy was not sufficient to justify the extra computing time in routine calibration runs. Many routine computer runs with the time increment set at 180 days had mass balances closer to 1. Shorter time increments would be recommended only for model applications where early-time transient results are important. Trials also showed that a convergence criterion (maximum difference in concentration at any cell between successive iterations) of 1 µg/L was adequate for calibration runs. Reducing this criterion did not significantly improve the global mass balance, but greatly increased execution time.

### 6.2.5 Source Loading Estimation

Calibration of 2DSOL involved successive trials in which uranium source loading rates and the distribution coefficients were modified within acceptable ranges to approach a match between observed and calculated uranium concentrations. No direct information on the rate of seepage of uranium to the aquifer was available. Consequently, source loading rates were made part of the calibration of the model. The procedure to generate the initial estimates of source loading involved the following steps:

- Calculating an initial estimate of the total amount of uranium present in the plumes
- Reviewing available documents containing information related to possible source locations and uranium discharge rates
- Choosing source areas based on the above review
- Estimating the proportion of the uranium in the plume south of the storm sewer outfall ditch, and assigning that uranium to the storm sewer outfall ditch source area and Paddys Run immediately downstream from the storm sewer outfall ditch
- Assigning the remaining uranium to other potential source areas, as follows:
  - Dividing the discharge time into periods when uranium discharge to the aquifer was probably significantly different from preceding and succeeding periods
  - Prorating the amount of uranium from the various sources to the time periods.

Calculation of initial estimates of the amount of uranium in the plumes was generated from an isoconcentration plot of observed uranium data. The volume of the aquifer was estimated by use of planimetry. A porosity of 0.25 was used; and the distribution coefficient was taken as 0.005 cubic

foot per pound ($ft^3/lb$), which corresponds to the retardation factor of 3.5 selected for use in the preliminary analytical solute transport modeling. The distribution coefficient is a representation of the partitioning of the uranium between the soluble form and that adsorbed onto the solid matrix. (See Freeze and Cherry 1979 for a detailed definition.) An estimate of the uranium historically removed by pumping the Albright & Wilson Company pumping wells was also made and added to the estimated amount in the plume to obtain an initial estimate of the total amount of uranium to be introduced into the aquifer by the various source areas. This initial estimate was 4749 pounds. The estimate was only for initiating calibration and was expected to be superseded by values generated during model calibration. Although these initial estimates could be very inaccurate due to a lack of direct information, it was felt that starting with logically derived estimates would tend to yield better results after calibration than starting calibration with completely arbitrary estimates.

The documents reviewed to obtain information related to source locations and loading rates included Dames and Moore (1985); Eye (1961); Facemire (1959); GeoTrans (1985); Hartsock (1960); Spieker and Norris (1962); Thatcher and Phoenix (1987); U.S. Energy Research and Development Administration (ERDA) (1977); and WMCO (1987). The potential source areas chosen for inclusion in the model were the storm sewer outfall ditch area (including the flyash piles and Southfield), Paddys Run downstream from the storm sewer outfall ditch, Paddys Run between the storm sewer outfall ditch and the waste storage area, the waste pit area, the former production area, the silos area, the biodenitrification surge lagoon area, the lime sludge pond area, and the abandoned incinerator area at the sewage treatment plant. The biodenitrification surge lagoon and the lime sludge pond areas were assigned zero discharge rates in the initial run. No record of radiological materials being placed in the lime sludge ponds was found, and there is no significant radioactivity in the lime sludge ponds (Thatcher and Phoenix 1987). The biodenitrification surge lagoon has a double liner system that should prevent significant loss of uranium to the underlying glacial overburden, and no significant amount of uranium would be expected to pass through the overburden and reach the Great Miami Aquifer within the short period of operation. Figure 6-8 shows the locations of the source cells used in the models. In some areas, the loading sources are close to the boundary of the model. Since the SWIFT III code automatically takes into account the convection of contaminant through constant head and flux boundaries, the transport of contaminant in the simulation region can be evaluated accurately.

The proportion of uranium in the plume south of the storm sewer outfall ditch was estimated from the isoconcentration plot. The assignment of loading cells for the uranium in this plume area to the storm sewer outfall ditch and the reach of Paddys Run just below the storm sewer outfall ditch was based on groundwater vector maps from 3DFLOW, which showed water moving from these areas toward the observed location of the plume.

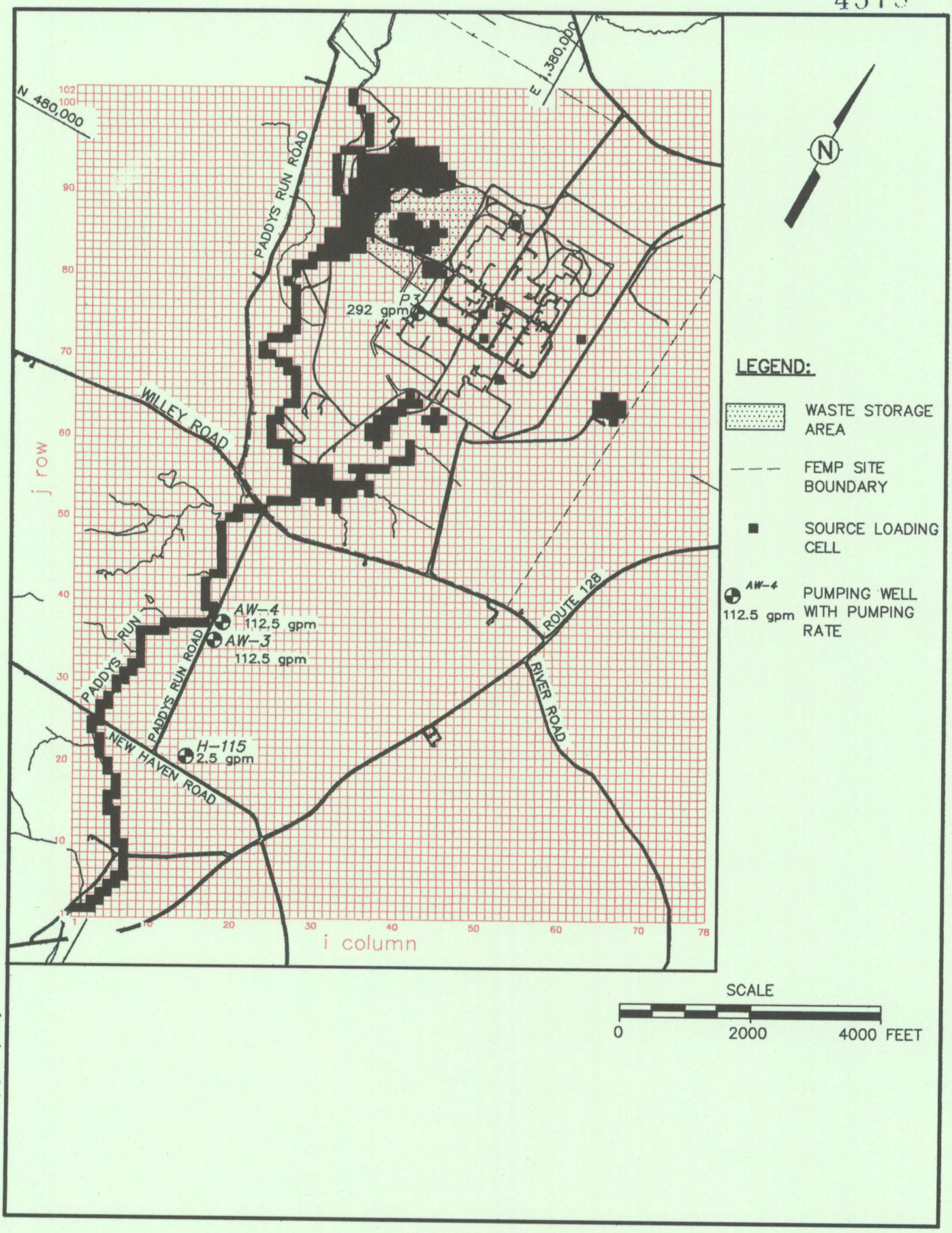


409195-A70 (GW) /01 (PGH)

FIGURE 6-8 3-DIMENSIONAL SOLUTE TRANSPORT MODEL SOURCE LOADING LOCATIONS AND PUMPING WELL RATES

The period of loading was divided into four source loading periods in the model. These periods correspond to periods of time when uranium-bearing water discharged to the storm sewer outfall ditch and Paddys Run was estimated to be significantly different from preceding and/or succeeding periods. The time periods were established by using estimated amounts of uranium discharged to the storm sewer outfall ditch as presented in Table 4-2. The first period is 1952 through 1958 and represents the early years of plant operation when uranium discharge rates to the storm sewer outfall ditch were relatively low and only two of the waste pits had been constructed. The second period is 1959 through 1966, an 8-year period when the rate of uranium discharge to the storm sewer outfall ditch was greater than during any other period and two more waste pits were put into operation, including Waste Pit 3. The third period is 1967 through 1975, a 9-year period when discharges to the storm sewer outfall ditch were moderate compared to the preceding period, and Waste Pit 3 was closed. The fourth period is 1976 through 1988, a 13-year period of lowest total discharges to the storm sewer outfall ditch. Retention basins were constructed at the storm sewer outfall ditch near the end of this period. These periods were for initial calibration runs and were changed as required for calibration of the model.

Initially, the estimated loading rates of total uranium discharged to the Great Miami Aquifer were 8, 60, 27, and 5 percent during the Periods 1, 2, 3, and 4, respectively. These source loading rates were later superseded by calibration of the solute transport models. They were only used as reasonable starting values to begin the calibration runs.

### 6.2.6 Model Calibration

Uranium data collected from monitoring wells beginning in 1985 and continuing through August 1989 were used for calibrating the model. These data were from the FEMP environmental monitoring data from National Lead of Ohio (NLO) and Westinghouse Materials Company of Ohio (WMCO), Resource Conservation and Recovery Act (RCRA) Sampling Rounds Nos. 1 through 5 (Dames and Moore 1986a, 1986b, 1987a, 1987b, 1987c), IT data (IT 1986b), RI/FS data, and data from Albright & Wilson Company. (1986).

No general trend in uranium concentration variation with time was found in these data. That is, the observed uranium concentration in each monitoring well was sufficiently stable. Consequently, the data at each monitoring well were treated as random sampling from a normal distribution, and calibration was based on this type of data. The scatter of the data at each monitoring well is thought to be due to short-term variations in recharge and source loading rates, and geochemical variability of the aquifer system combined with minor temporal variations in flow direction and rate.

The objective of the calibration was to reduce the difference between the uranium concentration calculated by the model at each monitoring well and the mean concentration of the actual population.

The population means for the monitoring wells are not known; however, for wells where many concentrations have been measured, the sample means were assumed to be close to the population means. For monitoring wells where only a few concentrations have been measured, the sample means may be very different from the population means. Consequently, an adequately calibrated model might show large residuals at monitoring wells where the number of measurements are small, and some large residuals were allowed under such conditions in the 2DSOL model.

The criteria for calibration were: (1) to avoid bias indicated by too many residuals having the same sign; (2) to avoid clustering of residuals of the same sign; and (3) to avoid creating residuals that were too high to be acceptable representations of actual field conditions. No attempt was made to closely match each mean concentration because this would involve matching random variation rather than the underlying representative concentration. Furthermore, the lateral concentration gradients in the south plume are very high. Consequently, a slight difference between natural and simulated isoconcentration lines can cause a large difference between measured and simulated concentrations at a point, even though the overall concentration distributions within the plumes are very similar.

During the 2DSOL calibration, the longitudinal dispersivity was held constant at 100 feet and the transverse dispersivity was held constant at 10 feet. The use of 100 feet for longitudinal dispersivity and 10 feet for transverse dispersivity was based on information on dispersivity in the scientific literature, as described in Section 6.1.2. Higher ratios (1/5, for example) are also reported, but since SWIFT III does not differentiate between lateral and vertical dispersivity and vertical dispersivity tends to be low, the value 1/10 was considered to be most representative.

The calibration included trials with distribution coefficients of 0.005, 0.026, 0.0063, and 0.010 $ft^3/lb$ corresponding to retardation factors of 3.5, 6, 4.13, and 14. Uranium source loading rates were also varied. The best calibration obtained without changing the longitudinal dispersivity from 100 feet was obtained using a distribution coefficient of 0.010 $ft^3/lb$; i.e., a retardation factor of 6. This calibration was considered sufficient for the purposes of 2DSOL; further refinement was postponed until the calibration of 3DSOL. A map of the plume produced by this transitional model and corresponding field data are presented in Figures 6-9 and 6-10. This map shows the concentrations calculated at the end of the last time period (1978 to 1988) used in the model. The contoured field data shows much sharper peaks and more defined plume boundaries than does the modeled plume. These discrepancies are due to the model's ability to interpolate into other regions. This results in a much broader plume south of the FEMP. The high peak shown in the area north of the storm sewer outfall ditch was not accounted for in the model due to the lack of a known sourcing

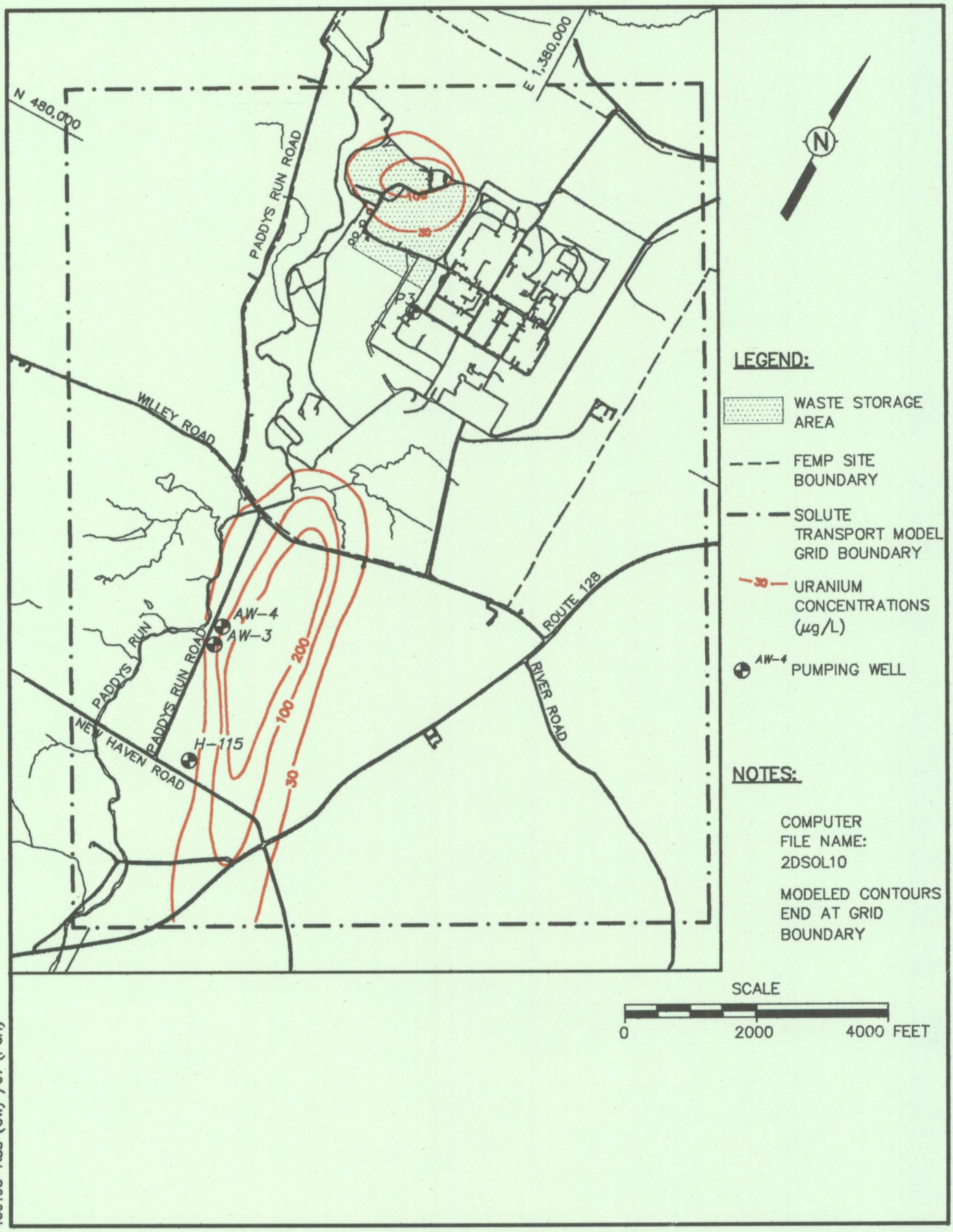


409195-A88 (GW) /01 (PGH)

FIGURE 6-9 2-DIMENSIONAL SOLUTE TRANSPORT MODEL SIMULATED URANIUM CONCENTRATIONS PRESENT CONDITIONS

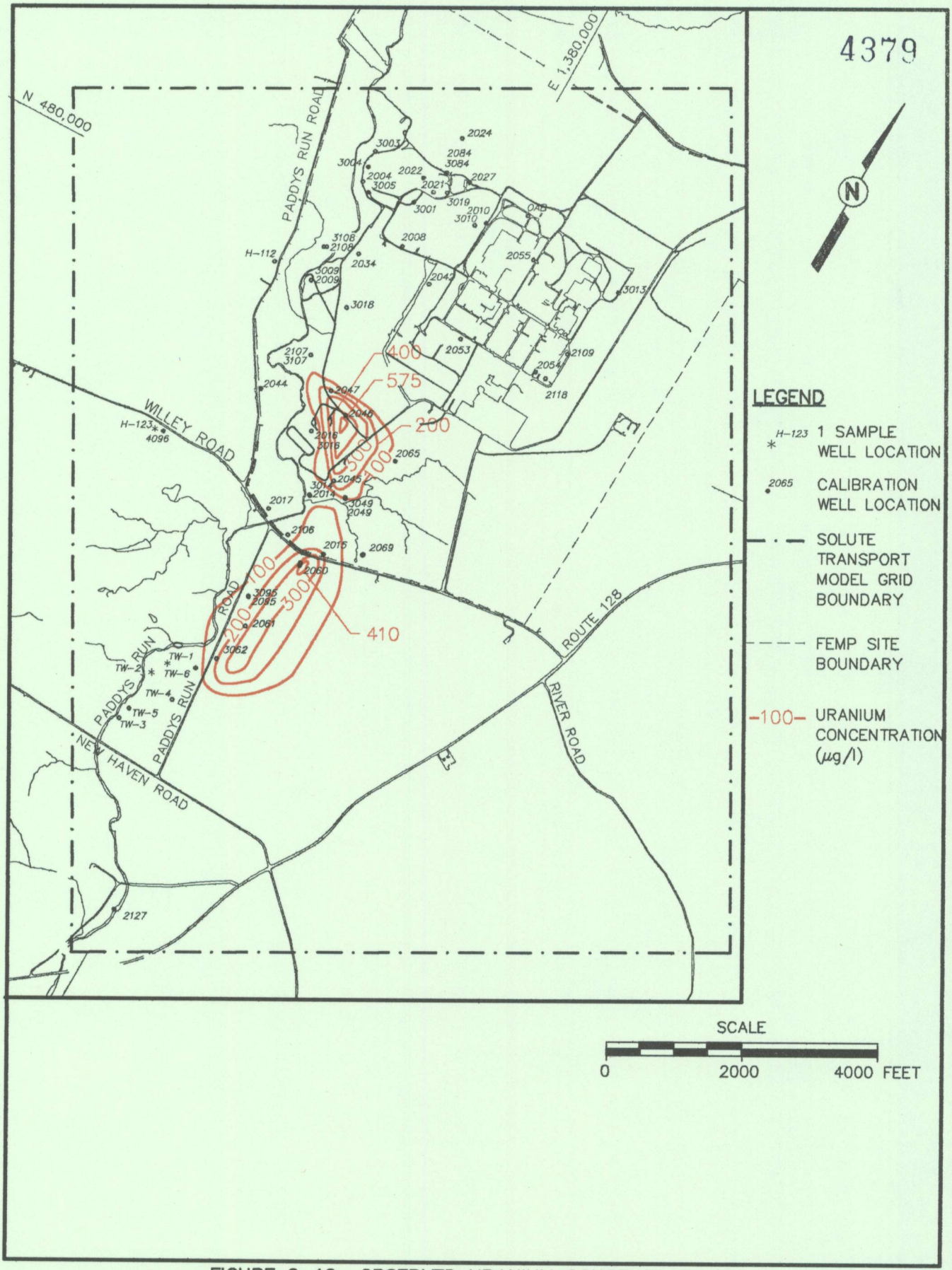


409195-A54 (GW) (PGH)

FIGURE 6-10 OBSERVED URANIUM CONCENTRATIONS
2000 SERIES WELLS

area for it and the large confidence interval which was generated for Monitoring Well 2046. These two factors caused the model to be calibrated without a large peak in this area.

### 6.2.7 Sensitivity Analysis

Experience with this model showed it to be most sensitive to the value of the uranium distribution coefficient and to the amount and location of source loading. The results of the trials showed that increasing the distribution coefficient shrinks the area of the plume and changes the concentrations in the plume if other factors are held constant. Increasing source loadings at all source cells increases the area of the plume and the concentrations if other factors are held constant. Consequently, various combinations of the source loading and the distribution coefficient can yield similar plumes. However, when the dispersion coefficient is held constant, the distribution coefficient controls the concentration gradients in the plume and the choice of parameters that yield a good calibration is limited. In this case, loading rates, retardation factors, and dispersion values are all mutually dependent on each other. Once a preferred dispersion value is selected and source areas are set, the retardation factor and loading rates are limited to achieve a proper calibration.

## 6.3 THREE-DIMENSIONAL SOLUTE TRANSPORT MODEL

The purpose of the 3DSOL transport model was to provide a useful representation of the transport of uranium in the groundwater system in the vicinity of the FEMP. Once completed, the model could then be used to predict the future migration of uranium under a no-action condition and the effects of various remedial alternatives for dealing with the uranium contamination. The 3DSOL model is a better representation of the groundwater system than 2DSOL for the following reasons:

- It allows source loading to be applied to the upper layer of cells only, and provides a better representation of the effects of adding the contaminant at the water table where it will spread downward as well as laterally as it moves away from the sources. Consequently, it allows the concentrations near the bottom of the simulated aquifer to be smaller than concentrations at the top, which is the known condition in the natural aquifer.

- It contains an explicit representation of the clay interbed that is present beneath the FEMP site. The bed impedes the downward movement of the contaminant, and it affects groundwater flow directions.

- It provides better estimates of source loading rates. In the two-dimensional model, concentrations had to be uniform with depth in the aquifer; whereas, in the three-dimensional model, concentrations decrease with depth. Most of the monitoring wells used for calibration are in the upper part of the aquifer. Consequently, the calibrated two-dimensional model contains more uranium in any vertical column of aquifer than the calibrated three-dimensional model; and the simulated plume in the two-dimensional model contains more uranium than the plume in the equivalent three-dimensional model. Since the mass of uranium in the plume has to balance with the mass of uranium

entering the plume at the sources, the source loading rates in the two-dimensional model tend to be too high.

- It provides a better tool for examining the feasibility of removing uranium by using extraction wells than 2DSOL, because it will not tend to exaggerate the amount of uranium in the aquifer, as noted above. It also provides a way to estimate the depth required for extraction wells because it can simulate the effectiveness of partially penetrating wells in pulling water up from the lower layers.

### 6.3.1 Model Grid and Boundary Conditions

The 3DSOL model used the same grid as 2DSOL, except that five layers were added in the vertical direction. These layers are the same as those of 3DFLOW and were imported from corresponding cells of 3DFLOW. The resulting model contained 39,780 cells, which caused the importation of data from the preceding models to be complex. The computer files to be generated were very large; therefore, data manipulation and transfer had to be done by developing computer programs to produce various parts of the 3DSOL input file. Solute transport execution times of 3 to 12 hours on a Prime EXL325 computer were required for each calibration run.

Boundary heads were imported directly from 3DFLOW. The head at the boundary face of each boundary cell in the solute transport model was taken directly from the cell in the flow model that contained the boundary. This was done for each layer so that the boundary head in the transport model varied with depth in accordance with the results of the flow model. Again, the constant-head boundary condition resulted in a convective flux boundary condition for radionuclide transport. Initial uranium concentrations throughout the aquifer were set at zero, as in 2DSOL.

### 6.3.2 Input Data and Groundwater Recalibration

Groundwater flow in the 3DSOL model was recalculated. All parameters related to flow simulation such as hydraulic conductivities, bedrock elevations, recharge rates, and pumping rates were imported from 3DFLOW. However, bedrock elevations were changed near Paddys Run along the western edge of the Paddys Run Outlet. The purpose of this change was to more accurately simulate the effects of Paddys Run. In the previous models, Paddys Run was simulated as crossing bedrock cells in this area, even though it is actually on thin alluvium. The latter condition could not be more realistically simulated until accommodated by the small cell size and layering in 3DSOL. The smaller cell size permitted simulating thin alluvium on a gradually sloping bedrock surface beneath Paddys Run. After this change was made, the hydraulic heads calculated in 3DSOL were compared with the corresponding heads in 3DFLOW to see if the simulated flow was significantly affected by the change. The maximum pressure head difference is less than 0.01 foot in the 3DSOL simulation region.

Along with the change in bedrock around Paddys Run, the recharge rates along Paddys Run were also refined. In transforming the input file from the flow model grid with large cell sizes to the solute

transport model grid with smaller cell sizes, much of the area occupied by Paddys Run in the flow model was lost when the stream was more accurately depicted by the smaller cells. To compensate for this, the rate of recharge to the smaller stream cells was increased until the total volume of recharge to Paddys Run matched that used in the flow model. This resulted in increasing the recharge rate from 14 in./yr to 32 in./yr to compensate for the loss in area in Paddys Run. The hydraulic heads in the model were checked again after this change was made.

Well No. H-115 (Rutgers-Nease chemical plant pumping well) was added to the model and assigned a pumping rate of 2.5 gpm. Again, the hydraulic heads in the model were checked to verify that the new well caused no significant change.

The time increment used in the transient solute transport modeling was maintained at 180 days.

### 6.3.3 Model Calibration

Calibration of 3DSOL involved successive trials in which uranium source rates, distribution coefficient, longitudinal dispersivity, and transverse dispersivity were varied. It was found that decreasing dispersivity increased concentration gradients by decreasing the spread of the plume, and the effect was somewhat similar to the effect of increasing the distribution coefficient. This condition allowed an acceptable calibration to be achieved through a range of distribution coefficients and dispersivity values by finding a balance between source loading rates, distribution coefficient, and dispersivities. Consequently, additional information was needed to find the most representative combination of these factors. During early stages of the modeling, additional information became available from preliminary results of geochemical modeling. During later stages of the solute transport modeling, the geochemical modeling had been completed and final results were available (IT 1989). This progressive change in the amount of geochemical data available resulted in the distribution coefficient being progressively increased to 0.016, which corresponds to a retardation factor of 9, and then to 0.022 $ft^3/lb$, which corresponds to a retardation factor of 12. A preliminary calibration, based on a distribution coefficient of 0.016 $ft^3/lb$, was used for the determination of locations of additional monitoring wells required to characterize the contaminant plume, and for the evaluation of an interim removal action to mitigate contaminant migration pending final action under the RI/FS (Appendix C). More recent RI/FS work is using the final, more-refined calibration that was accomplished with a retardation factor of 12.

#### 6.3.3.1 Preliminary Calibration Testing

The preliminary calibration was based on early geochemical results, which indicated that the dissolved uranium is in complexes with neutral and negative charges. Such charges imply low adsorption and low distribution coefficients. Information in the literature suggests that a scale-dependent dispersivity of less than 40 feet would be marginal in a system as large as the one treated in the present model.

For example, Walton (1985) shows representative longitudinal dispersivities for areal models of alluvial sediments and glacial deposits to be between 39 and 200 feet. The strategy, therefore, for obtaining a representative model for the FEMP was to use a low distribution coefficient that would allow calibration with a longitudinal dispersivity greater than 40 feet.

The calibration process was begun by importing initial source loading rates, distribution coefficient, and dispersivities from the transitional 2DSOL model. The monitoring well data used for 2DSOL calibration were also used for 3DSOL, and additional new data were used as they became available. The most recent data used for calibration were collected in August 1989. For calibration, only monitoring wells from which all samples contained uranium above the detection limit were included in calculations of nondetect means and other statistics. Monitoring wells that yielded any samples with nondetected uranium were treated as locations where calculated concentrations should be minimized, without attempting to actually match a mean concentration. Excluding these monitoring wells from calculations eliminated the problem of what concentration value to assign to such samples. Figure 6-11 shows these "nondetect" monitoring wells. For the purposes of calibration, the measured concentration data for each monitoring well with detectable concentrations were tested for outliers following the methods described by Grubbs (1969). Concentrations that tested as outliers at the 2.5 percent significance level (95 percent confidence interval) were not included in the calculation of means used for model calibration. The purpose of eliminating the outliers was to make the model more representative by not including questionable data in the calibration. The statistical procedure provides an objective method of identifying the questionable data. The rejected data are listed in Table 6-2. The monitoring wells used in the calibration are shown in Figure 6-12. In the calibration, the observed concentrations were compared with the concentrations calculated for the model layer in which the monitoring well was completed.

Attempts to calibrate the model using a distribution coefficient of zero (i.e.; where there is no adsorption) were not successful. A simulated plume that matched field data could not be produced because the simulated plumes proved to be too broad and too long even with longitudinal dispersivity as low as 30 feet. Furthermore, most uranium exited the south boundary of the model in all runs. This plume behavior is not in accordance with monitoring well data. A residential well located south of the intersection of Route 128 and New Haven Road, in the direction of movement of the plume, yielded a uranium concentration below a detection level of 1 µg/L, which is in the range of background levels. If a plume had extended to this area, the elevated concentration at this residential well would still be present because the source is still present. Consequently, the evidence indicates that the plume has never extended to this area. Model solutions with longitudinal dispersivity set lower than 30 feet (15 and 10 feet) failed to converge. Another observation for the zero distribution coefficient case was that when the higher concentration values in the simulated plume were made to approximate observed values, the highest concentrations in successively deeper layers shift southward.

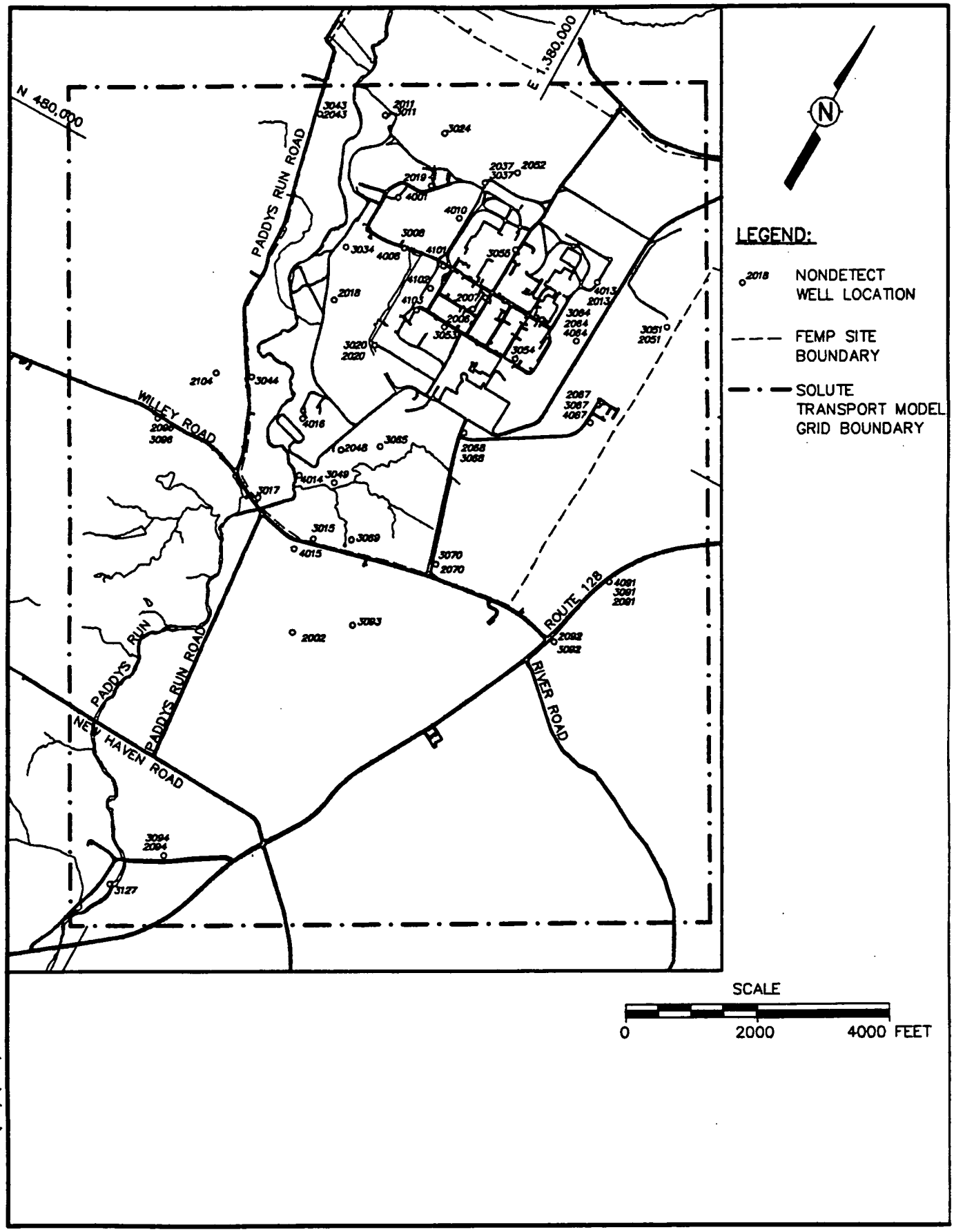


409195-A84 (GW) (PGH)

FIGURE 6-11 3-DIMENSIONAL SOLUTE TRANSPORT MODEL NONDETECT WELL LOCATIONS

## TABLE 6-2
## OUTLIER DATA ELIMINATED FOR URANIUM CONCENTRATION MODEL CALIBRATION

| Well Number | Cell I | Cell J | Cell K | Initial Number of Observations | Initial Range of Observed Concentrations µg/L Minimum | Maximum | Concentrations Rejected as Outliers µg/L | Mean[a] (µg/L) |
|---|---|---|---|---|---|---|---|---|
| EMR-13 | 31 | 40 | 1 | 47 | 0.3 | 1.9 | 1.9, 1.3 | 0.60 |
| EMR-14 | 59 | 38 | 1 | 48 | 0.34 | 1.7 | 0.34 | 1.10 |
| EMR-16 | 49 | 57 | 1 | 47 | 0.40 | 2.8 | 2.8, 1.5, 1.4 | 0.7 |
| EMR-20 | 19 | 15 | 4 | 30 | 0.1 | 0.8 | 0.8 | 0.3 |
| EMR-21 | 24 | 1 | 2 | 48 | 0.2 | 6.1 | 6.1 | 0.6 |
| EMR-22 | 22 | 62 | 1 | 44 | 0.6 | 2.3 | 2.3 | 1.1 |
| 2014 | 29 | 55 | 1 | 9 | 17.0 | 85.0 | 85.0 | 34.2 |
| 2015 | 30 | 48 | 1 | 9 | 154 | 401 | 401 | 201.2 |
| 2044 | 23 | 67 | 1 | 4 | 1 | 33.0 | 33.0 | 9.3 |
| 2060 | 28 | 47 | 1 | 56 | 105 | 591 | 591 | 248 |
| 2061 | 21 | 39 | 1 | 58 | 208 | 476 | 476 | 290 |
| 2027 | 48 | 92 | 1 | 4 | 6.0 | 7.0 | 7.0 | 6.3 |
| 3001 | 41 | 89 | 2 | 4 | 13.0 | 15.0 | 13.0 | 14.5 |
| 3005 | 36 | 90 | 2 | 4 | 3.0 | 10/0 | 10.0 | 4.8 |
| 3013 | 65 | 78 | 2 | 6 | 4.0 | 490 | 490 | 86.8 |
| 3062 | 18 | 35 | 2 | 47 | 31.0 | 110 | 110 | 51.2 |

[a]Mean was calculated without outliers.

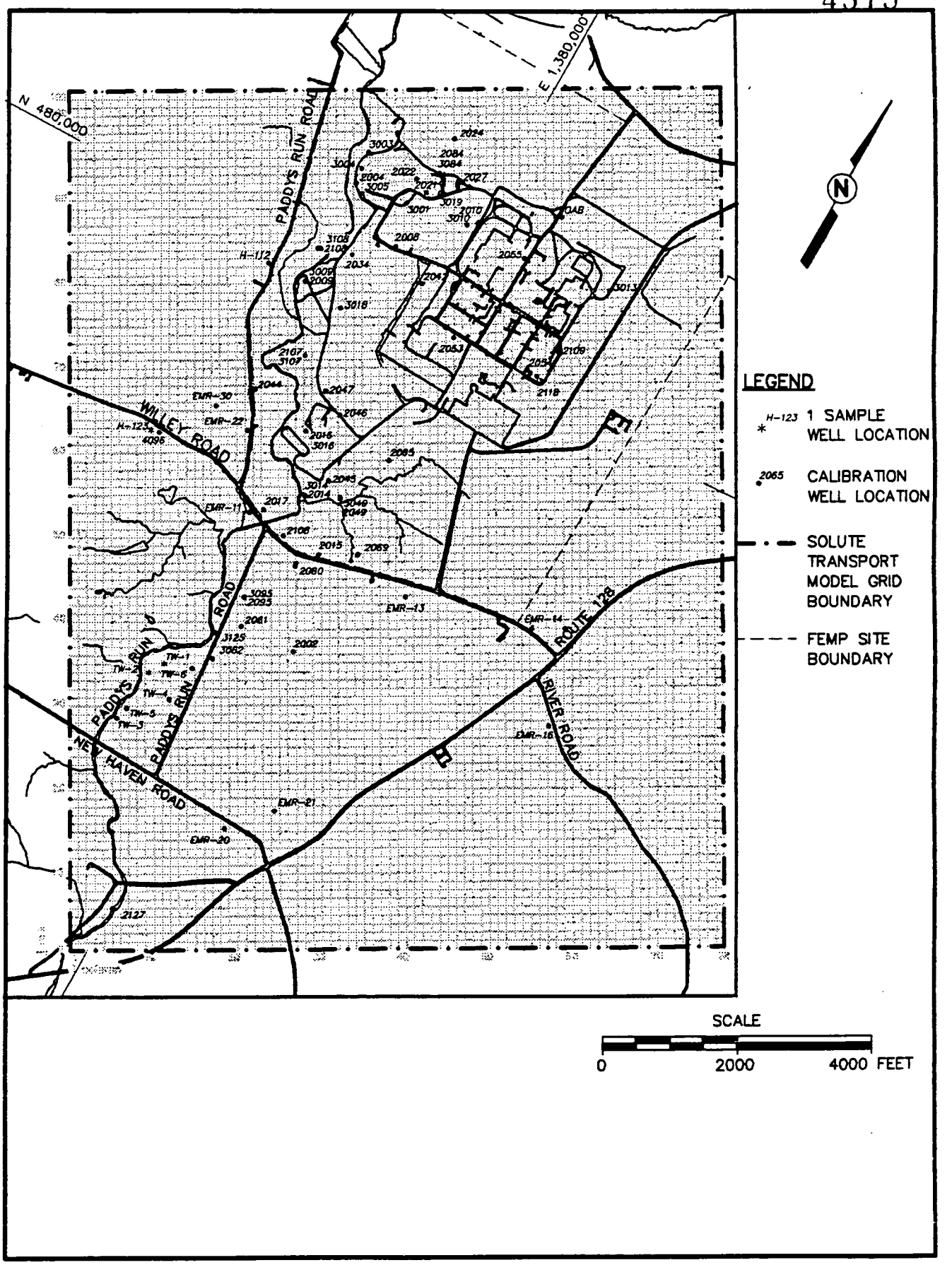


409195-A87 (GW) (PGH)

FIGURE 6-12
3-DIMENSIONAL
SOLUTE TRANSPORT MODEL
CALIBRATION WELL LOCATIONS

No evidence for such shift exists in the observed concentration profile. The evidence from numerous computer runs using a distribution coefficient of zero indicates that an acceptable calibration cannot be reached, and the solute transport model supplies convincing evidence that significant adsorption of uranium occurs in the natural system.

As noted in Section 6.2.2, any longitudinal dispersivity less than 62.5 feet violates the guideline on grid size needed to avoid overshoot and undershoot. All runs with longitudinal dispersivity less than 62.5 produced some negative concentrations in low concentration cells, interpreted as undershoot. This undershoot appeared to have only a minor effect on the plume concentrations, because the plumes produced at slightly higher dispersivities with no negative concentrations were very similar to the plumes containing evidence of undershoot. Experience with these runs suggests that significant undershoot is easily identified in this model by the appearance of negative concentrations. The observation that undershoot is identifiable in the results has also been made by at least one other modeler (Frind and Palmer 1980).

Runs with the distribution coefficient set at 0.002 and 0.004 $ft^3/lb$ (retardation factors of 2 and 3, respectively) also resulted in most of the uranium loaded at the source cells exiting the boundary of the model by the end of the 37-year simulation period. That is, the main body of the plume passed the boundary. Again, the background uranium concentration recorded in a private well south of the FEMP (Monitoring Well 5382) indicates the plume has never extended beyond its present terminus. Therefore, the evidence shows that a distribution coefficient of 0.004 $ft^3/lb$ or less will not produce a representative model. Conversely, simulation runs at distribution coefficients at 0.010 $ft^3/lb$ (retardation factor = 6) and higher result in less than 20 percent of the input uranium flowing out of the system. This amount of adsorption causes a plume to form in the south plume area that resembles the observed plume.

Attempts to calibrate the model using a distribution coefficient of 0.010 $ft^3/lb$ began by importing source loadings from the 2DSOL transport model, which was roughly calibrated with this distribution coefficient. Runs with longitudinal dispersivity of 100 feet and transverse dispersivity of 10 feet resulted in a plume with too much spread and was centered too far southeast. These results were judged to indicate the distribution coefficient was too low, and calibration moved on to a coefficient of 0.016 $ft^3/lb$ (retardation factor = 9) that was consistent with interim findings of the geochemical program. The calibration process and the corresponding results using the distribution coefficient of 0.016 $ft^3/lb$ are presented in Appendix C.

6.3.3.2 Final Calibration

The RI/FS geochemical investigation (IT 1989) determined that many uranium distribution coefficients calculated from results of an iron- and manganese-leaching procedure were higher than the distribution

coefficient 0.016 $ft^3/lb$ used in the preliminary solute transport modeling. Consequently, use of a higher distribution coefficient in the model would be consistent with the final results of the geochemical investigation, although not required by it. This geochemical finding allowed the distribution coefficient to be increased to 0.022 ft/lb (retardation factor 12), so that the longitudinal dispersivity could be increased back to the preferred value of 100 feet.

Values of the distribution coefficient greater than 0.022 $ft^3/lb$ were not considered because the occurrence of uranium in neutral and negatively charged complexes indicates a low value should be preferred, as previously discussed in this section. Other evidence for a low distribution coefficient is that Monitoring Well 2060 has yielded high uranium concentrations since February 1982. Particle tracking indicates that an unretarded particle would require over two years to move from the nearest source (Paddys Run) to this monitoring well. Since the FEMP had only been operating for 30 years by 1982, the concentrations at this monitoring well imply a retardation factor less than 15. Other local wells, such as the Albright and Wilson Company pumping well and the Rutgers-Nease pumping well, also agree with this conclusion, as their uranium concentration did not begin to peak until the mid- to late-1980s.

The available evidence points to a retardation factor greater than 9 and less than 15. Review of the retardation factor ($R_f$) calculations (Appendix A, page 32) indicates that a grain density of 2.66 grams per cubic centimeter (g/cc) was used as the value for rho, rather than the bulk density value of 1.77 g/cc. By replacing the value of 1.77 g/cc into the equation, the value of $R_f$ ranges from 8 to 31 for uranium. Although the $R_f$ of 9 occurs within this range, the available evidence indicated that the retardation factor of 12 was more representative of the $R_f$ range, and would allow for the preferred longitudinal dispersivity of 100 feet in the model. The value of 12 is, therefore, the preferred value within the acceptable $R_f$ range.

Calibration at a distribution coefficient of 0.022 $ft^3/lb$ (retardation factor of 12) was more refined than that at 0.016 $ft^3/lb$. As mentioned in Section 6.2.6, the calibration aimed at reducing the difference between the uranium concentration calculated by the model at each monitoring well and the mean concentration of the actual population. Consequently, an appropriate goal for calibration is to maximize the number of simulated concentrations within the 95 percent confidence interval of the true mean. Calculation of confidence intervals for the mean is described in Mood and Graybill (1963, pp. 251-253). Since the objective is to match the calculated concentration with the population mean rather than a sample distribution as in the outlier test, this test is more restrictive as it results in a smaller confidence interval. Consequently, its application to the final calibration resulted in a more conservative model. Hereafter, the 95 percent confidence interval for the true mean concentration at a well will be called the "range." It should be noted that for small sample size (less than 4), the statistical confidence limits are less meaningful. In cases where small sample sizes generated a wide

range for the confidence interval, the calculated interval was still used although the data range was also taken into account. This approach allowed for the incorporation of data from wells containing only limited sampling data. Rational judgment was used in calibration for those data groups. Lower confidence limits below zero were set equal to zero for the calibration.

The result of the calibration was that all of the calculated concentrations in Layer 1 were brought into range except the concentration at Monitoring Well 2061 and the concentrations at a few monitoring wells upgradient from any known sources. These upgradient monitoring wells are 2108, 2024, and H-112. Several concentrations at monitoring wells screened in the lower layers also could not be brought into range. The results are presented in Table 6-3. Figures 6-13 and 6-14 show the deviations of calculated concentrations from the mean of measured concentrations at the monitoring wells. Concentrations that are out of range are underlined.

Since the uranium concentration decreases with depth, it is more important to match concentrations in Layer 1 than in lower layers, because this layer contains a large proportion of the total mass of uranium in the ground.

Not matching lower concentrations might affect the calculation of the extent of the plume. The degree of matching obtained required detailed study of particle tracks connecting sources to monitoring wells and very refined adjustment of source loadings. Such adjustments had to bring concentrations at one well into range while not causing the calculated concentration at another well near the same track to fall outside of the range. The time of the source loading as well as its location had to be considered.

The concentration at Monitoring Well 2061 could not be brought into range because the measured concentrations at that monitoring well are higher than the concentrations at Monitoring Well 2095, which is upgradient on the same particle track. The monitoring wells are only about 375 feet apart. The concentration at Monitoring Well 2061 could have been brought into range while keeping Monitoring Well 2095 in range by taking advantage of lateral dispersion from Paddys Run downstream from Monitoring Well 2095. However, source rates at cells upgradient from Well 3062 (Albright & Wilson Company pumping well) would have to have been increased and the concentration at Monitoring Well 3062 would have increased too much. Breaking the source periods into smaller increments and varying source loadings to get a downgradient increase in concentration was not attempted, because the wells are close together and longitudinal dispersion would probably was too great to allow the development of a sufficient increase in concentration between the two wells. While this possibility remains untested, it is more likely that the anomalous concentration in Monitoring Well 2061 is the result of preferential fingering of the contaminant front through the porous matrix in the manner described by Freeze and Cherry (1979, p. 399). It was not practical to attempt a detailed simulation of such fingering in this study.

# TABLE 6-3

## OBSERVED CONCENTRATIONS
## 95 PERCENT CONFIDENCE INTERVALS FOR THE MEANS
## AND CALCULATED CONCENTRATIONS
## FOR THE THREE-DIMENSIONAL FINITE-DIFFERENCE SOLUTE TRANSPORT MODEL
## RETARDATION FACTOR 12

| Well No. | Cell | | | Number of Observations | Range of Observed Concentrations (µg/L) | | | 95% Confidence Intervals for the Means (µg/L) | | Model Calculated Concentrations |
|---|---|---|---|---|---|---|---|---|---|---|
| | I | J | K | | Minimum | Maximum | Mean | Lower End | Upper End | (µg/L) |
| 2002 | 30 | 35 | 1 | 2 | 1 | 2 | 1.5 | 0 | 7.9 | 7.8 |
| 2004 | 35 | 92 | 1 | 23 | 5.8 | 10 | 7.6 | 7.1 | 8.1 | 8.0 |
| 2008 | 40 | 84 | 1 | 4 | 5 | 21.5 | 15.9 | 3.7 | 28.1 | 6.1 |
| 2009 | 29 | 80 | 1 | 4 | 19 | 27 | 23 | 17.6 | 28.4 | 21.4 |
| 2010 | 48 | 87 | 1 | 4 | 2 | 21 | 12.3 | 0 | 28.4 | 2.9 |
| 2014 | 29 | 55 | 1 | 12 | 17 | 125 | 49.1 | 23.4 | 77.1 | 64.3 |
| 2015 | 30 | 48 | 1 | 10 | 132 | 200 | 174 | 159 | 189 | 160.5 |
| 2016 | 29 | 62 | 1 | 10 | 12 | 30 | 20.4 | 15.7 | 23.2 | 20.9 |
| 2017 | 24 | 53 | 1 | 8 | 2.6 | 5.1 | 3.7 | 3.0 | 4.4 | 32.0 |
| 2021 | 43 | 90 | 1 | 10 | 1 | 21.1 | 6.7 | 1.8 | 11.6 | 7.1 |
| 2022 | 42 | 92 | 1 | 7 | 3.2 | 6 | 4.3 | 3.4 | 5.2 | 4.8 |
| 2024 | 47 | 97 | 1 | 4 | 2 | 6 | 4.4 | 1.7 | 7.1 | 0.1 |
| 2027 | 48 | 92 | 1 | 3 | 6 | 6 | 6 | 6.0 | 6.0 | 3.9 |
| 2034 | 34 | 83 | 1 | 4 | 15 | 24 | 20.5 | 13.6 | 27.4 | 17.1 |

TABLE 6-3
(Continued)

| Well No. | Cell I | Cell J | Cell K | Number of Observations | Range of Observed Concentrations (µg/L) Minimum | Maximum | Mean | 95% Confidence Intervals for the Means (µg/L) Lower End | Upper End | Model Calculated Concentrations (µg/L) |
|---|---|---|---|---|---|---|---|---|---|---|
| 2042 | 43 | 80 | 1 | 4 | 1.5 | 4 | 2.6 | 0.9 | 4.4 | 1.3 |
| 2044 | 23 | 67 | 1 | 2 | 1 | 1 | 1 | 1.0 | 1.0 | 1.7 |
| 2045 | 31 | 56 | 1 | 4 | 278 | 462 | 341 | 249 | 312 | 275.4 |
| 2046 | 32 | 64 | 1 | 4 | 232 | 907 | 575 | 0 | 1,302 | 21.2 |
| 2047 | 32 | 68 | 1 | 4 | 9 | 15 | 12.0 | 3.4 | 19.3 | 7.6 |
| 2049 | 33 | 54 | 1 | 7 | 2.5 | 437 | 129 | 0 | 163 | 57.9 |
| 2053 | 47 | 72 | 1 | 2 | 1 | 6 | 3.5 | 0 | 35.3 | 23.3 |
| 2054 | 55 | 69 | 1 | 2 | 21 | 23 | 22 | 9.3 | 34.7 | 15.8 |
| 2055 | 55 | 82 | 1 | 2 | 3 | 4 | 3.5 | 0 | 9.9 | 0.2 |
| 2060 | 28 | 47 | 1 | 92 | 105 | 410 | 246 | 235 | 256 | 236.0 |
| 2061 | 21 | 39 | 1 | 93 | 208 | 578 | 335 | 318 | 352 | 173.4 |
| 2065 | 39 | 59 | 1 | 7 | 8 | 13 | 10.3 | 8.7 | 11.8 | 11.3 |
| 2069 | 35 | 48 | 1 | 5 | 6 | 14.8 | 11.6 | 7.5 | 15.7 | 10.9 |
| 2084 | 45 | 93 | 1 | 4 | 16 | 21 | 18.3 | 14.7 | 21.8 | 15.7 |
| 2095 | 21 | 42 | 1 | 5 | 87 | 201.5 | 154.1 | 137 | 210 | 191.6 |
| 2106 | 26 | 49 | 1 | 3 | 16 | 89 | 55.3 | 0 | 324 | 209.1 |
| 2107 | 28 | 71 | 1 | 2 | 9 | 14 | 11.5 | 0 | 43.3 | 9.7 |

**TABLE 6-3**
(Continued)

| Well No. | Cell I | Cell J | Cell K | Number of Observations | Range of Observed Concentrations (µg/L) Minimum | Maximum | Mean | 95% Confidence Intervals for the Means (µg/L) Lower End | Upper End | Model Calculated Concentrations (µg/L) |
|---|---|---|---|---|---|---|---|---|---|---|
| 2108 | 30 | 84 | 1 | 2 | 32 | 37 | 34.5 | 2.7 | 66.3 | 1.6 |
| 2109 | 59 | 71 | 1 | 2 | 2 | 35.5 | 18.8 | 0 | 232 | 5.2 |
| 2118 | 57 | 68 | 1 | 2 | 9 | 16 | 12.5 | 0 | 57.0 | 6.5 |
| 2127 | 5 | 5 | 1 | 3 | 6 | 37 | 19 | 0 | 59.0 | 15.3 |
| 3001 | 41 | 89 | 2 | 23 | 7.5 | 15 | 11.0 | 9.9 | 12.1 | 4.7 |
| 3003 | 36 | 95 | 2 | 21 | 2.1 | 4.3 | 3.0 | 2.7 | 3.3 | 2.4 |
| 3004 | 35 | 93 | 2 | 4 | 10 | 13 | 11.3 | 9.3 | 13.3 | 3.2 |
| 3005 | 36 | 90 | 2 | 24 | 3 | 6.3 | 4.3 | 3.9 | 4.7 | 4.1 |
| 3009 | 29 | 80 | 2 | 24 | 0.8 | 4 | 1.8 | 1.5 | 2.2 | 5.8 |
| 3010 | 49 | 87 | 2 | 22 | 13.1 | 29.2 | 20.9 | 18.7 | 23.1 | 1.3 |
| 3013 | 65 | 78 | 2 | 10 | 1.4 | 21 | 11.4 | 6.0 | 16.8 | 0.1 |
| 3014 | 29 | 54 | 2 | 10 | 19 | 38 | 27.5 | 22.3 | 31.0 | 43.9 |
| 3016 | 29 | 62 | 2 | 9 | 7 | 13.4 | 9.3 | 7.7 | 9.9 | 19.2 |
| 3018 | 33 | 77 | 2 | 9 | 0.85 | 2.9 | 1.8 | 1.3 | 2.2 | 4.8 |
| 3019 | 45 | 90 | 2 | 9 | 19 | 67 | 33.4 | 21.6 | 45.2 | 3.7 |
| 3062 | 18 | 35 | 2 | 79 | 31 | 78 | 53.0 | 50.7 | 55.3 | 53.4 |
| 3084 | 45 | 93 | 2 | 4 | 14 | 218 | 57.5 | 0 | 237 | 3.7 |

**TABLE 6-3**
(Continued)

| Well No. | Cell I | Cell J | Cell K | Number of Observations | Range of Observed Concentrations (µg/L) Minimum | Maximum | Mean | 95% Confidence Intervals for the Means (µg/L) Lower End | Upper End | Model Calculated Concentrations (µg/L) |
|---|---|---|---|---|---|---|---|---|---|---|
| 3095 | 21 | 42 | 2 | 5 | 4 | 13 | 7.4 | 0.5 | 13.5 | 123.6 |
| 3107 | 28 | 71 | 2 | 2 | 1 | 2 | 1.5 | 0 | 7.9 | 4.5 |
| 3108 | 30 | 84 | 2 | 2 | 31 | 33 | 32 | 19.3 | 44.7 | 0.7 |
| 3125 | 18 | 38 | 2 | 2 | 70.9 | 88.1 | 79.5 | 0 | 189 | 52.3 |
| 4096 | 11 | 62 | 5 | 4 | 0.5 | 2 | 1.0 | 0 | 2.1 | 0.0 |
| EMR-11 | 22 | 53 | 1 | 74 | 0.8 | 2 | 1.4 | 1.3 | 1.4 | 17.9 |
| EMR-13 | 40 | 42 | 1 | 75 | 0.3 | 1 | 0.6 | 0.6 | 0.7 | 0.0 |
| EMR-14 | 59 | 38 | 1 | 82 | 0.6 | 1.8 | 1.2 | 1.1 | 1.2 | 0.0 |
| EMR-16 | 57 | 27 | 2 | 78 | 0.3 | 1.5 | 0.7 | 0.7 | 0.8 | 0.0 |
| EMR-20 | 19 | 15 | 4 | 53 | 0.09 | 0.6 | 0.2 | 0.2 | 0.3 | 9.4 |
| EMR-21 | 24 | 17 | 4 | 79 | 0.2 | 0.8 | 0.4 | 0.4 | 0.5 | 13.0 |
| EMR-22 | 22 | 62 | 1 | 52 | 0.6 | 1.7 | 1.1 | 1.0 | 1.1 | 0.4 |
| EMR-30 | 18 | 66 | 4 | 19 | 0.4 | 0.8 | 0.6 | 0.5 | 0.6 | 0.0 |
| H-112 | 24 | 82 | 1 | 2 | 0.43 | 0.48 | 0.5 | 0.1 | 0.8 | 0.0 |
| TW-3 | 7 | 28 | 4 | 3 | 1.1 | 2.14 | 1.5 | 0.2 | 2.9 | 0.0 |
| TW-4 | 13 | 31 | 1 | 3 | 1.71 | 1.92 | 1.8 | 1.6 | 2.1 | 1.6 |
| TW-5 | 8 | 29 | 1 | 4 | 0.45 | 0.85 | 0.6 | 0.3 | 0.9 | 0.8 |

TABLE 6-3
(Continued)

| Well No. | Cell I | Cell J | Cell K | Number of Observations | Range of Observed Concentrations (µg/L) Minimum | Maximum | Mean | 95% Confidence Intervals for the Means (µg/L) Lower End | Upper End | Model Calculated Concentrations (µg/L) |
|---|---|---|---|---|---|---|---|---|---|---|
| TW-6 | 15 | 32 | 4 | 4 | 1.08 | 1.18 | 1.1 | 1.1 | 1.2 | 6.2 |
| OAB | 58 | 87 | 3 | 9 | 0.7 | 4.8 | 1.7 | 1.0 | 3.0 | 0.0 |

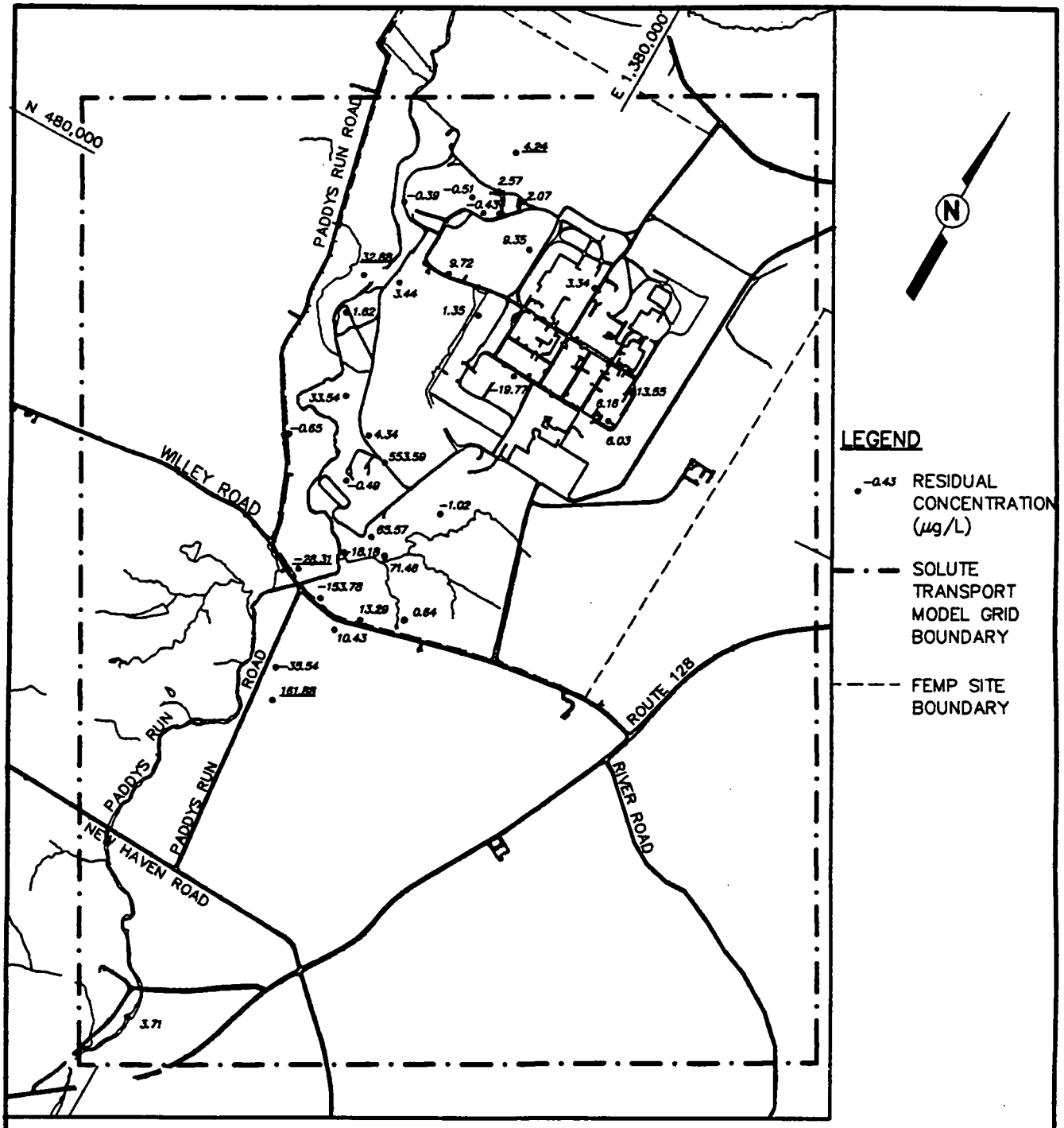


NOTES:

RESIDUAL IS THE OBSERVED MINUS COMPUTED URANIUM CONCENTRATION

UNDERLINED VALUES ARE OUTSIDE OF 95% CONFIDENCE RANGE

COMPUTER FILE NAME: 3DSOL12-60

SCALE

0 2000 4000 FEET

409195-A72 (GW) (PGH)

FIGURE 6-13 3-DIMENSIONAL SOLUTE TRANSPORT MODEL RESIDUAL CONCENTRATIONS FOR CALIBRATED RUN LAYER 1 RETARDATION FACTOR 12

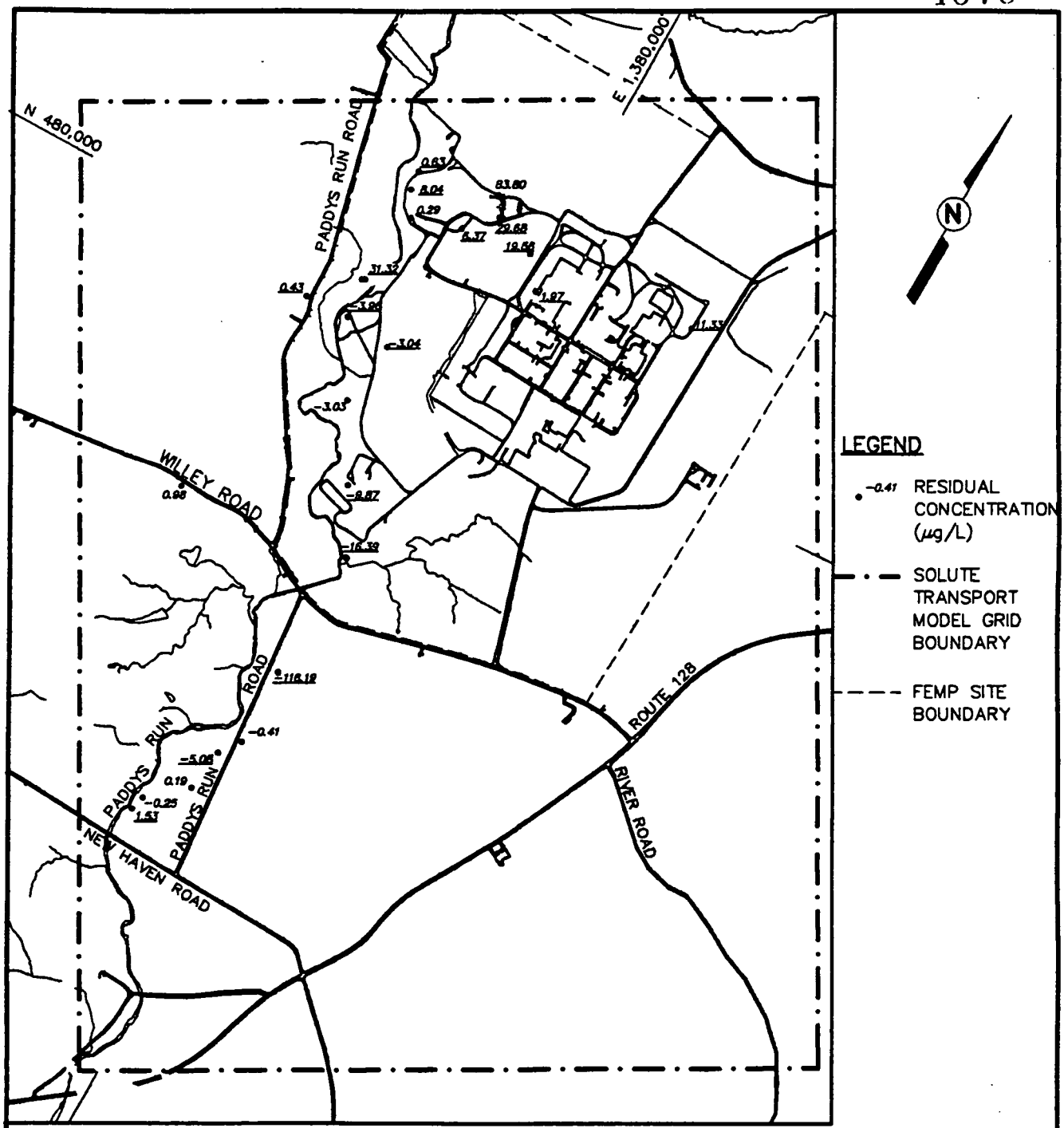


**NOTES:**

RESIDUAL IS THE OBSERVED MINUS COMPUTED URANIUM CONCENTRATION

UNDERLINED VALUES ARE OUTSIDE OF 95% CONFIDENCE RANGE

COMPUTER FILE NAME: 3DSOL12-60

SCALE

0 2000 4000 FEET

409195-A71 (GW) (PGH)

FIGURE 6-14 3-DIMENSIONAL SOLUTE TRANSPORT MODEL RESIDUAL CONCENTRATIONS FOR CALIBRATED RUN LAYERS 2 THROUGH 5 RETARDATION FACTOR 12

Monitoring Wells 2108 and H-112 are upgradient from Paddys Run. Minor westward movement of uranium from Paddys Run can occur due to the temporary reversal of groundwater flow direction caused by water table mounding under the stream during heavy runoff periods. However, the steady-state flow model cannot simulate such water movement. Since the calculated concentrations at these monitoring wells are less than 2 µg/L below the ranges, the representativeness of the model is not affected.

Monitoring Well 2024 is upgradient from any known contaminant source, so it is not possible to raise the calculated concentration at that location. Again, the calculated concentration is less than 2 µg/L below the range, and the representativeness of the model is not affected.

The calculated concentration at Monitoring Well 2017 is too high. This monitoring well is on the upgradient side of Paddys Run. The lack of fit here is related to the finite-difference simulation of source cells along Paddys Run. A source cell in the model is closer to the monitoring well than the stream actually is. The calculated concentration is 28 µg/L out of range and does not affect the representativeness of the model.

Several concentrations for monitoring wells screened in Layers 2 through 4 are out of range. Calculated concentrations tend to be too low in the northern part of the area and too high in the southern part of the area. A few concentrations are in range in both areas. All of the concentrations are less than 17 µg/L out of range, except the deviation at Monitoring Well 3095 where the calculated concentration is 110 µg/L above the range. These deviations are interpreted to be caused primarily by irregular vertical fingering in the contaminant plume. Since monitoring wells that are in range are scattered north-south through the model in Layer 2 or lower, the model is adequately simulating vertical dispersion even though the precision of the simulated vertical dispersion is not great enough to get all of the calculated concentrations in range. Since the wells monitoring the different layers are in clusters at the same location, transverse dispersivity would have to be varied throughout the model to bring the concentrations in the lower layers into range without causing the corresponding concentrations in Layer 1 to go out of range.

The sensitivity analysis for the 3DSOL model was calibrated using a distribution coefficient 0.016 $ft^3/lb$ (Appendix C). Since the ranges of the parameters varied in the sensitivity analysis overlap the parameters used in the final calibrated model (distribution coefficient of 0.22 $ft^3/lb$), a similar sensitivity behavior is expected for the final calibrated model.

The calibrated solute transport model shows that significant adsorption occurs within the aquifer system underlying the FEMP with a distribution coefficient of 0.022 $ft^3/lb$. Over 80 percent of the

estimated mass of uranium lost to the groundwater system is still located near the FEMP site within the boundaries of the local solute transport model grid.

The solute transport model is sensitive to the values of the dispersivities and distribution coefficient and to the amount and location of source loading. Balancing these three parameters can yield similar plumes. However, when the dispersion coefficient is held constant, the distribution coefficient controls the concentration gradients in the plume and the choice of parameters that yield a good calibration is limited.

The model was successfully calibrated with two different distribution coefficients, 0.016 $ft^3/lb$ and 0.022 $ft^3/lb$ (retardation factors 9 and 12, respectively). The calibration at 0.022 $ft^3/lb$ was more refined, because a more restrictive statistical test method was used and more residuals were below the confidence limit. Nevertheless, this result demonstrates that calibration can be accomplished using different distribution coefficients, if compensating adjustments are made in dispersivities and source loading rates. Longitudinal and transverse dispersivities of 50 feet and 1 foot, respectively, were used to calibrate with a distribution coefficient of 0.016 $ft^3/lb$, but these could be increased to the preferred values of 100 feet and 10 feet from literature for calibration with a dispersivity of 0.022 $ft^3/lb$. In order to compensate for the variation of the distribution coefficient from primary to final calibration, the loading rates were changed to consider the following:

- Source loading had to increase when the distribution coefficient was increased to effect a calibration, providing all other parameters remain unchanged. Concentrations of dissolved uranium in a calibrated plume were maintained roughly the same regardless of the distribution coefficient, so more uranium had to be supplied at the source cells to accommodate the increased adsorption at higher distribution coefficients.

- Some source loadings had to be shifted backward in time (i.e.; earlier releases) at higher distribution coefficients because the more travel time due to retardation effect must be accommodated in the calibration.

- Some source loading cells had to be shifted closer to affected monitoring wells with higher distribution coefficients because the retardation effect had to be accommodated in the calibration.

The source loading rates that resulted from the final calibration with a distribution coefficient of 0.022 $ft^3/lb$ are shown in Figures 6-15 through 6-19, and are summarized in Tables 6-4 and 6-5. As shown in Tables 6-4 and 6-5, a fifth period was added to represent the year 1989 in the final calibration of the model to update the uranium discharge into Paddys Run. This also allowed a closer match for the high concentration in Monitoring Well 2045 which is just east of Paddys Run. The information about the source loading rates for the preliminary calibration with a distribution coefficient of 0.016 $ft^3/lb$ is presented in Appendix C. Comparing two source loading patterns

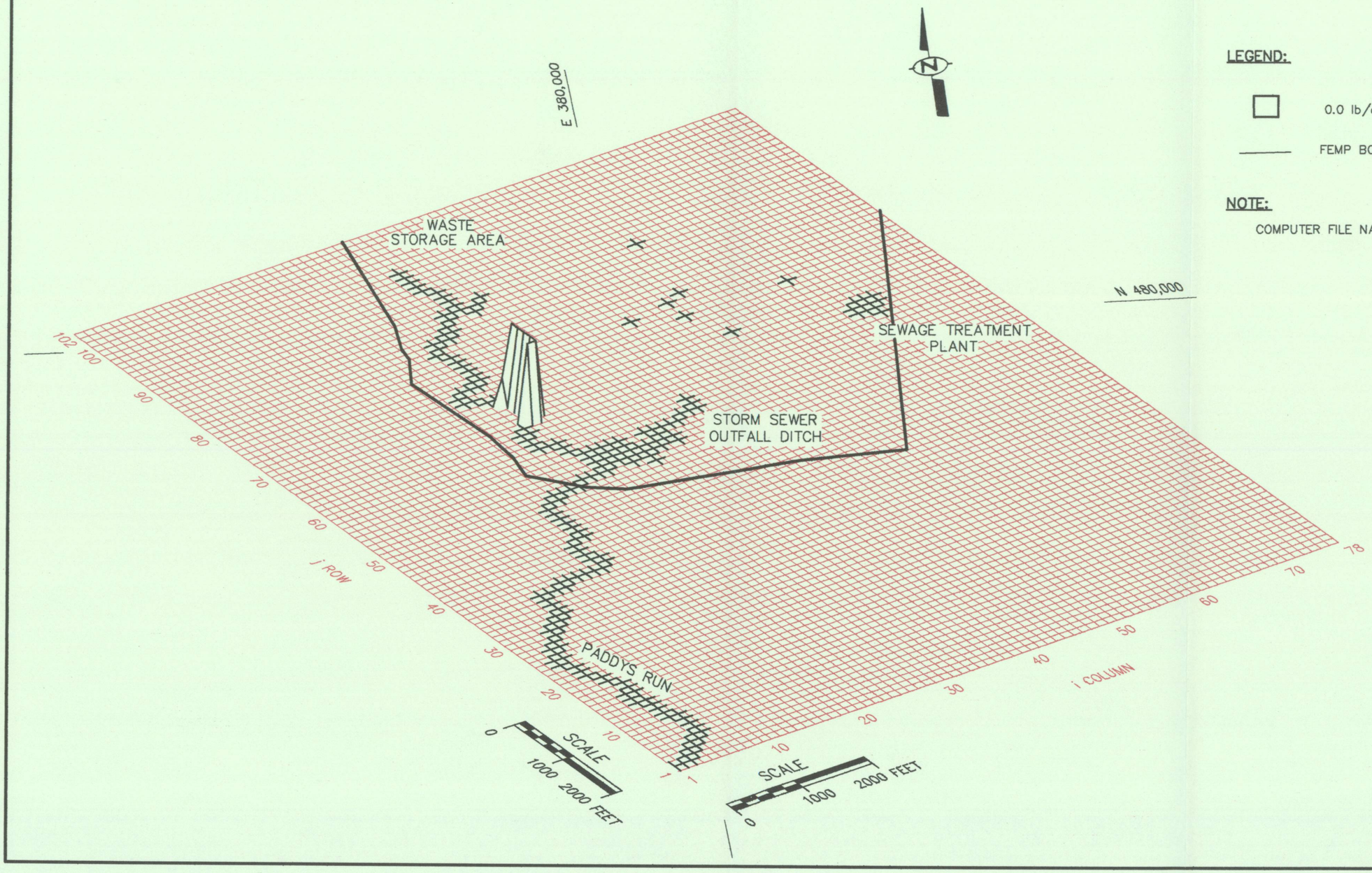


**LEGEND:**

0.0 lb/day to 0.1 lb/day

FEMP BOUNDARY

**NOTE:**

COMPUTER FILE NAME: 3DSOL12-60



FIGURE 6-15
3-DIMENSIONAL SOLUTE TRANSPORT MODEL
SOURCE LOADING RATES
SOURCE PERIOD 1
RETARDATION FACTOR 12

409195-B79 /01 (GW) (PGH)
409195-B79 /01 (100% RED

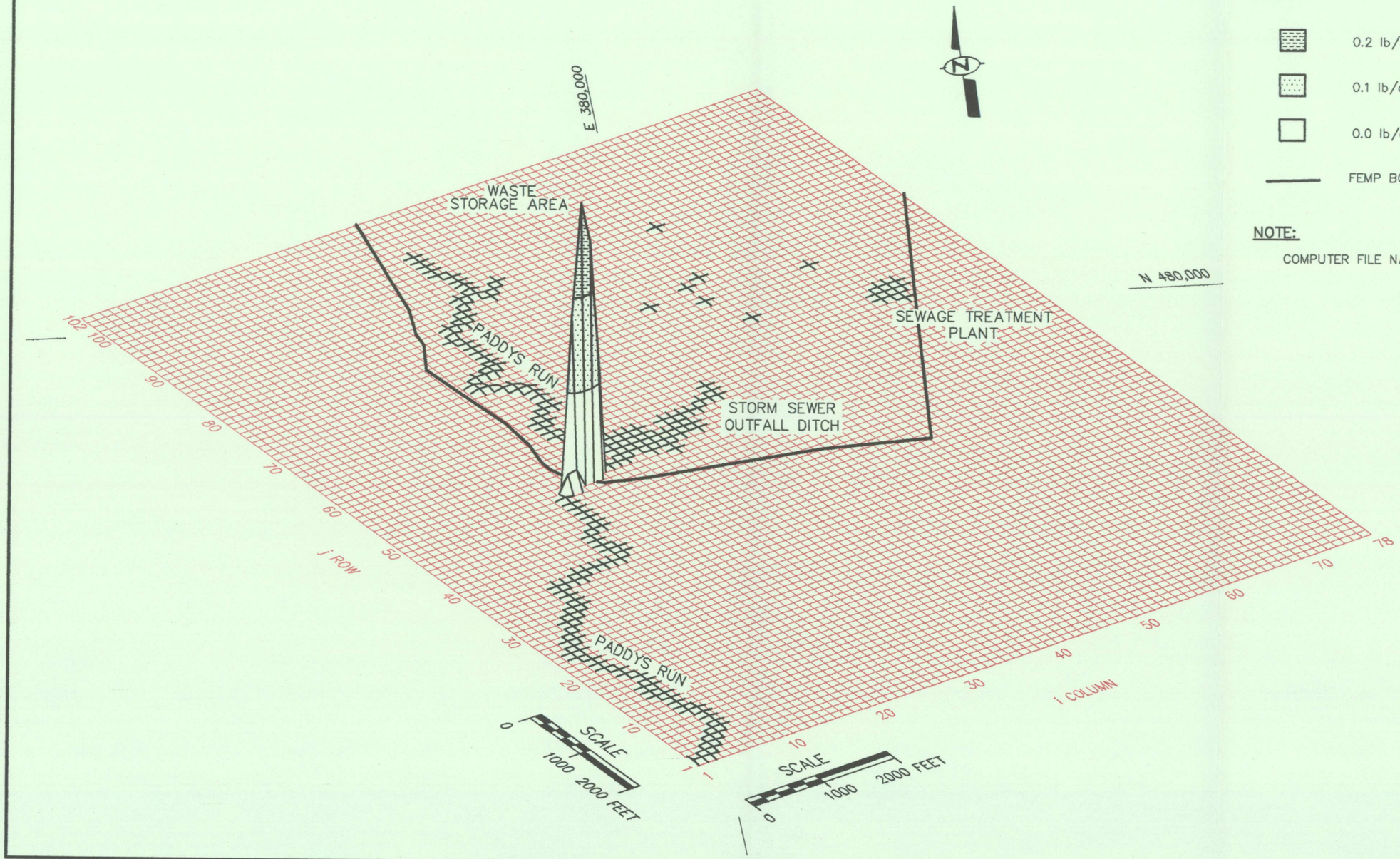


**LEGEND:**

- 0.2 lb/day to 0.3 lb/day
- 0.1 lb/day to 0.2 lb/day
- 0.0 lb/day to 0.1 lb/day
- FEMP BOUNDARY

**NOTE:**

COMPUTER FILE NAME: 3DSOL12-60



FIGURE 6-16
3-DIMENSIONAL SOLUTE TRANSPORT MODEL
SOURCE LOADING RATES
SOURCE PERIOD 2
RETARDATION FACTOR 12

409195-B73 (GW) 100% RED
409195-B73 /01 (GW) (PGH)

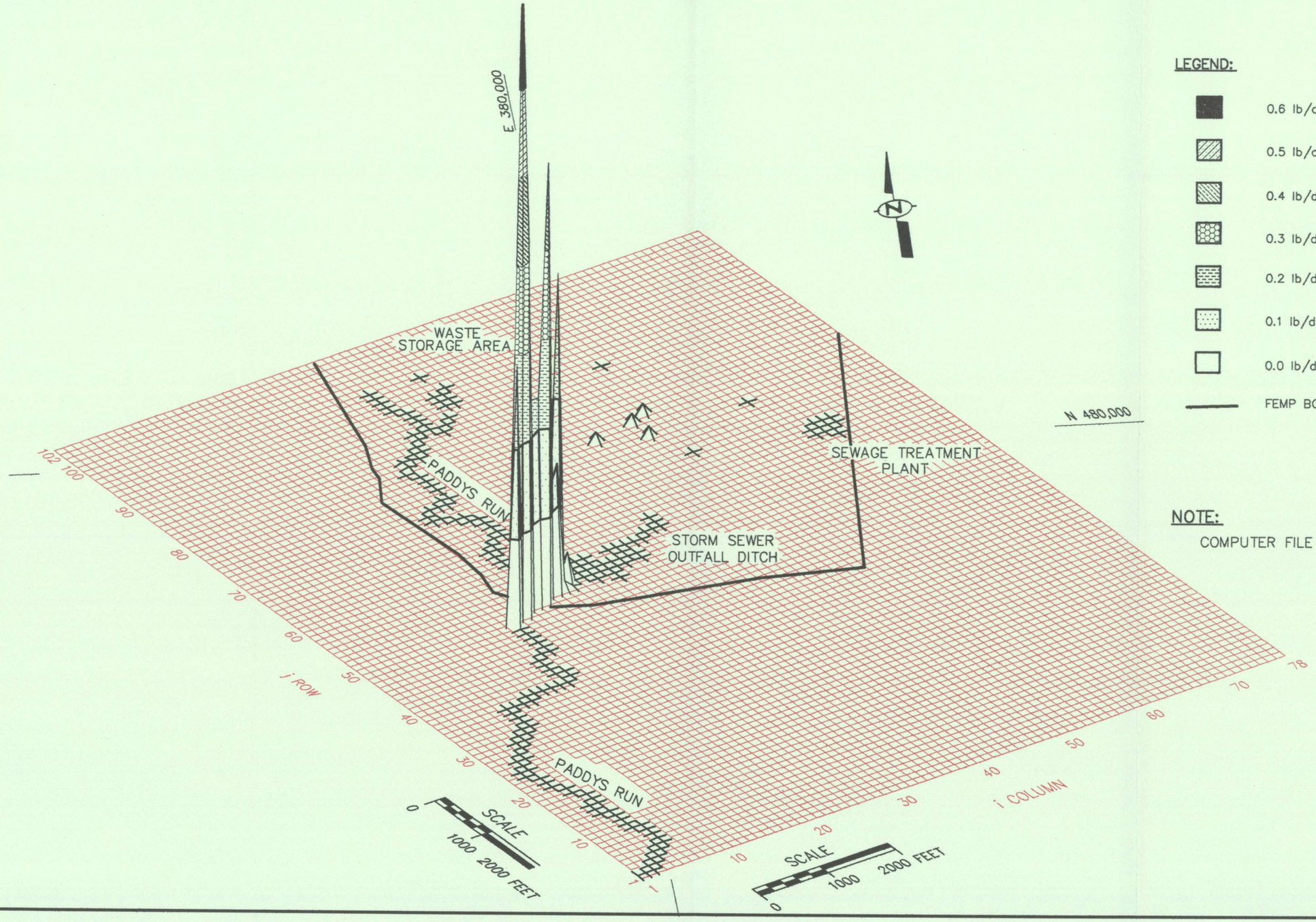


**LEGEND:**

- 0.6 lb/day to 0.7 lb/day
- 0.5 lb/day to 0.6 lb/day
- 0.4 lb/day to 0.5 lb/day
- 0.3 lb/day to 0.4 lb/day
- 0.2 lb/day to 0.3 lb/day
- 0.1 lb/day to 0.2 lb/day
- 0.0 lb/day to 0.1 lb/day
- FEMP BOUNDARY

**NOTE:**

COMPUTER FILE NAME: 3DSOL12-60



FIGURE 6-17
3-DIMENSIONAL SOLUTE TRANSPORT MODEL
SOURCE LOADING RATES
SOURCE PERIOD 3
RETARDATION FACTOR 12

409195-B74 100% RED
409195-B74 /01 (GW) (PGH)

**LEGEND:**

0.0 lb/day to 0.1 lb/day

FEMP BOUNDARY

**NOTE:**

COMPUTER FILE NAME: 3DSOL12-60



409195-B72 /01 (GW) (PGH)

FIGURE 6-18
3-DIMENSIONAL SOLUTE TRANSPORT MODEL
SOURCE LOADING RATES
SOURCE PERIOD 4
RETARDATION FACTOR 12

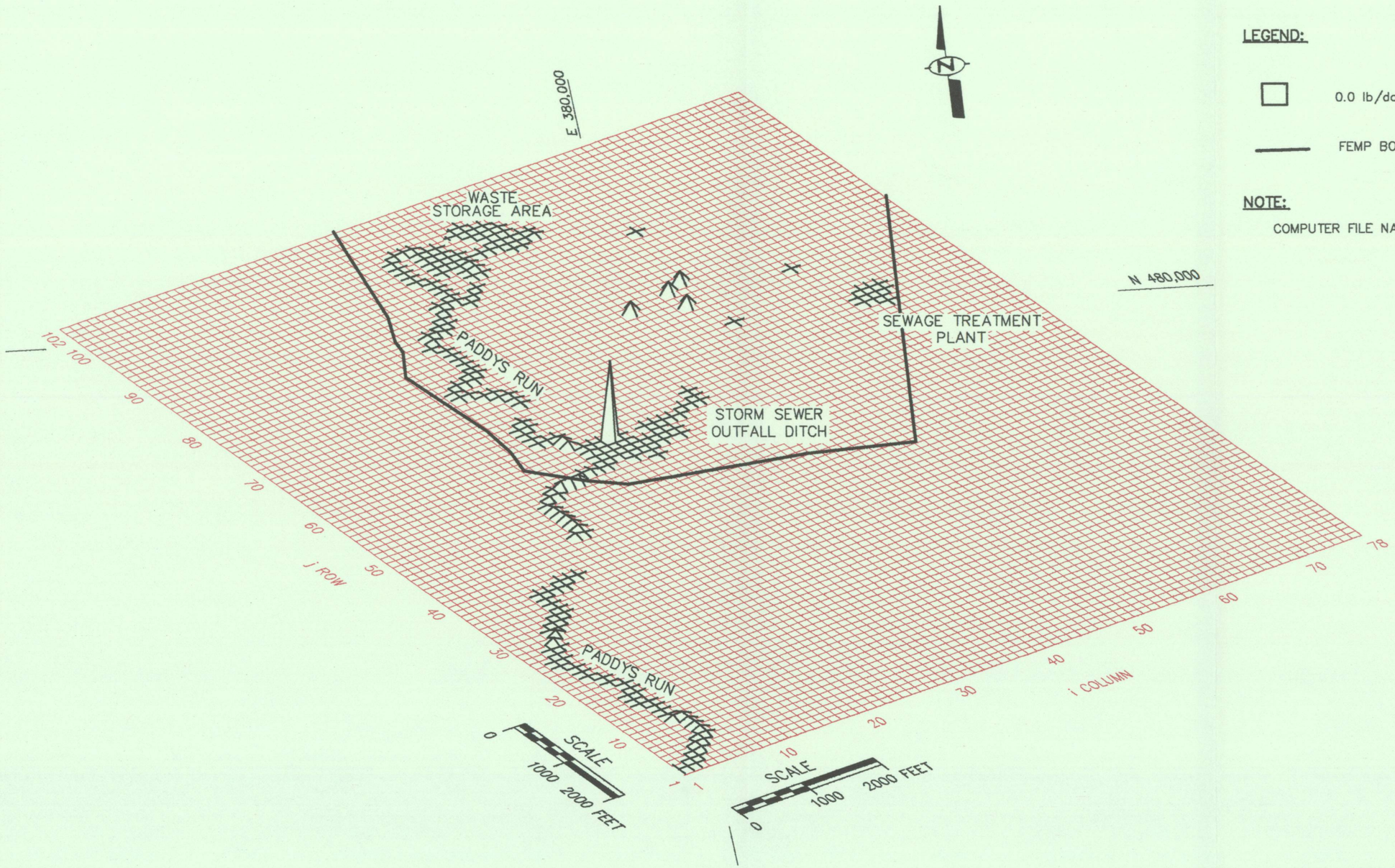


**LEGEND:**

0.0 lb/day to 0.1 lb/day

FEMP BOUNDARY

**NOTE:**

COMPUTER FILE NAME: 3DSOL12-60



FIGURE 6-19
3-DIMENSIONAL SOLUTE TRANSPORT MODEL
SOURCE LOADING RATES
SOURCE PERIOD 5
RETARDATION FACTOR 12

409195-B71 /01 (GW) (PGH)
409195-B71 /01 (GW) 100% RED

## TABLE 6-4

## URANIUM LOADING RATES FOR SOURCE AREAS IN THE THREE-DIMENSIONAL FINITE-DIFFERENCE SOLUTE TRANSPORT MODEL RETARDATION FACTOR 12, LONGITUDINAL DISPERSIVITY 100 FEET, AND TRANSVERSE DISPERSIVITY 10 FEET

| Source Loading Area | URANIUM SOURCE LOADING RATES (lb/day) | | | | | |
|---|---|---|---|---|---|---|
| | Period 1 1952-1958 | Period 2 1959-1966 | Period 3 1969-1975 | Period 4 1976-1988 | Period 5 1989-1989 | Area Totals |
| Paddys Run: | | | | | | |
| North of Waste Storage Area | 0.0000286 | 0.000373 | 0.000372 | 0.00464 | 0.00618 | 0.01159 |
| Waste Storage Area to Storm Sewer Outfall Ditch | 0.546 | 0.0492 | 0.0515 | 0.0486 | 0.0478 | 0.7431 |
| Storm Sewer Outfall Ditch to Albright & Wilson Company Wells | 0.000353 | 0.915 | 3.57 | 0.331 | 0.0662 | 4.8826 |
| South of Albright & Wilson Company Wells | 0.00292 | 0.0192 | 0.00769 | 0.111 | 0.0409 | 0.18171 |
| Waste Storage Area | 0.0 | 0.0 | 0.00291 | 0.0242 | 0.0231 | 0.05021 |
| Waste Storage Silo Area | 0.000197 | 0.000197 | 0.0014 | 0.002 | 0.000957 | 0.00475 |
| Biodenitrification Lagoon | 0.0 | 0.0 | 0.0 | 0.0 | 0.0 | 0.0 |
| Sludge Ponds | 0.0 | 0.0 | 0.0 | 0.0 | 0.0 | 0.0 |
| Former Production Area | 0.00178 | 0.00178 | 0.0488 | 0.0488 | 0.0488 | 0.14996 |
| Sewage Treatment Area | 0.000593 | 0.000593 | 0.000593 | 0.000593 | 0.000593 | 0.00297 |
| Storm Sewer Outfall Ditch | 0.0000052 | 0.0000034 | 0.0000593 | 0.000299 | 0.0831 | 0.08347 |
| PERIOD TOTALS | 0.5520 | 0.9865 | 3.6865 | 0.5703 | 0.3176 | 6.11 |

# TABLE 6-5

## TOTAL URANIUM LOADING FOR SOURCE AREAS IN THE THREE-DIMENSIONAL FINITE-DIFFERENCE SOLUTE TRANSPORT MODEL RETARDATION FACTOR 12, LONGITUDINAL DISPERSIVITY 100 FEET, AND TRANSVERSE DISPERSIVITY 10 FEET

| | Uranium Source Loadings (lb) | | | | | |
|---|---|---|---|---|---|---|
| Source Loading Area | Period 1 1952-1958 | Period 2 1959-1966 | Period 3 1967-1975 | Period 4 1976-1988 | Period 5 1989-1989 | Area Totals |
| Paddys Run | | | | | | |
| North of Waste Storage Area | 0.07 | 1.09 | 1.22 | 22.02 | 2.26 | 26.66 |
| Waste Storage Area to Storm Sewer Outfall Ditch | 1395 | 143.7 | 169.2 | 230.6 | 17.45 | 1956 |
| Storm Sewer Outfall Ditch to Albright & Wilson Company Wells | 0.90 | 2672 | 11730 | 1571 | 24.16 | 15,998 |
| South of Albright & Wilson Co. Wells | 7.46 | 56.1 | 25.3 | 526.7 | 14.93 | 630.4 |
| Waste Storage Area | 0.00 | 0.00 | 9.56 | 114.8 | 8.43 | 132.8 |
| Waste Storage Silo Area | 0.50 | 0.58 | 4.60 | 9.49 | 0.35 | 15.52 |
| Biodenitrification Lagoon | 0.00 | 0.00 | 0.00 | 0.00 | 0.00 | 0.00 |
| Sludge Ponds | 0.00 | 0.00 | 0.00 | 0.00 | 0.00 | 0.00 |
| Former Production Area | 4.55 | 5.20 | 160.3 | 231.6 | 17.81 | 419.4 |
| Sewage Treatment Area | 1.52 | 1.73 | 1.95 | 2.81 | 0.22 | 8.23 |
| Storm Sewer Outfall Ditch | 0.01 | 0.01 | 0.2 | 1.42 | 30.33 | 31.96 |
| TOTAL | 1410 | 2880 | 12102 | 2710 | 116 | 19,218 |

corresponding to preliminary and final calibration, higher total loading quantity and earlier loading peaks are shown in the model with a greater distribution coefficient.

The source loading rates from the final calibration do not represent a unique solution to the problem of estimating the historical loss of uranium to groundwater at the site. However, they are constrained by the following considerations:

- Concentrations in the model were consistent with concentrations measured in the field. Therefore, calibration of the concentration values in the model resulted in plumes that contained the best estimate of the amount of uranium in the groundwater system, including that which was adsorbed.

- The total source loading was equal to the sum of dissolved and adsorbed uranium in the simulated plume, plus uranium that had crossed the model boundaries, and uranium that had been removed from the system by water wells. Therefore, the total source loading was fairly accurate for a given distribution coefficient.

- The distribution of simulated source loading in time and space is severely limited by the constraints of calibration. It was necessary to introduce uranium via source cells at the proper place at the proper time to produce the desired effect on the calculated concentration at a monitoring well site.

Consequently, freedom in choosing location and time variation in source loading conditions was found to be limited if the distribution coefficient was held constant. The evidence that most loss of uranium to the groundwater system was in the vicinity of the confluence of the storm sewer outfall ditch and Paddys Run is very strong. The corollary is that the loss of uranium from the waste storage area and other areas of the FEMP site to the regional aquifer has been relatively small, unless such losses involve discharge to Paddys Run that would then be accounted for under the assumed principal source in Paddys Run. The source loading rates also indicate that uranium discharge to the Great Miami Aquifer was much greater in the past than it is now.

The plume resulting from the final calibration at distribution coefficient 0.022 $ft^3/lb$ is shown in Figures 6-20 through 6-24. As additional monitoring wells are installed in the future, it may be necessary to make minor modifications in this model to accommodate those data. The magnitude and location of the peak concentrations in the plume may not be exactly as shown by the model. Some unknown sources may exist, and they could be added to the model if they were discovered by field investigation.

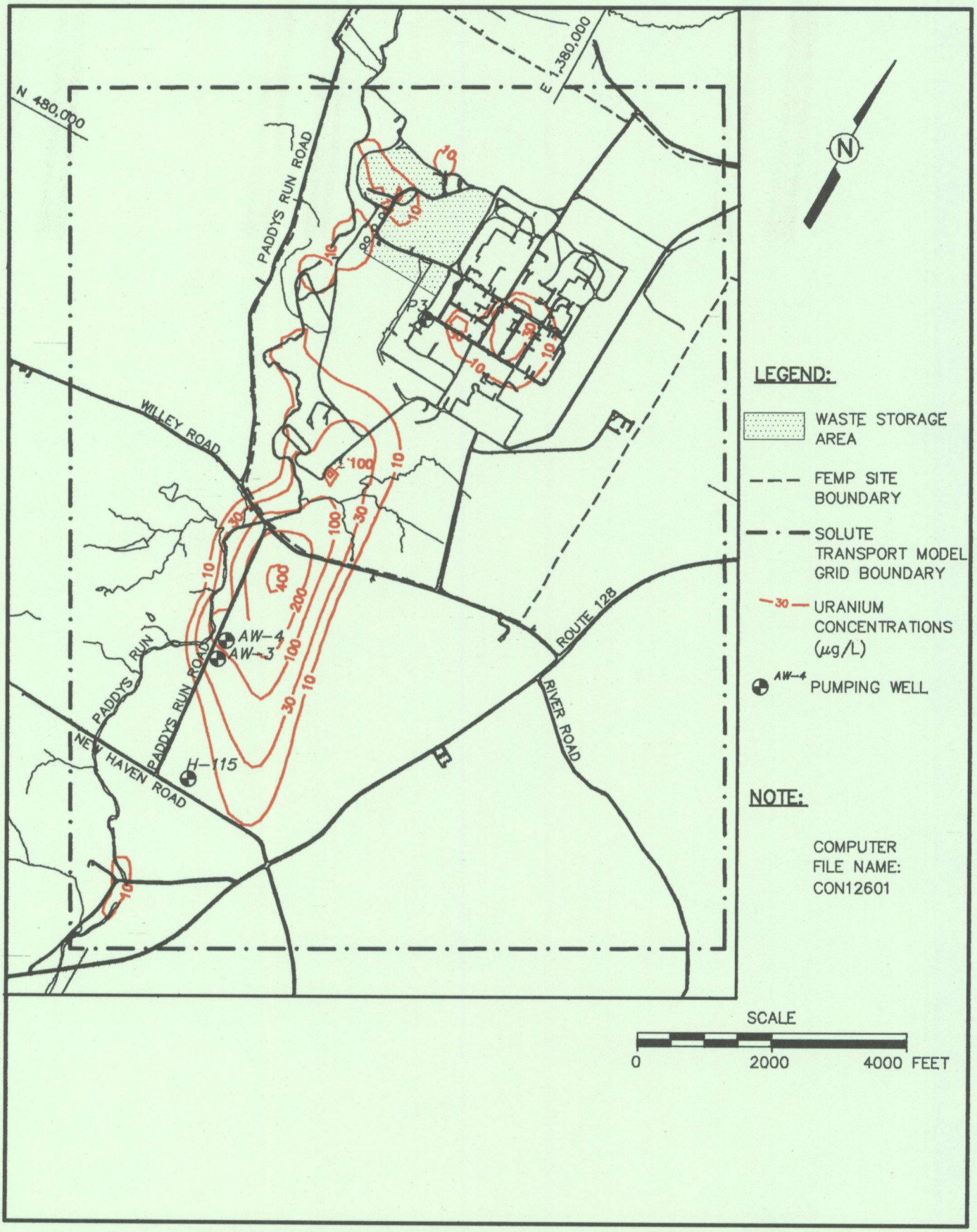


409195-A78 (GW) /01 (PGH)

FIGURE 6-20 3-DIMENSIONAL SOLUTE TRANSPORT MODEL
SIMULATED URANIUM CONCENTRATIONS
PRESENT CONDITIONS
LAYER 1
RETARDATION FACTOR 12

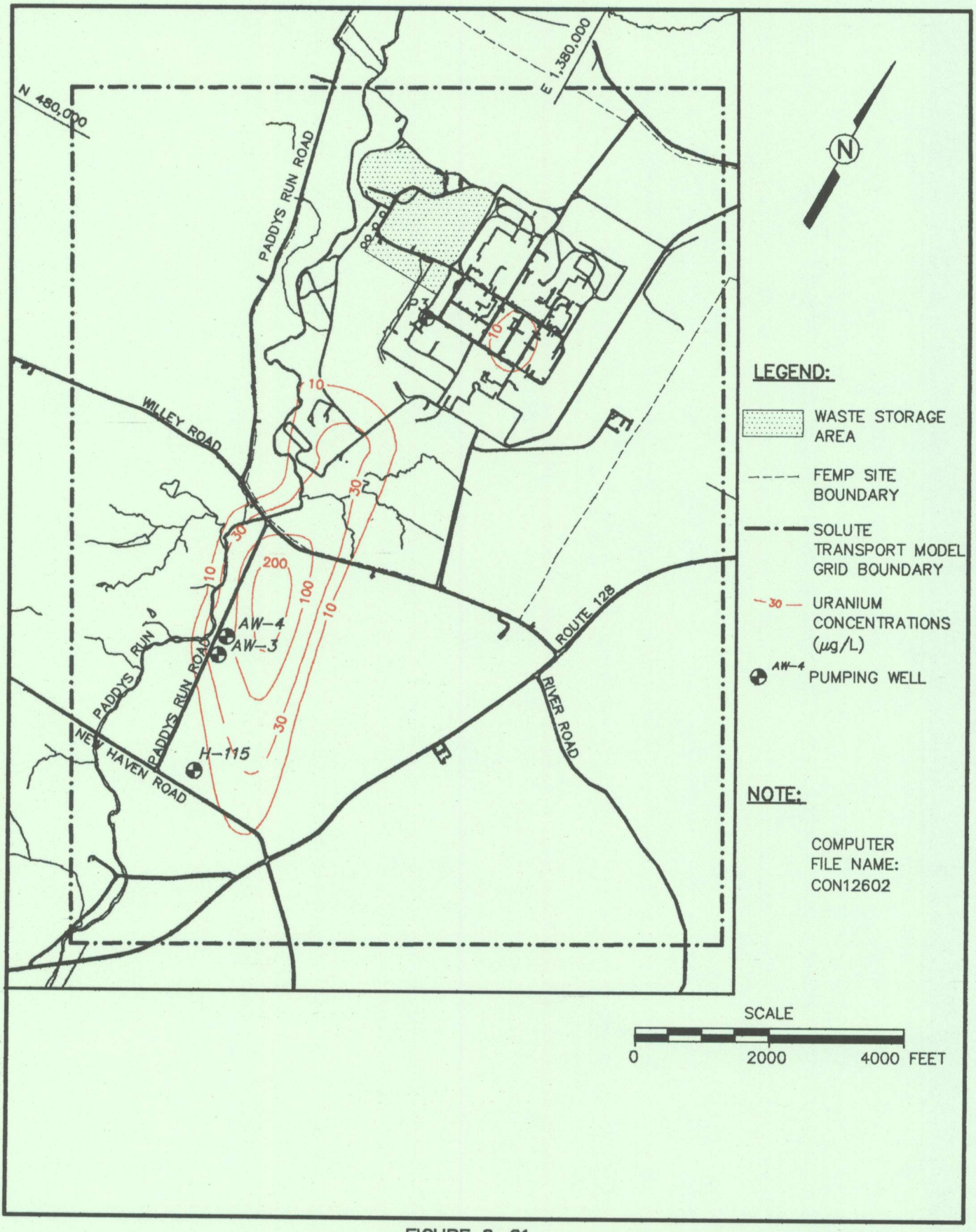


409195-A82 (GW) (PGH)

FIGURE 6-21
3-DIMENSIONAL SOLUTE TRANSPORT MODEL
SIMULATED URANIUM CONCENTRATIONS
PRESENT CONDITIONS
LAYER 2

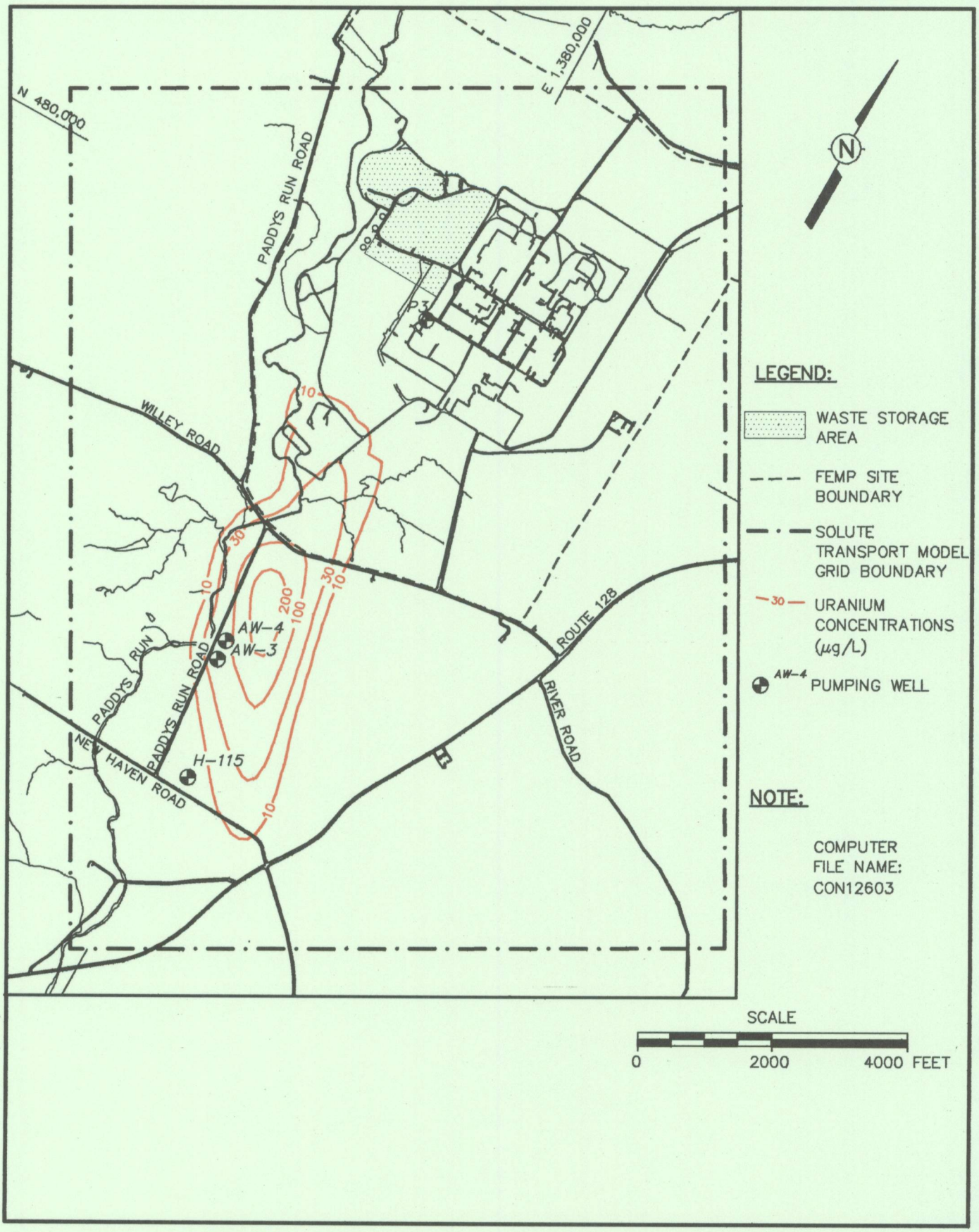


409195-A81 (GW) /01 (PGH)

FIGURE 6-22 3-DIMENSIONAL SOLUTE TRANSPORT MODEL
SIMULATED URANIUM CONCENTRATIONS
PRESENT CONDITIONS
LAYER 3
RETARDATION FACTOR 12

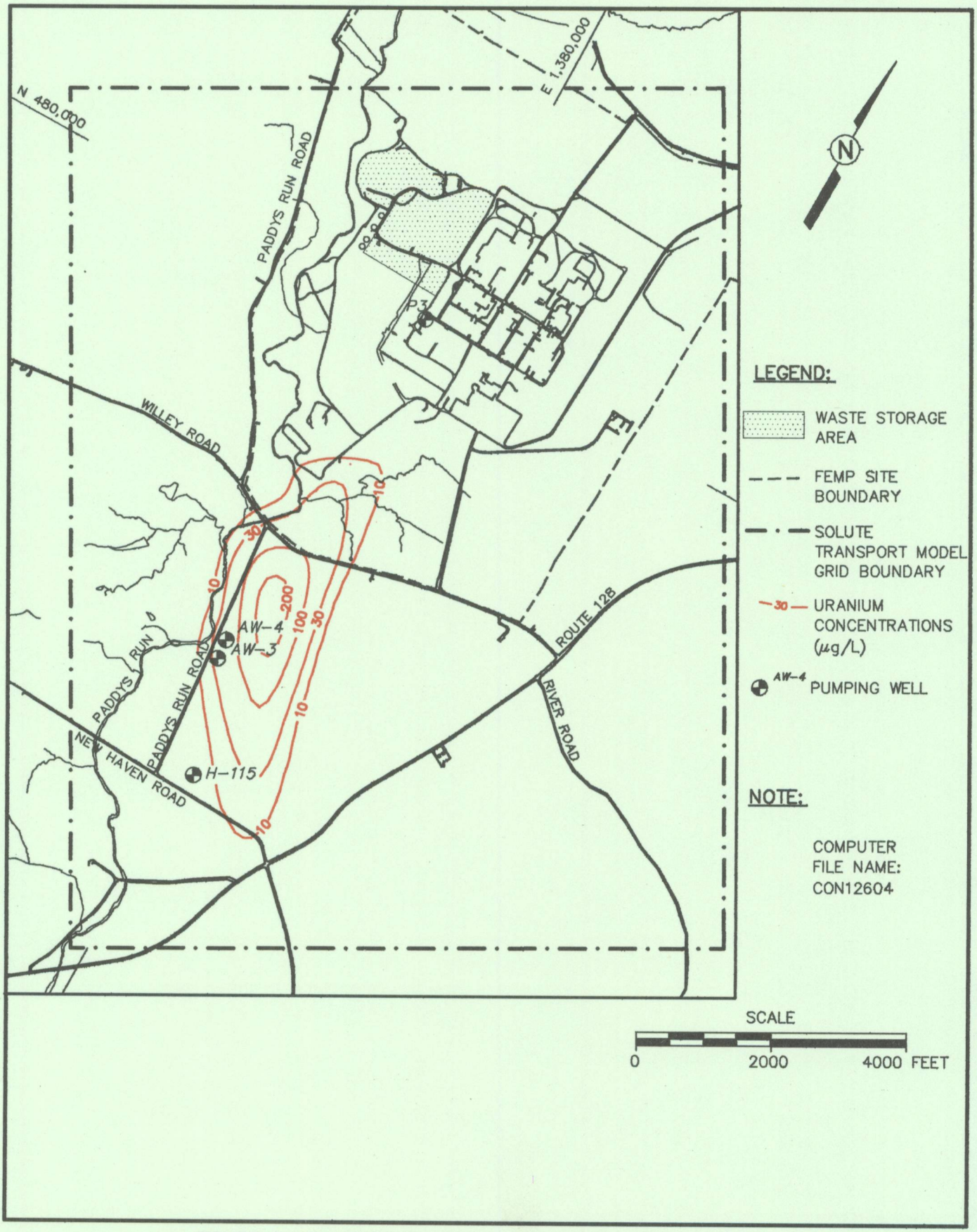


409195-A80 (GW) /01 (PGH)

FIGURE 6-23 3-DIMENSIONAL SOLUTE TRANSPORT MODEL
SIMULATED URANIUM CONCENTRATIONS
PRESENT CONDITIONS
LAYER 4
RETARDATION FACTOR 12

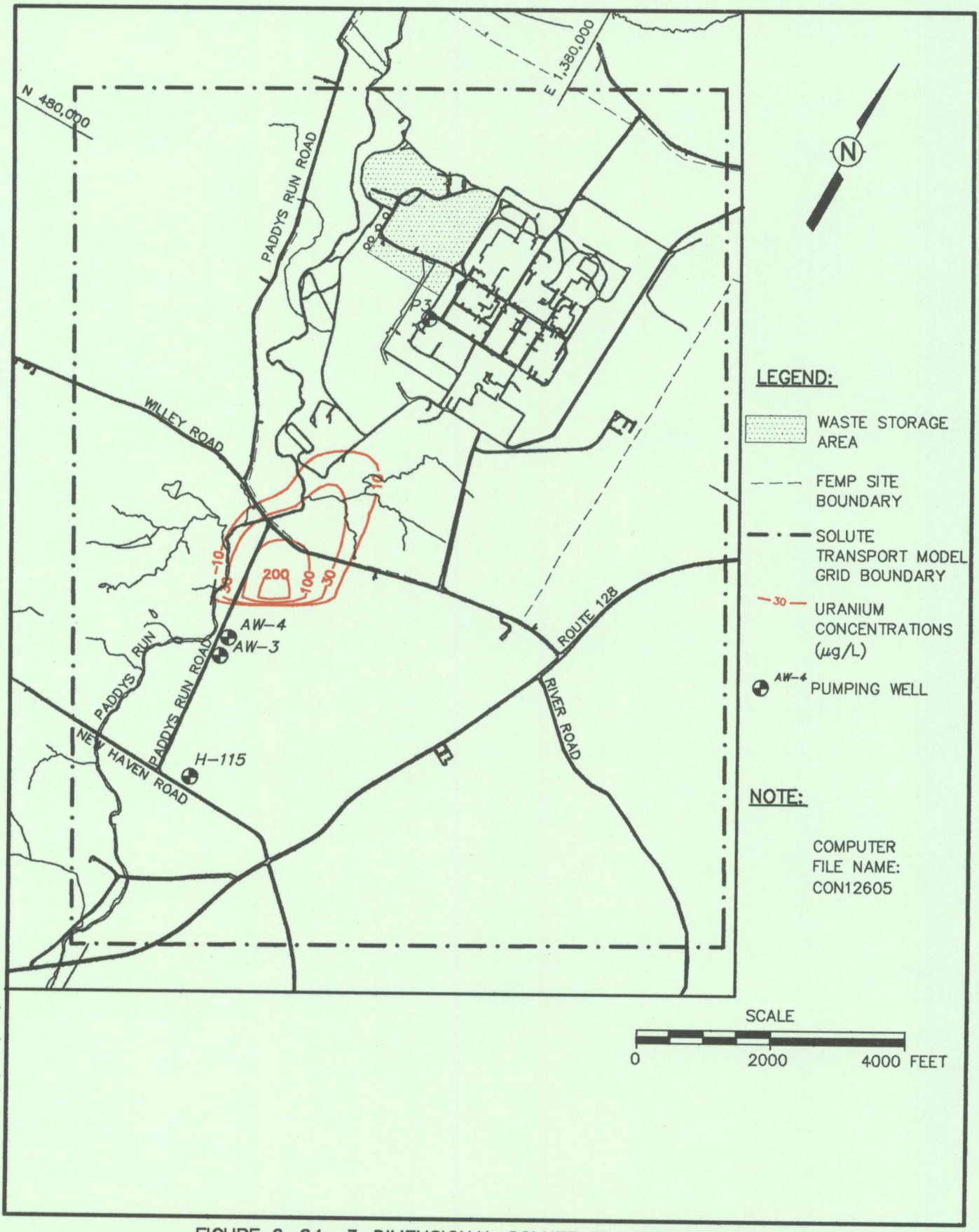


409195-A79 (GW) /01 (PGH)

FIGURE 6-24 3-DIMENSIONAL SOLUTE TRANSPORT MODEL
SIMULATED URANIUM CONCENTRATIONS
PRESENT CONDITIONS
LAYER 5
RETARDATION FACTOR 12

# REFERENCES

Albright & Wilson Company, 1986, Correspondence from S. R. Goodson, Plant Manager, to J. L. Hosler of IT Corporation, dated April 11, 1986.

Babu, D. K., G. F. Pinder, A. Niemi, and D. P. Ahlfeld, 1987, "Chemical Transport by Three-Dimensional Ground Water Flows," 84-WR-3, Department of Civil Engineering, Princeton University, Princeton, New Jersey.

Barari, A., 1983, "Hydrogeology of Glacial Till," unpublished, South Dakota Geological Survey, Vermillion, South Dakota.

Barari, A. and L. S. Hedges, 1985, "Movement of Water in Glacial Till," International Association of Hydrogeologists, Memoires, Vol. XVII, Part 1, Proceedings, Hydrogeology of Rocks of Low Permeability, Tucson, Arizona.

Batu, V., 1989, "A Generalized Two-Dimensional Analytical Solution for Hydrodynamic Dispersion in Bounded Media with the First-Type Boundary Condition at the Source," Water Resources Research, Vol. 25, No. 6, pp. 1125-1132.

Batu, V. and M. Th. van Genuchten, 1990, "First- and Third-Type Boundary Conditions in Two-Dimensional Solute Transport Modeling," Water Resources Research, Vol. 26, No. 2, pp. 339-350.

Beavers, J. E., W. E. Manrod, and W. C. Stoddart, 1982, Recommended Seismic Hazard Levels for the Oak Ridge, Tennessee; Paducah, Kentucky; Fernald, Ohio; and Portsmouth, Ohio, Department of Energy Reservations, Revision 1, K/BD-1025/R1, Oak Ridge National Laboratory, Oak Ridge, Tennessee.

Brockman, C. S., 1988, "Glacial Geologic Mapping in Hamilton County, Ohio," Ohio Department of Natural Resources, Division of Geological Survey, Columbus, Ohio.

Cravens, S. J., and L. C. Ruedisili, 1987, "Water Movement in Till of East-Central South Dakota," Groundwater, Vol. 25, No. 5, pp. 555-561.

Dames and Moore, 1985, Department of Energy Feed Materials Production Center, Groundwater Task C Report, prepared for National Lead of Ohio, Inc., Cincinnati, Ohio.

Dames and Moore, 1986a, "RCRA Groundwater Monitoring Report, Vol. 1, - Round 1 Sampling," prepared for Westinghouse Materials Company of Ohio, Fernald, Ohio.

Dames and Moore, 1986b, "RCRA Groundwater Monitoring Report, Vol. 2, - Round 1 Sampling," prepared for Westinghouse Materials Company of Ohio, Fernald, Ohio.

Dames and Moore, 1987a, "RCRA Groundwater Monitoring Report, Vol. 3, - Round 1 Sampling," prepared for Westinghouse Materials Company of Ohio, Fernald, Ohio.

Dames and Moore, 1987b, "RCRA Groundwater Monitoring Report, Vol. 4, - Round 1 Sampling," prepared for Westinghouse Materials Company of Ohio, Fernald, Ohio.

**REFERENCES**
**(Continued)**

Dames and Moore, 1987c, "RCRA Groundwater Monitoring Report, Vol. 5, - Round 1 Sampling," prepared for Westinghouse Materials Company of Ohio, Fernald, Ohio.

Dove, G. D., 1961, "A Hydrologic Study of the Valley-Fill Deposits in the Venice Area, Ohio," Technical Report No. 4, Ohio Department of Natural Resources, Division of Water, Columbus, Ohio.

Dove G. D., and S. E. Norris, 1951, "Conditions Governing the Occurrence of Groundwater in the Fernald Area, Ohio, with Reference to the Possibilities of Contamination by Disposal of Chemical Wastes," U.S. Geological Survey, Groundwater Branch, Columbus, Ohio, 10 pp. (plus tables and figures).

Driscoll, F. G., 1986, Groundwater and Wells, Second Edition, Johnson Division, St. Paul, Minnesota.

Durrell, R. H., 1961, "The Pleistocene Geology of the Cincinnati Area," Geological Society of America Guidebook Series, Cincinnati Meeting, pp. 47-57.

Eye, J. D., 1961, "Report on the Ground Water Pollution Potential in the Feed Materials Production Center Operated by the National Lead Company of Ohio," Report to National Lead Company of Ohio.

Facemire, C. G., 1985, "Feed Materials Production Center Environmental Monitoring Annual Report for 1984," NLO-2028, Special UC-41.

Fenneman, N. M., 1916, "The Geology of Cincinnati and Vicinity," Geological Society of Ohio, Bulletin 19, 207 pp., 2 maps.

Fetter, C. W., Jr., 1980, Applied Hydrogeology, Merrill Publishing, Columbus, Ohio.

Ford, J. P., 1974, "Bedrock Geology of the Cincinnati West Quadrangle and Part of the Covington Quadrangle, Hamilton County, Ohio," Ohio Department of Natural Resources, Division of Geological Survey, Report of Investigations No. 93, Columbus, Ohio.

Freeze, R. A. and J. A. Cherry, 1979, Groundwater, Prentice-Hall, New York, New York.

Frind, E. O., and C. D. Palmer, 1980, "Parametric Study of Potential Contaminant Transport at the Proposed Delmarva Power and Light Company Plant Site, Vienna, Maryland," Report prepared for Maryland Power Plant Siting Program, Annapolis, Maryland.

GeoTrans, Inc., 1985, "Preliminary Characterization of the Groundwater Flow System Near the Feed Materials Production Center, Great Miami River Valley-Fill Aquifer, Fernald, Ohio," prepared for the Ohio Environmental Protection Agency, Southwest District Office, Dayton, Ohio.

GeoTrans, Inc., 1987, "STLINE, Version 1.9," User's Manual.

GeoTrans, Inc., 1988, "SWIFT III Quality Assurance Benchmark Problem Execution Fiche," Herndon, Virginia.

Golden Software, Inc., 1989, "SURFER® Version 2," Reference Manual, Golden, Colorado.

## REFERENCES
## (Continued)

Grisak, G. E., J. A. Cherry; J. A. Vonhof, and J. P. Blumle, 1976, "Hydrogeologic and Hydrochemical Properties of Fractured Till in the Interior Plains Region," Glacial Till: An Interdisciplinary Study, R. F. Legget (ed.), Royal Society of Canada Special Publication 12, pp. 304-335.

Grubbs, F. E., 1969, "Procedures for Detecting Outlying Observations in Samples," Technometrics, Vol. 11, No. 1, pp. 1-21.

Hartsock, J. K., 1960, "Geologic Considerations of Waste Control at the Feed Materials Production Center, Fernald, Ohio", TID-12297, U.S. Atomic Energy Commission.

Hendry, M. J., 1982, "Hydraulic Conductivity of a Glacial Till in Alberta," Groundwater, Vol. 20, No. 2, pp. 162-169.

Hendry, M. J., 1988, "Hydrology of Clay Till in a Prairie Region of Canada," Groundwater, Vol. 26, No. 5, pp. 607-614.

IT Corporation, 1986, "GEOFLOW, Ground Water Flow and Solute Transport Computer program, User's Manual," Monroeville, Pennsylvania.

IT Corporation, 1986a, "Two-Dimensional General Analytical Solutions for Solute Transport Through a Bounded Porous Medium with the First-Type Boundary Condition and the Computer Program for a Strip Source, STRIB1B," Pittsburgh, Pennsylvania.

IT Corporation, 1986b, "Two-Dimensional General Analytical Solutions for Solute Transport Through a Bounded Porous Medium with the Third-Type Boundary Condition and the Computer Program for a Strip Source, STRIP1B-FBC-G," Pittsburgh, Pennsylvania.

IT Corporation, 1987, "GEOSTAT, A Statistical Program for Examining the Goodness of Fit of Ground Water Modeling Data," User's Manual, Monroeville, Pennsylvania.

IT Corporation, 1988, "Hydrogeologic Study of FMPC Discharge to the Great Miami River," prepared for U.S. Department of Energy, Oak Ridge Operations, Oak Ridge, Tennessee.

IT Corporation, 1988a, "Work Plan, Ground Water Flow/Solute Transport Modeling, Remedial Investigation, Feed Materials Production Center," prepared for U.S. Department of Energy, Oak Ridge Operations, Oak Ridge, Tennessee.

IT Corporation, 1988b, "Hydrogeologic Study of FMPC Discharge to the Great Miami River," prepared for U.S. Department of Energy, Oak Ridge Operations, Oak Ridge, Tennessee.

IT Corporation, 1989, "Preliminary Field Sampling and Laboratory Procedure Plan for the Geochemical Program," in support of the Remedial Investigation/Feasibility Study, Feed Materials Production Center, Fernald, Ohio, prepared for the U.S. Department of Energy, Oak Ridge Operations, Oak Ridge, Tennessee.

## REFERENCES
## (Continued)

IT Corporation, 1990, "Fernald RI/FS Groundwater Modeling, Flow and Solute Transport Computer code Verification," prepared for U.S. Department of Energy, Oak Ridge Operations, Oak Ridge, Tennessee.

Johnson, A. I., 1967, "Specific Yield - Compilation of Specific Yields for Various Materials," U.S.G.S. Water Supply Paper 1662-D.

Kazmann, Raphael Gabriel, 1950, "Hydrogeology and Water Resources (abs.)," Journal of the American Geophysical Union, Vol. 31, No. 2, p. 336.

Klaer, F. H., Jr., and Kazmann, R. G., 1943, "A Quantitative Study of the Well Field of the Mill Creek Valley Water Supply Project, Butler County, Ohio," U.S. Geological Survey Open-File Report.

Klaer, Fred H., Jr., 1968, "Well and Well Field Operations," Journal of the American Water Works Association, Vol. 60, No. 3, pp. 273-280.

Leow, J. A., 1985, "Top of Rock Map of Butler County, Ohio," Open File Map 224, Ohio Department of Natural Resources, Division of Geological Survey, Columbus, Ohio.

Lerch, N. K., W. F. Hale and D. D. Lemaster, 1980, "Soil Survey of Butler County, Ohio," U.S. Department of Agriculture, Soil Conservation Service, in Cooperation with Ohio Department of National Resources, Division of Lands and Soil and Ohio Agriculture Research and Development Center, Columbus, OH.

Lerch, N. K, W. F. Hale and D. D. Lemaster, 1982, "Soil Survey of Hamilton County, Ohio," U.S. Department of Agriculture, Soil Conservation Service, in Cooperation with Ohio Department of Natural Resources, Division of Lands and Soil and Ohio Agricultural Research and Development Center, Columbus, OH.

Lewis, R. C., 1968, "An Investigation of the Potential Yield of the Big Bend Wellfield," unpublished Master's dissertation, University of Cincinnati Graduate School, Cincinnati, Ohio.

Miami Conservancy District (MCD), 1985, Hydrologic Data for the Hamilton, Baltimore Area 1984, the Water Conservation Subdistrict of the Miami Conservancy District.

Mood, M. M. and F. A. Graybill, 1963, "Introduction to the Theory of Statistics," McGraw-Hill.

National Lead Company of Ohio (NLO), Inc., 1977, "Study of Radioactive Storage Areas at the Feed Materials Production Center," Report to U.S. Energy Research and Development Administration, Oak Ridge Operations Office.

National Lead Company of Ohio (NLO), Inc., 1979-1983, Waste Water Quality Report, NPDES Permit Parameters, Data Summary.

Plummer, Paul, July 24, 1990, personal communications, Miami Conservancy District, Dayton, Ohio.

## REFERENCES
## (Continued)

Reeves, M., D. S. Ward, N. D. Johns, and R. M. Cranwell, 1986, "Theory and Implementation for SWIFT II, the Sandia Waste-Isolation Flow and Transport Model for Fractured Media, Release 4.84," NUREG/CR-3328, SAND83-1159, Sandia National Laboratories, Albuquerque, New Mexico.

Sedam, A. C., 1985, "Occurrence of Uranium in Groundwater in the Vicinity of the U.S. Department of Energy Feed Materials Production Center, Fernald, Ohio," U.S. Geological Survey Open-File Report 85-099.

Smith, Robert C. and Associates, 1960, "Results of Investigation: Available Well Water Supply at Baldwin-Lima-Hamilton, Ohio," Technical Report for Champion Paper and Fibre Company, Hamilton, Ohio.

Smith, R. D., 1962, "Groundwater Development, Miami River Area," Consultant Report to City of Cincinnati, Water Works Department (see GeoTrans, 1985).

Spieker, A. M., 1968a, "Groundwater Hydrology and Geology of the Lower Great Miami River Valley Ohio," U.S. Geological Survey Professional Paper 605-A, U.S. Government Printing Office, Washington, D.C.

Spieker, A. M., 1968b, "Effect of Increased Pumping of Groundwater in the Fairfield-New Baltimore Area, Ohio--A Prediction of Analog-Model Study," U.S. Geological Survey Professional Paper 605-C, U.S. Government Printing Office, Washington, D.C.

Spieker, A. M., 1968c, "Future Development of the Groundwater Resource in the Lower Great Miami River, Ohio--Problems and Alternative Solutions," U.S. Geological Survey Professional Paper 605-D, U.S. Government Printing Office, Washington, D.C.

Spieker, A. M. and S. E. Norris, 1962, "Groundwater Movement and Contamination at the AEC Feed Materials Production Center Located Near Fernald, Ohio," U.S. Geological Survey Technical Report for the U.S. Atomic Energy Commission.

Streeter, V. L., ed. 1961, Handbook of Fluid Dynamics, p. 135, McGraw-Hill, New York.

Swinford, E. M., 1990, "Bedrock Geology of the Shandon Quadrangle (Hamilton County Portion)," Open File Map BG-B5C6, Ohio Department of Natural Resources, Division of Geological Survey, Columbus, Ohio.

Swinford, M. (in preparation), "Bedrock Geology of Hamilton County, Ohio," Department of Natural Resources, Division of Geological Survey, Columbus, Ohio.

Thatcher, B. K. and D. R. Phoenix, 1987, Characterization Investigation Study Report, prepared for Roy F. Weston, Inc., Contract DE-AC05-86OR21600.

Todd, D. K., 1959, Ground Water Hydrology, Wiley.

U.S. Army Corps of Engineers (USACE), September 1982 (Revised October 1984), "Generalized Computer Program, HEC-2 Water Surface Profiles," Programmers Manual.

**REFERENCES**
**(Continued)**

U.S. Army Corps of Engineers, Louisville District, 1987, Computer File: Hamilton County, Cincinnati, Amberley and Blue Ash, Ohio; Type 15 Flood Insurance Study; Great Miami River 100-Year Flood Study.

U.S. Department of Energy (DOE), 1985, "Report on Historic Uranium Releases from Current DOE, Oak Ridge Operations Office Facilities," Oak Ridge, Tennessee.

U.S. Department of Energy (DOE), 1988, "Remedial Investigation and Feasibility Study, Feed Materials Production Center, Fernald, Ohio, Work Plan Requirements," U.S. DOE Oak Ridge Operations Office, Oak Ridge, Tennessee.

U.S. Department of the Navy, 1971, Design Manual 7: Soil Mechanics, Foundations and Earth Structures, Second Edition, Naval Facilities Engineering Command, Alexandria, Virginia.

U.S. Energy Research and Development Administration, 1977, "Study of Radioactive Waste Storage Areas at the Feed Materials production Center," National Lead Company of Ohio NLCO-1143 (Special).

U.S. Environmental Protection Agency, 1986, "RCRA Ground-Water Monitoring Technical Enforcement Guidance Document (TEGD)," (OSWER Directive 9950.1), EPA Office of Emergency and Environmental Response, Washington, D.C.

Vormelker, J., 1985, "Top of Rock Map of Hamilton County Ohio," Open File Map 229, State of Ohio, Department of Natural Resources, Division of Geological Survey, Columbus, Ohio.

Walker, A. C. 1986, "Groundwater Resources of Hamilton County," Ohio Department of Natural Resources, Division of Water, Columbus, Ohio.

Walton, W. C. and E. J. Schaefer, 1956, "Report to the Southwestern Ohio Water Company on Evaluation of the Potential Yield of the Aquifer in the Big Bend Area, Ohio," Mimeographed Report.

Walton, W. C., 1985, Practical Aspects of Groundwater Modeling, National Water Well Association, Worthington, Ohio.

Ward, D. S. M. Reeves and L. E. Duda, 1984, "Verification and Field Comparison of the Sandia Waste-Isolation Flow and Transport Model (SWIFT)," NUREG/CR-3316, SAND83-1154, Sandia National Laboratories, Albuquerque, New Mexico.

Ward, D. S., D. R. Buss, J. W. Mercer, and S. S. Hughs, 1987, "Evaluation of a Groundwater Corrective Action at the Chem-Dyne Hazardous Waste Site Using a Telescopic Mesh Refinement Modeling Approach," Water Resources Research, Vol. 23, No. 4, pp. 603-617.

Watkins, J. S. and A. M. Spieker, 1971, "Seismic Refraction Survey of Pleistocene Drainage Channels in the Lower Great Miami River Valley, Ohio," U.S. Geological Survey, Professional Paper, 605-B, U.S. Government Printing Office, Washington, D.C.

Westinghouse Materials Company of Ohio, 1986, Personal Communication.

## REFERENCES
## (Continued)

Westinghouse Materials Company of Ohio, 1987, "Groundwater Quality Assessment Program Plan for Waste Pit No. 4 at the Feed Materials Production Center," prepared for U.S. Department of Energy, November, 1987.

Westinghouse Materials Company of Ohio, 1988, Environmental Monitoring Annual Report for 1987, prepared for U.S. Department of Energy, Oak Ridge Operations Office, Oak Ridge, Tennessee.

# APPENDIX A

# GEOCHEMICAL PROGRAMS: ISSUES 3 AND 5 REPORT

# REMEDIAL INVESTIGATION AND FEASIBILITY STUDY
# FEED MATERIAL PRODUCTION CENTER
# FERNALD, OHIO

Final Geochemical Report on Issues 3 and 5

# TABLE OF CONTENTS

PAGE

1.0 INTRODUCTION ..... 1
1.1 BACKGROUND ..... 1
1.2 ISSUES OF THE GEOCHEMICAL PROGRAM ..... 2
1.3 ISSUE THREE: PADDY'S RUN AND THE STORM-WATER-OUTFALL DITCH... 2
1.3.1 Purpose and Scope ..... 2
1.3.2 Analytical Methods and Field Sampling ..... 4
1.3.2.1 Field-Sampling Procedure for Subsurface Soils ..... 4
1.4 ISSUE FIVE: PARAMETERS FOR SOLUTE-TRANSPORT MODEL ..... 5
1.4.1 Purpose and Scope ..... 5
1.4.2 Analytical Methods and Field Sampling ..... 6
1.4.2.1 Field-Sampling Procedure for U+4 and Total U ..... 7
2.0 ANALYTICAL METHODS AND RESULTS ..... 7
2.1 ANALYTICAL METHODS ..... 7
2.1.1 Gamma Spectrometry ..... 8
2.1.2 Differential Leaching Tests for Uranium ..... 8
2.1.3 Leaching Technique for Iron and Manganese ..... 9
2.2 ANALYTICAL RESULTS ..... 10
2.2.1 Issue Three ..... 10
2.2.1.1 Subsurface Soils ..... 10
2.2.1.2 Surface Waters ..... 11
2.2.2 Issue Five ..... 12
2.2.2.1 Aquifer Solids ..... 12
2.2.2.2 Anomalous Uranium Results ..... 13
2.2.2.3 Groundwaters ..... 14
2.3 DISCUSSION ..... 15
2.3.1 Issue Three ..... 16
2.3.2 Issue Five ..... 17
3.0 GEOCHEMICAL MODELING ..... 18
3.1 SELECTION CRITERIA FOR GROUNDWATER SAMPLES ..... 19

## TABLE OF CONTENTS

PAGE

3.2 MODELING ASSUMPTIONS AND CONSTRAINTS ..... 19
3.2.1 Electrical Charge Imbalances ..... 20
3.2.2 Eh Calculations ..... 20
3.3 URANIUM SPECIATION ..... 21
3.3.1 Discussion ..... 22
3.3.1.1 Data Base Integrity ..... 22
4.0 URANIUM ADSORPTION ..... 24
4.1 SPECIATION AND EXPERIMENTAL STUDIES ..... 24
4.1.1 Adsorption of Uranyl-Carbonate Species by Montmorillonite ..... 24
4.1.2 Adsorption of Uranyl-Carbonate Species by Amorphous Ferric Oxyhdroxide ..... 25
4.1.3 Empirical Determination of a Uranium Distribution Coefficient ..... 26
4.2 AQUIFER SOLIDS, LEACHATES AND GROUNDWATERS ..... 29
4.3 COMPARISON OF EMPIRICAL AND CALCULATED $K_d$ VALUES ..... 30
4.4 ESTIMATION OF THE URANIUM $K_d$ FOR THE FERNALD SITE AQUIFER... 31
5.0 CONCLUSIONS ..... 33
5.1 ISSUE THREE ..... 33
5.2 ISSUE FIVE ..... 34
5.2.1 Best Estimate of the Uranium $K_d$ for the Aquifer ..... 35
REFERENCES ..... 37
APPENDIX A - ANALYTICAL RESULTS

## LIST OF TABLES


| TABLE NO. | TITLE |
|---|---|
| 1 | Uranium Speciation in Groundwaters |
| 2 | Uranium Speciation in Surface Waters |
| 3 | Empirical Uranium Distribution Coefficients |
| 4 | Calculated Uranium Distribution Coefficients |


## LIST OF FIGURES


| FIGURE NO. | TITLE |
|---|---|
| 1 | Sample Locations for Subsurface Soils and Surface Waters |
| 2 | Uranium Concentrations in Subsurface Soils of Paddy's Run |
| 3 | Uranium Concentrations in Subsurface Soils of the Storm-Water Outfall Ditch |
| 4 | Weight Percent of Silt and Clay versus Leachable Fe, Mn and U |
| 5 | Weight Percent of Silt and Clay versus Total Organic Carbon |
| 6 | Weight Percent of Silt and Clay versus Cation Exchange Capacity |
| 7 | Uranium Concentrations in Aquifer Solids |
| 8 | Results of the Uranium Differential-Leach Test |
| 9 | Location of Monitoring Wells for Groundwaters |
| 10 | Uranium Redox Ratio versus Total Iron |
| 11 | Uranium Speciaiton as a Function of Groundwater Eh |
| 12 | Calculated $K_d$ versus Predicted $K_d$ |

# 1.0 INTRODUCTION

## 1.1 BACKGROUND

A Work Plan for the sitewide Remedial Investigation and Feasibility Study (RI/FS) at the U.S. Department of Energy's (DOE's) Feed Materials Production Center (FMPC) in Fernald, Ohio was developed to evaluate potential uranium sources to the underlying aquifers and provide geochemical parameters for a three-dimensional model of groundwater flow and radionuclide transport. Recognizing the need for site-specific modeling data on the physiochemical processes that could affect radionuclide migration and attenuation, a geochemical testing program was included in the RI/FS Work Plan as part of the Subsurface Soils Sampling Plan. The geochemical program included analytical testing for total uranium, differential leaching of uranium, total cation exchange capacity, total organic carbon, leachable iron and manganese, and grain size on about 40 subsurface solid samples from three stratigraphic horizons below the FMPC. The purpose of the geochemical testing program was to quantify chemical parameters on aquifer solids which would enhance the evaluation of radionuclide migration and attenuation.

Subsequent to the submission of the original RI/FS Work Plan, a reconsideration of the geochemical data needs indicated a deficiency in some of the proposed analytical work. For groundwater samples, a field determination of dissolved oxygen and alkalinity, and laboratory analysis of calcium, potassium and phosphate, were considered critical additions to the program to satisfy the data needs for the geochemical modeling effort. For aquifer-solid samples, the leachates produced from the leachable iron and manganese test were split, and one split of each sample was retained for total fluorimetric uranium analysis. Each of these additional analytical procedures were eventually integrated into the geochemical testing program.

Because the groundwater-flow and solute-transport model will simulate only the sand and gravel aquifer underlying the FMPC and surrounding region, contamination reaching the aquifer as a result of vertical migration through the overlying till is dealt with as a source term to the model. That is, any past, present, or future uranium release from the till will be input to the model as a known quantity from each principal source. The role of the geochemical program was expanded to account for this model design and served as the focal point to evaluate the source terms for the model.

## 1.2 ISSUES OF THE GEOCHEMICAL PROGRAM

The geochemical program conducted in support of the RI/FS is designed to:

- Evaluate past, current and future releases of uranium from several primary sources to the underlying aquifer
- Develop representative values for geochemical parameters that will be used to model solute transport in the groundwater.

In order to provide the most substantive results in a cost-effective manner, the technical approach to satisfy these objectives was developed around five key, site-specific issues. These five issues are:

- Does soil contamination from air deposition represent a source of uranium to groundwater
- Do soluble uranium spills represent a past, continuing or future source of uranium to groundwater
- Does Paddy's Run and/or the storm-water-outfall ditch represent a past, continuing or future source of uranium to groundwater
- Do the waste pits represent a past, continuing or future source of uranium to the underlying aquifers
- Geochemical parameters for radionuclide transport and attenuation in the sand and gravel aquifer must be estimated for use in the solute transport model.

The first four issues focus on field and laboratory data to estimate the amount of uranium available from potential sources, while the fifth issue additionally utilizes geochemical modeling and published literature to quantify a uranium distribution coefficient ($K_d$) for the aquifer. The uranium distribution coefficient is defined as the concentration of sorbed uranium per kg of aquifer solid divided by the concentration of uranium per liter of ground water [$K_d$ = (mg/kg)/(mg/L) = L/kg]. This interim report will address issues three and five of the RI/FS Geochemical Program.

## 1.3 ISSUE THREE: PADDY'S RUN AND THE STORM-WATER-OUTFALL DITCH

### 1.3.1 Purpose and Scope

The purpose of issue three is to establish whether uranium-bearing surface water has infiltrated and/or continues to infiltrate vertically downward through the bottom of Paddy's Run and the storm-water-outfall ditch. Additionally, the disposition of this uranium prior to reaching the

underlying sand and gravel aquifer needs to be established. To address this issue, subsurface soils and surface waters from Paddy's Run and the storm-water-outfall ditch (Fig. 1) have been sampled and analyzed to evaluate the retention capability of the soils and the degree of infiltration of uranium-bearing surface water to the underlying aquifer. Surface-water samples were analyzed for chemical parameters and the analytical data used to construct an equilibrium geochemical model that predicts the dominant uranium specie in the surface water. This information, along with analytical results on leachable iron, manganese and uranium produced from the subsurface-soil samples, was used to evaluate the degree of uranium retardation (if any) by the sediment and soil beneath Paddy's Run and the storm-water-outfall ditch. The analytical results for subsurface-soil samples were used to investigate three cases:

- No attenuation of uranium as it passes through the sediment and soil into the underlying aquifer (i.e., the vertical distribution of uranium in the subsurface-soil samples is similar to background levels)
- Uranium is historically bound-up in the subsurface-soil samples (i.e., uranium is retarded by the sediment and subsurface soil but has not broken through to the underlying aquifer)
- Uranium is present in the underlying aquifer solids (i.e., uranium has partially or completely broken through to the underlying aquifer)

These cases were evaluated by analyzing stream-bed borings obtained from Paddy's Run and the storm-water-outfall ditch for total uranium. Boring locations are shown in Figure 1. In Paddy's Run, one boring (P1; 1408) was placed upstream just below the waste-pit area and K-65 silos. A second boring (P2; 1409) was located in an area considered to be a significant zone of recharge to the underlying aquifer. The third boring (P3;1410) is downstream from the confluence with the storm-water-outfall ditch. These locations were chosen to allow a comparison of segments of Paddy's Run impacted by the flow from the storm-water-outfall ditch and those segments upstream from the confluence.

In the storm-water-outfall ditch, the upstream location (S1; 1405) was placed above the spillover of the storm-water-retention basin to evaluate the level of uranium retained by an inactive reach of the storm-water-outfall ditch. The second location (S2; 1406) is on an existing depression in the channel bottom, thought to be the remnants of a small, abandoned settling

basin. This area is proximal to the easternmost fly-ash pile and could serve to account for any associated impacts of fly ash on the storm-water-outfall ditch and underlying aquifer. A third boring (S3; 1407) is located near the confluence with Paddy's Run, which accounts for cumulative effects of fly-ash piles and/or whether most uranium is lost prior to reaching this point.

### 1.3.2 Analytical Methods and Field Sampling

International Technology Analytical Services (ITAS-Oak Ridge) analyzed surface waters for chemical and radiological parameters and subsurface soils for total uranium. In addition, the parameters Eh, pH, dissolved oxygen, conductivity, temperature and alkalinity were measured during the collection of samples. The collection, handling and analysis of subsurface soils and surface waters conformed to the procedures and conventions established in Revision 3 of the FMPC RI/FS Work Plan and Quality Assurance Project Plan (QAPP). Modifications to the collection and analysis of subsurface-soil samples were addressed in the Field Sampling and Laboratory Procedure Plan for the Geochemical Program. A summary of the field-sampling procedure appears below, and analytical methods are discussed in Section 2.0.

#### 1.3.2.1 Field-Sampling Procedure for Subsurface Soils

Details on the procedures and conventions used for the collection, handling and analysis of subsurface soil samples can be found in Revision 3 of the FMPC RI/FS Work Plan and QAPP, and the Field Sampling and Laboratory Procedure Plan for the Geochemical Program. The field-sampling procedure is summarized as follows:

- Split-spoon samples were collected continuously in six-inch intervals from the stream bed surface to the sand- and gravel-aquifer water table
- Samples were two- to six-inch sections of the split-spoon core
- If the water table was not detected because of wet subsurface material throughout, borings were advanced to the following depths:
  - P1 (1408) to 24 feet
  - P2 (1409) to 20 feet
  - P3 (1410) to 20 feet
  - S1 (1405) to 34 feet
  - S2 (1406) to 17 feet
  - S3 (1407) to 9 feet

- Changes in lithology and/or geochemistry took precedence over the depth-interval sampling criterion (e.g., if iron staining begins at a depth of 12 feet, a new sample begins at 12 feet)
- The sample log recorded the percent recovery for a given 1.5-foot interval and any interval where soil was not recovered
- If the first or second split-spoon interval was refused, the boring was restarted from the ground surface
- Samples were bottled immediately after screening, and no samples were collected for volatile organic analysis (VOA), regardless of HNu or organic vapor analysis (OVA) reading
- Boring logs emphasized lithology, stratigraphy and geochemical descriptions
- A maximum of eight soil samples from each boring were sent to the laboratory for total uranium analysis
- Samples not analyzed were archived for future use, if necessary.

## 1.4 ISSUE FIVE: PARAMETERS FOR SOLUTE-TRANSPORT MODEL

### 1.4.1 Purpose and Scope

The purpose of issue five is to estimate a uranium distribution coefficient ($K_d$) for the sand and gravel aquifer. In developing a technical approach to satisfy this objective, the following assumptions were made:

- The application of the solute-transport model is limited to the sand and gravel aquifer
- The relatively uniform characteristics of the sand and gravel aquifer imply related published information could provide $K_d$ values without site-specific, laboratory-attenuation studies
- Only uranium is currently proposed for detailed consideration in the solute-transport model, and the $K_d$ value for uranium is the focus of this issue.

Two methods were proposed to determine a uranium $K_d$ value for the aquifer. The first method relied on analytical data from groundwaters as input to a geochemical equilibrium model (EQ3NR; Wolery, 1983) to predict the dominant uranium species in solution. This information was to be combined with mineralogic data on the sand and gravel aquifer and the two sets of site-specific data compared to results of published $K_d$ studies. A second method was proposed to evaluate independently the uranium $K_d$ by conducting laboratory sorption studies with the sand and gravel solids.

The first method was modified to exclude mineralogic identification of aquifer solids after initial geochemical modeling and aquifer-solid analyses indicated that the dominant uranium specie was $UO_2(CO_3)_3^{-4}$, a negatively-charged specie that would not exhibit significant sorption on clay minerals with high cation-exchange capacity. To resolve this problem, the analytical results on leachable iron were used to estimate the amount of amorphous iron (which has a strong affinity for negatively-charged complexes) that could be present as coatings on clay minerals and along fractures in the aquifer. Using these estimates, and a published study on uranium sorption by amorphous iron oxyhydroxide, empirical calculations were carried out to derive an apparent uranium $K_d$ value.

The second method cited above has not been carried out at this time. However, an alternative method was substituted to maintain two independent calculations of the uranium $K_d$ value. Using the total uranium values obtained on leachates derived from the leachable iron and manganese test, and uranium analyses of groundwater, a $K_d$ was calculated directly from the uranium concentration in the solid (after a correction for background levels) and groundwater [$K_d$ = (mg U/kg solid)/(mg U/L groundwater)].

1.4.2 Analytical Methods and Field Sampling

ITAS-Oak Ridge performed the differential leaching/total uranium analysis of aquifer solids and the chemical and radiological analyses of groundwaters. Field parameters were measured on all groundwaters. To assist in determining the redox potential (Eh) of groundwater, 16 wells were sampled and analyzed for $U^{+4}$ and total U ($U^{+6}$ = total U - $U^{+4}$). $U^{+4}$ and $U^{+6}$ are defined as the sum of all uranium species for each oxidation state. The $U^{+4}$ and total U analyses were done by United Nuclear Corporation Geotech Laboratories (UNC Geotech), Grand Junction, Colorado. In support of the partitioning studies, IT-Export carried out analyses on the aquifer solids for total cation-exchange capacity, total organic carbon, grain size, and leachable iron and manganese. A leachate split was sent to ITAS-Oak Ridge for total U analysis.

The collection, handling and analysis of aquifer solids and groundwaters conformed to the procedures and conventions established in Revision 3 of the FMPC RI/FS Work Plan and Quality Assurance Project Plan (QAPP). Detailed procedures for the differential leaching analysis of aquifer solids, and $U^{+4}$ and total U field sampling and analytical methods are given

in the Appendix of the Field Sampling and Laboratory Procedure Plan for the Geochemical Program. A summary of the $U^{+}4$ and total U field-sampling procedure appears below, and analytical methods are discussed in Section 2.0.

1.4.2.1 Field-Sampling Procedure for $U^{+4}$ and Total U

Groundwater samples were collected for total U and $U^{+}4$ analysis to estimate independently the Eh of the groundwater. The $U^{+4}$ in solution is complexed with cerium and precipitated with hydrofluoric acid. $U^{+6}$ is determined by the difference of total U and $U^{+4}$. The procedure is summarized as follows:

- Approximately 250 ml of sample is collected after filtering the groundwater through a 0.45 um filter
- The sample is split and half is acidified with $HNO_3$ to pH<2 and shipped to the laboratory for total U analysis
- 25 ml of the remaining filtered sample is placed into a 125 ml plastic bottle, and 0.125 ml of cerium solution is added to the sample and mixed well
- 1.25 ml of reagent grade HF is added to the solution, and the solution is mixed thoroughly and cooled for 15 minutes in a cooler
- The sample is removed from the cooler, shaken, and filtered through a 0.1 um filter
- The sample bottle is rinsed three times with distilled water and the rinse solution is passed through the 0.1 um filter
- The filter funnel and filter paper are rinsed with distilled water prior to placing the filter paper in a container for shipment to the laboratory, where it is analyzed for $U^{+4}$.

## 2.0 ANALYTICAL METHODS AND RESULTS

### 2.1 ANALYTICAL METHODS

Standard analytical methods (e.g., Methods for Chemical Analysis of Waste and Water; EPA-600 4-79-020) were used for the analysis of surface waters and groundwaters and will not be discussed here. Subsurface soils and aquifer solids were analyzed by gamma spectrometry for total uranium. Aquifer solids were also subjected to leaching tests to determine the amount of leachable iron, manganese and uranium. Leachates recovered from these tests were analyzed for iron, manganese and uranium by standard procedures (e.g, atomic absorption, inductively

coupled plasma or laser fluorimetry). Some of the analytical methods employed for subsurface soils and aquifer solids are site-specific applications and are summarized below. Detailed laboratory procedures for the leaching tests can be found in Revision 3 of the FMPC RI/FS Work Plan, the Work Plan for the Geochemical Program and the Field Sampling and Laboratory Procedure Plan for the Geochemical Program.

### 2.1.1 Gamma Spectrometry

Solid samples analyzed by the gamma-spectrometry method are generally 500 gram splits of crushed and homogenized material. After sample preparation is completed, the samples are placed in containers that will yield an analytical geometry identical to that of standards used to calibrate the instrument. The standards have known concentrations of each uranium isotope that emits gamma radiation and are used to construct a calibration curve prior to sample analysis. Most instruments used for this procedure employ sophisticated software that contains a complex algorithm to account for sample-instrument geometry, sample weight, the coefficient of absorbance for gamma radiation in the sample material, and interfering gamma radiation from other radionuclides present in the sample. The sample geometry and weight are given as input parameters prior to analysis and the algorithm calculates the total uranium concentration in the sample based on the contribution of each uranium isotope. Output from the algorithm is the total uranium concentration in ug/g (ppm).

### 2.1.2 Differential Leaching Tests for Uranium

The differential leaching tests distinguish between easily mobilized and available uranium (i.e., sorbed or amorphous uranium phases) from insoluble uranium (i.e., U in mineral lattices such as zircon) that is not available to the groundwater environment. The four leaching tests are designed to provide the following information:

- Uranium present in fine-grained carbonate minerals (i.e., pore cement)
- Uranium present as sorbed species on clay minerals and amorphous iron and aluminum oxyhydroxides
- Uranium present as sorbed species or within organics in the soils or wastes
- Uranium present in amorphous solids or oxide phases such as $UO_2$ or $U_3O_8$.

The uranium of most concern is probably bound on amorphous iron and aluminum oxyhydroxides that coat clay minerals, or is present with the organics and amorphous oxide phases. This uranium (if present) could be available for transport through the aquifer. Uranium which is present in the lattices of clay minerals, apatite, monazite and zircon is naturally occurring and generally immobile, and can be considered representative of the background concentration level.

The four-step extraction technique can be summarized as follows:

- Sodium acetate is used to digest the fine-grained carbonate minerals
- Disodium ethylenediaminetetracetic acid (EDTA) is used to strip sorbed uranium from clay minerals, and amorphous iron and aluminum oxyhydroxides
- Hydrogen peroxide is used to digest organic material
- Nitric acid (1:1 with distilled $H_2O$) is used to dissolve amorphous solids and oxides of uranium.

At each step, the reagent is agitated with the sample and the solution fraction (leachate) was recovered by centrifuging. The leachates were analyzed for total uranium by laser fluorimetry.

### 2.1.3 Leaching Technique for Iron and Manganese

This leaching technique recovers iron and manganese from amorphous-oxyhydroxide coatings on grains or fractures and crystalline oxide minerals using a solution of acetic acid and hydroxylamine hydrochloride. The solid is mixed with the leaching solution, agitated and the leachate recovered by centrifuging. Unlike the differential leaching procedure which recovers 'historical' uranium (i.e., recently bound uranium) this procedure will also recover ancient uranium locked in the mineral lattices of detrital grains or fracture coatings. Therefore, uranium sorbed to iron- and manganese-oxyhydroxide coatings on grain surfaces or fractures is removed and mixed with uranium recovered from the lattice sites in iron- and manganese-oxide minerals (i.e., detrital grains or fracture coatings of hematite or pyrolusite). The two uranium components cannot be distinguished in the analysis, and the background component (i.e., uranium in mineral lattices) must be estimated from aquifer solids which are known to be uncontaminated.

## 2.2 ANALYTICAL RESULTS

Analytical results for samples of subsurface soils, surface waters, aquifer solids and groundwaters are given in Appendix A. Groundwater analyses reported in Appendix A are limited to the samples chosen for geochemical modeling. The analytical results for uranium on subsurface-soil and surface-water samples obtained from Paddy's Run and the storm-water-outfall ditch were used to evaluate a source term for these drainages (issue three). Analytical results on groundwaters and aquifer solids were used to calculate apparent uranium distribution coefficients for the sand and gravel aquifer (issue five).

### 2.2.1 Issue Three

Analytical results for total uranium were obtained on subsurface soils and surface waters in Paddy's Run and the storm-water-outfall ditch to evaluate a source term for these drainages.

#### 2.2.1.1 Subsurface Soils

Samples of subsurface soils obtained from Paddy's Run and the storm-water-outfall ditch (Fig. 1) were analyzed for total uranium by gamma spectrometry. The samples consist primarily of well-graded sand and gravel with horizons of poorly-graded sand and silty clay. Borehole depth ranged from 20 to 24 feet and 9 to 34 feet, respectively, in Paddy's Run and the storm-water-outfall ditch. The deepest borehole in the storm-water-outfall ditch (S1; 1405) penetrated an iron- and manganese-stained horizon between 25 and 30 feet below the surface, which was interpreted as a possible redox zone. Uranium results for six of the sampling sites are illustrated in Figures 2 and 3.

Soil samples recovered from Paddy's Run (Fig. 2) had total uranium concentrations of less than 1 to 4 ug/g (ppm). However, significant 2-sigma counting errors (generally > 50 % and up to 100 % of the reported value) precludes any discussion of significant variation in the uranium concentration with depth (i.e., no variation observed within the range of 2-sigma counting errors; Fig. 2). Additionally, for uranium concentrations in these soil samples, it is not possible to separate components of contamination (if present) from regional background levels, which in common rocks are: carbonates, 2.2 ppm; shales, 3.7 ppm; and granites, 5 ppm (Faure, 1977; Krauskopf, 1979). Site environmental-monitoring data has established uranium background levels of 1 to 3 ppm in the aquifer solids.

Total uranium values for soil samples recovered from the storm-water-outfall ditch ranged from 1 to 10 ppm (Fig. 3). Large 2-sigma counting errors makes discussion of uranium variation with depth equivocal for site S3 (1407). However, the soil profiles from sites S1 (1405) and S2 (1406) show uranium variation that is significant (i.e., greater than 3 ppm). Site S1 (1405) is most proximal to the Fernald compound (Fig. 1) and is located above the spillover for the storm-water-retention basin. Soil samples recovered from this boring indicate a decrease in the uranium concentration from 10 to 4 ppm within the top 4 feet of soil (Fig. 3). The high uranium concentrations in the upper 3 feet of this boring coincide with a clay-rich horizon between 0.5 and 2 feet, suggesting uranium may have sorbed onto the clay (see Section 2.5.1).

Site S2 (1406) is located near a fly-ash pile and in a depression which may be an abandoned settling basin. Very little (if any) soil is present at site S2 (1406), and the boring penetrates the top of the sand and gravel aquifer. The uranium profile from this site indicates uranium concentrations of 6 to 8 ppm over the interval of 5 to 15 feet (background uranium is less than 3 ppm). Because the soil present at this site is negligible, the profile indicates 'historical' uranium is present in the aquifer.

2.2.1.2 Surface Waters

Analytical results for three surface-water samples (W-7, W-11 and ASIT003; sampled 05/14/89) are given in Appendix A. Samples were collected in each flowage above the confluence of Paddy's Run and the storm-water-outfall ditch (W-11 and ASIT003, respectively), and below the confluence (W-7; Fig. 1). The surface samples are oxygenated waters (Eh approximately 450 mV) with a pH of about 8.5 and their solution chemistry is dominated by $HCO_3^-$ (> 200 mg/L) and Ca (> 70 mg/L), reflecting the interaction of these waters with carbonate rock in the subsurface. Uranium concentrations in the surface-water samples ranged from 0.002 (ASIT003) to 0.015 (W-07) mg/L. The sample obtained from the storm-water-outfall ditch (ASIT003) has a uranium concentration similar to background levels established for Paddy's Run (0.001 to 0.004 mg/L), using site-specific environmental-monitoring data. Samples recovered from Paddy's Run, above and below the confluence with the storm-water-outfall ditch, have uranium concentrations above the background level maximum, indicating these surface waters might

contribute uranium to the underlying aquifer by vertical infiltration. Modeling results for uranium speciation are presented in Section 3.3.

2.2.2 Issue Five

Analytical results for total uranium were obtained on aquifer solids and groundwaters to calculate an apparent distribution coefficient [$K_d$ = (mg U/kg solid)/(mg U/L groundwater)] for the sand and gravel aquifer. Additionally, geochemical modeling on the speciation of uranium in groundwater was combined with analytical results on leachable iron to derive empirically a distribution coefficient.

2.2.2.1 Aquifer Solids

Thirty-one subsurface samples consisting of gravel, sand, silt and clay were analyzed for leachable iron, manganese and uranium, total organic carbon, total cation exchange capacity and grain-size variation. Thirteen of these sample were also utilized for total uranium analysis (6) and differential-leaching uranium analysis (7). Analytical results are given in Appendix A and illustrated in Figures 4 to 6.

Figure 4 is a plot of leachable iron, manganese and uranium against the particle size of the sample. Based on the sieve analysis, two sample populations exist: (1) silt + clay greater than 50 weight percent and (2) silt + clay less than 25 weight percent. The leachable fraction of iron, manganese and uranium in the majority of aquifer-solid samples is not a function of the particle size, because the range of values for the metals is similar for the two sample populations. This observation suggests that the majority of iron and manganese solids accessed by the groundwater are present as amorphous- or crystalline-oxyhydroxide coatings along fractures in the fluid-flow path, rather than as detrital grains or surface coatings on the aquifer particles. This hypothesis is consistent with sample preparation procedures which avoided crushing the sample below its natural aggregated size (i.e., clay minerals were not mechanically disaggregated prior to the leaching test).

Three clay samples in the first population have leachable iron values greater than 2 mg/g, suggesting surface coatings on clay minerals and/or complexation with organic-carbon (see

below) controls the leachable fraction of iron in these samples. A lack of correlation between the sum of leachable iron and manganese versus total uranium (inset Fig. 4) indicates that:

- Sorption of uranium on amorphous iron- and manganese-oxyhydroxide coatings may not be occurring in the aquifer or
- The leachable iron and manganese in the solids is primarily from the digestion of crystalline oxyhydroxide phases.

Results for total organic carbon versus grain size are illustrated in Figure 5. As in Figure 4, there is no correlation between the total-organic-carbon content of the aquifer solids and the weight percent of silt and clay in the sample. The majority of samples, irrespective of silt and clay content, have total-organic-carbon values below 8 mg/g. Two samples obtained from a major clay interbed in the sand and gravel aquifer contain 15 to 16 mg/g of total organic carbon. These two samples are coincident with the highest leachable iron values in Figure 4. The correlation of high organic carbon content to high leachable iron values implies iron is associated with or adsorbed on organic materials in the clay interbed.

In contrast to results presented in Figures 4 and 5, the cation exchange capacity of the aquifer solids is a strong function of the silt and clay content (Fig. 6). Samples containing less than 25 weight percent of silt and clay have a total cation exchange capacity (CEC) of less than 0.04 meq/g, whereas those samples with greater than 50 weight percent silt and clay have CEC up to 0.28 meq/g.

2.2.2.2 Anomalous Uranium Results

Thirteen aquifer-solid samples were chosen for total-uranium analysis by gamma spectrometry. Seven of the 13 samples were selected for a differential-leaching procedure designed to strip uranium sequentially from the solids using a series of four progressively stronger leaching reagents (see analytical methods in the Appendix of the Field Sampling and Laboratory Procedure Plan for the Geochemical Program). Results for the total-uranium and differential-leaching analysis are reported in Appendix A and illustrated in Figures 7 and 8. It is emphasized that these results are anomalous with respect to those obtained previously for total uranium of aquifer solids.

Figure 7 is a plot of total uranium (ug/g or ppm) versus sample depth for six of the thirteen samples. Mean uranium concentrations in these aquifer solids range from about 11 to 16 ppm, but show no variation within their 2-sigma counting errors. The mean uranium values are about 3 to 5 times higher than the maximum uranium background level of 3 ppm (based on uranium analyses of subsurface solids from uncontaminated wells). Possible causes of the elevated uranium values are:

- Uranium sorption on particles along the flow path
- Precipitation of uranium solids along the flow path
- The presence of naturally-occurring uranium-bearing minerals (i.e., zircon, apatite or monazite) in the aquifer sands
- Problems with the procedures and analytical methods used to determine the uranium concentration (see Section 2.5.2).

Uranium results from the differential-leaching procedure are shown in Figure 8. The seven samples analyzed had mean uranium concentrations of 95 to 150 ppm prior to leaching and, within their 2-sigma counting error, were unchanged after leaching. Additionally, sample-to-sample variation in uranium concentration is not observed within the 2-sigma counting error. These solids have uranium concentrations 1 to 2 orders of magnitude higher than background uranium concentrations (see above), and an order of magnitude higher than the results shown in Figure 7. Sorption and precipitation of uranium along the flow path cannot be responsible for the high concentrations in these samples, because the leachates (analyzed by laser fluorimetry) from the solids had less than 2.5 ppb of uranium. Likewise, the uranium-bearing mineral apatite, and to a lesser degree monazite, cannot contribute significantly to the high uranium concentrations because they are soluble in nitric acid (used in final leaching step). The results presented in Figure 8 can be explained by high concentrations of insoluble uranium-bearing minerals (i.e., zircon) in the aquifer sands or problems with the analytical procedures and methods (see Section 2.5.2).

2.2.2.3 Groundwaters

Analytical results for groundwater samples used in the geochemical modeling appear in Appendix A. These groundwaters were collected from 20 monitoring wells (locations shown in Fig. 9) during Round 3 (Fourth Quarter, 1988) and Round 4 (First Quarter, 1989) sampling.

The dominant chemical characteristics of the groundwaters include: near-neutral pH values (6 - 8), Eh values of 50 to 450 mV, $HCO_3^-$ concentrations of 200 to 400 mg/L, and Ca concentrations of 70 to 200 mg/L. These chemical characteristics suggest the groundwaters are in equilibrium with carbonate rocks in the aquifer. Uranium concentrations in these samples vary from 0.005 to 4.38 mg/L, with most modeling samples having concentrations greater than expected for natural waters (i.e., U > 0.0001 to 0.010 mg/L; Hem, 1970). Modeling results for the uranium speciation are presented in Section 3.3.

## 2.3 DISCUSSION

### 2.3.1. Issue Three

Uranium concentrations in most subsurface-soil samples overlap with the range of values reported for common rock types (i.e., 2-5 ppm) and do not appear to reflect the sorption and/or precipitation of uranium from infiltrating groundwater. The lack of uranium contamination in the majority of the soil samples suggests any one or all of the following:

- The soils were not exposed to uranium-bearing water
- Uranium that had sorbed onto the soils has been subsequently desorbed by uncontaminated water
- Uranium was in the form of non-sorptive species.

Therefore, the soil profiles from sites P1 (1408), P2 (1409), P3 (1410), and S3 (1407) may conform to the case one scenario (Section 1.3.1), which states that if surface waters with high uranium concentrations infiltrated these soils, no attenuation took place (i.e., the soil profile for uranium reveals background levels). This scenario supports the speciation results for surface waters (Section 3.3, Table 2), which indicate the neutral complex $UO_2(H_2PO_4)_2^*$ is present and little (if any) attenuation of uranium will occur as surface waters vertically infiltrate to the underlying aquifer. The scenario also supports modeling results which indicate the anionic uranyl-carbonate species are present if amorphous iron oxyhydroxide is absent (i.e., no sorption on the soil-particles).

Exceptions are sites S1 (1405) and S2 (1406). At site S1 (1405), uranium values up to 10 ppm in the upper 2-3 feet of soil suggest uranium sorption and/or precipitation may have occurred.

Site S1 (Fig. 3) is proximal to the discharge point for the storm-water-outfall ditch, and higher uranium concentrations in these subsurface-soil samples are in agreement with known periodic discharges of uranium-bearing waters. The elevated uranium concentrations in the upper 3 feet of this boring are coincident with a clay rich horizon between 0.5 and 2 feet. This observation suggests that uranium is being retarded by sorption processes in this area. Therefore, this uranium is a potential source for future releases to the underlying aquifer.

Site S2 (1406) shows slightly elevated uranium concentrations (6 to 8 ppm) over a depth interval of 5 to 15 feet. However, this observation cannot be correlated with clay-rich horizons found in the soil profile at site S1, because little (if any) soil is present at this site. This site is proximal to a fly-ash pile and may also be situated on the remnants of an abandoned settling basin. Either of these observations could account for the presence of 'historical' uranium in the S2 profile. Uranium may be retarded along this profile by sorption onto iron- and manganese-oxyhdroxide coatings, which formed along the fluid-flow path, or by precipitation of amorphous uranium compounds. Because site S2 (1406) is located in an area where the till is absent, this uranium is currently present in the aquifer, and is a potential source for future release and transport through the aquifer.

The soil profile from site S1 (1405) supports the case two scenario (Section 1.3.1), which states that uranium present above the expected background level is 'historical' uranium bound in the subsurface soil (i.e., no breakthrough has occurred to the underlying aquifer). However, the profile from site S2 (1406) indicates partial breakthrough of uranium to the sand and gravel aquifer (case three, Section 1.3.1). For both of these cases, modeling results which predict the dominant uranium specie as $UO_2(CO_3)_3^{-4}$ (Section 3.3, Table 2) support the hypothesis of uranium sorption on amorphous iron- and aluminum-oxyhydroxide films. Alternatively, uranium may be retarded by precipitation of amorphous uranium compounds.

2.3.2 Issue Five

Analytical results for uranium concentrations in aquifer solids are highly suspect because the differential-leaching procedure did not lower uranium values in aquifer solids that are 1 to 2 orders of magnitude larger than background uranium concentrations. Those samples which did

not undergo the differential-leaching procedure had uranium concentrations 2 to 8 times higher than common rocks, but are also suspect because the differential-leaching procedure indicates a lack of sorbed or amorphous uranium (i.e., all uranium present is within mineral lattice structures), which is in contrast to uranium results obtained on leachates derived from the iron and manganese experiments (see below). Petrographic data on the composition of aquifer sands is not available, although it is unlikely that high concentrations of an insoluble uranium-bearing phase such as zircon would be found to account for the elevated uranium concentrations. The most probable cause of the anomalously high uranium concentrations is a variation in the standard analytical procedure or method.

Gamma spectrometry is used to analyze for total uranium in the aquifer solids. This analytical method is sensitive to the mass of solid analyzed and the geometry of the sample with respect to the detector. Standards used to calibrate the instrument are 500 gram aliquots that are dried and ground to homogenize the solid prior to analysis. Aquifer-solid samples of 4 to 40 grams were analyzed without drying and homogenizing the material, and the small sample volumes resulted in poor geometry configurations with respect to the detector. These deviations from standard procedures requires that the analytical results for total uranium in aquifer solids be treated as qualitative.

In contrast, the total uranium in the leachate fractions produced from the differential-leaching procedure were analyzed by laser fluorimetry and results are considered to be quantitative. These results indicate that less than 2.5 ppb of uranium is sorbed onto the aquifer solids, which is in contrast to uranium values of 33 to 783 ppb obtained from the leachate produced by the iron- and manganese-oxyhydroxide stripping procedure. Reagents specific to each procedure can account for the difference in uranium results, as the analytical method was identical for all leachates. The differential leaching is a four-step procedure; initial leaching with sodium acetate followed by EDTA, hydrogen peroxide, and nitric acid solutions. This procedure removes:

- Uranium sorbed to inorganic and organic particles
- Uranium complexed within amorphous aluminum, iron or manganese oxyhydroxides
- Amorphous uranium solids present in the sample.

In contrast, the iron- and manganese-oxyhydroxide procedure utilizes acetic acid and hydroxylamine hydrochloride to attack amorphous and crystalline iron- and manganese-oxyhydroxide minerals (Chester and Hughes, 1967). Therefore, the latter procedure will contain a uranium component derived from crystallized iron and manganese minerals (i.e., detrital minerals older than the Holocene), while the former will not. The uranium in the detrital minerals is not of recent origin, and the concentrations of less than 1 ppm are well below the average of 3.7 ppm reported for shales (Krauskopf, 1979).

Because of the suspect nature of the uranium analytical results for aquifer solids and leachates, calculated distribution coefficients ($K_d$) should be interpreted cautiously. However, the calculations are useful as an independent check on partitioning estimates based on speciation modeling (Section 3.3) and experimental studies (Section 4.1).

## 3.0 GEOCHEMICAL MODELING

Geochemical modeling of the uranium speciation in surface waters was carried out to assist in the evaluation of the potential source term in Paddy's Run and the storm-water-outfall ditch (issue three), and in groundwaters to support the calculation of the uranium distribution coefficient for the aquifer (issue five). Modeling was conducted with the EQ3NR geochemical code (ver. 3245; Wolery, 1983), which is an industry standard, speciation/solubility code developed by Lawrence Livermore National Laboratory for use in predicting the behavior of metals, radionuclides, and other contaminants in the natural environment. The code accesses a data base containing the thermodynamic properties of 47 elements, 686 aqueous species, 713 minerals, and 11 gases. This data base includes 49 uranium- bearing aqueous species and 53 uranium-bearing minerals, constituting the most complete data base available for modeling the behavior of uranium in natural waters.

Modeling results must be interpreted cautiously. Values for thermodynamic parameters utilized by the EQ3NR code for speciation and solubility calculations are experimentally determined by many investigators, and the quality of their results is variable. Personnel at Lawrence Livermore National Laboratory have qualified the thermodynamic data utilized by the code by

indicating whether the data is poor, fair, good or uncertain. Uncertain generally indicates that independent workers have reached conflicting results for the indicated value and the problem is currently unresolved. All aqueous-uranium species and uranium minerals considered in this investigation have thermodynamic values which have been judged to be good.

Additionally, it must be emphasized that results obtained from geochemical modeling of natural systems are not unique. At best, modeling can present a snapshot of a point in time for the dynamic natural system. However, modeling studies are useful to establish boundary conditions for a system, which may enhance the development of remediation techniques and/or the solution to contaminant problems.

## 3.1 SELECTION CRITERIA FOR GROUNDWATER SAMPLES

Over 100 groundwater analyses from Round 3 (Fourth Quarter, 1988) and Round 4 (First Quarter, 1989) were available for modeling. Because of the large number of analyses received, selection criteria were developed to choose samples from the entire spectrum of analyses, thus reducing the number of analyses to model. All groundwaters with reported uranium concentrations greater than 0.3 mg/L (7 analyses) were modeled. Analyses deemed to be representative of 'typical' local groundwaters were screened for uranium content, and 14 samples were chosen that had uranium concentrations of 0.005 to 0.3 mg/L (greater than 50 percent of the samples received had reported uranium concentrations of less than 0.005 mg/L). Additional criteria focused on anomalous concentrations of calcium, phosphorous, potassium and sulfate, and Eh values (based on platinum electrode measurements) that were below 100 mV (6 analyses). It is important to reiterate that the selection criteria for groundwater samples used in the geochemical modeling is biased toward those analyses with high uranium concentrations.

## 3.2 MODELING ASSUMPTIONS AND CONSTRAINTS

Analytical results received for surface and groundwaters did not contain values for total dissolved solids (TDS) and specific gravity (SG). Many results also lacked a reported value for the redox potential (Eh) of the water. Values for these parameters must be included on the input file for the EQ3NR code and were estimated as follows:

- TDS was calculated by summing the concentrations (in mg/L) of analytes that were above the detection limit
- SG was assumed to be 1 g/cc, based on the low TDS values (400 - 600 mg/L)
- Eh was calculated by the EQ3NR code using the $NH_4^+/NO_3^-$ and $O_2/H_2O$ redox couples, and with solubility constraints based on pyrolusite ($MnO_2$) and uraninite ($UO_2$) saturation (Eh calculations are discussed in detail in Section 3.2.2).

### 3.2.1 Electrical Charge Imbalances

The 26 water analyses utilized for modeling had electrical charge balances ranging from -27 to +64 percent of the total charge (Table 1). About half of the analyses have reasonable charge balances that lie between -5 and +5 percent of the total charge. Electrical imbalances greater than +5 or less than -5 percent suggest either errors in the analysis of a major constituent or the omission of a major constituent in the analysis. The omission of a major constituent will usually cause a consistent bias (positive or negative) in the electrical imbalance, thus the range of imbalances observed here suggests random errors in the analyses. A reduced level of confidence should be placed on those analyses with large electrical imbalances (i.e., those that lie outside of the range -5 to +5 percent) and the corresponding uranium speciation calculated from the analytical data. However, uranium speciation will probably not be affected by large electrical imbalances resulting from analytical errors in the determination of calcium, potassium, magnesium, sodium or sulfate, but can be affected if the phosphorous concentration, alkalinity, or pH is in error (see discussion of uranium speciation in Section 3.3).

### 3.2.2 Eh Calculations

Platinum-electrode measurements were not provided with all groundwater analyses and a variety of redox couples and mineral-solubility limits were utilized to constrain the system Eh. Eh values were calculated with the $O_2/H_2O$ (770 to 800 mV), $NH_4^+/NO_3^-$ (324 to 350 mV) and $U^{+4}/UO_2^{+2}$ (-120 to -160 mV) redox couples, and by lowering the $O_2/H_2O$ redox value in increments until the solution reached saturation with respect to, first, pyrolusite ($MnO_2$; 575 to 605 mV) and then uraninite ($UO_2$; 35 to 50 mV). Eh values bounded by the pyrolusite and uraninite solubility limits overlap with the range obtained by platinum-electrode measurements in the field (454 to 75 mV).

The $O_2/H_2O$ and $U^{+4}/U^{+6}$ redox couples overestimated and underestimated, respectively, the redox state of the groundwaters. For the $O_2/H_2O$ couple, the high Eh value may be due to addition of atmospheric $O_2$ during sample collection or the inability of the geochemical code to evaluate the kinetic rate of the $O_2$-$H_2O$ half-cell reaction. Calculation of the groundwater Eh with the $U^{+4}/U^{+6}$ couple produced values inconsistent with mineral solubilities and platinum-electrode measurements. Low uranium redox values (-120 to -160 mV) indicate concentrations of $U^{+4}$ are too high. The high $U^{+4}/U^{+6}$ ratios measured in these groundwaters are attributed to the sorption of uranyl species on iron-bearing colloids (Fig. 10), which comprised a portion of the filtered residue analyzed for $U^{+4}$ (see field sampling technique for $U^{+4}$ and total U in Field Sampling and Laboratory Procedure Plan for the Geochemical Program).

Because a wide range of Eh values were used to model uranium speciation, several groundwater compositions were modeled over an Eh range of 50 to 650 mV to determine the affect (if any) of Eh variation. Results for this test are shown in Figure 11, and indicate that variation in the Eh estimate of groundwaters does not affect the speciation results for uranium.

### 3.3 URANIUM SPECIATION

Uranium speciation was investigated in 26 groundwater samples (20 unique wells) and 3 surface-water samples. Results for the speciation modeling are presented in Tables 1 and 2. Speciation results for the groundwaters support calculations to estimate a uranium distribution coefficient for the aquifer (issue five). Table 1 reveals that 11 samples had greater than 99 percent of the uranium partitioned into the aqueous specie $UO_2(H_2PO_4)_2^{\bullet}$, 9 samples (phosphorous not reported or below the detection limit) had greater than 99 percent of the uranium partitioned into the aqueous species $UO_2(CO_3)_3^{-4}$, $UO_2(CO_3)_2^{-2}$ and $UO_2(CO_3)^{\bullet}$, and 6 samples (five with uranium greater than 0.3 mg/L) partitioned the uranium into a combination of the above three species. These results indicate that uranyl ion ($UO_2^{+2}$) will form negatively charged complexes with carbonate ion ($CO_3^{-2}$) in this environment only if the molar concentration (moles per liter) of uranium is greater than one-half the molar concentration of phosphorous (i.e., [U] > 0.5[P]). When uranyl-carbonate complexes form, $UO_2(CO_3)_3^{-4}$ is the dominant specie in these groundwaters at neutral and slightly alkaline pH.

Three surface waters were chosen for uranium-speciation modeling to evaluate the potential of introducing uranium to the underlying aquifer by vertically infiltrating surface waters (issue three). Analyses for these three samples reported uranium concentrations of 0.002 to 0.015 mg/L, with phosphorous ranging from below the detection limit (<0.02 mg/L) to 0.16 mg/L (Appendix A). Because of the relatively low uranium concentrations in these surface waters, all uranium was partitioned into the neutral phosphate complex in waters which contained detectable amounts of phosphorous (Table 2). Surface waters without reportable phosphorous concentrations (i.e., W-11; Table 2) partitioned uranium into the anionic carbonate complexes.

### 3.3.1 Discussion

Preliminary results on the feasibility of recovering uranium from groundwaters by anion-exchange processes show 90 percent of the uranium is recovered by this method (personal communication, Khan, 1989). The experimental results are in good agreement with the majority of modeling results (i.e., negatively-charged uranyl-carbonate species). However, modeling results also indicate that uranium is complexed as the neutral $UO_2(H_2PO_4)_2^{\circ}$ specie in 11 of 26 groundwaters.

Several factors could account for the observed sorptive behavior of uranium. First, phosphorous (measured as total P and converted to phosphate) may form organic complexes in the groundwaters, which would reduce the activity of the phosphate complex and decrease the amount of $UO_2(H_2PO_4)_2^{\circ}$ formed. Organic-phosphate speciation was not modeled because thermodynamic data is limited to inorganic-phosphate complexes, which results in $UO_2(H_2PO_4)_2^{\circ}$ concentrations that may be over estimated. Second, the association constant for $UO_2(HPO_4)_2^{-2}$ may not be correct (see 3.3.1.1 below) and, therefore, significant partitioning of uranium into this specie cannot be ruled out. The presence of $UO_2(HPO_4)_2^{-2}$ in the groundwaters would be consistent with removal of uranium by anion exchange. Finally, the $UO_2(H_2PO_4)_2^{\circ}$ specie may exhibit weak dipole properties (similar to $H_2O$) that, despite the neutral charge, result in retardation along the flow path in an anion-exchange column.

#### 3.3.1.1 Data Base Integrity

The speciation results for surface and groundwaters indicate that the uranyl ion has a strong affinity to form an uncharged complex with phosphate. A phosphorous concentration of 0.02

mg/L (the limit of detection) would allow up to 0.071 mg/L uranium to be complexed as $UO_2(H_2PO_4)_2^{\bullet}$. Since the majority of analyses received (not modeled) have uranium concentrations less than 0.071 mg/L and phosphate values greater than 0.02 mg/L, the modeling results suggest carbonate complexation may not occur in these groundwaters. However, the speciation results for groundwaters containing phosphorous appear to be in conflict with published studies (Scanlan, 1977; Tripathi, 1984; Koss, 1988), which indicate $UO_2^{+2}$ will form carbonate complexes in bicarbonate waters at neutral pH. In addition, studies by Moskvin et al. (1967) and Dongarra and Langmuir (1980) concluded that the dominant uranyl-phosphate complex in natural waters of neutral pH is the single-protonated, negatively-charged $UO_2(HPO_4)_2^{-2}$ complex, which is in contrast to the neutral, double-protonated $UO_2(H_2PO_4)_2^{\bullet}$ specie predicted by the EQ3NR code.

To resolve this apparent discrepancy, the thermodynamic values for the aqueous uranium species active in this study were checked to ensure data base integrity. Association constants for $UO_2(H_2PO_4)_2^{\bullet}$ (log K = 45.24; Baes, 1956; Tripathi, 1984), $UO_2(CO_3)_2^{-2}$ and $UO_2(CO_3)_3^{-4}$ (log K = 17.08 and 21.70, respectively; Scanlan, 1977; Tripathi, 1984)) were verified to be correctly entered in the thermodynamic data base. However, single-protonated uranyl-phosphate complexes (e.g., $UO_2HPO_4^{\bullet}$ and $UO_2(HPO_4)_2^{-2}$) were not present in the thermodynamic data base. Lawrence Livermore National Laboratory removed single-protonated uranyl-phosphate complexes from the EQ3NR data base as a result of the conclusions reached by Tripathi (1984). Tripathi argued that the studies of Moskvin et al. (1967) and Dongarra and Langmuir (1980), who concluded that $UO_2(HPO_4)_2^{-2}$ (association log K = 18.3) is the dominant specie in oxygenated waters with pH between 4 and 8, are not valid because their experiments were carried out with acidic solutions (pH = 0 to 4) and uranyl complexation with $H_2PO_4^-$ and $H_3PO_4$ was not considered. The omission of the single-protonated uranyl-phosphate complex from the data base was hypothesized to be insignificant because of the much larger association constant for $UO_2(H_2PO_4)_2^{\bullet}$ relative to $UO_2(HPO_4)_2^{-2}$ (log K = 45.24 versus 18.3, respectively). This hypothesis was verified by reinserting the thermodynamic data of Dongarra and Langmuir (1980) into the data base and finding no change in the speciation after rerunning several groundwaters.

# 4.0 URANIUM ADSORPTION

Partitioning of uranium between aquifer solids and groundwater was evaluated to calculate an apparent distribution coefficient [$K_d$ = (mg U/kg solid)/(mg U/L groundwater)] for uranium in the sand and gravel aquifer. This task was carried out to meet the objectives of issue five. Uranium adsorption was evaluated by:

- Modeling the uranium speciation of groundwater using the EQ3NR geochemical code and comparing the speciation output to published $K_d$ studies
- Calculating distribution coefficients based on uranium concentrations reported for archived aquifer solids, leachates, and groundwaters.

## 4.1 SPECIATION AND EXPERIMENTAL STUDIES

Speciation results presented in Section 3.3 indicate the expected uranium complexes in groundwaters recovered from Fernald monitoring wells are dominantly $UO_2(CO_3)_3^{-4}$ and $UO_2(CO_3)_2^{-2}$, and $UO_2(H_2PO_4)_2^{\circ}$ when phosphorous is present. The modeling results are in good agreement with studies by Ferri et al. (1981), which show uranium is present as the $UO_2(CO_3)_3^{-4}$ complex in carbonate solutions between pH 7 and 12. Neutral aqueous species (e.g., $UO_2(H_2PO_4)_2^{\circ}$) are not expected to sorb appreciably (perhaps slightly if the molecule has a strong dipole) and, consequently, are not considered in experimental studies. Therefore, this discussion focuses on studies which have addressed the adsorption of uranium from carbonate solutions.

### 4.1.1 Adsorption of Uranyl-Carbonate Species by Montmorillonite

Canterford and Sparrow (1983) studied the adsorption of uranium using a montmorillonite and carbonate solution mixture. A simple solution was prepared by adding 4 g of $Na_2CO_3$ and 8.4 g of $UO_2(NO_3)_2 \cdot 6H_2O$ to one liter of distilled water, yielding $CO_3^{-2}$ and U concentrations of, respectively, 2.26 g/L (0.038 mole/L) and 3.97 g/L (0.017 mole/L) at a final pH of 7.7. The montmorillonite suspension was 0.48 weight percent solids at a pH of 7.6. Five ml of the uranium solution was added to 195 ml of the montmorillonite suspension and samples were stirred and agitated for 96 hours. Results for this experiment indicate an apparent $K_d$ for uranium of 65.78 L/kg at a final pH of 8.

However, the large $K_d$ value for uranium in this simple system is suspect with respect to sorption of anionic uranyl-carbonate species by montmorillonite. Note that the experiments of Canterford and Sparrow (1983) had about 0.004 mole/L of excess uranium that could not be complexed as the specie $UO_2(CO_3)_3^{-4}$ (the dominant specie at pH = 8; Ferri and Salvatore, 1981). That is, the amount of carbonate ion in the system, 0.038 mole/L, requires only 0.0127 mole/L of the available 0.017 mole/L of uranium to form $UO_2(CO_3)_3^{-4}$. Therefore, the excess 0.004 mole/L of uranium could be present as the $UO_2^{+2}$ specie, which would readily sorb to montmorillonite in these neutral and slightly alkaline pH waters because of its low zero point of charge (montmorillonite $pH_{zpc}$ = 2.5; Stumm and Morgan, 1981).

The pH at which a clay mineral surface has a zero point of charge ($pH_{zpc}$) is very important with respect to sorption of charged aqueous species. At a solution pH value below the $pH_{zpc}$, the surface of the clay mineral contains only free positively-charged sites, which would attract negatively-charged ions (e.g., $UO_2(CO_3)_3^{-4}$). Similarly, for solution pH values above the $pH_{zpc}$, a clay mineral surface will have only free negatively-charged sites and sorb positively-charged ions (e.g., $UO_2^{+2}$).

An alternate hypothesis for the large $K_d$ value reported by Canterford and Sparrow (1983) is that uranium partitioning is balanced to allow for $UO_2(CO_3)_3^{-4}$ (U = 0.004 moles/L) and $UO_2(CO_3)_2^{-2}$ (U = 0.013 moles/L) complexation without $UO_2^{+2}$. If this latter hypothesis holds, then the large $K_d$ value for this system suggests amorphous AlOOH and FeOOH ($pH_{zpc}$ = 8.2 and 7.8, respectively; Stumm and Morgan, 1981) films on the montmorillonite surface are sorbing the anionic complexes. This latter scenario is less credible because the dominant uranium specie in the solutions of pH = 8 (Canterford and Sparrow, 1983) would have to be $UO_2(CO_3)_2^{-2}$, which is in contrast to the $UO_2(CO_3)_3^{-4}$ specie predicted by experimental studies (Ferri et al., 1981) and modeling results.

4.1.2 Adsorption of Uranyl-Carbonate Species by Amorphous Ferric Oxyhdroxide

Ames et al. (1983) investigated sorption of uranium on amorphous ferric oxyhydroxide ($pH_{zpc}$ = 7.8 to 8.5; Stumm and Morgan, 1981) at 25° and 60°C from 0.01 molar (moles/liter) $NaHCO_3$ solutions over an initial uranium concentration range of 0.0001 to 0.00000055 molar (23.8 to

0.13 mg/L). Their amorphous ferric oxyhydroxide was prepared by mixing 1 ml of 0.1 molar $FeCl_3$ with 30 ml of 0.01 molar NaOH. Uranyl-carbonate solutions were added to the ferric oxyhdroxide precipitate to yield an iron mass to solution volume ratio of 0.279 g/L. Solutions and ferric oxyhydroxide were sealed in polypropylene tubes and agitated for seven days. Blanks containing uranyl-carbonate solutions but no ferric oxyhydroxide indicated less than 2 percent tube-wall sorption. A count on the initial and final solutions determined the sorbed uranium by difference. Apparent $K_d$ values at 25°C and average final pH of 8.6 to 8.7 ranged from about 4,000 L/kg at U = 23.8 mg/L to about 26,000 L/kg at U = 0.13 mg/L The apparent $K_d$ values increased to, respectively, 5,000 and 34,000 L/kg at 60°C.

The results of Ames et al. (1983) indicate a strong potential for sorption of anionic uranyl-carbonate species onto amorphous ferric-oxyhydroxide surfaces in slightly alkaline solutions (maximum loading = 3.116 moles U per kg ferric oxyhydroxide). However, these apparent $K_d$ values were calculated for a simple system and do not take into account the presence of other ligands (e.g, $SO_4^{-2}$, $PO_4^{-3}$, etc) in natural waters. Sulfate and phosphate complexes would compete for the available anion sorption sites on ferric oxyhydroxide and lower uranium $K_d$ values considerably, primarily due to the much greater concentrations of sulfate and phosphate, relative to uranium, in solution.

4.1.3 Empirical Determination of a Uranium Distribution Coefficient

Using the maximum uranium loading on ferric oxyhydroxide (3.116 moles/kg; Ames et al., 1983), an apparent $K_d$ between aquifer solids and groundwater was calculated. The calculation is based on the following assumptions:

- Groundwater and aquifer solids are in equilibrium at 25°C
- The composition of the groundwater is the same prior to and at equilibrium
- All uranium is speciated into $UO_2(CO_3)_3^{-4}$
- The experimentally determined maximum uranium loading on ferric oxyhydroxide (3.116 moles/kg) is taken as the total moles of anionic species that can be sorbed
- All Fe leached from the aquifer solids was in the form FeOOH
- Each sorption site on FeOOH is occupied by either $HCO_3^-$, $NO_3^-$, $HPO_4^{-2}$, $SO_4^{-2}$, or $UO_2(CO_3)_3^{-4}$

- The affinity of a molecule to sorb on FeOOH is proportional to its charge and concentration.

Assumptions three and five may introduce the greatest uncertainty in the $K_d$ calculation. For instance, modeling results for uranium speciation in groundwaters (Table 1) indicates $UO_2(H_2PO_4)_2^{\cdot}$ and $UO_2(CO_3)_2^{-2}$ are important species in addition to $UO_2(CO_3)_3^{-4}$. This uncertainty can be estimated by comparing the calculated $K_d$ value based on the assumptions above with that calculated for speciation based on modeling results (Table 3). Partitioning of all iron into amorphous ferric oxyhydroxide is the most tenuous assumption, as the analytical leaching technique is known to recover iron from both amorphous- and crystalline-oxyhydroxide phases, and it is not possible to distinguish between these two iron components. However, even if the partitioning of iron among these components was known, the $K_d$ value would probably not decrease by more than a factor of two, and this uncertainty is probably no greater than uncertainties associated with the remaining assumptions.

Noting the limitations of the above assumptions, empirical $K_d$ values were calculated for all wells (17) with groundwater and aquifer-solid analyses (Table 3). The 1000 series wells (2) are in a discontinuous glacial-till horizon which overlies the sand and gravel aquifer (i.e., the till is not part of the regional aquifer). Groundwater from well 3016 has been paired with a clay interbed sample that is probably impermeable and, therefore, not interacting with groundwater in the aquifer. These three well numbers have been excluded from discussions which refer to the range and average $K_d$ value. The remaining groundwater-solid pairs (14) have $K_d$ values that range from 0 to 3.89 L/kg, and individual wells had variation in their $K_d$ values from round to round (Table 3). For example, the $K_d$ value calculated for the Round 3 (Fourth Quarter, 1988) groundwater analysis of well 2010 is less than that of the Round 4 (First Quarter, 1989) $K_d$ value because of the larger sulfate value reported for the Round 3 analysis (i.e., less FeOOH sites available for uranium species in Round 3 groundwater).

Empirical $K_d$ values are dependent on the amount of leachable iron (i.e., FeOOH) present in the aquifer solids, the concentration and speciation of uranium in the groundwater, and the

aqueous concentrations of remaining ligands. In general, all anionic complexes except uranium being fixed, the uranium $K_d$ value will:

- Double if the leachable iron in the aquifer solids is doubled, while holding the uranium concentration constant
- Double if the uranium concentration in solution is doubled, while holding leachable iron constant
- Decrease by half if the leachable iron in the aquifer solids is decreased by half, with uranium concentration held constant
- Decrease by half if the uranium concentration in solution decreases by half, with leachable iron held constant
- Decrease by half to zero if all uranium is partitioned into $UO_2(CO_3)_2^{-2}$ or $UO_2(H_2PO_4)_2^{\bullet}$, respectively, while leachable iron is held constant.

Points three and five merit special emphasis because of their sensitivity to the assumptions used in calculating the $K_d$ values. As noted above, iron leached from the aquifer solids can be derived from amorphous- and crystalline-oxyhydroxide grains, and organic complexes. Unfortunately, there is no quantitative way to separate these components and refine the amount of Fe that is partitioned solely into amorphous ferric oxyhydroxide. Therefore, the empirically calculated $K_d$ values overestimate the 'true' $K_d$ value.

Point five is important because speciation modeling predicts most wells to have phosphate concentrations in excess of that required to complex uranium as $UO_2(H_2PO_4)_2^{\bullet}$ (see Section 3.3). Table 3 reports the $K_d$ value for the empirical model based on the available speciation results for a limited number of groundwaters. Note that $K_d$ values approach zero for those wells which partition greater than 99 percent of the uranium into the neutral phosphate complex (e.g.,1082, 2046, 2095). Based on the present modeling results for uranium speciation, the groundwater-aquifer-solid pairs in Table 3 that were not modeled for speciation would probably have $K_d$ values close to zero, because the phosphate and uranium concentrations suggest most uranium will be partitioned into the neutral phosphate complex. However, for reasons discussed in Section 3.3.1, it is unlikely that the neutral phosphate complex plays as significant a role as predicted by the EQ3NR geochemical code and, if present, this complex would still exhibit some sorptive capacity due to dipole attractions. Therefore, empirical $K_d$ values based

on the partitioning of greater than 99 percent of the uranium into $UO_2(H_2PO_4)_2^{\bullet}$ will probably underestimate the 'true' $K_d$ of the aquifer.

## 4.2 AQUIFER SOLIDS, LEACHATES AND GROUNDWATERS

Analytical results for uranium concentrations in groundwaters, leachates and aquifer solids were used to calculate apparent distribution coefficients for 17 monitoring sites. The following assumptions were used in calculating the apparent $K_d$'s:

- The analyzed groundwater samples were in equilibrium with their respective aquifer solids (i.e., kinetic rates for uranium sorption were faster than solution flow rates through a given volume element)
- All uranium species sorb at the same rate
- The background concentration of uranium in the aquifer solids is 3 mg/kg and in the leachates 0.142 mg/kg
- The adsorbed uranium concentration is equal to the concentration of uranium obtained for the aquifer solid or leachate minus the background concentration of uranium
- The apparent $K_d$ is equal to the sorbed uranium concentration (mg/kg) divided by the groundwater uranium concentration (mg/L).

Apparent distribution coefficients were calculated from reported uranium concentrations for aquifer solids from wells 2046 (U = 16 mg/kg) and 4010 (U = 13.8 mg/kg), and round 4 groundwater analyses from wells 2046 (U = 0.309 mg/L) and 4010 (<0.001 mg/L). These samples were chosen because they bound the range of aqueous uranium concentrations available for groundwater analyses that can be matched to the aquifer solids. Using the uranium values cited above, $K_d$'s for wells 2046 and 4010 are, respectively, 42 and 10,800 L/kg. The $K_d$ for well 4010 was calculated with the uranium detection-limit value of 0.001 mg/L. Utilizing the 2-sigma error range for uranium concentrations in the aquifer solids (12.3 to 19.7 mg/kg and 9.7 to 17.9 mg/kg, respectively), the corresponding range in $K_d$ for the respective wells is 30 to 54 L/kg and 6,700 to 14,900 L/kg. Because of the similar uranium concentrations reported for the unleached aquifer solids, the $K_d$ is primarily a function of the uranium concentration in the groundwater. It is important to reemphasize that the uranium concentrations reported for aquifer solids analyzed by gamma spectrometry are suspect, and $K_d$ calculations using these anomalous results yield partition coefficients that are too great for the aquifer.

Results for total uranium concentrations in the leachate fractions derived from the differential-leaching procedure indicate less than 2.5 ppb of uranium is sorbed on aquifer solids (i.e., $K_d$ = 0). In contrast, a range of 33 to 783 ppb of uranium was reported for leachates derived from aquifer solids which underwent the iron- and manganese-leaching procedure (see Section 2.5.2). Utilizing the above assumptions, and a background uranium concentration in the leachates of 0.142 mg/kg (obtained by averaging the leachate uranium values obtained from samples 7790, 10407, 10460, 10607 and 10696, which have reported uranium concentrations in groundwater of less than 1 ppb), $K_d$ values calculated for 14 aquifer wells (1000 series wells and clay interbed sample are not included) ranged from 0 to 68.2 L/kg (Table 4). About a third of the samples have a $K_d$ value of zero, but most of these are from wells considered to be representative of uranium background levels and do not reflect 'true' $K_d$ values. Three samples have distribution coefficients greater than 10. The samples which produced high $K_d$ values were obtained from the waste-pit region bounding the northwest corner of the Fernald compound, and may indicate that precipitated uranium solids are contributing to the sorption $K_d$ value.

## 4.3 COMPARISON OF EMPIRICAL AND CALCULATED $K_d$ VALUES

Figure 12 is a plot of the calculated $K_d$ from groundwater and leachate analyses versus the predicted $K_d$ based on the empirical sorption model. Wells in the regional aquifer were broken down into areas adjacent to and within the Feed Material Production Center (FMPC) compound. The areas are identified as the south plume (south of the FMPC), waste pit (northwest of the FMPC), and within the FMPC compound. The 1000-series wells in the glacial till are in the waste-pit area but have been plotted separately because they are not part of the regional aquifer. The plot was constructed with the data in Tables 3 and 4 after averaging multiple $K_d$ values for individual wells and omitting well 3016, which had groundwater matched to an anomalous clay-interbed sample.

Monitoring wells in the regional aquifer, representing the south-plume and waste-pit areas, were identified and plotted separately to construct regression lines for these areas. A slope of one on this plot, and a correlation coefficient (r) near one, would indicate a perfect fit between the calculated and predicted $K_d$. The regression line for the south-plume data has a slope of 0.87, but a less than ideal r value of 0.65. Data points representing the waste-pit area define a regression line with a slope of 6.44 and a r value of 0.29, indicating a poor fit between the

predicted and calculated $K_d$ values. Wells within the FMPC compound and glacial till lie near the south plume regression line (but have not been used in the calculation of the regression line). The poor fit between predicted and calculated $K_d$ values for aquifer samples from the waste pit may indicate that precipitation of amorphous uranium solids has occurred in those samples with calculated $K_d$ values greater than 30 (e.g., 2007, 2010, 2027). If precipitation and sorption are mechanisms responsible for retardation of uranium in the waste-pit area, the empirical model would not be expected to predict accurately the $K_d$ because it is based only on the sorption of uranium.

The precipitation hypothesis is supported by uranium concentrations in groundwater recovered from waste-pit area wells 1073 and 1082 (0.8 to 4.4 mg/L), and 3010 (0.015 to 0.020 mg/L). These samples were obtained from the glacial till above the aquifer (1073 and 1082) and, within the aquifer, from below (3010) the 2000 series samples with high $K_d$ values. If uranium-rich waters in the glacial till vertically infiltrated to the underlying aquifer, mixing at the till/aquifer interface could have resulted in precipitation of amorphous uranium solids in the 2000-series horizon, thus limiting breakthrough to the 3000-series horizon.

### 4.4 ESTIMATION OF THE URANIUM $K_d$ FOR THE FERNALD SITE AQUIFER

Results presented in Tables 3 and 4, and Figure 12, indicate that the most reliable indicators of uranium $K_d$ values in the Fernald site aquifer come from well locations in the south-plume area. This conclusion is based on the similarity of $K_d$ estimates derived from two independent methods. Wells in the waste-pit area are not considered in the estimation of the aquifer $K_d$, because large calculated values for 2000-series wells (Table 4) suggest uranium is also present as amorphous oxide solids. Additionally, calculated $K_d$ values (Table 4), rather than empirical $K_d$ values (Table 3), were used to estimate the site $K_d$ because assumptions based on the former are more valid and defensible.

To derive the estimate of the aquifer $K_d$, 2000- and 3000-series wells from the south-plume area (Table 4) were averaged (if Round 3 and Round 4 values were reported) to produce a single $K_d$ value for each well. Wells with reported $K_d$ values of zero were not considered because of the inability to estimate a reasonable $K_d$ (i.e., a distribution coefficient is a finite

number). A simple average of the $K_d$ value for each well was considered to be the best approach, because there is no basis on which to weigh individual wells at this time. After satisfying the preceding criteria, four wells (2016, 2046, 2095 and 3095) were used to estimate the aquifer $K_d$. The mean $K_d$ value for the four wells is 2.38, with a standard deviation of 1.42.

The mean uranium $K_d$ value can be converted to a retardation factor with the relationship:

$$R_f = 1 + (rho/n) \bullet K_d$$

where:

$R_f$ = retardation factor
rho = density
n = porosity
$K_d$ = distribution coefficient

Using the mean $K_d$ value of 2.38 L/kg (note: a L/kg = ml/g), and typical values for rho (2.6 g/cc; cc = ml) and n (0.25) in the sand and gravel aquifer, the $R_f$ value is 25.8. This retardation factor implies that uranium species present in the groundwater will move 1 meter for every 25.8 meters traversed by the groundwater front. Unfortunately, this retardation value is based on the uranium recovered from the iron and manganese leachates, and the uranium present as 'historical' uranium (if any) is estimated from subtracting an 'estimated' background level from the total. Additionally, recall that the differential-leaching of aquifer solids (6 samples) for uranium recovered less than 2.5 ppb uranium, which suggests the above retardation factor is far too great. Resolving these problems will require additional data on the mineral composition of aquifer solids (i.e., petrographic and x-ray diffraction studies to estimate detrital iron-oxide minerals) and a larger sample-size population for the differential-leaching analysis.

Noting the limitations of the present estimate of the aquifer $K_d$, it is recommended that the solute-transport model be evaluated using the limits defined by the standard deviation of the mean $K_d$ value. This approach requires two runs of the model at bounding conditions of 0.96

L/kg (estimated lower limit) and 3.80 L/kg (estimated upper limit), and would bracket the majority of $K_d$ values calculated for the site (excluding 2000-series wells in the waste-pit area). The bounding conditions can be cautiously applied to the waste-pit area, noting that additional analytical data is required to evaluate the retardation process occurring in these 2000-series wells. Given the current data base available to work with, this is the recommended application of the estimated $K_d$ value to the solute-transport model.

## 5.0 CONCLUSIONS

### 5.1 ISSUE THREE

Subsurface soils and surface waters from Paddy's Run and the storm-water-outfall ditch (Fig. 1) have been sampled and analyzed to evaluate the degree of infiltration of uranium-bearing surface water to the underlying aquifer. Presently, there is no indication of contamination at four of the six soil-sample sites. If uranium-rich waters had infiltrated these soil horizons, the present observation suggests uranium was not attenuated (e.g., the dominant specie in the infiltrating waters may have been $UO_2(H_2PO_4)_2^{\circ}$) and/or uranium that had sorbed (e.g, $UO_2(CO_3)_3^{-4}$) or precipitated was desorbed or dissolved prior to sampling and analysis of the soils. Both of these scenarios are compatible with the modeling results, which predict the presence of neutral uranyl-phosphate and anionic uranyl-carbonate species in the surface waters (Table 2).

The top ten feet of material at sites S1 (1405) and S2 (1406) have concentrations of uranium that are about twice the level of background values. This observation indicates uranium has been retarded at these sites by sorption or precipitation processes occurring in the soil (site S1) and regional aquifer (site S2). The uranium profiles for these sites (Fig. 3) are compatible with scenarios of no breakthrough to the underlying aquifer (i.e., all uranium is retarded by the soil, site S1) and partial breakthrough to the aquifer (i.e., 'historical' uranium is present in the aquifer, site S2). If the retardation of soluble uranium by the soil and aquifer solids is taking place via a sorption process in the unsaturated zone, modeling results indicate the uranium is in the form of anionic uranyl-carbonate species (Table 2). The presence of sorbed or precipitated uranium at these sites presents the potential for future releases to the underlying aquifer.

## 5.2 ISSUE FIVE

Partitioning of uranium between aquifer solids and groundwater (see Fig. 9 for well locations) was evaluated to calculate an apparent distribution coefficient ($K_d$) for uranium in the sand and gravel aquifer. The $K_d$ was evaluated by:

- Modeling the uranium speciation of groundwater using the EQ3NR geochemical code and comparing the speciation output to published $K_d$ studies (i.e., the empirical method)
- Obtaining analyses for total uranium on archived aquifer solids, leachates and groundwaters to calculate a $K_d$ directly.

Empirically derived $K_d$ values for well sites in the regional aquifer ranged from 0 to 3.89 L/kg (Table 3). Distribution coefficients near zero for wells that have greater than 99 percent of their uranium partitioned into $UO_2(H_2PO_4)_2^{\bullet}$ (e.g., 2046 and 2095, Table 3) are probably too low, and reflect the inability to model organic phosphate complexation and sorption processes that take credit for molecular dipole attraction. Speciation results were not available for all groundwaters evaluated with the $K_d$ model, and $UO_2(CO_3)_3^{-4}$ was assumed to be the specie present. This assumption is supported by:

- Speciation results which indicate $UO_2(CO_3)_3^{-4}$ is the dominant specie if phosphate concentrations are below the detection limit of 0.02 mg/L (Table 1)
- Experimental anion-exchange tests that recovered greater than 90 percent of the uranium from site groundwater samples (Khan, 1989; personal communication)
- Documented experimental studies that indicate the dominant uranyl ion in bicarbonate solutions at neutral and slightly alkaline pH is $UO_2(CO_3)_3^{-4}$ (Ferri et al., 1981).

Additionally, the empirical $K_d$ values are strongly dependent on the amount of iron that is partitioned into amorphous ferric oxyhydroxide. Because it is not possible to separate the leachable iron into amorphous and crystalline components, all iron was assumed to be partitioned into the amorphous phase. This assumption yields $K_d$ values that overestimate the 'true' $K_d$ of the aquifer.

Distribution coefficients calculated directly from analyses of uranium in aquifer solids, leachates and groundwaters range from 0 to greater than 10,000 L/kg. Calculations of distribution

coefficients based on gamma-spectrometry analysis of uranium in aquifer solids (30 to 14,900 L/kg) are not reliable, and are excluded from interpretations based on the leaching results. The differential-leaching procedure revealed that less than 2.5 ppb of uranium is present as sorbed or amorphous uranium products, which suggests the uranium $K_d$ is zero for these samples. However, the iron- and manganese-leaching technique recovered 33 to 783 ppb of uranium from the aquifer solids, resulting in a range of 0 to 68 L/kg for calculated $K_d$ values (Table 4). A background level was subtracted from the uranium values obtained from the iron and manganese leachate prior to the calculation (adsorbed U = total U - background U), and about a third of the samples had a calculated concentration of adsorbed uranium equal to zero, which resulted in a $K_d$ of zero for that sample. It is important to note that those wells with calculated $K_d$ values of zero are mainly from 3000 and 4000 series horizons, which in general show no indication of uranium contamination.

5.2.1 Best Estimate of the Uranium $K_d$ for the Aquifer

The best estimate of the uranium $K_d$ value for the aquifer was derived from calculated $K_d$ values for south-plume wells. Empirical $K_d$ values were not used because the assumptions supporting the derivation are not as valid and defensible as the calculated $K_d$ assumptions. Calculated $K_d$ values for waste-pit area wells were also excluded from the estimate of the site $K_d$, because 2000-series wells in this area have apparent $K_d$ values that are anomalously high with respect to values calculated for the majority of wells (Fig. 12). These anomalous values may indicate uranium is being retarded by sorption and precipitation processes in the waste-pit area.

Using the calculated $K_d$ values from four south-plume wells (2016, 2046, 2095 and 3095; Table 4), the aquifer $K_d$ was estimated as 2.38 L/kg. This $K_d$ indicates the retardation factor for uranium in the aquifer will be close to 26, which appears to be too great as evidenced by the differential-leaching tests. However, it is recommended that the solute-transport model be evaluated at the lower (0.96 L/kg) and upper (3.80 L/kg) standard-deviation limits. These two bounding cases would bracket the majority of $K_d$ values calculated for the south-plume and waste-pit area wells (excluding the 2000-series waste-pit wells). The bounding cases may be cautiously applied to the waste-pit area, but additional analytical work on aquifer solids is

required to evaluate critically how the mechanisms of sorption and precipitation retard uranium in 2000-series wells from this area.

## REFERENCES


Ames, L. L., J. E. McGarrah, B. A. Walker, and P. F. Salter, 1983, "Uranium and Radium Sorption on Amorphous Ferric Oxyhydroxide," Chemical Geology, Vol. 40, pp. 135-148.

Baes, C. F., 1956, "A Spectrophotometric Investigation of Uranyl Phosphate Complex Formation in Perchloric Acid Solution," Journal of Physical Chemistry, Vol. 60, pp. 878-883.

Canterford, J. H., and G. J. Sparrow, 1983, Adsorption of Uranium from Carbonate Media, Society of Mining Engineers of AIME, Vol. 83-305, 10 pp.

Chester, R., and M. J. Hughes, 1967, "A Chemical Technique for the Separation of Ferro-Manganese Minerals, Carbonate Minerals and Adsorbed Trace Elements from Pelagic Sediments," Chemical Geology, Vol. 2, pp. 249-262.

Dongarra, G., and D. Langmuir, 1980, "The Stability of $UO_2OH^-$ and $UO_2(HPO_4)_2^{-2}$ Complexes at 25°C," Geochimica et Cosmochimica Acta, Vol. 44, pp. 1747-1751.

Environmental Protection Agency, Methods for Chemical Analysis of Waste, EPA-600, 4-79-020.

Faure, G., 1977, Principles of Isotope Geology, John Wiley & Sons, New York, 464 pp.

Ferri, D., I. Grenthe, and F. Salvatore, 1981, "Dioxouranium (IV) Carbonate Complexes in Neutral and Alkaline Solutions," Acta Chemica Scandinavia, Vol. A35, pp. 165-168.

Hem, J. D., 1970, "Study and Interpretation of the Chemical Characteristics of Natural Water," U.S. Geological Survey, Water-Supply Paper 1473, 363 pp.

International Technology Corporation, 1989, "Field Sampling and Laboratory Procedure Plan for the Geochemical Program: In Support of the Remedial Investigation Feasibility Study, Feed Materials Production Center, Fernald, Ohio."

International Technology Corporation, 1988, "Remedial Investigation and Feasibility Study at the U.S. Department of Energy's Feed Materials Production Center, Fernald, Ohio."

Kahn, M, 1989, Personal communication to Jon Myers.

Koss, V., 1988, "Modeling of Uranium (IV) Sorption and Speciation in a Natural Sediment-Groundwater System," Radiochimica Acta, Vol. 44/45, pp. 403-406.

Krauskopf, K. B., 1979, Introduction to Geochemistry, McGraw-Hill, San Francisco, 533 pp.

Moskvin, A. I., A. M. Shelyakina, and P. S. Perminov, 1967, "Solubility Product of Uranyl Phosphate and the Composition and Dissociation Constants of Uranyl Phosphato- Complexes," Russian Journal of Inorganic Chemistry, Vol. 12, pp. 1756-1760.

Scanlan, J. P., 1977, "Equilibria in Uranyl Carbonate Systems, II: The Overall Stability Constant of $UO_2(CO_3)_2^{-2}$ and the Third Formation Constant of $UO_2(CO_3)_3^{-4}$," Journal of Inorganic Nuclear Chemistry, Vol. 39, pp. 635-639.

Stumm, W., and J. J. Morgan, 1981, Aquatic Chemistry, John Wiley & Sons, New York, 780 pp.

Tripathi, V. S., 1984, "Uranium (VI) Transport Modeling: Geochemical Data and Submodels," Ph.D. Dissertation, Stanford University, Stanford, California.

Wolery, T. J., 1983, EQ3NR, A Computer Program for Geochemical Aqueous Speciation-Solubility Calculations: User's Guide and Documentation, UCRL-53414, Lawrence Livermore National Laboratory, Livermore, California.

## TABLE 1

## RESULTS FOR URANIUM SPECIATION IN WATERS RECOVERED FROM FERNALD MONITORING WELLS

| WELL # | ROUND | pH | Eh mV | U mg/L | P mg/L | SPECIES | % | CB[a] |
|---|---|---|---|---|---|---|---|---|
| 1019 | 3 | 7 | 386[b] | 0.818 | 0.061 | $UO_2(CO_3)_3^{-4}$<br>$UO_2(H_2PO_4)_2^{o}$<br>$UO_2(CO_3)_2^{-2}$ | 52<br>29<br>19 | +14.84[c] |
| 1019 | 4 | 7 | 371[b] | 0.739 | 0.12 | $UO_2(H_2PO_4)_2^{o}$<br>$UO_2(CO_3)_3^{-4}$<br>$UO_2(CO_3)_2^{-2}$ | 62<br>26<br>12 | + 7.99 |
| 1073 | 3 | 7.6 | 321[b] | 3.297 | 0.493 | $UO_2(H_2PO_4)_2^{o}$<br>$UO_2(CO_3)_3^{-4}$<br>$UO_2(CO_3)_2^{-2}$ | 57<br>39<br>3 | + 2.60 |
| 1073 | 4 | 7.1 | 366[b] | 4.38 | NR | $UO_2(CO_3)_3^{-4}$<br>$UO_2(CO_3)_2^{-2}$ | 92<br>8 | +64.16[e] |
| 1082 | 3 | 7 | 350[f] | 1.079 | 3.79 | $UO_2(H_2PO_4)_2^{o}$ | >99 | -26.85[g] |
| 1082 | 4 | 7.35 | 350[f] | 0.81 | 0.65 | $UO_2(H_2PO_4)_2^{o}$ | >99 | +19.61[h] |
| 2013 | 3 | 6.85 | 137[i] | 0.008 | <0.02 | $UO_2(CO_3)_2^{-2}$<br>$UO_2(CO_3)_3^{-4}$<br>$UO_2(CO_3)^{o}$ | 67<br>31<br>2 | + 4.55 |
| 2024 | 3 | 7.30 | 152[i] | 0.005 | 0.342 | $UO_2(H_2PO_4)_2^{o}$ | >99 | - 9.46 |
| 2044 | 3 | 7.47 | 331[j] | 0.033 | 0.024 | $UO_2(H_2PO_4)_2^{o}$ | >99 | - 9.82 |
| 2045 | 4 | 7.3 | 324[k] | 0.283 | NR | $UO_2(CO_3)_3^{-4}$<br>$UO_2(CO_3)_2^{-2}$ | 59<br>41 | + 5.79 |
| 2046 | 4 | 7.0 | 324[k] | 0.309 | 0.39 | $UO_2(H_2PO_4)_2^{o}$ | >99 | + 8.68 |
| 2060 | 3 | 7.50 | 605[l] | 0.171 | <0.02 | $UO_2(CO_3)_3^{-4}$<br>$UO_2(CO_3)_2^{-2}$ | 61<br>39 | + 4.07 |
| 2060 | 4 | 7.4 | 324[k] | 0.250 | 0.03 | $UO_2(H_2PO_4)_2^{o}$<br>$UO_2(CO_3)_3^{-4}$<br>$UO_2(CO_3)_2^{-2}$ | 45<br>32<br>23 | + 3.74 |
| 2061 | 4 | 7.6 | 324[b] | 0.292 | 0.02 | $UO_2(CO_3)_3^{-4}$<br>$UO_2(H_2PO_4)_2^{o}$<br>$UO_2(CO_3)_2^{-2}$ | 50<br>25<br>24 | + 4.87 |
| 2094 | 4 | 7.1 | 75[i] | 0.0045 | 1.92 | $UO_2(H_2PO_4)_2^{o}$ | >99 | +54.91[m] |
| 2095 | 3 | 7.33 | 331[j] | 0.177 | 0.063 | $UO_2(H_2PO_4)_2^{o}$ | >99 | +14.65[n] |

# TABLE 1

## RESULTS FOR URANIUM SPECIATION IN WATERS RECOVERED FROM FERNALD MONITORING WELLS
(CONTINUED)

| WELL # | ROUND | pH | Eh mV | U mg/L | P mg/L | SPECIES | % | CB[a] |
|---|---|---|---|---|---|---|---|---|
| 3001 | 3 | 8 | 81[o] | 0.015 | <0.02 | $UO_2(CO_3)_3^{-4}$<br>$UO_2(CO_3)_2^{-2}$ | 89<br>11 | +20.52[p] |
| 3001 | 4 | 7.1 | 81[i] | 0.015 | 0.12 | $UO_2(H_2PO_4)_2^o$ | >99 | + 6.00 |
| 3013 | 3 | 6.30 | 139[o] | 0.011 | <0.02 | $UO_2(CO_3)_2^{-2}$<br>$UO_2(CO_3)_3^{-4}$<br>$UO_2(CO_3)^o$ | 77<br>19<br>4 | + 4.83 |
| 3013 | 4 | 8.4 | 139[i] | 0.49 | 0.02 | $UO_2(CO_3)_3^{-4}$<br>$UO_2(H_2PO_4)_2^o$<br>$UO_2(CO_3)_2^{-2}$ | 79<br>15<br>6 | + 1.22 |
| 3014 | 3 | 7.75 | 575[l] | 0.028 | <0.02 | $UO_2(CO_3)_3^{-4}$<br>$UO_2(CO_3)_2^{-2}$ | 70<br>30 | + 1.56 |
| 3016 | 3 | 7.60 | 331[j] | 0.008 | <0.05 | $UO_2(CO_3)_3^{-4}$<br>$UO_2(CO_3)_2^{-2}$ | 64<br>35 | -15.24[q] |
| 3062 | 3 | 7.90 | 331[b] | 0.041 | <0.02 | $UO_2(CO_3)_3^{-4}$<br>$UO_2(CO_3)_2^{-2}$ | 83<br>17 | + 6.59 |
| 3069 | 3 | 7.60 | 331[j] | 0.005 | 0.662 | $UO_2(H_2PO_4)_2^o$ | >99 | - 5.92 |
| 3094 | 4 | 7.1 | 99[i] | 0.0006 | 0.88 | $UO_2(H_2PO_4)_2^o$ | >99 | +58.57[m] |
| 4097 | 4 | 7.1 | 221[i] | 0.0019 | 0.11 | $UO_2(H_2PO_4)_2^o$ | >99 | + 1.77 |

NR = no analysis reported.
[a]Charge balance expressed as percent of total charge.
[b]Eh estimated from the $NH_4^+/NO_3^-$ redox couple.
[c]Excessive charge balance probably due to high Mg or Na concentrations (159 and 437 mg/L, respectively).
[d]EQ3NR calculations indicate the groundwater sample is supersaturated with respect to thorianite, and the dominant aqueous Th-specie (>99 %) is $Th(OH)_4$.
[e]Excessive charge balance probably results from high Ca concentration (4000 mg/L).
[f]Eh estimated from results of $NH_4^+/NO_3^-$ redox couple in wells 1019 and 1073.
[g]Excessive charge balance probably due to high $SO_4^{-2}$ concentration (510 mg/L).
[h]Excessive charge balance probably due to low $SO_4^{-2}$ concentration (19.6 mg/L).
[i]Platinum-electrode measurement.
[j]Eh value estimated from $NH_4^+/NO_3^-$ redox couple for well 3062.
[k]Eh value estimated from $NH_4^+/NO_3^-$ redox couple for well 2061.
[l]Eh based on pyrolusite saturation.
[m]Excessive charge balance probably results from high K concentration (1800-1830 mg/L).
[n]Excessive charge balance probably due to low Cl concentrartion (4 mg/L).
[o]Eh value obtained from round 4 analysis of same well number.
[p]Excessive charge balance probably due to high Ca and Na concentrations (173 and 24.4 mg/L, respectively), relative to round 4 analysis of same well.
[q]Excessive charge balance probably due to high $SO_4^{-2}$ concentration (174 mg/L).

## TABLE 2

## RESULTS FOR URANIUM SPECIATION IN SURFACE WATERS RECOVERED FROM PADDY'S RUN, FERNALD SITE

| SAMPLE # | pH | Eh mV | P ----mg/L----- | U | SPECIES | % | CB[a] |
|---|---|---|---|---|---|---|---|
| W-07 | 8.38 | 451 | 0.032 | 0.015 | $UO_2(H_2PO_4)_2^0$ | >99 | +2.99 |
| W-11 | 8.58 | 441 | BDL | 0.009 | $UO_2(CO_3)_3^{-4}$<br>$UO_2(CO_3)_2^{-2}$ | 90<br>10 | +3.36 |
| ASIT003 | 8.57 | 452 | 0.161 | 0.002 | $UO_2(H_2PO_4)_2^0$ | >99 | +1.99 |

BDL = below detection limit
[a]Charge balance expressed as percent of total charge.

## TABLE 3

## EMPIRICAL URANIUM DISTRIBUTION COEFFICIENTS FOR SELECTED MONITORING WELLS

| WELL | GW[a] | $HCO_3^-$ mg/L | $NO_3^-$ mg/L | $HPO_4^{-2}$ mg/L | $SO_4^{-2}$ mg/L | U mg/L | AS[b] | Fe[c] mg/g | $K_d$[d] L/kg | $K_d$[e] L/kg |
|---|---|---|---|---|---|---|---|---|---|---|
| REGIONAL AQUIFER | | | | | | | | | | |
| South-Plume Area | | | | | | | | | | |
| 2016 | rd1[f] | 292 | <22 | 0.87 | 59 | 0.021 | 10437 | 0.69 | 2.27 | NA[g] |
| 2046 | 3997 | 355 | 5.98 | 1.21 | 74 | 0.309 | 8956 | 0.81 | 2.15 | 0.02 |
| 2095 | 3787 | 352 | 77.5 | 0.20 | 18 | 0.177 | 10038 | 0.66 | 1.77 | 0.02 |
| 2095 | 3976 | 349 | 13.1 | 2.7 | 137 | 0.146 | 10038 | 0.66 | 1.48 | NA[g] |
| 3095 | 3786 | 370 | <0.4 | 0.409 | 18 | 0.005 | 10049 | 1.00 | 3.08 | NA[g] |
| 3095 | 3971 | 335 | <0.4 | 2.98 | 90 | 0.006 | 10049 | 1.00 | 2.67 | NA[g] |
| 4014 | rd4[f] | 285 | <0.4 | NR[h] | 58 | <0.001 | 10407 | 1.08 | 0.00 | NA[g] |
| 4016 | rd4[f] | 313 | <0.4 | NR[h] | 98 | <0.001 | 10460 | 0.38 | 0.00 | NA[g] |
| Waste-Pit Area | | | | | | | | | | |
| 2007 | rd5[f] | 311 | <0.4 | 4.25 | 123 | 0.005 | 10796 | 1.08 | 2.76 | NA[g] |
| 2010 | 3715 | 368 | <0.4 | 0.17 | 271 | 0.005 | 8426 | 1.50 | 2.55 | NA[g] |
| 2010 | 3902 | 382 | <0.08 | 8.1 | 140 | 0.021 | 8426 | 1.50 | 3.18 | NA[g] |
| 2027 | 3941 | 406 | <0.08 | 0.06 | 245 | 0.007 | 7874 | 1.58 | 2.67 | 2.45 |
| 2034 | 3646 | 287 | 9.74 | 0.136 | 39 | 0.024 | 8286 | 0.78 | 2.73 | 2.51 |
| 3010 | 3714 | 428 | 12.3 | <0.06 | 712 | 0.020 | 10611 | 3.50 | 3.15 | NA[g] |
| 3010 | 3901 | 426 | 0.84 | 0.06 | 520 | 0.015 | 10611 | 3.50 | 3.89 | NA[g] |
| 4010 | rd4[f] | 399 | <0.08 | 0.25 | 36 | <0.001 | 10607 | 1.08 | 0.00 | NA[g] |
| FMPC Compound | | | | | | | | | | |
| 2013 | 3709 | 328 | <0.4 | <0.06 | 97 | 0.008 | 10670 | 0.65 | 1.74 | 1.12 |
| 2013 | 3900 | 311 | 0.13 | 0.37 | 110 | 0.036 | 10670 | 0.65 | 1.74 | NA[g] |
| 2054 | rd5[f] | 402 | <0.4 | 0.82 | 666 | 0.023 | 8645 | 1.17 | 1.13 | NA[g] |
| Clay Interbed | | | | | | | | | | |
| 3016 | rd1[f] | 270.2 | 0.4 | <0.15 | 56 | 0.011 | 10449 | 4.83 | 17.1 | 13.9 |
| 3016 | rd4[f] | 242.8 | 11.6 | 0.22 | 60 | 0.007 | 10449 | 4.83 | 17.7 | NA[g] |
| GLACIAL TILL | | | | | | | | | | |
| Waste-Pit Area | | | | | | | | | | |
| 1073 | 3775 | 481 | 420 | 1.53 | 612 | 3.297 | 8561 | 1.00 | 0.72 | 0.29 |
| 1073 | 3951 | 455 | 872 | NR[h] | 428 | 4.380 | 8561 | 1.00 | 0.65 | 0.62 |
| 1082 | 3765 | 531 | <0.4 | 11.75 | 510 | 1.079 | 7667 | 0.81 | 0.82 | 0.01 |
| 1082 | 3949 | 518 | <0.4 | 2.01 | 20 | 0.810 | 7667 | 0.81 | 1.80 | 0.02 |

[a]Groundwater sample ID
[b]Aquifer-solid sample ID
[c]Leachable iron obtained from aquifer solid
[d]Distribution coefficient based on all U partitioned into $UO_2(CO_3)_3^{-4}$
[e]Distribution coefficient based on speciation in Table 1
[f]Round number indicated because sample ID not available
[g]Speciation results not available
[h]Analysis not reported

# TABLE 4

## CALCULATED URANIUM DISTRIBUTION COEFFICIENTS FOR SELECTED MONITORING WELLS

| WELL | GW[a] | U mg/L | AQ[b] | U mg/kg | $U_{ads}$[c] mg/kg | $K_d$[d] L/kg |
|---|---|---|---|---|---|---|
| REGIONAL AQUIFER | | | | | | |
| South-Plume Area | | | | | | |
| 2016 | rd1[e] | 0.021 | 10437 | 0.158 | 0.016 | 0.76 |
| 2046 | 3997 | 0.309 | 8956 | 0.675 | 0.533 | 1.72 |
| 2095 | 3787 | 0.177 | 10038 | 0.783 | 0.641 | 3.62 |
| 2095 | 3976 | 0.146 | 10038 | 0.783 | 0.641 | 4.39 |
| 3095 | 3786 | 0.005 | 10049 | 0.158 | 0.016 | 3.20 |
| 3095 | 3971 | 0.006 | 10049 | 0.158 | 0.016 | 2.67 |
| 4014 | rd4[e] | <0.001 | 10407 | 0.117 | 0 | 0 |
| 4016 | rd4[e] | <0.001 | 10460 | 0.033 | 0 | 0 |
| Waste-Pit Area | | | | | | |
| 2007 | rd5[e] | 0.005 | 10796 | 0.483 | 0.341 | 68.2 |
| 2010 | 3715 | 0.005 | 8426 | 0.408 | 0.266 | 53.2 |
| 2010 | 3902 | 0.021 | 8426 | 0.408 | 0.266 | 12.7 |
| 2027 | 3941 | 0.007 | 7874 | 0.383 | 0.241 | 34.4 |
| 2034 | 3646 | 0.024 | 8286 | 0.117 | 0 | 0 |
| 3010 | 3714 | 0.020 | 10611 | 0.183 | 0.041 | 2.05 |
| 3010 | 3901 | 0.015 | 10611 | 0.183 | 0.041 | 2.73 |
| 4010 | rd4[e] | <0.001 | 10607 | 0.217 | 0.075 | 0 |
| FMPC Compound | | | | | | |
| 2013 | 3709 | 0.008 | 10670 | 0.092 | 0 | 0 |
| 2013 | 3900 | 0.036 | 10670 | 0.092 | 0 | 0 |
| 2054 | rd5[e] | 0.023 | 8645 | 0.333 | 0.191 | 8.3 |
| Clay Interbed | | | | | | |
| 3016 | rd1[e] | 0.011 | 10449 | 0.133 | 0 | 0 |
| 3016 | rd4[e] | 0.007 | 10449 | 0.133 | 0 | 0 |
| GLACIAL TILL | | | | | | |
| Waste-Pit Area | | | | | | |
| 1073 | 3775 | 3.297 | 8561 | 0.675 | 0.533 | 0.16 |
| 1073 | 3951 | 4.38 | 8561 | 0.675 | 0.533 | 0.12 |
| 1082 | 3765 | 1.079 | 7667 | 0.367 | 0.225 | 0.21 |
| 1082 | 3949 | 0.81 | 7667 | 0.367 | 0.225 | 0.28 |

[a]Groundwater sample number
[b]Aquifer-solid sample number
[c]Adsorbed uranium (total uranium - background of 0.142)
[d]Distribution coefficient calculated from adsorbed uranium and groundwater uranium values
[e]Round number indicated because sample ID not available

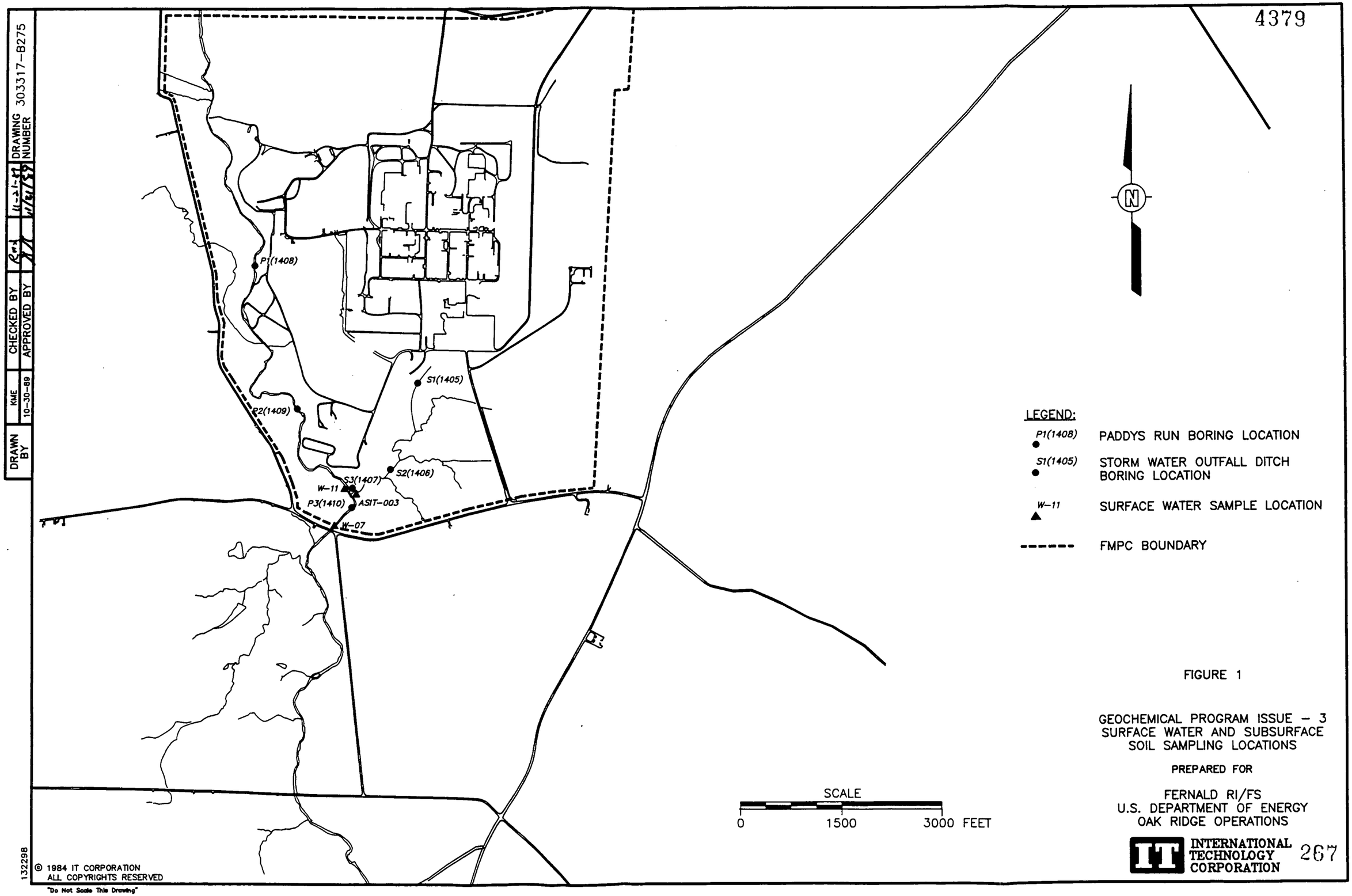


FIGURE 1

GEOCHEMICAL PROGRAM ISSUE – 3
SURFACE WATER AND SUBSURFACE
SOIL SAMPLING LOCATIONS

PREPARED FOR

FERNALD RI/FS
U.S. DEPARTMENT OF ENERGY
OAK RIDGE OPERATIONS

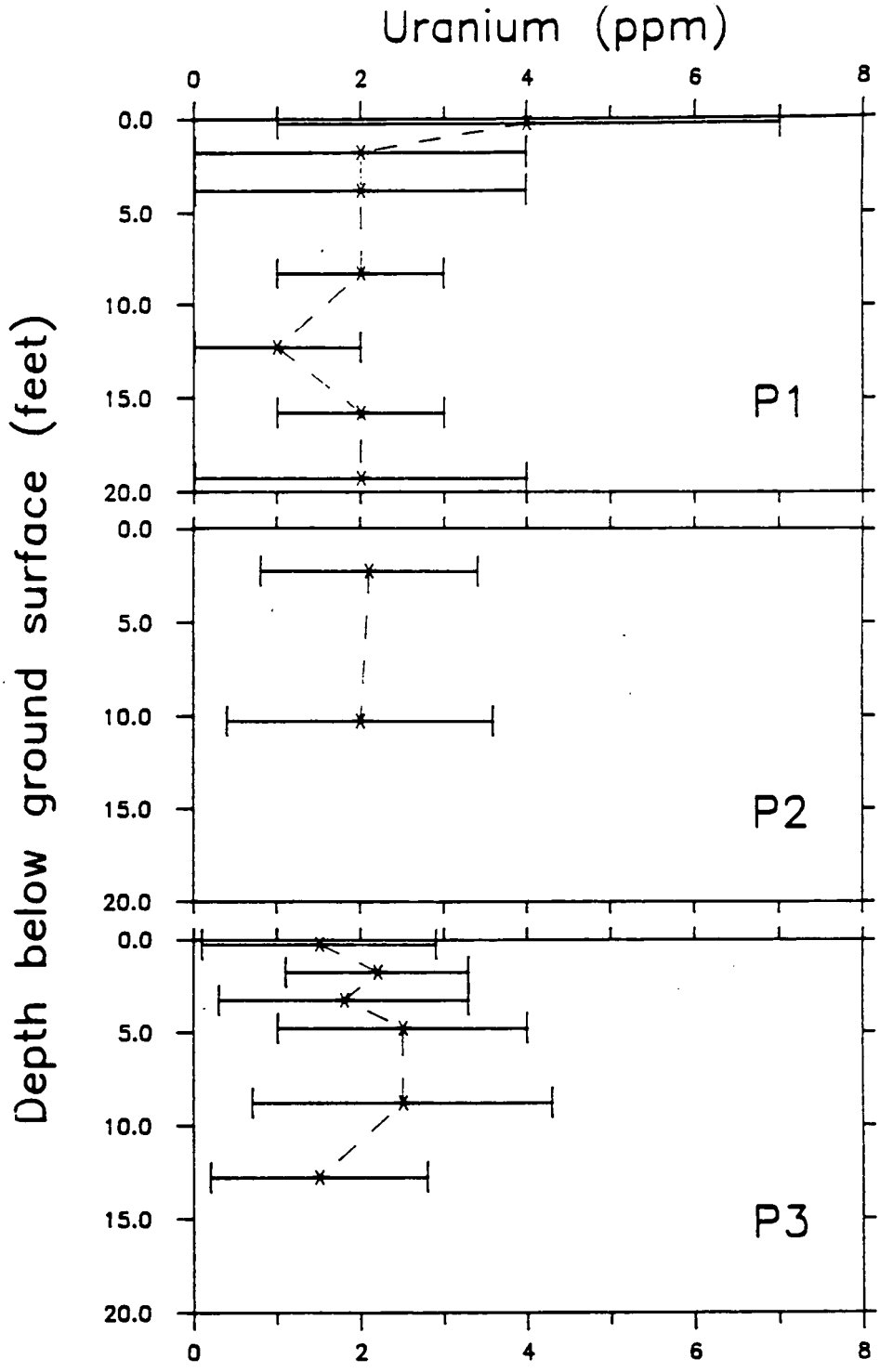


FIGURE 2

URANIUM CONCENTRATIONS IN SUBSURFACE SOILS OF PADDY'S RUN

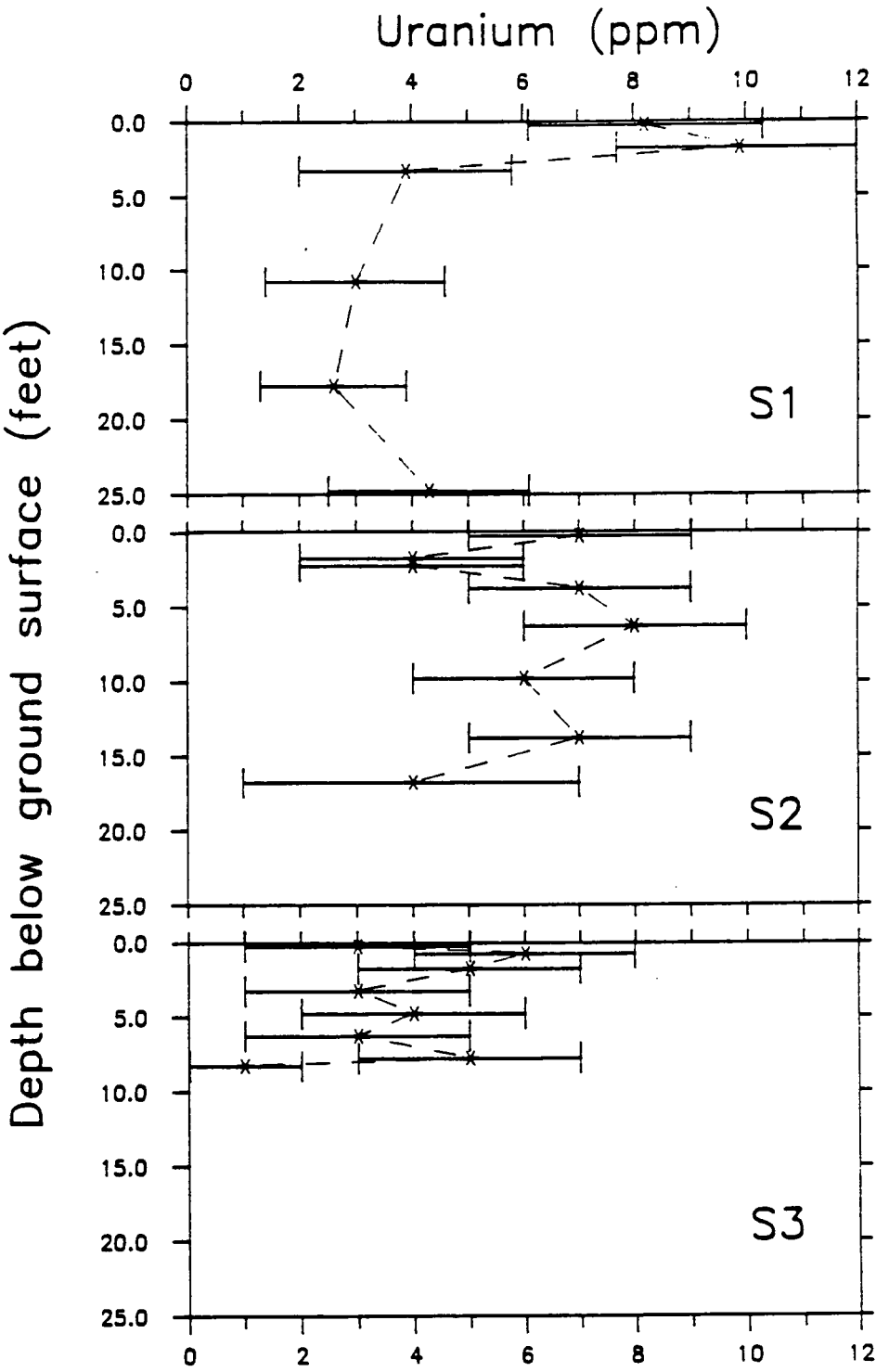


FIGURE 3

URANIUM CONCENTRATIONS IN SUBSURFACE SOILS OF THE STORM-WATER-OUTFALL DITCH

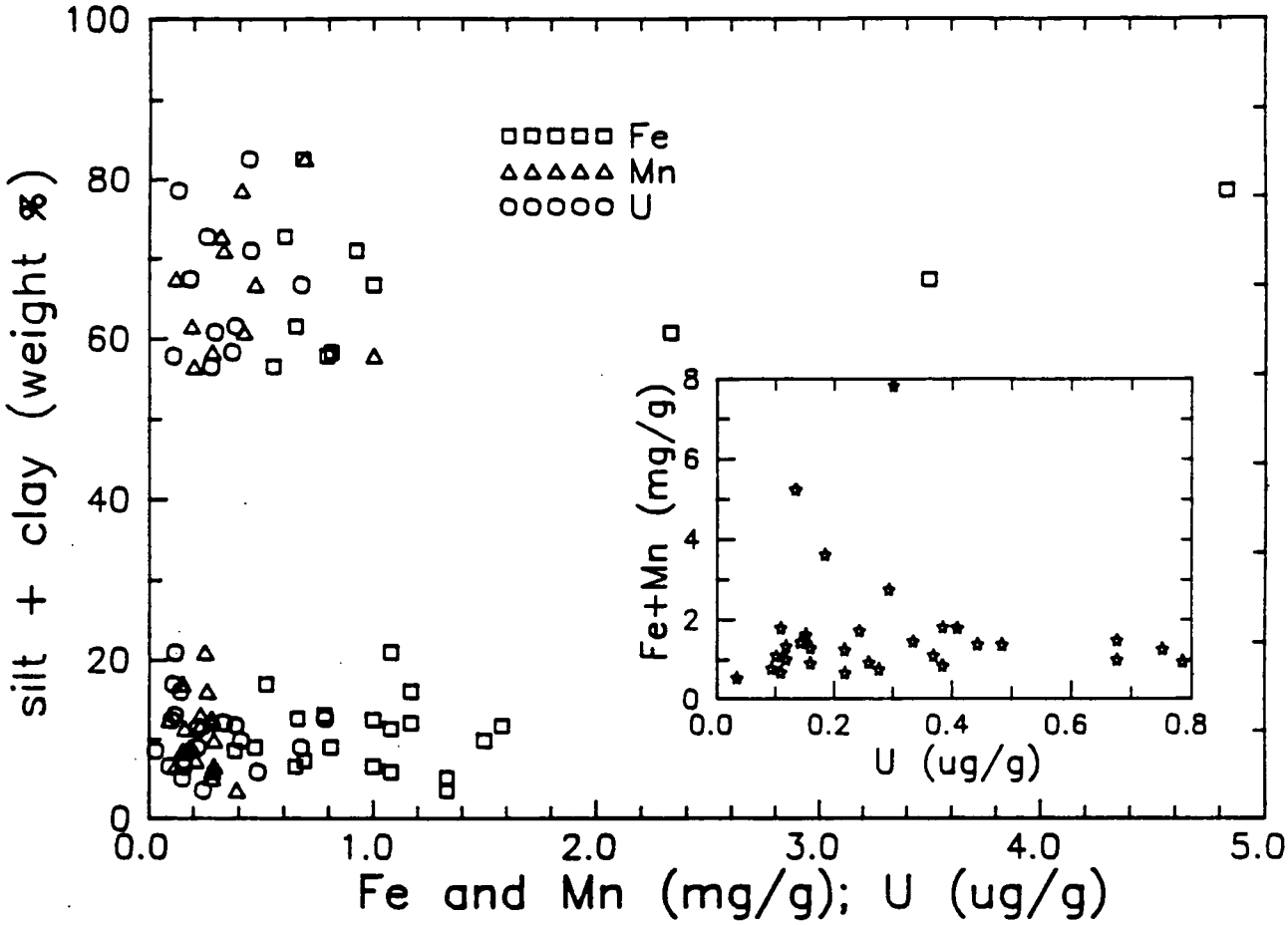


FIGURE 4

WEIGHT PERCENT OF SILT + CLAY VERSUS LEACHABLE IRON, MANGANESE AND URANIUM

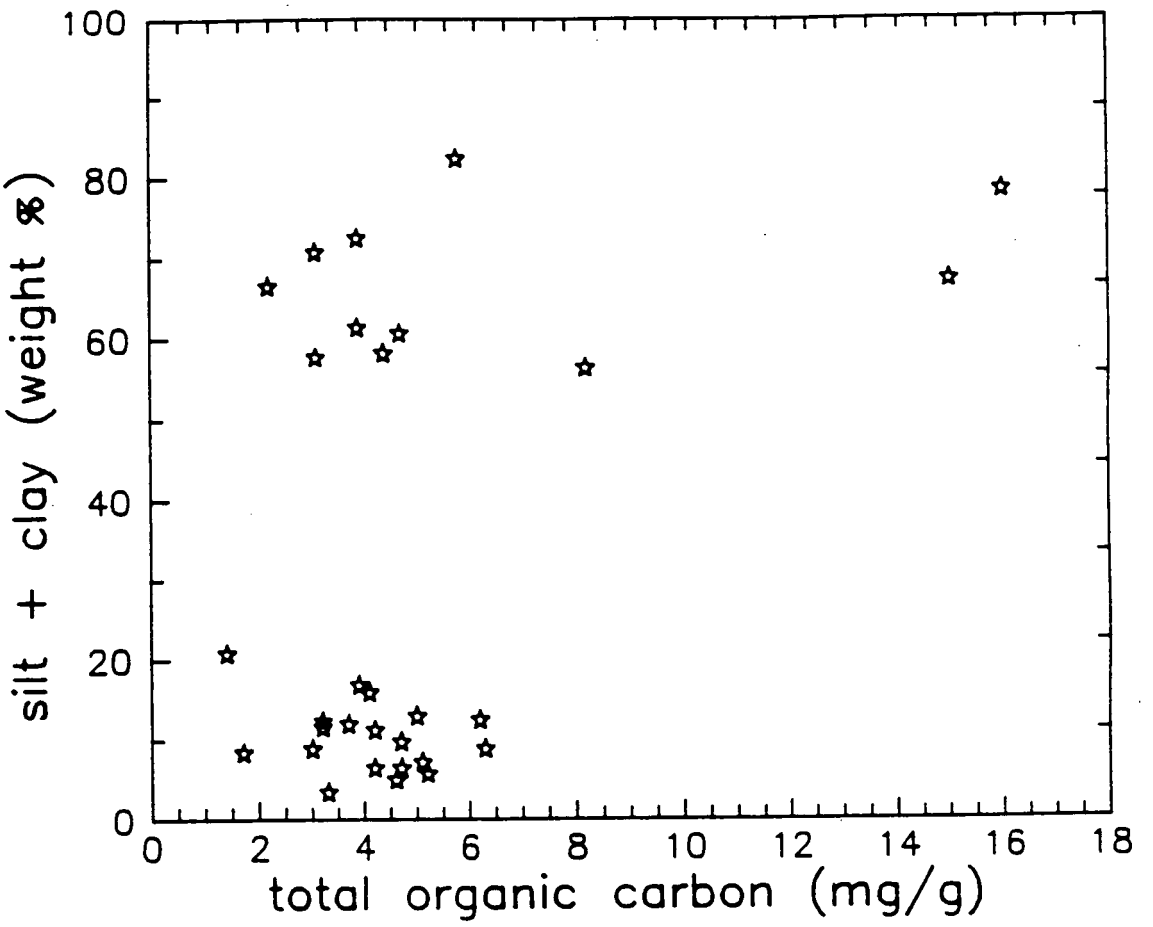


FIGURE 5

WEIGHT PERCENT OF SILT + CLAY VERSUS TOTAL ORGANIC CARBON

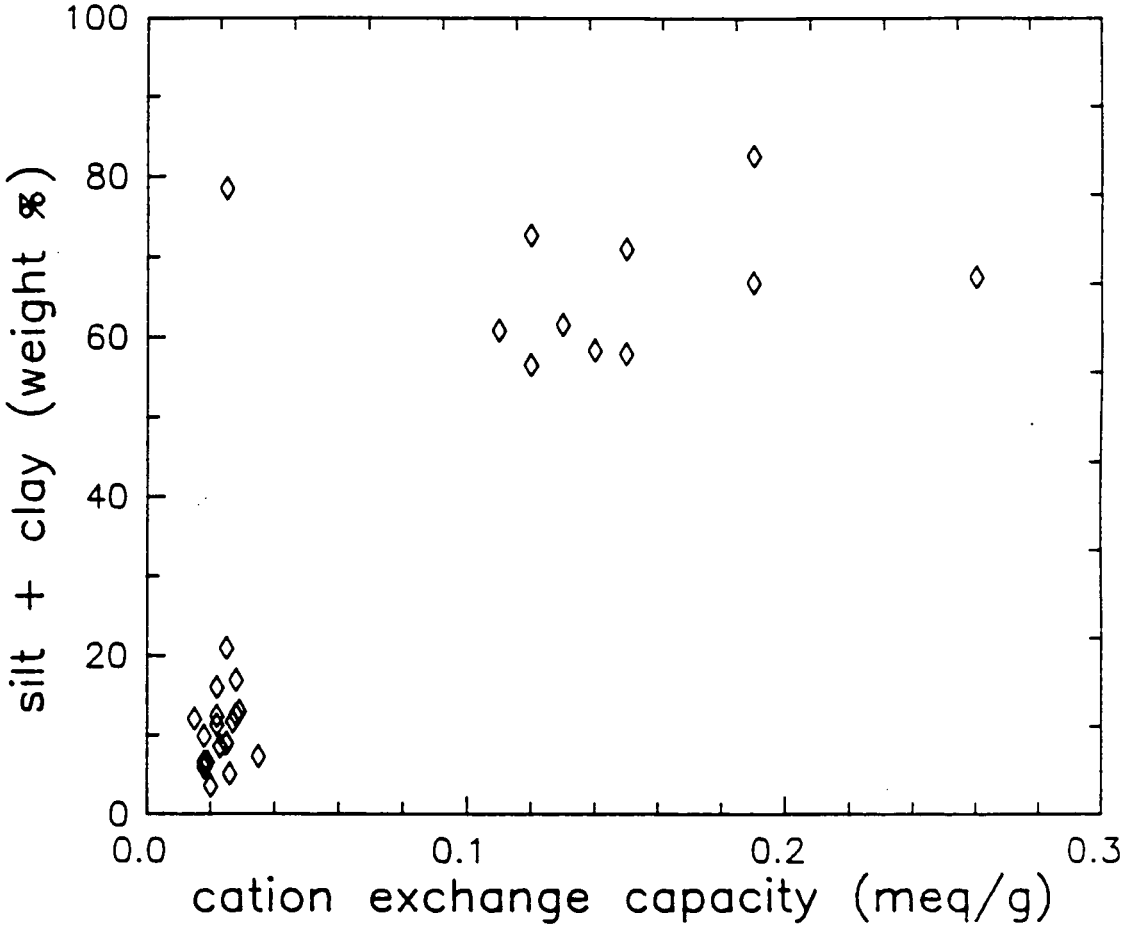


FIGURE 6

WEIGHT PERCENT OF SILT + CLAY VERSUS CATION EXCHANGE CAPACITY

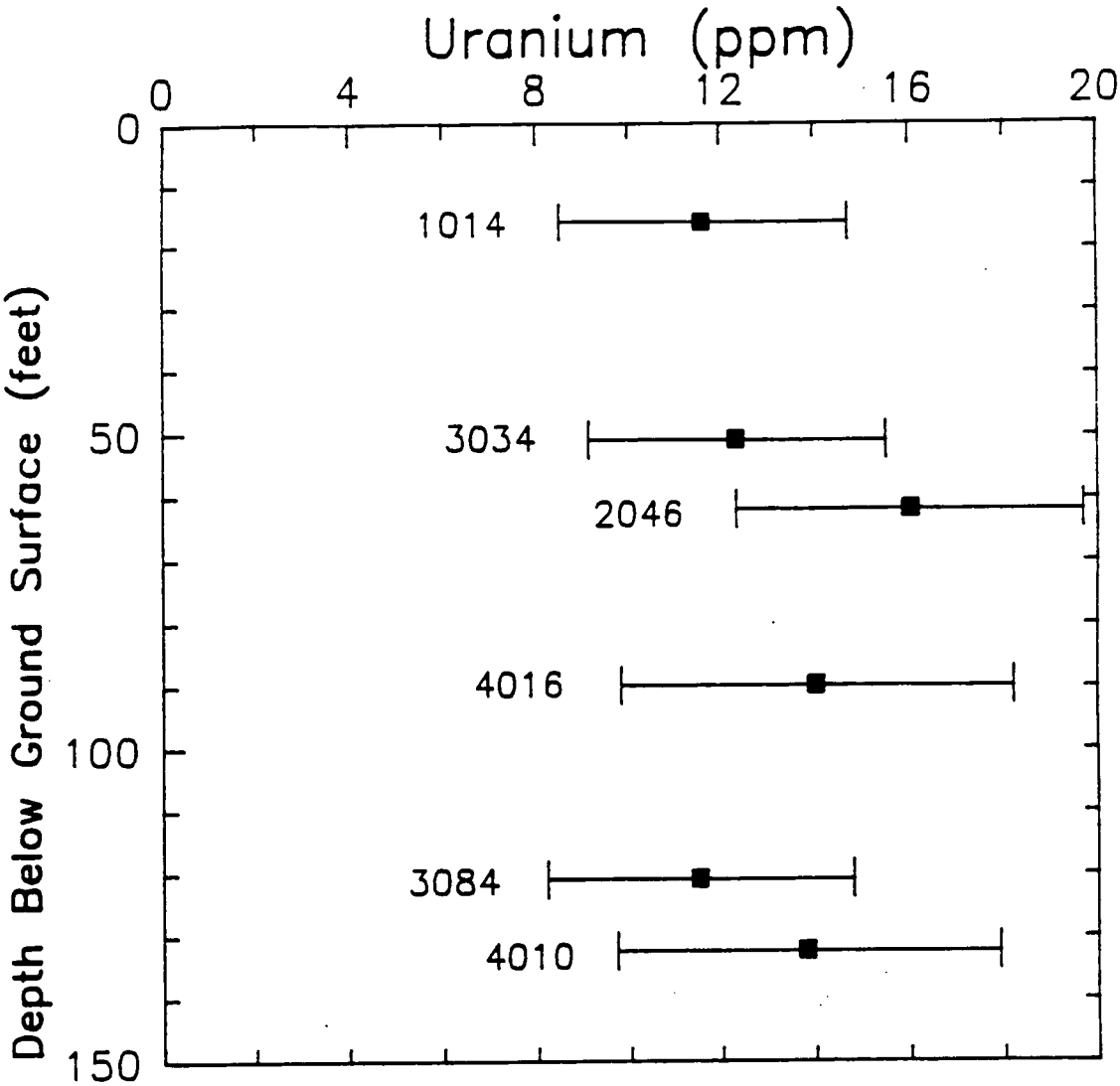


FIGURE 7

URANIUM CONCENTRATIONS IN AQUIFER SOLIDS

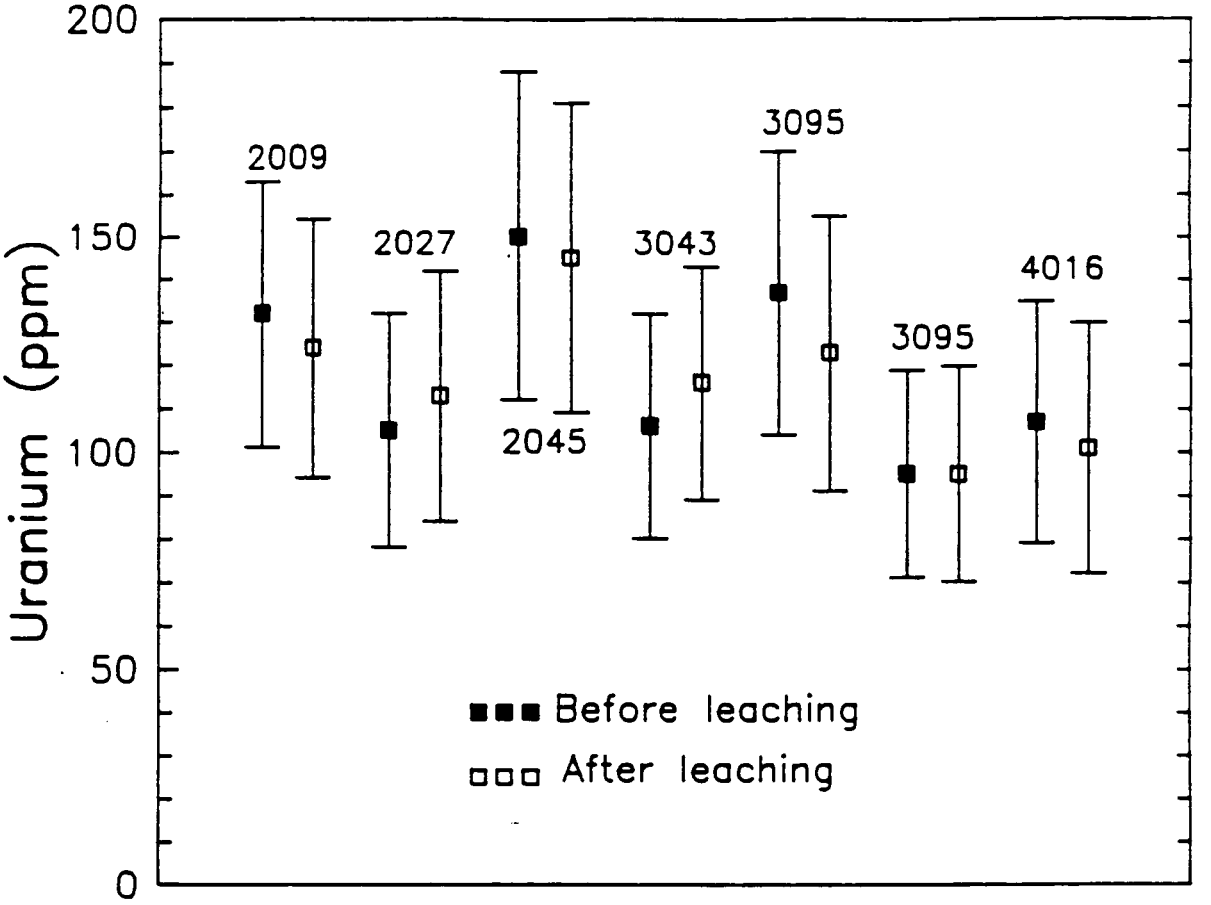


FIGURE 8

RESULTS OF THE URANIUM DIFFERENTIAL-LEACH TEST

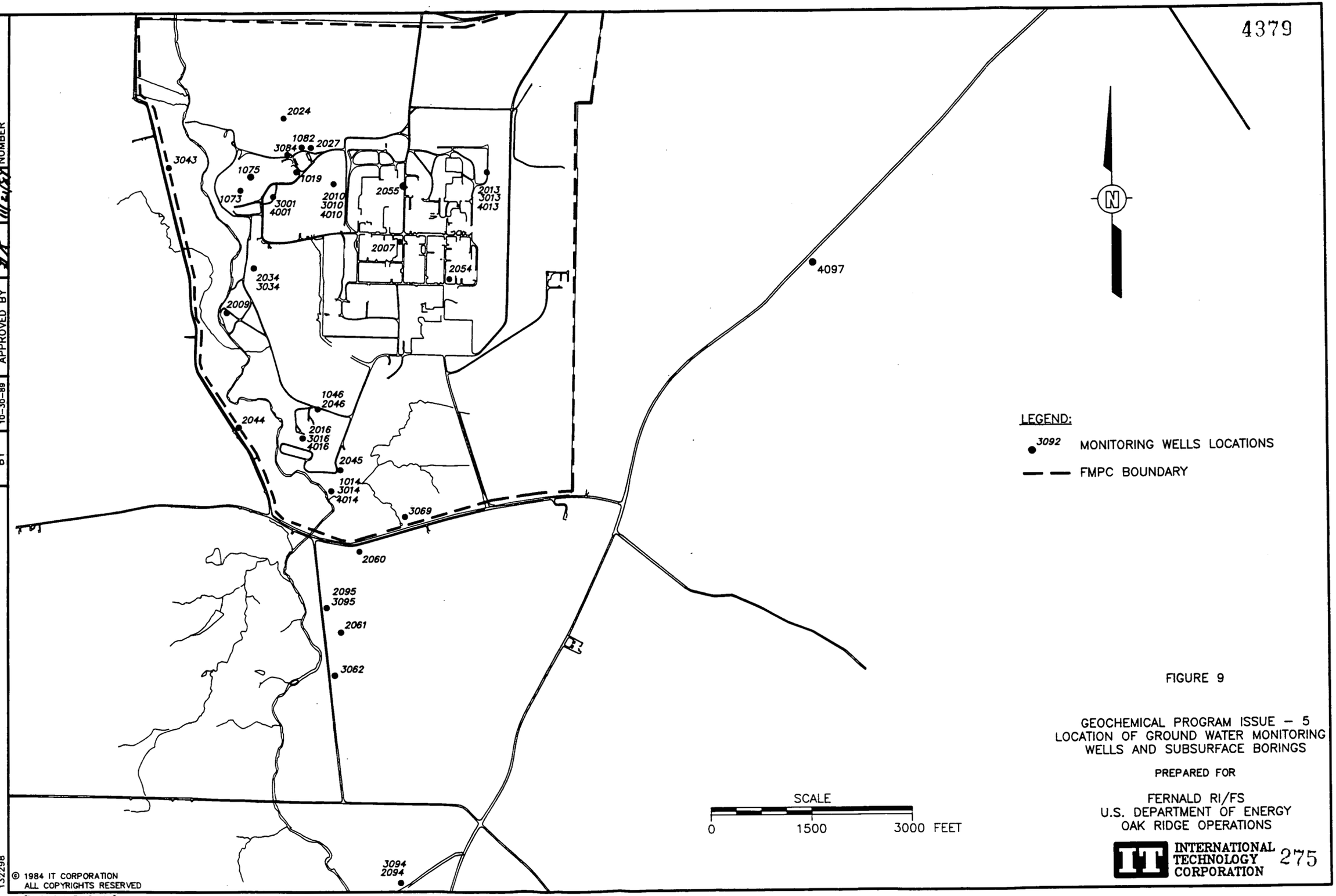


FIGURE 9

GEOCHEMICAL PROGRAM ISSUE – 5
LOCATION OF GROUND WATER MONITORING WELLS AND SUBSURFACE BORINGS

PREPARED FOR

FERNALD RI/FS
U.S. DEPARTMENT OF ENERGY
OAK RIDGE OPERATIONS

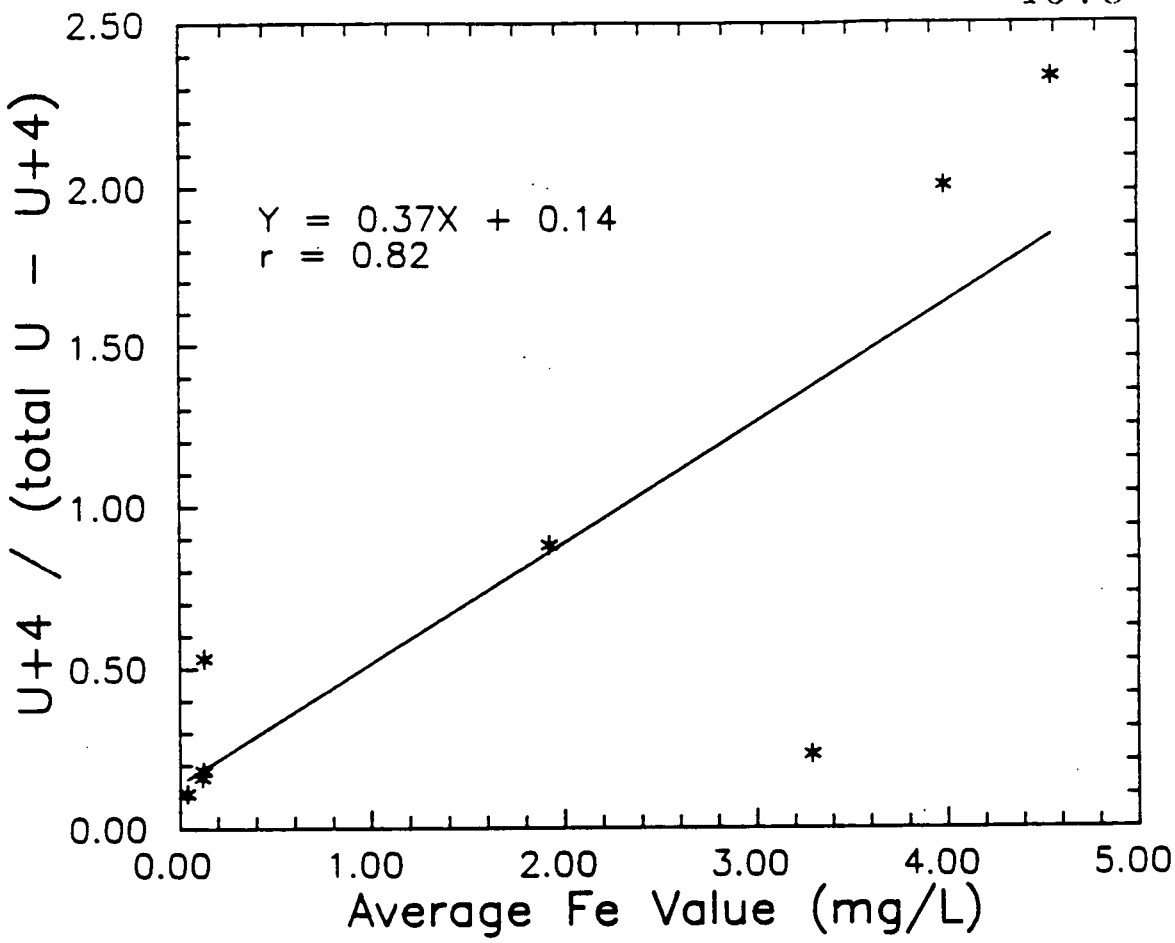


FIGURE 10

URANIUM REDOX RATIO VERSUS TOTAL IRON

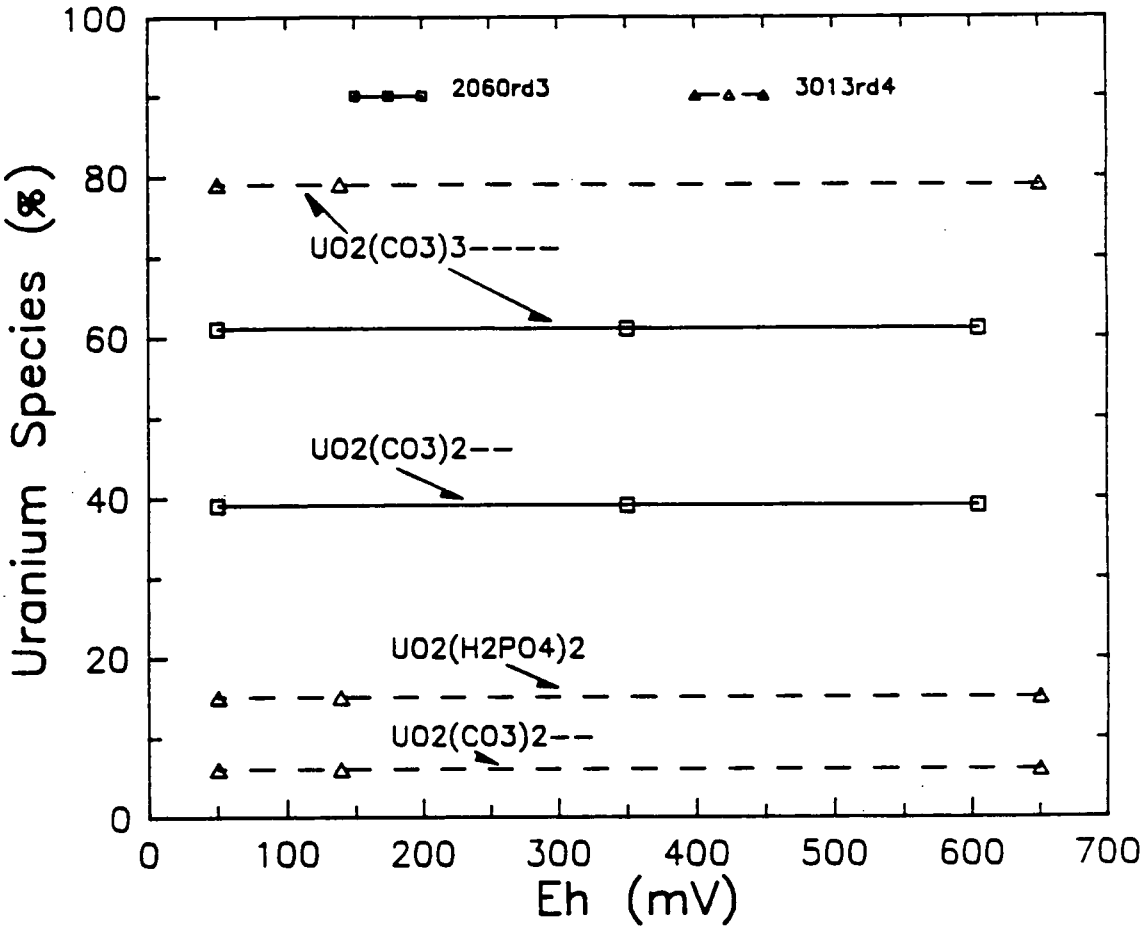


FIGURE 11

URANIUM SPECIATION AS A FUNCTION OF THE GROUNDWATER Eh

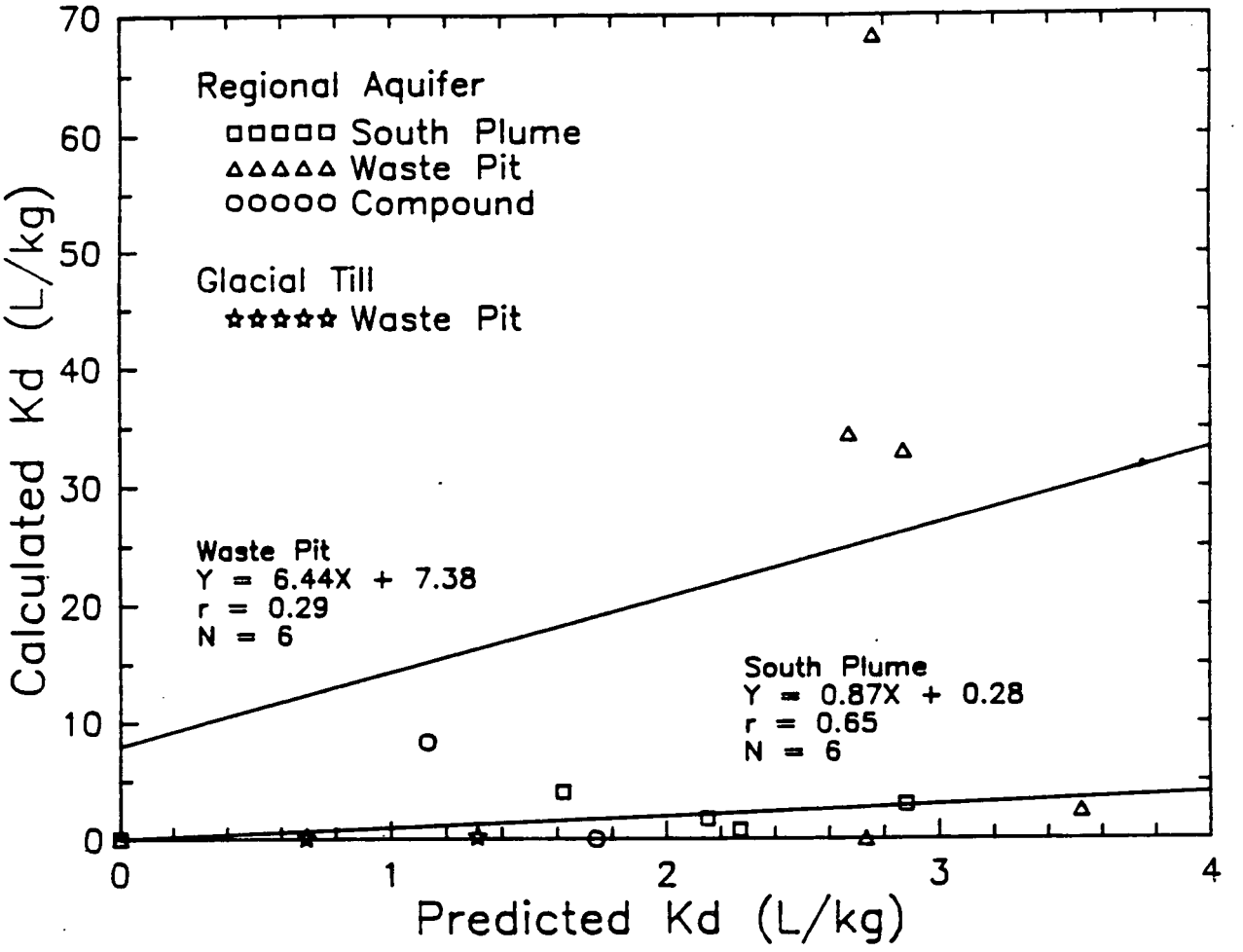


FIGURE 12

CALCULATED Kd VERSUS PREDICTED Kd

# APPENDIX A

# ANALYTICAL RESULTS

# APPENDIX A
## ANALYTICAL RESULTS FOR SOIL SAMPLES

| | | | | | |
|---|---|---|---|---|---|
| SITE # | P1 | P1 | P1 | P1 | P1 |
| Sample ID | 98152 | 98153 | 98155 | 98162 | 98168 |
| Sample Date | 06/02/89 | 06/02/89 | 06/02/89 | 06/02/89 | 06/02/89 |
| Sample Depth (ft) | 0.0-0.5 | 1.5-2.0 | 3.5-4.0 | 8.0-8.5 | 12.0-12.5 |
| U-total (ug/g) | 4 | 2 | 2 | 2 | 1 |
| 2-sigma error | 3 | 2 | 2 | 1 | 1 |

| | | | | | |
|---|---|---|---|---|---|
| SITE # | P1 | P1 | P1 | P2 | P2 |
| Sample ID | 98174 | 98180 | 98189 | 98116 | 98117 |
| Sample Date | 06/02/89 | 06/02/89 | 06/02/89 | 05/31/89 | 05/31/89 |
| Sample Depth (ft) | 15.5-16.0 | 19.0-19.5 | 23.5-24.0 | 0.0-0.5 | 1.5-2.0 |
| U-total (ug/g) | 2 | 2 | <2 | <2 | <3 |
| 2-sigma error | 1 | 2 | | | |

| | | | | | |
|---|---|---|---|---|---|
| SITE # | P2 | P2 | P2 | P2 | P2 |
| Sample ID | 98118 | 98119 | 98125 | 98132 | 98143 |
| Sample Date | 05/31/89 | 05/31/89 | 05/31/89 | 05/31/89 | 05/31/89 |
| Sample Depth (ft) | 2.0-2.5 | 3.0-3.5 | 6.5-7.0 | 10.0-10.5 | 15.5-16.0 |
| U-total (ug/g) | 2.1 | <3.5 | <3.0 | 2.0 | <2.5 |
| 2-sigma error | 1.3 | | | 1.6 | |

| | | | | | |
|---|---|---|---|---|---|
| SITE # | P2 | P3 | P3 | P3 | P3 |
| Sample ID | 98151 | 98029 | 98030 | 98032 | 98034 |
| Sample Date | 05/31/89 | 05/16/89 | 05/16/89 | 05/16/89 | 05/16/89 |
| Sample Depth (ft) | 19.5-20.0 | 0.0-0.5 | 1.5-2.0 | 3.0-3.5 | 4.5-5.0 |
| U-total (ug/g) | <3.4 | 1.5 | 2.2 | 1.8 | 2.5 |
| 2-sigma error | | 1.4 | 1.1 | 1.5 | 1.5 |

| | | | | |
|---|---|---|---|---|
| SITE # | P3 | P3 | P3 | P3 |
| Sample ID | 98040 | 98047 | 98054 | 98061 |
| Sample Date | 05/22/89 | 05/22/89 | 05/22/89 | 05/22/89 |
| Sample Depth (ft) | 8.5-9.0 | 12.5-13.0 | 16.0-16.5 | 19.5-20.0 |
| U-total (ug/g) | 2.5 | 1.5 | <2.9 | <2.8 |
| 2-sigma error | 1.8 | 1.3 | | |

# APPENDIX A
## ANALYTICAL RESULTS FOR SOIL SAMPLES

| | | | | | |
|---|---|---|---|---|---|
| SITE # | S1 | S1 | S1 | S1 | S1 |
| Sample ID | 98062 | 98064 | 98066 | 98077 | 98089 |
| Sample Date | 05/24/89 | 05/24/89 | 05/24/89 | 05/24/89 | 05/24/89 |
| Sample Depth (ft) | 0.0-0.5 | 1.5-2.0 | 3.0-3.5 | 10.5-11.0 | 17.5-18.0 |
| U-total (ug/g) | 8.2 | 9.9 | 3.9 | 3.0 | 2.6 |
| 2-sigma error | 2.1 | 2.2 | 1.9 | 1.6 | 1.3 |

| | | | | | |
|---|---|---|---|---|---|
| SITE # | S1 | S1 | S1 | S2 | S2 |
| Sample ID | 98100 | 98106 | 98115 | 98010 | 98011 |
| Sample Date | 05/24/89 | 05/24/89 | 05/24/89 | 05/16/89 | 05/16/89 |
| Sample Depth (ft) | 24.5-25.0 | 28.5-29.0 | 33.5-34.0 | 0.0-0.5 | 1.5-2.0 |
| U-total (ug/g) | 4.3 | <3.0 | 2.7 | 7 | 4 |
| 2-sigma error | 1.8 | | 1.3 | 2 | 2 |

| | | | | | |
|---|---|---|---|---|---|
| SITE # | S2 | S2 | S2 | S2 | S2 |
| Sample ID | 98012 | 98014 | 98017 | 98020 | 98024 |
| Sample Date | 05/16/89 | 05/16/89 | 05/16/89 | 05/16/89 | 05/16/89 |
| Sample Depth (ft) | 2.0-2.5 | 3.5-4.0 | 6.0-6.5 | 9.5-10.0 | 13.5-14.0 |
| U-total (ug/g) | 4 | 7 | 8 | 6 | 7 |
| 2-sigma error | 2 | 2 | 2 | 2 | 2 |

| | | | | | |
|---|---|---|---|---|---|
| SITE # | S2 | S3 | S3 | S3 | S3 |
| Sample ID | 98028 | 98000 | 98001 | 98002 | 98003 |
| Sample Date | 05/16/89 | 05/16/89 | 05/16/89 | 05/16/89 | 05/16/89 |
| Sample Depth (ft) | 16.5-17.0 | 0.0-0.5 | 0.5-1.0 | 1.5-2.0 | 3.0-3.5 |
| U-total (ug/g) | 4 | 3 | 6 | 5 | 3 |
| 2-sigma error | 3 | 2 | 2 | 2 | 2 |

| | | | | |
|---|---|---|---|---|
| SITE # | S3 | S3 | S3 | S3 |
| Sample ID | 98004 | 98006 | 98008 | 98009 |
| Sample Date | 05/16/89 | 05/16/89 | 05/16/89 | 05/16/89 |
| Sample Depth (ft) | 4.5-5.0 | 6.0-6.5 | 7.5-8.0 | 8.0-8.5 |
| U-total (ug/g) | 4 | 3 | 5 | 1 |
| 2-sigma error | 2 | 2 | 2 | 1 |

# APPENDIX A
## ANALYTICAL RESULTS FOR SURFACE WATERS

| Sample ID | ASIT003 | W-07 | W-11 |
|---|---|---|---|
| Sample Date | 05/14/89 | 05/14/89 | 05/14/89 |
| pH | 8.57 | 8.38 | 8.58 |
| Eh (mV) | 452 | 451 | 441 |
| $O_2$ (mg/L) | 8.6 | 10.2 | 11.8 |
| T ($^oC$) | 15.5 | 13 | 18 |
| Cl (mg/L) | 34 | 18.19 | 19.99 |
| F (mg/L) | 0.19 | 0.21 | 0.18 |
| $HCO_3^-$ (mg/L) | 200.5 | 256.5 | 212 |
| $NH_4^+$ (mg/L) | 0.162 | <0.1[a] | <0.1 |
| $NO_3^-$ (mg/L) | 24.08 | 11.95 | 10.23 |
| P (mg/L) | 0.161 | 0.032 | <0.02 |
| $SO_4^{-2}$ (mg/L) | 51.3 | 57.36 | 57.36 |
| Ag (mg/L) | <0.01 | <0.01 | <0.01 |
| Al (mg/L) | 0.0866 | <0.06 | 0.0764 |
| As (mg/L) | <0.002 | <0.002 | <0.002 |
| Ba (mg/L) | 0.0399 | 0.0374 | 0.0313 |
| Ca (mg/L) | 72.3 | 84.7 | 71.8 |
| Cd (mg/L) | <0.002 | <0.002 | <0.002 |
| Cr (mg/L) | <0.01 | <0.01 | <0.01 |
| Cu (mg/L) | <0.01 | <0.01 | <0.01 |
| Fe (mg/L) | 0.0659 | 0.0286 | 0.0415 |
| Hg (mg/L) | <0.0002 | 0.0002 | 0.0003 |
| K (mg/L) | 1.84 | 1.55 | 1.68 |
| Mg (mg/L) | 19.9 | 21.4 | 20.9 |
| Mn (mg/L) | 0.0097 | 0.0152 | 0.0121 |
| Mo (mg/L) | <0.01 | <0.01 | <0.01 |
| Na (mg/L) | 14.6 | 9.93 | 9.69 |
| Ni (mg/L) | <0.02 | <0.02 | <0.02 |
| Pb (mg/L) | 0.0026 | 0.0093 | 0.0074 |
| Se (mg/L) | <0.002 | <0.002 | <0.002 |
| Si (mg/L) | 3.89 | 1.73 | 2.25 |
| Th (mg/L) | <0.006 | <0.002 | <0.006 |
| U (mg/L) | 0.002 | 0.015 | 0.009 |
| V (mg/L) | <0.01 | <0.01 | <0.01 |

[a]Less than sign indicates value is below detection limit.

## APPENDIX A
## ANALYTICAL RESULTS FOR AQUIFER SOLIDS

| WELL # | 1014 | 1046 | 1073 | 1075 | 1082 |
|---|---|---|---|---|---|
| Sample ID | 07363 | 08016 | 08561 | 08572 | 07667 |
| Sample Depth (ft) | 15.0-16.5 | 3.0-4.5 | 18.0-19.5 | 21.0-22.5 | 13.5-15.0 |
| Leached Metals[a] | | | | | |
| Fe (mg/g) | 1.33 | 0.68 | 1.00 | 0.92 | 0.81 |
| Mn (mg/g) | 0.28 | 0.69 | 0.47 | 0.33 | 0.28 |
| U-total (ug/g) | 0.150 | 0.442 | 0.675 | 0.750 | 0.367 |
| 2-sigma error | 0.017 | 0.050 | 0.067 | 0.083 | 0.042 |
| TOC[b] (mg/g) | 4.6 | 5.8 | 2.2 | 3.1 | 4.4 |
| CEC[c] (meq/g) | 0.026 | 0.190 | 0.190 | 0.150 | 0.140 |
| <200 mesh[d] (wt %) | 5.03 | 82.50 | 66.63 | 70.90 | 58.24 |
| U-total (ug/g) | 11.6 | NA[e] | NA | NA | NA |
| 2-sigma error | 3.1 | | | | |

| WELL # | 2007 | 2007 | 2009 | 2010 | 2027 |
|---|---|---|---|---|---|
| Sample ID | 10779 | 10796 | 07084 | 08426 | 07874 |
| Sample Depth (ft) | 13.5-15.0 | 65.0-66.5 | 38.5-40.0 | 70.0-71.5 | 65.0-66.5 |
| Leached Metals | | | | | |
| Fe (mg/g) | 2.33 | 1.08 | 0.52 | 1.50 | 1.58 |
| Mn (mg/g) | 0.42 | 0.28 | 0.15 | 0.29 | 0.23 |
| U-total (ug/g) | 0.292 | 0.483 | 0.108 | 0.408 | 0.383 |
| 2-sigma error | 0.033 | 0.058 | 0.017 | 0.042 | 0.042 |
| TOC (mg/g) | 4.7 | 5.2 | 3.9 | 4.7 | 3.2 |
| CEC (meq/g) | 0.110 | 0.018 | 0.028 | 0.018 | 0.027 |
| <200 mesh (wt %) | 60.74 | 5.83 | 16.85 | 9.79 | 11.63 |
| U-initial[f] (ug/g) | NA | NA | 132 | NA | 105 |
| 2-sigma error | | | 31 | | 27 |
| U-final[g] (ug/g) | NA | NA | 124 | NA | 113 |
| 2-sigma error | | | 30 | | 29 |

[a]Sample leached with a solution of acetic acid and hydroxylamine hydrochloride
[b]TOC = total organic carbon
[c]CEC = cation exchange capacity
[d]Weight percent of sample less than 0.075 mm (silt + clay)
[e]Analysis not available
[f]Total uranium before differential-leaching analysis
[g]Total uranium after differential-leaching analysis

## APPENDIX A
## ANALYTICAL RESULTS FOR AQUIFER SOLIDS

| | | | | | |
|---|---|---|---|---|---|
| WELL # | 2045 | 2046 | 2054 | 2054 | 2054 |
| Sample ID | 08947 | 08956 | 10414 | 10416 | 08645 |
| Sample Depth (ft) | 30.0-31.5 | 61.0-62.5 | 6.0-7.5 | 9.0-10.5 | 70.0-71.5 |
| Leached Metals[a] | | | | | |
| Fe (mg/g) | 0.47 | 0.81 | 0.55 | 0.65 | 1.17 |
| Mn (mg/g) | 0.19 | 0.18 | 0.20 | 0.19 | 0.28 |
| U-total (ug/g) | 0.217 | 0.675 | 0.275 | 0.383 | 0.333 |
| 2-sigma error | 0.025 | 0.075 | 0.025 | 0.042 | 0.033 |
| TOC[b] (mg/g) | 3.0 | 6.3 | 8.2 | 3.9 | 3.7 |
| CEC[c] (meq/g) | 0.025 | 0.025 | 0.120 | 0.130 | 0.015 |
| <200 mesh[d] (wt %) | 8.92 | 8.92 | 56.44 | 61.46 | 11.98 |
| U-total (ug/g) | NA[e] | 16 | NA | NA | NA |
| 2-sigma error | | 3.7 | | | |
| U-initial[f] (ug/g) | 150 | NA | NA | NA | NA |
| 2-sigma error | 38 | | | | |
| U-final[g] (ug/g) | 145 | NA | NA | NA | NA |
| 2-sigma error | 36 | | | | |

| | | | | | |
|---|---|---|---|---|---|
| WELL # | 2055 | 2055 | 3034 | 3043 | 3043 |
| Sample ID | 10736 | 10766 | 08286 | 07619 | 07790 |
| Sample Depth (ft) | 1.5-3.0 | 70.0-71.5 | 50.0-51.5 | 7.5-9.0 | 108.0-109.5 |
| Leached Metals | | | | | |
| Fe (mg/g) | 0.79 | 1.17 | 0.78 | 0.60 | 1.00 |
| Mn (mg/g) | 1.00 | 0.26 | 0.23 | 0.32 | 0.09 |
| U-total (ug/g) | 0.108 | 0.142 | 0.117 | 0.258 | 0.100 |
| 2-sigma error | 0.008 | 0.017 | 0.017 | 0.033 | 0.008 |
| TOC (mg/g) | 3.1 | 4.1 | 5.0 | 3.9 | 3.2 |
| CEC (meq/g) | 0.150 | 0.022 | 0.029 | 0.120 | 0.022 |
| <200 mesh (wt %) | 57.80 | 15.95 | 12.96 | 72.64 | 12.34 |
| U-total (ug/g) | NA | NA | 12.3 | NA | NA |
| 2-sigma error | | | 3.2 | | |
| U-initial (ug/g) | NA | NA | NA | NA | 106 |
| 2-sigma error | | | | | 26 |
| U-final (ug/g) | NA | NA | NA | NA | 116 |
| 2-sigma error | | | | | 27 |

[a]Sample leached with a solution of acetic acid and hydroxylamine hydrochloride
[b]TOC = total organic carbon
[c]CEC = cation exchange capacity
[d]Weight percent of sample less than 0.075 mm (silt + clay)
[e]Analysis not available
[f]Total uranium before differential-leaching analysis
[g]Total uranium after differential-leaching analysis

# APPENDIX A
## ANALYTICAL RESULTS FOR AQUIFER SOLIDS

| | | | | | |
|---|---|---|---|---|---|
| WELL # | 3084 | 3095 | 3095 | 4010 | 4010 |
| Sample ID | 07558 | 10038 | 10049 | 10611 | 10607 |
| Sample Depth (ft) | 120.0-121.5 | 20.0-21.5 | 75.0-76.5 | 131.5-132 | 195.0-196.5 |
| Leached Metals[a] | | | | | |
| Fe (mg/g) | 7.67 | 0.66 | 1.00 | 3.50 | 1.08 |
| Mn (mg/g) | 0.16 | 0.28 | 0.29 | 0.12 | 0.16 |
| U-total (ug/g) | 0.300 | 0.783 | 0.158 | 0.183 | 0.216 |
| 2-sigma error | 0.033 | 0.083 | 0.017 | 0.017 | 0.025 |
| TOC[b] (mg/g) | 3.3 | 6.2 | 4.7 | 15.0 | 4.2 |
| CEC[c] (meq/g) | 0.250 | 0.028 | 0.018 | 0.260 | 0.022 |
| <200 mesh[d] (wt %) | NA[e] | 12.52 | 6.52 | 67.38 | 11.26 |
| U-total (ug/g) | 11.5 | NA | NA | 13.8 | NA |
| 2-sigma error | 3.3 | | | 4.1 | |
| U-initial[f] (ug/g) | NA | 137 | 95 | NA | NA |
| 2-sigma error | | 33 | 24 | | |
| U-final[g] (ug/g) | NA | 123 | 93 | NA | NA |
| 2-sigma error | | 32 | 25 | | |

| | | | | | |
|---|---|---|---|---|---|
| WELL # | 4013 | 4013 | 4014 | 4016 | 4016 |
| Sample ID | 10670 | 10696 | 10407 | 10437 | 10449 |
| Sample Depth (ft) | 75.0-76.5 | 205.0-206.5 | 135.0-136.5 | 30.0-31.5 | 89.3-89.6 |
| Leached Metals | | | | | |
| Fe (mg/g) | 0.65 | 1.33 | 1.08 | 0.69 | 4.83 |
| Mn (mg/g) | 0.12 | 0.39 | 0.25 | 0.21 | 0.41 |
| U-total (ug/g) | 0.092 | 0.242 | 0.117 | 0.158 | 0.133 |
| 2-sigma error | 0.008 | 0.025 | 0.017 | 0.017 | 0.017 |
| TOC (mg/g) | 4.2 | 3.3 | 1.4 | 5.1 | 16.0 |
| CEC (meq/g) | 0.019 | 0.020 | 0.025 | 0.035 | 0.190 |
| <200 mesh (wt %) | 6.54 | 3.50 | 20.88 | 7.24 | 78.50 |
| U-total (ug/g) | NA | NA | NA | NA | 14.0 |
| 2-sigma error | | | | | 4.2 |
| U-initial (ug/g) | NA | NA | NA | 107 | NA |
| 2-sigma error | | | | 28 | |
| U-final (ug/g) | NA | NA | NA | 101 | NA |
| 2-sigma error | | | | 29 | |

[a]Sample leached with a solution of acetic acid and hydroxylamine hydrochloride
[b]TOC = total organic carbon
[c]CEC = cation exchange capacity
[d]Weight percent of sample less than 0.075 mm (silt + clay)
[e]Analysis not available
[f]Total uranium before differential-leaching analysis
[g]Total uranium after differential-leaching analysis

## APPENDIX A
## ANALYTICAL RESULTS FOR AQUIFER SOLIDS

| | |
|---|---|
| WELL # | 4016 |
| Sample ID | 10460 |
| Sample Depth (ft) | 145.0-146.5 |
| | |
| Leached Metals[a] | |
| Fe (mg/g) | 0.38 |
| Mn (mg/g) | 0.15 |
| U-total (ug/g) | 0.033 |
| 2-sigma error | 0.008 |
| | |
| TOC[b] (mg/g) | 1.7 |
| CEC[c] (meq/g) | 0.023 |
| <200 mesh[d] (wt %) | 8.50 |

[a]Sample leached with a solution of acetic acid and hydroxylamine hydrochloride
[b]TOC = total organic carbon
[c]CEC = cation exchange capacity
[d]Weight percent of sample less than 0.075 mm (silt + clay)

## APPENDIX A
## ANALYTICAL RESULTS FOR MODELED GROUNDWATERS

| WELL # | 1019 | 1019 | 1073 | 1073 | 1082 |
|---|---|---|---|---|---|
| Sample ID | 3748 | 3944 | 3775 | 3951 | 3765 |
| Sample Date | 12/04/88 | 03/08/89 | 12/04/88 | 03/12/89 | 11/20/88 |
| Round # | 3 | 4 | 3 | 4 | 3 |
| pH | 7 | 7 | 7.6 | 7.1 | 7 |
| Eh (mV) | NR[a] | NR | NR | NR | NR |
| $O_2$ (mg/L) | 10.6 | 2.8 | 6.25 | 8.1 | 8 |
| T ($^oC$) | 11 | 7 | 12.5 | 10.5 | 13 |
| Cl (mg/L) | 1160 | 490 | 1030 | 1170 | 2 |
| F (mg/L) | 0.48 | 0.5 | 6.25 | 7.25 | 1.25 |
| $HCO_3^-$ (mg/L) | 403.8 | 395.8 | 480.6 | 454.9 | 530.8 |
| $NH_4^+$ (mg/L) | 0.139 | 0.5 | 80.2 | 71.6 | <0.1[b] |
| $NO_3^-$ (mg/L) | 56.7 | 0.9 | 419.7 | 872 | <0.4 |
| P (mg/L) | 0.061 | 0.12 | 0.493 | NR | 3.79 |
| $SO_4^{-2}$ (mg/L) | 224 | 250 | 612 | 428 | 510 |
| Ag (mg/L) | <0.02 | 0.01 | <0.02 | <0.0005 | <0.0005 |
| As (mg/L) | 0.004 | <0.003 | 0.002 | <0.002 | <0.002 |
| Ba (mg/L) | 0.195 | 0.1 | 0.138 | 0.126 | 0.044 |
| Ca (mg/L) | 522 | 300 | 413 | 4000 | 129 |
| Cd (mg/L) | 0.002 | 0.006 | 0.002 | 0.0364 | <0.002 |
| Cr (mg/L) | <0.02 | 0.04 | <0.02 | 0.0464 | <0.02 |
| Cu (mg/L) | <0.01 | <0.01 | 0.014 | 0.0836 | <0.01 |
| Fe (mg/L) | 1.51 | 0.87 | 0.073 | 0.172 | 0.015 |
| Hg (mg/L) | <0.0002 | <0.0002 | 0.0007 | 30.2 | <0.0002 |
| K (mg/L) | 1.47 | 0.86 | 33 | 0.0007 | 2.42 |
| Mg (mg/L) | 159 | 86 | 325 | 364 | 65 |
| Mn (mg/L) | 1.61 | 1.1 | 2.1 | 0.689 | 0.008 |
| Mo (mg/L) | <0.02 | 0.02 | 0.533 | 0.58 | 0.033 |
| Na (mg/L) | 437 | 170 | 149 | 178 | 13.3 |
| Ni (mg/L) | <0.02 | <0.03 | 0.066 | 0.114 | <0.02 |
| Pb (mg/L) | 0.003 | <0.002 | 0.004 | <0.002 | <0.002 |
| Se (mg/L) | <0.002 | <0.005 | <0.002 | <0.002 | 0.002 |
| Th (mg/L) | <0.004 | <0.005 | 0.012 | 0.025 | <0.006 |
| U (mg/L) | 0.818 | 0.739 | 3.297 | 4.38 | 1.079 |

[a]NR = analysis not reported
[b]Less than sign indicates below detection limit value

# APPENDIX A
## ANALYTICAL REUSULTS FOR MODELED GROUNDWATERS

| WELL # | 1082 | 2013 | 2024 | 2044 | 2045 |
|---|---|---|---|---|---|
| Sample ID | 3949 | 3709 | 3656 | 3682 | 3993 |
| Sample Date | 02/05/89 | 11/15/88 | 11/02/88 | 11/03/88 | 01/23/89 |
| Round # | 4 | 3 | 3 | 3 | 4 |
| pH | 7.35 | 6.85 | 7.30 | 7.47 | 7.3 |
| Eh (mV) | NR[a] | NR | 152 | NR | NR |
| $O_2$ (mg/L) | 8 | 1.3 | 0.4 | 4.39 | 3.6 |
| T ($^oC$) | 10 | 13 | 10 | 10 | 7 |
| Cl (mg/L) | 19 | 26.5 | 19 | 38 | 15 |
| F (mg/L) | 0.72 | 0.185 | <0.5[b] | 0.17 | 0.17 |
| $HCO_3^-$ (mg/L) | 517.6 | 328.3 | 422.7 | 308.3 | 344.3 |
| $NH_4^+$ (mg/L) | <0.1 | <0.1 | 0.44 | <0.1 | <0.1 |
| $NO_3^-$ (mg/L) | <0.4 | <0.4 | 0.584 | 1.32 | 8.72 |
| P (mg/L) | 0.65 | <0.02 | 0.342 | 0.024 | NR |
| $SO_4^{-2}$ (mg/L) | 19.6 | 97.2 | 385 | 121 | 54.2 |
| Ag (mg/L) | <0.0005 | <0.01 | <0.01 | <0.01 | <0.0005 |
| As (mg/L) | <0.002 | <0.002 | <0.002 | <0.002 | <0.002 |
| Ba (mg/L) | 0.077 | 0.072 | 0.090 | 0.05 | 0.044 |
| Ca (mg/L) | 143 | 119 | 196 | 88.6 | 108 |
| Cd (mg/L) | 0.011 | <0.002 | <0.002 | <0.002 | 0.004 |
| Cr (mg/L) | 0.039 | <0.02 | <0.02 | <0.02 | 0.025 |
| Cu (mg/L) | 0.018 | <0.01 | <0.01 | <0.01 | 0.012 |
| Fe (mg/L) | 0.062 | 2.67 | 4.30 | 0.02 | 0.043 |
| Hg (mg/L) | 0.0012 | <0.0002 | <0.0002 | <0.0002 | 0.0006 |
| K (mg/L) | 2.01 | 2.16 | 1.35 | 2.62 | 2.1 |
| Mg (mg/L) | 72.8 | 27.9 | 33.8 | 24.2 | 25.7 |
| Mn (mg/L) | 0.01 | 0.198 | 0.40 | 0.03 | 0.012 |
| Mo (mg/L) | <0.02 | <0.033 | <0.02 | <0.02 | <0.02 |
| Na (mg/L) | 15.4 | 11.6 | 9.5 | 16.8 | 9.12 |
| Ni (mg/L) | 0.034 | <0.02 | <0.02 | <0.02 | <0.02 |
| Pb (mg/L) | <0.002 | <0.002 | 0.032 | 0.003 | <0.002 |
| Se (mg/L) | <0.002 | <0.002 | <0.002 | <0.002 | <0.002 |
| Th (mg/L) | <0.008 | <0.002 | <0.004 | <0.002 | 0.005 |
| U (mg/L) | 0.81 | 0.008 | 0.005 | 0.033 | 0.283 |

[a]NR = analysis not reported
[b]Less than sign indicates below detection limit value

## APPENDIX A
## ANALYTICAL RESULTS FOR MODELED GROUNDWATERS

| WELL # | 2046 | 2060 | 2060 | 2061 | 2094 |
|---|---|---|---|---|---|
| Sample ID | 3997 | 3696 | 3889 | 3890 | 3872 |
| Sample Date | 02/02/89 | 10/25/88 | 02/01/89 | 02/07/89 | 02/01/89 |
| Round # | 4 | 3 | 4 | 4 | 4 |
| pH | 7.1 | 7.5 | 7.4 | 7.6 | 7.1 |
| Eh (mV) | 441 | NR[a] | 477 | 415 | 75 |
| $O_2$ (mg/L) | 4 | 3.2 | 2 | 0.7 | 0.4 |
| T ($^oC$) | 9 | 11 | 8 | 6 | 15 |
| Cl (mg/L) | 3 | 21 | 22 | 19.5 | 185 |
| F (mg/L) | 0.15 | 0.54 | 0.48 | 0.33 | 0.17 |
| $HCO_3^-$ (mg/L) | 355.3 | 265.5 | 276.6 | 262.5 | 716.6 |
| $NH_4^+$ (mg/L) | <0.1[b] | <0.1 | <0.1 | 0.266 | <0.1 |
| $NO_3^-$ (mg/L) | 5.98 | 32.8 | 1.51 | 1.73 | <0.4 |
| P (mg/L) | 0.39 | <0.02 | 0.03 | 0.02 | 1.92 |
| $SO_4^{-2}$ (mg/L) | 73.5 | 36 | 78.3 | 61.8 | 33 |
| Ag (mg/L) | <0.0005 | <0.01 | <0.0005 | <0.0005 | <0.0005 |
| As (mg/L) | <0.002 | <0.002 | <0.002 | <0.002 | 0.21 |
| Ba (mg/L) | 0.067 | 0.039 | 0.054 | 0.044 | 1.25 |
| Ca (mg/L) | 111 | 81.8 | 90.6 | 87 | 74 |
| Cd (mg/L) | 0.006 | <0.002 | <.02 | 0.006 | 0.011 |
| Cr (mg/L) | 0.023 | <0.02 | 0.03 | 0.026 | 0.03 |
| Cu (mg/L) | 0.021 | <0.01 | 0.018 | 0.027 | 0.026 |
| Fe (mg/L) | 0.117 | 0.011 | 0.161 | 0.18 | 21.2 |
| Hg (mg/L) | <0.0002 | <0.0002 | 0.001 | <0.0002 | 0.0085 |
| K (mg/L) | 2.86 | 2.27 | 5.58 | 2.77 | 1800 |
| Mg (mg/L) | 31.8 | 20.8 | 24.3 | 22.6 | 49.4 |
| Mn (mg/L) | 0.017 | 0.001 | 0.01 | 0.016 | 0.256 |
| Mo (mg/L) | <0.02 | <0.02 | <0.02 | <0.02 | <0.02 |
| Na (mg/L) | 10.2 | 10.6 | 13.6 | 10.6 | 109 |
| Ni (mg/L) | 0.02 | <0.02 | <0.02 | <0.02 | 0.052 |
| Pb (mg/L) | 0.006 | <0.002 | <0.002 | 0.004 | <0.002 |
| Se (mg/L) | 0.003 | <0.002 | <0.002 | 0.002 | <0.002 |
| Th (mg/L) | <0.002 | <0.007 | <0.003 | <0.003 | <0.004 |
| U (mg/L) | 0.309 | 0.171 | 0.25 | 0.292 | 0.0045 |

[a]NR = analysis not reported
[b]Less than sign indicates below detection limit value

## APPENDIX A
## ANALYTICAL RESULTS FOR MODELED GROUNDWATERS

| WELL # | 2095 | 3001 | 3001 | 3013 | 3013 |
|---|---|---|---|---|---|
| Sample ID | 3787 | 3783 | 3936 | 3703 | 3899 |
| Sample Date | 12/06/88 | 12/05/88 | 02/28/89 | 11/14/88 | 02/22/89 |
| Round # | 3 | 3 | 4 | 3 | 4 |
| pH | 7.33 | 8 | 7.1 | 6.3 | 8.4 |
| Eh (mV) | NR[a] | NR | 81 | NR | 139 |
| $O_2$ (mg/L) | 4.1 | 9.5 | 0.7 | 1.9 | NR |
| T ($^oC$) | 11 | 9 | 11 | 13.5 | 7 |
| Cl (mg/L) | 4 | 19.1 | 21 | 60 | 21 |
| F (mg/L) | 0.24 | 0.19 | 0.1 | 0.113 | 0.45 |
| $HCO_3^-$ (mg/L) | 352.2 | 300.7 | 300.9 | 480.5 | 302.2 |
| $NH_4^+$ (mg/L) | <0.1 | .131 | 0.5 | <0.1 | 0.1 |
| $NO_3^-$ (mg/L) | 77.5 | <0.4 | <0.08 | <0.4 | 0.4 |
| P (mg/L) | 0.063 | <0.02 | 0.12 | <0.02 | 0.02 |
| $SO_4^{-2}$ (mg/L) | 17.5 | 176 | 67 | 252 | 130 |
| Ag (mg/L) | <0.02 | <0.02 | <0.01 | <0.01 | <0.01 |
| As (mg/L) | <0.002 | <0.002 | <0.003 | <0.002 | <0.003 |
| Ba (mg/L) | 0.05 | 0.085 | 0.053 | 0.089 | 0.071 |
| Ca (mg/L) | 100 | 173 | 100 | 202 | 68 |
| Cd (mg/L) | <0.002 | <0.002 | <0.005 | 0.007 | 0.007 |
| Cr (mg/L) | <0.02 | <0.02 | 0.02 | <0.02 | 0.4 |
| Cu (mg/L) | 0.014 | <0.01 | <0.01 | <0.01 | 0.01 |
| Fe (mg/L) | 0.032 | 4.5 | 2.5 | 7.21 | 0.05 |
| Hg (mg/L) | 0.0004 | <0.0002 | <0.0002 | <0.0002 | <0.0002 |
| K (mg/L)B | 2.5 | 5.56 | 2.3 | 3.85 | 2 |
| Mg (mg/L) | 23.3 | 37.9 | 25 | 45.2 | 52 |
| Mn (mg/L) | 0.003 | 0.362 | 0.61 | 0.382 | 0.02 |
| Mo (mg/L) | <0.02 | <0.02 | 0.01 | 0.041 | 0.02 |
| Na (mg/L) | 24.6 | 24.4 | 11 | 45.7 | 18 |
| Ni (mg/L) | <0.02 | <0.02 | <0.03 | <0.02 | <0.03 |
| Pb (mg/L) | <0.002 | <0.002 | <0.002 | 0.004 | <0.002 |
| Se (mg/L) | <0.002 | <0.002 | <0.005 | <0.002 | <0.005 |
| Th (mg/L) | <0.004 | <0.006 | <0.003 | <0.006 | <0.003 |
| U (mg/L) | 0.177 | 0.015 | 0.015 | 0.011 | 0.490 |

[a]NR = analysis not reported
[b]Less than sign indicates below detection limit value

## APPENDIX A
## ANALYTICAL RESULTS FOR MODELED GROUNDWATERS

| WELL # | 3014 | 3016 | 3062 | 3069 | 3094 |
|---|---|---|---|---|---|
| Sample ID | 3672 | 3686 | 3780 | 3663 | 3874 |
| Sample Date | 11/06/88 | 11/04/88 | 10/25/88 | 11/07/88 | 02/01/89 |
| Round # | 3 | 3 | 3 | 3 | 4 |
| pH | 7.75 | 7.6 | 7.9 | 7.6 | 7.1 |
| Eh (mV) | NR[a] | NR | NR | NR | 99 |
| $O_2$ (mg/L) | 6.2 | 5.1 | 6.8 | 3.82 | 0.6 |
| T ($^oC$) | 12 | 13.5 | 11 | 9.5 | 15 |
| Cl (mg/L) | 25.8 | 25.6 | 19.9 | 24.5 | 140 |
| F (mg/L) | 0.16 | 0.15 | 0.32 | 0.18 | 0.13 |
| $HCO_3^-$ (mg/L) | 229.4 | 251.4 | 312.8 | 261.0 | 710.6 |
| $NH_4^+$ (mg/L) | <0.1[b] | <0.1 | <0.1 | 0.17 | 2.4 |
| $NO_3^-$ (mg/L) | 7.44 | 13.5 | <0.4 | 2.97 | <0.4 |
| P (mg/L) | <0.02 | <0.02 | <0.02 | 0.662 | 0.88 |
| $SO_4^{-2}$ (mg/L) | 51.4 | 174 | 29 | 92.7 | 41.2 |
| Ag (mg/L) | <0.01 | <0.01 | <0.01 | <0.01 | <0.0005 |
| As (mg/L) | <0.002 | <0.002 | <0.002 | <0.002 | 0.003 |
| Ba (mg/L) | 0.03 | 0.040 | 0.063 | 0.050 | 0.382 |
| Ca (mg/L) | 74.1 | 82.9 | 92.3 | 79.6 | 106 |
| Cd (mg/L) | 0.004 | <0.002 | <0.002 | <0.002 | 0.007 |
| Cr (mg/L) | <0.02 | <0.02 | <0.02 | <0.02 | 0.032 |
| Cu (mg/L) | <0.01 | <0.01 | <0.01 | <0.01 | 0.02 |
| Fe (mg/L) | 0.03 | 0.10 | 1 | 0.10 | 4.43 |
| Hg (mg/L) | <0.0002 | <0.0002 | <0.0002 | <0.0002 | 0.0023 |
| K (mg/L) | 1.94 | 2.53 | 2.16 | 2.15 | 1830 |
| Mg (mg/L) | 18.7 | 21.4 | 22.7 | 20.6 | 58.1 |
| Mn (mg/L) | <0.001 | 0.050 | 0.396 | 0.10 | 0.241 |
| Mo (mg/L) | <0.02 | <0.02 | <0.02 | <0.02 | <0.02 |
| Na (mg/L) | 10.9 | 11.3 | 12.9 | 11.4 | 90.1 |
| Ni (mg/L) | <0.02 | <0.02 | <0.02 | <0.02 | 0.066 |
| Pb (mg/L) | 0.016 | 0.003 | <0.002 | 0.010 | <0.002 |
| Se (mg/L) | 0.002 | 0.002 | <0.002 | 0.002 | <0.002 |
| Th (mg/L) | <0.007 | NR | <0.002 | NR | <0.003 |
| U (mg/L) | 0.028 | 0.008 | 0.041 | 0.005 | 0.0006 |

[a]NR = analysis not reported
[b]Less than sign indicates below detection limit value

# APPENDIX A
## ANALYTICAL RESULTS FOR MODELED GROUNDWATERS

| | |
|---|---|
| WELL # | 4097 |
| Sample ID | 3988 |
| Sample Date | 02/08/89 |
| Round # | 4 |
| | |
| pH | 7.1 |
| Eh (mV) | 221 |
| $O_2$ (mg/L) | 0.5 |
| T ($^oC$) | 11 |
| | |
| Cl (mg/L) | 25 |
| F (mg/L) | 0.16 |
| $HCO_3^-$ (mg/L) | 329.7 |
| $NH_4^+$ (mg/L) | .247 |
| $NO_3^-$ (mg/L) | .53 |
| P (mg/L) | 0.11 |
| $SO_4^{-2}$ (mg/L) | 66.4 |
| Ag (mg/L) | <0.0005[a] |
| As (mg/L) | <0.002 |
| Ba (mg/L) | 0.055 |
| Ca (mg/L) | 94.7 |
| Cd (mg/L) | 0.006 |
| Cr (mg/L) | 0.024 |
| Cu (mg/L) | 0.01 |
| Fe (mg/L) | 0.743 |
| Hg (mg/L) | 0.0006 |
| K (mg/L) | 2.17 |
| Mg (mg/L) | 27.6 |
| Mn (mg/L) | 0.243 |
| Mo (mg/L) | <0.02 |
| Na (mg/L) | 15.1 |
| Ni (mg/L) | <0.02 |
| Pb (mg/L) | <0.002 |
| Se (mg/L) | 0.003 |
| Th (mg/L) | <0.002 |
| U (mg/L) | 0.019 |

[a]Less than sign indicates below detection limit value

# APPENDIX B
# 2D FLOW MODEL EVALUATION

# APPENDIX B

## 2DFLOW Model Evaluation

The 2DFLOW model was evaluated by using the May 1988 water level data, which includes a large number of water level measurements made during a severe drought. The use of these data provided a test of model performance when hydrologic input is significantly different from that of the calibration conditions. A large amount of water level data were available for this month. The hydrograph for Monitoring Well 02E shown in Figure 3-11 demonstrates that the groundwater level was abnormally low compared to water levels in the preceding years. These low water levels may not representative of long-term conditions.

The model was successful in matching the 1988 drought data without changing the values of hydraulic conductivities or any other basic parameters. Matching the drought conditions only involved reducing infiltration rates, the Great Miami River stage, and external boundary heads. Infiltration rates were reduced to 10 in./yr where they had been 14 in./yr and to 4 in./yr where they had been 6 in./yr. The Great Miami River stage was reduced 3.6 feet in accordance with the actual difference in river stage between April 1986 and May 1988; and external boundary heads were reduced 3.5 feet in accordance with the average reduction in water levels in monitoring wells compared with the April 1986 data. The pumping rates of the collector wells were also changed to conform to reported pumping rates. The combined pumping rate of the collector wells (1 and 2) was increased from 12,052 gpm (17.35 Mgd) in the 1986 period to 12,844 gpm (18.55 Mgd) in the 1988 period. The change was an increase of 832 gpm (1.2 Mgd), or about 7 percent.

The degree of calibration is indicated by the statistical results presented in Table B-1. The criteria related to the size of the residuals are satisfied. Other results indicate clumping of positive and negative residuals. The clumping is considered acceptable in this case because the residuals are small, and further refinement of the parameter values is not necessary for validation of the model. This model of drought conditions will not be used in future applications.

These results show that the model is capable of adequately simulating two different sets of hydrologic conditions, while leaving parameters related to unchanging geologic conditions constant. This step, which demonstrated model performance under conditions significantly different than those used in the model calibration, provides additional grounds for confidence in model applications that involve changing hydrologic input.

The results of the sensitivity analysis applied to the model of 1988 conditions are shown in Table B-2. These results merely confirm that the model is sensitive to river leakage factor. It is also noteworthy that the model is sensitive to hydraulic heads assigned to the Great Miami Aquifer at

**TABLE B-1**

**STATISTICAL TESTS FOR 2DFLOW MODEL EVALUATION BASED ON MAY 1988 DATA**

| Statistical Measure | Predetermined Criteria | 2-D Flow 1988 (2DFLOW) |
|---|---|---|
| Mean Residual (Observed Minus Computed Head) (ft) | $\pm$ 0.5 | 0.083 |
| Mean of The Absolute Residuals (ft) | $\leq$ 2 | 1.080 |
| Standard Deviation of Differences (ft) | $\leq$ 3 | 0.138 |
| Regression Coefficient Between Measured and Computed Values | 1 $\pm$ 0.05 | 0.89 |
| Nearest Neighbor Autocorrelation Unit Normal Deviate | < 1.645 | 3.493 |

**TABLE B-2**

**RESULTS OF THE SENSITIVITY ANALYSIS FOR THE TWO-DIMENSIONAL FLOW MODEL BASED ON MAY 1988 DATA UTILIZING RUN 2DFLOW**

| | | | | Sensitivity Run[a] Statistics | |
|---|---|---|---|---|---|
| Sensitivity Run Number | Parameter | 2DFLOW Value | Sensitivity Run Value | Mean Residual (ft) | Mean Absolute Residual (ft) |
| 1 | River Bed Leakage Factor | 0.5 | 0.25 | 0.851 | 0.949 |
| 2 | River Bed Leakage Factor | 0.5 | 0.375 | 0.357 | 0.759 |
| 3 | River Bed Leakage Factor | 0.5 | 0.625 | -0.082 | 0.872 |
| 4 | River Bed Leakage Factor | 0.5 | 0.750 | -0.200 | 0.923 |
| 5 | River Bed Leakage Factor | 0.5 | 1.0 | -0.354 | 1.005 |
| | | 2DFLOW STATISTICS: | | 0.100 | 1.077 |

[a]Mean Residual is the mean of the differences between observed heads and calculated heads. Mean Absolute Residual is the mean of the absolute differences between observed heads and calculated heads.

external boundaries. Consequently, if the model is used to simulate drought conditions or other extreme events, the external boundary heads must be changed in addition to recharge rates and river stage. It should be noted that any differences between the boundary heads and what may actually occur in the real system have little effect on calibration results in the vicinity of the FEMP, which is of principal concern in subsequent applications. These parts are the FEMP area and the areas hydraulically downgradient from the FEMP, extending southward from the FEMP to the Great Miami River and eastward from the FEMP to the collector wells and the Great Miami River.

# APPENDIX C
# 3DSOL CALIBRATION USING RETARDATION FACTOR OF 9

# APPENDIX C

## C.1 MODEL CALIBRATION

Calibration runs with the distribution coefficient of 0.016 $ft^3/lb$ (retardation factor = 9) began with the longitudinal dispersivity set at the preferred value of 100 feet and the transverse dispersivity set at 10 feet. The plume produced by using 100 feet for the longitudinal dispersivity had too much spread; however, it was close enough to matching field concentrations that runs were made with lower dispersivity values in an attempt to refine the calibration without requiring a higher distribution coefficient. An acceptable calibration was accomplished. The final calibrated run had a longitudinal dispersivity of 50 feet and a transverse dispersivity of 1 foot. This reduction in dispersivity was needed to make the concentration gradients high enough (that is, make the shape of the plume sharp enough) to match the high concentrations near the axis of the plume, while matching very low concentrations at the edge of the plume a short distance east of the axis. The 50/1 dispersivity ratio was needed to increase the sharpness of the plume and to get a decrease in concentration with depth near the source areas, since the model uses transverse dispersivity for vertical dispersivity. This calibrated model is called 3DSOL9.

A comparison of the mean observed concentrations at 41 individual monitoring wells and the calculated concentrations in the model cells containing the monitoring wells is presented in Table C-1. As mentioned above, the mean of observed concentrations at a monitoring well where only a few concentrations have been measured may not be an accurate estimate of the most representative value for that monitoring well; consequently, such means were not matched more closely than their representativeness warranted. Instead, the model calibration emphasized (1) avoidance of excessive clustering of positive or negative residuals (observed mean minus calculated concentration), and (2) keeping the absolute values of the residuals reasonably low.

The clustering criterion is examined by calculating the unit normal deviate from a modification of Moran's I (IT 1987). A value greater than 1.645 indicates a nonrandom distribution of residuals at the 0.05 level of significance. The optimal value is zero. The value calculated for the calibrated run was 0.144.

The reasonably low absolute values of residuals corresponding to the second calibration criterion may be examined by using a statistical procedure to determine whether the calculated concentration at an observation well differs by an improbable amount from the mean concentration observed at the well. The statistical testing procedure used for this purpose followed methods described by Grubbs (1969). This method of testing goodness of fit is more informative than simply measuring deviations from means because it includes uncertainty related to the representativeness of the observed concentrations at a given monitoring well. It allows less deviation from means of large samples and/or samples with

# TABLE C-1
## INLIER CONCENTRATIONS CALCULATED BY THE THREE-DIMENSIONAL FINITE-DIFFERENCE SOLUTE TRANSPORT MODEL RETARDATION FACTOR 9

| Well No. | Cell | | | Number of Observed Concentrations | Observed Concentrations (µg/l) | | | Calculated Concentrations (µg/l) |
|---|---|---|---|---|---|---|---|---|
| | I | J | K | | Minimum | Maximum | Mean | |
| EMR-13 | 40 | 42 | 1 | 45 | 0.3 | 1 | 0.55 | 0.1 |
| EMR-16 | 49 | 57 | 1 | 44 | 0.4 | 1.1 | 0.59 | 0.1 |
| 2004 | 34 | 83 | 1 | 4 | 7 | 18 | 11 | 0.4 |
| 2008 | 40 | 84 | 1 | 4 | 5 | 22 | 15.3 | 11.7 |
| 2009 | 29 | 80 | 1 | 4 | 17 | 24 | 20.5 | 18.5 |
| 2010 | 48 | 87 | 1 | 4 | 2 | 21 | 12.3 | 16 |
| 2014 | 29 | 55 | 1 | 8 | 17 | 35 | 27.1 | 45.1 |
| 2015 | 30 | 48 | 1 | 8 | 154 | 200 | 176 | 168 |
| 2016 | 29 | 62 | 1 | 8 | 12.0 | 22.0 | 18.1 | 29.1 |
| 2022 | 42 | 92 | 1 | 4 | 4 | 10 | 6.3 | 19.4 |
| 2024 | 47 | 97 | 1 | 4 | 2 | 6 | 4.5 | 0.1 |
| 2034 | 34 | 83 | 1 | 4 | 15 | 24 | 20.5 | 21.5 |
| 2042 | 43 | 80 | 1 | 4 | 2 | 4 | 2.8 | 6.9 |
| 2044 | 23 | 67 | 1 | 3 | 1 | 2 | 1.33 | 0.3 |
| 2046 | 10 | 32 | 1 | 3 | 232 | 850 | 464 | 23.3 |
| 2047 | 11 | 32 | 1 | 3 | 9 | 15 | 11.3 | 19.2 |
| 2049 | 33 | 54 | 1 | 6 | 2.5 | 175 | 78.1 | 14.6 |
| 2054 | 55 | 69 | 1 | 2 | 21 | 23 | 22 | 1.5 |
| 2060 | 28 | 47 | 1 | 55 | 105 | 410 | 243 | 144 |
| 2061 | 21 | 39 | 1 | 57 | 208 | 378 | 287 | 180 |
| 2065 | 39 | 59 | 1 | 5 | 7 | 11.5 | 9.2 | 0.7 |
| 2069 | 35 | 38 | 1 | 5 | 6 | 14.8 | 11.6 | 5.3 |
| 2084 | 45 | 93 | 1 | 4 | 16 | 21 | 18.3 | 14.4 |
| 2106 | 26 | 49 | 1 | 2 | 16 | 61 | 38.5 | 5.4 |
| 2107 | 28 | 71 | 1 | 2 | 32 | 37 | 34.5 | 0.1 |

**TABLE C-1**
(Continued)

| Well No. | Cell | | | Number of Observed Concentrations | Observed Concentrations (µg/l) | | | Calculated Concentrations (µg/l) |
|---|---|---|---|---|---|---|---|---|
| | I | J | K | | Minimum | Maximum | Mean | |
| 2109 | 59 | 71 | 1 | 2 | 2 | 34 | 18 | 0.7 |
| 2118 | 57 | 68 | 1 | 2 | 9 | 16 | 12.5 | 1.1 |
| 2127 | 5 | 5 | 1 | 3 | 6 | 37 | 19 | 0.4 |
| 3003 | 36 | 95 | 2 | 3 | 3 | 4 | 3.3 | 0.1 |
| 3009 | 29 | 80 | 2 | 4 | 2 | 4 | 2.8 | 1.4 |
| 3010 | 49 | 87 | 2 | 4 | 15 | 20 | 17 | 4 |
| 3019 | 45 | 90 | 2 | 4 | 20 | 45 | 32 | 4.4 |
| 3014 | 29 | 54 | 2 | 9 | 19 | 38 | 26.7 | 13.5 |
| 3016 | 29 | 62 | 2 | 8 | 7 | 11 | 8.8 | 6.5 |
| 3062 | 18 | 35 | 2 | 46 | 31 | 76 | 49.9 | 42.5 |
| 3084 | 45 | 93 | 2 | 4 | 23 | 218 | 90.5 | 0.9 |
| 3095 | 21 | 42 | 2 | 4 | 4 | 13 | 7 | 32.3 |
| 4096 | 11 | 62 | 5 | 4 | 0.5 | 2 | 0.98 | 0.1 |
| H-112 | 24 | 82 | 4 | 2 | 0.43 | 0.48 | 0.46 | 0.1 |
| TW-3 | 7 | 28 | 2 | 3 | 1.1 | 2.1 | 1.53 | 0.1 |
| TW-5 | 8 | 29 | 1 | 4 | 0.45 | 0.85 | 0.58 | 0.1 |

little variation in values, and greater deviation from means based on only a few samples and/or means based on samples with a large variation in values. As is the case when simply comparing computed concentrations with observed means, judgment must still be used in interpreting the results with regard to goodness of fit. However, the statistical procedure provides information upon which to base that judgment.

Calculated concentrations that tested as being improbable in the real system at a significance level of 2.5 percent are listed in Table C-2 along with the observed mean, the number of measured concentrations, and the range of the observed concentrations. These results show that two calculated concentrations within the main plume was significantly different from the observed mean for the monitoring wells in these cells (Monitoring Wells 2045 and 2095). These deviations were greatly reduced in the final calibration (R=12). The remaining 15 monitoring wells with calculated concentrations that exhibit statistically significant deviations from the observed means (Table C-2) are all located peripherally to the main plume. Since these are all cases where both the observed and calculated concentrations are very low, the actual difference between observed and calculated concentrations is also low. The effect on the overall fit of the model is negligible, and it is not practical to attempt to match these data more closely. Such additional calibration might be very difficult for the following reasons:

- Concentration gradients on the flanks of the southern plume are high, and the finite-difference approximation may be causing a slight undershooting of the real values where the concentrations are approaching zero near the edge of the main plume.

- Some of the statistically significant deviations may be caused by rounding off the concentrations reported for the samples. Some observed concentrations are reported as one-digit integers, which tends to hide the true variation of the concentration and cause the statistical procedure to underestimate the range of likely concentrations.

- Monitoring Wells 2096, 2108, 3108, 2044, 3044, 2104, 2017, 3017, and 2127 located west of Paddys Run yielded observed concentrations that were above background. The monitoring wells are at nine different locations. The highest concentration found in any of them was 37 µg/L in Monitoring Well 2108. These elevated concentrations are thought to be caused by temporary seasonal reversals in hydraulic gradient near Paddys Run. Such reversals could intermittently carry small amounts of uranium a short distance westward from Paddys Run, but they cannot be simulated by the steady-state flow model.

It is noteworthy in Table C-1 that Monitoring Well 2046 has calculated concentrations considerably below their mean observed concentrations. The calculated concentration for this monitoring well does not test as outlier due the small number of observed concentrations and the large range in the observed

# TABLE C-2
## OUTLIER CONCENTRATIONS CALCULATED BY THE THREE-DIMENSIONAL FINITE-DIFFERENCE SOLUTE TRANSPORT MODEL RETARDATION FACTOR 9

| Well No. | Cell | | | Number of Observed Concentrations | Observed Concentrations (µg/l) | | | Calculated Concentrations (µg/l) |
|---|---|---|---|---|---|---|---|---|
| | I | J | K | | Minimum | Maximum | Mean | |
| EMR-11 | 22 | 53 | 1 | 46 | 0.9 | 1.8 | 1.46 | 0.1 |
| EMR-14 | 59 | 38 | 1 | 47 | 0.7 | 1.7 | 1.09 | 0.1 |
| EMR-20 | 19 | 15 | 4 | 30 | 0.1 | 0.8 | 1.34 | 7.6 |
| EMR-21 | 24 | 17 | 2 | 47 | 0.2 | 0.7 | 0.43 | 3.6 |
| EMR-22 | 22 | 62 | 1 | 43 | 0.6 | 1.6 | 1.07 | 0.1 |
| EMR-29 | 17 | 46 | 4 | 12 | 1.7 | 2.2 | 1.9 | 0.1 |
| EMR-30 | 18 | 66 | 4 | 19 | 0.4 | 0.8 | 0.6 | 0.1 |
| 2027 | 48 | 92 | 1 | 4 | 6 | 6 | 6 | 5.3 |
| 2045 | 31 | 56 | 1 | 3 | 278 | 341 | 301 | 19.7 |
| 2095 | 22 | 43 | 1 | 4 | 146 | 202 | 173 | 349 |
| 3001 | 41 | 89 | 2 | 3 | 15 | 15 | 15 | 3.6 |
| 3004 | 35 | 93 | 2 | 4 | 10 | 13 | 11.3 | 0.1 |
| 3005 | 36 | 90 | 2 | 3 | 3 | 3 | 3 | 0.9 |
| 3013 | 65 | 78 | 2 | 3 | 4 | 4 | 4 | 0.1 |
| 3108 | 30 | 84 | 2 | 31 | 33 | 32 | 32 | 0.1 |
| TW-4 | 13 | 31 | 1 | 3 | 1.71 | 1.92 | 1.82 | 0.1 |
| TW-6 | 15 | 34 | 4 | 4 | 1.08 | 1.18 | 1.13 | 0.1 |

concentrations. The source of uranium in the monitoring well remains uncertain and continues to be investigated in the RI/FS.

## C.2 LOADING RATES AND CONCENTRATION DISTRIBUTION

The uranium source loading rates for each period that resulted from this calibration are shown in Figure C-1 through C-4, and summarized in terms of loading rates and total mass loading in Table C-3 and C-4. The corresponding uranium plume resulting from this calibration is shown for the respective vertical layers in Figures C-5 through C-9.

## C.3 SENSITIVITY ANALYSIS

Results of sensitivity analyses for the models described in previous sections also apply to 3DSOL. No new parameters were introduced into 3DSOL. As in 2DSOL, the model is to be most sensitive to the value of the uranium distribution coefficient and to the amount and location of source loading. However, since varying the dispersivities may have a different effect in 3DSOL than they did in 2DSOL, they were subjected to sensitivity analysis. The model with the distribution coefficient set at 0.016 (3DSOL9) was used for the analysis. The results are shown in Table C-5. Increasing dispersivities caused the plume to spread and decreasing dispersivities had the opposite effect. This property of the model was instrumental in model calibration, as mentioned above.

The effect of increasing the hydraulic conductivity of the clay interbed beneath the FEMP was also checked. It was found to have virtually no effect on model calibration (Table C-5). The change in the calculated vertical head difference across the clay was from 0.90 to 0.05 feet at the location of Monitoring Wells 2008 and 3008 in 3DSOL9. The decrease in vertical hydraulic gradient was associated with a decrease in hydraulic head above the clay interbed and an increase below it.

Changes in flow model parameters in the flow modeling sensitivity analysis did not significantly affect the flow field within the solute transport model area. The most impact areas are the regions near the Great Miami River and collection monitoring wells, as shown in Section 5.2.4. Consequently, the sensitivity of the solute transport model to these parameters was not investigated. Experience with the present model suggests that the calibrated three-dimensional solute transport model would not be significantly affected by variations in most of the parameters.

409195-B69 /01 (GW) 100% RED



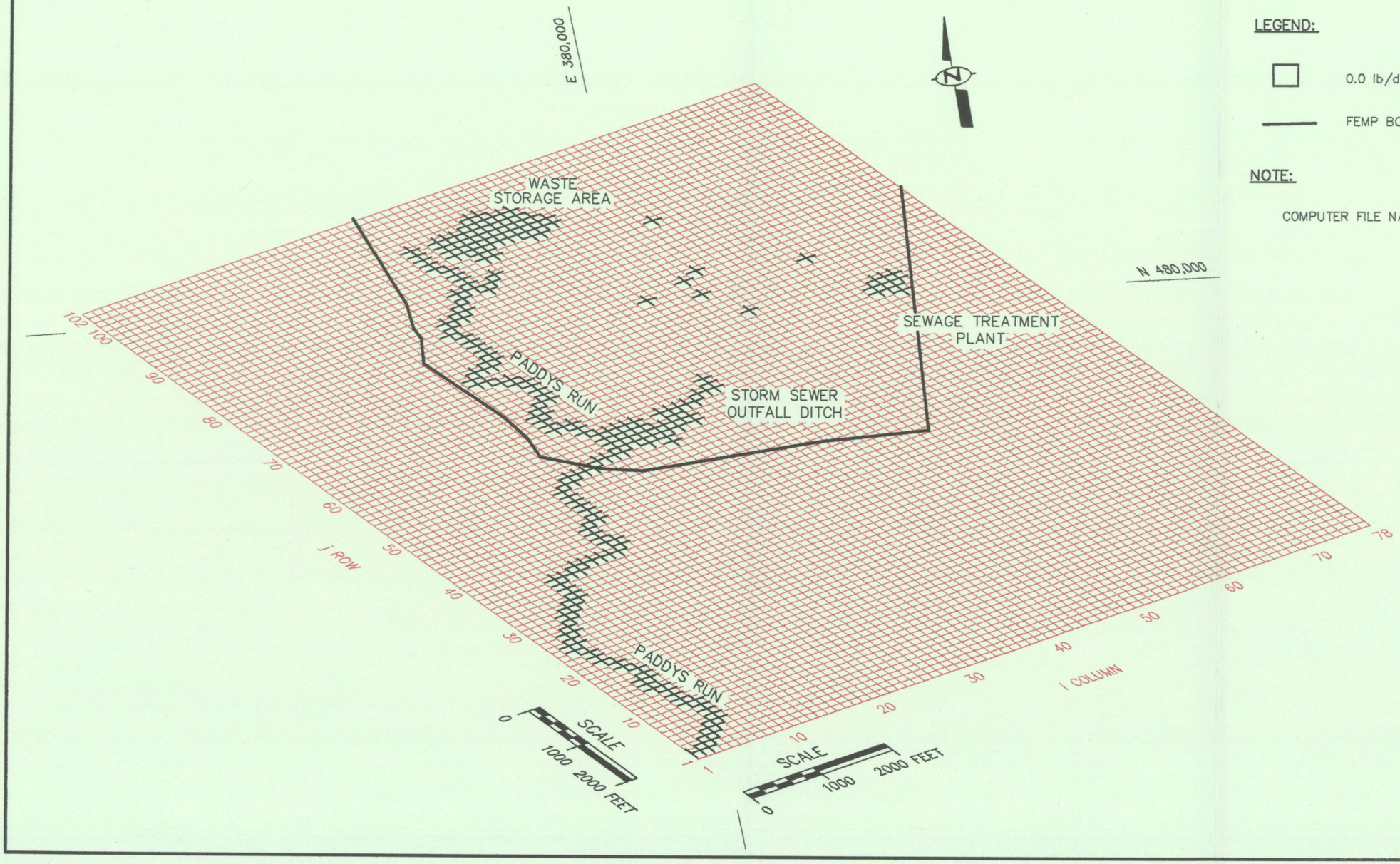


**LEGEND:**

0.0 lb/day to 0.1 lb/day

FEMP BOUNDARY

**NOTE:**

COMPUTER FILE NAME: 3DSOL9-64



409195-B69 /01 (GW) (PGH)

FIGURE C-1
3-DIMENSIONAL SOLUTE TRANSPORT MODEL
SOURCE LOADING RATES
SOURCE PERIOD 1
RETARDATION FACTOR 9

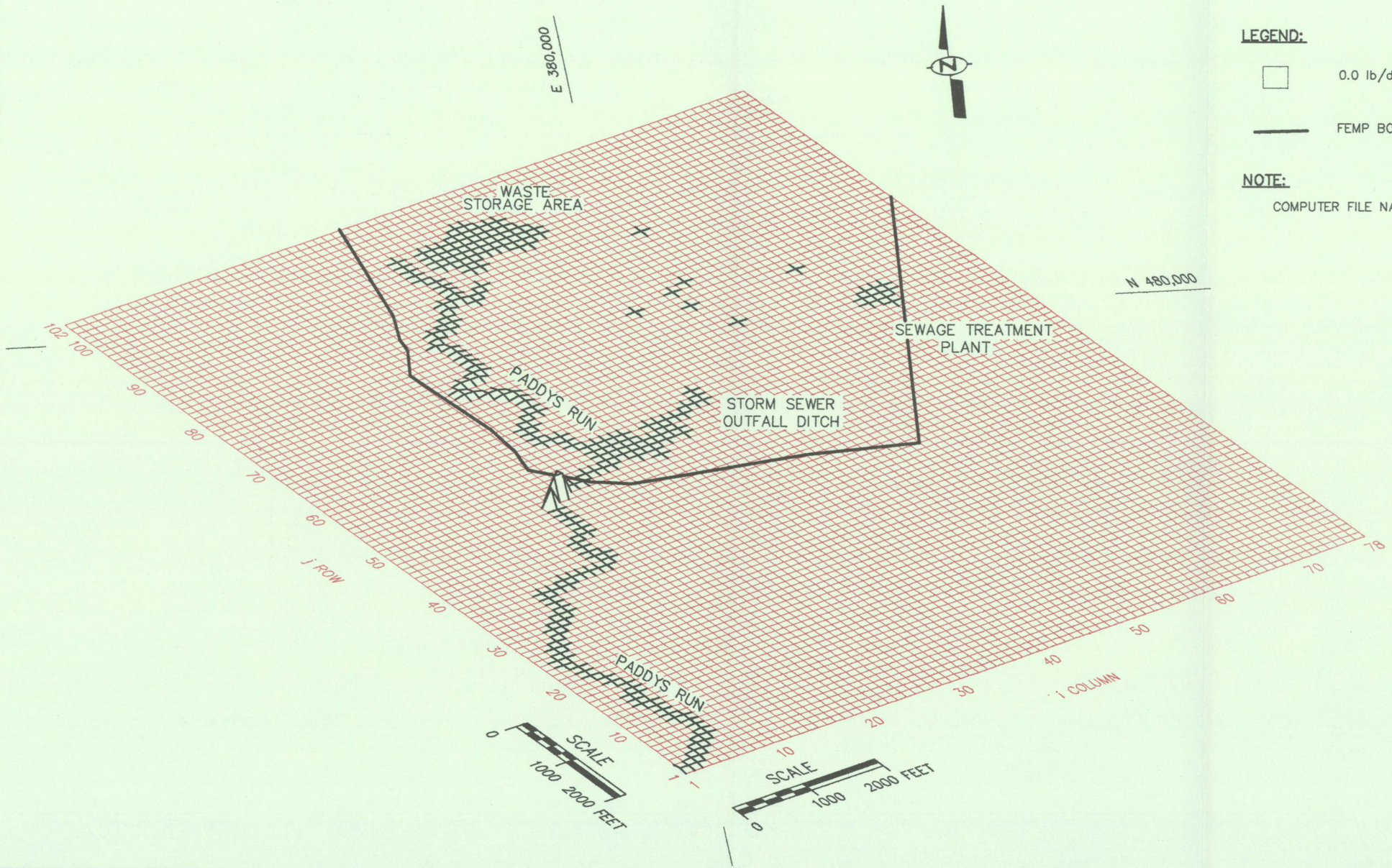


**LEGEND:**

0.0 lb/day to 0.1 lb./day

FEMP BOUNDARY

**NOTE:**

COMPUTER FILE NAME: 3DSOL9-64



409195-B77 /01 (GW) (PGH)

FIGURE C-2
3-DIMENSIONAL SOLUTE TRANSPORT MODEL
SOURCE LOADING RATES
SOURCE PERIOD 2
RETARDATION FACTOR 9

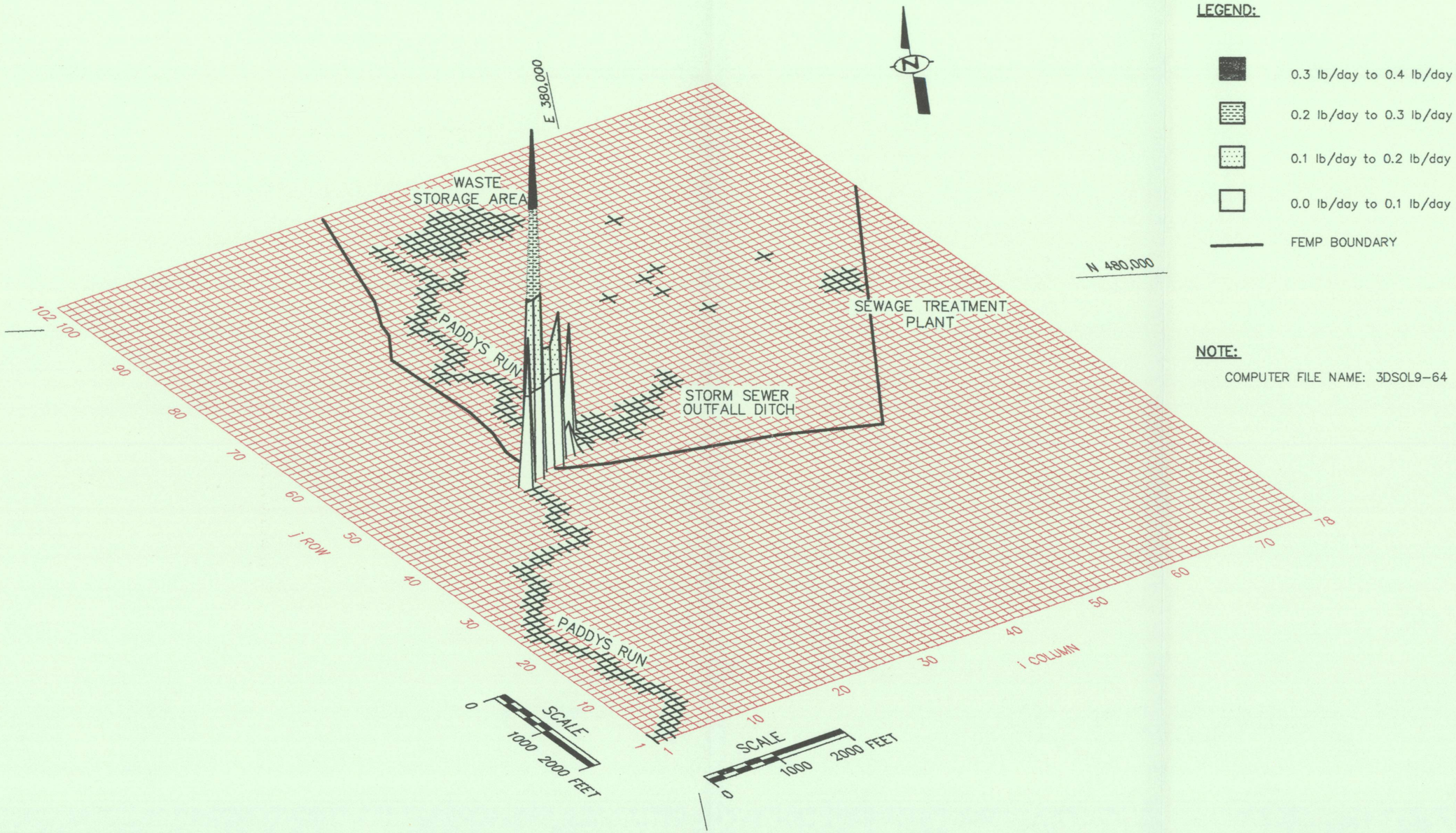


**LEGEND:**

- 0.3 lb/day to 0.4 lb/day
- 0.2 lb/day to 0.3 lb/day
- 0.1 lb/day to 0.2 lb/day
- 0.0 lb/day to 0.1 lb/day
- FEMP BOUNDARY

**NOTE:**

COMPUTER FILE NAME: 3DSOL9-64

409195-B70 /01 (GW) (PGH)



FIGURE C-3
3-DIMENSIONAL SOLUTE TRANSPORT MODEL
SOURCE LOADING RATES
SOURCE PERIOD 3
RETARDATION FACTOR 9

LEGEND:

0.0 lb/day to 0.1 lb/day

FEMP BOUNDARY

NOTE:

COMPUTER FILE NAME: 3DSOL9-64



FIGURE C-4
3-DIMENSIONAL SOLUTE TRANSPORT MODEL
SOURCE LOADING RATES
SOURCE PERIOD 4
RETARDATION FACTOR 9

409195-B78 /01 (GW) (PGH)
409195-B7P- (GW) /01 100%

# TABLE C-3

## URANIUM LOADING RATES FOR SOURCE AREAS IN THE THREE-DIMENSIONAL FINITE-DIFFERENCE SOLUTE TRANSPORT MODEL RETARDATION FACTOR 9, LONGITUDINAL DISPERSIVITY 50 FEET, AND TRANSVERSE DISPERSIVITY 1 FOOT

| | Uranium Source Loading Rates (lb/day) | | | |
|---|---|---|---|---|
| Source Loading Area | Period 1 1952-1958 | Period 2 1959-1966 | Period 3 1967-1975 | Period 4 1976-1988 |
| Paddys Run: | | | | |
| North of Waste Storage Area | 0.0000286 | 0.000373 | 0.000372 | 0.000372 |
| Waste Storage Area to Storm Sewer Outfall Ditch | 0.00319 | 0.0602 | 0.0559 | 0.0559 |
| Storm Sewer Outfall Ditch to Albright & Wilson Co. Wells | 0.000428 | 0.0875 | 1.68 | 0.332 |
| South of Albright & Wilson Co. Wells | 0.00292 | 0.0192 | 0.00769 | 0.00101 |
| Waste Storage Area | 0.00262 | 0.0209 | 0.0209 | 0.0209 |
| Waste Storage Silo Area | 0.000197 | 0.000197 | 0.000197 | 0.000197 |
| Biodenitrification Lagoon | 0.0000000 | 0.0000000 | 0.0000000 | 0.0000000 |
| Sludge Ponds | 0.0000000 | 0.0000000 | 0.0000000 | 0.0000000 |
| Production Area | 0.00178 | 0.00178 | 0.00178 | 0.00178 |
| Sewage Treatment Area | 0.000593 | 0.000593 | 0.000593 | 0.000593 |
| Storm Sewer Outfall Ditch | 0.000521 | 0.00342 | 0.001960 | 0.000252 |
| Total | 0.0123 | 0.194 | 1.77 | 0.413 |

# TABLE C-4

## TOTAL URANIUM LOADINGS FOR SOURCE AREAS IN THE THREE-DIMENSIONAL FINITE-DIFFERENCE SOLUTE TRANSPORT MODEL RETARDATION FACTOR 9, LONGITUDINAL DISPERSIVITY 50 FEET, AND TRANSVERSE DISPERSIVITY 1 FOOT

| | Total Uranium Source Loadings (lb) | | | | |
|---|---|---|---|---|---|
| Source Loading Area | Period 1 1952-1958 | Period 2 1959-1966 | Period 3 1967-1975 | Period 4 1976-1988 | Total |
| Paddys Run: | | | | | |
| North of Waste Storage Area | 0.073 | 1.09 | 12.20 | 1.77 | 15.10 |
| Waste Storage Area to Storm Sewer Outfall Ditch | 8.15 | 176.00 | 184.00 | 265.00 | 633.00 |
| Storm Sewer Outfall Ditch to Albright & Wilson Co. Wells | 1.09 | 256.00 | 5510.00 | 1580.00 | 7647.00 |
| South of Albright & Wilson Co. Wells | 7.47 | 56.00 | 25.30 | 4.81 | 93.60 |
| Waste Storage Area | 6.69 | 0.576 | 68.80 | 99.40 | 236.00 |
| Waste Storage Silo Area | 0.504 | 0.00 | 0.648 | 0.937 | 2.66 |
| Biodenitrification Lagoon | 0.00 | 0.00 | 0.00 | 0.00 | 0.00 |
| Sludge Ponds | 0.00 | 0.00 | 0.00 | 0.00 | 0.00 |
| Production Area | 4.54 | 5.19 | 5.84 | 8.43 | 24.00 |
| Sewage Treatment Area | 1.51 | 1.73 | 1.95 | 2.81 | 8.00 |
| Storm Sewer Outfall Ditch | 1.33 | 10.00 | 6.45 | 1.20 | 19.00 |
| Total | 31.40 | 568.00 | 5815.00 | 1964.00 | 8378.00 |

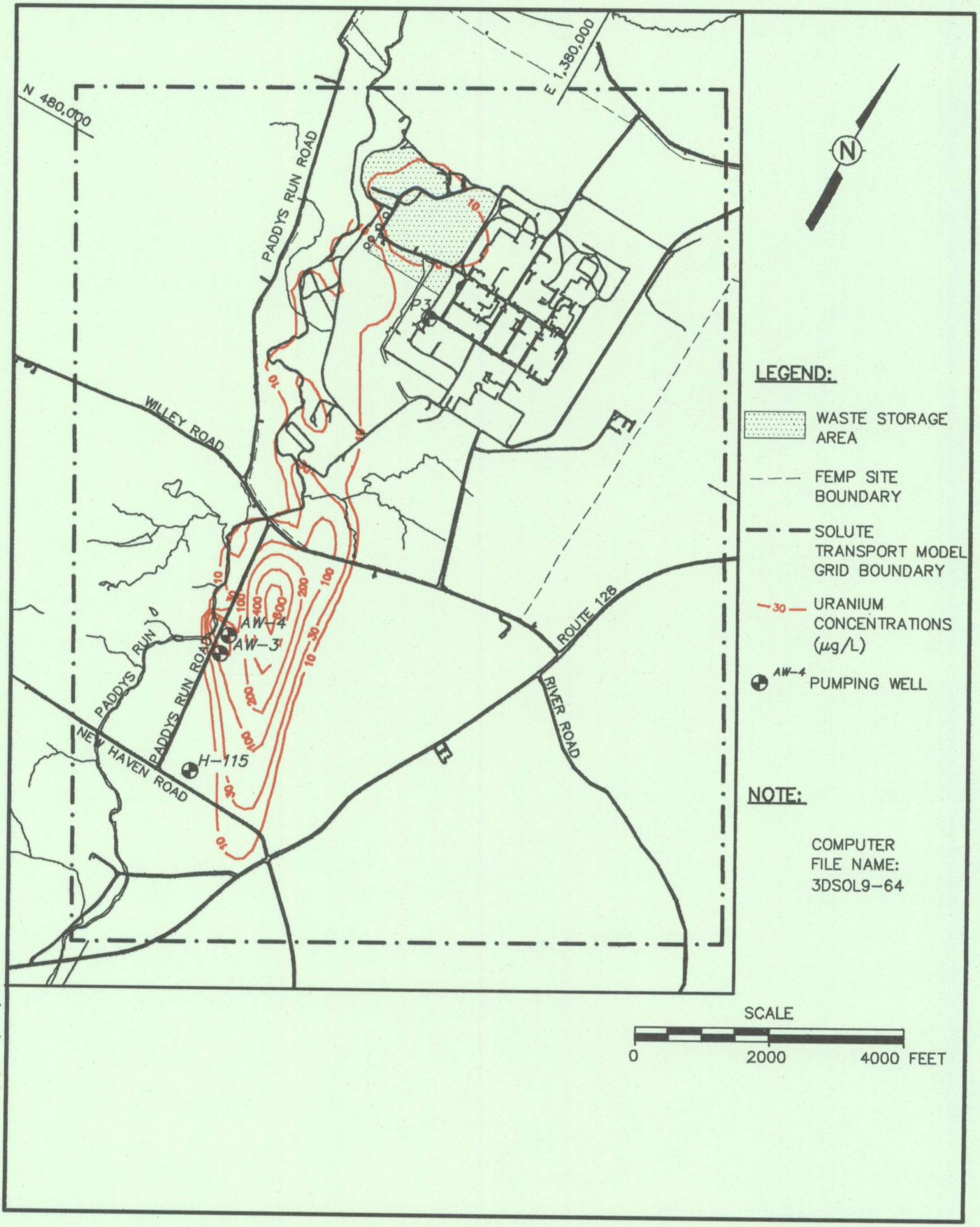


409195-A73 (GW) /01 (PGH)

FIGURE C-5 3-DIMENSIONAL SOLUTE TRANSPORT MODEL
SIMULATED URANIUM CONCENTRATIONS
PRESENT CONDITIONS
LAYER 1
RETARDATION FACTOR 9

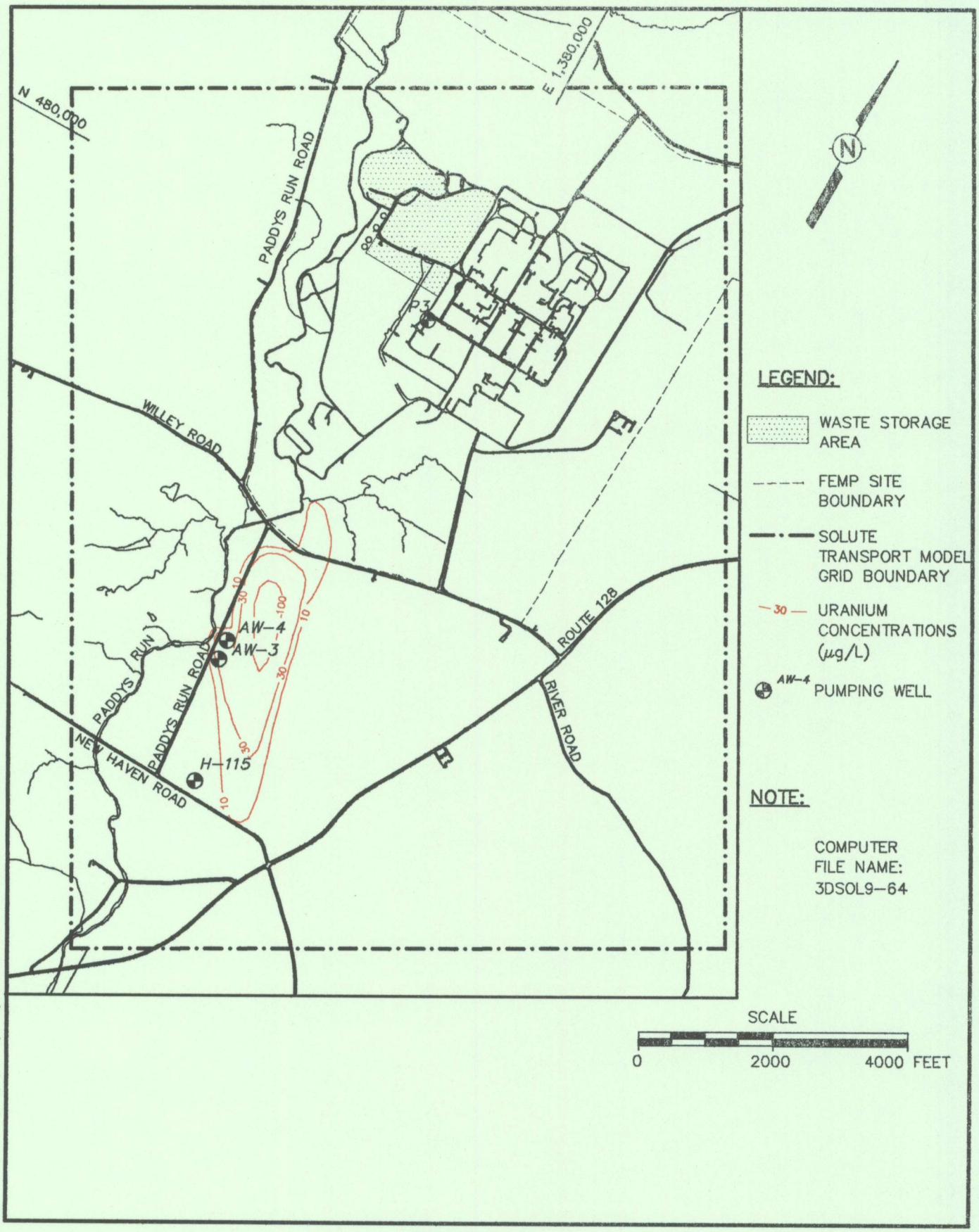


303317-A158 (GW) /01 (PGH)

FIGURE C-6
3-DIMENSIONAL SOLUTE TRANSPORT MODEL
SIMULATED URANIUM CONCENTRATIONS
PRESENT CONDITIONS
LAYER 2
RETARDATION FACTOR 9

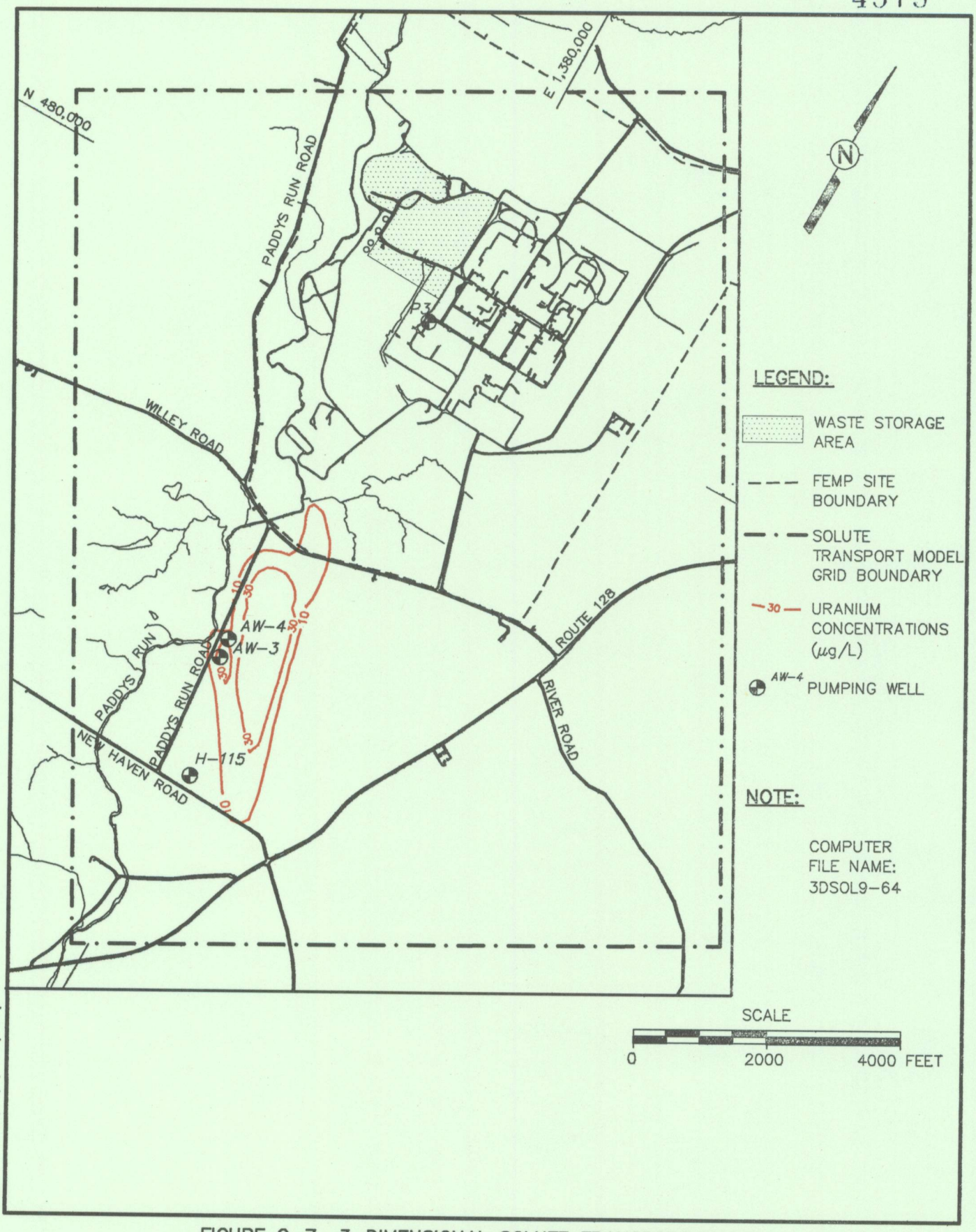


409195-A75 (GW) /01 (PGH)

FIGURE C-7 3-DIMENSIONAL SOLUTE TRANSPORT MODEL
SIMULATED URANIUM CONCENTRATIONS
PRESENT CONDITIONS
LAYER 3
RETARDATION FACTOR 9

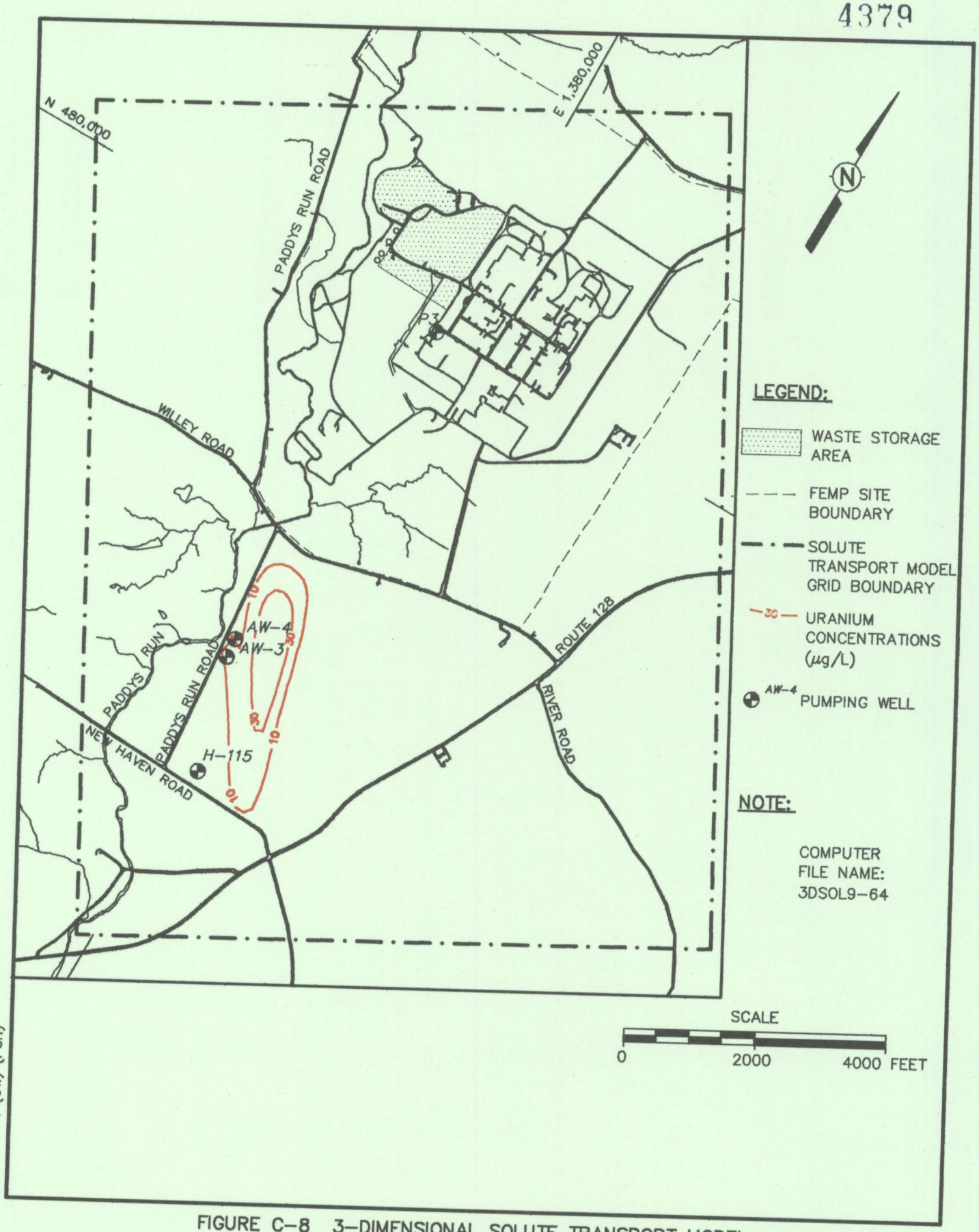


409195-A74 (GW) (PGH)

FIGURE C-8 3-DIMENSIONAL SOLUTE TRANSPORT MODEL
SIMULATED URANIUM CONCENTRATIONS
PRESENT CONDITIONS
LAYER 4
RETARDATION FACTOR 9

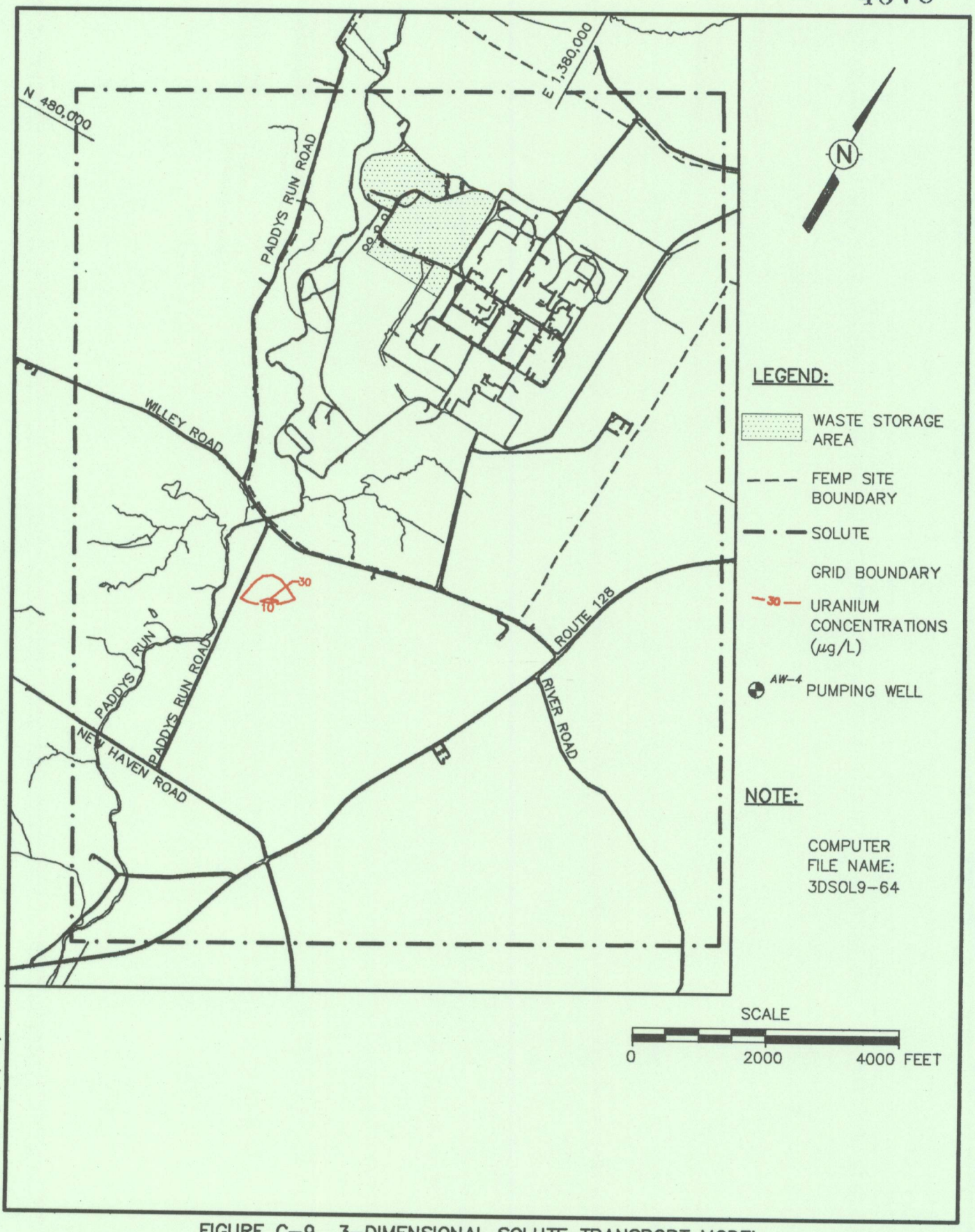


409195-A76 (GW) (PGH)

FIGURE C-9 3-DIMENSIONAL SOLUTE TRANSPORT MODEL
SIMULATED URANIUM CONCENTRATIONS
PRESENT CONDITIONS
LAYER 5
RETARDATION FACTOR 9

## TABLE C-5

## RESULTS OF THE SENSITIVITY ANALYSIS FOR THE THREE-DIMENSIONAL FINITE-DIFFERENCE SOLUTE TRANSPORT MODEL RETARDATION FACTOR 9

| Sensitivity Run Number | Parameter | 3DSOL Value | Sensitivity Run Value | Sensitivity Run Statistics[a] Mean Residual (µg/L) | Sensitivity Run Statistics[a] Mean Absolute Residual (µg/L) |
|---|---|---|---|---|---|
| 1 | Longitudinal Dispersivity<br>Transverse Dispersivity | 50 ft<br>1 ft | 50 ft<br>5 ft | 25.31 | 30.36 |
| 2 | Longitudinal Dispersivity<br>Transverse Dispersivity | 50 ft<br>1 ft | 50 ft<br>25 ft | 29.67 | 32.23 |
| 3 | Longitudinal Dispersivity<br>Transverse Dispersivity | 50 ft<br>1 ft | 300 ft<br>6 ft | 27.29 | 33.34 |
| 4 | Clay Interbed Horizontal Conductivity<br>Clay Interbed Vertical Conductivity | 0.0003 ft/day<br>0.00003 ft/day | 0.4 ft/day<br>0.4 ft/day | 17.68 | 28.16 |
| | | 3DSOL STATISTICS: | | 17.85 | 28.16 |

[a]Mean Residual is the mean of the differences between observed concentrations and calculated concentrations. Mean Absolute Residual is the mean of the absolute difference between observed concentrations and calculated concentrations.